Characterization of Metal-Mediated Base Pairs in Duplex DNA Using Fluorescent Nucleoside Analogs and NMR Spectroscopy

---

Dissertation

zur Erlangung der naturwissenschaftlichen Doktorwürde

(Dr. sc. nat.)

vorgelegt der

Mathematisch-naturwissenschaftlichen Fakultät

der Universität Zürich

von

Olivia P. Schmidt

von Zürich

Promotionskommission

Prof. Dr. Nathan W. Luedtke (Vorsitz)

Prof. Dr. Roland K.O. Sigel

Prof. Dr. Benjamin Schuler

Zürich, 2018

Acknowledgments

I would like to express my special thanks of gratitude to the following people for their support, contributions, and enjoyable time during my studies:

I would like to thank my mentor Dr. Nathan Luedtke for his inspiring passion for science and his enthusiasm to pass on his knowledge, for his guidance along my Ph.D. thesis and during my studies, and for his enormous support for my future.

I am very grateful to Dr. Roland Sigel and Dr. Benjamin Schuler for serving on my committee and their input and support of this work. Further, I would like to thank Dr. Shana Sturla for her expert review of my thesis. I would like to thank the Swiss National Science Foundation, the University of Zurich and CMSZH, for their generous financial support.

I would like to thank all past and present members of the Luedtke group for their inspiring scientific discussions, their support, and the incredible fun we had in the lab. I have had a wonderful time in this group. From the Luedkte's I would especially like to thank Dr. Guillaume Mata, for starting this project and for his input, and to Andrea Benz "Bisi" for all her support, enthusiasm and great work on the project. I would also like to thank Anaelle Dumas for her support and knowledge during my project practicum and for initiating my excitement about nucleic acids, Marco Brandstätter for the great time spent during our Master's thesis, Dr. Jawad Alzeer for constantly supporting me and for giving me my favorite five minutes of the day drinking coffee with him. Special thanks goes to Pony, Bisi, and Banana for their wonderful friendship, for creating a fun atmosphere in the lab, all their "panic checks", and the nice time spent together outside of the University.

All the members of the Zerbe group have given me constant support for all my NMR and computer questions. I had an incredibly fun time "Zerbe lunchin" with them and I thoroughly enjoyed getting to know them. I would especially like to thank Laurens the "moustache man" for all his help, the great NMR lectures I received from him and for always answering my tiiinsy NMR questions, Matthias for proof reading all my texts, especially the german ones and Stefano for all our non-scientific discussions, for making me laugh at least once a day, and for enriching my life in so many ways. My deepest gratitude goes to Simon Jurt for his support and interest in my NMR project. I would like to thank him for the fun and interesting time we spent sitting infront of the NMR machines, his enthusiasm for solving "NMR puzzles" and his immense knowledge. Further, I would like to thank the entire Nevado group, for the great atmosphere on the floor and all their scientific discussions on catalysis and the Jessen group for the great fun I had during their stay in our lab. I would especially like to thank Igor, Scarfy, and Luis for their really fun friendship

and Roopi for teaching me Hindi and all his support during my SNF application time. I direct my further gratitude to the Sigel and the Freisinger group for their helpful discussions. My special thanks goes to Dr. Silke Johannsen for her support and knowledge on NMR studies of nucleic acids, to Jelena Habjanić and Kenneth Adea for all their helpful discussions. Many thanks I also direct to the Schuler group for all their help with the fluorescent measurements and for all their "pushin start" for the k_{on} measurements. My special thanks goes to Franziska Zosel for her great input and help. I would like to direct my further thanks to Dr. Thomas Fox for always being so enthusiastic about discussing NMR problems, Sasha Giger for his help with installing and explaining computer programs, and the MS-teams of the University, in particular, Urs Stalder and Serge Chesnov, for measuring all my DNA samples. I would also like to thank Dr. Stefan Bienz for providing me with a wonderful "thesis-writing place" and the best office-buddy Vicky for making the last few months in front of the computer so enjoyable. I direct my further thanks to Clepto, for her friendship and all her support, and to my friends outside of the University, in particular Vanda, Sabrina, Anna-laura, and Julia.

My very special gratitude I direct to my family, my parents Thomas and Margaritha, my sisters Martina and Julia and their partners Niko and Tieni, my nephews Benno and Levi, and my nieces Rosa and Clementine, and to the entire family Zarth; Christian, Ursula, Mirjam, Roger, Raphael, Regula, Cucci, Jelle, Niels, Linus, Jonathan, and Emma. I consider myself incredibly lucky to have such a wonderful family and thank them for all their love, their support, and encouragement. I would especially like to thank Thomas, from whom I like to believe I have inherited my passion for science, for giving me the nicest imaginable start to every week during my studies; discussing math over coffee. Most importantly, I owe my deepest gratitude to Andreas for his love, his understanding, for being so patient with me, and for his constant encouragement.

Table of Contents

Chapter 1

Introduction

All biological information essential for life is stored and encoded in nucleic acids. The isolation and analysis of DNA molecules in 1869 by *Miescher* laid the cornerstone for unravelling the molecular basis of life.[1,2] In 1919, *Levene* reported the isolation of the nucleoside building blocks of DNA and RNA, including adenosine (A), guanosine (G), cytidine (C) and thymidine (T) and described nucleic acids as being polynucleotide chains composed of nucleotide units.[3] Years after its initial discovery, the importance of studying the structure and functions of DNA was revived, when *Avery*, *McLoad*, and *McCarty* proposed DNA rather than proteins as carrier of genetic information.[4] This was unambiguously proven in 1952 by *Hershey* and *Chase.*[5] *Chargaff* helped pave the way to elucidate the secondary structure of DNA by his discovery of a 1:1 ratio between adenine and thymidine, and guanosine and cytosine.[6] This information, together with X-ray diffraction data collected by *Franklin* and *Wilkinson* enabled *Watson* and *Crick* to propose the B-form duplex structure of DNA in 1953, thereby dramatically improving our mechanistic understanding of DNA as the carrier of genetic information.[7]

Nucleic acids have intrigued scientist for decades. Despite the ground breaking revelations and wealth of information obtained since its first discovery, our understanding of DNA is far from complete. Investigating various structures and functions of DNA is of great importance and continues to fascinate those devoted to its study.

1.1. DNA Structure and Function

The primary role of deoxyribonucleic acid (DNA) is the storage and encoding of genetic information. Transfer of the genetic information from DNA to RNA to proteins was first proposed by *Francis Crick* in 1958 and became known as the "central dogma of biology" (Figure 1.1a).[8] In his publication, *Crick* described three possible information transfer pathways; the "general transfers", "special transfers", and the "unknown transfers". The "general" information transfer from DNA to RNA to protein can occur in all cells, whereas "special" transfers such as RNA to DNA have been observed in virus-infected cells.[8] Transmission of misfolded states from prions to other proteins provides an example of an "unknown" transfer.[9] After the publication of the central dogma in 1958, it was often reformulated by other scientists in simpler and more restrictive ways.[10] An example is *Watson's* depiction of the central dogma (Figure 1.1b),[11] where DNA acts as a template for self-replication and only a unidirectional flow of information occurs from DNA to RNA and from RNA to protein.[11]

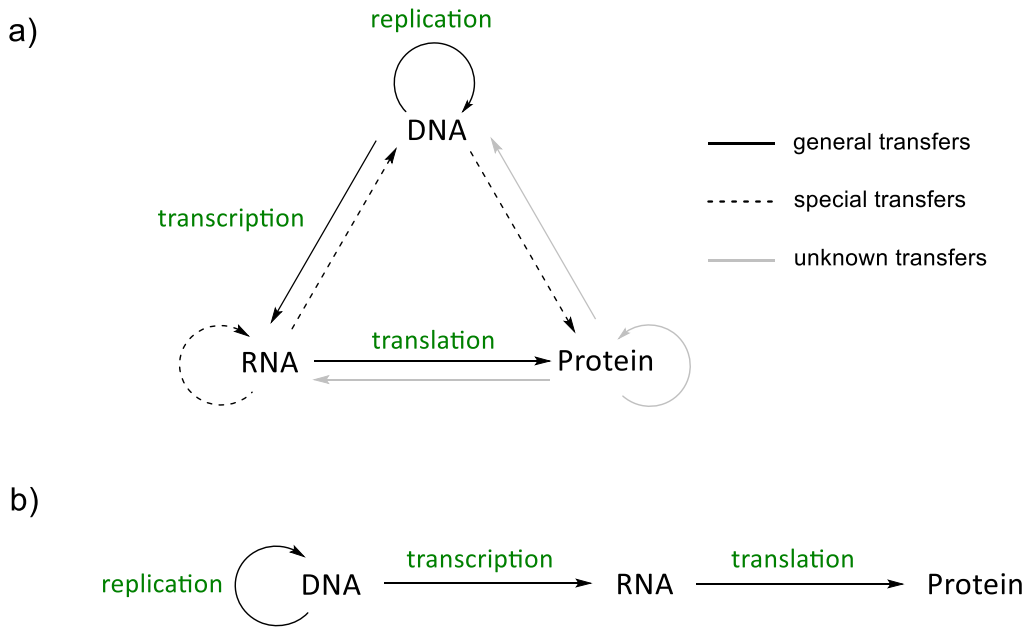

Figure 1.1. *The Central Dogma of Molecular Biology.* a) Model for flow of genetic information showing all possible transfers: "general transfers" can occur in all cells are shown as solid black arrows, "special transfers" are depicted in dashed arrows, and "unknown transfers" are depicted in grey arrows.[8] b) The simplified central dogma of biology depicted by Watson in 1965.

Since its first formulation in 1958,[8] notable exceptions to *Watson's* simplified depiction of the central dogma have been reported.[10] For example, the vast majority of RNA present in cells perform structural, catalytic, and regulatory functions and only a small fraction of RNA is produced as mRNA.[12–16] Investigations of the mechanism of replication of viruses demonstrated the existence of "special" transfer of information from RNA to RNA and RNA to DNA, as well as the fact that RNA rather than DNA can be the primary storage of genetic information.[17] The splicing mechanism of the primary RNA transcripts to mature mRNA demonstrated that protein sequences are not continuously encoded in DNA, leading to the discovery of non-coding sequences in genes.[18] Such non-coding regions make up to 98% of the human genome and there is increasing evidence that these sequences are of functional significance including transcriptional regulation, recombination sites, and chromatin structure.[16,19–21] Epigenetics provides another striking expansion of the central dogma. Covalent modifications of DNA and histone proteins provide examples of gene expression regulation which is not encoded directly by the sequence of the DNA.[22] Modifications of histone proteins, including methylation, acetylation, and phosphorylation, influence the chromatin structure and provide a regulatory mechanism for gene activation and silencing.[23] The discovery that the non-canonical "5th base" 5-methyldeoxycytosine can silence specific genes demonstrated that nucleobases themselves can act as regulatory elements for transcriptional activity.[24,25] Other non-canonical bases have recently been

discovered, expanding the variability of information contained in DNA.[26] These epigenetic "marks" include 5-hydroxymethylcytosine,[27,28] 5-formyldeoxycytosine,[29] 5-carboxydeoxycytosine,[30] and possibly 8-oxo-deoxyguanosine.[31,32]

1.1.1. Double Helix Structures

DNA is a linear polymer consisting of deoxyribonucleotides composed of a cyclic five-carbon sugar (ß-D-2'-deoxyribose) with a phosphate group at the 5' position and a nucleobase at the C1' position (Figure 1.2). The four common nucleobases are adenine (A) and guanine (G), cytosine (C), and thymine (T). The deoxyribonucleotide units are linked together via phosphodiester groups that connect the 3' and 5' positions of deoxyribose. At neutral pH the phosphate groups are deprotonated, rendering the DNA an anionic polymer.[33]

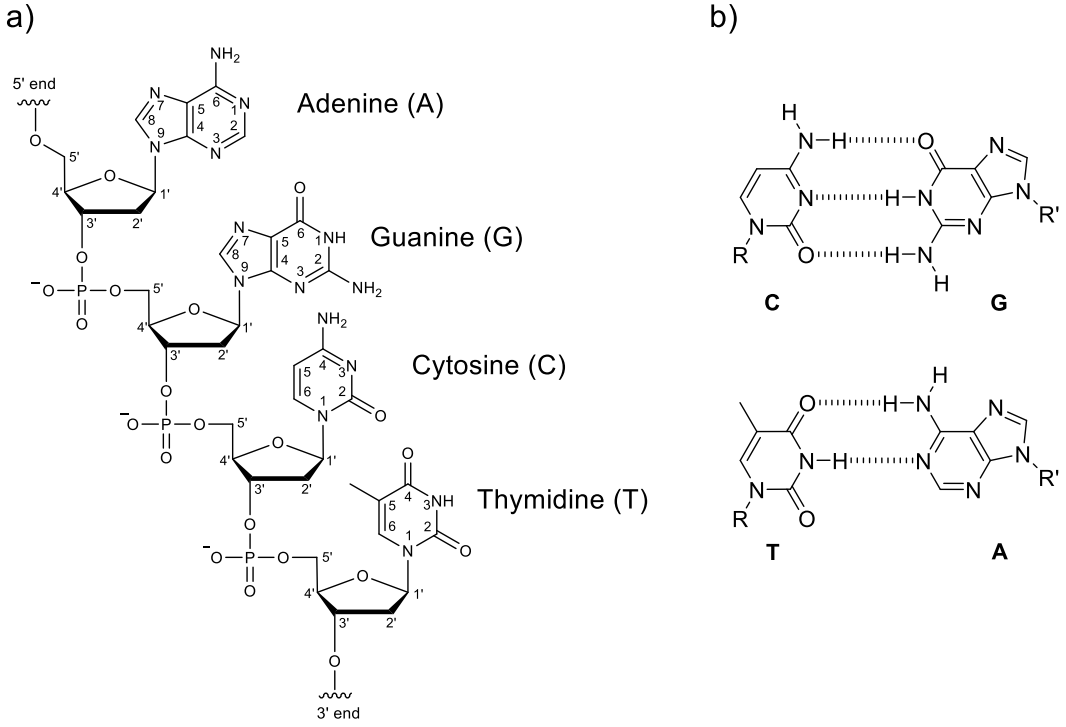

Figure 1.2. a) The primary structure of DNA. b) Watson and Crick base pairs; G pairs with C via three hydrogen bonds and A pairs with T via two hydrogen bonds (R, R' = deoxyribose-phosphate backbone) .[7]

An important DNA secondary structure is the B-form double helix which was first described by *Watson* and *Crick* (Figure 1.3b).[7] This double helix consists of two complementary polynucleotide DNA chains which coil around a central axis. The negatively charged phosphate groups are located on the outside of the helical structure and the nucleobases occupy the hydrophobic core of the helix. The nucleobases form specific base pairs, where guanosine pairs with cytosine and adenine bonds with thymidine to give G-C and A-T *Watson* and *Crick* base pairs (Figure 1.2b).[7] The formation G-C and A-T base pairs stabilize the helix by hydrogen bonding and base stacking interactions.[34] In the B-form duplex DNA, the two strands coil in a right-handed fashion around an internal axis and asymmetric winding along the axis results in the formation of a wide major groove and a narrow minor groove. The B-helix has a diameter of 20 Å with 10 base pairs per turn and a pitch (rise per turn) of 34 Å. The base pairs are stacked nearly perpendicular (6°) to the helical axis. The ß-D-2'-deoxyribose sugars have limited flexibility and adopt a non-planar C2'-*endo* sugar pucker in the B-form helix (Figure 1.4a).

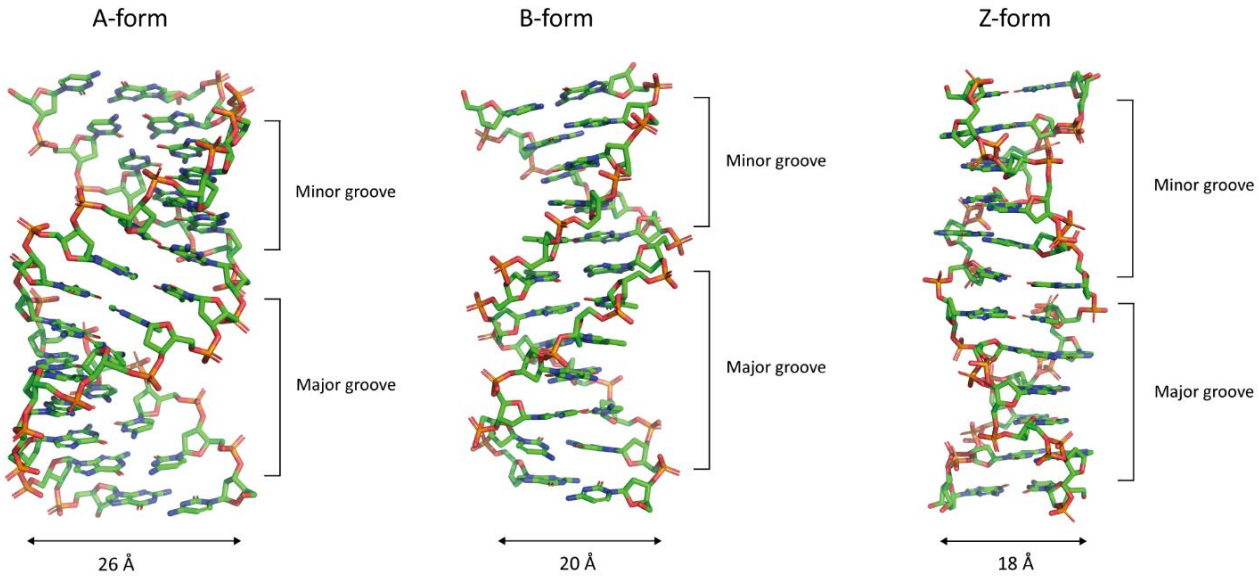

Figure 1.3. Structural variations between A, B, and Z-form duplex DNA (from left to right). Coordinates were taken from the PDB files 3V9D,[35] 2BNA,[36] and 4ocb,[37] respectively.

Alternative helical structures of double-stranded DNA have been reported, such as A-form and Z-form (Figure 1.3).[38–40] Under dehydrating conditions, the B-form duplex can undergo a conformational change to the A-form duplex.[39] Like the B-form, the A-form duplex also forms a right-handed double helix, but increase in base pair per turn (11.6) leads to a wider helix with a diameter of 26 Å (Figure 1.3a).[39] A prominent feature of the A-form helix is the displacement of the base pairs from the center of the helix, thereby creating an axial "hole".[41] Each base pair is displaced by ~4° towards the minor groove giving a helix with a deeper major groove and a shallower minor groove

(Figure 1.3a).[39] Another striking feature of the A-form duplex is the distinct tilting of the base pairs with respect to the helical axis by 20° and C3'-*endo* conformation of the deoxyribose units (Figure 1.4a).

In contrast to B- and A-form, the Z-form duplex adopts a left-handed helical structure (Figure 1.3c).[40,42] Z-DNA has 12 base pairs per turn and a large helical twist (60°) per base pair and a large helix rise (44 Å) per turn. The base pairs are displaced in the direction of the major groove, giving rise to a helix with a deep minor groove with similar dimensions as the major groove. The Z-form duplex DNA usually forms from polynucleotides with alternating purine and pyrimidine residues such as poly d(CG) at high salt concentrations. In B- and A-DNA, both pyridine and purine residues have *anti*-glycosidic bonds, where the plane of the ribose points away from the minor groove. In the Z-form conformation, however, the purine residues rotate 180° about the gylcosidic bond into the *syn* conformation, leading to a zig-zag backbone conformation where the sugars adopt a C2'-*endo* conformation for pyrimidine, and C3'-*endo* for purine residues (Figure 1.4a).[40,42]

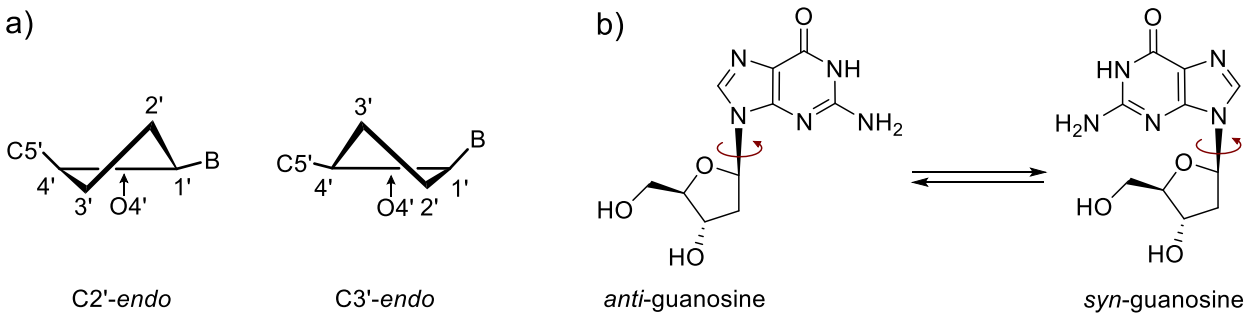

Figure 1.4. a) Common sugar puckers, C2'-*endo* (left) and C3'-*endo* (right). b) *Anti*- and *syn*-conformations of guanosine's glycosidic bond.

Transitions between conformations, such as B- to A-form transitions, B- to Z-form transitions or alterations of the B-form duplex to intermediate helical states have been suggested to occur in vivo and can play important roles for biological processes.[43–48] For example, crystal structures of TATA-sequences found in the promotor regions of genes demonstrated that protein binding induces a local A-form type helix.[46,49–51] DNA-RNA hybrid duplexes which occur during transcription and initiation of DNA replication adopt A-form conformations or intermediate A- and B-form structures. Such hybrids act as regulators of gene expression, DNA replication, and DNA repair.[52–54] Z-DNA has been proposed to form in response to supercoiling which occurs during replication, transcription, and recombination processes, and can serve as a distinct binding site for certain proteins such as ADAR1.[55]

Rather than being a static molecule, double helical DNA structures can exhibit considerable conformational flexibility. In particular, DNA bending has been suggested to be a critical component for the specificity of DNA recognition by proteins.[56–61]

1.1.2. Single-Stranded Secondary Structures

During DNA replication, transcription and repair, duplex DNA must dissociate into single strands. This allows the kinetic access to single-stranded secondary structures, such as hairpin, triplex, G-quadruplex or i-motif structures (Figure 1.5).[62,63] These types of structures have been implicated in a wide variety of different biological functions.[20,21,64,65]

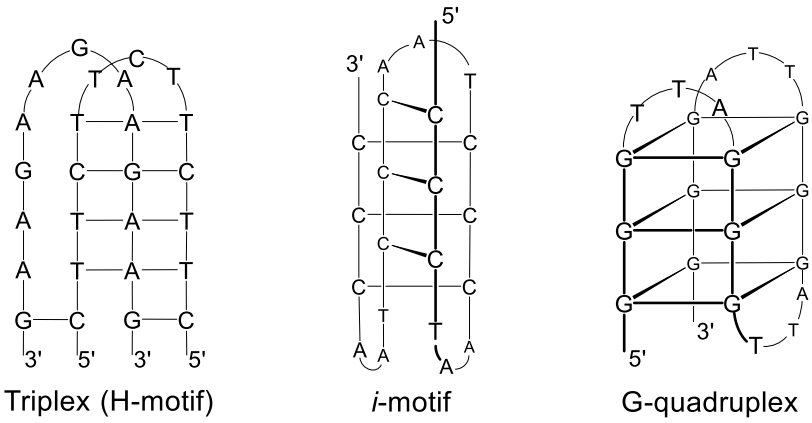

Figure 1.5. Schematic representation of selected DNA secondary structures triplex, *i*-motif, and G-quadruplex.

Intermolecular triplex DNA formation occurs by sequence-specific binding of a triplex-forming oligonucleotide (TFO) to a duplex DNA.[66,67] TFO's bind to the major groove of duplex DNA either in a parallel or anti-parallel fashion. Binding of the TFO to duplex DNA occurs via non-canonical *Hoogsteen* hydrogen bonding without disrupting the *Watson-Crick* hydrogen bond of the duplex DNA to form base triads. (Figure 1.6) Polypyrimidine TFO's bind to purine rich duplexes via the formation of C^+-GC and T-AT triads in a parallel fashion (Figure 1.6b). Polypurine TFO's bind in an antiparallel fashion via A-AT, G-GC, and T-AT triads.[66,67] Intramolcular triplex (H-motif) structures can be formed from single-stranded DNA in an analogeous fashion (Figure 1.5) and are thought to form in certain regions of the genome.[66,67]

Nucleic acid sequences containing stretches of sequential guanosines can fold into a four stranded structure commonly known as G-quadruplex or G_4-DNA (Figure 1.5).[68,69] A G-quadruplex consists of planar G-tetrads stacked

upon each other with a monovalent ion such as K^+ or Na^+ intercalated between each tetrad (Figure 1.7). Four guanosines associate via *Watson-Crick* and *Hoogsteen* base pairing to form each tetrad (Figure 1.6a and Figure 1.7). A wide variety of different G-quadruplex conformations have been reported.[68–71] They can form in an intermolecular fashion to give tetrameric, dimeric, or monomeric G-quadruplexes, or can be assembled in an intramolecular fashion. The adjacent strands can have either a parallel or and antiparallel orientation. Depending on the type of G-quadruplex, the glycosidic bonds can be *syn* or *anti*.[72]

C-rich sequences can fold into *i*-motif structures at slightly acidic pH. (Figure 1.5)[73] Two strands of duplex DNA containing hemiprotonated C-C^+ base pairs (Figure 1.6a) can intercalate in an *anti*-parallel fashion to form a four stranded *i*-motif structure. Alternatively, a single-strand can form an *i*-motif in an intramolecular fashion. Various types of different *i*-motif structures can form depending on the number of base pairs, loop topology, and environmental conditions.[63,74–76]

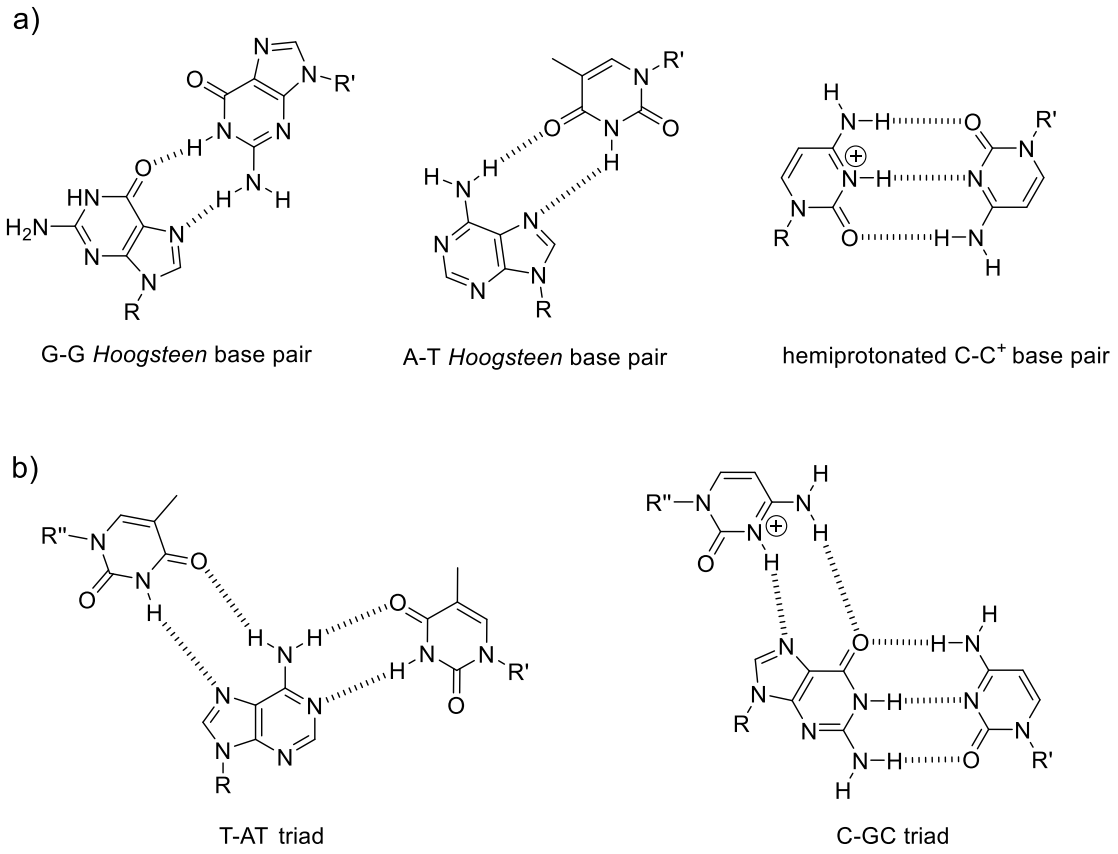

Figure 1.6. a) Examples of non-canonical base pairs. b) Examples of triads formed in triplex DNA structures. (R, R', R'' = 2'-D-deoxyribose)

These examples of non-duplex secondary structures are topologically distinct, providing unique recognition sites for proteins and small molecules that together mediate gene expression, recombination, and chromosome stability.[20,21,64,65] For example, it was suggested that triplex DNA may act as a regulator of DNA replication or transcription by blocking DNA or RNA polymerase and thereby initiating termination of DNA/RNA synthesis.[77,78] G-quadruplex and *i*-motif forming sequences can be found throughout the entire human genome with a high frequency in the telomeric regions of eukaryotic chromosomes and in the promotor regions of many proto-oncogenes.[79–81] Mounting evidence suggests that G-quadruplexes play roles in regulating gene expression, recombination and programmed cell death.[79,82]

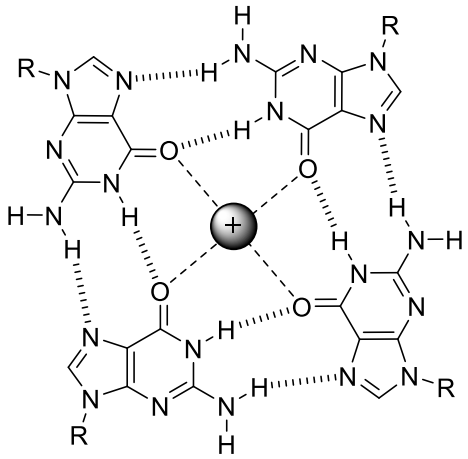

G-tetrad

Figure 1.7. Cation-bound G-tetrad present in G-quadruplex structures.

1.2. Metal Ions and Nucleic Acids

At neutral pH the phosphate linkages in DNA are deprotonated, giving an anionic polymer.[33] DNA and RNA molecules are therefore accompanied by cations at pH = 7.[83,84] The interactions between metal ions and DNA include non-specific diffuse binding, sequence-specific binding through inner-shell water ligands, and/or direct coordination which is accompanied by a release of all or part of the hydration shell.[85–87] Biologically relevant metal ions such as Na^+, K^+, Mg^{2+}, Zn^{2+}, or Ca^{2+} mediate specific functions of biological nucleic acids.[88–90] In addition to stabilizing duplex DNA structures, metal ions can induce conformational changes,[91–94] mediate protein-DNA binding interactions,[95] and act as catalytic cofactors in ribozyme catalysis.[96–98] In addition to the importance of metal ions to the vital functions of living systems, numerous applications in medicine,[99] nucleic acid diagnostics,[100–103] and material sciences[104,105] have emerged in recent years which utilize metal ion-DNA interactions.

1.2.1. Metal Ions Stabilize Secondary Structures of Nucleic Acids

One of the main functions of metal ions is to maintain the structural integrity of the secondary structures of nucleic acids and to facilitate proper folding by shielding the negative charges of the phosphate groups from one another. This can be accomplished by biologically available metal ions including Na^+, K^+, Mg^{2+}, Ca^{2+}, Cu^{2+}, and Zn^{2+}, or by polyamines.[88] They are condensed in proximity to the nucleic acid, thereby neutralizing the negative charge of the nucleic acid by electrostatic interactions.[106]

The identity of metal ions can induce different types of DNA structures. For example, metal ions are involved in the transition from B-DNA to A-DNA, where A-DNA can be formed in presence of Na^+ [107] but not Li^+ ions, which induces duplex conformation similar to B-DNA form.[108,109] It has also been suggested that binding of metal ions such as Ba^{2+} or $[Co(NH_3)_6]^{3+}$ could induce the formation of A-DNA, depending on the sequence of the DNA.[110] B- to Z-DNA transitions can be triggered by the addition of various metal ions.[111] The shorter distances of the phosphate groups in Z-DNA requires higher concentrations of monovalent ions or coordination of divalent ions such as Mg^{2+} to trigger B- to Z-DNA transitions for DNA containing poly d(GC) sequences.[112,113] Coordination of Co^{2+} and Ni^{2+} salts to *N7* of guanosine[114] and highly charged $[Co(NH_3)_6]^{3+}$ and $[Ru(NH_3)_6]^{3+}$ complexes have also been reported to induce B- to Z-form transformations.[113]

Metal ions also play an important role in the formation of higher-order nucleic acid structures, such as helical junctions, triplex DNA or G-quadruplexes.[115] Helical junctions occur in DNA as intermediates in recombination events and are common structures adopted by many functional RNA molceules.[92,116] The increase in charge density upon formation of triplex DNA and helical junctions requires high concentrations of divalent metal ions such as Mg^{2+} to effectively shield the electrostatic repulsion of the phosphate groups.[117] Recent evidence suggests that site-specific binding of divalent metal ions at the junction site also may be important for the structural integrity of helical junctions.[92] G-quadruplex is a highly polymorphic structure and many different topologies have been reported.[63,68–71] A characteristic feature of all G-quadruplex structures is their axial channel generated by the vertical stacking of G-tetrads. In addition to *Hoogsteen* hydrogen bonding, the stability of G-quadruplex structures is strongly influenced by the cation occupancy of this channel (Figure 1.7).[70,115,118] K^+ and Na^+ are the predominant metal ions shown to stabilize G-quadruplexes, but other monovalent and divalent cations, such as Rb^+, Cs^+, Li^+, Ca^{2+}, Pb^{2+}, or Ba^{2+} have also been reported.[119] The metal ions are bound via direct coordination to four to eight *O6* carbonyl oxygens of the guanosine residues, and depending on the size of the cations they can be located in the plane of the G-tetrads or in between them.[115,120]

The presence of metal ions is also required for stabilizing the secondary structures of ribonucleic acids.[88] RNA is known to fold into a variety of different secondary structures. Many of these motifs contain non-*Watson and Crick* base pairs and metal ions can play a crucial role for their formation. To form catalytically active tertiary structures of RNA, typically divalent metal cations are needed, most commonly Mg^{2+}, but monovalent potassium cations can also play a role in stabilization of tertiary structures.[121] Ribozymes, as well as DNAzymes can also utilize metal ions directly in their active sites.[121]

1.2.2. Metal Ion Binding by Nucleobases in Duplex DNA

The binding site of metal ions is largely determined by the relative hardness and softness of the metal ion and respective ligand sphere. "Hard" metal ions preferentially coordinate to non-bridging, negatively charged oxygens of the phosphate groups, or to the exocyclic oxygen atoms of the nucleobase, whereas "soft" metal ions exhibit higher tendency for direct nucleobase coordination, mainly to the endocyclic nitrogen atoms.[33,122] Because of the high basicity, good accessibility, and favorable electrostatic potential of the major groove, the *N7* of guanosine is one of the major coordination sites of softer metal ions in nucleic acids.[123,124] A prominent example of *N7* coordination occurs in the formation of inter- and intrastrand crosslinks by Pt^{II}. This crosslinking is thought to be responsible for the antitumor activity of cisplatin.[125] The slightly lower basicity of *N7*-adenosine may explain the higher preference of metal ions to bind to guanine residues. Other purine target sites include *N1* and *N3* of adenosine and *N1* of deprotonated guanosine. Metal binding to cytosine can occur through *N3, O2, N4*, and *C5* and to thymidine and uracil via *N3, O2, O4*. For uracil, binding to *C5* via electrophilic aromatic substitution has also been observed.[33]

1.2.3. Metal-Mediated Base Pairs

The investigation of metal-ion pyrimidine interactions has gained increasing attention in recent years, due to the discovery that certain transition metal ions can selectively bind to mismatched pyrimidines in duplex DNA and form so-called "metal-mediated" base pairs.[126] Various metal-mediated base pairs with wild-type or artificial nucleobase mimic have been reported, however, only a small number of duplex DNA containing "all-natural" metallo base pairs have been well characterized.[127–133]

First reported in the early 1960s,[134–136] T-Hg^{II}-T base pairs provided the first examples of "all natural" metal-mediated base pairs composed of pyrimidine-pyrimidine mismatches coordinated to a transition metal ion (Figure 1.8). In 2006, *Ono* and co-workers reported that T-T mismatches in duplex DNA exhibited stoichiometric binding

of Hg^{II} ions *in vitro*, giving duplexes with approximately the same thermal stabilities as duplexes containing T-A base pairs.[137] NMR studies using ^{15}N-labeled oligonucleotides provided direct proof of the coordination mode of Hg^{II} to T-T mismatch-containing oligonucleotides (Figure 1.8a).[138] ^{15}N -^{15}N J^2-coupling across mercury demonstrated that the preferred Hg^{II} binding site was to the *N*3 positions of two deprotonated thymine residues.[139] Interestingly, this was the same binding mode originally proposed by *Katz* in 1963.[135] A crystal structure,[140] as well as a NMR solution structure[141] of duplex DNA containing two such T-Hg^{II}-T base pairs revealed minimal distortion of the B-form duplex (Figure 1.8). The *N3*-Hg^{II}-*N3* bond lengths were 2 Å with a linear coordination geometry of the central Hg^{II} ion.[140] A notable propeller twist angles of -20 ° of the metallo base pair was ascribed to the absence of additional hydrogen bonds and repulsion of the carbonyl groups between thymidine residues. The distance of 3.4 Å between the consecutive Hg^{II} ions suggested some metal-metal attraction. The *C*1'- *C*1' distance between the thymidines of T-Hg^{II}-T (9.5 – 9.6 Å) were 1 Å shorter than for canonical *Watson-Crick* base pairs in B-form duplex DNA (~10.7 Å). This, however, caused only minimal distortion, giving a duplex with very similar local helical parameters, intra base pair parameters, and pseudorotation phase angles as the standard B-form duplex (Figure 1.8). Interestingly, a positive change in entropy was measured upon T-Hg^{II}-T formation. This was explained by the release of ordered water molecules from Hg^{II} upon binding the T-T mismatch.[141]

In addition to structural similarities, T-Hg^{II}-T can serve as a functional mimic of T-A base pairs by stabilizing T-T during DNA primer extension,[142] and by causing the enzymatic misincorporation of dTTP across from thymidine during primer extension to give T-Hg^{II}-T base pairs.[143] These activities provide a potential mechanism for the formation of T-Hg^{II}-T base pairs in S-phase cells and could explain some of the point mutations known to occur in cells treated with Hg^{II}.[144–146]

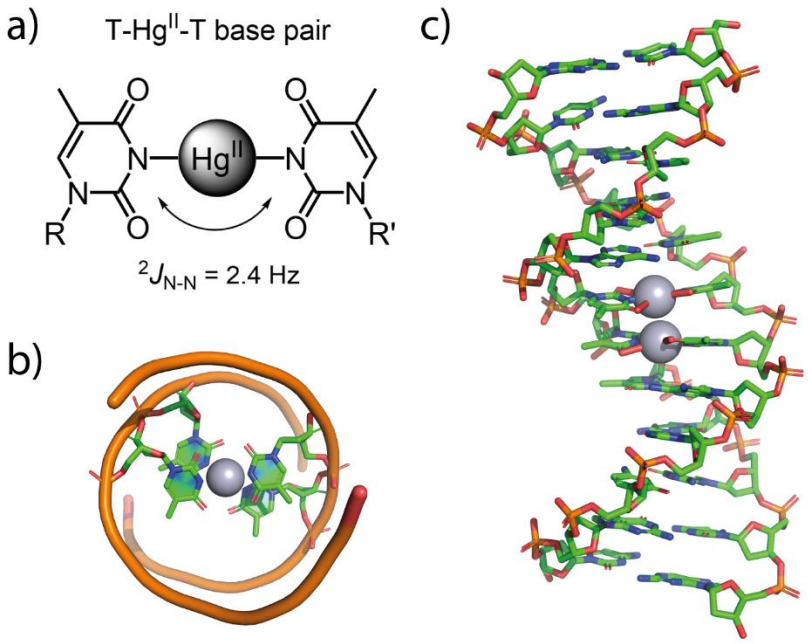

Figure 1.8. a) Nitrogen-nitrogen coupling (^{2}J = 2.4 Hz) across Hg^{II} in T-Hg^{II}-T base pairs. b) Top view and c) side view of duplex DNA containing two consecutive T-Hg^{II}-T base pairs. Coordinates were taken from the PDB file 4L24.[141]

In addition to T-Hg^{II}-T, C-Ag^{I}-C base pairs have also been well characterized (Figure 1.9a).[127–133] A crystal structure of a RNA duplex containing C-Ag^{I}-C base pairs demonstrated coordination of Ag^{I} to the *N3* positions of cytosine.[147] High-resolution structure analysis by NMR of a C-Ag^{I}-C-containing duplex DNA revealed a B-form helical structure in solution, with coordination of Ag^{I} to the *N3* positions of cytosine according to direct ^{15}N-Ag^{I} coupling.[148] The ^{1}J(^{15}N-Ag^{I}) coupling constants (83 and 84 Hz) were of the same magnitude as previously reported for a duplex DNA containing three consecutive imidazole-Ag^{I}-imidazole base pairs (86 Hz).[149] The cisoid orientation of the cytosines explained the large propeller twist angle (-18°) of this metallo base pair.[148]

A wide variety of other all-natural metallo base pairs have been formed in crystals of non-B-form nucleic acids.[150–152] For example, a G-Au^{III}-C base pair was observed in the initiation site of HIV-1 RNA and a C-Hg^{II}-T base pair was found in short, A-form duplex DNA where the metal ion was unexpectedly bound to the exocyclic amine (*N4*) of a deprotonated cytosine residue and to the *N3* of a deprotonated thymidine (Figure 1.9b).[151] A solid-state "wire" containing C-Ag^{I}-C, G-Ag^{I}-G, G-Ag^{I}-C, and T-Ag^{I}-T base pairs was also recently reported (Figure 1.9c),[150] as well as a short, non-helical DNA structure containing two C-Ag^{I}-C and one G-Ag^{I}-G base pair.[152]

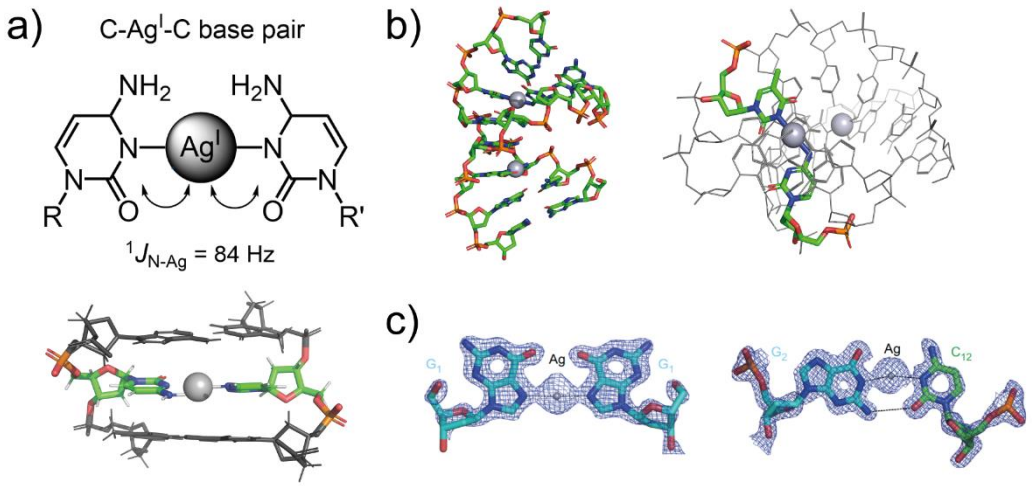

Figure 1.9. Selected examples of metallo base pairs. a) Ag^{I} binding to a C-C mismatch in duplex DNA determined by direct ^{15}N-Ag^{I} coupling (top) and side view of C-Ag^{I}-C-binding in duplex DNA (bottom). Coordinates were taken from the PDB entry 2RVP.[148] b) Side view of an A-form-like duplex DNA containing two C-Hg^{II}-T base pairs (left) and top view highlighting the unusual (*N3*)C-Hg^{II}-(*N3*)T binding mode. Coordinates were taken from PDB entry 5WSQ.[151] c) Two examples of metallo base pairs observed in a solid state "wire": G-Ag^{I}-G- (left) and G-Ag^{I}-C base pair (right). Figure was reproduced from *Kondo* et al.[150]

All natural, metal-mediated base pairs are potentially important in both biological and materials sciences.[153–165] A wide variety of applications of DNA containing metallo-base pairs have been developed, including their use as metal sensors,[166,167] single-nucleotide polymorphism detectors,[168,169] epigenetic marker detection,[162] molecular wires,[170–173] and for metal-responsive, functional DNA molecules.[174,175] In most cases, however, little is known about the kinetic or thermodynamic parameters of metallo base pair formation in solution. A detailed understanding of kinetic and thermodynamic properties is essential for gauging their potential applications in devices as well as their ability to interfere with biological processes.[143,176,177]

1.3. Fluorescent Nucleobase Analogs to Study Nucleic Acids

A wide variety of spectroscopic methods have been used to characterize structure and properties of nucleic acids *in vitro*, including UV absorption,[178,179] circular dichroism(CD),[180] NMR spectroscopy,[181–184] X-ray crystallography,[185] and fluorescence.[186] UV absorbance and CD spectroscopy are widely used to study the global structural properties of DNA.[187,188] Changes in absorbance of ultra-violet light can be used to monitor transitions of folded to unfolded states of nucleic acids.[188] The conformational chirality of DNA molecules gives rise to differences in absorbance of left- versus right handed circularly polarized light, making it a simple and powerful method to determine secondary structures of nucleic acids.[187] Given the wide availability of UV- and CD spectroscopy, these methods are commonly used, but they suffer from low sensitivity and only information regarding global structural changes can be obtained. In contrast, NMR and X-ray can provide highly detailed structural information.[181–185,189] The excellent resolution of these methods can facilitate determination of the exact three-dimensional structure with atomic-level resolution, thereby revealing base pair step parameters, and local binding interactions to ligands and other small molecules such as metal ions. The intrinsically low sensitivity of NMR spectroscopy, however, requires highly concentrated, pure DNA samples.[190,191]

1.3.1. Fluorescent DNA Labeling Strategies

The above mentioned biophysical techniques typically require pure samples and are not suitable for analyses in vivo. With excellent sensitivity, fluorescence spectroscopy is a powerful method to study conformation, folding, ligand binding, and localization of nucleic acids.[186] Fluorescence offers great versatility with a wide variety of experimental approaches such as steady-state and time-resolved intensity measurements,[186,192] *Förster* resonance energy transfer can adress distances and global conformations,[193–195] and fluorescence anisotropy reports dynamic motions.[196,197] In addition, fluorescence spectroscopy can be used in whole biological systems and provide information on dynamics and location of nucleic acids in their native environment.[198–204] The low quantum yields of the natural nucleobases ($\phi = 0.5 - 1.2 \times 10^{-4}$)[205] requires strategic DNA labeling techniques, but also provides a low background environment for fluorescent probes. Fluorescent DNA labeling strategies can be divided into three main classes (Figure 1.10): external probes (a), conjugated probes (b), and internal probes (c).

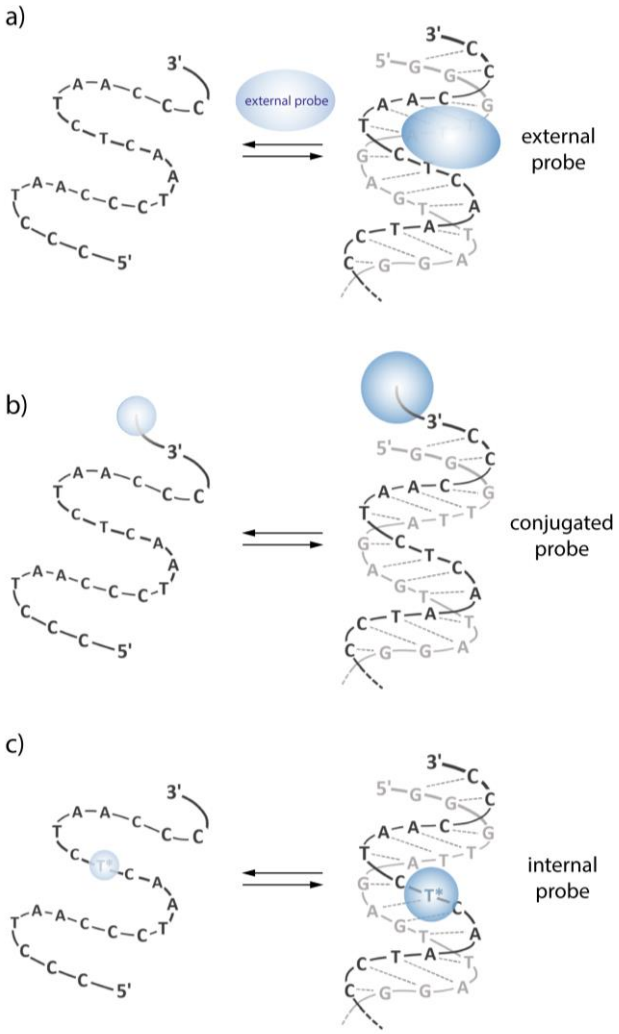

Figure 1.10. Fluorescent DNA labeling strategies. a) external probes, b) conjugated probes, and c) internal probes.

Exogenous fluorescent molecules can bind to nucleic acids either by hydrogen bonding, base stacking interactions, and/or electrostatic interactions that recognize specific structural features or local conformations of DNA (Figure 1.10a). For example, ethidium bromide is known to bind to DNA either via electrostatic interactions to the surface of nucleic acids and/or by intercalating in between complementary stacked base pairs, depending on the ionic strength, and is a commonly used as external fluorescent probe for staining of double stranded DNA in gel-electrophoreses experiments (Figure 1.11a).[206] Exogenous fluorescent probes DAPI[207] and Hoechst[208] are commonly used as DNA staining agents in cellular imagining techniques (Figure 1.11a). Restricted rotational freedom of the molecules upon binding the minor-groove of AT-rich regions of duplex DNA induces a large increase in fluorescence which accounts for the low background signal of these dyes. Disadvantages of this labeling strategy is the lack of specificity towards different DNA conformations and their propensity to perturb the conformational preferences of the DNA that they bind to.[194,209]

Conjugated probes can be described as the covalent attachment of large fluorescent molecules to the ends or within oligonucleotide sequences, but outside of the base stack (Figure 1.10b).[186] Changes in fluorescence can be monitored to determine DNA folding and ligand binding in vitro.[210–216] Bright fluorophores such as fluorescein, BODIPY, TAMRA, or Cy-dyes are examples of commonly used probes for conjugation to oligonucleotides (Figure 1.11b).[215] A widely-used application of conjugated probes is *Förster* resonance energy transfer (FRET) from a donor to an acceptor molecule.[192,217] Transfer of energy between conjugated probes depends on the distance (10 – 80 Å) as well as the spectral overlap between donor emission and acceptor excitation. An example for an excellent FRET-pair is fluorescein and rhodamine due to their good spectral overlap, high extinction coefficients and quantum yields (Figure 1.11b).[218] FRET-based experiments can be used to measure distances within a DNA molecule and therefore global conformational changes upon DNA folding.[215] The main drawbacks of this labeling technique is that fluorescent signal changes are limited to large conformational changes, and the probes themselves can impact the conformational preferences of the DNA.[219]

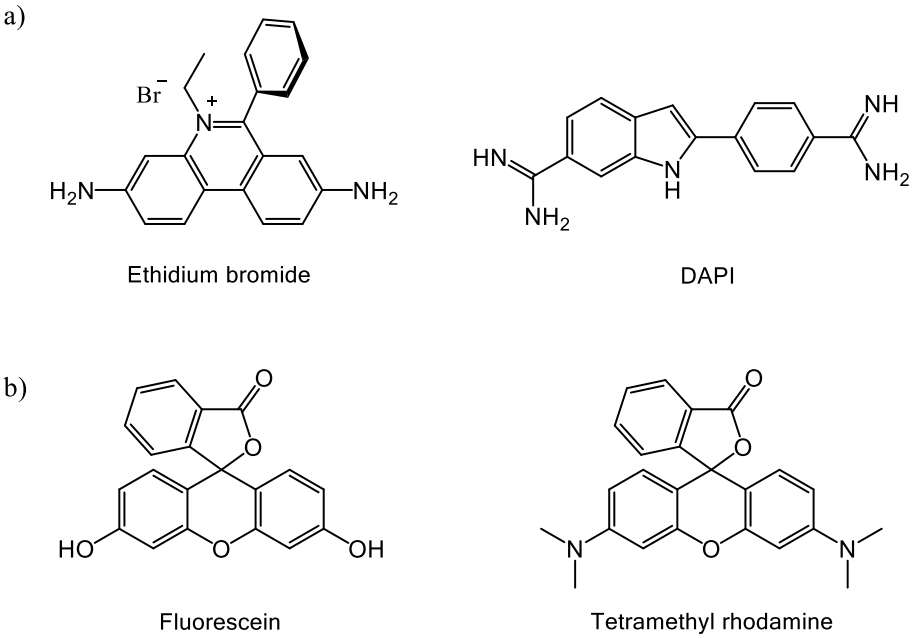

Figure 1.11. a) Examples of external fluorescent probes. b) Examples of fluorophores used as conjugated probes.

With their small size and predictable location, internal fluorescent probes can facilitate highly sensitive biophysical measurements with excellent spatial and temporal resolution and offer unique advantages over exogenous and conjugated fluorescent probes (Figure 1.10c).[186,220–223] By maintaining the structure and electronic characteristics of natural nucleobases, well designed internal probes can have a minimal impact on the structure and stability of DNA. Fluorescent nucleobase analogs can be derived by structural modifications to the natural nucleobases. The difficulty in designing fluorescent nucleobase analogs lies in the requirement to generate a

fluorescent molecule which retains a high quantum yield in the context of folded nucleic acids with red-shifted wavelengths of excitation and emission, while minimizing structural impact by the modification. If properly designed, fluorescent nucleobase analogs can mimic the natural nucleobase by preserving the shape, base pairing face and glycosidic bond conformation. Such probes can also possess favorable photophysical properties that are sensitive to the local environment.[186,220–224] Fluorescent nucleobase analogs can thereby provide powerful tools to report conformational changes and binding interactions with single nucleotide resolution.[225–232]

1.3.2. Fluorescent Pyrimidine Analogs

The instrinsic fluorescence of the five canonical nucleobases is very weak with quantum yields in the range of $\phi = 0.5 - 1.2 \times 10^{-4}$.[205] Introducing small chemical modifications to the natural structure can impart desirable photophysical properties to the nucleobases.[233] With stronger base stacking interactions and redshifted excitation/emission wavelengths, purine analogs offer advantages over pyrimidine derivatives as emissive nucleobase analogs.[68,69,234–236] Nevertheless, numerous fluorescent pyrimidine analogs have been reported (Figure 1.12).[186,220–223] These can broadly be categorized into three main groups. (1) Chromophore-conjugated pyrimidine analogs, (2) expanded pyrimidine nucleobase analogs, and (3) isomorphic pyrimidine analogs. (Figure 1.12)

Chromophore-conjugated nucleobases consist of a fluorescent metal complex or organic fluorophore attached to a natural nucleobase via a linker.[237,238] By using a saturated linker the photophysical properties of the fluorophore are retained, whereas expanding the π-system by using a conjugated, unsaturated linker generates a chromophore with unique photophysical properties.[186] The impact on the stability and structure of the DNA containing a conjugated nucleobase analog is dependent on the size and shape of the attached fluorophore. Perturbation by the analog can be minimized by attaching the chromophore to the *C*5 position of deoxyuridine or deoxycytidine, thereby retaining the hydrogen bonding pattern while directing the chromophore to the major groove.[239–242]

Extending the π-conjugation of the natural bases can yield in highly emissive chromophores (Figure 1.12). First applied to purine analogs,[243–246] this strategy has also been applied to pyrimidine analogs. Fusion of additional rings to the pyrimidine core can result in expanded aromatic systems with high emission quantum yields and red-shifted excitation and emission wavelengths. In well-designed analogs, this can be accomplished without disruption of the hydrogen bonding face of the nucleobase.[247–249] Isomorphic pyrimidine analogs possess high structural similarity to native nucleobases and maintain their hydrogen bonding patterns.[250–253] Given their close resemblance to canonical nucleobases they offer the clear advantage of being minimally perturbing to stability and structure of DNA (Figure 1.12).

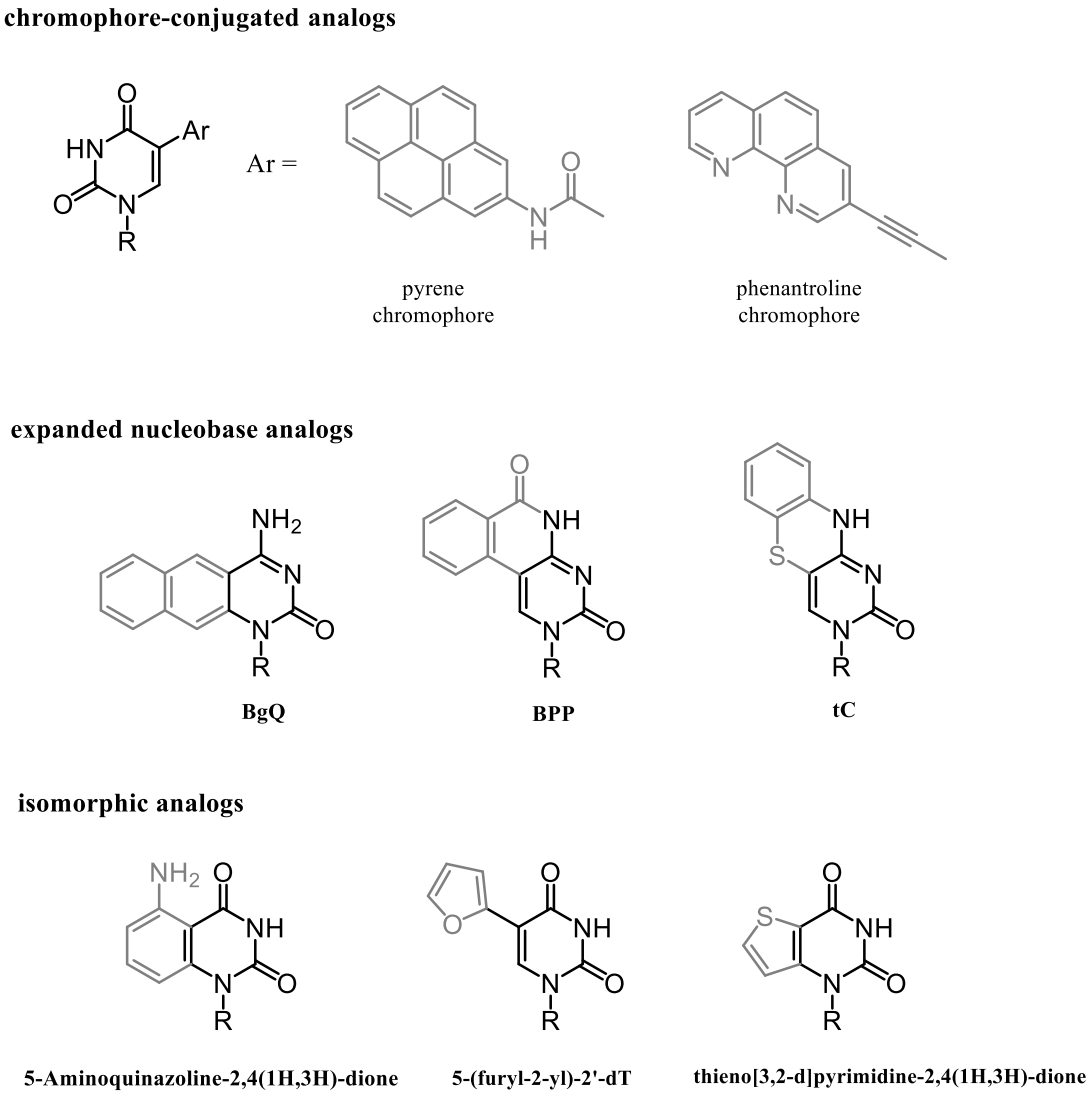

Figure 1.12. Selected examples fluorescent pyrimidine analgos. Chromophore conjugated-pyrimidine analogs with pyrene[239] or phenanthroline[240] attached to the *C*5-position of deoxyuridine (R = deoxyribose) (top), "BgQ",[248] "BPP",[247] and "tC"[249] as selected examples of pyrimidine nucleosides containing expanded π-systems (middle), and isomorphic pyrimidine analogs which exhibit minimal perturbation of duplex DNA (bottom).[227,251,253]

1.3.3. Fluorescent Cytosine Analog ^{DMA}C

In 2015, *Mata* and *Luedtke* reported a new fluorescent cytosine analog as a sensitive probe for *i*-motif folding.[254] "*N*,*N*-dimethylaniline-2'-deoxycytosine" or "^{DMA}C" is composed of a dimethylaniline unit fused to canonical 2'-deoxycytosine, giving a nucleoside analog with a quinazoline core structure (Figure 1.13).[254] The dimethylamino group at *C*6 of the quinazoline core generated a cytosine analog with photophysical properties that were sensitive to local environment, without effecting the ionization properties of natural cytosine. With same pK_a and base pairing characteristics, ^{DMA}C is an excellent mimic of native cytosine and provided the first fluorescent probe to be directly incorporated into C-G and C-C$^+$ base pairs without perturbing the stability or structure of duplex or *i*-motif structures (Figure 1.13). The excellent correlation between Stokes' shift and solvent polarity suggested that the shift in electron density from dimethylaniline to cytosine upon photoexcitation was stabilized by polar solvents, demonstrating the "push–pull" character of ^{DMA}C. Large red shifting of the absorbance maximum upon ^{DMA}C protonation at *N3* (λ_{abs} = 395 → 425 nm) facilitated its use as a "turn-on" fluorescent probe for *i*-motif formation by selective excitation of protonated ^{DMA}C. The environmental-sensitive photophysical properties of ^{DMA}C provided a conformation-specific fluorescent probe of *i*-motif formation. Measuring ^{DMA}C emission maxima, fluorescence anisotropy values, and energy transfer efficiencies enabled unambiguous assignment of the folded state of the DNA containing it. By monitoring changes in fluorescence as a function of time, ^{DMA}C was used to probe real-time DNA dynamics and the kinetic parameters of *i*-motif folding. In a novel strand displacement assay, the rate constants of *i*-motif formation were determined by addition of an excess of unlabeled DNA to a duplex DNA containing ^{DMA}C and a 5' overhang. Comparing the rates of strand displacement upon addition of an unfolded DNA versus *i*-motif DNA revealed that *i*-motif structures have high kinetic stabilities that pose large kinetic barriers for duplex DNA formation.[254]

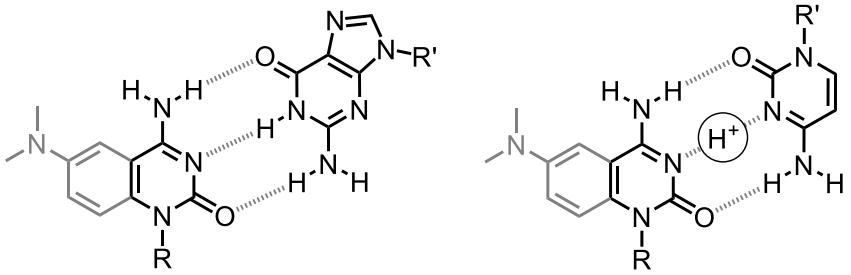

Figure 1.13. ^{DMA}C-G base pair and hemi-protonated ^{DMA}C-C$^+$ base pair (R, R' = duplex DNA). Figure was reproduced from *Mata* et al.[254]

A thymidine analog ^{DMA}T has recently been reported that has close structural homology with ^{DMA}C.[255] ^{DMA}T was designed to have the same *Watson-Crick* face, glycosidic bond conformation, and pK_a as thymidine and it exhibited the same base pairing characteristics as native thymidine residues. It is important to note that the vast majority of fluorescent nucleoside analogs are quenched by their incorporation into duplex nucleic acids.[186] In contrast, the quantum yield of ^{DMA}T(ϕ = 0.03 in water) increased upon its incorporation into duplex DNA (ϕ = 0.11 – 0.20). The fluorescent properties of ^{DMA}T were highly sensitive to nucleobase hydration, ionization, base pairing, and metal binding. A detailed description of the fluorescent thymidine mimic ^{DMA}T will be provided in Chapter 2.

1.4. Objectives and Scientific Goals

The formation and properties of "all-natural" metallo base pairs such as T-Hg^{II}-T and C-Ag^{I}-C have broad implications in materials and biological sciences. The kinetic and thermodynamic parameters of local, site-specific metal-mediated base pair formation in duplex DNA are important for understanding their potential biological impact and material properties, however, there are no previous studies that report these values. Our goal was to develop a fluorescence based assay to detect and characterize metallo base pair formation and investigate their potential impact on dynamic processes involving DNA. Our approach focused on the incorporation of fluorescent thymidine and cytosine analogs into oligonucleotides to determine kinetic and thermodynamic parameters of Hg^{II}-mediated base pairs and thereby shed light on potential mechanisms for the cytotoxic and mutagenic activities associated with Hg^{II} exposure.

This thesis is divided into the following chapters:

I. In Chapter 1, an introduction to DNA structures and biological functions is presented. The interactions of metal ions and nucleic acids are discussed, as well as biophysical techniques to study nucleic acids with a special emphasis on fluorescent labeling techniques.

II. The fluorescent thymidine mimic ^{DMA}T will be described in Chapter 2. The fluorescent properties, global structures, thermal stabilities, and metal binding properties of ^{DMA}T-containing sequences will be presented. The results described in Chapter 2 were published as part of: Mata, G., Schmidt, O.P., Luedtke, N. W., *Chem. Commun.,* 2016, *52,* 4718.

III. Chapter 3 describes the development of a fluorescence-based assay to study direct, site-specific metal binding reactions involving unmodified nucleobases in duplex DNA using ^{DMA}T-containing oligonucleotides. The kinetic and thermodynamic parameters of wild-type T-Hg^{II}-T base pairs will be described and the effects of this metallo base pair on DNA metabolism will be presented. The results described in Chapter 3 were published as part of: Schmidt, O. P., Mata, G., Luedtke, N. W. *J. Am. Chem. Soc.* 2016, *138*, 14733.

IV. In Chapter 4 the use of fluorescent nucleobase analogs ^{DMA}T and ^{DMA}C as an attractive alternative method for the identification and study of DNA-metal binding interactions will be described. The fluorescence based assay developed in Chapter 3 was used to evaluate site-selective metal binding of Hg^{II} or Ag^{I} to C-T mismatches. The results described in Chapter 4 were published as part of Schmidt, O. P., Benz, A. S., Mata, G., Luedkte, N. W., *Nucleic Acids Res.* 2018, *46*, 6470.

V. Chapter 5 describes the detailed investigation of Hg^{II} binding sites to C-T mismatch-containing duplex DNA using ^{15}N-labeled oligonucleotides and NMR spectrocopy. The global helical structures of duplex DNA containing C-Hg^{II}-T base pairs will be presented and a metal-coupled switch of alternative helical structures of DNA in dynamic equilibrium will be described. The results in Chapter 5 will soon be submitted for review to *Nature Chemistry*.

VI. In Chapter 6 materials and methods are described. Experimental details and additional spectra for DNA synthesis, CD spectroscopy, thermal denaturation, kinetic and thermodynamic measurements and analysis, strand displacement reactions, primer extension reactions, NMR measurements and structure calculations will be provided.

REFERENCES

[1] F. Miescher, *Med. Untersuchungen* 1871, *4*, 502–509.

[2] R. Dahm, *Hum. Genet.* 2008, *122*, 565–581.

[3] P. A. Levene, *J. Biol. Chem.* 1919, *40*, 415–424.

[4] O. T. Avery, C. M. MacLeod, M. McCarty, *J. Exp. Med.* 1944, *79*, 137–158.

[5] A. D. Hershey, M. Chase, *J. Gen. Physiol.* 1952, *36*, 39–56.

[6] D. Elson, E. Chargaff, *Experientia* 1952, *8*, 143–145.

[7] J. D. Watson, F. H. C. Crick, *Nature,* 1953, *171*, 737–738.

[8] F. Crick, *Nature,* 1970, *227*, 561–563.

[9] S. B. Prusiner, *Science,* 1982, *216*, 136–144.

[10] D. Thieffry, S. Sarkar, *Trends Biochem. Sci.* 1998, *23*, 312–316.

[11] J. D. Watson, *Molecular Biology of the Gene*, Benjamin, W. A., New York, 1965.

[12] A. Kornberg, T. Baker, *DNA Replication*, University Science Books,U.S., Sausalito, 1992.

[13] E. H. Blackburn, in *RNA Struct. Funct.* (Eds.: R.W. Simons, M. Grunberg-Manago), Cold Spring Harbor Laboratory Press, 1998, pp. 669–693.

[14] J. B. Hartford, T. A. Rouault, in *RNA Struct. Funct.* (Eds.: R.W. Simons, M. Grunberg-Manago), Cold Spring Harbor Laboratory Press, 1998, pp. 575–602.

[15] S. R. Eddy, *Nat. Rev. Genet.* 2001, *2*, 919–929.

[16] G. Elgar, T. Vavouri, *Trends Genet.* 2008, *24*, 344–52.

[17] B. N. Fields, D. M. Knipe, P. M. (Eds. . Howley, *Fundamental Virology*, Lippencott-Raven Pubs., 1996.

[18] T. W. Nilsen, in *RNA Struct. Funct.* (Eds.: R.W. Simons, M. Grunberg-Manago), Cold Spring Harbor Laboratory Press, 1998, pp. 279–307.

[19] N. Ahituv, Y. Zhu, A. Visel, A. Holt, V. Afzal, L. A. Pennacchio, E. M. Rubin, *PLoS Biol.* 2007, *5*, 1906–11.

[20] L. A. Cahoon, H. S. Seifert, *Science,* 2009, *325*, 764–767.

[21] G. Biffi, D. Tannahill, J. McCafferty, S. Balasubramanian, *Nat. Chem.* 2013, *5*, 182–186.

[22] C. Martin, Y. Zhang, *Curr. Opin. Cell Biol.* 2007, *19*, 266–272.

[23] A. J. Bannister, T. Kouzarides, *Cell Res.* 2011, *3*, 381–395.

[24] G. R. Wyatt, *Nature,* 1950, *166*, 237–238.

[25] R. Jaenish, A. Bird, *Nat. Genet.* 2003, *33*, 245–254.

[26] T. Carell, M. Q. Kurz, M. Müller, M. Rossa, F. Spada, *Angew. Chemie - Int. Ed.* 2018, *57*, 2–19.

[27] S. Kriaucionis, N. Heintz, *Science,* 2009, *324*, 929–930.

[28] M. Tahiliani, K. P. Koh, Y. H. Shen, W. A. Pastor, H. Bandukwala, Y. Brudno, L. M. Agarwal, S. Iyer, D. R. Liu, L. Aravind, A. Rao, *Science,* 2009, *324*, 930–935.

[29] T. Pfaffeneder, B. Hackner, M. Truss, M. Münzel, M. Müller, C. A. Deiml, C. Hagemeier, T. Carell, *Angew. Chemie - Int. Ed.* 2011, *50*, 7008–7012.

[30] Y.-F. He, B.-Z. Li, Z. Li, P. Liu, Y. Wang, Q. Tang, J. Ding, Y. Jia, Z. Chen, L. Li, et al., *Science,* 2011, *333*, 1303–1307.

[31] A. M. Flemming, C. J. Burrows, *DNA Repair (Amst).* 2017, *56*, 75–83.

[32] A. M. Flemming, Y. Ding, C. J. Burrows, *Proc. Natl. Acad. Sci.* 2017, 2604–2609.

[33] B. Lippert, *Coord. Chem. Rev.* 2000, *200*, 487–516.

[34] E. T. Kool, *Annu. Rev. Biophys. Biomol. Struct.* 2001, *30*, 1–22.

[35] P. K. Mandal, S. Venkadesh, N. Gauthan, *Acta Crystallogr. Sect. F- Struct. Biol. Cryst. Commun.* 2012, *68*, 393–399.

[36] H. R. Drew, S. Samson, R. E. Dickerson, *Proc. Natl. Acad. Sci.* 1982, *79*, 4040–4044.

[37] Z. Luo, M. Dauter, Z. Dauter, *Acta Crystallogr. Sect. D* 2014, *70*, 1790–1800.

[38] R. Dickerson, in *Methods Enzymol.* (Eds.: D. Lilley, J. Dahlberg, J. Abelson, M. Simon), Academic Press, Inc., 1992, pp. 67–111.

[39] V. I. Ivanov, D. Y. Krylov, in *Methods Enzymol.* (Eds.: D. Lilley, J. Dahlberg, J. Abelson, M. Simon), Academic Press, Inc., 1992, pp. 111–127.

[40] B. H. Johnston, in *Methods Enzymol.* (Eds.: D. Lilley, J. Dahlberg, J. Abelson, M. Simon), Academic Press, Inc., n.d., pp. 127–158.

[41] R. E. Dickerson, *Sci. Am.* 1983, *94*, 94–111.

[42] A. Rich, A. Nordheim, A. H.-J. Wang, *Annu. Rev. Biochem.* 1984, *53*, 791–846.

[43] S. C. Parker, L. Hansen, H. O. Abaan, T. D. Tullius, E. H. Margulies, *Science,* 2009, *324*, 389–392.

[44] A. G. Tsai, A. E. Engelhart, M. M. Hatmal, S. I. Houston, N. V. Hud, I. S. Haworth, M. R. Lieber, *J. Biol. Chem.* 2009, *284*, 7157–7164.

[45] S. Harteis, S. Schneider, *Int. J. Mol. Sci.* 2014, *15*,

12335–12363.

[46] G. Guzikevich-Guerstein, Z. Shakked, *Nat. Struct. Biol.* 1996, *3*, 32–37.

[47] A. Rich, S. Zhang, *Nat. Rev. Genet.* 2003, *4*, 566–572.

[48] R. D. Wells, *J. Biol. Chem.* 2009, *284*, 8997–9009.

[49] Z. Shakked, D. Rabinovich, *J. Mol. Biol.* 1983, *166*, 183–201.

[50] Y. Kim, J. H. Geiger, S. Hahn, P. B. Sigler, *Nature,* 1993, *365*, 512–520.

[51] D. B. Nikolov, H. Chen, E. D. Halay, A. A. Usheva, K. Hisatake, D. K. Lee, R. G. Roeder, S. K. Burley, *Nature,* 1995, *377*, 119–128.

[52] J. M. Santos-Pereira, A. Aguilera, *Nat. Rev. Genet.* 2015, *16*, 583–597.

[53] J. Sollier, K. A. Cimprich, *Trends Cell Biol.* 2015, *25*, 514–522.

[54] K. Skourti-Stathaki, N. J. Proudfoot, *Genes Dev.* 2014, *28*, 1384–1396.

[55] A. Herbert, A. Rich, *Genetica* 1999, *106*, 37–47.

[56] M. A. El Hassan, C. R. Calladine, *J. Mol. Biol.* 1998, *282*, 331–343.

[57] R. Rohs, S. M. West, A. Sosinsky, P. Liu, R. S. Mann, B. Honig, *Nature,* 2009, *461*, 1248–1254.

[58] A. A. Travers, *Nat. Struct. Biol.* 1995, *2*, 615–618.

[59] J. L. Kim, S. K. Burley, *Nat. Struct. Biol.* 1994, *1*, 638–653.

[60] A. Tissier, P. Kannouche, P. Mauffrey, I. Allemand, G. Frelat, R. Devoret, J. F. Angulo, *Genomics* 1996, *38*, 238–242.

[61] R. Spurio, M. Falconi, A. Brandi, C. L. Pon, C. O. Gualerzi, *EMBO J.* 1997, *16*, 1795–1805.

[62] J. Choi, T. Majima, *Chem. Soc. Rev.* 2011, *40*, 5893–5909.

[63] D. J. Patel, A. T. Phan, V. Kuryavyi, *Nucleic Acids Res.* 2007, *35*, 7429–7455.

[64] J. S. Smith, C. Q., L. A. Yatsunyk, J. M. Nicoludis, M. S. Garcia, R. Kranaster, S. Balasubramanian, D. Monchaud, M. P. Teulade-Fichou, L. Abramowitz, et al., *Nat. Struct. Mol. Biol.* 2011, *18*, 478–485.

[65] A. Bacolla, R. D. Wells, *Mol. Carcinog.* 2009, *48*, 273–285.

[66] K. M. Vasquez, P. M. Glazer, *Q. Rev. Biophys.* 2002, *35*, 89–107.

[67] M. D. Frank-Kamenetskii, S. M. Mirkin, *Annu. Rev. Biochem.* 1995, *64*, 65–95.

[68] D. Sen, W. Gilbert, *Nature,* 1988, *334*, 364–366.

[69] W. I. Sundquist, A. Klug, *Nature,* 1989, *342*, 825–829.

[70] S. Burge, G. N. Parkinson, P. Hazel, A. K. Todd, S. Neidle, *Nucleic Acids Res.* 2006, *34*, 5402–5415.

[71] A. N. Lane, J. B. Chaires, R. D. Gray, J. O. Trent, *Nucleic Acids Res.* 2008, *36*, 5482–5515.

[72] W. A. Harrell Jr, *Quadruplex Nucleic Acids*, The Royal Society Of Chemistry, 2006.

[73] K. Gehring, J. L. Leroy, M. A. Gueron, *Nature,* 1993, *363*, 561–565.

[74] J.-L. Mergny, L. Lacrois, X. Han, J.-L. Leroy, C. Helene, *J. Am. Chem. Soc.* 1995, *117*, 8887–8898.

[75] S. Kendrick, Y. Akiyama, S. M. Hecht, L. H. Hurley, *J. Am. Chem. Soc.* 2009, *131*, 17667–17676.

[76] D. Miyoshi, H. Karimata, N. Sugimoto, *J. Am. Chem. Soc.* 2006, *128*, 7957–7963.

[77] E. H. Postel, S. J. Flint, D. J. Kessler, M. E. Hogan, *Proc. Natl. Acad. Sci.* 1991, *88*, 8227–8231.

[78] D. Praseuth, A. L. Guieysse, C. Helene, *Biochim. Biophys. Acta* 1999, *1489*, 181–206.

[79] J. L. Huppert, S. Balasubramanian, *Nucleic Acids Res.* 2005, *33*, 2908–2916.

[80] A. K. Todd, M. Johnston, S. Neidle, *Nucleic Acids Res.* 2005, *33*, 2901–2907.

[81] M. L. Bochman, K. Paeschke, V. A. Zakian, *Nat. Rev. Genet.* 2012, *11*, 770–780.

[82] G. Pennarun, C. Granotier, L. M. Gauthier, D. Gomez, F. Hoffschir, E. Mandine, J.-F. Riou, J.-L. Mergny, P. Mailliet, F. D. Boussin, *Oncogene,* 2005, *24*, 2971–2928.

[83] D. E. Draper, D. Grilley, A. M. Soto, *Annu. Rev. Biophys. Biomol. Struct.* 2005, *34*, 221–243.

[84] G. S. Manning, *Acc. Chem. Res.* 1979, *12*, 443–449.

[85] M. Pechlaner, R. K. . Sigel, in *Met. Ions Life Sci.* (Eds.: A. Sigel, H. Sigel, R.K.. Sigel), Springer, Dordrecht, 2012, pp. 1–42.

[86] B. Lippert, *Coord. Chem. Rev.* 2000, *200-202*, 487–516.

[87] P. K. Bhattacharya, J. Cha, J. K. Barton, *Nucleic Acids Res.* 2002, *30*, 4740–4750.

[88] J. Müller, *Metallomics* 2010, *2*, 318–327.

[89] A. Sigel, H. Sigel, R. K. . Sigel, *Metal Ions in Life Sciences*, Springer, Dordrecht, 2012.

[90] N. Hadjiliadis, E. Sletten, *Metal Complex-DNA Interactions*, Wiley, Chichester, 2009.

[91] A. M. Pyle, O. Fedorova, C. Waldsich, *Trends Biochem. Sci.* 2007, *32*, 138–145.

[92] D. M. J. Lilley, *Q. Rev. Biophys.* 2000, *33*, 109–159.

[93] N. V. Hud, V. Sklenar, J. Feigon, *J. Mol. Biol.* 1999, *286*, 651–660.

[94] M. Guéron, J. P. Demaret, M. Filoche, *Biophys. Chem.* 2000, *78*, 1070–1083.

[95] B. Zambelli, F. Musiani, S. Ciurli, in *Interplay between Met. Ions Nucleic Acids* (Eds.: A. Sigel, H. Sigel, R.K.. Sigel), Dordrecht, 2012, pp. 136–169.

[96] J.-H. Chen, R. Yajima, D. M. Chadalavada, E. Chase, P. C. Bevilacqua, B. L. Golden, *Biochemistry* 2010, *49*, 6508–6518.

[97] N. Toor, K. S. Keating, S. D. Taylor, A. M. Pyle, *Science,* 2008, *320*, 77–82.

[98] M. R. Stahley, S. A. Strobel, *Science,* 2005, *309*, 1587–1590.

[99] B. Lippert, M. Leng, in *DNA Interact. (Top. Biol. Inorg. Chem.)* (Eds.: M.J. Clarke, P.J. Sadler), Springer, Berlin, 1999, p. 117.

[100] J. Wang, *Chem. Eur. J.* 1999, *5*, 1681–1685.

[101] P. K.-L. Fu, C. Turro, *J. Am. Chem. Soc.* 1999, *121*, 1–7.

[102] A. C. Ontko, P. M. Armistead, S. R. Kircus, H. H. Thorp, *Inorg. Chem.* 1999, *38*, 1842–1846.

[103] B. N. Trawick, A. T. Daniher, J. H. Bashkin, *Chem. Rev.* 1998, *98*, 939–960.

[104] J. J. Storhoff, C. A. Mirkin, *Chem. Rev.* 1999, *99*, 1849–1862.

[105] E. Braun, Y. Eichen, U. Sivan, G. Ben-Yoseph, *Nature,* 1998, *391*, 775–778.

[106] V. K. Misra, R. Shiman, D. E. Draper, *Biopolymers* 2003, *69*, 118–136.

[107] R. E. Franklin, R. G. Gosling, *Nature,* 1953, *171*, 740–741.

[108] D. A. Marvin, M. Spencer, M. H. F. Wilkings, L. D. Hamilton, *Nature,* 1958, *182*, 387–388.

[109] S. Arnott, E. Selsing, *J. Mol. Biol.* 1975, *98*, 265–269.

[110] M. C. Wahl, M. Sundaralingam, in *Oxford Handb. Nucleic Acid Struct.* (Ed.: S. Neidle), Oxford University Press, 1999, pp. 117–144.

[111] T. Theophanides, H. A. Tajmir-Riahi, *J. Biomol. Struct. Dyn.* 1985, *2*, 995–1004.

[112] F. M. Pohl, T. M. Jovin, *J. Mol. Biol.* 1972, *67*, 375–396.

[113] B. Basham, B. F. Eichman, P. S. Ho, in *Oxford Handb. Nucleic Acid Struct.* (Ed.: S. Neidle), Oxford University Press, 1999, pp. 199–252.

[114] S. Adam, P. Bourtayre, J. Liquier, E. Taillandier, *Nucleic Acids Res.* 1986, *14*, 3501–3513.

[115] J. Plavec, in *Met. DNA Interact.* (Eds.: N. Hadjiliadis, E. Sletten), Wiley, Chichester, 2009, pp. 55–94.

[116] D. R. Duckett, A. I. H. Murchie, D. M. J. Lilley, *Cell* 1995, *83*, 1027–1036.

[117] D. M. J. Lilley, R. M. Clegg, *Annu. Rev. Biophys. Biomol. Struct.* 1993, *22*, 299–328.

[118] T. I. Gaynutdinov, P. Brown, R. D. Neumann, I. G. Panyutin, *Biochemistry* 2009, *48*, 11169–11177.

[119] A. Wong, G. Wu, *J. Am. Chem. Soc.* 2003, *125*, 13859–13905.

[120] S. Basu, A. A. Szewczak, M. Coco, S. A. Strobel, *J. Am. Chem. Soc.* 2000, *122*, 3240–3241.

[121] R. K. O. Sigel, *Eur. J. Inorg. Chem.* 2005, 2281–2292.

[122] R. K. O. Sigel, H. Sigel, *Acc. Chem. Res.* 2010, *43*, 974–984.

[123] A. Pullman, B. Pullman, *Q. Rev. Biophys.* 1981, *14*, 289–380.

[124] J. Sponer, J. Leszczynski, P. Hobza, *J. Phys. Chem.* 1996, *100*, 1965–1974.

[125] E. R. Jamieson, S. J. Lippard, *Chem. Rev.* 1999, *99*, 2467–2498.

[126] B. Lippert, P. J. S. Miguel, *Acc. Chem. Res.* 2016, *49*, 1537–1545.

[127] G. H. Clever, C. Kaul, T. Carell, *Angew. Chemie - Int. Ed.* 2007, *46*, 6226–6236.

[128] Y. Takezawa, M. Shionoya, *Acc. Chem. Res.* 2012, *45*, 2066–2076.

[129] P. Scharf, J. Müller, *Chempluschem* 2013, *78*, 20–34.

[130] Y. Tanaka, J. Kondo, V. Sychrovský, J. Šebera, T. Dairaku, H. Saneyoshi, H. Urata, H. Torigoe, A. Ono, *Chem. Commun.* 2015, *51*, 17434–17360.

[131] Y. Takezawa, J. Müller, M. Shionoya, *Chem. Lett.* 2017, *46*, 622–633.

[132] B. Jash, J. Müller, *Chem. Eur. J.* 2017, *23*, 17166–17178.

[133] A. Ono, H. Torigoe, Y. Tanaka, I. Okamoto, *Chem. Soc. Rev.* 2011, *40*, 5855–5866.

[134] S. Katz, *Nature,* 1962, *194*, 569.

[135] S. Katz, *Biochim. Biophys. Acta* 1963, *68*, 240–253.

[136] T. Yamane, N. Davidson, *J. Am. Chem. Soc.* 1961, *83*, 2599–2607.

[137] Y. Miyake, H. Togashi, M. Tashiro, H. Yamaguchi, S. Oda, M. Kudo, Y. Tanaka, Y. Kondo, R. Sawa, T. Fujimoto, et al., *J. Am. Chem. Soc.* 2006, *128*, 2172–2173.

[138] Y. Tanaka, S. Oda, H. Yamaguchi, Y. Kondo, C. Kojima, A. Ono, *J. Am. Chem. Soc.* 2007, *129*, 244–245.

[139] Y. Tanaka, S. Oda, H. Yamaguchi, Y. Kondo, C. Kojima, A. Ono, *J. Am. Chem. Soc.* 2007, *129*, 244–245.

[140] J. Kondo, T. Yamada, C. Hirose, I. Okamoto, Y. Tanaka, A. Ono, *Angew. Chem. Int. Ed. Engl.* 2014, *53*, 2385–2388.

[141] H. Yamaguchi, Y. Sebera, J. Kondo, S. Oda, T. Komuro, T. Kawamura, T. Dairaku, Y. Kondo, I. Okamoto, A. Ono, et al., *Nucleic Acids Res.* 2014, *42*, 4094–4099.

[142] K. S. Park, C. Jung, H. G. Park, *Angew. Chemie - Int. Ed.* 2010, *49*, 9757–9760.

[143] H. Urata, E. Yamaguchi, T. Funai, Y. Matsumura, S.-I. Wada, *Angew. Chem. Int. Ed. Engl.* 2010, *49*, 6516–6519.

[144] J. C. Codina, C. Pérez-Torrente, A. Pérez-Garc'ia, F. M. Cazorla, A. de Vicente, *Arch. Environ. Contam. Toxicol.* 1995, *29*, 260–265.

[145] M. E. Ariza, M. V Williams, *J. Biochem. Mol. Toxicol.* 1999, *13*, 107–112.

[146] F. Schurz, M. Sabater-Vilar, J. Fink-Gremmels, *Mutagen.* 2000, *15* , 525–530.

[147] J. Kondo, Y. Tada, T. Dairaku, H. Saneyoshi, I. Okamoto, Y. Tanaka, A. Ono, *Angew. Chemie - Int. Ed.* 2015, *54*, 13323–13326.

[148] T. Dairaku, K. Furuita, H. Sato, J. Šebera, K. Nakashima, J. Kondo, D. Yamanaka, Y. Kondo, I. Okamoto, A. Ono, et al., *Chem. Eur. J.* 2016, *6*, 13028–13031.

[149] S. Johannsen, N. Megger, D. Bo, R. K. O. Sigel, J. Müller, *Nat. Chem.* 2010, *2*, 229–234.

[150] J. Kondo, Y. Tada, T. Dairaku, Y. Hattori, H. Saneyoshi, A. Ono, Y. Tanaka, *Nat. Chem.* 2017, *9*, 956–960.

[151] H. Liu, C. Cai, P. Haruehanroengra, Q. Yao, Y. Chen, C. Yang, Q. Luo, B. Wu, J. Li, J. Ma, et al., *Nucleic Acids Res.* 2017, *45*, 2910–2918.

[152] Hehua,L., F. Shen, P. Haruehanroengra, Q. Yao, Y. Cheng, Y. Chen, C. Yang, J. Zhang, B. Wu, Q. Luo, et al., *Angew. Chemie - Int. Ed.* 2017, *56*, 9430–9434.

[153] L. Y., Y. Lu, *Angew. Chemie - Int. Ed.* 2007, *46*, 7587–7590.

[154] Y.-W. Lin, H.-T. Ho, C. C. Huang, H.-T. Chang, *Nucleic Acids Res.* 2008, *36*, e123.

[155] G. Mor-Piperberg, R. Tel-Vered, J. Elbaz, I. Willner, *J. Am. Chem. Soc.* 2010, *132*, 6878–6879.

[156] Z.-G. Wang, I. Elbaz, I. Willner, *Nano Lett.* 2011, *11*, 304–309.

[157] S. Wen, T. Zeng, L. Liu, K. Zhao, Y. Zhao, X. Liu, H.-C. Wu, *J. Am. Chem. Soc.* 2011, *133*, 18312–18317.

[158] J. M. Thomas, H.-Z. Yu, D. Sen, *J. Am. Chem. Soc.* 2012, *134*, 13738–13748.

[159] S. J. Xiao, P. P. Hu, G. F. Xiao, Y. Wang, Y. Liu, C. Z. Huang, *J. Phys. Chem. B* 2012, *116*, 9565–9569.

[160] I. Kang, Y. Wang, C. Reagan, Y. Fu, M. X. Wang, L.-Q. Gu, *Sci. Rep.* 2013, *3*, 2381.

[161] S. Bi, B. Ji, Z. Zhang, J.-J. Zhu, *Chem. Sci.* 2013, *4*, 1858–1863.

[162] Y. Wang, B. Ritzo, L.-Q. Gu, *RSC Adv.* 2015, *5*, 2655–2658.

[163] T. Hong, Y. Yuan, T. Wang, J. Ma, Q. Yao, X. Hua, Y. Xia, X. Zhou, *Chem. Sci.* 2017, *8*, 200–205.

[164] X. Guo, F. Seela, *Chem. Eur. J.* 2017, *23*, 11776–11779.

[165] K. S. Park, C. Y. Lee, H. G. Park, *Chem. Commun.* 2016, *52*, 4868–4871.

[166] E. M. Nolan, S. J. Lippert, *Chem. Rev.* 2008, *108*, 3443–3480.

[167] D.-L. Ma, D. S.-H. Chan, B. Y.-W. Man, C. H. Leung, *Chem.-Asian J.* 2011, *6*, 986–1003.

[168] H. Torigoe, K. Kawahashi, A. Takamori, A. Ono, *Nucleosides. Nucleotides Nucleic Acids* 2005, *24*, 915–917.

[169] H. Torigoe, A. Ono, T. Kazasa, *Transit. Met. Chem.* 2011, *36*, 131–144.

[170] K. Tanaka, A. Tengeiji, T. Kato, N. Toyama, M. Shionoya, *Science,* 2003, *299*, 1212–1213.

[171] T. Carell, C. Behrens, J. Gierlich, *Org. Biomol. Chem.* 2003, *1*, 2221–2228.

[172] T. Ehrenschwender, W. Schmucker, C. Wellner, T. Augenstein, P. Carl, J. Hamer, F. Breher, H.-A. Wagenknecht, *Chem. Eur. J.* 2013, *19*, 12547–12552.

[173] J. C. Leon, Z. She, A. Kamal, M. H. Shamsi, J. Müller, H. B. Kraatz, *Angew. Chemie - Int. Ed.* 2017, *56*, 6098–6102.

[174] X. Liu, C.-H. Lu, I. Willner, *Acc. Chem. Res.* 2014, *47*, 1673–1680.

[175] A. Porchetta, A. Vallée-Bélisle, K. W. Plaxco, F. Ricci, *J. Am. Chem. Soc.* 2013, *135*, 13238–13241.

[176] T. Funai, Y. Miyazaki, M. Aotani, E. Yamaguchi, O. Nakagawa, S.-I. Wada, H. Torigoe, A. Ono, H. Urata, *Angew. Chemie - Int. Ed.* 2012, *51*, 6464–6466.

[177] O. P. Schmidt, G. Mata, N. W. Luedtke, *J. Am. Chem. Soc.* 2016, *1383*, 14733–14739.

[178] J. L. Mergny, A. T. Phan, L. Lacroix, *FEBS Lett.* 1998, *435*, 74–78.

[179] A. T. Phan, J. L. Mergny, *Nucleic Acids Res.* 2002, *30*, 4618–4625.

[180] R. Z. Jin, B. L. Gaffney, C. Wang, R. A. Jones, K. J. Breslauer, *Proc. Natl. Acad. Sci.* 1992, *89*, 8832–8836.

[181] A. T. Phan, K. N. Luu, D. J. Patel, *Nucleic Acids Res.* 2006, *34*, 5715–5719.

[182] A. Ambrus, D. Chen, J. X. Dai, R. A. Jones, D. Z. Yang, *Biochemistry* 2005, *44*, 2048.

[183] A. T. Phan, V. Kuryavyi, S. Burge, S. Neidle, D. J. Patel, *J. Am. Chem. Soc.* 2007, *129*, 4386.

[184] J. X. Dai, A. Ambrus, L. H. Hurley, D. Z. Yang, *J. Am. Chem. Soc.* 2009, *131*, 6102.

[185] G. N. Parkinson, M. P. H. Lee, S. Neidle, *Nature,* 2002, *417*, 876.

[186] R. W. Sinkeldam, N. J. Greco, Y. Tor, *Chem. Rev.* 2010, *110*, 2579–2619.

[187] J. Kypr, I. Kejnovska, D. Renciuk, M. Vorlickova, *Nucleic Acids Res.* 2009, *37*, 1713–1725.

[188] J. L. Mergny, J. Li, L. Lacroix, S. Amrane, J. B. Chaires, *Nucleic Acids Res.* 2005, *33*, e138.

[189] Dairaku,T., K. Furuita, H. Sato, J. Šebera, K. Nakashima, J. Kondo, D. Yamanaka, Y. Kondo, I. Okamoto, A. Ono, et al., *Chem. Eur. J.* n.d., *2016*, 13028–13031.

[190] G. C. K. Roberts, *NMR of Macromolecules*, Oxford University Press, New York, 1995.

[191] O. Zerbe, S. Jurt, *Applied NMR Spectroscopy for Chemists and Life Scientists*, Wiley, Weinheim, 2013.

[192] J. R. Lakowicz, *Principles of Fluorescence Spectroscopy*, Springer, New York, 2006.

[193] F. He, Y. L. Tang, S. Wang, Y. L. Li, D. B. Zhu, *J. Am. Chem. Soc.* 2005, *127*, 12343.

[194] J. L. Mergny, J. C. Maurizot, *ChemBioChem* 2001, *2*, 124.

[195] S. Nagatoishi, T. Nojima, E. Galezowska, J. B., S. Takenaka, *ChemBioChem* 2006, *7*, 1730.

[196] D. S. . Liu, S. A. Balasubramanian, *Angew. Chemie - Int. Ed.* 2003, *42*, 5734.

[197] J. . Choi, S. . Kim, T. . Tachikawa, M. . Fujitsuka, T. Majima, *J. Am. Chem. Soc.* 2011, *133*, 16146.

[198] A. B. . Neef, F. . Samain, N. W. Luedtke, *ChemBioChem* 2012, *13*, 1750.

[199] A. B. . Neef, N. W. Luedtke, *Proc. Natl. Acad. Sci.* 2011, *108*, 20404.

[200] J. . Zhang, R. E. . Campbell, A. Y. . Ting, R. Y. Tsien, *Nat. Rev. Mol. Cell Biol.* 2002, *3*, 906.

[201] A. B. Neef, N. W. Luedkte, *ChemBioChem* 2014, *15*, 789.

[202] B. N. G. . Giepmans, S. R. . Adams, M. H. . Ellisman, R. Y. Tsien, *Science,* 2006, *312*, 217.

[203] U. Rieder, N. W. Luedkte, *Proc. Natl. Acad. Sci.* 2014, *53*, 9168.

[204] T. Triemer, A. Messikommer, S. M. K. Glasauer, J. Alzeer, M. H. Paulisch, N. W. Luedtke, *Proc. Natl. Acad. Sci.* 2018, *115*, E1366–E1373.

[205] J. Peon, A. H. Zewail, *Chem. Phys. Lett.* 2001, *348*, 255–262.

[206] J. B. LePecq, C. Paoletti, *J. Mol. Biol.* 1967, *27*, 87.

[207] G. . Cosa, K. S. . Focsaneanu, J. R. N. . McLean, J. P. . McNamee, J. C. Scaiano, *Photochem. Photobiol.* 2001, *73*, 585.

[208] S. A. Latt, G. Stetten, L. A. Juergens, H. F. Willard, C. D. Scher, *J. Histochem. Cytochem.* 1975, *23*, 493.

[209] J. Alzeer, N. W. Luedtke, *Biochemistry2* 2010, *49*, 4339–4348.

[210] P. J. Somerharju, J. A. Virtanen, K. K. Eklund, P. Vianio, P. K. J. Kinnunen, *Biochemistry* 1985, *24*, 2773.

[211] D. Tang, P. L. G. Chong, *Biophys. J.* 1992, *63*, 903.

[212] P. L. G. Chong, D. Tang, I. P. Sugar, *Biophys. J.* 1994, *66*, 2029.

[213] K. Nicolay, R. Hovius, R. Bron, K. Wirtz, B. Dekruijff, *Biochim. Biophys. Acta* 1990, *1025*, 49.

[214] M. Langner, S. W. Hui, *Biochim. Biophys. Acta* 2000, *1463*, 439.

[215] B. Juskowiak, *Anal Bioanal Chem* 2011, *399*, 3157–3176.

[216] E. J. Merino, K. M. Weeks, *J. Am. Chem. Soc.* 2003, *125*, 12370–12371.

[217] R. M. Clegg, *Methods Enzymol.* 1992, *211*, 353–388.

[218] R. F. Delgadillo, L. J. Parkhurst, *Photchemistry Photobiol.* 2010, *86*, 261–272.

[219] B. G. Moreira, Y. You, M. A. Behlke, R. Owczarzy, *Biochem. Biophys. Res. Commun.* 2005, *327*, 473–484.

[220] A. Okamoto, Y. Saito, I. Saito, *J. Photochem. Photobiol. Photochem. Rev.* 2005, *6*, 108.

[221] L. M. Wilhelmsson, *Q. Rev. Biophys.* 2010, *43*, 159.

[222] A. A. Tanpure, M. G. Pawar, S. G. Srivatsan, *Isr. J. Chem.* 2013, *53*, 366.

[223] A. Matarazzo, R. H. E. Hudson, *Tetrahedron,* 2015, *71*, 1627.

[224] A. C. Jones, R. K. Neely, *Q. Rev. Biophys.* 2015, *48*, 244.

[225] S. G. Svrivatsan, H. Weizman, Y. Tor, *Org. Biomol. Chem.* 2008, *6*.

[226] M. J. Rist, J. P. Marino, *Curr. Org. Chem.* 2002, *6*, 775.

[227] N. J. Greco, Y. Tor, *Tetrahedron,* 2007, *63*, 3515.

[228] R. S. Butler, P. Cohn, P. Tenzel, K. A. Abboud, R. K. Castellano, *J. Am. Chem. Soc.* 2009, *131*, 623.

[229] M. E. Hawkings, *Fluoresc. Spectrosc* 2008, *450*, 201–231.

[230] R. D. Gray, L. Petraccone, J. O. Trent, J. B. Chaires, *Biochemistry* 2010, *49*, 179–194.

[231] S. R. Kirk, N. W. Luedtke, Y. Tor, *Bioorg. Med. Chem* 2001, *9*, 2295–2301.

[232] H.-A. Wagenknecht, *Ann. N. Y. Acad. Sci.* 2008, *1130*, 122–130.

[233] D. Shin, R. W. Sinkeldam, Y. Tor, *J. Am. Chem. Soc.* 2011, *133*, 14912–14915.

[234] A. Dumas, N. W. Luedtke, *J. Am. Chem. Soc.* 2010, *132*, 18004–18007.

[235] D. G. Xu, T. M. Nordlund, *Biophys. J.* 2000, *78*, 1042–1058.

[236] T. E. Haran, U. Mohanty, *Q. Rev. Biophys.* 2009, *42*, 41–81.

[237] A. Okamoto, K. Kanatani, I. Saito, *J. Am. Chem. Soc.* 2004, *126*, 4820–4827.

[238] T. Ehrenschwender, H.-A. Wagenknecht, *Synthesis,* 2008, *22*, 3657–3662.

[239] T. L. Netzel, M. Zhao, K. Nafisik, J. Headrick, S. M. S., B. E. Eaton, *J. Am. Chem. Soc.* 1995, *117*, 9119–9128.

[240] D. J. Hurley, S. E. Seaman, J. C. Mazura, Y. Tor, *Org. Lett.* 2002, *4*, 2305–2308.

[241] A. Okamoto, K. Tainaka, T. Unzai, I. Saito, *Tetrahedron,* 2007, *63*, 3465–3470.

[242] Q. Xiao, R. T. Ranasinghe, A. M. P. Tang, T. Brown, *Tetrahedron,* 2007, *63*, 3484–3490.

[243] J. A. Secrist, J. R. Barrio, N. J. Leonard, *Science,* 1972, *175*, 646–647.

[244] A. Holmen, B. Albinsson, B. Norden, *J. Phys. Chem* 1994, *98*, 13460–13469.

[245] F. Seela, E. Schweinberger, K. Xu, V. R. Sirivolu, H. Rosemeyer, E.-M. Becker, *Tetrahedron,* 2007, *63*, 3471–3482.

[246] N. J. Leonard, *Acc. Chem. Res.* 1982, *15*, 128–135.

[247] A. Okamoto, K. Tanaka, T. Fukuta, I. Saito, *J. Am. Chem. Soc.* 2003, *125*, 9296–9297.

[248] F. Godde, J. J. Toulme, S. Moreau, *Nucleic Acids Res.* 2000, *28*, 2977–2985.

[249] L. M. Wilhelmsson, A. Holmen, P. Lincoln, P. E. Nielson, B. Norden, *J. Am. Chem. Soc.* 2001, *123*, 2434–2435.

[250] Y. Tor, S. Del Valle, D. Jaramillo, S. G. Srivatsan, A. Rios, H. Weizman, *Tetrahedron,* 2007, *63*, 3608–3614.

[251] Y. Xie, T. Maxson, Y. Tor, *J. Am. Chem. Soc.* 2010, *132*, 11896–11897.

[252] Y. Xie, A. V. Dix, Y. Tor, *J. Am. Chem. Soc.* 2009, *131*, 17605–17614.

[253] N. J. Greco, Y. Tor, *Org. Lett.* 2009, *11*, 1115–1118.

[254] G. Mata, N. W. Luedtke, *J. Am. Chem. Soc.* 2015, *137*, 699–707.

[255] G. Mata, O. P. Schmidt, N. W. Luedkte, *Chem Commun* 2016, *52*, 4718.

Chapter 2

A Fluorescent Surrogate of Thymidine in Duplex DNA[1]

2.1. Introduction

Nucleobase analogs constitute an important family of fluorescent probes.[1] They can be positioned in nucleic acid structures with high precision, and their photophysical properties are highly sensitive to local polarity,[2] viscosity,[3] and pH.[4] Together these features facilitate specific monitoring of biochemical transformations,[5] conformational changes,[6] metal binding,[7] and base pairing interactions.[8] Nucleobase ionization can mediate proton-coupled folding,[9] metal binding,[10] and/or the catalytic activities of certain nucleic acids at neutral pH.[11] Thymidine (T) and uracil (U) are among the most inherently acidic residues,[12] but fluorescent analogs capable of reporting pyrimidine ionization in nucleic acids are scarce. Previously reported examples utilized biaryl or triaryl fluorophores,[4c-d] having unreported or highly perturbed pK_a values ($pK_a \approx 6.8$) as compared to unmodified T and U residues ($pK_a \approx 9.5$).[12]

2.2. Ionization Properties and Environmental Sensitivity of ^{DMA}T

Recently, a new fluorescent thymidine analog "*N*,*N*-dimethylaniline-2'-deoxythymidine" or "^{DMA}T" was reported (Figure 2.1).[13] To generate a push-pull fluorophore, an electron donating group was incorporated at the *C*6 position of a quinazoline core.[9,14] This position was selected because it is not in conjugation with *N*3-H, and therefore had little to no impact on its acidity. Molecular orbital calculations predicted a charge transfer from a dimethylaniline-centered HOMO to a pyrimidine-centered LUMO with a HOMO-LUMO energy gap (ΔE) = 2.44 eV in the neutral form and a pyrimidine-centered HOMO, and a larger

[1] Published by Mata, G., Schmidt, O.P., Luedtke, N. W., *Chem. Commun.,* 2016, *52,* 4718.

$\Delta E = 2.81$ eV in the anionic form (Figure 2.1). Consistent with these calculations, ^{DMA}T exhibits an exceptionally large Stoke's shift, with an absorbance maximum (λ_{abs}) = 357 nm and emission maximum (λ_{em}) = 522 nm (Figure 2.2a, Table 2.1). A linear correlation ($R^2 = 0.980$) with a large slope of 177 cm^{-1} / kcal mol^{-1} was obtained by plotting the Stoke's shift of ^{DMA}T measured in various water/dioxane mixtures against Reichardt's solvent polarity parameter (E_T^{30}),[15,16] demonstrating ^{DMA}T to be an environmentally sensitive, push-pull fluorophore (Figure 2.2a). Interestingly, ^{DMA}T exhibited a two-fold higher quantum yield in D_2O ($\phi = 0.07$) than H_2O ($\phi = 0.03$) (Table 2.1), suggesting that proton transfer with bulk solvent provides an effective nonradiative decay pathway.[4a]

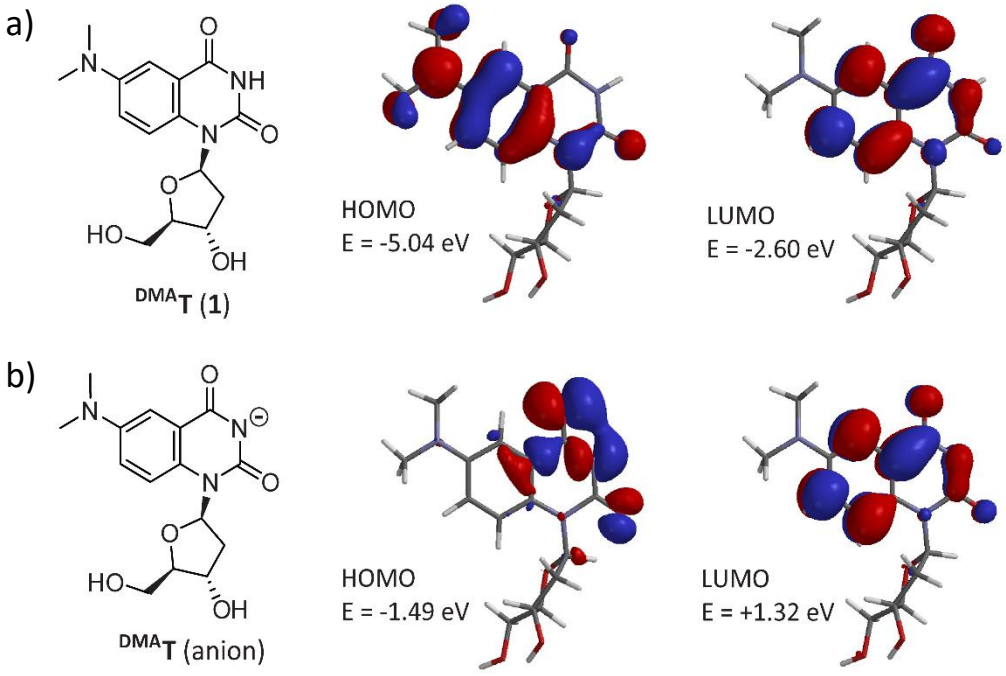

Figure 2.1. a) Structure of the ^{DMA}T nucleoside, and b) its conjugate base. HOMOs, LUMOs, and their relative energies were calculated from DFT-optimized geometries using LSDA/pBP86/DN**.

The fluorescence sensitivity of ^{DMA}T towards nucleobase ionization was evaluated by recording its absorbance and emission spectra at different pH values. Consistent with DFT calculations, the emission maximum of ^{DMA}T shifted towards the blue with increasing pH (Table 2.1). This was accompanied by a dramatic increase in fluorescence intensity. By plotting absorbance and fluorescent changes against pH a pK_a value of 9.5 ± 0.1 was determined, corresponding to the pK_a of thymidine and uracil (Figure 2.2b).[12]

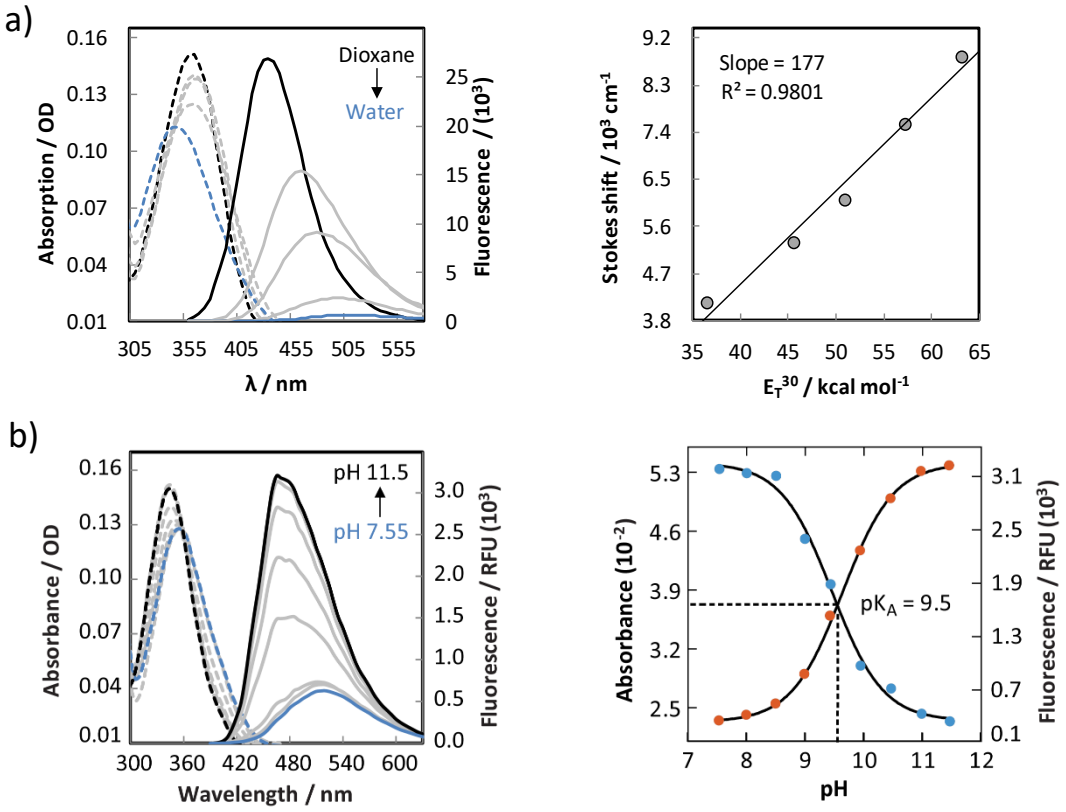

Figure 2.2. a) Absorbance (---) and emission (—) spectra (λ_{ex} = 370 nm) of ^{DMA}T (1) at 40 µM in dioxane (black), water (blue), and various mixtures (grey) (left). Linear relationship between the Stokes shift and the E_T^{30} (right). b) Absorbance (---) and emission (—) spectra (λ_{ex} = 360 nm) of 40 µM ^{DMA}T in phosphate citric acid buffer (200 mM of Na_2HPO_4, 100 mM of citric acid and 100 mM NaCl) (left). Single-wavelength analyses of the pH-dependent absorbance (400 nm, blue dots) and emission (470 nm, red dots) of ^{DMA}T (right).

Table 2.1 Photophysical Data of ^{DMA}T and its Conjugate Base.[a]

Solvent	λ_{abs}[a]	λ_{em}[b]	$\varepsilon_{(260)}$[c]	$\varepsilon_{(\lambda abs)}$[d]	ϕ[e]
H_2O	357	522	15.0	2.9	0.03
pH = 11.0	345	480	17.1	3.9	0.09
D_2O	355	520	13.0	2.7	0.07
pD = 11.0	345	480	14.3	3.4	0.19

[a]Absorbance maxima (λ_{abs}) in nm. [b]Emission maxima (λ_{em}) in nm. [c-d]Extinction coefficients (ε) in 10^3 M^{-1} cm^{-1} were measured at 260 nm and at λ_{abs}. [e]Quantum yields (ϕ) were calculated using quinine hemisulfate in 0.5 M H_2SO_4 as a fluorescent standard.[17] Reproducibility is within ± 10% of each reported ϕ value.

2.3. ^{DMA}T as a Fluorescent Thymidine Mimic in DNA

Using standard phosphoramidite chemistry, ^{DMA}T was incorporated at one of four positions within the same, 21-residue DNA sequence (Figure 2.3). Three positions near the middle of the sequence (X13, X14 and X15) and a single position near the 5' terminus (X2) were selected in order to evaluate the impact on fluorescence properties of the probe due to variable flanking sequences and DNA end "breathing" motions, respectively. Circular dichroism and thermal denaturation experiments revealed that ^{DMA}T had little to no impact on the global structure or stability of duplex DNA. CD measurements gave spectra consistent with formation of B-form helices (Figures A1 and A2, Appendix). ^{DMA}T–A-containing duplexes exhibited nearly identical T_m values as the corresponding wild-type duplexes containing T–A base pairs (ΔT_m = –0.2 to –1.7 °C) (Table 2.2, Figure A2, Appendix). In contrast, duplexes containing a single C–A, A–A, ^{DMA}T–T or T–T mismatch at positions X13–X15 caused a large loss in thermal stability (ΔT_m = –4.8 to –7.9 °C). DNA end breathing motions of the duplex explain the relatively small impacts on T_m when the mismatch was positioned at X2 (Table 2.2, Figure A2, Appendix).

Table 2.2 Thermal Denaturation Melting (T_m) Temperatures (°C) of duplexes.[a]

Position	T-A	^{DMA}T-A	C-A	A-A	^{DMA}T-T	T-T
X2	69.0	68.8	67.3	67.5	68.0	67.0
X13	68.8	67.1	60.9	62.4	62.3	61.5
X14	68.7	67.3	61.3	63.9	62.5	61.5
X15	68.9	68.0	61.2	62.7	64.0	62.8

[a] All samples contained 5 μM of DNA in phosphate citric acid buffer (200 mM of Na_2HPO_4, 100 mM of citric acid, and 100 mM NaCl or $NaNO_3$) at pH = 7.35. Reproducibility is within ± 0.3 °C of each reported value. For duplex DNA sequences see Figure 2.3 and Table 6.2, Materials and Methods.

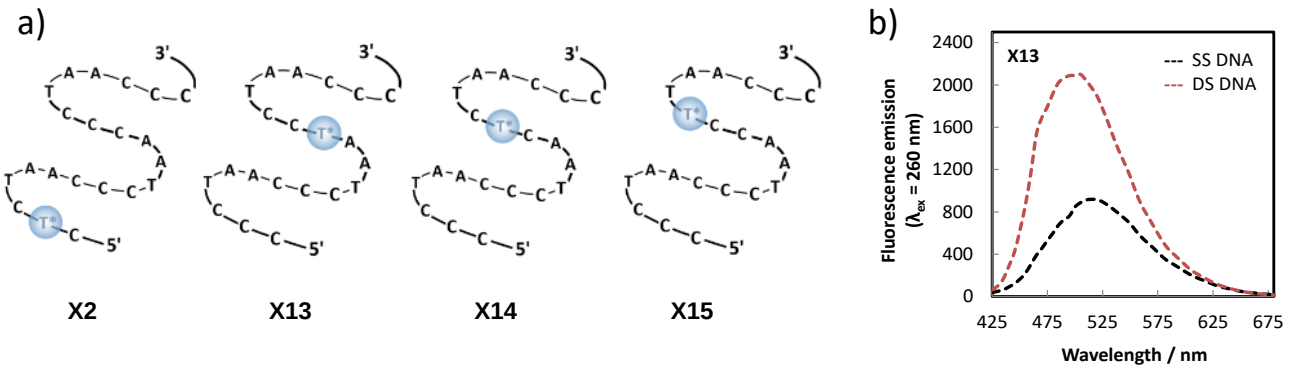

Figure 2.3. a) Oligonucleotides containing ^{DMA}T at different positions. b) Fluorescent emission spectra of "X13" (λ_{ex} = 260 nm) in unstructured single stranded form ("SS") and in double stranded DNA ("DS"). For spectra of "X2", "X14", and "X15" see Figure A3, Appendix.

The fluorescence properties of ^{DMA}T were highly sensitive to the global structure of the DNA containing it (Table 2.3). At all three internal positions X13–X15, ^{DMA}T exhibited a two-fold higher quantum yield and blue-shifted λ_{em} in duplex versus single-stranded DNA (Table 2.3, Figure 2.3b, Figure A3, Appendix). Decreased probe hydration upon duplex formation is probably responsible, because the ^{DMA}T nucleoside exhibited higher quantum yields and blue-shifted λ_{em} in organic versus aqueous solvents (Table 2.3). At all four positions of incorporation, higher fluorescence anisotropy was observed in duplex DNA (r = 0.09–0.18) as compared to unfolded structures (r = 0.03–0.06), consistent with large losses in dynamic motions of the probe upon duplex formation (Table 2.3).

The photophysical properties of ^{DMA}T were sensitive to matched versus mismatched base pairing in duplex DNA (Table 2.4). In oligonucleotide X15, for example, ^{DMA}T exhibited a higher quantum yield and blue-shifted λ_{abs} and λ_{em} in ^{DMA}T–A base pairs (λ_{abs} = 355 nm, λ_{em} = 486 nm, ϕ = 0.11) as compared to ^{DMA}T–T, ^{DMA}T–G and ^{DMA}T–C mismatches ((λ_{abs} = 365 – 370 nm, λ_{em} = 500 – 505 nm, ϕ = 0.05 – 0.08). Changes in probe hydration and base stacking are likely responsible for these differences, because similar trends were also observed when comparing duplex versus single-stranded DNA containing ^{DMA}T (Table 2.3). Together with the thermal denaturation results (Table 2.2), these data demonstrated that ^{DMA}T exhibits the same base pairing specificity as T.

Table 2.3 Photophysical Properties of ^{DMA}T in Single-Stranded and Duplex DNA (X = ^{DMA}T).

Structure	Position	λ_{abs}[a]	λ_{em}[b]	r[c]	ϕ[d]
Duplex	X2	355	505	0.18	0.03
	X13	355	504	0.09	0.20
	X14	355	492	0.14	0.13
	X15	355	486	0.15	0.11
Unfolded	X2	365	515	0.03	0.05
	X13	365	515	0.05	0.09
	X14	365	516	0.06	0.06
	X15	365	515	0.05	0.05

[a]Absorbance maxima (λ_{abs}) in nm. [b]Emission maxima (λ_{em}) in nm. [c]Fluorescence anisotropy (r) with λ_{ex} = 375 nm and λ_{em} = 500 nm. [d]Quantum yields (ϕ) calculated using the ^{DMA}T nucleoside (ϕ = 0.03) as a fluorescent standard. Reproducibility is within ± 30% of each reported ϕ value. All samples contained 4 µM of DNA in a buffer containing 20 mM of Na_2HPO_4, 10 mM of citric acid and 10 mM NaCl (pH = 7.35). For duplex DNA sequences see Figure 2.3 and Table 6.2, Materials and Methods.

Table 2.4 Photophysical Properties of ^{DMA}T in Duplex DNA (X = ^{DMA}T).[a]

Position	Pairing	λ_{abs}	λ_{em}	r	ϕ
X13	^{DMA}T–A	355	504	0.09	0.20
	^{DMA}T–T	365	505	0.09	0.13
	^{DMA}T–G	365	508	0.10	0.09
	^{DMA}T–C	365	498	0.10	0.12
X15	^{DMA}T–A	355	486	0.15	0.11
	^{DMA}T–T	365	500	0.12	0.08
	^{DMA}T–G	370	505	0.12	0.06
	^{DMA}T–C	370	502	0.17	0.05

[a] See Table 2.3 footnotes for experimental details and symbol definitions.

2.4. ^{DMA}T Can Report Site-Specific Hg^{II}-DNA Binding

Metal-mediated base pairing interactions serve as important recognition motifs in biological and material sciences.[10] For example, Hg^{II} ions specifically bind to opposing thymine residues to form T–Hg^{II}–T base pairs[19] that can cause miscoding of DNA synthesis *in vitro* and possibly *in vivo*.[20] Thermal melting temperature analysis measured in the presence or absence of 1.0 equiv. of Hg^{II} were used to demonstrate the ability of ^{DMA}T–T to mimic T–T in duplex DNA (Table 2.5, Figure A4, Appendix). Only small increases in thermal stabilities (ΔT_m = +0.8 to +1.5 °C) were observed when Hg^{II} was added to duplexes containing a ^{DMA}T–T or T–T at position X2, whereas much larger increases were observed at positions X13–X15 (ΔT_m = +2.9 to +6.0 °C, Table 2.4, Figure 2.4a, Figure A4, Appendix). At all four positions, the same T_m values were obtained for duplexes containing ^{DMA}T–Hg^{II}–T as T–Hg^{II}–T (Table 2.5). In contrast, the addition of 1.0 equiv. of Hg^{II} to duplexes containing a C–T mismatch resulted in no increase in thermal stability as compared to the mismatch alone (Table 2.4). These results demonstrated the excellent mimicry of ^{DMA}T for thymidine residues in the demanding context of T–Hg^{II}–T base pairs.

Table 2.5 Thermal Denaturation Melting (T_m) Temperatures (°C) of Unmodified or ^{DMA}T-Containing Duplexes.

Position	T-T	T-T +Hg^{II}	^{DMA}T-T	^{DMA}T-T +Hg^{II}	C-T	C-T +Hg^{II}
X2	67.0	68.5	68.0	68.8	66.8	66.3
X13	61.5	67.5	62.3	67.1	60.4	61.1
X14	61.5	65.1	62.5	65.7	60.4	60.3
X15	62.8	65.7	64.0	66.9	60.6	60.9

[a] All samples contained 5 μM of DNA in phosphate citric acid buffer (200 mM of Na_2HPO_4, 100 mM of citric acid, and 100 mM NaCl or $NaNO_3$) at pH = 7.35. Reproducibility is within ± 0.3 °C of each reported value. For duplex DNA sequences see Figure 2.3 and Table 6.2, Materials and Methods).

The fluorescence properties of ^{DMA}T were utilized to monitor site-specific binding of Hg^{II} ions to ^{DMA}T–T sites (Figure 2.4, Table A1, Figure A5, Appendix). Bi-phasic fluorescence quenching was observed upon addition of Hg^{II} to duplex DNA containing a ^{DMA}T–T mismatch, giving a 95% decrease in fluorescence intensity upon addition of 3 eq. of Hg^{II} (Figure 2.4b). The biphasic quenching mirrored the increases in T_m values obtained when Hg^{II} is added to duplexes containing a T–T mismatch (Figure 2.4b). A comparison of these results revealed that the steep slopes observed between 0.0 to 1.0 equiv. of added Hg^{II} are a result of T–T-specific binding, and the shallow slopes between 2.0 to 3.0 equiv. are due to non-specific interactions. In contrast to ^{DMA}T–T, very little fluorescence quenching (~20%) was observed upon the addition of Hg^{II} ions to duplex DNA containing a ^{DMA}T–A base pair, or a ^{DMA}T–G mismatch (Table A2, Figure A6, Appendix). Conversely, the addition of Zn^{II}, Cu^{II}, Mg^{II}, Fe^{II}, Ca^{II}, Ag^{I}, Cd^{II}, Pd^{II} and Ni^{II} ions to duplexes containing a ^{DMA}T–T mismatch resulted in little or no change in ^{DMA}T fluorescence (Figure 2.4c). These results are consistent with previous studies demonstrating a high degree of specificity between T–T mismatches and Hg^{II} ions using thermal denaturation.[19] These results provided the first example of using a fluorescent nucleobase analog to monitor a specific binding reaction between DNA and Hg^{II} ions. ^{DMA}T will therefore enable detailed kinetics analyses and large-scale screening efforts that are not currently feasible using other analytical techniques.[10d]

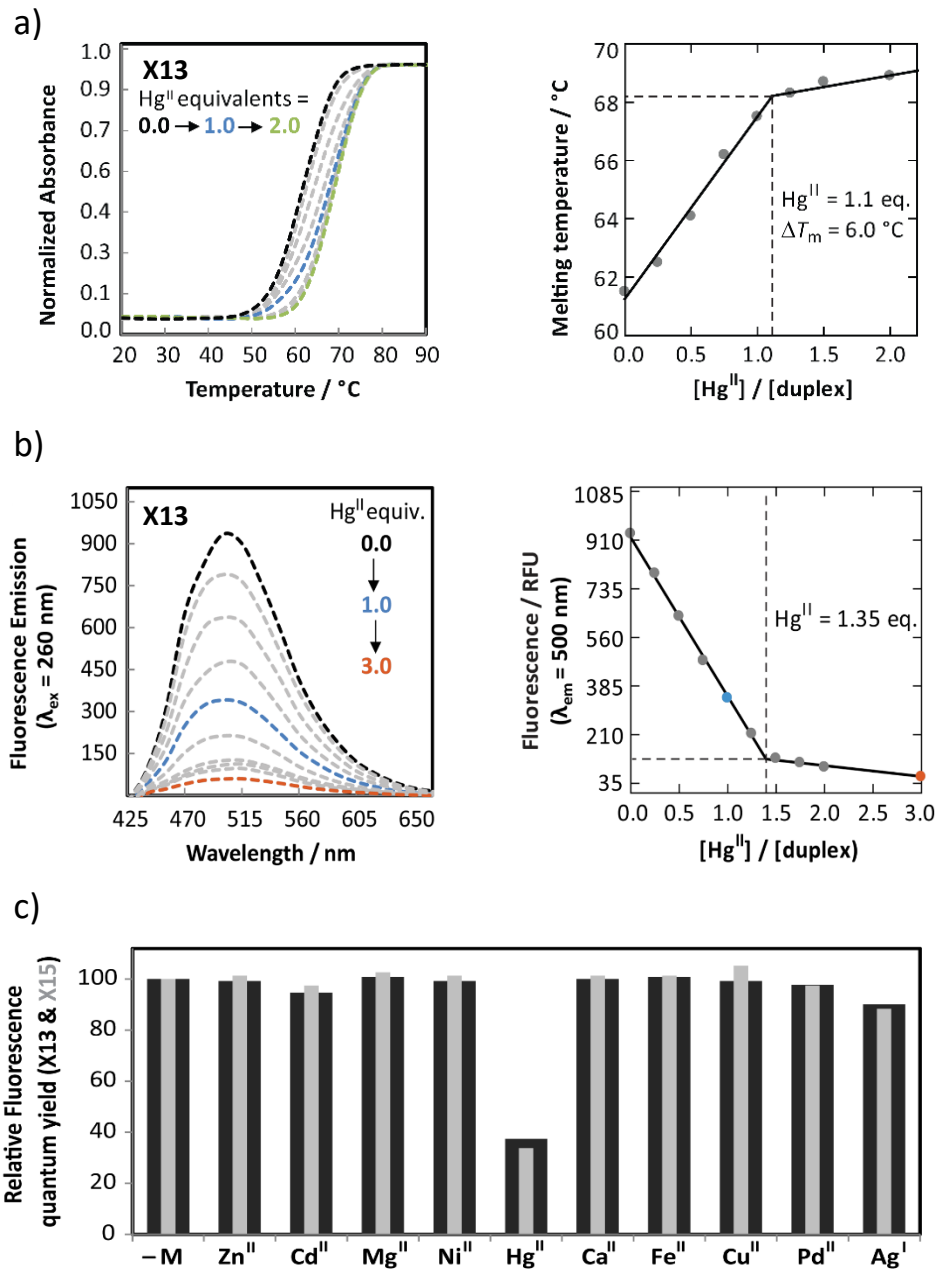

Figure 2.4. a) Thermal denaturation curves of duplex X13 in the absence (black) and in the presence of $Hg(ClO_4)_2$ (1.0 equiv. (blue), 2.0 equiv. (green) and intermediate (grey)) (left). Plot of the melting temperature versus equivalents of Hg^{II} ions (right). The complementary strand contained a "T" mismatched opposite to the "X13" base. b) Fluorescence spectra (λ_{ex} = 260 nm) of duplex X13 in the absence (black) and in the presence of variable $Hg(ClO_4)_2$ (left) and plot of fluorescence intensity (λ_{em} = 500 nm) versus equiv. of Hg^{II} ions (right). c) Relative quantum yield of ^{DMA}T-T mismatched duplex DNA X13 (black) or X15 (grey) upon addition of metal ions (1.0 equiv.): $Hg(ClO_4)_2$, $ZnCl_2$, $CuCl_2$, $MgCl_2$, $FeCl_2$, $CaCl_2$, $CdCl_2$, $PdCl_2$, $NiCl_2$, or $AgNO_3$. All samples were measured in phosphate citric acid buffer (200 mM of Na_2HPO_4, 100 mM of citric acid and 100 mM $NaNO_3$). For duplex DNA sequences see Figure 2.3 and Table 6.2, Materials and Methods).

REFERENCES

1 (*a*) M. E. Hawkins, *Cell Biochem. Biophys*., 2001, *34*, 257. (b) A. T. Krueger, H. Lu, A. H. Lee, E. T. Kool, *Acc. Chem. Res*. 2007, *40*, 141; (*b*) R. W. Sinkeldam, N. J. Greco, Y. Tor, *Chem. Rev.*, 2010, *110*, 2579; (*c*) L. M. Wilhelmsson, *Q. Rev. Biophys.*, 2010, *43*, 159; (*d*) A. A. Tanpure, M. G. Pawar, S. G. Srivatsan, *Isr. J. Chem.,* 2013, *53*, 366; (*e*) M. Weinberger, F. Berndt, R. Mahrwald, N. P. Ernsting, H. A. Wagenknecht, *J. Org. Chem.*, 2013, *78*, 2589; (*f*) A. Matarazzo, R. H. E. Hudson, *Tetrahedron*, 2015, *71*, 1627.

2 R. W. Sinkeldam, N. J. Greco, Y. Tor, *ChemBioChem*, 2008, *9*, 706.

3 R. W. Sinkeldam, A. J. Wheat, H. Boyaci, Y. Tor, *ChemPhysChem*, 2011, *12*, 567.

4 (*a*) K. M. Sun, C. K. McLaughlin, D. R. Lantero, R. A. Manderville, *J. Am. Chem. Soc.,* 2007, *129*, 1894; (*b*) D. Jiang, F. Seela, *J. Am. Chem. Soc.*, 2010, *132*, 4016; (*c*) J. Riedl, R. Pohl, L. Rulisek, M. Hocek, *J. Org. Chem.*, 2012, *77*, 1026; (d) R. W. Sinkeldam, P. A. Hopkins, Y. Tor, *Chemphyschem*, 2012, *13*, 3350.

5 (*a*) R. A. Mizrahi, D. Shin, R. W. Sinkeldam, K. J. Phelp, A. Fin, D. J. Tantillo, Y. Tor, P. A. Beal, *Angew. Chem. Int. Ed.*, 2015, *54*, 8713; (*b*) A. C. Jones, R. K. Neely, *Q. Rev. Biophys.*, 2015, *48*, 244.

6 (*a*) F. Godde, J. J. Toulmé, S. Moreau, *Biochemistry*, 1998, *37*, 13765; (*b*) Y. Hikida, M. Kimoto, S. Yokoyama, I. Hirao, *Nat. Protoc*., 2010, *5*, 1312; (*c*) A. Dumas, N. W. Luedtke, *Nucleic Acids Res*., 2011, *39*, 6825; (*d*) A. Dumas, N. W. Luedtke, *ChemBioChem*, 2011, *12*, 2044; (*e*) M. Sholokh, R. Sharma, D. Shin, R. Das, O. A. Zaporozhets, Y. Tor, Y. Mély, *J. Am. Chem. Soc.*, 2015, *137*, 3185; (*f*) A. A. Tanpure, S. G. Srivatsan, *Nucleic Acids Res.*, 2015, *43*, e149.

7 (*a*) A. Dumas, N. W. Luedtke, *Chem. Eur. J.*, 2012, *18*, 245; (*b*) A. Omumi, C. K. McLaughlin, D. Ben-Israel, R. A. Manderville, *J. Phys. Chem. B*, 2012, *116*, 6158; (*c*) S. K. Jana, X. Guo, H. Mei, F. Seela, *Chem. Commun*., 2015, *51*, 17301.

8 (*a*) J. Michel, G. Gueguen, J. Vercauteren, S. Moreau, *Tetrahedron*, 1997, *53*, 8457; (b) A. Okamoto, K. Tainaka, I. Saito, *J. Am. Chem. Soc.* 2003, *125*, 4972; (*c*) H.-A. Wagenknecht, *Ann. N.Y. Acad. Sci.*, 2008, *1130*, 122; (*d*) Y. Xie, A. V. Dix, Y. Tor, *J. Am. Chem. Soc.*, 2009, *131*, 17605; (*e*) N. J. Greco, R. W. Sinkeldam, Y. Tor, *Org. Lett.,* 2009, *11*, 1115; (*f*) X. Ming, F. Seela, *Chem. Eur. J.*, 2012, *18*, 9590; (*g*) Y. Saito, A. Suzuki, Y. Okada, Y. Yamasaka, N. Nemoto, I. Saito, *Chem. Commun*., 2013, *49*, 5684.

9 G. Mata, N. W. Luedtke, *J. Am. Chem. Soc.*, 2015, *137*, 699.

10 (*a*) G. H. Clever, C. Kaul, T. Carell, *Angew. Chem. Int. Ed.*, 2007, *46*, 6226; (*b*) J. Müller, *Metallomics*, 2010, *2*, 318-327; (*c*) G. H. Clever, M. Shionoya, *Met. Ions. Life. Sci.*, 2012, *10*, 269; (d) Y. Tanaka, J. Kondo, V. Sychrovský, J. Šebera, T. Dairaku, H. Saneyoshi, H. Urata, H. Torigoe, A. Ono, *Chem. Commun.*, 2015, *51*, 17343.

11 (*a*) P. L. Nixon, D. P. Giedroc, *J. Mol. Biol.*, 2000, *296*, 659; (*b*) S. R. Das, J. A. Piccirilli, *Nat. Chem. Biol.*, 2005, *1*, 45.

12 R. M. Izatt, J. J. Christensen, H. Rytting, *Chem. Rev.*, 1971, *71*, 439.

13 G. Mata, O. P. Schmidt, N. W. Luedtke *Chem. Commun.* 2016, *52*, 4718.

14 (*a*) Y. Xie, T. Maxson, Y. Tor, *J. Am. Chem. Soc.*, 2010, *132*, 11896; (*b*) G. Mata, N. W. Luedtke, *Org. Lett.*, 2013, *15*, 2462; (*c*) D. Liu, Z. Y. Zhang, H. Z. Zhang, Y. Wang, *Chem. Commun.*, 2013, *49*, 10001; (*d*) S. Achelle, J. Rodriguez-Lopez, F. Robin-le Guen, *J. Org. Chem*., 2014, *79*, 7564.

15 (*a*) C. Reichardt, *Chem. Rev.*, 1994, *94*, 2319; (*b*) R. W. Sinkeldam, Y. Tor, *Org. Biomol. Chem.*, 2007, *5*, 2523.

16 (*a*) T. L. Netzel, M. Zhao, K. Nafisi, J. Headrick, M. S. Sigman, B. E. Eaton, *J. Am. Chem. Soc.*, 1995, *117*, 9119; (*b*) R. S. Butler, P. Cohn, P. Tenzel, K. A. Abboud, R. K. Castellano, *J. Am. Chem. Soc.*, 2009, *131*, 623.

17 W. H. Melhuish, *J. Phys. Chem.*, 1961, *65*, 229.

18 (*a*) D. M. Gray, R. L. Ratliff, M. R. Vaughan, *Methods Enzymol*., 1992, *211*, 389; (*b*) J. Kypr, I. Kejnovska, D. Renciuk, M. Vorlickova, *Nucleic Acids Res.*, 2009, *37*, 1713.

19 Y. Miyake, H. Togashi, M. Tashiro, H. Yamaguchi, S. Oda, M. Kudo, Y. Tanaka, Y. Kondo, R. Sawa, T. Fujimoto, T. Machinami, A. Ono, *J. Am. Chem. Soc.*, 2006, *128*, 2172.

Chapter 3

Fluorescent Base Analog Reveals T-Hg^{II}-T Base Pairs Have High Kinetic Stabilities that Perturb DNA Metabolism[2]

The thymidine analog ^{DMA}T was used for the first fluorescence-based study of direct, site-specific metal binding reactions involving unmodified nucleobases in duplex DNA. The fluorescence properties of ^{DMA}T-A base pairs were highly sensitive to mercury binding reactions at T-T mismatches located at an adjacent site or one base pair away. This allowed for precise determination of the local kinetic and thermodynamic parameters of T-Hg^{II}-T binding reactions. The on- and off-rates of Hg^{II} were surprisingly slow, with association rate constants (k_{on}) $\approx 10^4 - 10^5$ $M^{-1}s^{-1}$, and dissociation rate constants (k_{off}) $\approx 10^{-4} - 10^{-3}$ s^{-1}; giving equilibrium dissociation constants (K_d) = 8 – 50 nM. In contrast, duplexes lacking a T-T mismatch exhibited local, non-specific Hg^{II} binding affinities in the range of K_d = 0.2 – 2.0 μM, depending on the buffer conditions. The exceptionally high kinetic stabilities of T-Hg^{II}-T metallo-base pairs (half-lives = 0.3 – 1.3 h) perturbed dynamic processes including DNA strand displacement and primer extension by DNA polymerases that resulted in premature chain termination of DNA synthesis. In addition to providing the first detailed kinetic and thermodynamic parameters of site-specific T-Hg^{II}-T binding reactions in duplex DNA, these results demonstrate that T-Hg^{II}-T base pairs have a high potential to disrupt DNA metabolism *in vivo*.

[2] Published by Schmidt, O. P., Mata, G., Luedtke, N. W. *J. Am. Chem. Soc.* 2016, *138*, 14733.

3.1 Introduction

Hg^{II} is infamous for being cytotoxic and mutagenic,[1] but the exact mechanisms for these activities are still unclear. In addition to oxidative stress,[2] Hg^{II} causes DNA point mutations,[3] DNA strand breaks,[4,5] and the inhibition of DNA synthesis and repair in live cells.[5,6] These activities could be the result of direct mercury-DNA binding interactions. When 5 μM of $HgCl_2$ was applied to live cells for 4 h and the DNA harvested and analyzed, approximately 0.3 % of base pairs contained mercury.[7] After 30 years of study, however, little is known about the composition or structure of these complexes. While many different metal-DNA binding modes are possible,[8] Hg^{II} preferentially binds to *N1* or *N7* of purines and to *N3* of thymidine residues *in vitro*.[9] In 2006, Ono and co-workers reported that T-T mismatches in duplex DNA exhibited stoichiometric binding of Hg^{II} ions *in vitro*, giving duplexes with approximately the same thermal stabilities as duplexes containing T-A base pairs.[10] The preferred Hg^{II} binding site was found to be the *N3* positions of two deprotonated thymine residues (Figure 3.1a).[11] A crystal structure of duplex DNA containing two such T-Hg^{II}-T base pairs revealed minimal distortion of the B-form duplex.[12] In addition to structural similarities, T-Hg^{II}-T can serve as a functional mimic of T-A base pairs by stabilizing T-T during DNA primer extension,[13] and by causing the enzymatic misincorporation of dTTP across from thymidine to give T-Hg^{II}-T base pairs.[14] These activities provide a potential mechanism for the formation of T-Hg^{II}-T base pairs in S-phase cells.

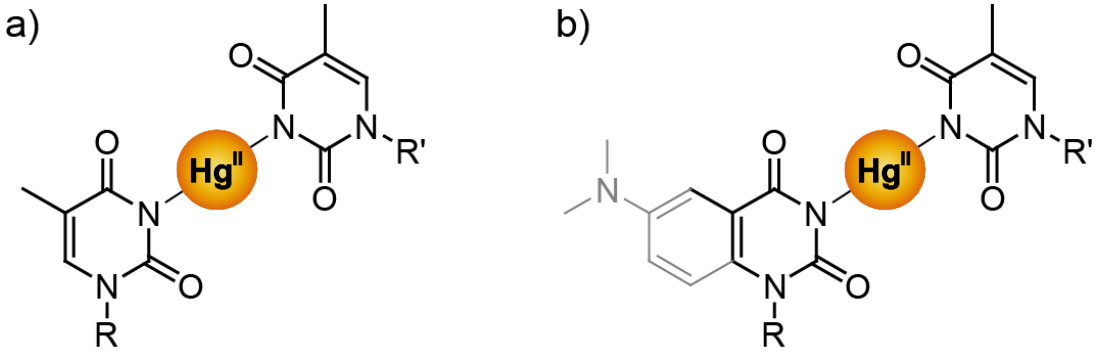

Figure 3.1. a) T-Hg^{II}-T base pair. b) ^{DMA}T-Hg^{II}-T base pair (R, R' = duplex DNA).

Given the potentially broad importance of T-Hg^{II}-T base pairs in both biological and material sciences,[15] a wide variety of spectroscopic methods have been used to characterize their properties including UV,[10,16] Raman,[17] CD,[18] NMR,[19] ITC,[20] and fluorescence.[21] With the exception of high resolution structural analyses by Raman and NMR, these methods report changes in global properties resulting from both specific and non-specific binding interactions.

To our knowledge, there are no previous studies that report the exact kinetic and thermodynamic parameters of local, site-specific T-Hg^{II}-T binding reactions in duplex DNA. These values are important for understanding the potential biological impact and material properties of T-Hg^{II}-T base pairs.

Fluorescent nucleobase analogs (FBAs) can facilitate highly sensitive biophysical measurements with single-base resolution.[22,23] FBAs are therefore ideal candidates for characterizing local binding interactions,[24] but only a few previous studies have utilized FBAs as probes of transition metal binding.[25] In these cases, the FBA directly participated in the binding reaction and therefore it provided little or no information about native DNA-metal interactions. In other examples,[24] ligand binding caused conformational changes that impacted the FBA's microenvironment and therefore its fluorescence properties in an indirect way. There are no previous examples of native, site-specific metal-nucleobase binding interactions being directly reported by an FBA. This would provide a powerful tool for determining the kinetic and thermodynamic parameters of local metal binding reactions. With this goal, we recently synthesized a new fluorescent thymidine mimic "^{DMA}T" that exhibits same base pairing preferences as native thymine residues.[26] Duplexes containing ^{DMA}T-A or ^{DMA}T-Hg^{II}-T base pairs (Figure 3.1b) exhibited the same global structures, thermal stabilities, and metal binding properties as wild-type duplexes containing T-A or T-Hg^{II}-T, respectively. Here we report the use of ^{DMA}T-T and ^{DMA}T-A for directly assessing the local kinetic and thermodynamic parameters of T-Hg^{II}-T binding reactions. Surprisingly, T-Hg^{II}-T complexes exhibited slow association and dissociation kinetics and perturbed dynamic processes including DNA strand displacement and enzymatic synthesis. T-Hg^{II}-T complexes therefore have a high potential to disrupt DNA metabolism *in vivo*.

3.2 Thermodynamic Analysis of T-Hg^{II}-T Binding

To the best of our knowledge, isothermal titration calorimetry (ITC) was the only technique previously used to assess the thermodynamic parameters of Hg^{II} binding to T-T mismatches in duplex DNA.[20] In this approach, Hg^{II} was titrated into concentrated solutions of DNA (40 μM) and the changes in heat flow were measured. The results suggested a modest equilibrium dissociation constant (K_d) = ~2 μM for DNA sequences containing a single T-T mismatch.[20] Given the exceptionally high sensitivity of fluorescence measurements, we were able to use dilute solutions of DNA (25 nM, Figure 3.2) for equilibrium titrations (Figures 3.3 – 3.6 and Figure A7, Appendix). DNA oligonucleotides containing a single ^{DMA}T residue at variable positions "X" were synthesized using phosphoramidite chemistry, purified and characterized as previously reported.[26] ^{DMA}T fluorescence quenching upon mercury addition was used to track Hg^{II} association to duplex DNA.

Figure 3.2. Variable regions (underlined) and names of DNA sequences used in these studies: X13: 5'-CCC-TAA-CCC-TAA-XCC-TAA-CCC-3'; X14: 5'-CCC-TAA-CCC-TAA-CXC-TAA-CCC-3'; X15: 5'-CCC-TAA-CCC-TAA-CCX-TAA-CCC-3'; where X = T or T* (^{DMA}T). See Tables 6.3 – 6.4, Chapter 6 for a complete list of all reported duplexes.

Initial binding experiments were conducted in the same non-coordinating buffer previously reported for ITC-based measurements (10 mM cacodylic acid, 100 mM $NaClO_4$ (pH = 6.8)).[20] Hg^{II} was titrated into solutions of 21-mer duplex DNA containing either a ^{DMA}T-T mismatch (red circles, Figure 3.3b), or a ^{DMA}T-A base pair at position X13 (red triangles, Figure 3.3b, Figure 3.4). After equilibrating the DNA with variable Hg^{II} concentrations for 1 h at 25 °C, the fluorescence intensities of each sample were measured. By fitting the data to a monophasic equation, K_d values were determined (eq. 1 – 4, Chapter 6). To our surprise, both duplexes exhibited very high Hg^{II} affinities under these conditions, with a K_d = 43 ± 6 nM for the duplex containing the ^{DMA}T-T mismatch and a K_d = 210 ± 40 nM for the DNA containing a ^{DMA}T-A base pair with no T-T mismatch. We reasoned that this small, 5-fold difference between mismatch-specific and non-specific DNA binding affinities would complicate the study of association kinetics under these conditions. To increase the specificity of binding (blue symbols, Figure 3.3b, Figure 3.5), the stringency of the reaction was increased by using a phosphate-citrate buffer (200 mM Na_2HPO_4, 100 mM citric acid and 100 mM $NaNO_3$ (pH = 7.35)) that reversibly coordinates to mercury ions.[27] Remarkably, a very similar affinity was measured for the DNA containing a ^{DMA}T-T mismatch in both coordinating (K_d = 77 ± 4 nM) and non-coordinating buffers (K_d = 43 ± 6 nM). In contrast, DNA containing ^{DMA}T-A and no T-T mismatch exhibited a 10-fold lower affinity (K_d = 1.97 ± 0.08 μM) in the coordinating versus non-coordinating buffers. Given the large improvement in binding specificity, we selected the high-stringency buffer for subsequent experiments.

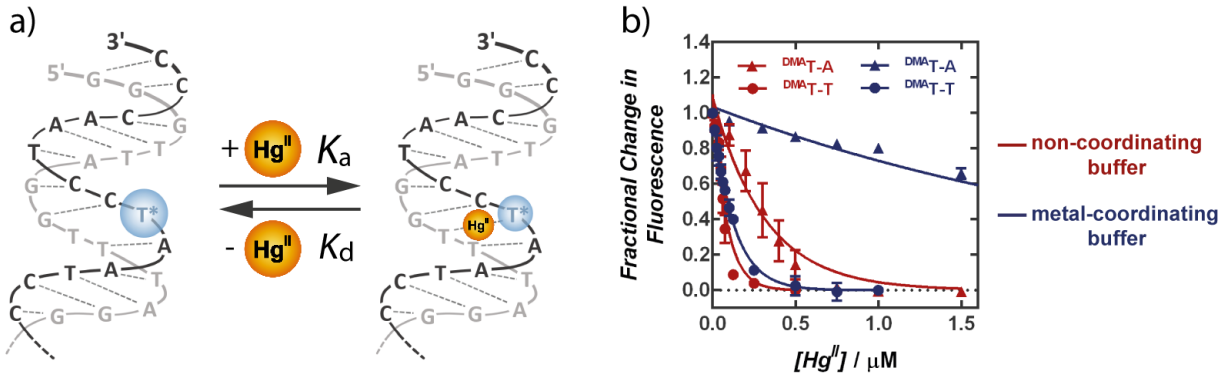

Figure 3.3. a) Schematic representation of dissociation equilibrium (K_d) of Hg^{II} to X13 ^{DMA}T-T, where T* = ^{DMA}T. b) Normalized changes in fluorescence of "X13 ^{DMA}T-A" (triangles) or "X13 ^{DMA}T-T" (circles) upon addition of Hg^{II} in a non-coordinating buffer (red) or metal-coordinating buffer (blue). See Table 6.3, Chapter 6 for complete sequence.

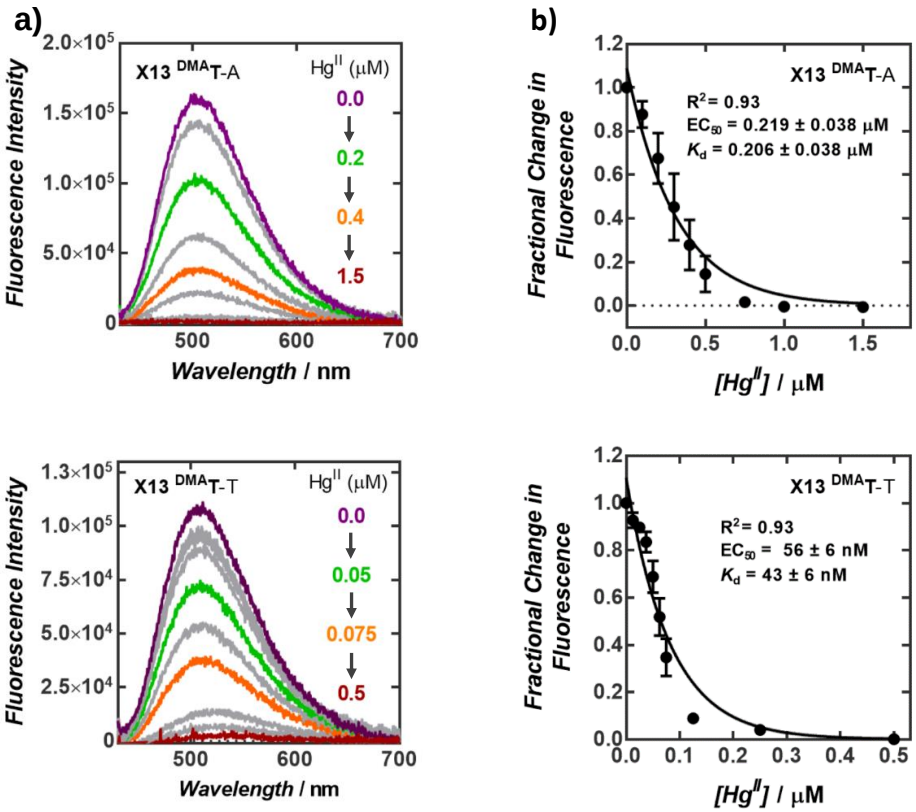

Figure 3.4. Fluorescence quenching of duplex DNA X13 containing a ^{DMA}T-A base pair (top) or a ^{DMA}T-T mismatch (bottom) upon addition of Hg^{II} in a noncoordinating buffer. a) Fluorescence spectra (λ_{ex} = 370 nm) of ^{DMA}T-containing duplex DNA in the absence (purple) and in the presence of variable concentrations of Hg^{II}. b) Plot of fluorescence intensity (λ_{em} = 500 nm) versus concentration of Hg^{II}. All samples contained 25 nM DNA in aqueous buffer (10 mM cacodylic acid and 100 mM $NaClO_4$) at pH = 6.80 and were incubated with $Hg(ClO_4)_2$ at 25 °C for 1 h prior to reading.

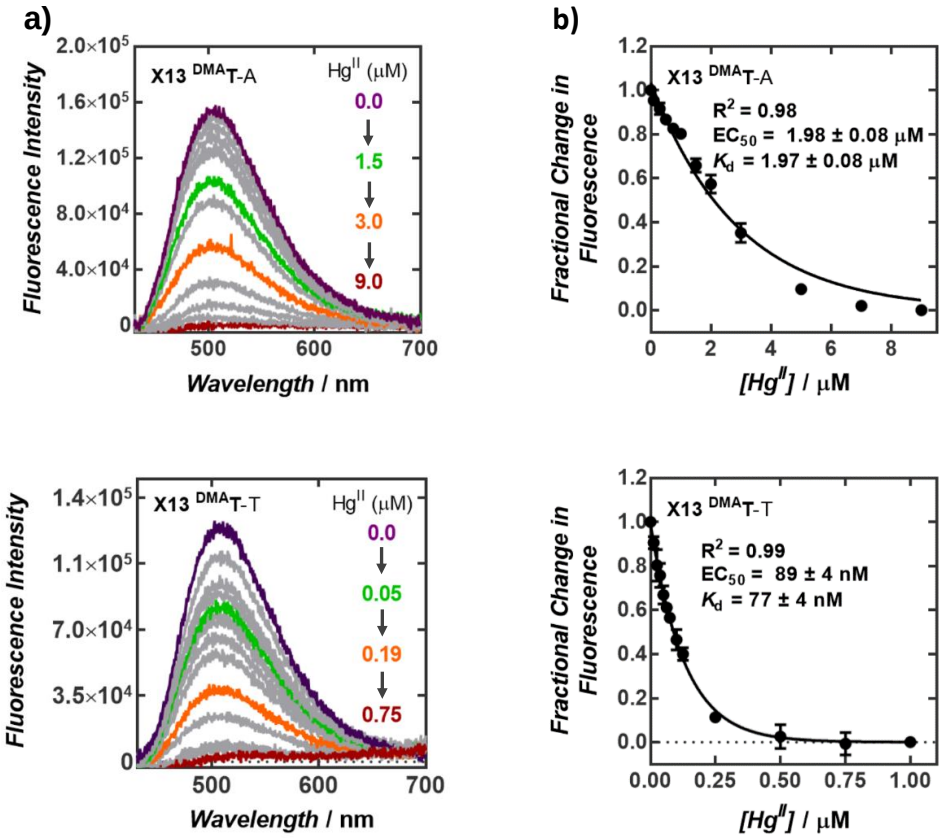

Figure 3.5. Fluorescence quenching of duplex DNA X13 containing a ^{DMA}T-A base pair (top) or a ^{DMA}T-T mismatch (bottom) upon addition of Hg^{II} in metal-coordinating buffer. a) Fluorescence spectra (λ_{ex} = 370 nm) of ^{DMA}T-containing duplex DNA in the absence (purple) and in the presence of variable concentrations of Hg^{II}. b) Plot of fluorescence intensity (λ_{em} = 500 nm) versus concentration of Hg^{II}. All samples contained 25 nM DNA in aqueous buffer (200 mM Na_2HPO_4, 100 mM citric acid and 100 mM $NaNO_3$) at pH = 7.35 and were incubated with $Hg(ClO_4)_2$ at 25 °C for 1 h prior to reading.

To evaluate the ability of a ^{DMA}T-A base pair to report the formation of a wild-type T-Hg^{II}-T complex at a neighboring or proximal site, duplexes were prepared containing a T-T mismatch at position X16 and a ^{DMA}T-A base pair at position X13, X14, or X15 (Figure 3.2). The duplex "X13 ^{DMA}T-A, X16 T-T" containing two intervening base pairs between ^{DMA}T-A and T-T exhibited the same concentration-dependent fluorescence response (apparent K_d = 1.96 ± 0.05 μM, Figure 3.6) as did duplex "X13 ^{DMA}T-A" containing no T-T mismatch (K_d = 1.97 ± 0.08 μM, Table 3.1). This indicated that in the case of "X13 ^{DMA}T-A, X16 T-T" the probe was positioned too far away (~ 10 Å) from T-T to report site-specific T-Hg^{II}-T association. This is consistent with heavy-atom fluorescence quenching effects that act over very short distances. In contrast, the duplex "X15 ^{DMA}T-A, X16 T-T" with no intervening base pair between ^{DMA}T-A and T-T exhibited the same apparent affinity (K_d = 57 ± 7 nM) as observed for duplex "X13 ^{DMA}T-T" (K_d = 77 ± 4 nM, Table 3.1). These results suggest that the ^{DMA}T-A base pair can report Hg^{II} binding of a neighboring T-T mismatch with little or no impact on the affinity of the reaction. Kinetics analyses (Table 3.2)

further support this conclusion. Interestingly, the duplex "X14 ^{DMA}T-A, X16 T-T" containing a single intervening base pair between ^{DMA}T-A and T-T exhibited a pronounced bi-phasic quenching curve (green squares, Figure 3.6). The first component saturated at a 0.7 fractional decrease in fluorescence with an affinity consistent with specific T-Hg^{II}-T binding (K_d = 34 ± 12 nM), while the second component exhibited an apparent affinity indicative of non-specific binding (apparent K_d = 2.20 ± 0.09 μM, Table 3.1, overall goodness of fit (R^2) = 0.98). These results provided the first example of an experiment where both the specific and non-specific Hg^{II} binding affinities could be derived from a single titration.

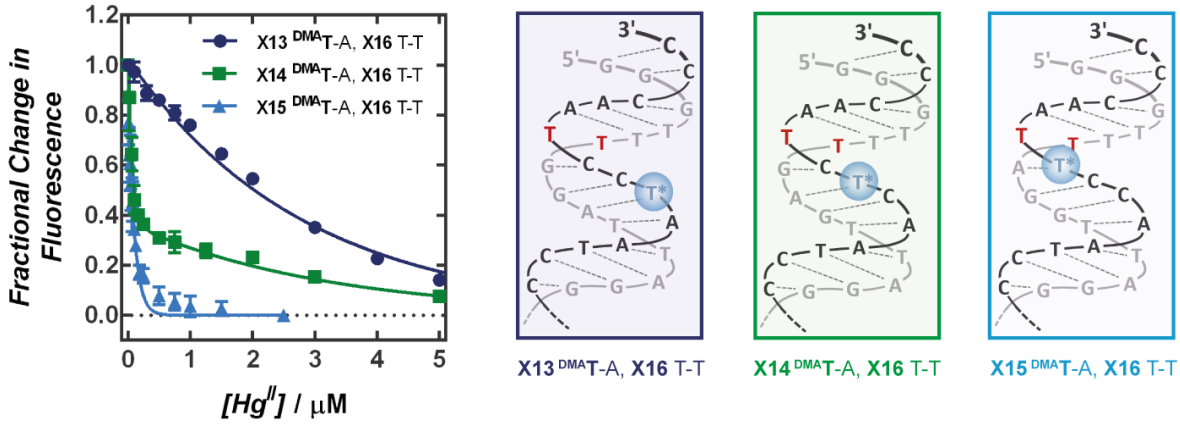

Figure 3.6. Fluorescence quenching of three different duplexes containing a T-T mismatch fixed at position X16 and a ^{DMA}T-A base pair at position X13, X14, or X15. All DNA samples (25 nM) were incubated with variable concentrations of $Hg(ClO_4)_2$ at 25 °C for 1 h prior to reading (λ_{ex} = 370 nm, λ_{em} = 500 nm). Samples were prepared in aqueous buffer (200 mM of Na_2HPO_4, 100 mM of citric acid, 100 mM $NaNO_3$ (pH = 7.35)). See Figure A7, Appendix for raw data. See Table 6.3, Chapter 6 for complete sequence.

Table 3.1 Equilibrium Binding Affinity (K_d) of Hg^{II} Binding to ^{DMA}T-Containing Duplex DNAs.[a]

Sequence	K_d (nM) non-specific	K_d (nM) T-T-specific
X13 ^{DMA}T-A	1970 ± 80	*n.o.*[b]
X13 ^{DMA}T-T	*n.o.*[b]	77 ± 4
X13 ^{DMA}T-A, X16 T-T	1960 ± 50	*n.o.*[b]
X14 ^{DMA}T-A, X16 T-T	2200 ± 90	34 ± 12
X15 ^{DMA}T-A, X16 T-T	*n.o.*[b]	57 ± 7

[a] Reported values = mean ± standard deviation from three independent measurements. Samples contained 25 nM of DNA in an aqueous buffer containing 200 mM of Na_2HPO_4, 100 mM citric acid and 100 mM $NaNO_3$ (pH = 7.35). K_d values were calculated by fitting quenching data to a monoexponential curve (eq. 1 – 4, Chapter 6), except for "X14 ^{DMA}T-A, X16 T-T" which was fit to a biphasic curve (eq. 5, Chapter 6). In all cases, R^2 values were $\geq$ 0.94. For duplex DNA sequences see Table 6.3. [b] "*n.o*" = not observed.

3.3 Kinetic Analysis of T-Hg^{II}-T Binding

To determine association and dissociation kinetics of T-Hg^{II}-T base pairs, we utilized time-dependent changes in fluorescence intensities of duplexes containing a single ^{DMA}T-T mismatch at position X13 or X15, or an unmodified T-T mismatch adjacent to a ^{DMA}T-A base pair in "X15 ^{DMA}T-A, X16 T-T" (Figure 3.7). ^{DMA}T fluorescence quenching upon formation T-Hg^{II}-T base pairs was used to track Hg^{II} association. Control experiments with duplexes containing a ^{DMA}T-A base pair but no T-T mismatch exhibited an extremely rapid and small magnitude of fluorescence quenching (<10%) upon addition of Hg^{II} (Figure 3.8, Figure A8, Appendix). This non-specific component was excluded from our data analysis. Association rates and rate constants (k_{on}) were determined using pseudo-first-order approximations (eq. 6 – 9, Chapter 6) at three mercury concentrations. Very similar k_{on} values of 0.8×10^4 $M^{-1}s^{-1}$ and 1.9×10^4 $M^{-1}s^{-1}$ were observed for ^{DMA}T-T at positions X13 and X15 (Table 3.2, Figure 3.9). The probe itself had little or no impact on k_{on}, because duplex DNA containing a ^{DMA}T-A base pair at position X15 and an unmodified T-T mismatch at position X16 gave a similar k_{on} of 9.0×10^4 $M^{-1}s^{-1}$ (Table 3.2). These rate constants are about 10^5-fold lower than those reported for outer-sphere binding of divalent ions to polynucleotides.[28] This is consistent with the fact that T-Hg^{II}-T binding requires *N3*-H deprotonation to give a stable complex. It was unclear how this multi-step process might impact our kinetics analyses, but the excellent agreement between the K_d values determined by both kinetic and thermodynamic methods indicate a negligible effect (Tables 3.1 – 3.2).

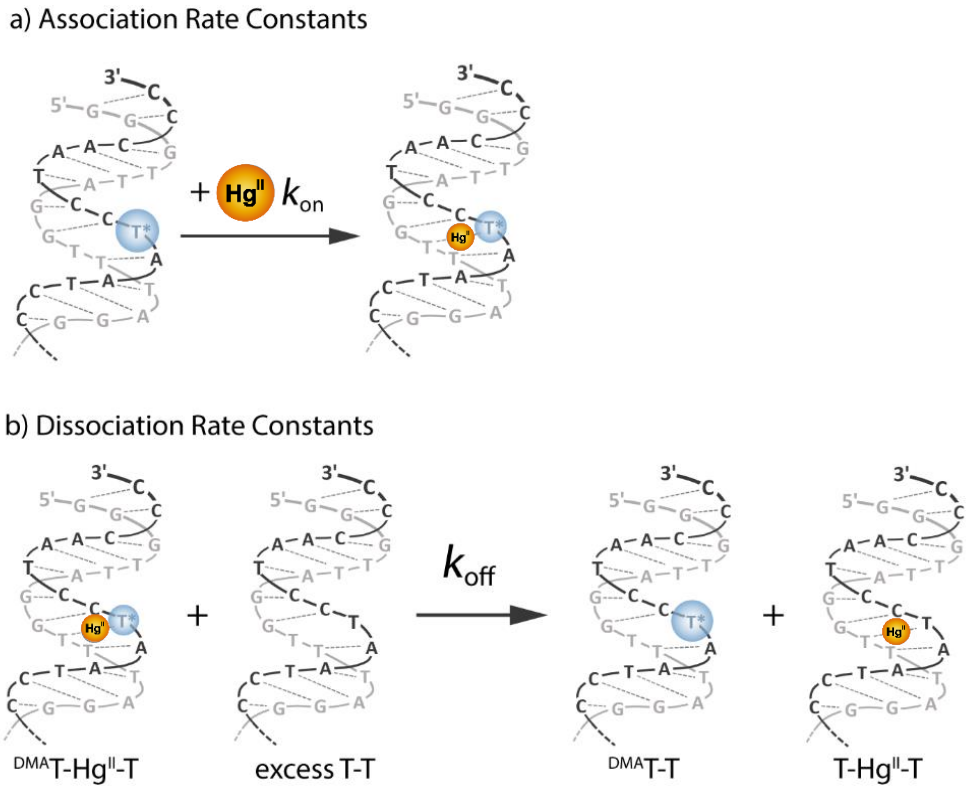

Figure 3.7. a) Schematic representation of association of Hg^{II} to ^{DMA}T-T mismatch containing duplex DNA and b) dissociation of Hg^{II} from ^{DMA}T-Hg^{II}-T upon addition of an excess of unlabeled, T-T-containing duplex DNA of the same sequence. (T* =^{DMA}T).

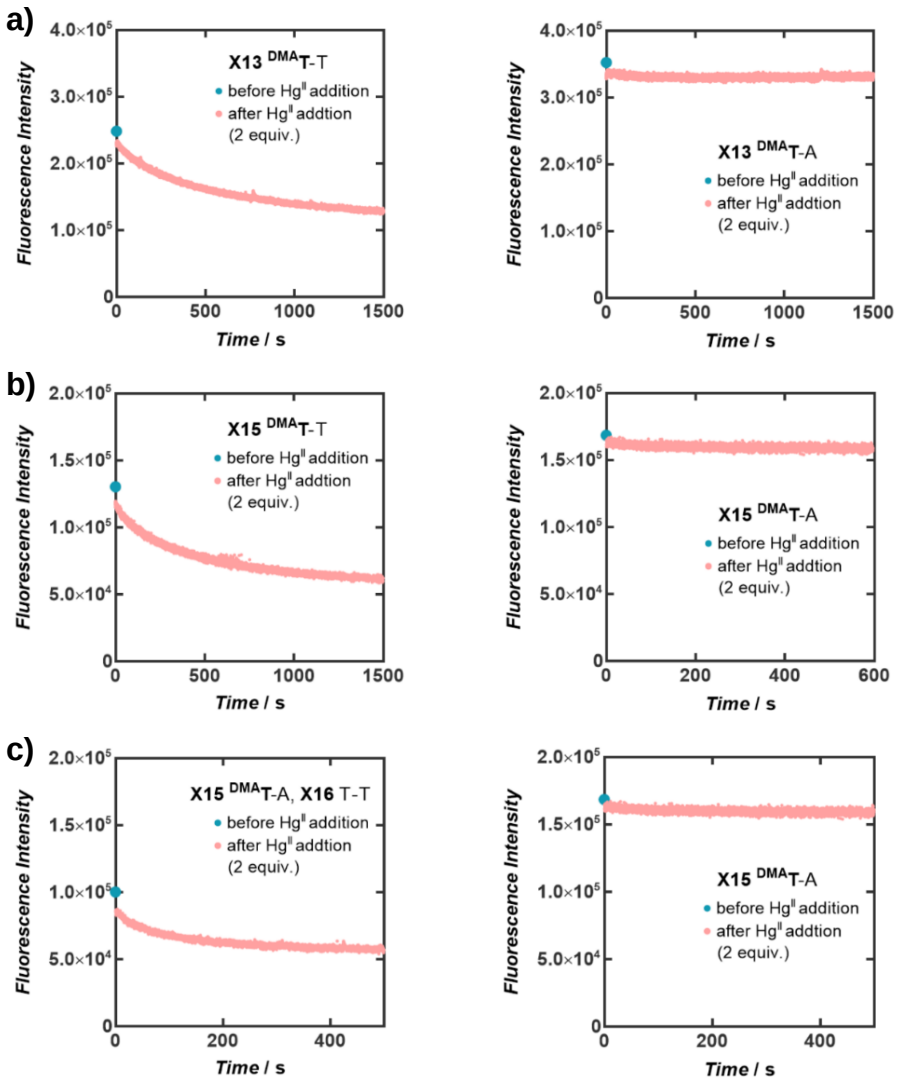

Figure 3.8. Addition of Hg^{II} (2 equiv) to duplex DNA containing a ^{DMA}T-T mismatch or a T-T mismatch (left), or to a duplex containing a ^{DMA}T-A base pair and no T-T mismatch (right). a) X13 ^{DMA}T-T, b) X15 ^{DMA}T-T, c) X15 ^{DMA}T-A, X16 T-T. Samples were excited at 370 nm and fluorescence was monitored at 500 nm. All samples contained 0.1 μM DNA in aqueous buffer (200 mM Na_2HPO_4, 100 mM citric acid and 100 mM $NaNO_3$) at pH = 7.35. For additional equiv of Hg^{II} see Figure A8, Appendix.

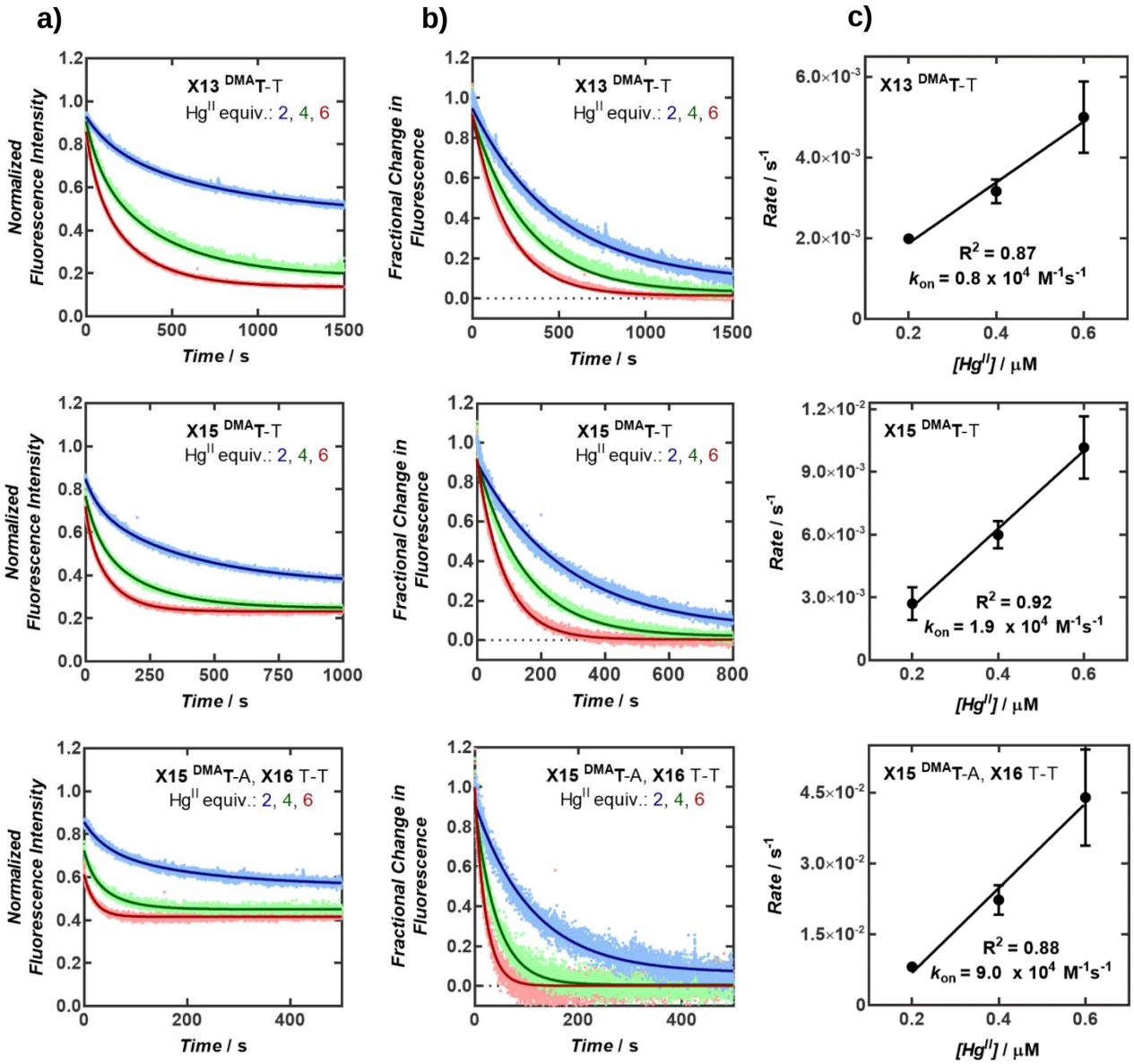

Figure 3.9. Site-selective binding of Hg^{II} to X13 ^{DMA}T-T (top), X15 ^{DMA}T-T (middle) and X15 ^{DMA}T-A, X16 T-T (bottom) according to fluorescence changes after addition of 2, 4, and 6 equiv of Hg^{II}. a) Fluorescent changes upon Hg^{II} binding normalized to fluorescence intensity prior to Hg^{II} addition, and fitted with a biphasic curve. b) Change in fluorescence as a fraction of y_0 and plateau of (a). Rate of binding was determined by fitting with a monoexponential curve (eq 9, Chapter 6). c) Pseudo-first-order rate versus Hg^{II} concentration. The slope of the linear regression provides the rate constant k_{on}. Samples were excited at 370 nm and fluorescence was monitored at 500 nm. All samples contained 0.1 μM DNA in aqueous buffer (200 mM Na_2HPO_4, 100 mM citric acid and 100 mM $NaNO_3$) at pH = 7.35.

To measure the rate constants of mercury dissociation (k_{off}) from duplexes containing ^{DMA}T-Hg^{II}-T or T-Hg^{II}-T, a large excess of an analogous, non-fluorescent duplex DNA containing a T-T mismatch was added as a passive Hg^{II} scavenger (Figure 3.7). The addition of 40 equiv. of unlabeled DNA was needed to obtain a concentration-independent, first order dissociation curve (Figure 3.10a). By fitting the data to a single-order decay process, k_{off} was calculated from the obtained half-lives ($t_{1/2}$) (eq. 11 – 12, Chapter 6). Similar k_{off} values were obtained for all three duplexes evaluated, ranging from 1.5 – 9.0 x 10^{-4} s^{-1} (Figure 3.10, Table 3.2), corresponding to $t_{1/2}$ values of 0.3 – 1.3 h.

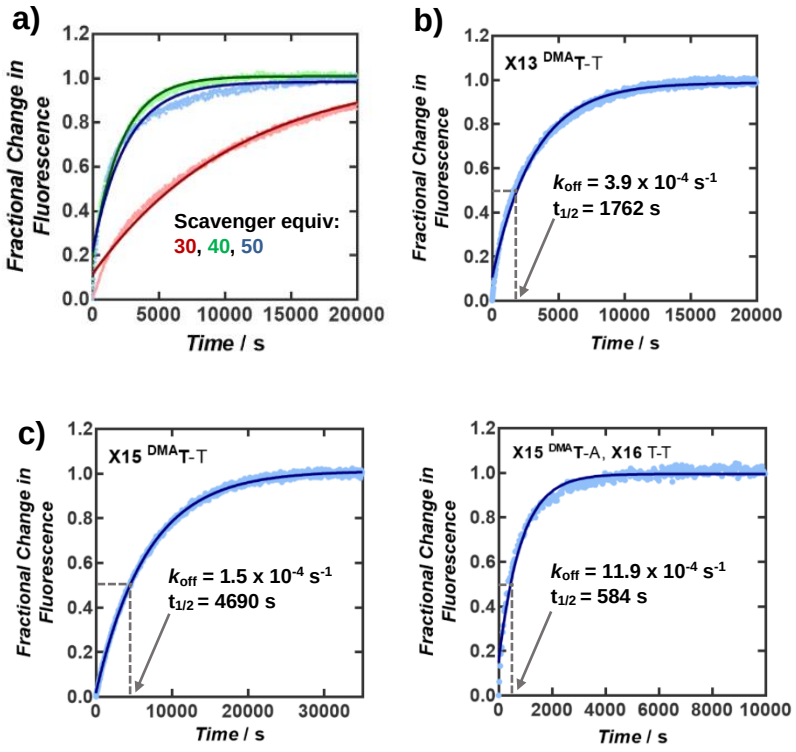

Figure 3.10. a) Dissociation of Hg^{II} from "X13 ^{DMA}T-T" upon the addition of various equiv of unlabeled, T-T-containing "scavenger" duplex DNA. b) Hg^{II} dissociation from X13 containing a ^{DMA}T-Hg^{II}-T base pair. c) Hg^{II} dissociation from X15 containing a ^{DMA}T-Hg^{II}-T base pair (left) or a T-Hg^{II}-T base pair in position 16 (right) according to fractional change in fluorescence intensity (λ_{ex} = 370 nm, λ_{em} = 500 nm). All samples contained 4 μM DNA in aqueous buffer (200 mM Na_2HPO_4, 100 mM citric acid and 100 mM $NaNO_3$) at pH = 7.35. Prior to the addition of scavenger, the fluorescent DNA duplexes were incubated with Hg^{II} (2 equiv) for 3 h.

Table 3.2 Rate Constants of Association (k_{on}), Dissociation (k_{off}), and Calculated Equilibrium Affinities (K_d) of Hg^{II} Binding to ^{DMA}T-T or T-T in Duplex DNA.[a]

Sequence	k_{on} ($M^{-1}s^{-1}$)	k_{off} (s^{-1})	K_d (nM)[c]
X13 ^{DMA}T-T	$0.8 \pm 0.2 \times 10^{4}$	$4.0 \pm 0.5 \times 10^{-4}$	50 ± 14
X15 ^{DMA}T-T[b]	$1.9 \pm 0.1 \times 10^{4}$	$1.5 \pm 0.2 \times 10^{-4}$	8.0 ± 1.1
X15 ^{DMA}T-A, X16 T-T	$9.0 \pm 2.0 \times 10^{4}$	$9.0 \pm 4.0 \times 10^{-4}$	10 ± 5.0

[a] Reported values = mean ± standard deviation from three independent measurements. Dissociation rate constants were determined by addition of 50 equiv. of unlabeled DNA containing a T-T mismatch. All samples were prepared in aqueous buffer (200 mM of Na_2HPO_4, 100 mM of citric acid and 100 mM $NaNO_3$ (pH = 7.35)). [b] Similar rates constants of association and dissociation were also observed for duplex X15 ^{DMA}T-T when measurements were conducted in a buffer containing 10 mM cacodylic acid and 100 mM $NaClO_4$ (pH = 6.8). [c] Equilibrium dissociation constants (K_d) calculated as $K_d = k_{off} / k_{on}$.

3.4 T-Hg^{II}-T Base Pairs Inhibit DNA-DNA Strand Displacement

Most biochemical processes take place on time scales ranging from microseconds to seconds. The exceptionally high kinetic stabilities of T-Hg^{II}-T base pairs could therefore pose significant barriers to DNA metabolism. To evaluate this possibility, DNA-DNA strand displacement was selected as a model system for T-loop and R-loop dynamics.[29] Duplexes with a short single-stranded overhang (green, Figure 3.11 and Table 6.4, Chapter 6) were prepared containing either ^{DMA}T-Hg^{II}-T or a ^{DMA}T-A base pair located 3 to 4 base pairs away from an unmodified T-Hg^{II}-T. Strand displacement of the ^{DMA}T-containing strand was initiated by adding a large excess of an unlabeled invading strand "I" to give a longer, thermodynamically more stable duplex as the product. Changes in ^{DMA}T fluorescence were used to track strand displacement reactions in real time (Figures 3.13 – 3.14, Figures A9 – A10, Appendix).

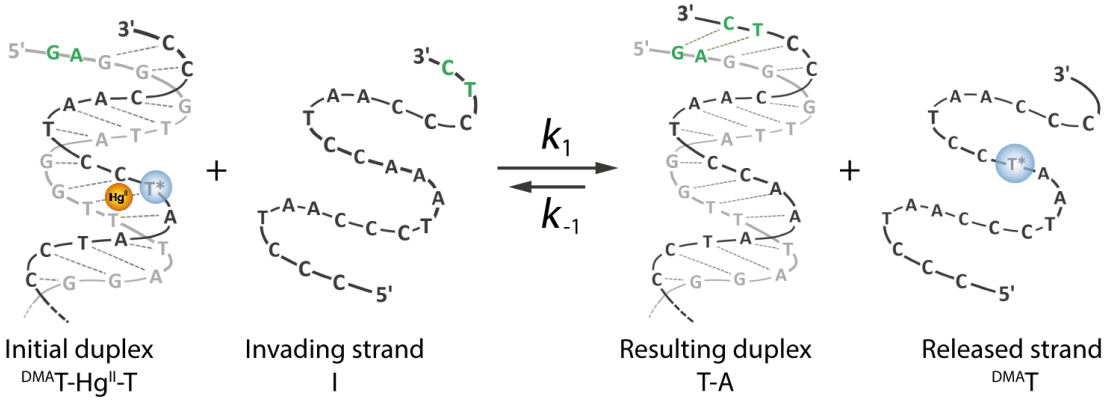

Figure 3.11. Schematic representation of a strand-displacement reaction, where T* = ^{DMA}T.

Second-order rate constants were calculated under pseudo-first order conditions (eq. 14, Chapter 6) by adding 4, 6, 8, or 10 equiv. of the invading strand. In the absence of Hg^{II}, the rate constants for all duplexes ranged from 29 – 247 $M^{-1}s^{-1}$, corresponding to experimental half-lives of 1.5 – 33 min. In contrast, 100 to 2000-fold lower rate constants (k = 0.05 – 0.47 $M^{-1}s^{-1}$) were measured for the same duplexes containing a single ^{DMA}T-Hg^{II}-T or T-Hg^{II}-T, corresponding to experimental half-lives of 10 – 77 hours. Duplexes lacking a T-T mismatch exhibited the same displacement rates in both the presence and absence of Hg^{II} (Table 3.3, Figure 3.12b, Figure A9, Appendix), indicating that non-specific Hg^{II}-DNA binding had little or no impact on strand displacement kinetics. Taken together, these results demonstrate that T-Hg^{II}-T base pairs impose a large and specific kinetic barrier to passive DNA-DNA strand-displacement reactions.

Table 3.3 Second-Order Rate Constants k ($M^{-1}s^{-1}$) of Strand Displacement in the Absence or Presence of Hg^{II}.[a]

Initial Duplex	k ($M^{-1}s^{-1}$), no Hg^{II}	k ($M^{-1}s^{-1}$), + Hg^{II}
X13 ^{DMA}T-T	97 ± 12	0.05 ± 0.01
X13 ^{DMA}T-A, X10 T-T	55 ± 15	0.47 ± 0.03
X13 ^{DMA}T-A, X16 T-T	247 ± 16	0.21 ± 0.06
X13 ^{DMA}T-A	29 ± 3.0	22 ± 3.0[b]
X14 ^{DMA}T-T	171 ± 13	0.64 ± 0.07
X14 ^{DMA}T-A, X10 T-T	90 ± 8	0.18 ± 0.02
X14 ^{DMA}T-A	45 ± 7	31 ± 0.3 [b]

[a] Rate constants (k) were calculated by fitting the fractional change in fluorescence intensity to a monoexponential curve (eq 14, Chapter 6). All samples contained 4 μM preannealed duplex DNA in aqueous buffer (200 mM Na_2HPO_4, 100 mM citric acid and 100 mM $NaNO_3$) at pH = 7.35. ^{DMA}T-Hg^{II}-T and T-Hg^{II}-T base pairs were generated by incubation with 2 equiv of $Hg(ClO_4)_2$ for 3 h. For duplex sequences see Table 6.4. [b] Estimated from a single concentration of added invading strand (I_0), see Figures 3.12 and Figure A9, Appendix.

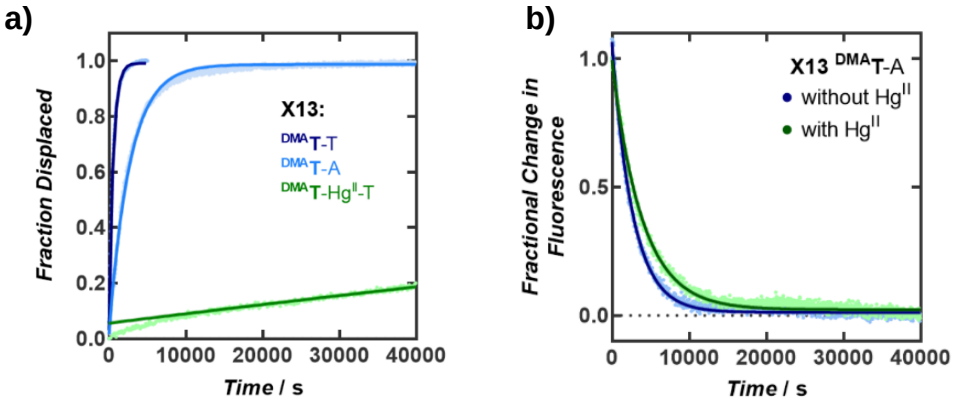

Figure 3.12. a) Strand displacement of X13 containing either a ^{DMA}T-A base pair (light blue), a ^{DMA}T-T mismatch (dark blue), or a ^{DMA}T-Hg^{II}-T base pair (green). b) Strand displacement of X13 ^{DMA}T-A with and without Hg^{II}.

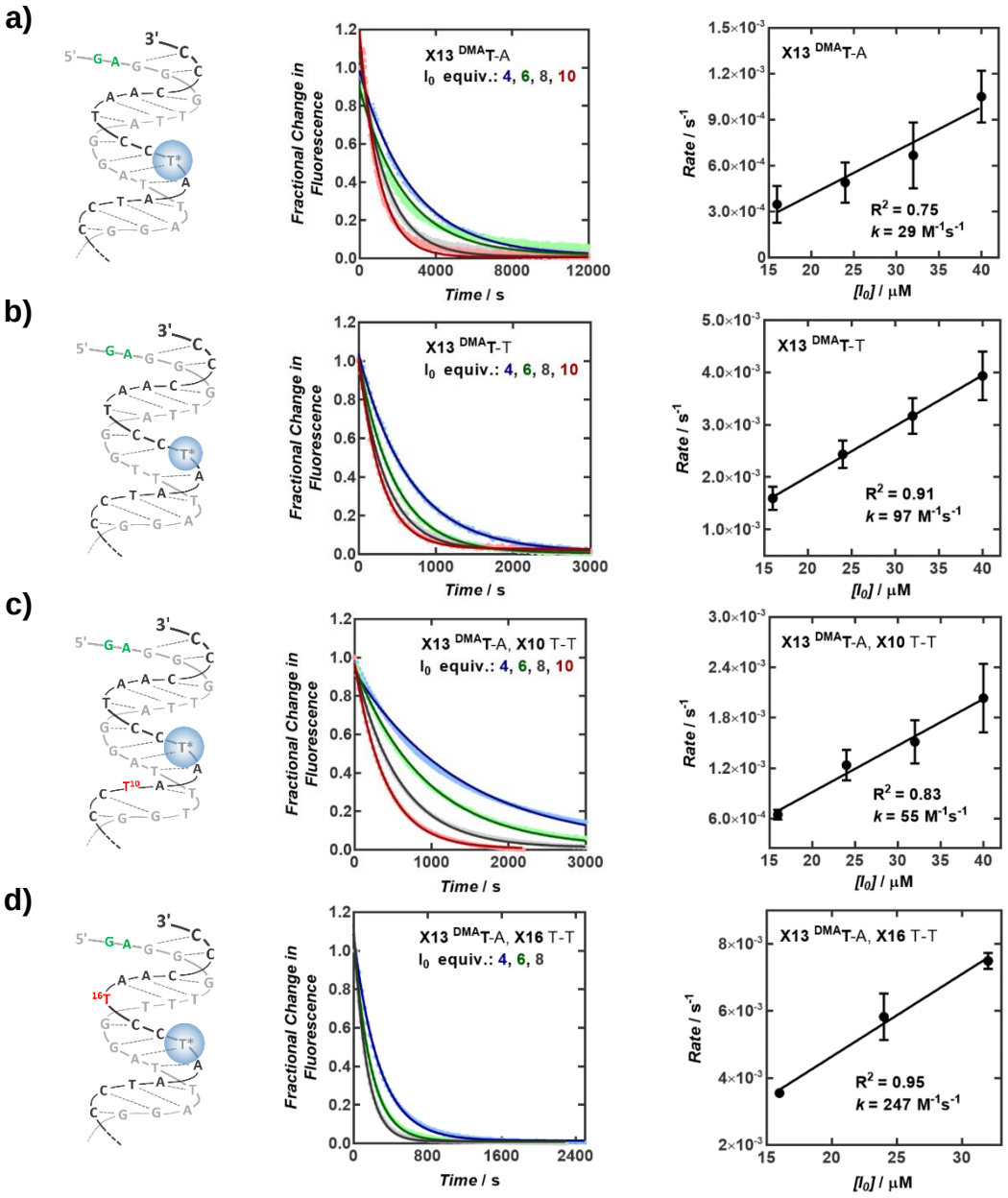

Figure 3.13. Duplex DNA structures (T* = ^{DMA}T) and rates of strand displacement versus invading strand (I_0) concentration for X13 containing a) ^{DMA}T-A base pair, b) ^{DMA}T-T mismatch, c) ^{DMA}T-A base pair and a T-T mismatch in position 10, d) ^{DMA}T-A base pair and a T-T mismatch in position 16.

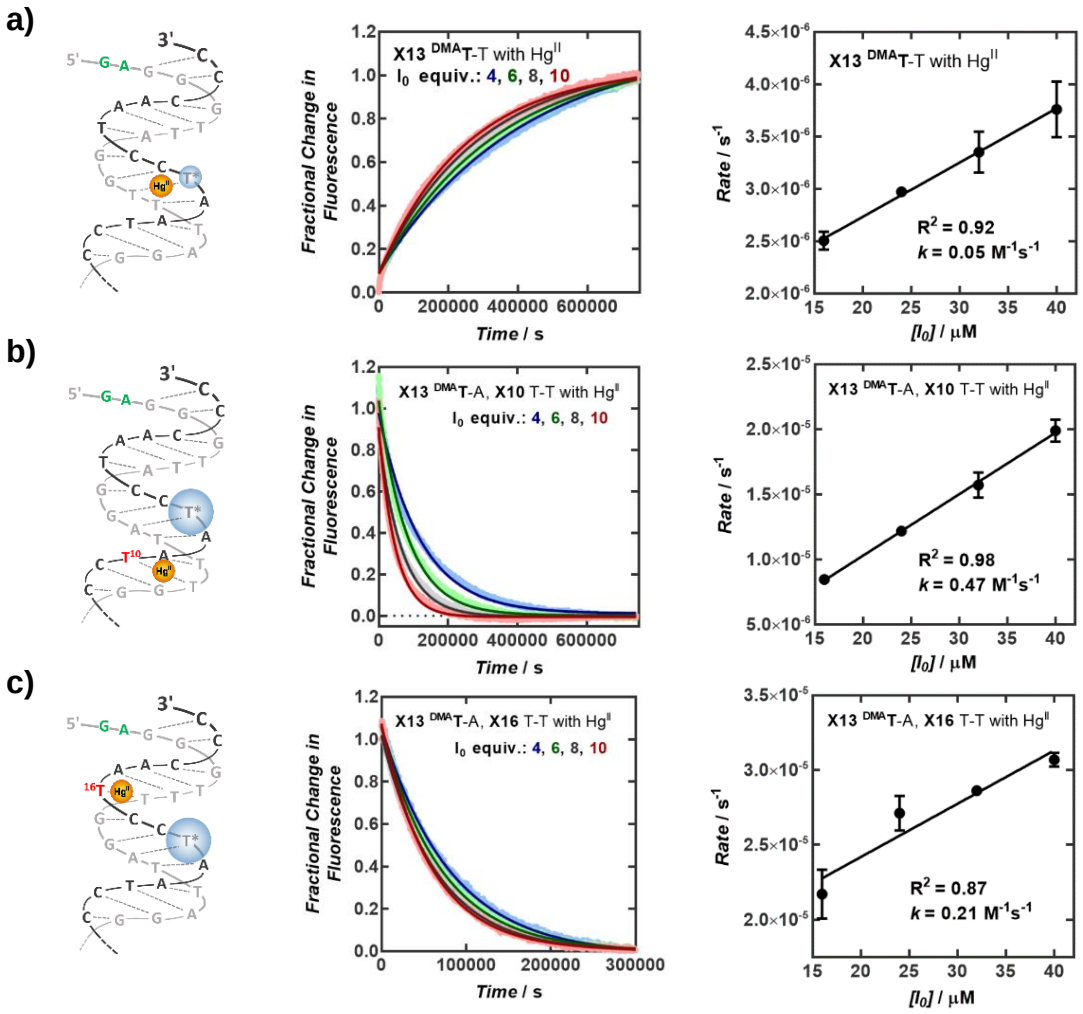

Figure 3.14. Duplex DNA structures (T* = ^{DMA}T) and rates of strand displacement versus invading strand (I_0) concentration for X13 containing a) ^{DMA}T-Hg^{II}-T base pair, b) T-Hg^{II}-T base pair in position 10, and c) T-Hg^{II}-T base pair in position 16.

3.5 T-Hg^{II}-T Base Pairs Inhibit DNA Polymerases

To evaluate the potential impact of T-Hg^{II}-T base pairs on energy-dependent strand-displacement reactions, we investigated enzymatic DNA synthesis by two different DNA polymerases differing only in their exonuclease (*exo*) activities: DNA Pol I from *E. coli* (5' to 3' *exo*+), and the derived "Klenow Fragment" (5' to 3' *exo*-). Primer extension assays were conducted using DNA duplexes containing either a T-T or T-A base pair at position #1 (ODN1) or position #7 (ODN2) downstream of a nicked site (arrow, Figure 3.15a). DNA synthesis therefore requires displacement or degradation of the non-template "displaced strand" DNA. The primer-template constructs were incubated with variable concentrations of Hg^{II} (0 – 20 μM) for three hours, followed by addition of nucleotide triphosphates and a DNA polymerase. Aliquots from each reaction were removed as a function of time, quenched with EDTA and analyzed by denaturing polyacrylamide gel electrophoresis (PAGE, Figure 3.15, Figures A11 – A14, Appendix).

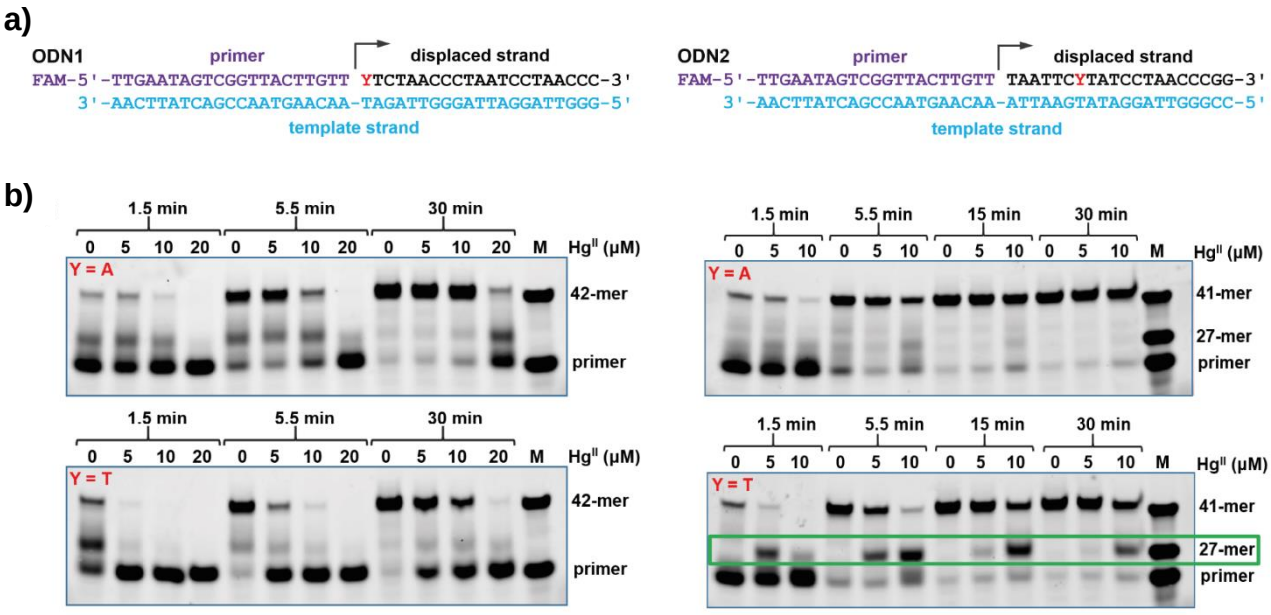

Figure 3.15. a) Duplex DNAs "ODN1" and "ODN2" containing a *Watson-Crick* base pair (Y=A), or T-T mismatch (Y=T) where "FAM" = fluorescein. b) PAGE analysis of ODN1 (left) and ODN2 (right) primer extension by the Klenow Fragment at various Hg^{II} concentrations and time points. "M" = marker for primer and full-length sequence.

Hg^{II} caused both specific and non-specific inhibition of primer extension as revealed by duplexes containing T-T versus T-A, respectively. DNA synthesis by the Klenow Fragment (*exo*-) requires DNA strand displacement of the non-template strand in a 5' to 3' direction. As such, a 2.7-fold higher rate of primer extension was observed for ODN1 containing T-T versus T-A in the absence of Hg^{II} (Table 3.4, Figure 3.16). Upon adding $5 - 10\ \mu M$ of Hg^{II}, a 7 to 13-fold decrease in k_{obs} was observed for ODN1 containing T-T, whereas little or no change was observed for the same duplex containing a T-A base pair (Klenow, Table 3.4, Figure 3.16). Given the relatively slow k_{on} rates for Hg^{II} binding to T-T (Table 3.2), the inhibition of Klenow by T-Hg^{II}-T must be the result of a slow off rate of Hg^{II} from the duplex-enzyme complex. Similar inhibitory effects of a smaller magnitude were observed for ODN2 that exhibited a pronounced stalling and termination of DNA synthesis at the T-Hg^{II}-T site (Figure 3.15b, Figure 3.17 Table 3.4).

In contrast to the Klenow Fragment, DNA synthesis by *E. coli* DNA Pol I involves the enzymatic degradation of the non-template DNA strand in a 5' to 3' direction. As such, in the absence of Hg^{II}, the same rates of primer extension were observed for ODN1 containing T-A versus T-T (Figure 3.18, Table 3.4). Interestingly, upon adding $5 - 10\ \mu M$ of Hg^{II}, a 2-fold decrease in k_{obs} was observed for ODN1 containing T-T, whereas a roughly 2-fold increase in k_{obs} was observed for ODN1 containing T-A (Pol I, Table 3.4). These results demonstrate that T-Hg^{II}-T sites impose a specific barrier to DNA synthesis that cannot be entirely overcome by exonuclease activity. Interestingly, the Hg^{II} concentrations needed for DNA polymerase inhibition *in vitro* ($IC_{50} = 6.3\ \mu M - 17.5\ \mu M$, Figure 3.16 and 3.18) were in the same concentration range as those reported to perturb DNA synthesis in living cells.[5b]

Table 3.4 Observed Rates (k_{obs}) of ODN 1 and ODN2 Primer Extension by Klenow Fragment (*exo*-) or *E. coli* DNA Pol I (*exo*+).[a]

Hg^{II} (μM)	Duplex DNA	"Y"	Klenow (*exo*-) k_{obs} (min^{-1})	k_{obs} rel (*exo*-)	Pol I (*exo*+) k_{obs} (min^{-1})	k_{obs} rel (*exo*+)
0	ODN1	A	0.18 ± 0.05	1.0	0.20 ± 0.02	1.0
		T	0.48 ± 0.12	1.0	0.21 ± 0.04	1.0
5	ODN1	A	0.23 ± 0.07	1.3	0.23 ± 0.06	1.2
		T	0.07 ± 0.01	0.15	0.16 ± 0.06	0.76
10	ODN1	A	0.14 ± 0.05	0.8	0.35 ± 0.16	1.8
		T	0.038 ± 0.002	0.08	0.11 ± 0.05	0.52
20	ODN1	A	0.044 ± 0.005	0.24	0.17 ± 0.10	0.85
		T	0.04 ± 0.02	0.08	0.05 ± 0.01	0.24
0	ODN2	A	0.28 ± 0.04	1.0	0.069 ± 0.003	1.0
		T	0.25 ± 0.03	1.0	0.087 ± 0.022	1.0
5	ODN2	A	0.29 ± 0.04	1.04	0.059 ± 0.003	0.86
		T	0.17 ± 0.03	0.68	0.048 ± 0.005	0.55
10	ODN2	A	0.18 ± 0.03	0.64	0.035 ± 0.005	0.51
		T	0.066 ± 0.009	0.26	0.027 ± 0.009	0.31
20	ODN2	A	n.d.	n.d.	0.011 ± 0.003	0.16
		T	n.d.	n.d.	0.005 ± 0.003	0.06

[a] For experimental details see Materials and Methods. The relative rates "k_{obs} rel" = k_{obs} (X μM Hg) / k_{obs} (0 μM Hg), where X = 5, 10 or 20. "n.d."= not determined.

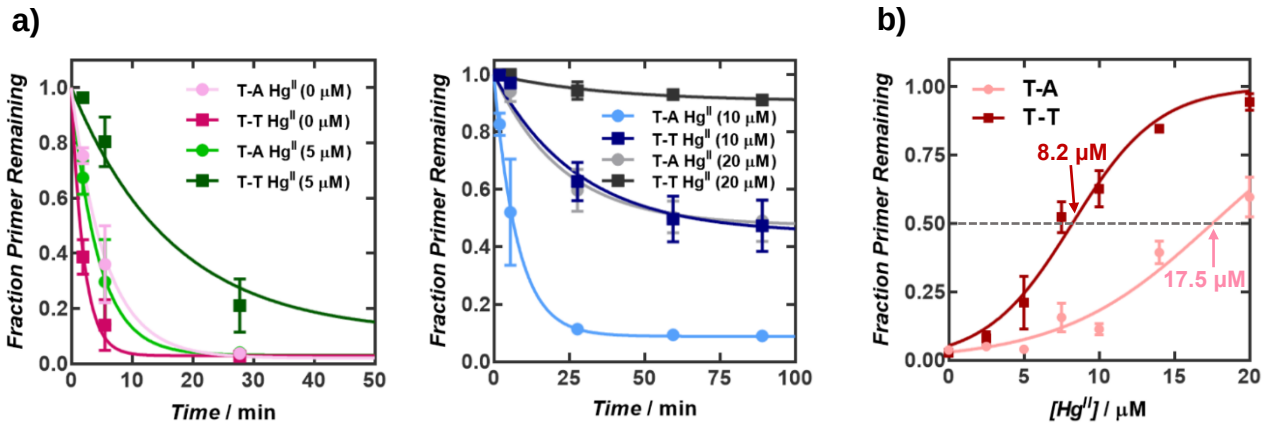

Figure 3.16. a) Observed rates of DNA synthesis of ODN1 with Klenow Fragment (*exo*-) according to fraction primer remaining at various Hg^{II} concentrations. b) IC_{50} values obtained by plot of fraction primer remaining versus Hg^{II} concentration at 30 min. For raw data see Figure 3.15 and Figure A11, Appendix.

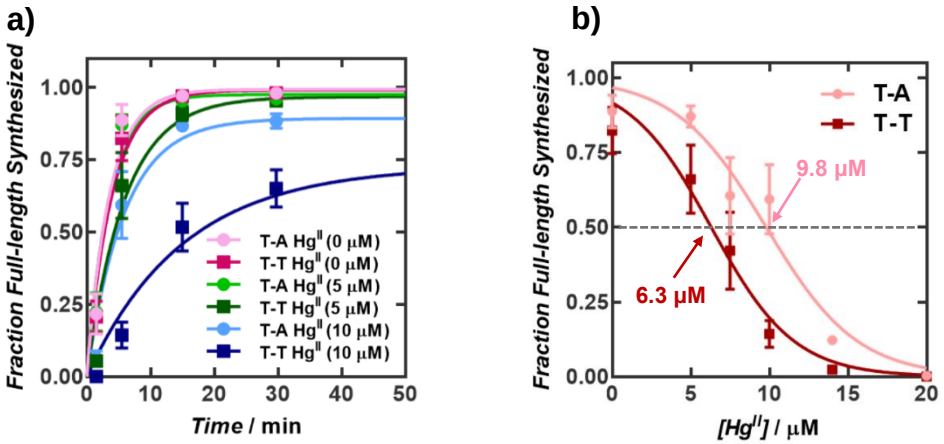

Figure 3.17. a) Observed rates of DNA synthesis ODN2 with Klenow Fragment (*exo*-) according to fraction full-length synthesized at various Hg^{II} concentrations. b) IC_{50} values obtained by plot of fraction full-length synthesized versus Hg^{II} concentration at 5 min. For raw data see Figure 3.15 and Figure A13, Appendix.

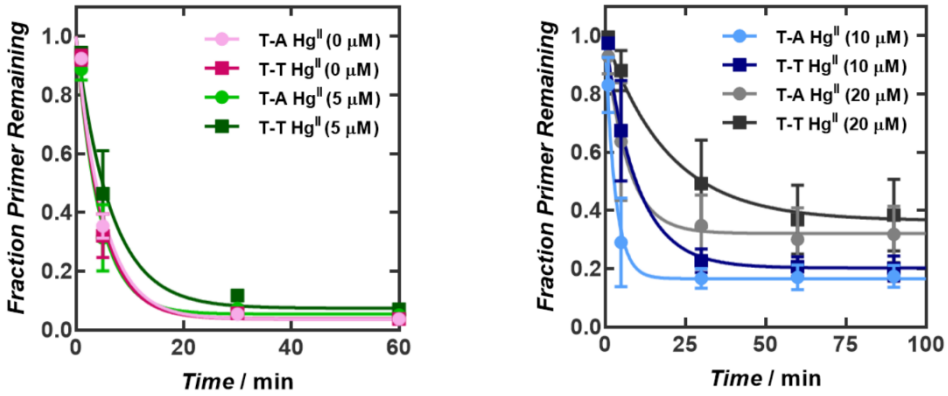

Figure 3.18. Observed rates of DNA synthesis of ODN1 with DNA Pol I (*E. coli*) according to fraction primer remaining at various Hg^{II} concentrations. For raw data see Figure A12, Appendix.

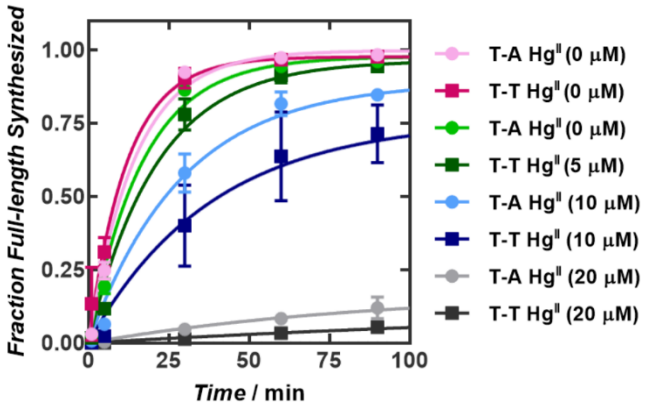

Figure 3.19. Observed rates of DNA synthesis of ODN2 with DNA Pol I (*E. coli*) according to fraction full-length synthesized at various Hg^{II} concentrations. For raw data see Figure A14, Appendix.

3.6 Discussion and Conclusions

The formation and properties of "all-natural" metallo base pairs such as T-Hg^{II}-T and C-Ag^{I}-C have broad implications in materials and biological sciences.[30] Previous studies have demonstrated that T-Hg^{II}-T base pairs exhibit similar thermal stabilities and structural features as T-A base pairs in duplex DNA.[10-12] The perception of analogous behavior of T-Hg^{II}-T and T-A was further enhanced by studies showing that T-Hg^{II}-T could serve as a substitute for T-A in primer hybridization,[13] and by the enzymatic misincorporation of dTTP across from thymidine to give T-Hg^{II}-T base pairs in the new duplex.[14] This activity could provide a pathway for the formation of T-Hg^{II}-T base pairs in genomic DNA that explains some of the point mutations known to occur in cells treated with Hg^{II}.[3]

The kinetic parameters of mercury binding reactions are expected to be highly relevant *in vivo*, where high concentrations of protein thiols and glutathione (20 – 50 mM total) would be expected to easily out-compete DNA for Hg^{II} binding.[31] Amazingly, the addition of micromolar concentrations of Hg^{II} (5 μM) to living cells resulted in the formation of high-stability DNA-Hg^{II} adducts at a frequency of 0.3% of all base pairs.[7] This is approximately the same concentration of Hg^{II} that was needed to inhibit DNA polymerase inhibition *in vitro* (Table 3.4) and to perturb DNA synthesis in living cells.[5b] Given the vast excess of intracellular thiols and irreversible binding of S-Hg^{II}-S, thermodynamic parameters alone cannot explain these observations.

Here we report the first kinetic analysis of Hg^{II} binding to T-T sites in duplex DNA. Contrary to the common perception of analogous structural and functional properties of T-Hg^{II}-T and T-A,[10-14] our results demonstrate that T-Hg^{II}-T base pairs are kinetically distinct from T-A base pairs. The slow on-rates and extremely slow off-rates of

Hg^{II} from T-T are consistent with the formation and breakage of partially covalent bonds. Agreements between our kinetic and thermodynamic analyses were remarkably good, both giving affinities in the range of K_d = 8 – 77 nM. In contrast, duplexes lacking a T-T mismatch exhibited local, "non-specific" Hg^{II} binding affinities of K_d = 0.20 – 2.0 μM, depending on the coordination strength of the buffer. The non-specific components of Hg^{II} association reactions were extremely rapid (Figure 3.8 and Figure A8, Appendix), consistent with outer-sphere binding of divalent ions that are near the diffusion limits.[28] Given these observations together, we propose a model for Hg^{II} exposure of living cells, where long-range electrostatic interactions faciliate rapid, non-specific association of Hg^{II} to the *N1* or *N7* positions of purines[9] that offer some temporary protection from cellular thiols. Cells in S-phase then incorporate Hg^{II} ions into DNA as T-Hg^{II}-T mismatches that exhibit high kinetic stabilities and therefore disrupt a wide variety of processes. Here we demonstrate that T-Hg^{II}-T base pairs are inhibitors of DNA polymerases that would normally displace or degrade the non-template DNA strand during DNA synthesis. These activities are required for DNA repair and the completion of DNA lagging strand synthesis.[32] Indeed, Hg^{II} is known to cause the inhibition of both DNA synthesis and repair in living cells.[5,6] The ability of Hg^{II} to inhibit DNA polymerases *in vitro* also reveals a potential mechanism for its reported ability to cause DNA strand breaks *in vivo*,[4,5] where molecules that generate DNA-DNA interstrand crosslinks can cause DNA strand breaks due to cellular metabolism.[33] The premature termination of DNA synthesis is one such mechanism by which this can occur (Figure 3.15b). It is possible that other dynamic processes such as transcription and DNA repair are also directly inhibited by the high kinetic stabilities of T-Hg^{II}-T base pairs.

REFERENCES

(1) Park, J.-D.; Zheng, W. *J. Prev. Med. Public Heal.* 2012, *45*, 344.

(2) Monteiro, D. A.; Rantin, F. T.; Kalinin, A. L.; *Ecotoxicology*, 2010, *19*, 105.

(3) a) Schurz, F.; Sabater-Vilar, M.; Fink-Gremmels, J.; *Mutagen.* 2000, *15*, 525; b) Codina, J. C.; Pérez-Torrente, C.; Pérez-Garcia, A.; Cazorla, F. M.; deVicente, A.; *Arch. Environ. Contam. Toxicol.* 1995, *29*, 260. c) Ariza M. E.; Williams, M. V. *J. Biochem. Mol. Toxicol.* 1999, *13*, 107.

(4) Cantoni, O.; Evans, R. M.; Costa, M. *Biochem. Biophys. Res. Commun.* 1982, *108*, 614.

(5) Williams, M. V.; Winters, T.; Waddell, K. S. *Mol. Pharmacol.* 1987, *31*, 200.

(6) Christie, N. T.; Cantoni, O.; Sugiyama, M.; Cattabeni, F.; Costa, M. *Mol. Pharmacol.* 1986, *29*, 173.

(7) Cantoni, O.; Christie, N. T.; Swann, A.; Drath, D. B.; Costa, M. *Mol. Pharmacol.* 1984, *26*, 360.

(8) a) Clever, G. H.; Kaul, C.; Carell, T. *Angew. Chem. Int. Ed.* 2007, *46*, 6226; b) Megger, D. A.; Megger, N.; Müller J. in *Metal Ions in Life Sciences, Vol. 10* (Eds.: Sigel, A.; Sigel, H.; Sigel R. K. O.), Springer, Dordrecht, 2012, 295-317; c) Takezawa, Y.; Shionoya, M. *Acc. Chem. Res.* 2012, *45*, 2066; d) Clever, G. H.; Shionoya M. in *Metal Ions in Life Sciences, Vol. 10* (Eds.: Sigel, A.; Sigel, H.; Sigel R. K. O.), Springer, Dordrecht, 2012, 269-294.

(9) a) Simpson, R. B. *J. Am. Chem. Soc.* 1964, *86*, 2059; b) Buchanan, G. W.; Stothers, J. B. *Can. J. Chem.* 1982, *60*, 787; c) Polak, M.; Plavec, J. *Eur. J. Inorg. Chem.* 1999, 547; d) Eichhorn, G. L.; Clark, P. *J. Am. Chem. Soc.* 1963, *85*, 4020.

(10) Miyake, Y.; Togashi, H.; Tashiro, M.; Yamaguchi, H.; Oda, S.; Kudo, M.; Tanaka, Y.; Kondo, Y.; Sawa, R.; Fujimoto, T.; Machinami, T.; Ono, A. *J. Am. Chem. Soc.* 2006, *128*, 2172.

(11) Tanaka, Y.; Oda, S.; Yamaguchi, H.; Kondo, Y.; Kojima, C.; Ono, A. *J. Am. Chem. Soc.* 2007, *129*, 244.

(12) Kondo, J.; Yamada, T.; Hirose, C.; Okamoto, I.; Tanaka, Y.; Ono, A. *Angew. Chem. Int. Ed.* 2014, *53*, 2385.

(13) Park, K. S.; Jung, C.; Park, H. G. *Angew. Chem. Int. Ed.* 2010, *49*, 9757.

(14) Urata, H.; Yamaguchi, E.; Funai, T.; Matsumura, Y.; Wada, S.-I. *Angew. Chem. Int. Ed.* 2010, *49*, 6516.

(15) a) Liu, J.; Lu, Y. *Angew. Chem. Int. Ed.* 2007, *46*, 7587; b) Li, D.; Wieckowska, A.; Willner, I. *Angew. Chem. Int. Ed.* 2008, *47*, 3927; c) Liu, C.-W.; Lin, Y.-W.; Huang, C.-C.; Chang, H.-T. *Biosens. Bioelectron.* 2009, *24*, 2541; d) Mor-Piperberg, G.; Tel-Vered, R.; Elbaz, J.; Willner, I. *J. Am. Chem. Soc.* 2010, *132*, 6878; e) Wang, Z.-G.; Elbaz, J.; Willner, I. *Nano Lett.* 2011, *11*, 304; f) Wen, S.; Zeng, T.; Liu, L.; Zhao, K.; Zhao, Y.; Liu, X.; Wu, H.-C. *J. Am. Chem. Soc.* 2011, *133*, 18312; g) Thomas, J. M.; Yu, H.-Z.; Sen, D. *J. Am. Chem. Soc.* 2012, *134*, 13738; h) Xiao, S. J.; Hu, P. P.; Xiao, G. F.; Wang, Y.; Liu, Y.; Huang, C. Z. *J. Phys. Chem. B*, 2012, *116*, 9565; i) Kang, I.; Wang, Y.; Reagan, C.; Fu, Y.; Wang, M. X.; Gu, L.-Q. *Sci. Rep.* 2013, *3*, 2381; j) Scharf, P.; Müller, J. *ChemPlusChem*, 2013, *78*, 20.

(16) a) Gruenwedel, D. W.; Cruikshank, M. K.; Smith, G. M. *J. Inorg. Biochem.* 1993, *52*, 251; b) Gruenwedel, D. W. *Biophys. Chem.* 1994, *52*, 115; c) Tanaka, Y.; Yamaguchi, H.; Oda, S.; Kondo, Y.; Nomura, M.; Kojima, C.; Ono, A. *Nucleosides, Nucleotides and Nucleic Acids*, 2006, *25*, 613.

(17) a) Chrisman, R. W.; Mansy, S.; Peresie, H. J.; Ranade, A.; Berg, T. A.; Tobias, R. S. *Bioinorg. Chem.* 1977, *7*, 245; b) Uchiyama, T.; Miura, T.; Takeuchi, H.; Dairaku, T.; Komuro, T.; Kawamura, T.; Kondo, Y.; Benda, L.; Sychrovský, V.; Bouř, P.; Okamoto, I.; Ono A.; and Tanaka, Y. *Nucleic Acids Res.* 2012, *40*, 5766.

(18) a) Gruenwedel, D. W. *J. Inorg. Biochem.* 1994, *56*, 201; b) Kuklenyik, Z.; Marzilli, L. G. *Inorg. Chem.* 1996, *35*, 5654.

(19) a) Tanaka, Y.; Ono, A. *Dalton Trans.* 2008, 4965; b) Dairaku, T.; Furuita, K.; Sato, H.; Šebera, J.; Yamanaka, D.; Otaki, H.; Kikkawa, S.; Kondo, Y.; Katahira, R.; Bickelhaupt, F. M.; Guerra, C. F.; Ono, A.; Sychrovský, V.; Kojima, C.; Tanaka, Y. *Chem. Commun.* 2015, *51*, 8488.

(20) a) Torigoe, H.; Ono, A.; Kozasa, T. *Chem. Eur. J.* 2010, *16*, 13218; b) Torigoe, H.; Miyakawa, Y.; Ono, A.; Kozasa, T. *Thermochim. Acta,* 2012, *532*, 28. c)

(21) a) Ono, A.; Togashi, H. *Angew. Chem. Int. Ed.* 2004, *43*, 4300; b) Liu, C.-W.; Hsieh, Y.-T.; Huang, C.-C.; Lin, Z.-H.; Chang, H.-T. *Chem. Commun.* 2008, 2242; c) Wang, J.; Liu, B. *Chem. Commun.* 2008, 4759; d) Xue, X.; Wang, F.; Liu, X. *J. Am. Chem. Soc.* 2008, *130*, 3244; e) Yang, R.; Jin, J.; Long, L.; Wang, Y.; Wang, H.; Tan, W. *Chem. Commun.* 2009, 322.

(22) For review articles see: a) Okamoto, A.; Saito, Y.; Saito, I. *J. Photochem. Photobiol. Photochem. Rev.* 2005, *6*, 108; b) Sinkeldam, R. W.; Greco, N. J.; Tor, Y. *Chem. Rev.* 2010, *110*, 2579; c) Wilhelmsson, L. M.; *Q. Rev. Biophys.* 2010, *43*, 159; d) Tanpure, A. A.; Pawar, M. G.; Srivatsan,

S. G. *Isr. J. Chem.,* 2013, *53*, 366; e) Jones, A. C.; Neely, R. K. *Q. Rev. Biophys.*, 2015, *48*, 244. f) Matarazzo, A.; Hudson, R. H. E. *Tetrahedron*, 2015, *71*, 1627.

(23) For selected examples see: a) Okamoto, A.; Tainaka, K.; Saito, I. *J. Am. Chem. Soc.* 2003, *125*, 4972; b) Sun, K. M.; McLaughlin, C. K.; Lantero, D. R.; Manderville, R. A. *J. Am. Chem. Soc.* 2007, *129*, 1894; c) Jiang, D.; Seela, F.; *J. Am. Chem. Soc.* 2010, *132*, 4016; d) Dumas, A.; Luedtke, N. W. *Nucleic Acids Res.* 2011, *39*, 6825; e) Dumas, A.; Luedtke, N. W. *ChemBioChem*, 2011, *12*, 2044; f) Riedl, J.; Pohl, R.; Rulisek, L.; Hocek, M. *J. Org. Chem.* 2012, *77*, 1026; g) Segal, M.; Fischer, B. *Org. Biomol. Chem.* 2012, *10*, 1571; h) Saito, Y.; Suzuki, A.; Okada, Y.; Yamasaka, Y.; Nemoto, N.; Saito, I. *Chem. Commun.* 2013, *49*, 5684; i) Seio, K.; Kanamori, T.; Tokugawa, M.; Ohzeki, H.; Masaki, Y.; Tsunoda, H.; Ohkubo, A.; Sekine, M. *Bioorg. Med. Chem.* 2013, *21*, 3197; j) Weinberger, M.; Berndt, F.; Mahrwald, R.; Ernsting, N. P.; Wagenknecht, H. A. *J. Org. Chem.*, 2013, *78*, 2589; k) Rodgers, B. J.; Elsharif, N. A.; Vashisht, N.; Mingus, M. M.; Mulvahill, M. A.; Stengel, G.; Kuchta, R. D.; Purse, B. W. *Chem. Eur. J.* 2014, *20*, 2010; l) Suchy, M.; Hudson, R. H. E. *J. Org. Chem.* 2014, *79*, 3336; m) McCoy, L. S.; Shin, D.; Tor, Y. *J. Am. Chem. Soc.* 2014, *136*, 15176; n) Kanamori, T.; Ohzeki, H.; Masaki, Y.; Ohkubo, A.; Takahashi, M.; Tsudo, K.; Ito, T.; Shirouzu, M.; Kuwasako, K.; Muto, Y.; Sekine, M.; Seio, K. *ChemBioChem*, 2015, *16*, 167; o) Larsen, A. F.; Dumat, B.; Wranne, M. S.; Lawson, C. P.; Preus, S.; Bood, M.; Gradén, H.; Wilhelmsson, L. M.; Grøtli, M. *Nat. Publ. Gr.* 2015, 1; p) Sholokh, M.; Sharma, R.; Shin, D.; Das, R.; Zaporozhets, O. A.; Tor, Y.; Mély, Y. *J. Am. Chem. Soc.* 2015, *137*, 3185; q) Mata, G.; Luedtke, N. W. *J. Am. Chem. Soc.* 2015, *137*, 699; r) Mizrahi, R. A.; Shin, D.; Sinkeldam, R. W.; Phelps, K. J.; Fin, A.; Tantillo, D. J.; Tor, Y.; Beal, P. A. *Angew. Chem. Int. Ed.* 2015, *54*, 8713; s) Tanpure, A. A.; Srivatsan, S. G. *Nucleic Acids Res.* 2015, *43*, e149.

(24) a) Fedoriw, A. M.; Liu, H.; Anderson, V. E.; deHaseth, P. L. *Biochemistry,* 1998, *37*, 11971; b) Arzumanov, A.; Godde, F.; Moreau, S.; Toulme, J.; Weeds, A.; Gait, M. J. *Helv. Chim. Acta,* 2000, *83*, 1424; c) Bradrick, T. D.; Marino, J. P. *RNA*, 2004, *10*, 1459; d) Gilbert, S. D.; Stoddard, C. D.; Wise, S. J.; Batey, R. T. *J. Mol. Biol.* 2006, *359*, 754; e) Kimura, T.; Kawai, K.; Fujitsuka, M.; Majima, T. *Tetrahedron*, 2007, *63*, 3585; f) Parsons, J.; Hermann, T. *Tetrahedron*, 2007, *63*, 3548; g) Lang, K.; Rieder, R.; Micura, R. *Nucleic Acids Res.* 2007, *35*, 5370; h) Barbieri, C. M.; Kaul, M.; Pilch, D. S. *Tetrahedron*, 2007, *63*, 3567; i) Xie, Y.; Dix, A. V.; Tor, Y. *J. Am. Chem. Soc.* 2009, *131*, 17605; j) Velmurugu, Y.; Chen, X.; Sevilla, P. S.; Min, J.-H.; Ansari, A. *Proc. Natl. Acad. Sci.* 2016, *113*, E2296.

(25) a) Kim, S. J.; Kool, E. T. *J. Am. Chem. Soc.* 2006, *128*, 6164; b) Dumas, A.; Luedtke, N. W. *Chem. Eur. J.* 2012, *18*, 245; c) Omumi, A.; McLaughlin, C. K.; Ben-Israel, D.; Manderville, R. A. *J. Phys. Chem. B*, 2012, *116*, 6158; d) Jana, S. K.; Guo, X.; Mei, H.; Seela, F. *Chem. Commun.* 2015, *51*, 17301.

(26) Mata, G.; Schmidt, O. P.; Luedtke, N. W. *Chem. Commun.* 2016, *52*, 4718.

(27) Martell, A. E.; Smith, R. M. *Critical Stability Constants*, *Vol. 4*, Plenum Press., New York, 1979, 394.

(28) a) Pörschke, D. *Biophys. Chem.* 1976, *4*, 383; b) Granot, J.; Feigon, J.; Kearns, D. R. *Biopolymers*, 1982, *21*, 181.

(29) a) Yurke, B.; Turberfield, A. J.; Mills, A. P.; Simmel, F. C.; Neumann, J. L. *Nature,* 2000, *406*, 605; b) Turberfield, A. J.; Mitchell, J. C.; Yurke, B.; Mills, A. P.; Blakey, M. I.; Simmel, F. C. *Phys. Rev. Lett.* 2003, *90*, 118102; c) Zhang, D. Y.; Winfree, E. *J. Am. Chem. Soc.* 2009, *131*, 17303; d) Zhang, D. Y.; Seelig, G.; *Nat. Chem.* 2011, *3*, 103; e) Genot, A. J.; Zhang, D. Y.; Bath, J.; Turberfield, A. J.; *J. Am. Chem. Soc.* 2011, *133*, 2177; f) Tang, W.; Wang, H.; Wang, D.; Zhao, Y.; Li, N.; Liu, F. *J. Am. Chem. Soc.* 2013, *135*, 13628.

(30) Tanaka, Y.; Kondo, J.; Sychrovský, V.; Šebera, J.; Dairaku, T.; Saneyoshi, H.; Urata, H.; Torigoe, H.; Ono, A. *Chem. Commun.* 2015, *51*, 17343.

(31) Prakash, M.; Shetty, M.S.; Tilak, P.; Anwar, N. *Online J Health Allied Scs.* 2009, *8*, 1.

(32) a) Dianov, G. L.; Prasad, R.; Wilson, S. H.; Bohr, V. A. *J Biol. Chem.* 1999, *274*, 13741. b) Maga, G.; Villani, G.; Tillement, V.; Stucki, M.; Locatelli, G. A.; Frouin, I.; Spadari, S.; Hübscher, U. *Proc. Natl. Acad. Sci. U.S.A.*, 2001, *98*, 14298.

(33) Frankenberg-Schwager, M.; Kirchermeier, D.; Greif, G.; Baer, K.; Becker, M.; Frankenberg, D. *Toxicology*, 2005, *212*, 175.

Chapter 4

Hg^{II} Binds to C-T Mismatches with High Affinity[3]

Binding reactions of Hg^{II} and Ag^{I} to pyrimidine-pyrimidine mismatches in duplex DNA were characterized using fluorescent nucleobase analogs, thermal denaturation and ^{1}H NMR. Unlike Ag^{I}, Hg^{II} exhibited stoichiometric, site-specific binding of C-T mismatches. The on- and off-rates of Hg^{II} binding were approximately 10-fold faster to C-T mismatches ($k_{on} \approx 10^{5}$ $M^{-1}s^{-1}$, $k_{off} \approx 10^{-3}s^{-1}$) as compared to T-T mismatches ($k_{on} \approx 10^{4}$ $M^{-1}s^{-1}$, $k_{off} \approx 10^{-4}s^{-1}$), resulting in very similar equilibrium binding affinities for both types of "all natural" metallo base pairs ($K_{d} \approx 10 - 150$ nM). These results are in contrast to thermal denaturation analyses, where much larger increases in the thermal stabilities of duplexes containing T-T mismatches were observed upon addition of Hg^{II} ($\Delta\Delta T_{m} = 6 - 19$ °C), as compared to C-T mismatches ($\Delta\Delta T_{m} = 1 - 4$ °C) . In addition to revealing the high thermodynamic and kinetic stabilities of C-Hg^{II}-T base pairs, our results demonstrate that fluorescent nucleobase analogs enable highly sensitive detection and characterization of metal-mediated base pairs – even in situations where metal binding has little or no impact on the thermal stability of the duplex.

[3] Published by Schmidt, O. P.; Benz, A. S.; Mata, G.; Luedtke, N. W., *Nucleic Acids Res.,* 2018, *46*, 6470.

4.1 Introduction

First reported in the early 1960s,[1-3] T-Hg^{II}-T base pairs provided the first examples of "all natural" metal-mediated base pairs composed of pyrimidine-pyrimidine mismatches coordinated to a transition metal ion. High-resolution structural studies revealed that Hg^{II} binds to T-T mismatches via *N3* coordination of two deprotonated thymidine residues (Figure 4.1a).[4] Structurally analogous C-Ag^{I}-C base pairs have also been well characterized.[5] In both cases, little or no impact on the global structure of the B-form duplex was observed.[4-7] A wide variety of other metallated base pairs have been observed in crystals of non-B-form nucleic acids.[8-10] For example, a G-Au^{III}-C base pair was observed in the initiation site of HIV-1 RNA,[11] and a C-Hg^{II}-T base pair was found in short, A-form duplex DNA where the metal ion was unexpectedly bound to the exocyclic amine (*N4*) of a deprotonated cytosine residue and to the *N3* of a deprotonated thymidine.[9] A solid-state "wire" containing C-Ag^{I}-C, G-Ag^{I}-G, G-Ag^{I}-C, and T-Ag^{I}-T base pairs was recently reported,[8] as well as a short, non-helical DNA structure containing one G-Ag^{I}-G and two C-Ag^{I}-C base pairs.[10] In most such cases, very little or nothing is known about the kinetic and thermodynamic parameters of metallo base pair formation in solution.

All-natural, metal-mediated base pairs are potentially important in both biological and materials sciences.[12-25] A detailed understanding of kinetic and thermodynamic properties is essential for gauging their potential applications in devices as well as their ability to interfere with biological processes.[26-29] The energetics of metallo base pair formation has been characterized using a wide variety of techniques.[30-44] High affinity, stoichiometric binding of Hg^{II} and Ag^{I} to DNA duplexes containing T-T or C-C mismatches, respectively, was initially revealed using thermal denaturation studies, isothermal titration calorimetry and ^{1}H NMR spectroscopy.[36-42] Remarkably, duplexes containing T-Hg^{II}-T base pairs or C-Ag^{I}-C base pairs exhibited similar thermal stabilities as duplexes containing canonical T-A or G-C base pairs.[38,39] In contrast, little or no change was observed in the thermal melting temperatures of duplexes containing C-T mismatches upon addition of Hg^{II}.[44] This result could be interpreted as the absence of a strong binding interaction, however, in some cases, high-affinity metal binding can decrease the thermal stability of duplex DNA.[45,46]

Fluorescent nucleobase analogs provide highly sensitive probes for the real-time study of molecular binding interactions.[47-57] In contrast to NMR, isothermal calorimetry, and absorbance-based thermal denaturation analyses, very dilute (nM) solutions of fluorescent nucleic acids can be used to directly characterize the thermodynamic and kinetic parameters of DNA-metal binding reactions.[29,58-60] In practice, this enables the measurement of equilibrium binding constants (K_d) in the low nM range, something that is not feasible by analyzing binding data collected using DNA solutions in the μM to mM concentration range. This limitation is especially relevant to the characterization of metal-DNA binding interactions, where non-specific Hg^{II} binding by canonical, duplex DNA occurs with

relatively high affinity (K_d = 0.2 – 2.0 μM in non-coordinating and metal-coordinating buffers, respectively).[29] We recently reported a novel fluorescence-based assay to investigate site-selective T-Hg^{II}-T base pair formation using the fluorescent nucleobase analog ^{DMA}T (Figure 4.1b).[43] By monitoring the real-time changes in ^{DMA}T-fluorescence upon addition of Hg^{II} or a Hg^{II} scavenger, the Hg^{II} binding affinity (K_d), and association/dissociation rate constants (k_{on} and k_{off}) of T-T mismatches were determined under various conditions.[29] Even in the presence of metal-coordinating buffers containing phosphate and citrate, T-Hg^{II}-T base pairs exhibited high thermodynamic stabilities (K_d = 8 – 50 nM) and high kinetic stabilities (half-lives = 0.3 – 1.3 h) that interfered with dynamic processes such as DNA-DNA strand displacement and enzymatic primer extension reactions. The use of non-coordinating buffers such as sodium cacodylate had little impact on the thermodynamic or kinetic stabilities of T-Hg^{II}-T base pairs, but caused a 10-fold increase in the non-specific binding affinity of Hg^{II} to duplexes lacking a base pair mismatch.[29]

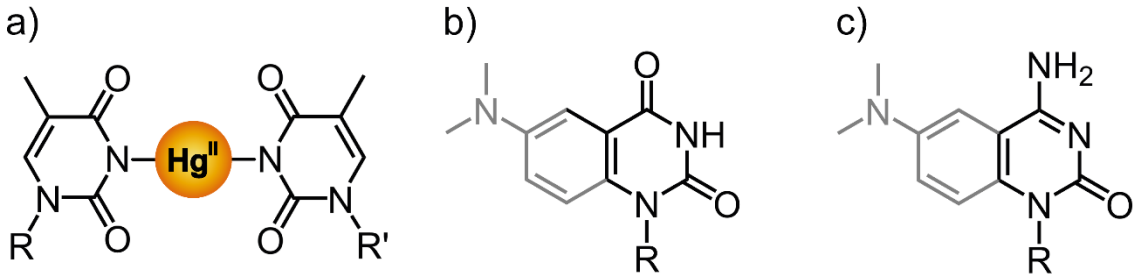

Figure 4.1. a) T-Hg^{II}-T base pair.[4] b) Fluorescent thymidine analog ^{DMA}T.[43] c) Fluorescent cytosine analog ^{DMA}C.[61]

Here we report the use of DNA duplexes containing a fluorescent thymidine mimic ^{DMA}T (Figure 4.1b),[43] or an analogous cytosine mimic ^{DMA}C[61] (Figure 4.1c) to evaluate site-selective metal binding of Hg^{II} or Ag^{I} to C-T mismatches. Together with ^{1}H NMR experiments, our results demonstrate that Hg^{II}, but not Ag^{I}, exhibits high-affinity, stoichiometric binding of C-T mismatches in duplex DNA. C-Hg^{II}-T base pairs exhibited thermodynamic stabilities (K_d = 10 – 153 nM) that were very similar to those of widely-studied T-Hg^{II}-T base pairs.[29] These affinities are approximately 10 – 200 times higher than non-specific binding of Hg^{II} to duplexes lacking a mismatch ($K_d \approx 2$ μM) in a metal-coordinating buffer containing citrate and phosphate. Remarkably, temperature-dependent K_d measurements revealed that C-T mismatches exhibited a three-fold *higher* Hg^{II} affinity at 4 °C versus 25 °C, whereas T-T mismatches exhibited a two-fold *lower* Hg^{II} affinity at 4 °C versus 25 °C. Taken together, these results suggest that the less favorable entropy changes of C-Hg^{II}-T versus T-Hg^{II}-T formation are responsible for the negligible

impact that Hg^{II} had on the thermal stabilities of DNA duplexes containing C-T mismatches (ΔT_m = 1 – 4 °C) as compared to T-T mismatches (ΔT_m = 6 – 19 °C). In addition to revealing the high thermodynamic and kinetic stabilities of C-Hg^{II}-T base pairs, our results have revealed that the on- and off-rates of Hg^{II} binding were approximately 10-fold faster to C-T mismatches ($k_{on} \approx 10^5$ $M^{-1}s^{-1}$, $k_{off} \approx 10^{-3}s^{-1}$) as compared to T-T mismatches ($k_{on} \approx 10^4$ $M^{-1}s^{-1}$, $k_{off} = 10^{-4}s^{-1}$). Taken together with the differences in their formation entropies, these results suggest that C-Hg^{II}-T and T-Hg^{II}-T base pairs exhibit different metal binding modes.

4.2 Metal Ion Screening

Fluorescent nucleobase analogs provide highly sensitive and rapid means to screen for new metal-nucleobase binding reactions.[57-60] To evaluate the abilities of metals to selectively bind to C-T mismatches in duplex DNA, 2.0 equiv of various metal ions (Hg^{II}, Ag^{I}, Cd^{II}, Mg^{II}, Fe^{II}, Ni^{II}, Pd^{II}, Zn^{II}, or Ca^{II}) were incubated with pre-formed duplexes "X14" containing either a ^{DMA}T-C or ^{DMA}C-T mismatch. Among the metal ions evaluated, only Hg^{II} and Ag^{I} caused significant changes in fluorescence intensities (Figure 4.2). Consistent with the formation of ^{DMA}T-Hg^{II}-C and ^{DMA}C-Hg^{II}-T base pairs, the addition of Hg^{II} caused fluorescence quenching of both duplexes. In contrast, Ag^{I} ions caused fluorescence quenching of the duplex containing ^{DMA}T-C, yet enhanced fluorescence of the ^{DMA}C-T duplex. This unexpected enhancement is not consistent with direct ^{DMA}C-Ag^{I} binding, as the titration of Ag^{I} to solutions of free ^{DMA}C nucleoside caused fluorescence quenching (Figure 4.3). The addition of Hg^{II} to duplexes X13 or X15 containing a ^{DMA}T-G mismatch or a ^{DMA}T-A base pair resulted in minimal changes in fluorescence intensity (Figure A15, Appendix).

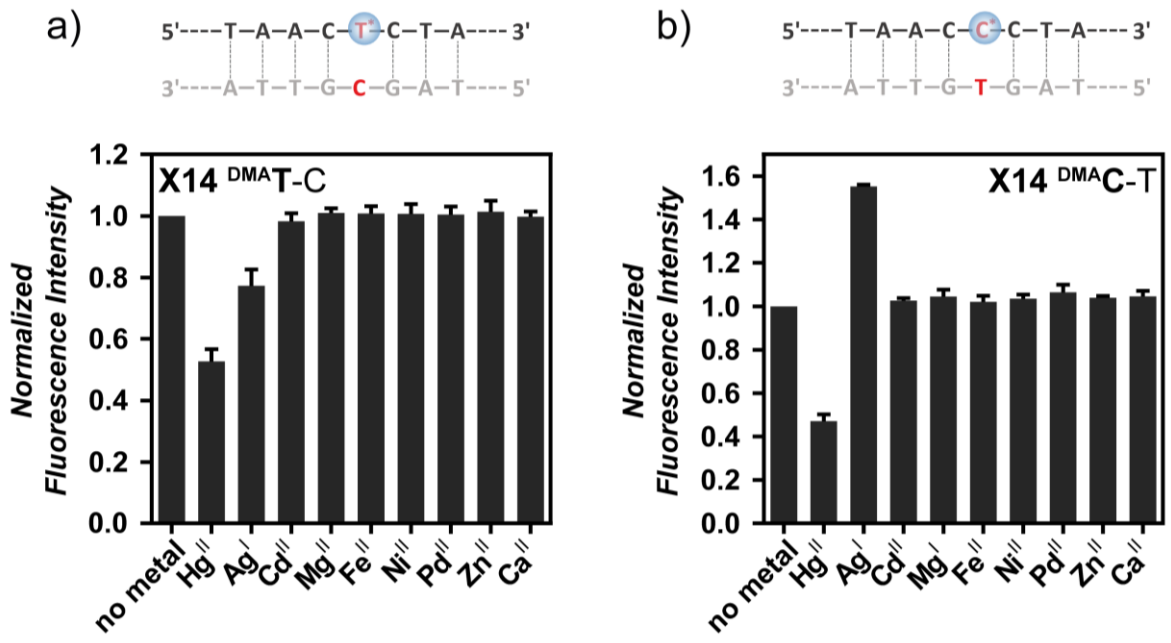

Figure 4.2. a) Fluorescence changes of duplex X14 containing a ^{DMA}T-C mismatch, or, b) ^{DMA}C-T mismatch upon addition of various metal ions (2.0 equiv). The addition of Hg^{II} to duplexes X13 or X15 containing a ^{DMA}T-G mismatch or a ^{DMA}T-A base pair resulted in minimal changes in fluorescence intensity (Figure A15, Appendix). All samples contained 4 μM of DNA in aqueous buffer (200 mM of Na_2HPO_4, 100 mM of citric acid and 100 mM $NaNO_3$ (pH = 7.35)) and were incubated with metal ions for 3 h prior to measuring. For complete sequence see Table 6.5, Chapter 6.

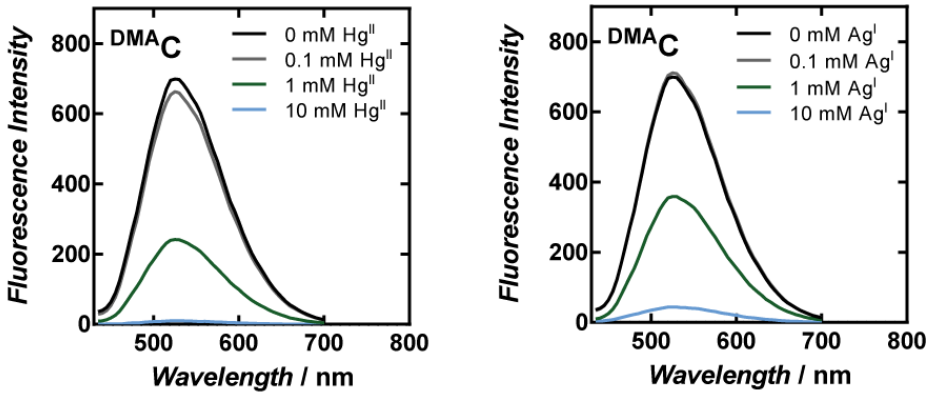

Figure 4.3. Fluorescence quenching of ^{DMA}C-nucleoside upon addition of Hg^{II} and Ag^{I}. All samples contained 40 μM of ^{DMA}C in aqueous buffer (200 mM of Na_2HPO_4, 100 mM of citric acid and 100 mM $NaNO_3$ (pH = 7.35)) and were incubated with metal ions for 40 min prior to measuring.

4.3 ^{1}H NMR Titrations

To further evaluate C-Hg^{II}-T and C-Ag^{I}-T formation, we monitored imino-proton resonances[38,66] of a 14-mer, palindromic DNA[67] containing two C-T-mismatches (ODN[15] "C-T") upon addition of Hg^{II} or Ag^{I} at 4 °C (Figure 4.4). Temperature and DNA concentration-dependent CD measurements confirmed that this sequence forms a stable, intermolecular duplex at temperatures ≤ 20 °C (Figure 4.5). In the absence of Hg^{II}, an imino-proton signal was observed at 10.9 ppm, corresponding to the mismatched thymidine *NH*.[38,66,67] The addition of two equivalents of Hg^{II} (1:1 with respect to the number of mismatches present) caused stoichiometric disappearance of this unpaired thymidine *NH*-resonance. Some shifting of the other imino protons was also observed, but the total number remained six upon saturation with Hg^{II} (Figure 4.4a). Taken together, these results indicate site-specific binding of Hg^{II} to the mismatched T. In contrast, the addition of $AgNO_3$ did not result in the disappearance of the unpaired thymidine *NH*-resonance, instead giving a complex mixture of new imino signals (Figure 4.4b). Taken together with the results of our fluorescence-based screening, these NMR data are consistent with the formation of site-specific, 1:1 complexes between Hg^{II} and C-T mismatches, but not between Ag^{I} and C-T mismatches.

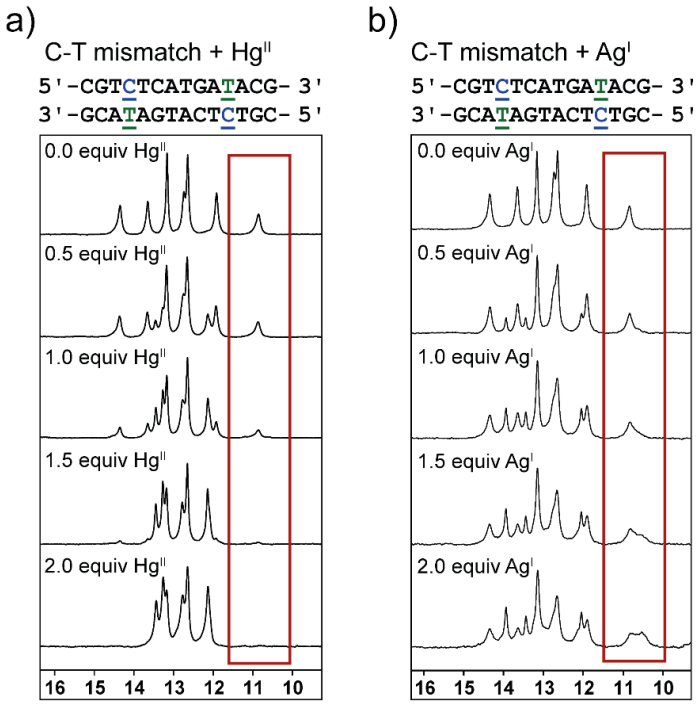

Figure 4.4. a) Site-specific binding of Hg^{II} to C-T mismatches in 14-mer duplex DNA (ODN[15] "C-T") according to disappearance of imino-resonance of the mismatched thymidine upon addition of Hg^{II}. b) Heterogenous binding of Ag^{I} to the same DNA upon addition of Ag^{I}. The number of metal ion equivalents are with respect to the number of mismatches present in the DNA. Samples were measured at 4 °C and contained 0.5 mM of pre-folded duplex DNA in aqueous buffer (200 mM $NaClO_4$, 50 mM cacodylic acid at pH = 7.0).

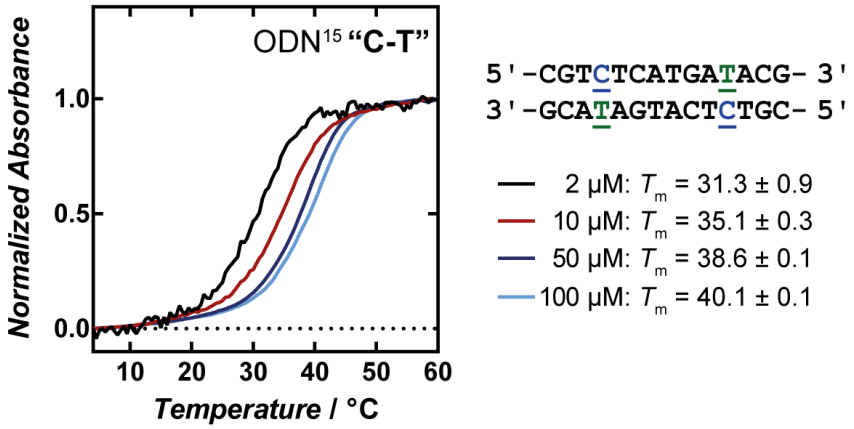

Figure 4.5. Melting temperature curves and T_m values of ODN[15] "C-T" at variable DNA concentrations. Duplex DNA were prepared in aqueous buffer (200 mM $NaClO_4$, 50 mM cacodylic acid at pH = 7.0). Reported values = mean ± standard deviation from three independent measurements.

4.4 Thermal Denaturation Studies

Thermal denaturation studies are widely used to investigate formation of metal-mediated base pairs in duplex DNA.[36] Thermal melting temperatures (T_m) were determined using palindromic 14-mer duplex DNAs containing two C-T, T-T, or G-T mismatches or two canonical A-T base pairs upon addition of Hg^{II} or Ag^{I} (Figure 4.6 and 4.7, Table 4.1). As expected from previous studies,[38] the addition of Hg^{II} to ODN[16] duplex "T-T" induced a large increase in melting temperature (ΔT_m = +19.4 °C), yet only a small increase in T_m was observed for ODN[15] duplex "C-T" (ΔT_m = +4.2 °C, Figure 4.6, Table 4.1). Hg^{II} caused small *decreases* in T_m values of a similar magnitude (ΔT_m = -3.9 and -5.7 °C) for ODN[18] "A-T" and ODN[17] "G-T", respectively. Melting experiments conducted using 21-mer duplexes X13, X14, and X15 containing a single C-T or T-T mismatch revealed little if any changes in melting temperatures upon addition of Hg^{II} to duplexes containing C-T mismatches (ΔT_m = -0.1 to +0.7 °C), and much larger changes (ΔT_m = +2.9 to +6.0 °C) upon addition of Hg^{II} to the duplexes containing T-T mismatches (Table 6.5, Chapter 6, Table A3, Figure A16, Appendix). According to CD spectroscopy, the addition of Hg^{II} caused little or no change in the global structures of B-form duplexes ODN[15], X13, X14, and X15 containing C-T mismatches (Figure 4.8, Figure A17, Appendix). Taken together with previous studies,[36,43] these results demonstrate that the formation of C-Hg^{II}-T base pairs have little or no impact on the thermal stability of B-form duplex DNA containing C-T mismatches. The apparent lack of C-T thermal stabilization is in stark contrast to the high affinity, stoichiometric binding of Hg^{II} to C-T according to our fluorescence screening and ^{1}H NMR experiments. To the best of our knowledge, there are no previous reports of the thermodynamic or kinetic parameters of Hg^{II} binding to C-T mismatches in DNA or RNA.

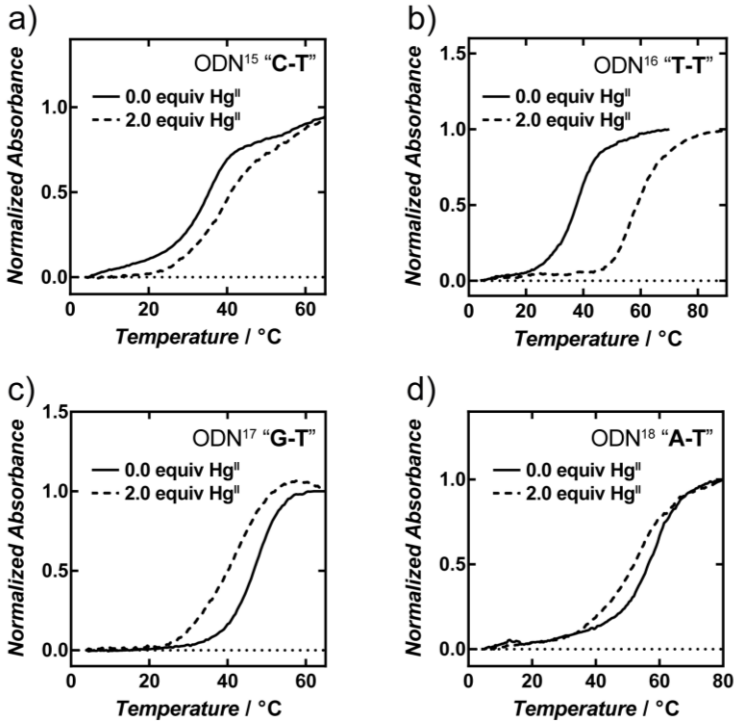

Figure 4.6. Thermal denaturation curves for a) ODN^{15} "C-T" b) ODN^{16} "T-T", c) ODN^{17} "G-T", d) ODN^{18} "A-T" in the presence and absence of 2.0 equiv of Hg^{II} (equiv of Hg^{II} according to mismatch). DNA samples contained 10 μM of pre-folded duplex DNA in aqueous buffer (200 mM $NaClO_4$, 50 mM cacodylic acid at pH = 7.0).

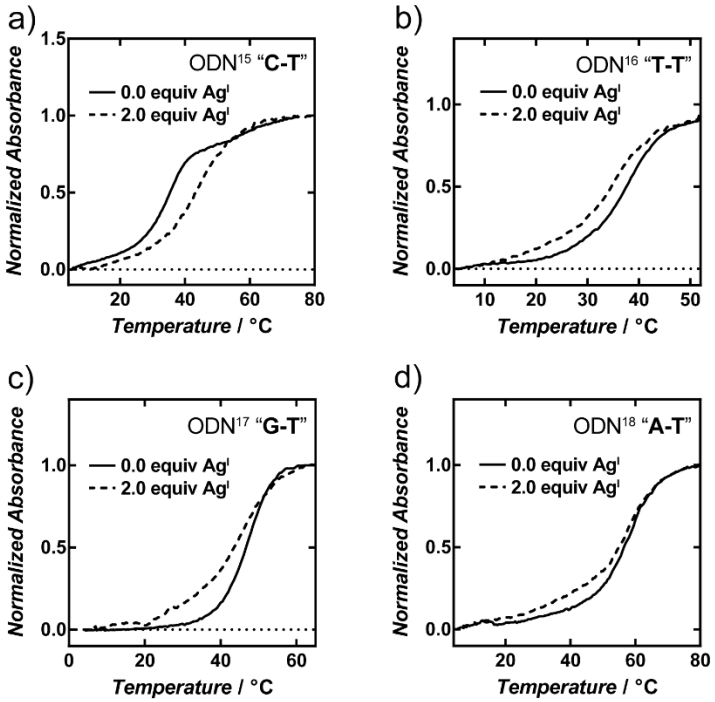

Figure 4.7. Thermal denaturation curves for a) ODN^{15} "C-T" b) ODN^{16} "T-T", c) ODN^{17} "G-T", d) ODN^{18} "A-T" in the presence and absence of 2.0 equiv of Ag^{I} (equiv of Ag^{I} according to mismatch). DNA samples contained 10 μM of pre-folded duplex DNA in aqueous buffer (200 mM $NaClO_4$, 50 mM cacodylic acid at pH = 7.0).

Table 4.1: Melting Temperatures (T_m) of Duplex DNA Containing C-T, G-T, or T-T Mismatches or A-T Base Pairs in the Presence and Absence of 2 Equiv of Hg^{II} and Ag^{I}.[a]

Sequence	T_m (°C) no metal ions	T_m (°C), (ΔT_m) with Hg^{II}	T_m (°C), (ΔT_m) with Ag^{I}
ODN[15] "C-T"	35.1 ± 0.3	39.3 ± 0.2 (+4.2)	44.0 ± 0.2 (+8.9)
ODN[16] "T-T"	37.9 ± 0.1	57.3 ± 0.1 (+19.4)	36.2 ± 0.5 (-1.7)
ODN[17] "G-T"	47.3 ± 0.4	41.6 ± 0.8 (-5.7)	45.5 ± 0.4 (-1.8)
ODN[18] "A-T"	57.1 ± 0.1	53.2 ± 0.8 (-3.9)	57.2 ± 0.7 (+0.1)

[a] Reported values = mean ± standard deviation from three independent measurements. ΔT_m reflects the difference in T_m upon addition of 2 equiv metal ions per mismatch present. All samples contained 10 μM of duplex DNA in aqueous buffer (200 mM $NaClO_4$, 50 mM cacodylic acid at pH = 7.0). For duplex sequences see Figure 4.4 and Table 6.6, Chapter 6, Experimental Procedures. For raw melting data see Figures 4.6 – 4.7.

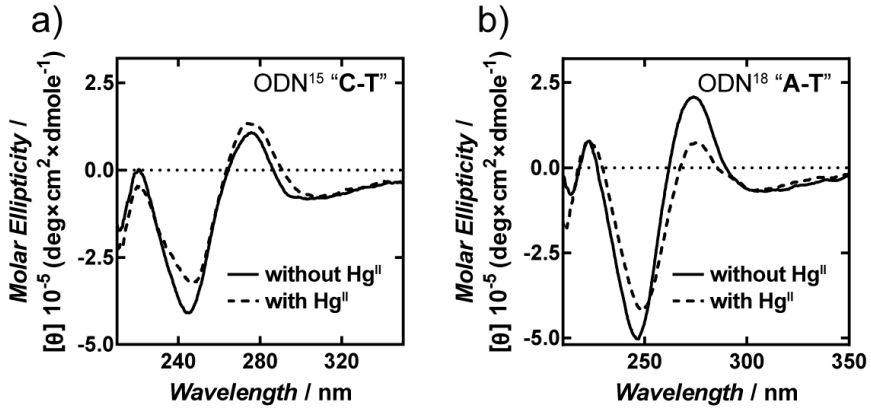

Figure 4.8. CD spectra of a) ODN[15] "C-T" and b) ODN[18] "A-T" in the presence and absence of Hg^{II}. DNA samples contained 10 μM of pre-folded duplex DNA in aqueous buffer (200 mM $NaClO_4$, 50 mM cacodylic acid at pH = 7.8) and were incubated with 2.0 equiv of Hg^{II} for 3 h prior to use.

4.5 Association and Dissociation Rate Constants of Hg^{II} Binding C-T Mismatches

To evaluate the kinetic parameters of C-Hg^{II}-T formation, the changes in fluorescence intensities of 21-mer duplex DNA X13 or X15 containing a single ^{DMA}T-C mismatch, ^{DMA}C-T mismatch, or a wild-type C-T mismatch placed adjacent to a ^{DMA}C-G base pair were monitored as a function of time and Hg^{II} concentration (Figure 4.9, Figures 4.10 and 4.11). Rate constants of association (k_{on}) were determined using pseudo-first-order approximations (eq 6 - 9, Chapter 6). For all four constructs evaluated, the second-order rate constants of Hg^{II} association to C-T mismatches were in a similar range of $7.6 \times 10^4 - 8.5 \times 10^5$ $M^{-1}s^{-1}$ (Table 4.2). ^{DMA}C-containing duplexes lacking a C-T mismatch exhibited little or no time-dependent quenching under the same conditions (Figure A19, Appendix).

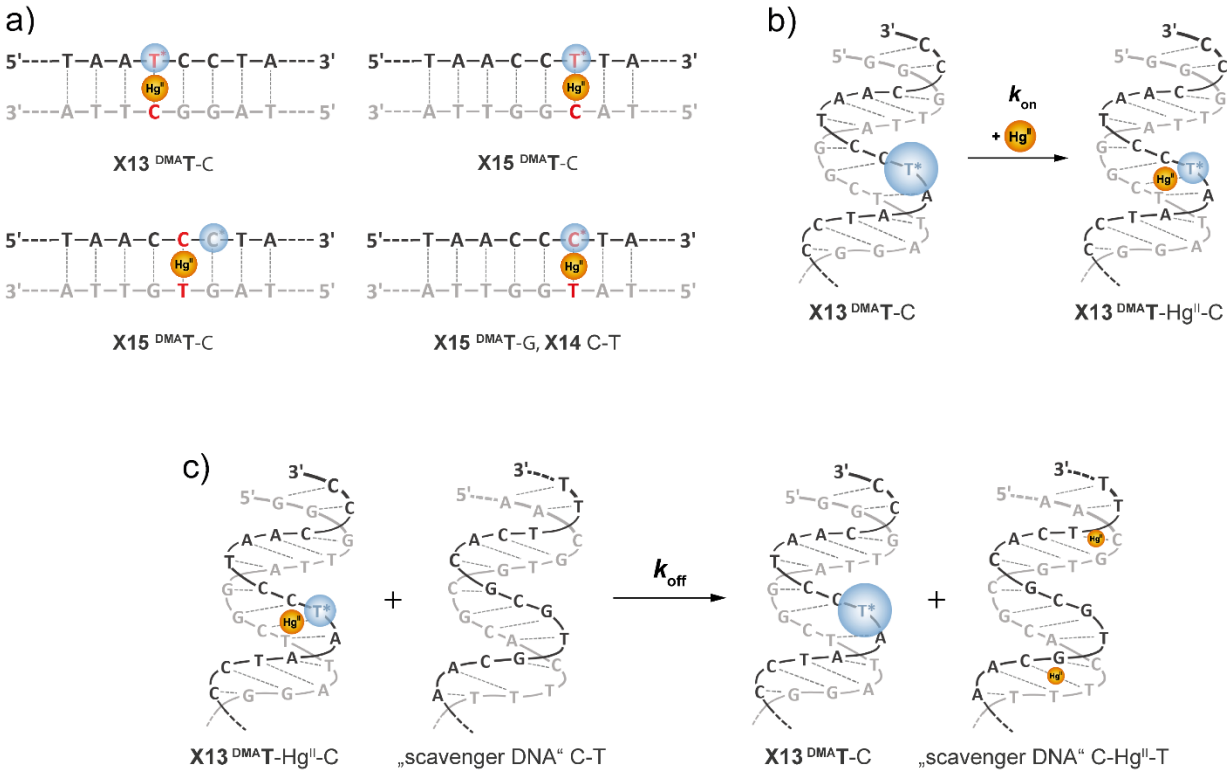

Figure 4.9. a) Variable regions (underlined) and names of DNA sequences used in these kinetic studies: X13: 5'-CCC-TAA-CCC-TAA-XCC-TAA-CCC-3'; X15: 5'-CCC-TAA-CCC-TAA-CCX-TAA-CCC-3'; where X = C, T*, or C* (^{DMA}T or ^{DMA}C, respectively). See Tables 6.5, Chapter 6, Experimental Procedures for a complete list of all reported duplexes. b) Schematic representation of Hg^{II} association to "X13 ^{DMA}T-C" and c) Schematic representation of dissociation of Hg^{II} from "X13 ^{DMA}T-Hg^{II}-C" (T* = ^{DMA}T).

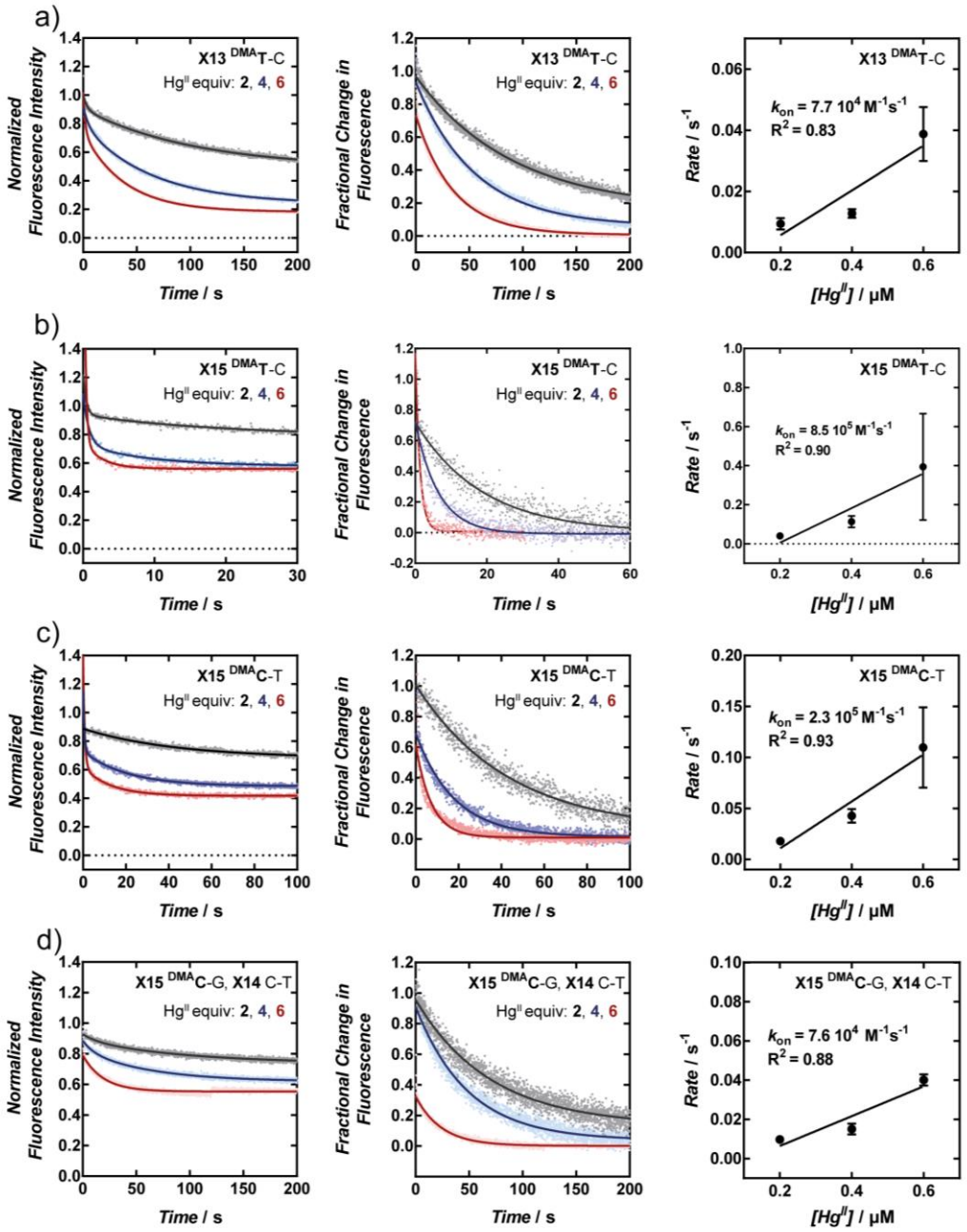

Figure 4.10. Site-selective binding of Hg^{II} to a) "X13 ^{DMA}T-C", b) "X15 ^{DMA}T-C", c) "X15 ^{DMA}C-T", and d) "X15 ^{DMA}C-G, X14 C-T" according to fluorescence quenching upon addition of 2, 4, and 6 equiv of Hg^{II}. Fluorescence changes upon Hg^{II} coordination normalized to fluorescence intensity prior to Hg^{II} addition, and fitted with a biphasic curve (left). Change in fluorescence as a fraction of y_0 and plateau of fit of normalized fluorescence intensity fit with a monoexponential decay to determine rate of binding (middle). k_{on} determined by slope of the linear regression from the plot of pseudo-first-order rate versus Hg^{II} concentration. Samples were excited at 370 nm and fluorescence was monitored at 500 nm (^{DMA}T) or 510 nm (^{DMA}C). All samples contained 0.1 µM DNA in aqueous buffer (200 mM Na_2HPO_4, 100 mM citric acid and 100 mM $NaNO_3$) at pH = 7.35.

To evaluate the rates of Hg^{II} dissociation from C-T mismatches, pre-formed duplexes containing a single ^{DMA}T-Hg^{II}-C, ^{DMA}C-Hg^{II}-T, or wild-type C-Hg^{II}-T complex adjacent to a ^{DMA}C-G base pair were monitored upon addition of 50 equiv of a non-fluorescent, passive Hg^{II} "scavenger" DNA containing two C-T mismatches (ODN[14], Figure 4.9c, Figure 4.11, Table 6.5, Chapter 6, Experimental Procedures). Consistent with the dissociation of Hg^{II}, increased fluorescence was observed as a function of time (Figure 4.11). Control experiments revealed that the use of 30, 40, and 50 equiv of scavenger gave the same apparent first-order rates (Figure A20, Appendix). Data obtained using 50 equiv of scavenger DNA were fit to monoexponential curves (eq 11 - 12, Chapter 6) and the first-order dissociation constants (k_{off}) were calculated from the dissociation half-lives ($t_{1/2}$) of the complexes. With half-lives ranging from 27 – 820 s (Figure 4.11), similar dissociation constants were obtained for all four constructs (k_{off} = 9.4 x 10^{-4} – 2.7 x 10^{-2} s^{-1}). Remarkably, the duplexes exhibiting faster Hg^{II} dissociation (such as X15 ^{DMA}T-C) also exhibited more rapid Hg^{II} association. The ratios of dissociation and association rate constants (k_{off} / k_{on} = K_d) were therefore nearly identical for all four constructs evaluated (K_d = 10 – 32 nM, Table 4.2).

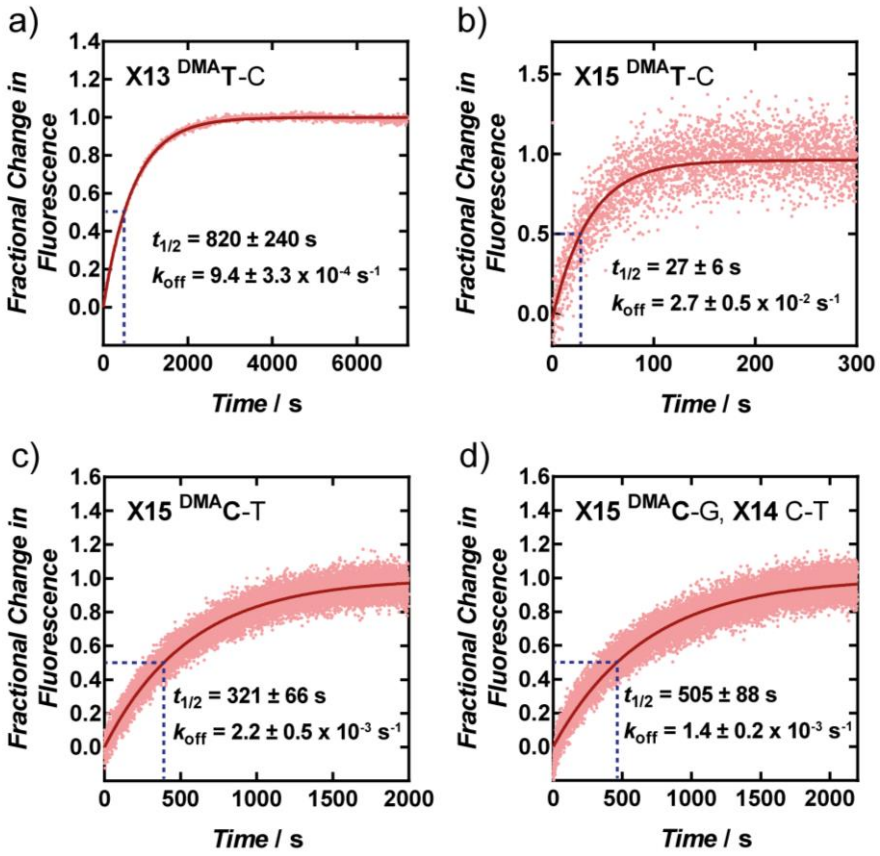

Figure 4.11. Dissociation of Hg^{II} from a) X13 ^{DMA}T-Hg^{II}-C, b) X15 ^{DMA}T-Hg^{II}-C, c) X15 ^{DMA}C-Hg^{II}-T, and d) X15 ^{DMA}C-G, X14 C- Hg^{II}-T upon addition 50 equiv of unlabeled, C-T-containing 'scavenger' duplex DNA. C-Hg^{II}-T base pairs were formed by pre-incubation of duplex DNA with 2.0 equiv of $Hg(ClO_4)_2$ for 3 h prior to addition of scavenger DNA. Samples contained either 0.1 or 4 μM C-Hg^{II}-T-containing duplex DNA in aqueous buffer (200 mM Na_2HPO_4, 100 mM citric acid and 100 mM $NaNO_3$) at pH = 7.35.

Table 4.2: Rate Constants of Association (k_{on}), Dissociation (k_{off}), and Calculated Equilibrium Dissociation Constants ($K_d = k_{off} / k_{on}$) of Hg^{II} Binding to ^{DMA}T-C, ^{DMA}C-T or C-T in Duplex DNA.[a]

Sequence	k_{on} ($M^{-1}s^{-1}$)	k_{off} (s^{-1})	K_d (nM)[b]
X13 ^{DMA}T-C	$7.7 \pm 1.4 \times 10^{4}$	$9.4 \pm 3.3 \times 10^{-4}$	12 ± 5.0
X15 ^{DMA}T-C	$8.5 \pm 6.7 \times 10^{5}$	$2.7 \pm 0.5 \times 10^{-2}$	32 ± 26
X15 ^{DMA}C-T	$2.3 \pm 1.0 \times 10^{5}$	$2.2 \pm 0.5 \times 10^{-3}$	10 ± 5.0
X15 ^{DMA}C-G, X14 C-T	$7.6 \pm 0.8 \times 10^{4}$	$1.4 \pm 0.2 \times 10^{-3}$	18 ± 3.0

[a] Reported values = mean ± standard deviation from three independent measurements. Dissociation rate constants were determined by addition of 50 equiv of unlabeled DNA. For duplex sequences see Table 6.5, Chapter 6, Experimental Procedures. [b] Equilibrium dissociation constants (K_d) calculated as $K_d = k_{off} / k_{on}$.

4.6 Equilibrium Measurements of C-Hg^{II}-T Formation

To further evaluate the thermodynamic parameters of C-Hg^{II}-T formation, the changes in fluorescence intensities of 21-mer duplex DNA X13 or X15 containing a single ^{DMA}T-C mismatch, ^{DMA}C-T mismatch, or a wild-type C-T mismatch placed adjacent to a ^{DMA}C-G base pair were monitored as a function of Hg^{II} concentration following one hour equilibration at 4 °C or 25 °C (Figure 4.12 and 4.13, Figures A20, Appendix). K_d values were calculated from the equilibrium quenching data with the assumption of 1:1 binding stoichiometry by curve-fitting the raw data to mono- or bi-phasic binding curves (eq 1 - 5, Chapter 6). Duplexes lacking any base pair mismatch and containing a ^{DMA}C-G base pair exhibited a mono-phasic "non-specific" binding curve with a modest apparent affinity of K_d = 2.3 +/- 0.1 μM (green triangles, Figure 4.12, Table 4.3). Similar results were also previously obtained for duplexes containing ^{DMA}T-A and lacking a base pair mismatch.[29] Duplexes containing a ^{DMA}C-G base pair placed adjacent to a wild-type C-T mismatch exhibited a bi-phasic binding curve (blue circles, Figure 4.12b), with a low affinity component having the same apparent affinity as the non-specific binding (K_d (1) = 2.2 +/- 0.4 μM) and a high-affinity component (K_d (2) = 107 +/- 45 nM, Figure 4.12b, Table 4.3) exhibiting a similar affinity as determined from the ratio of kinetic rate constants (Table 4.2). Similar values were obtained for the duplexes containing a single ^{DMA}T-C, ^{DMA}C-T, or ^{DMA}T-T mismatch (Table 4.3, Figure 4.12, Figure A21, Appendix). These results demonstrate that Hg^{II} exhibits high affinity for C-T mismatches in duplex DNA – even in the high salt, metal-coordinating buffer conditions (200 mM of Na_2HPO_4, 100 mM of citric acid and 100 mM $NaNO_3$ (pH = 7.35)) that were previously shown to minimize non-specific binding interactions with duplex DNA.[29]

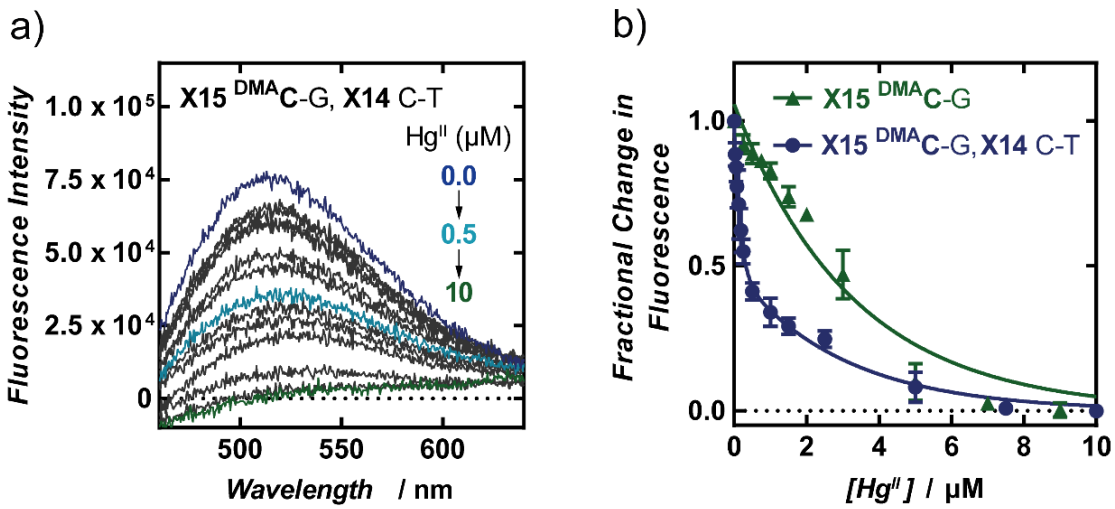

Figure 4.12. a) Fluorescence quenching of X15 ^{DMA}C-G, X14 C-T upon addition of Hg^{II}. Fluorescence spectra (λ_{ex} = 370 nm) of ^{DMA}C-containing sequences in the absence (dark blue) and in the presence of variable concentrations of Hg^{II}. b) Fluorescence quenching of X15 ^{DMA}C-G and X15 ^{DMA}C-G, X14 C-T fit to a monoexponential (eq 4, Chapter 6) or biphasic curve (eq, 5 Chapter 6), respectively. Samples contained 25 nM duplex DNA in aqueous buffer (200 mM of Na_2HPO_4, 100 mM of citric acid and 100 mM $NaNO_3$ (pH = 7.35)) and were equilibrated with variable concentrations of $Hg(ClO_4)_2$ at 25 °C for 1 h prior to measuring.

Table 4.3: Steady-State Equilibrium Dissociation Constants (K_d) of Hg^{II} Binding to ^{DMA}T-C, ^{DMA}C-T, ^{DMA}T-T or Wild-Type C-T in Duplex DNA.[a]

Sequence	Temperature	K_d (nM) non-specific	K_d (nM) mismatch specific
X13 ^{DMA}T-C	25 °C	–	152 ± 4
X13 ^{DMA}T-C	4 °C	–	56 ± 4
X15 ^{DMA}T-C	25 °C	1300 ± 300	123 ± 76
X15 ^{DMA}C-T	25 °C	2300 ± 300	153 ± 27
X15 ^{DMA}C-G, X14 C-T	25 °C	2200 ± 400	107 ± 45
X15 ^{DMA}C-G	25 °C	2260 ± 130	–
X13 ^{DMA}T-T	25 °C	–	77 ± 4
X13 ^{DMA}T-T	4 °C	–	144 ± 27

[a] Reported values = mean ± standard deviation from three independent measurements. Samples contained 25 nM of DNA in an aqueous buffer containing 200 mM Na_2HPO_4, 100 mM citric acid and 100 mM $NaNO_3$ (pH = 7.35). K_d values were calculated by fitting quenching data to either a monoexponential curve (eq 4, Chapter 6) or to a biphasic curve (eq 5, Chapter 6). All R^2 values were $\geq$ 0.97 (Figures 4.12 – 4.13, Figure A21, Appendix). For duplex sequences see Table 6.5, Chapter 6, Experimental Procedures.

Temperature-dependent K_d measurements revealed that the specific binding affinities of ^{DMA}T-C mismatches to Hg^{II} are three-fold higher at 4 °C (K_d = 56 nM) than at 25 °C (K_d = 152 nM, Figure 4.13, Table 4.3). In contrast, ^{DMA}T-T mismatches exhibited a two-fold lower affinity for Hg^{II} at 4 °C (K_d = 144 nM) than at 25 °C (K_d = 77 nM, Figure 4.13, Table 4.3). This latter result is consistent with the positive entropy of formation (ΔS) previously reported for T-Hg^{II}-T base pairs determined using isothermal titration calorimetry.[44] By plotting the free energies of formation (ΔG) calculated from K_d measurements at 4 °C and 25 °C, and assuming a constant enthalpy change (ΔH) over this small temperature range, our data suggest that the formation of C-Hg^{II}-T base pairs involve very little to no positive entropy, whereas the formation of T-Hg^{II}-T base pairs exhibit a relatively large positive entropy change (Figure 4.14).

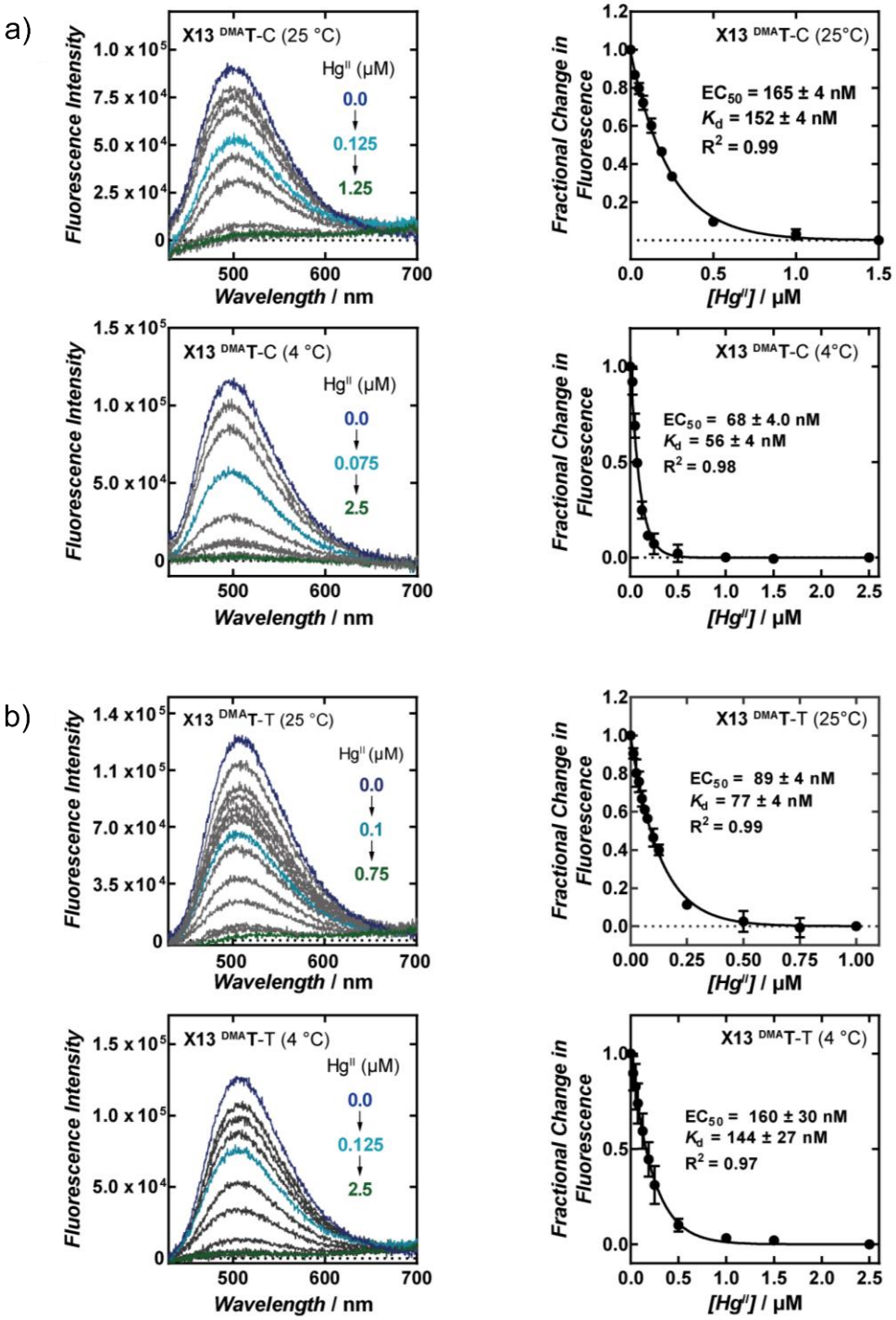

Figure 4.13. Fluorescence quenching of a) X13 ^{DMA}T-C at 25 °C (top) and 4°C (bottom) and b) X13 ^{DMA}T-T at 25 °C (top) and 4°C (bottom) upon addition of Hg^{II}. Fluorescence spectra (λ_{ex} = 370 nm) of ^{DMA}T-containing sequences in the absence (dark blue) and in the presence of variable concentrations of Hg^{II} (left). Plot of fluorescence intensity (λ_{em} = 500 nm (^{DMA}T) or 510 nm (^{DMA}C) versus concentration of Hg^{II} (right) fit with a monoexponential equation (eq 4, Chapter 6). All samples contained 25 nM duplex DNA in aqueous buffer (200 mM of Na_2HPO_4, 100 mM of citric acid and 100 mM $NaNO_3$ (pH = 7.35)) and were incubated at the indicated temperature with $Hg(ClO_4)_2$ for 1 h prior to measuring.

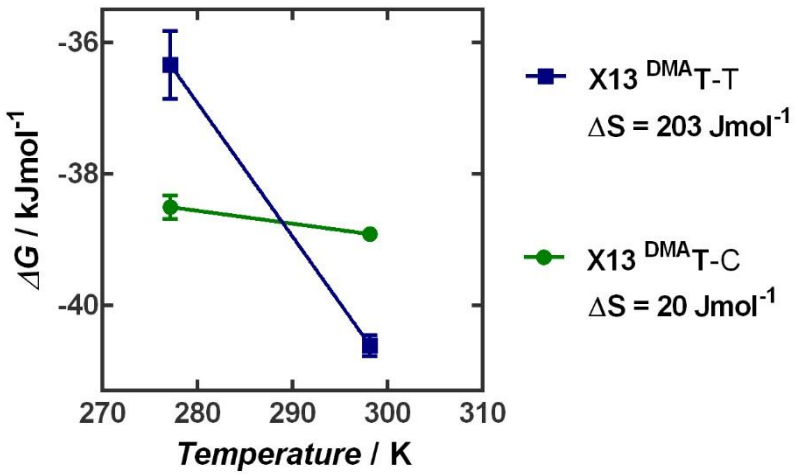

Figure 4.14. Change in entropy (ΔS) for X13 ^{DMA}T-T and X13 ^{DMA}T-C determined by slope of linear regression from plot of ΔG versus temperature. ΔG was calculated as $\Delta G = -RT\ln(1/K_d)$. All samples contained 25 nM duplex DNA in aqueous buffer (200 mM of Na_2HPO_4, 100 mM of citric acid and 100 mM $NaNO_3$ (pH = 7.35)).

4.7 Discussion and Conclusions

Here we report the use of fluorescent nucleobase analogs ^{DMA}T and ^{DMA}C for the characterization of site-selective Hg^{II} binding to C-T mismatches in duplex DNA. Our fluorescence and ^{1}H NMR data reveal that Hg^{II} selectively and stoichiometrically binds to C-T mismatches with high affinity (K_d = 10 – 153 nM). These affinities are very similar to those of Hg^{II} binding to T-T mismatches under the same conditions (Table 4.3 and reference (29)). Unlike the widely studied T-Hg^{II}-T metallo base pair, C-Hg^{II}-T formation was previously undetected by thermal melting temperature analyses.[44] Despite their high-affinity binding, little or no increase in T_m was observed for duplexes containing C-T mismatches upon addition of Hg^{II} (Table 4.1 and Table A3, Appendix). This apparent contradiction is likely a result of the lower Hg^{II} affinity to C-T mismatches at higher temperatures, whereas T-T mismatches exhibit higher Hg^{II} affinity with increasing temperatures (Table 4.3). These results highlight the fact that ΔT_m values must be interpreted with great caution, and that fluorescent nucleobase analogs offer an attractive alternative for the identification and study of DNA-metal binding interactions.

Despite their similar equilibrium binding affinities, there are some notable differences between the formation of T-Hg^{II}-T and C-Hg^{II}-T metallo base pairs in duplex DNA. Hg^{II} exhibits approximately a 10-fold higher rate constant

of association to C-T as compared to T-T mismatches. This observation is consistent with the fact that two protons must be removed from the T-T mismatch upon binding Hg^{II}, whereas only one or two protons are removed upon binding C-T (Figure 4.15). Furthermore, the ΔS of formation of C-Hg^{II}-T is much smaller than the ΔS of formation of T-Hg^{II}-T (Figure 4.14). The unusual positive ΔS of T-Hg^{II}-T formation was previously ascribed to the release of water molecules from Hg^{II} upon DNA binding.[6,44] The smaller ΔS of C-Hg^{II}-T formation therefore suggests that less water is released from Hg^{II} upon binding C-T mismatches as compared to T-T mismatches. The 10-fold larger rate constants of Hg^{II} dissociation from C-Hg^{II}-T (Table 4.2) versus T-Hg^{II}-T[29] are also consistent with a kinetically less stable, more solvent-exposed coordination site of Hg^{II} in C-Hg^{II}-T (Table 4.2) as compared to T-Hg^{II}-T[29] Taken together, these observations are consistent with a recently reported X-ray crystal structure of a C-Hg^{II}-T base pair in an A-form duplex DNA crystal structure[9] where the metal ion was unexpectedly bound to the exocyclic amine (*N4*) of a deprotonated cytosine residue and to the *N3* of a deprotonated thymidine (Figure 4.15). Additional studies using ^{15}N-NMR[4-5] will be required to determine if one or both of these metal binding modes are present in duplex DNA containing C-Hg^{II}-T base pairs in solution.

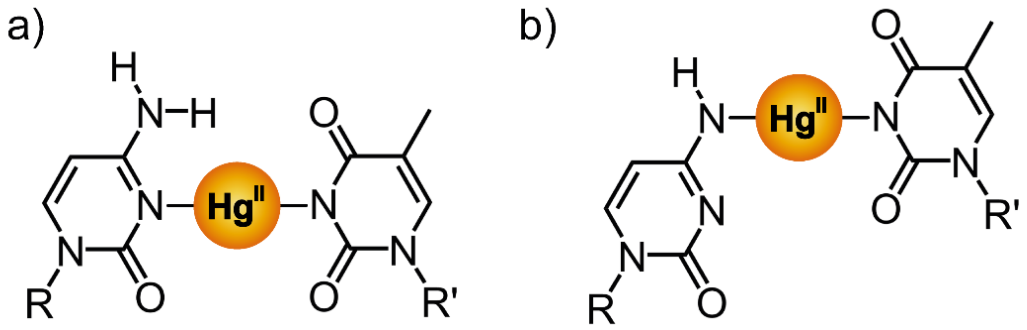

Figure 4.15. a) Structure of proposed, hypothetical (*N3*)C-Hg^{II}-(*N3*)T coordination complex (36) based upon structural analogy with T-Hg^{II}-T (4,37) and C-Ag^{I}-C (5,8,10). b) Structure of (*N4*)C-Hg^{II}-(*N3*)T coordination complex recently observed in an X-ray crystal structure of a short, A-form duplex DNA containing a C-T mismatch bound to Hg^{II} (9). (R, R' = duplex DNA).

REFERENCES

1. Yamane,T., Davidson,N. (1961) On the complexing of desoxyribonucleic acid (DNA) by mercuric ion. *J. Am. Chem. Soc.,* 83, 2599-2607.
2. Katz,S. (1962) Mechanism of the reaction of polynucleotides and Hg^{II}. *Nature*, 194, 569.
3. Katz,S. (1963) The reversible reaction of Hg(II) and double-stranded polynucleotides a step-function theory and its significance. *Biochim. Biophys. Acta*, 68, 240-253.
4. Tanaka,Y., Oda,S., Yamaguchi,H., Kondo,Y., Kojima,C. Ono,A., (2007) ^{15}N-^{15}N J-coupling across Hg^{II}: Direct observation of Hg^{II}-mediated T-T base pairs in a DNA duplex. *J. Am. Chem. Soc.*, 129, 244-245.
5. Dairaku,T., Furuita,K., Sato,H., Šebera,J., Nakashima,K., Kondo,J., Yamanaka,D., Kondo,Y., Okamoto,I., Ono,A., Sychrovský,V., Kojima,C., Tanaka,Y., (2016) Structure determination of an Ag^{I}-mediated cytosine-cytosine base pair within DNA duplex in solution with $^{1}H/^{15}N/^{109}Ag$ NMR spectroscopy. *Chem. Eur. J.*, 22, 13028-13031.
6. Yamaguchi,H., Sebera,J., Kondo,J., Oda,S., Komuro,T., Kawamura,T., Dairaku,T., Kondo,Y., Okamoto,T., Ono,A., Burda,J.V., Kojima,C., Sychrovsky,V., Tanaka,Y., (2014) The structure of metallo-DNA with consecutive thymine-Hg^{II}-thymine base pairs explains positive entropy for the metallo base pair. *Nucleic Acids Res.*, 42, 4094-4099.
7. Kondo,J., Yamada,T., Hirose,C., Okamoto,I., Tanaka,Y., Ono,A., (2014) Crystal structure of metallo DNA duplex containing consecutive Watson-Crick-like T-Hg(II)-T base pairs. *Angew. Chem. Int. Ed.*, 53, 2385.
8. Kondo,J., Tada,Y., Dairaku,T., Hattori,Y., Saneyoshi,H., Ono,A., Tanaka,Y., (2017) A metallo-DNA nanowire with interrupted one-dimensional silver array. *Nat. Chem.,* 9, 956-960.
9. Liu,H., Cai,C., Haruehanroengra,P., Yao,Q., Chen,Y., Yang,C., Luo,Q., Wu,B., Li,J., Ma,J., Sheng,J., Gan,J., (2017) Flexibility and stabilization of Hg^{II}-mediated C:T and T:T base pairs in DNA duplex. *Nucleic Acids Res.,* 45, 2910-2918.
10. Hehua,L., Shen,F., Haruehanroengra,P., Yao,Q., Cheng,Y., Chen,Y., Yang,C., Zhang,J., Wu,B., Luo,Q., Cui,R., Li,J., Ma,J., Sheng,J., Gan,J., (2017) A DNA structure containing Ag^{I}-mediated G:G and C:C base pairs. *Angew. Chem. Int. Ed.,* 56, 9430-9434.
11. Ennifar,E., Walter,P., Dumas,P., (2003) A crystallographic study of the binding of 13 metal ions to two related RNA duplexes. *Nucleic Acids Res.*, 31, 2671–2682.
12. Liu,J., Lu,Y., (2007) Rational design of "turn-on" allosteric DNAzyme catalytic beacons for aqueous mercury ions with ultrahigh sensitivity and selectivity. *Angew. Chem. Int. Ed.* 46, 7587-7590.
13. Lin,Y.-W., Ho,H.-T., Huang, C.-C., Chang,H.-T., (2008) Fluorescence detection of single nucleotide polymorphisms using a universal molecular beacon. *Nucleic Acids Res.,* 36, e123.
14. Mor-Piperberg,G., Tel-Vered,R., Elbaz,J., Willner,I., (2010) Nanoengineered electrically contacted enzymes on DNA scaffolds: Functional assemblies for the selective analysis of Hg^{2+} ions. *J. Am. Chem. Soc.*, 132, 6878-6879.
15. Park,K.S., Jung,C., Park,H.G., (2010) "Illusionary" polymerase activity triggered by metal ions: Use for molecular logic-gate operations. *Angew. Chem. Int. Ed.*, 49, 9757-9760.
16. Wang,Z.-G.,Elbaz,J., Willner,I., (2011) DNA machines: Bipedal walker and stepper. *Nano Lett.*, 11, 304-309.
17. Wen,S., Zeng,T., Liu,L., Zhao,K., Zhao,Y., Liu,X., Wu,H.-C., (2011) Highly sensitive and selective DNA-based detection of mercury(II) with α-hemolysin nanopore. *J. Am. Chem. Soc.*, 133, 18312-18317.
18. Thomas,J.M., Yu,H.-Z., Sen,D., (2012) A mechano-electronic DNA switch. *J. Am. Chem. Soc.*, 134, 13738-13748.
19. Xiao,S.J., Hu,P.P., Xiao,G.F., Wang,Y., Liu,Y., Huang,C.Z., (2012) Label-free detection of prion protein with its DNA aptamer through the formation of T-Hg^{2+}-T configuration. *J. Phys. Chem. B*, 116, 9565-9569.
20. Kang,I., Wang,Y., Reagan,C., Fu,Y., Wang,M.X., Gu,L.-Q., (2013) Designing DNA interstrand lock for locus-specific methylation detection in a nanopore. *Sci. Rep.*, 3, 2381.
21. Bi,S., Ji,B., Zhang,Z., Zhu,J.-J., (2013) Metal ions triggered ligase activity for rolling circle amplification and its application in molecular logic gate operations. *Chem. Sci.,* 4, 1858-1863.
22. Wang,Y., Ritzo,B., Gu,L.-Q., (2015) Silver(I) ions modulate the stability of DNA duplexes containing cytosine, methylcytosine and

hydroxymethylcytosine at different salt concentrations. *RSC Adv.,* 5, 2655-2658.
23. Park,K.S., Lee,C.Y., Park,H.G., (2016) Metal ion triggers for reversible switching of DNA polymerase. *Chem. Commun*., 52, 4868-4871.
24. Hong,T., Yuan,Y., Wang,T., Ma,J., Yao,Q., Hua,X., Xia,Y., Zhou,X., (2017) Selective detection of N6-methyladenine in DNA *via* metal ion-mediated replication and rolling circle amplification. *Chem. Sci.*, 8, 200– 205.
25. Guo,X., Seela,F., (2017) Anomeric 2'-deoxcytidines and silver ions: Hybrid base pairs with greatly enhanced stability and efficient DNA mismatch detection with α-dC. *Chem. Eur. J.,* 23, 11776-11779.
26. Urata,H., Yamaguchi,E., Funai,T., Matsumura,Y., Wada,S.-I., (2010) Incorporation of thymine nucleotides by DNA polymerases through T-Hg^{II}-T base pairing. *Angew. Chem. Int. Ed.,* 49, 6516-6519.
27. Funai,T., Miyazaki,Y., Aotani,M., Yamaguchi,E., Nakagawa,O., Wada,S.-I., Torigoe,H., Ono,A., Urata,H., (2012) Ag^{I} ion mediated formation of a C-A mispair by DNA polymerases. *Angew. Chem. Int. Ed.*, 51, 6464-6466.
28. Funai,T., Nakamura,J., Miyazaki,Y., Kiriu,R., Nakagawa,O., Wada,S.-I., Ono,A., Urata,H., (2014) Regulated incorporation of two different metal ions into programmed sites in a duplex by DNA polymerase catalyzed primer extension. *Angew. Chem. Int. Ed.,* 53, 6624-6627.
29. Schmidt,O.P., Mata,G., Luedtke,N.W., (2016) Fluorescent base analogue reveals T-Hg^{II}-T base pairs have high kinetic stabilities that perturb DNA metabolism. *J. Am. Chem. Soc.,* 138, 14733-14739.
30. Clever,G.H., Kaul,C., Carell,T., (2007) DNA-metal base pairs. *Angew. Chem. Int. Ed.,* 46, 6226-6236.
31. Takezawa,Y., Shionoya,M., (2012) Metal-mediated DNA base pairing: Alternatives to hydrogen-bonded Watson–Crick base pairs. *Acc. Chem. Res.,* 45, 2066-2076.
32. Scharf,P., Müller,J., (2013) Nucleic acids with metal-mediated base pairs and their application. *ChemPlusChem*, 78, 20-34.
33. Tanaka,Y., Kondo,J., Sychrovský,V., Šebera,J., Dairaku,T., Saneyoshi,H., Urata,H., Torigoe,H., Ono,A., (2015) Structures, physiochemical properties, and applications of T-Hg^{II}-T, C-Ag^{I}-C, and other metallo-base-pairs. *Chem. Commun.,* 51, 17343-17360.
34. Takezawa,Y., Müller,J., Shionoya,M., (2017) Artificial DNA base pairing mediated by diverse metal ions. *Chem. Lett.,* 46, 622-633.
35. Jash,B., Müller,J., (2017) Metal-mediated base pairs: from characterization to application. *Chem. Eur. J.* 23, 17166-17178.
36. Ono,A., Torigoe,H., Tanaka,Y., Okamoto,I., (2011) Binding of metal ions by pyrimidine base pairs in DNA duplexes. *Chem. Soc. Rev.*, 40, 5855-5866.
37. Tanaka,Y., Yamaguchi,H., Oda,S., Kondo,Y., Nomura,M., Kojima,C., Ono,A., (2006) The structure of metallo-DNA with consecutive thymine-Hg^{II}-thymine base pairs explains positive entropy for the metallo base pair formation. *Nucleic Acids Res.* 2006, *25*, 613-624.
38. Miyake,Y., Togashi,H., Tashiro,M., Yamaguchi,H., Oda,S., Kudo,M., Tanaka,Y., Kondo,Y., Sawa,R., Fujimoto,T., Machinami,T., Ono,A., (2006) $Mercury^{II}$-mediated formation of thymine-Hg^{II}-thymine base pairs in DNA duplexes. *J. Am. Chem. Soc.*, 128, 2172-2173.
39. Ono,A., Cao,S., Togashi,H., Tashiro,M., Fujimoto,T., Machinami,T., Oda,S., Miyake,Y., Okamoto,I., Tanaka,Y., (2008) Specific interactions between silver(I) ions and cytosine-cytosine pairs in DNA duplexes. *Chem. Commun.*, 0, 4825-4827.
40. Torigoe,H., Miyakawa,Y., Ono,A., Kozasa,T., (2011) Thermodynamic properties of the specific binding between Ag^{+} ions and C:C mismatched base pairs in duplex DNA. *Nucleosides, Nucleotides and Nucleic Acids,* 30, 149-167.
41. Torigoe,H., Miyake,Y., Ono,A., Kozasa,T., (2012) Positive cooperativity of the specific binding between Hg^{2+} ion and T:T mismatched base pairs in duplex DNA. *Thermochim. Acta,* 532, 28-35.
42. Torigoe,H., Okamoto,I., Dairaku,T., Tanaka,Y., Ono,A., Kozasa,T., (2012) Thermodynamic and structural properties of the specific binding between Ag^{+} ion and C:C mismatched base pair in duplex DNA to form C-Ag-C metal-mediated base pair. *Biochimie*, 94, 2431-2440.
43. Mata,G., Schmidt,O.P., Luedtke,N.W., (2016) A fluorescent surrogate of thymidine in duplex DNA. *Chem. Commun.,* 52, 4718-4721.
44. Torigoe,H., Ono,A., Kozasa,T., (2010) Hg^{II} ion specifically binds with T:T mismatched base

pairs in duplex DNA. *Chem. Eur. J.,* 16, 13218-13225.
45. Hofr,C., Brabec,V., (2001) Thermal and thermodynamic properties of duplex DNA containing site-specific interstrand cross-link of antitumor cisplatin or its clinically ineffective trans isomer. *J. Biol. Chem.,* 276, 9655-9661.
46. Rodriguez-Ramos,M.M., Wilker,J.J., (2010) Metal-bipyridine complexes in DNA backbones and effects on thermal stability. *J. Biol. Inorg. Chem.,* 15, 629-639.
47. Fedoriw,A.M., Liu,H., Anderson,V.E., deHaseth,P.L., (1998) Equilibrium and kinetic parameters of the sequence-specific interaction of *Escherichia coli* RNA polymerase with nontemplate strand oligodeoxyribonucleotides. *Biochemistry*, 37, 11971-11979.
48. Arzumanov,A., Godde,F., Moreau,S., Toulmé,J.-J., Weeds,A., Gait,M.J., (2000) Use of the fluorescent nucleoside analogue benzo[*g*]quinazoline 2'-*O*-methyl-ß-D-ribofuranoside to monitor the binding of the HIV-1 Tat protein or of antisense oligonucleotides to the TAR RNA stem-loop. *Helv. Chim. Acta*, 83, 1424-1436.
49. Bradrick,T.D., Marino, J.P., (2004) Ligand-induced changes in 2-aminopurine fluorescence as a probe for small molecule binding to HIV-1 TAR RNA. *RNA*, 10, 1459-1468.
50. Gilbert,S.D., Stoddard,C.D., Wise,S.J., Batey,R.T., (2006) Thermodynamic and kinetic characterization of ligand binding to the purine riboswitch aptamer domain. *J. Mol. Biol.,* 359, 754-768.
51. Kimura,T., Kawai,K., Fujitsuka,M., Majima,T., (2007) Monitoring G-quadruplex structures and G-quadruplex-ligand complex using 2-aminopurine modified oligonucleotides. *Tetrahedron*, 63, 3585-3590.
52. Parsons,J., Hermann,T., (2007) Conformational flexibility of ribosomal decoding-site RNA monitored by fluorescent pteridine base analogues. *Tetrahedron*, 63, 3548-3552.
53. Lang,K., Rieder,R., Micura,R., (2007) Ligand-induced folding of the *thiM* TPP riboswitch investigated by a structure-based fluorescence spectroscopic approach. *Nucleic Acids Res.* 35, 5370-5378.
54. Barbieri,C.M., Kaul,M., Pilch,D.S., (2007) Use of 2-aminopurine as a fluorescent tool for characterizing antibiotic recognition of the bacterial rRNA A-site. *Tetrahedron*, 63, 3567-6574.
55. Xie,Y., Dix,A.V., Tor,Y., (2009) FRET enabled real time detection of RNA-small molecule binding. *J. Am. Chem. Soc.,* 131, 17605-17614.
56. Velmurugu,Y., Chen,X., Sevilla,P.S., Min,J.-H., Ansari,A., (2016) Twist-open mechanism of DNA damage recognition by the Rad4/XPC nucleotide excision repair complex. *Proc. Natl. Acad. Sci. U. S. A.,* 113, E2296-E2305.
57. Kim,S.J., Kool,E.T., (2006) Sensing metal ions with DNA building blocks: Fluorescent pyridobenzimidazole nucleosides. *J. Am. Chem. Soc.,* 128, 6164-6171.
58. Dumas,A., Luedtke,N.W., (2012) Site-specific control of *N*7-metal coordination in DNA by a fluorescent purine derivative. *Chem. Eur. J.,* 18, 245-254.
59. Omumi,A., McLaughlin,C.K., Ben-Israel,D., Manderville,R.A., (2012) Application of a fluorescent *C*-linked phenolic purine adduct for selective N7-metalation of DNA. *J. Phys. Chem. B*, 116, 6158-6165.
60. Jana,S.K., Guo,X., Mei,H., Seela,F., (2015) Robust silver-mediated imidazolo-dC base pairs in metal DNA: dinuclear silver bridges with exceptional stability in double helices with parallel and antiparallel strand orientation. *Chem. Commun.,* 51, 17301-17304.
61. Mata,G., Luedtke,N.W., (2015) A fluorescent probe for proton-coupled folding reveals slow exchange of i-motif and duplex DNA. *J. Am. Chem. Soc.,* 137, 699-707.
62. Schulhof,J.C., Molko,D., Teoule,R., (1987) The final deprotection step in oligonucleotide synthesis is reduced to a mild and rapid ammonia treatment by using labile base-protecting groups. *Nucleic Acids Res.,* 15, 397-416.
63. Cantor,C.R., Warshaw,M.M., Shapiro,H., (1970) Oligonucleotide interactions. III. Circular dichroism studies of the conformation of deoxyoligonucleotides. *Biopolymers*, 9, 1059-1077.
64. Borer,P.N., (1975) Optical properties of nucleic acids, absorption and circular dichroism spectra, in *Handbook of Biochemistry and Molecular Biology*: *Nucleic Acids*, Vol. 1, 3rd Ed., Fasman,G.D. (Ed.), CRC Press, Cleveland, Ohio, 589-595.
65. Brown,T., Brown,D.J.S., 1991, Modern machine-aided methods of oligodeoxyribonucleotide synthesis, In *Oligonucleotides and Analogues. A*

practical approach (F.Eckstein, ed.), Oxford: IRL Press, p. 1-24.

66. Bhaumik,S.R., Chary,K.V.R., Govil,G., Liu,K., Miles,H.T., (1997) Homopurine and homopyrimidine strands complementary in parallel orientation form an antiparallel duplex at neutral pH with A-C,G-T, and T-C mismatched base pairs. *Biopolymers*, 41, 773-784.
67. Allawi,H.T., SantaLucia Jr,J., (1998) Thermodynamics of internal C•T mismatches in DNA. *Nucleic Acids Res.,* 26, 2694-2701.

Chapter 5

Dynamic Structural Polymorphism of a Metallo DNA Double Helix

Metal-mediated base pairs expand the repertoire of helical structures and dynamics available to duplex nucleic acids, thereby tuning their biological and materials properties. Here we report solution structures of a DNA double helix containing two C-Hg^{II}-T base pairs separated by six canonical base pairs. NMR experiments revealed two well-resolved duplexes in dynamic equilibrium, each with its own characteristic nucleobase-metal-nucleobase connectivity. Both structures exhibited characteristics of "mixed" A/B-form duplex DNA. The major species (~75%) containing two identical (*N3*)C-Hg^{II}-(*N3*)T coordination sites resembled a B-form duplex. The minor species (~25%) containing two (*C4-NH*)C-Hg^{II}-(*N3*)T base pairs adopted a more A-form like structure. Dynamic changes in local metal ion coordination were directly coupled to the global interconversion of the two duplexes. The rates of their exchange (k_1 = 4.3 ± 0.6 s^{-1}, k_{-1} = 8.8 ± 0.9 s^{-1}) were on the same time scale as many biochemical and materials processes and can therefore serve as a low-energy barrier switch between two functional states of a duplex.

5.1 Introduction

DNA molecules fold into a variety of double helical structures. Transitions between A- and B- form duplexes resulting from variable hydration were first described using X-ray fiber diffraction analyses.[1–3] In terms of biological significance, protein binding can cause partial dehydration of the double helix, giving rise to A-form viral genomes,[4] as well as local B-to-A deformations in crystal structures of DNA bound to eukaryotic enzymes.[5] Small molecules such as polyamines[6–8] and cisplatin[9–11] can also induce local B -> A conformational changes upon DNA binding, this, in turn, can impact protein binding and therefore the biological function of the DNA.[12] The first high-resolution structure of duplex DNA was determined using an alternating sequence of (GC)n that adopted a Z-form duplex at high salt concentrations.[13] In addition to certain proteins,[14] the Z-form duplex can be stabilized via binding of transition metal ions and complexes to the N7 position of purine residues.[15,16] Transition metal ions exhibit a wide variety of binding sites on nucleic acids[17] and in some cases, can dramatically stabilize the pairing interactions between synthetic and "all natural" nucleobases.[18–25] In addition to their broad implications in biology,[26–29] metal-based switching of DNA conformation has been widely utilized in the development of new materials and devices.[30,31,40–43,32–39]

T-Hg^{II}-T base pairs provided the first examples of "all natural" metal-mediated base pairs composed of nucleobase mismatches coordinated to a transition metal ion.[44–46] T-Hg^{II}-T can serve as a functional mimic of T-A base pairs by stabilizing T-T during DNA primer extension,[34] and by causing the enzymatic misincorporation of dTTP across from thymidine to give T-Hg^{II}-T base pairs in vitro and possibly in vivo.[26] High-resolution structural studies revealed that Hg^{II} binds to T-T mismatches via *N3* coordination of two deprotonated thymidine residues.[47] Structurally analogous C-Ag^{I}-C base pairs have also been reported,[48] and in both cases, little or no impact on the global structure of the B-form duplex was observed.[48–50] More recently, C-T mismatches have been found to bind Hg^{II} with high affinity,[51] yet metal binding causes little or no thermal stabilization of the C-T mismatch in duplex DNA.[51,52] A crystal structure of a short A-form duplex-forming sequence containing a C-T mismatch exhibited metal binding via the exocyclic amine (*N4*) of a deprotonated cytosine residue and to the *N3* of a deprotonated thymidine.[53] The purely A-form structure observed in the crystal was inconsistent with CD data of B-form duplex structures containing C-Hg^{II}-T base pairs in solution.[51] It was therefore unclear what type of metal coordination and global helical structure(s) are exhibited by duplex DNA containing these metallo base pairs.

Here we report C-Hg^{II}-T formation via two distinct coordination modes upon addition of Hg^{II} to C-T-mismatch containing duplex DNA to give a major species (~75 %) containing (*N3*)C-Hg^{II}-(*N3*)T coordination sites and a minor species (~25 %) with (*C4-NH*)C-Hg^{II}-(*N3*)T base pairs. The different nucleobase-metal-nucleobase connectivities resulted in duplex DNA with different helical structures. Both structures exhibited characteristics of

a "mixed" A/B-form duplex DNA, with the major duplex adopting a more B-form-like and the minor a more A-form-like duplex. Dynamic changes in local metal ion coordination were directly coupled to global interconversion of the two duplexes, with slow rate constants of interconversion (k_1 = 4.3 ± 0.6 s^{-1}, k_{-1} = 8.8 ± 0.9 s^{-1}), that are on similar time scale as many biochemical and material processes. These results provide the first example of a reversible, metal-coupled switch of alternative helical structures of DNA in dynamic equilibrium.

5.2 Stoichiometric Binding of Hg^{II} to C-T Mismatches in Duplex DNA

With the goal of investigating C-Hg^{II}-T base pair formation, we measured the imino proton resonances of a 14-mer, palindromic DNA containing two mismatches (ODN[1] "C-T") at 4 °C in the presence and absence of Hg^{II} (Figure 5.1, Table 6.7, Chapter 6, Experimental Procedures). This sequence had previously been shown to form a stable, intermolecular duplex at temperatures ≤ 25 °C according to both temperature and DNA concentration-dependent CD measurements.[51] Temperature-dependent ^{1}H NMR spectroscopy confirmed this result (Figure 5.2, Figure A24, Appendix). In the absence of Hg^{II}, a mismatched thymidine imino-proton signal was observed at 10.9 ppm (Figure 5.1).[51,54–56] The addition of two equivalents of Hg^{II} (1:1 with respect to the number of mismatches present) caused the stoichiometric disappearance of this unpaired thymidine *NH*-resonance.[51] Similar results were obtained for ODN[2] "T-T" upon formation of a T-Hg^{II}-T base pair. In contrast, addition of Hg^{II} to the analogous sequence containing two G-T mismatches (ODN[3] "G-T") did not induce deprotonation of the mismatched thymidine (Figure 5.1). [^{1}H,^{1}H]-NOESY cross peaks between *NH* of thymidine and guanine residues and between thymidine *NH* and H2 of adenine residues enabled the assignment of all imino-proton signals in the presence and absence of Hg^{II} (Figures 5.3 – 5.4). The imino proton resonances of the thymidine residues flanking the C-T mismatch exhibited the largest chemical shift changes upon C-Hg^{II}-T base pair formation, to give a spectrum with similar imino proton chemical shifts as for "T-T" upon addition of 2.0 equiv of Hg^{II} (Figure 5.1, Figures 5.3 – 5.4, Table A4, Appendix). These results suggest that deprotonation and coordination of Hg^{II} to thymidine *N3* occur without significantly perturbing the duplex DNA structure. The stoichiometry of binding is consistent with the formation of site-specific 1:1 complexes between Hg^{II} and C-T mismatches.[51]

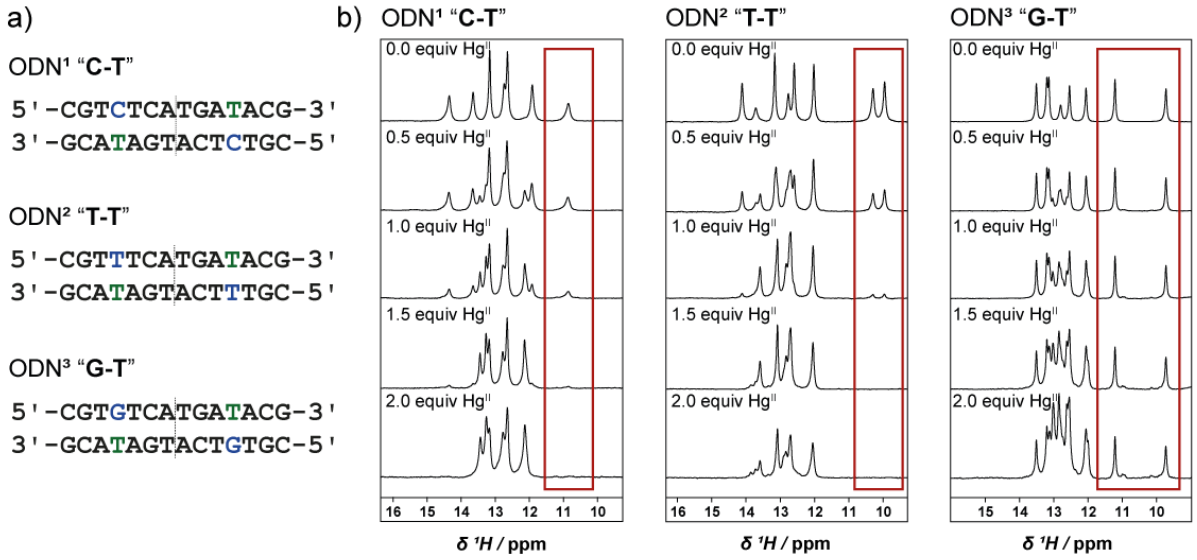

Figure 5.1. a) Names and sequences of palindromic, 14-mer duplex DNA "C-T" and "T-T", and "G-T". b) Stoichiometric binding of Hg^{II} to C-T- (left) and T-T-mismatch (middle) but not to G-T mismatches (right) according to the disappearance of thymidine imino proton resonance upon addition of Hg^{II}. All samples contained 0.5 mM of duplex DNA in aqueous buffer (200 mM $NaClO_4$, 50 mM cacodylic acid (pH = 7.0)). DNA samples were incubated with variable concentrations of $Hg(ClO_4)_2$ at r.t. for 15 min, followed by cooling at 4 °C for 15 min. (equiv of Hg^{II} given relative to mismatch).

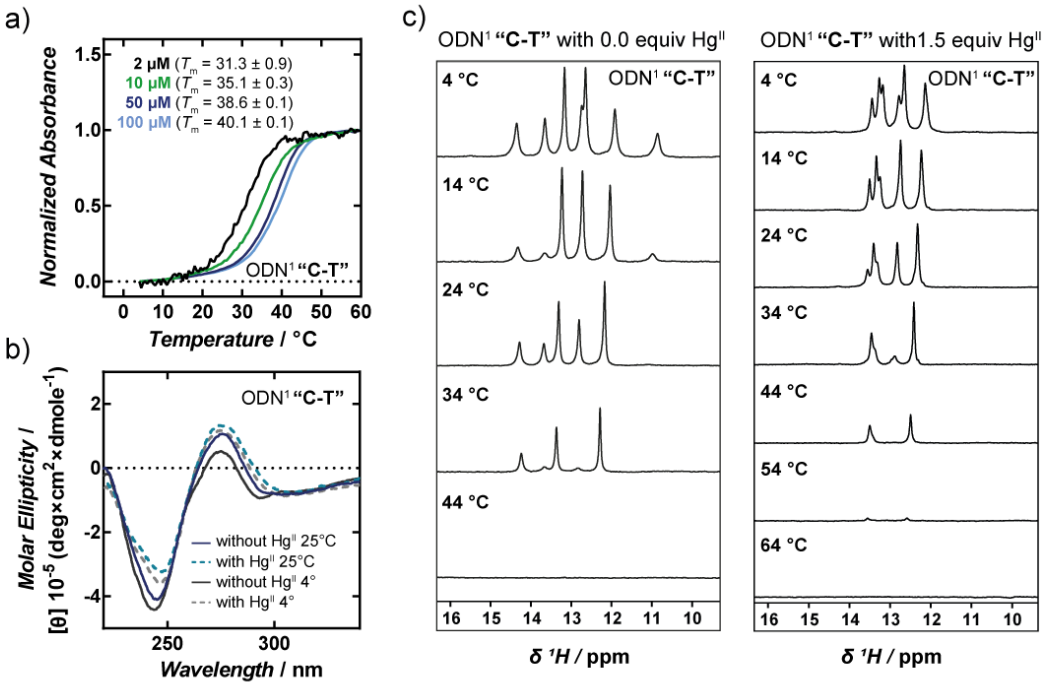

Figure 5.2. a) Thermal melting of ODN^1 "C-T" at variable DNA concentrations. b) CD spectra of ODN^1 "C-T" in the presence and absence of Hg^{II} at 4 °C and 25 °C. c) ^1H NMR spectra of ODN^1 "C-T" in the presence and absence of Hg^{II} at variable temperatures. For duplex sequence see Figure 5.1 and Table 6.7, Chapter 6, Experimental Procedures.

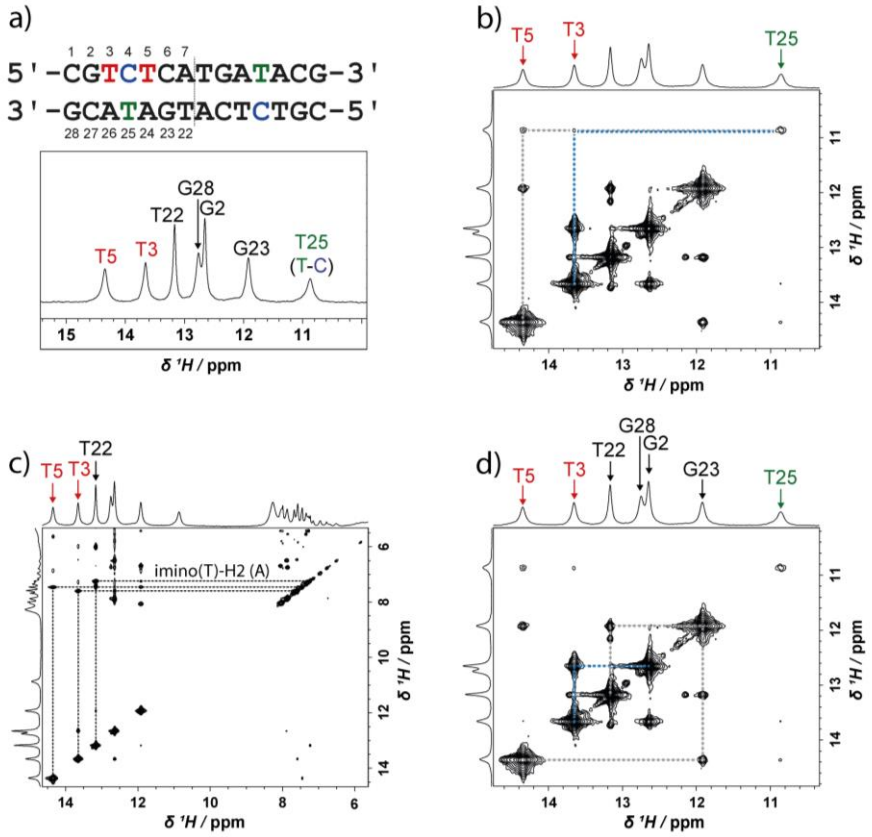

Figure 5.3. Assignment of *NH*-imino protons of the duplex ODN[1] "**C**-**T**". a) "**C**-**T**" sequence and imino region of ^{1}H NMR spectrum. b) Assignment of thymidine residues flanking the C-T mismatch according to NOE cross peaks between *NH*-imino protons of thymidine. c) Assignment of thymidine imino protons according to coupling of *NH*-imino signals of thymidine to H2 of adenine. d) Assignment of guanosine residues of "**C**-**T**" according to NOE cross peaks. The DNA sample contained 0.5 mM duplex DNA in aqueous buffer (200 mM $NaClO_4$, 50 mM cacodylic acid in H_2O / D_2O (9:1) at pH = 7.0). Spectra were recorded at 4 °C.

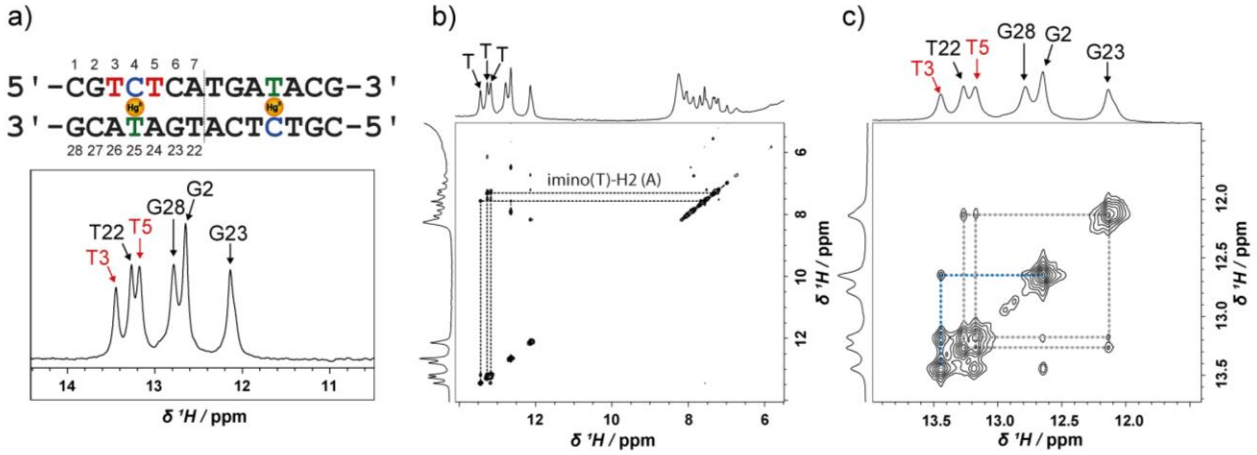

Figure 5.4. Assignment of *NH*-imino protons of ODN[1] "**C**-**T**" in the presence of Hg^{II}. a) "**C**-**T**" sequence and imino region of ^{1}H NMR spectrum. b) Assignment of thymidine imino protons according to coupling of *NH*-imino signals of thymidine residues to H2 of adenine. c) Assignment of thymidine and guanosine imino proton signals in the presence of Hg^{II} according to NOE cross peaks. The DNA sample contained 0.5 mM duplex DNA in aqueous buffer (200 mM $NaClO_4$, 50 mM cacodylic acid in H_2O / D_2O (9:1) at pH = 7.0). Spectra were recorded at 4 °C.

5.3 Nucleobase-Metal-Nucleobase Connectivity of C-Hg^{II}-T

^{15}N NMR is a powerful tool to determine the exact binding mode of metal ions to nucleotide residues.[47,48,57,58] To determine the metal coordination of C-Hg^{II}-T base pairs, we synthesized a ^{15}N-labeled ODN[1]* "C*-T*" by site-selectively incorporating a ^{15}N-labeled C-T mismatch using standard phosphoramidite chemistry. In the absence of Hg^{II}, ^{1}J ^{1}H,^{15}N coupling of thymidine *N3-H* was observed with a coupling constant of J = 88 Hz (Figure 5.5 a). Given the C_2 symmetry of the duplex DNA, five ^{15}N signals were observed in the 1D ^{15}N NMR spectrum (Figure 5.5b). ^{15}N-resonances were assigned by proton-coupled and proton-decoupled ^{15}N NMR spectra, ^{1}J ^{1}H,^{15}N coupling of thymidine *N3-H* and cytosine *NH*$_2$ by [^{15}N,^{1}H]-heteronuclear single quantum coherence spectrum (HSQC), and ^{3}J ^{1}H,^{15}N- and ^{2}J ^{1}H,^{15}N coupling between *N1* and H5 and/or H6 by long-range [^{15}N,^{1}H]-HSQC spectrum (Figure 5.6).

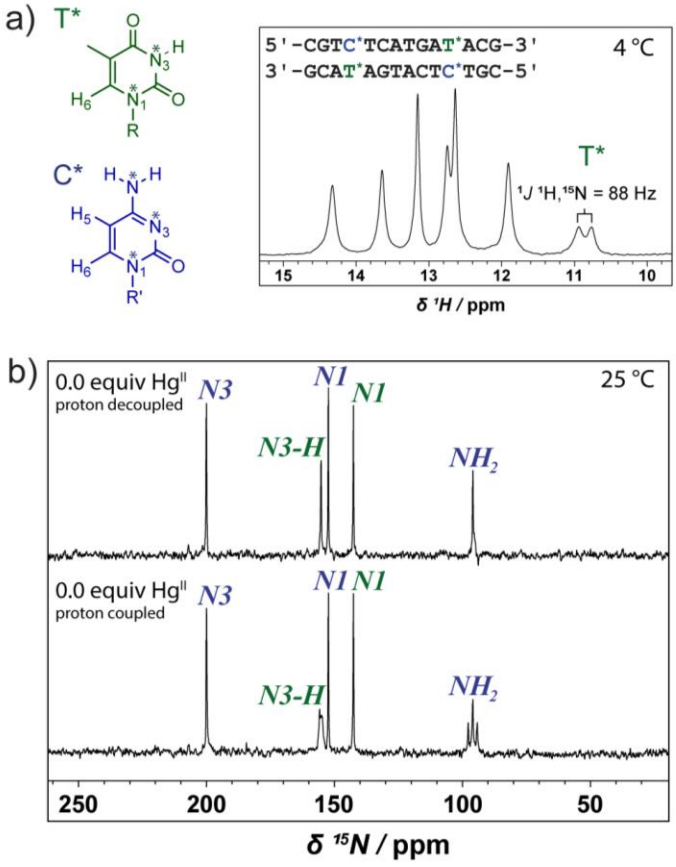

Figure 5.5. a) ^{1}H,^{15}N coupling (^{1}J = 88 Hz) of *N3-H* imino proton of thymidine according to ^{1}H NMR spectrum of "C*-T*" containing a site-selective, ^{15}N-labeled C-T mismatch at 4 °C (N* = ^{15}N). b) Assigned proton decoupled (top) and proton coupled (bottom) ^{15}N NMR spectra of "**C*-T***" at 25 °C. DNA samples contained 0.5 mM (^{1}H) and 1 mM (^{15}N) duplex DNA in aqueous buffer (200 mM $NaClO_4$, 50 mM cacodylic acid in H_2O / D_2O (9:1) at pH = 7.8).

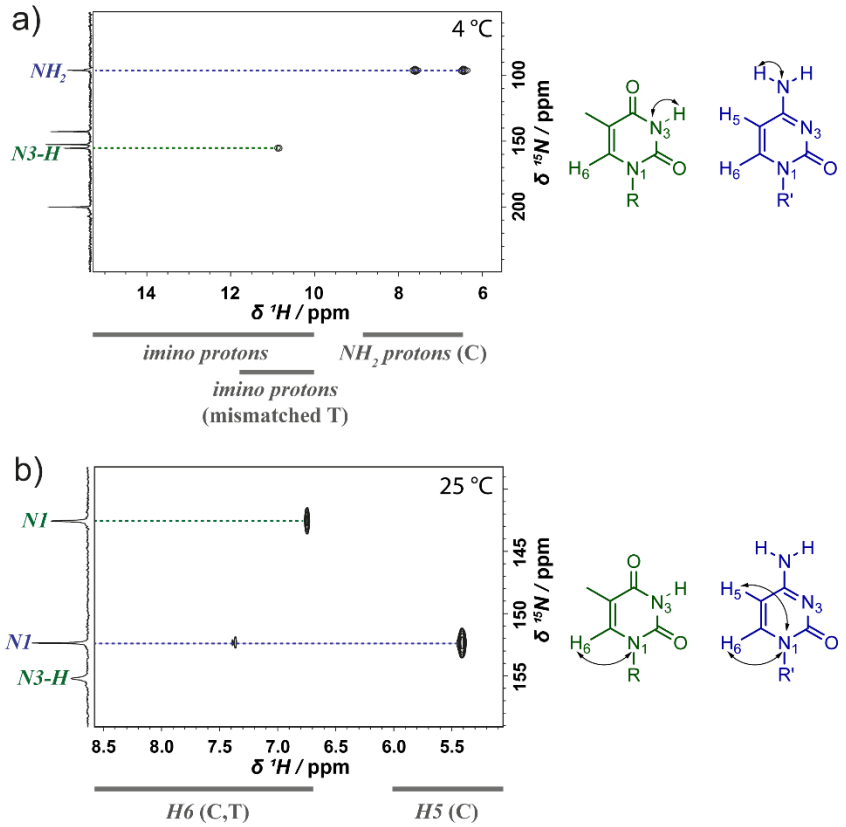

Figure 5.6. a) ^{1}J ^{1}H,^{15}N coupling of thymidine *N3*-H (green) and ^{1}J ^{1}H,^{15}N coupling of cytosine exocyclic amine (blue) according to [^{15}N,^{1}H]-HSQC spectrum at 4 °C. b) ^{3}J ^{1}H,^{15}N coupling between thymidine *N1* and H5 (green) and ^{3}J ^{1}H,^{15}N- and ^{2}J ^{1}H,^{15}N coupling between cytosine *N1* and H5 and H6 (blue) observed in the long-range [^{15}N,^{1}H]-HSQC spectrum at 25 °C. DNA samples contained 1.0 mM duplex DNA in aqueous buffer (200 mM $NaClO_4$, 50 mM cacodylic acid in H_2O / D_2O (9:1) at pH = 7.8) and were measured at the indicated temperature.

Upon addition of 1.5 equiv of Hg^{II} to "C*-T*" two sets of ^{15}N-resonances could be observed, corresponding to a major and a minor species in a ratio ~75% and ~25%, respectively (Figure 5.7). In the presence of only 1.0 equiv of Hg^{II}, these same signals were observed, in addition to those of unbound DNA, confirming that the formation of the minor species was not due to the small excess of Hg^{II} (Figure A25, Appendix). 1D ^{15}N spectroscopy and [^{15}N,^{1}H]-HSQC spectra allowed assignment of all ^{15}N signals and the metal coordination site for both the major and minor binding modes (Figure 5.7 – 5.9). The major species contained two (*N3*)C-Hg^{II}-(*N3*)T base pairs, and the minor species (*C4-NH*)C-Hg^{II}-(*N3*)T base pairs (Figure 5.7 a). Disappearance of the imino signal in ^{1}H NMR and of the *N3-H* cross peak in the ^{1}J [^{15}N,^{1}H]-HSQC spectrum demonstrated deprotonation of thymidine *N3* upon addition of 1.5 equiv of Hg^{II} (Figure 5.8). Consistent with previous reports,[47] the large downfield shift of thymidine $N3^{major}$ (Δppm = +29) and $N3^{minor}$ (Δppm = +28) suggested direct (T)*N3*-Hg^{II} coordination for both binding modes (Figure 5.7, Tables A5 – A6, Appendix). ^{3}J ^{1}H,^{15}N- and ^{2}J ^{1}H,^{15}N coupling of *N1* to H5 and/or H6 observed in the long-range [^{15}N,^{1}H]-HSQC spectrum allowed the assignment of $N1^{major}$ and $N1^{minor}$ resonances, as well as H5 and

H6 protons for cytosine and H6 of thymidine (Figure 5.9). The appearance of a single cross peak in the direct [^{15}N,^{1}H]-HSQC spectrum at 124/6.39 ppm indicated deprotonation of cytosine (*C4-NH^{minor}*) in the minor binding mode (Figure 5.8 a). The large downfield shift of cytosine *C4-NH^{minor}* (Δppm = +28, Figure 5.7, Table A5 – A6, Appendix) and a doublet observed in the proton-coupled [^{15}N,^{1}H]-HSQC (*J* = 86 Hz, Figure 5.8 c) suggested direct Hg^{II} coordination to the *N4* in the minor species. NOE cross peak between *C4-NH*^{minor} (6.39 ppm) to cytosine H5 confirmed the identity of the *^{15}N*-resonance (124 ppm) as being the deprotonated exocyclic amine of cytosine (Figure 5.10). ^{3}J ^{1}H,^{15}N-coupling of the ^{15}N-signal at 207 ppm to *C4-NH*^{minor} as well as to *C4-NH$_2^{major}$* was observed in a band-selective, long-range [^{15}N,^{1}H]-HSQC spectrum (Figure 5.9 b). This allowed the assignment of the overlapping *^{15}N*-resonances of the *N3^{major}* and *N3^{minor}* of cytosine. It was unclear, however, whether Hg^{II} coordinated to cytosine *N3^{major}*.

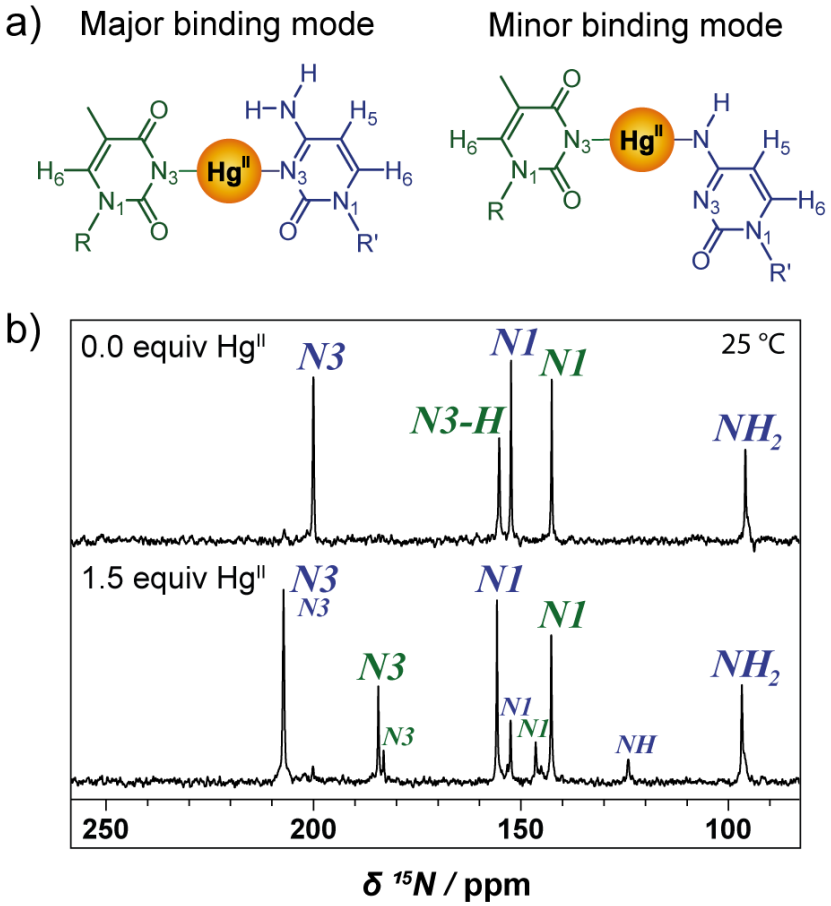

Figure 5.7. a) Major and minor coordination mode of Hg^{II} to a C-T mismatch. b) Formation of C-Hg^{II}-T according to ^{15}N NMR spectra of "C*-T*" upon addition of Hg^{II}. DNA samples contained 1 mM duplex DNA and 3 mM Hg^{II} (1.5 equiv relative to the mismatches) in aqueous buffer (200 mM $NaClO_4$, 50 mM cacodylic acid in H_2O / D_2O (9:1) at pH = 7.8) and were measured at 25 °C.

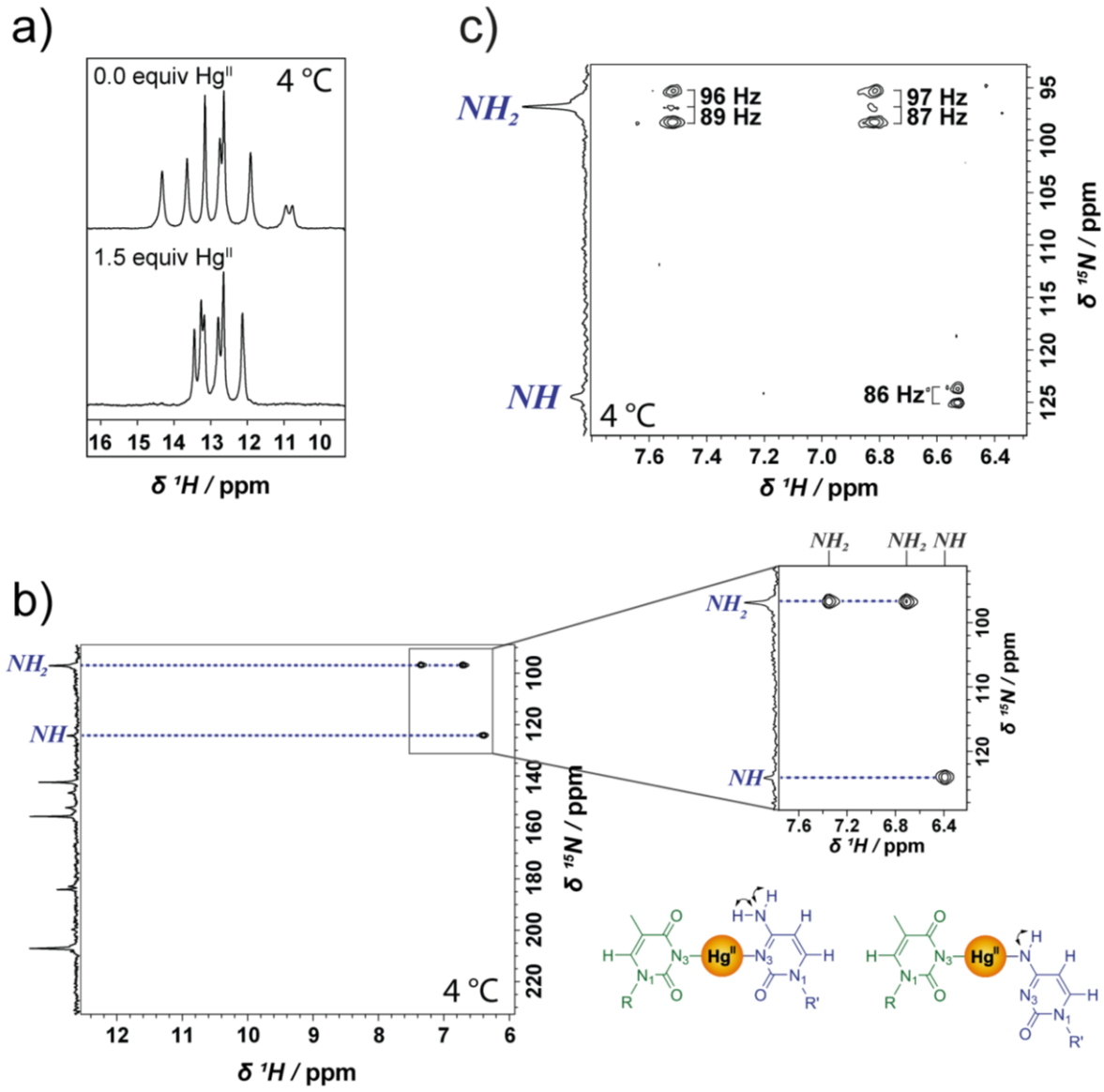

Figure 5.8. a) Deprotonation of thymidine *N3-H* upon addition of Hg^{II}. b) $^{1}J^{1}H,^{15}N$ coupling between thymidine *C4-NH*^{minor} and *C4-NH*$_2^{major}$ of cytosine according to [$^{15}N,^{1}H$]-HSQC spectrum. c) Doublet (124 ppm, ^{1}J = 86 Hz) observed in the proton-coupled [$^{15}N,^{1}H$]-HSQC spectrum confirming deprotonation of exocyclic amine in the minor binding mode. DNA samples contained 0.5 mM duplex DNA and 1.5 mM Hg^{II} (1.5 equiv relative to mismatch) in aqueous buffer (200 mM $NaClO_4$, 50 mM cacodylic acid in H_2O / D_2O (9:1) at pH = 7.8) and were measured at the indicated temperature.

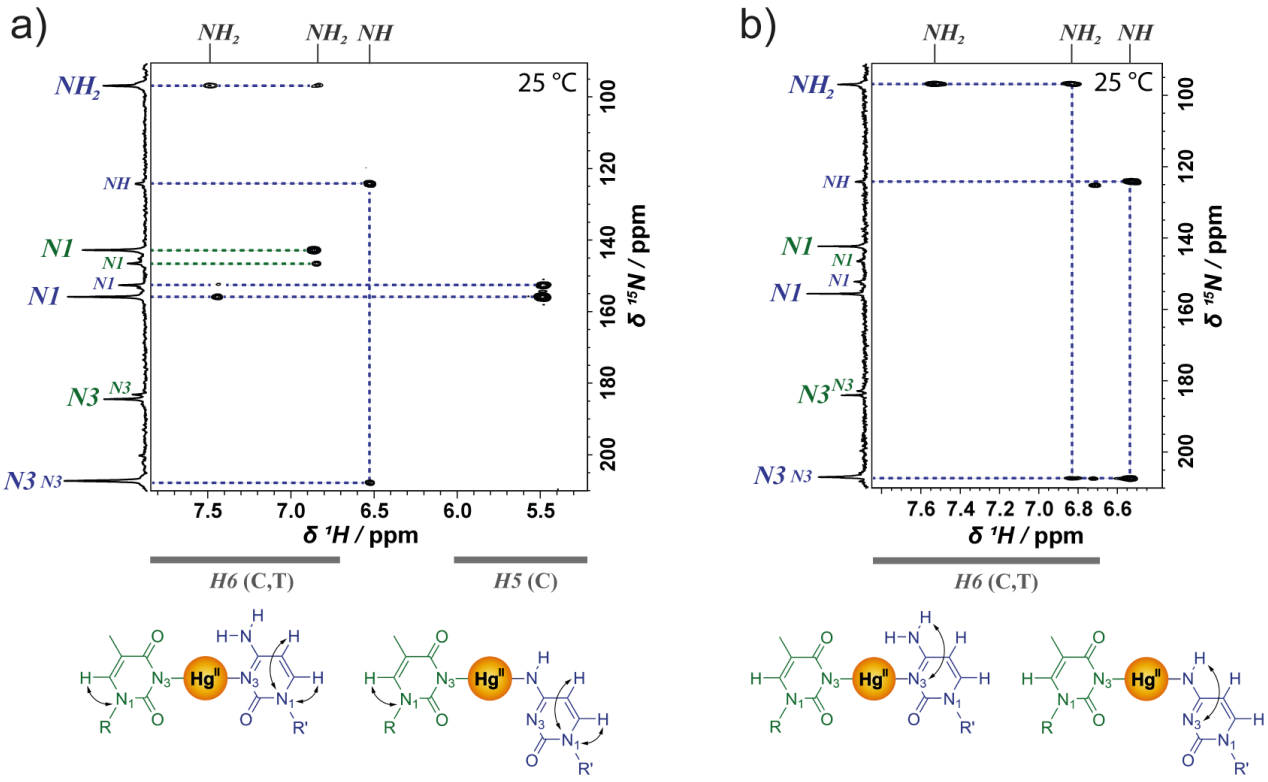

Figure 5.9. a) Assignment of *N1*^{major} and *N1*^{minor} of thymidine and cytosine by ^{3}J ^{1}H,^{15}N- and ^{2}J ^{1}H,^{15}N coupling between *N1* and H5 and/or H6 in the long-range [^{15}N,^{1}H]-HSQC spectrum. b) Assignment of *N3*^{major} and *N3*^{minor} of cytosine according to ^{3}J-coupling to *C4-NH*^{minor} and *C4-NH*$_2$^{major} in the band-selective, long-range [^{15}N,^{1}H]-HSQC spectrum at 25 °C. DNA samples contained 0.5 mM (a) and 1 mM (b) duplex DNA and 1.5 equiv of $Hg(ClO_4)_2$ in aqueous buffer (200 mM $NaClO_4$, 50 mM cacodylic acid in H_2O / D_2O (9:1) at pH = 7.8). Equiv of Hg^{II} are given relative to mismatch.

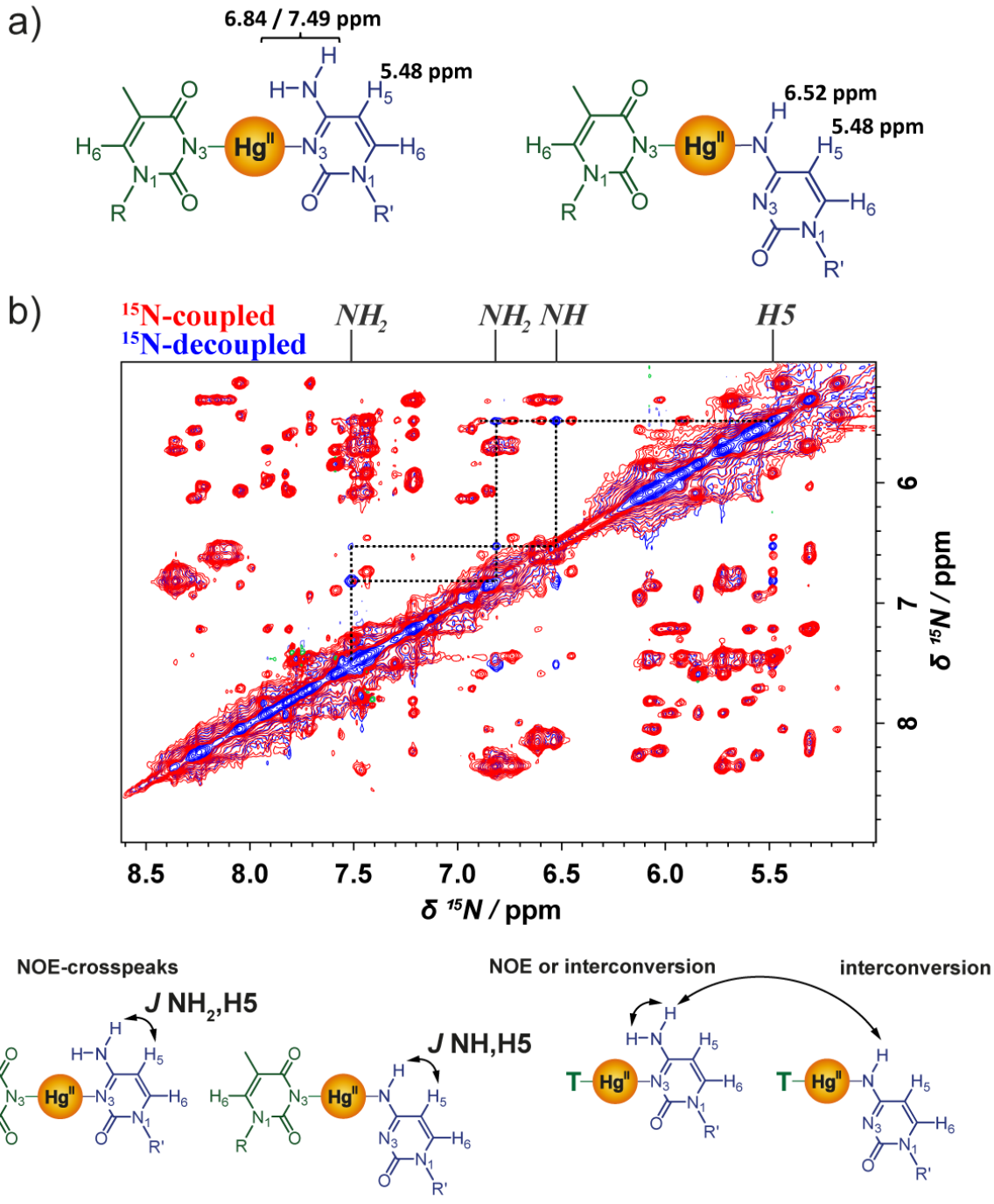

Figure 5.10. a) Chemical shift values of cytosine H5, *C4-NH*$_2^{major}$ and *C4-NH*^{minor} derived from [^{15}N,^{1}H]-HSQC and band-selective, long-range [^{15}N,^{1}H]-HSQC spectra. b) *NH*$_2$,H5 and *NH*,H5 NOE cross peaks and *NH*$_2$,*NH* exchange cross peaks observed in the ^{15}N-coupled and ^{15}N-decoupled [^{1}H,^{1}H]-NOESY spectra at 25 °C. The DNA sample contained 1 mM duplex DNA 3 mM of $Hg(ClO_4)_2$ in aqueous buffer (200 mM $NaClO_4$, 50 mM cacodylic acid in H_2O / D_2O (9:1) at pH = 7.8).

Direct detection of mercury-nitrogen binding by ^{1}J $^{15}N,^{199}Hg$ coupling has recently been reported for a T-Hg^{II}-T nucleoside complex.[59] To unambiguously determine the metal-nucleobase connectivity, we monitored changes in ^{15}N NMR spectrum of ODN1* "C*-T*" upon addition of ^{199}Hg-isotopically enriched $Hg(ClO_4)_2$ (Figure 5.11a). For the major binding mode, doublets for both cytosine and thymidine *N3*-resonances provided direct evidence for their coordination to Hg^{II} (Figure 5.11a). The exceptionally large ^{1}J $^{15}N,^{199}Hg$ coupling constant of 1095 Hz for thymidine Hg^{II}-$N3^{major}$ is consistent with previous reports on *N3*-Hg^{II} binding for a T-Hg^{II}-T nucleoside complex.[47] Cytosine $N3^{major}$-Hg^{II} bond exhibited a smaller coupling constant of ^{1}J $^{15}N,^{199}Hg$ = 114 Hz, possibly because of its weaker N-Hg^{II} bond (Figure 5.11a). A doublet of cytosine *C4-NH*^{minor} ^{15}N-resonance with a coupling constant of ^{1}J $^{15}N,^{199}Hg$ = 1052 Hz[4] demonstrated direct Hg^{II} coordination to cytosine *C4-NH*^{minor} (Figure 5.11a and b). In addition, a ^{1}H-^{199}Hg through-bond coupling with ^{2}J $^{15}N,^{199}Hg$ = 168 Hz was observed in the [^{15}N,^{1}H]-HSQC spectrum, consistent with previous reports of ^{1}H-^{199}Hg coupling over nitrogen (Figure 5.11b).[60] A doublet in the cross peak between cytosine $N3^{major}$ and *C4-*NH_2^{major} in the band-selective, long-range [^{15}N,^{1}H]-HSQC confirmed our assignment as $N3^{major}$ of cytosine (Figure 5.11c).

Taken together, these results provided the exact binding mode of Hg^{II} to duplex DNA containing C-T mismatches. Surprisingly, Hg^{II} binds via two distinct coordination modes. The major binding site (~75%) is *N3* of cytosine and *N3* of deprotonated thymidine to give (*N3*)C-Hg^{II}-(*N3*)T base pairs. The minor C-Hg^{II}-T binding mode (~25%), is via *N3* of deprotonated thymidine and deprotonated *C4-NH* of cytosine. The ratio of major/minor C-Hg^{II}-T base pair connectivity was determined by integration of ^{15}N signals in the 1D ^{15}N NMR spectra.

[4] Because of the higher signal-to-noise ratio in the [^{15}N,^{1}H]-HSQC spectra for the *C4-NH* signal the ^{1}J $^{15}N,^{199}Hg$ coupling constant determined from the [^{15}N,^{1}H]-HSQC spectra is reported.

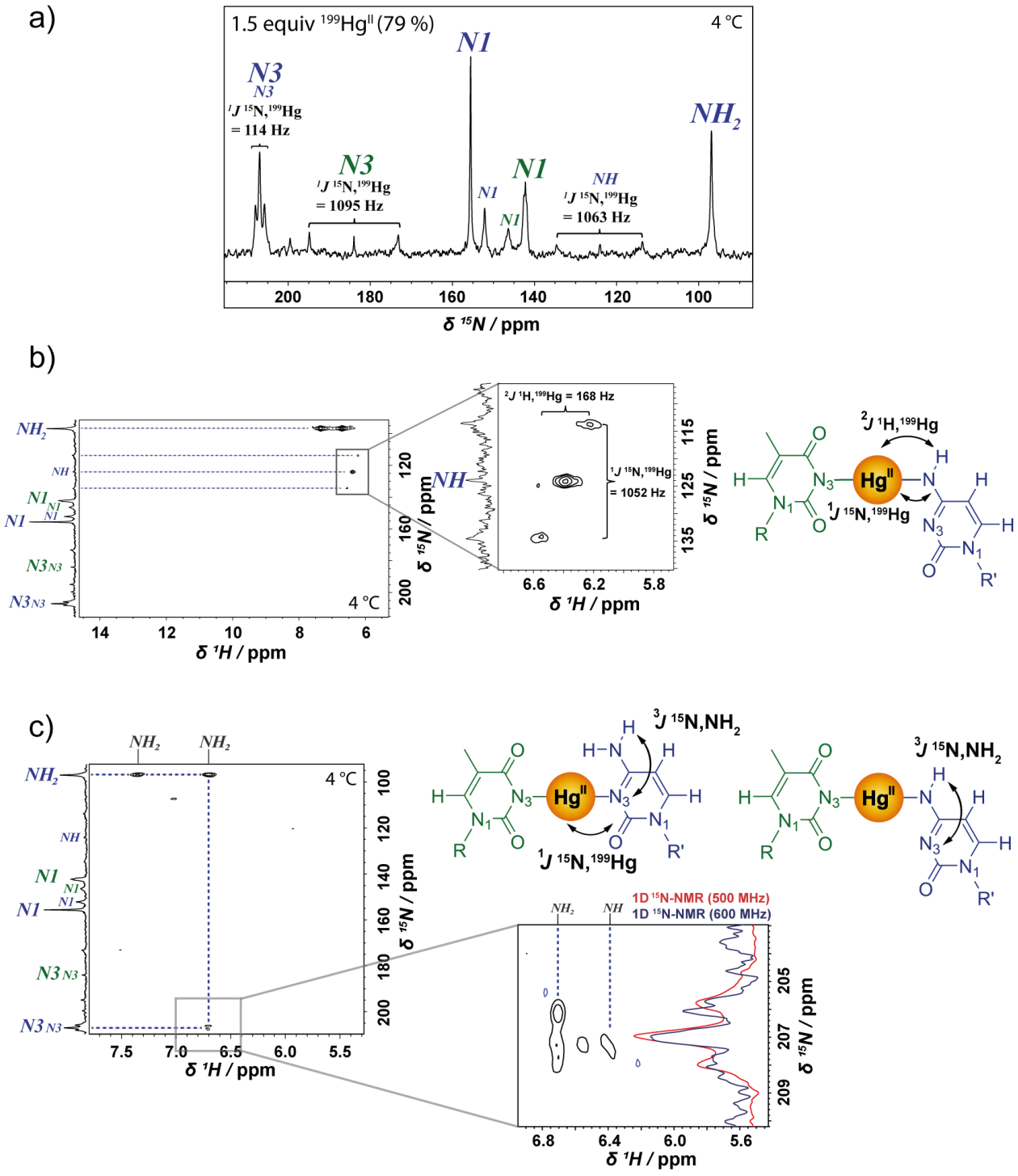

Figure 5.11. a) ^{1}J ^{15}N,^{199}Hg coupling according to ^{15}N NMR spectrum of ODN[1]* "C*-T*" with 1.5 equiv of ^{199}Hg-enriched $Hg(ClO_4)_2$ (79 % enriched). b) ^{1}J ^{15}N,^{199}Hg and ^{2}J ^{1}H,^{199}Hg coupling according to [^{15}N,^{1}H]-HSQC. c) ^{3}J ^{1}H, ^{15}N coupling between *N3*^{major} and C*4-NH*$_2$ of cytosine and ^{3}J ^{1}H,^{15}N coupling between *N3*^{minor} and deprotonated C*4-NH* of cytosine observed in the band-selective, long-range [^{15}N,^{1}H]-HSQC spectrum. The DNA sample contained 1 mM duplex DNA and 3 mM of ^{199}Hg-enriched $Hg(ClO_4)_2$ in aqueous buffer (200 mM $NaClO_4$, 50 mM cacodylic acid in H_2O / D_2O (9:1) at pH = 7.8), and the spectra were measured at 4 °C.

5.4 Global Helical Structures of Duplex DNA Containing C-Hg^{II}-T Base Pairs With Major and Minor Connectivity

Various biological processes depend on the structural polymorphism exhibited by DNA. In addition to recognition of bases by hydrogen bonding interactions,[61] the intrinsic conformational flexibility of duplex DNA can play an important role in mediating DNA-protein binding.[62] Local transitions between B-form and A-form or more subtle variations observed in A/B-intermediate states can provide specific recognition sites for protein binding.[4,5,63] Ligand-induced conformational changes have also been reported to enhance selectivity of DNA recognition.[62,64]

To investigate the impact of C-Hg^{II}-T formation on the global helical structure of duplex DNA, we solved the solution structures of ODN^1 "C-Hg^{II}-T" (Figure 5.12). The chemical shift differences of H1', H2', H2'', and the aromatic signals of major- and minor species (Figure 5.13) allowed for determination of the major duplex structure containing two (*N3*)C-Hg^{II}-(*N3*)T base pairs, as well as the minor duplex structure containing two (*C4-NH*)C-Hg^{II}-(*N3*)T base pairs (Figure 5.12b-c). The largest chemical shift differences between major- and minor duplex occurred at the C-Hg^{II}-T base pair sites and for residues T8 and G9 in the center of the duplex (Figure 5.13). The assignments of the proton resonances for each duplex were based on sequential walking along H1' and aromatic protons (H1'$_n$→ H6/H8$_{n+1}$ → H1'$_{n+1}$) (Figure 5.14). As cross references for our assignment the H2'/aromatic, H2''/aromatic (H2'/H2''$_n$ → H6/H8$_{n+1}$ → H2'/H2''$_{n+1}$), and aromatic/aromatic (H6/H8$_n$ → H6/H8$_{n+1}$ → H6/H8$_{n+2}$) regions in the [^{1}H,^{1}H]-NOESY spectrum, [^{1}H,^{1}H]-COSY spectrum (H1' → H2'/H2'') and [^{15}N,^{1}H]-HSQC spectra (aliphatic and aromatic regions) were used. Except for the first and last residues of the duplexes (C1 and G14), the signals of major and minor duplexes were well resolved and the sequential walk could be followed through the entire sequence for both species. Models for major and minor duplex were constructed based on 646 and 640 NOE conformationally restrictive distance restraints, respectively (Table 5.1). Given the experimental C_2 symmetry of the duplex observed in all NMR spectra, a non-crystallographic symmetry term was introduced for the structure calculations. Superimposition of the 20 lowest energy structures gives an overall root mean square deviation (r.m.s.d) of all heavy atoms of 1.21 ± 0.42 Å for the major duplex and 1.09 ± 0.35 Å for the minor duplex (Figure 5.12b, Table 5.1). The r.m.s.d. of all heavy atoms for the major C-Hg^{II}-T and minor C-Hg^{II}-T residues is 0.76 ± 0.28 Å and 0.75 ± 0.29 Å, respectively (Table 5.1).

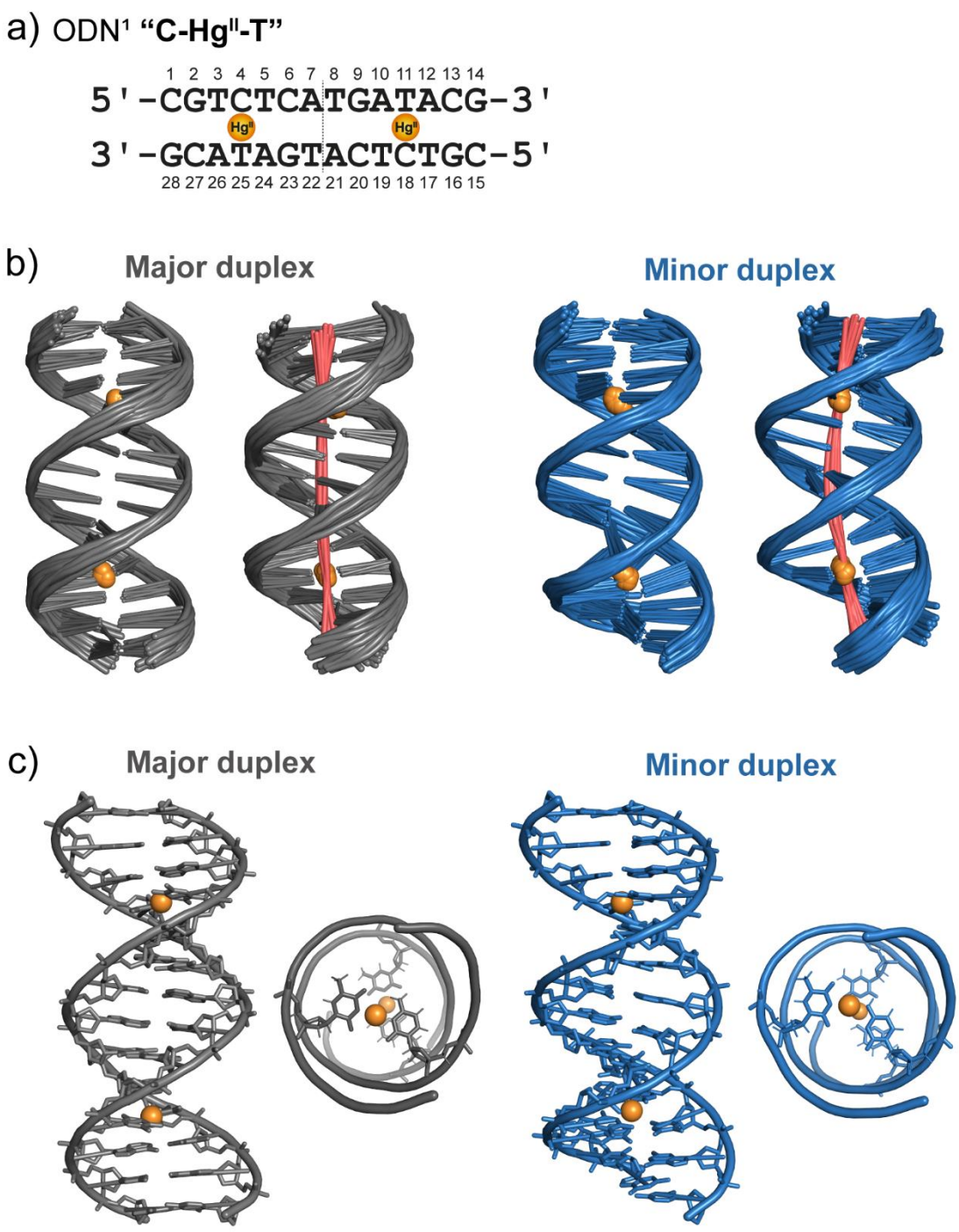

Figure 5.12. a) DNA sequence used for solution structures. b) Side-view overlay of 20 lowest energy conformations for major duplex species (right, grey) and minor duplex species (left, blue) with the helical axis reference (right, pink) calculated using Curves+.[65] From the 200 refined structures, the 20 lowest energy structures were visualized and analyzed. The structure with zero outliers in the geometric quality criteria was chosen as representative model for visualization for each major- and minor duplex (major: model 1, minor: model 6) (See Chapter 6, Experimental Procedures for a more detailed description of structures calculations and geometric quality criteria). 20 duplexes were aligned to the representative model. c) Side view and top view of representative major duplex (model 1, grey) and minor duplex (model 6, blue). In the top view only the C-Hg^{II}-T base pairs are shown. Hg^{II} ions are depicted in gold. All duplexes were visualized using PyMOL.[66]

Table 5.1. NMR Restraints and Statistics for Major and Minor Duplex Structures[a]

	Major duplex	Minor duplex
NOE-derived distance restraints[b]	646	640
Intra-nucleotide	266	264
Inter-nucleotide (*i-j* = 1)	306	302
Long-range (*i-j* = ≥ 2)	74	74
C-Hg^{II}-T base pair	158	148
Repulsive	0	0
NOE restraints per residue	23.07	22.86
NOE violation > 0.2 Å	0	0
Dihedral restraints[b,c]	168	168
Dihedral violations > 5.0 °	0	0
Hydrogen-bond restraints[b,c]	62	62
Planarity[c]	24	24
r.m.s.d (for all heavy atoms to the best structure, Å)		
Overall	1.21 ± 0.42 Å	1.09 ± 0.35 Å
Helix	1.35 ± 0.45 Å	1.20 ± 0.35 Å
C-Hg^{II}-T base pairs	0.76 ± 0.28 Å	0.75 ± 0.29 Å

[a] All statistic values are given for the 20 lowest energy structures from 200 calculated structures. [b]Experimentally derived contraints. [c]Introduced contraints. For detailed restraints values see Appendix.

^{13}P resonances (-2.0 – 0.0 ppm, Figure 5.15) were in a region of sugar-phosphate backbones reported for regular A- and B-form duplex DNA.[67] For the major species, all sugar protons were assigned by [^{1}H,^{1}H]-NOESY, [^{1}H,^{1}H]-COSY, and [^{1}H,^{1}H]-TOCSY experiments. Given the overlapping signals in the sugar regions and lower peak intensities of the minor species, only the H1', H2', and H2'' resonances were assigned for the minor duplex species and the same NOE-coupling patterns and NOE intensities were used as for the major species for H3', H4', H5' and H5'' for modelling calculations (See Appendix). ^{3}J-coupling constants between H1',H2' and H1',H2'' were determined for the major species by [^{1}H,^{1}H]-E.COSY measurements (Figure 5.16a, Table 5.2). Interestingly, the ^{3}J H1',H2' coupling constants for Hg^{II}-coordinated cytosine residue (^{3}J H1',H2' = 6.5) was smaller than the other residues (^{3}J H1',H2' = 7.8 – 9.3) (Figure 5.16a, Table 5.2) and is an intermediate value of those reported for C2'-endo (^{3}J H1',H2' = 9.5)[68] and C3'-endo (^{3}J H1',H2' = 1.5)[68] sugar conformations, indicating an unusual sugar pucker conformation at this position. The H1',H2'' coupling constants were similar for all residues, ranging from ^{3}J H1',H2'' = 6.6 – 7.1). These values were intermediate between those reported for C2'-endo- and C3'-endo

conformations (C2'-endo: ^{3}J H1',H2" = 5.8; C3'-endo: ^{3}J H1',H2" = 7.7) (Table 5.2). Given their lower signal intensities, the coupling constants for the minor duplex's sugar protons were not determined. However, the shape of H1',H2' and H1',H2" cross peaks in the [^{1}H,^{1}H]-COSY spectrum for Hg^{II}-bound thymidine of the minor duplex indicated similar coupling constants as for Hg^{II}-coordinated cytosine of the major duplex (Figure 5.16 b and c, Table 5.2). For these reasons, the torsion angles of all C-Hg^{II}-T base pair residues were left unconstrained for calculations of major and minor duplex structures.

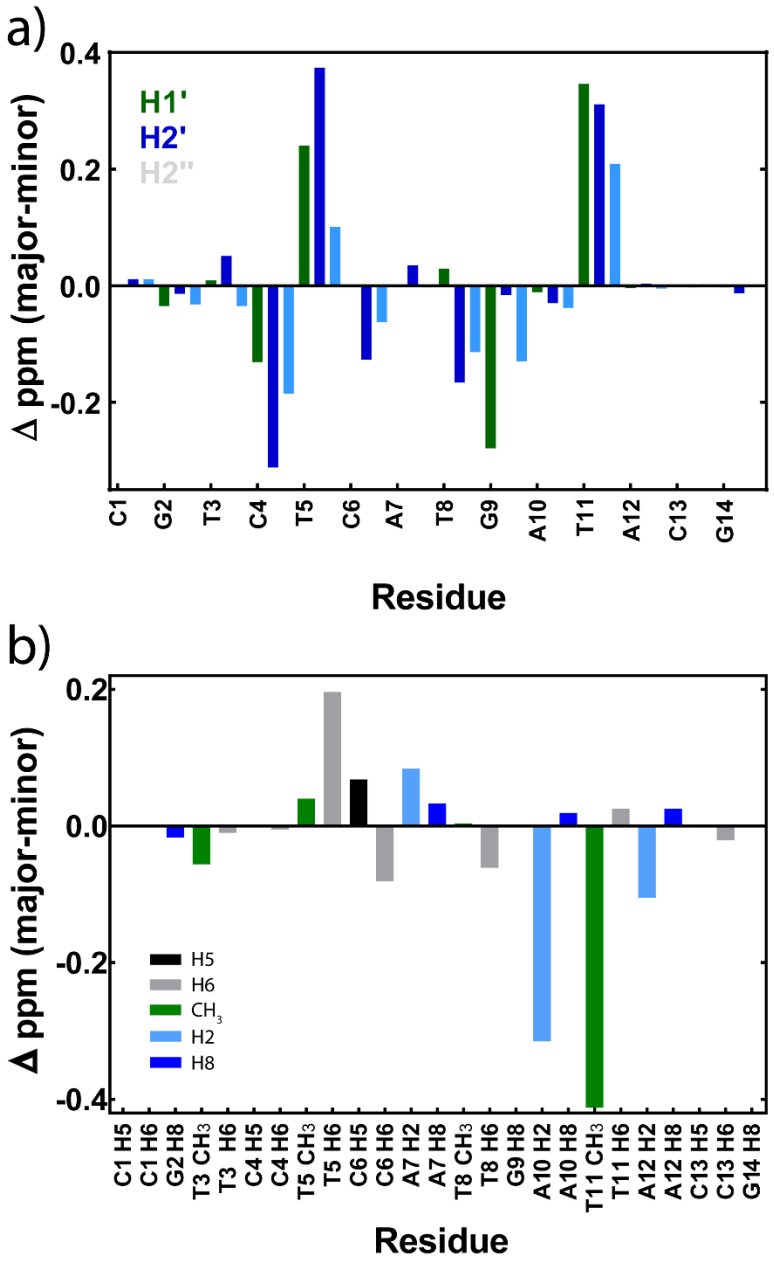

Figure 5.13. Chemical shift differences between major and minor duplexes of a) H1', H2', and H2" sugar proton signals, and b) of aromatic nucleobase signals. Δppm calculated as ppm(major) – ppm(minor). The DNA sample contained 0.4 mM duplex DNA and 1.2 mM Hg^{II} in aqueous solution of $NaClO_4$ (50 mM, D_2O, pD = 7.75) and was measured at 25 °C.

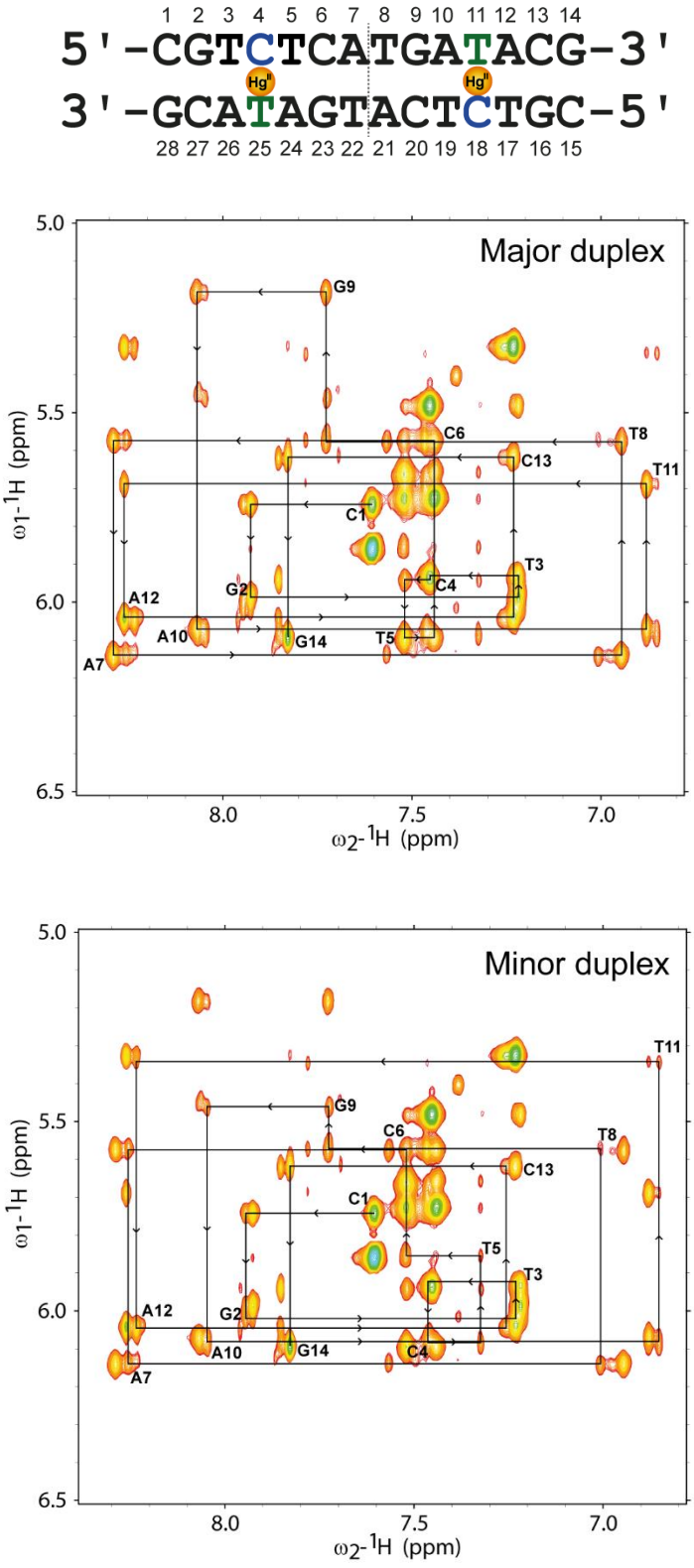

Figure 5.14. Sequential walk along H1' and aromatic protons through the entire sequence from residues C1 to G14 for major (top) and minor (bottom) duplex DNA. The DNA sample contained 0.4 mM duplex DNA and 1.2 mM Hg^{II} in aqueous solution of $NaClO_4$ (50 mM, D_2O, pD = 7.75) and was measured at 25 °C.

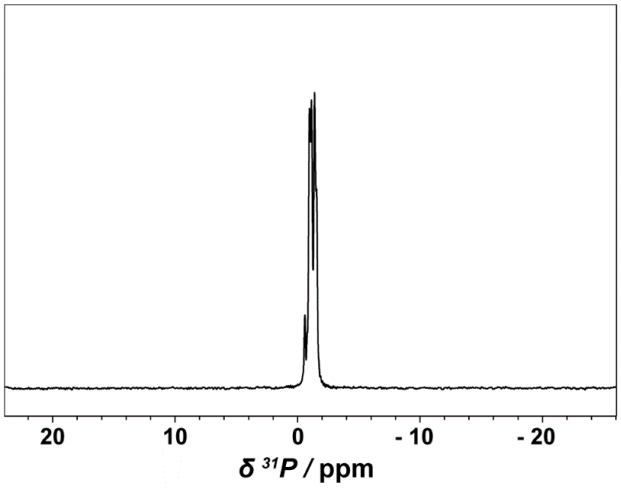

Figure 5.15. ^{31}P NMR of duplex ODN[1] "C-T" containing 0.4 mM duplex DNA and 1.2 mM Hg^{II} in aqueous solution of $NaClO_4$ (50 mM, D_2O, pD = 7.75) at 25 °C.

Table 5.2. ^3J-Coupling Constants H1',H2', H1',H2'', and H2',H2'' .[a]

Residue	H1',H2'	H1',H2''	H2',H2''
C1	7.8	6.9	13.8
G2	9.2	6.6	13.2
T3	8.6	6.9	13.7
C4	6.5	6.6	14.6
T5	n. d.	n. d.	n. d.
C6	8.4	7.1	13.5
A7	9	6.6	14.1
T8	n. d.	n. d.	n. d.
G9	n. d.	n. d.	n. d.
A10	n. d.	n. d.	n. d.
T11	9.3	6.9	14.9
A12	n. d.	n. d.	n. d.
C13	8.3	6.6	13.8
G14	8.4	6.6	13.9
S-type (C2'-endo)[68]	9.5	5.8	14.1
N-type (C3'-endo)[68]	1.5	7.7	14.1

[a] The DNA sample contained 0.4 mM duplex DNA and 1.2 mM Hg^{II} in aqueous solution of $NaClO_4$ (50 mM, D_2O, pD = 7.75) and was measured at 25 °C. n.d. = not determined.

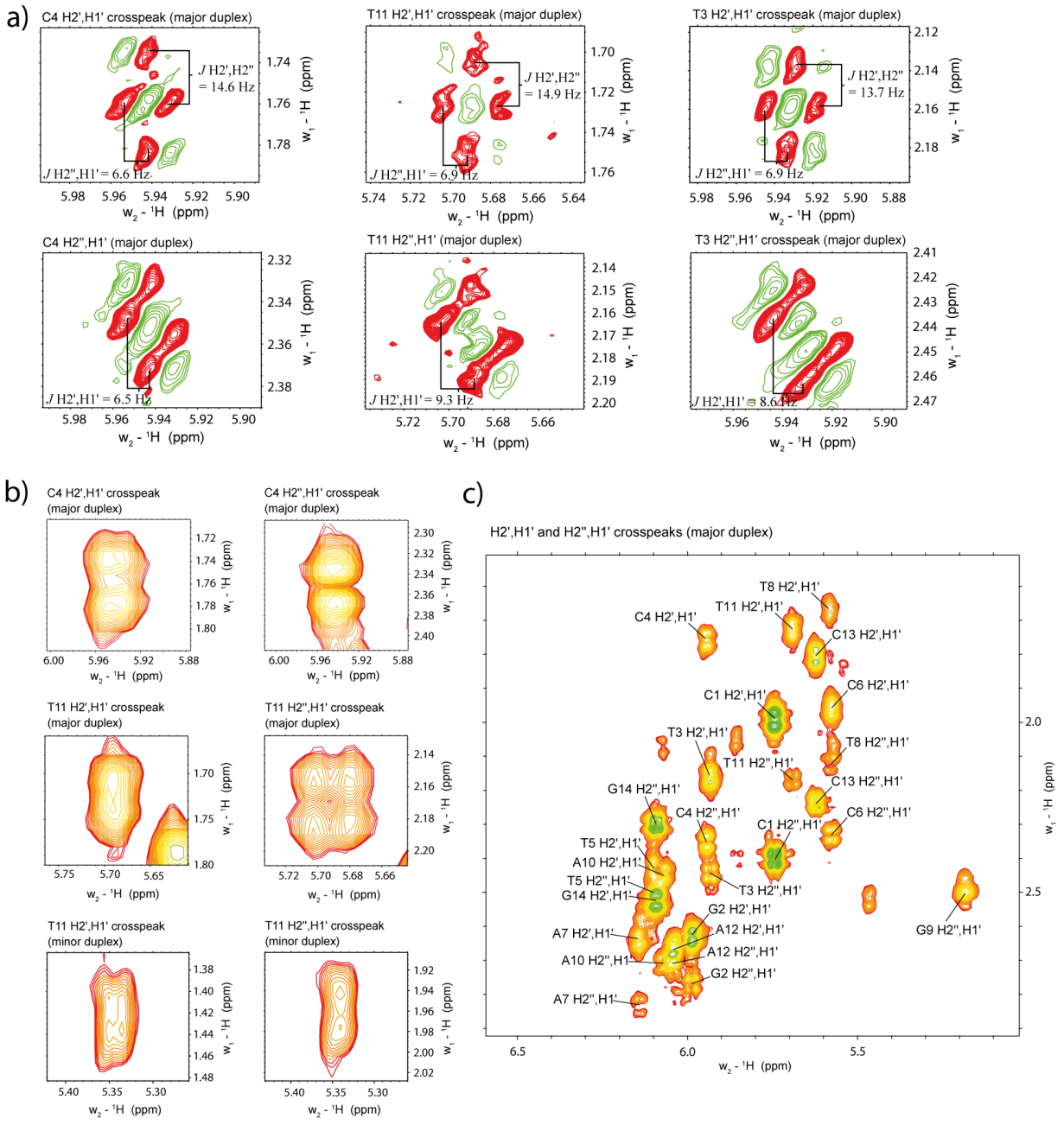

Figure 5.16. H1',H2' and H1',H2" cross peaks in [^{1}H,^{1}H]-E.COSY and magnitude-processed [^{1}H,^{1}H]-COSY. a) Coupling constants determined by [^{1}H,^{1}H]-E.COSY spectrum for Hg^{II}-bound residues C4 and T11 (left and middle) and coupling constants of T3 as a selected example for a Hg^{II} unbound residue. b) H1'-H2' and H1'-H2" cross peaks in magnitude processed [^{1}H,^{1}H]-COSY for Hg^{II}-coordinated residues. c) H1'-H2' and H1'-H2" cross peaks of the major duplex in the magnitude processed [^{1}H,^{1}H]-COSY spectrum. The DNA sample contained 0.4 mM duplex DNA and 1.2 mM Hg^{II} in aqueous solution of $NaClO_4$ (50 mM, D_2O, pD = 7.75) and was measured at 25 °C.

To investigate the conformations of the major and minor duplexes in detail, we analyzed their helical and base pair parameters calculated by Curves+[65] and 3DNA[69,70] (Figures 5.17 – 5.22, Figure A26 – A27, Appendix). Both duplexes exhibited an overall "mixed" A/B-form topology. The major species adopted a more B-form-like structure, whereas the minor species exhibited more A-form-like characteristics. Changes in CD spectra upon addition of Hg^{II} resembled differences reported for "mixed" A/B-type RNA/DNA hybrid duplexes versus B-form DNA/DNA duplex analog, thereby providing support for the mixed A/B-form of C-Hg^{II}-T-containing oligonucleotides.[71] Both duplexes exhibited shorter C1'-C1' distances (9.6 – 10 Å) between cytosine and thymidine of C-Hg^{II}-T base pairs as compared to the non-metallated residues (~10.6 Å) (Figure 5.17a). One structural parameter in characterizing A-, B- and "mixed" A/B intermediate helical structures is the Zp parameter, which describes the displacement of the phosphate group from the middle of a base pair.[72] For both duplexes, the positioning of the phosphate groups closely corresponded to B-form duplex DNA (Figure 5.17b). However, no single parameter alone can be used for the assignment of duplex conformations.[69,70] DNA conformation and variations from pure B- and A-form can also be investigated by structural parameters such as major- and minor groove dimensions, sugar pucker conformation, torsion angles, base pair displacements and inclination, helical rise, helical twist and base stacking parameters. Notable differences of these parameters are observed between major and minor species of C-Hg^{II}-T-containing duplex DNA.

B- to A-form transitions result in changes in the major- and minor groove widths and depths. The negative X-displacement (translation of the base pairs towards the grooves) results in an A-form duplex with a narrower and deeper major groove and a wider and shallower minor groove compared to B-form duplex.[73,74] The major C-Hg^{II}-T-containing duplex exhibited major groove dimensions and minor groove depths similar to canonical B-form duplex DNA and minor groove widths intermediate between standard A- and B-forms(Figure 5.17c-d). The minor C-Hg^{II}-T-containing duplex showed larger deviations from B-form duplex, with a decreased major groove width, increased major groove depth, and increased minor groove width, making this helix more A-form like than the major duplex species (Figure 5.17c-d, Figure 5.19a). A prominent feature of A-form duplex DNA is the distinct tilting of the base pairs with respect to the helical axis by 20 °.[65] The minor duplex DNA exhibited larger tip angles (rotation around the long axis of the base pair) compared to the major duplex DNA, and for both duplexes the tilting of the base pairs (mean inclination angle ~9 °) was intermediate between B- and A-form duplexes (0 ° and 20 °, respectively) (Figures 5.18a-b).[65] Interestingly, the minor C-Hg^{II}-T-containing duplex exhibited smaller inclination angles (~5.5 °) for the base pairs located 3' and 5' from the C-Hg^{II}-T base pairs, and larger angles in the center of the duplex (~12 °) (Figure 5.18b, Figure 5.19b). Local twist polymorphisms have been suggested to be structural recognition sites for protein binding and play important roles in regulatory regions such as d(CpG) motifs.[64] Interestingly, the minor C-Hg^{II}-T-containing duplex DNA exhibited a pronounced unwinding at the C-Hg^{II}-T base

pair site (helical twist = 28 °) and a higher twist to the neighboring step (helical twist = 42°) (Figure 5.18c). This resulted in a lower helical rise at the C-Hg^{II}-T base pair site (2.7 Å) which corresponds to the helical rise of standard A-form duplex DNA (A-form: 2.72 Å; B-form: 3.35 Å).[65] A decreased helical rise at the C-Hg^{II}-T site was also observed in the major duplex species (2.95 Å) (Figure 5.18c). The same twist trends could also be observed in the rise- and twist parameters which reflect the base pair stacking geometries at a dimer step level (Figure 5.18d). Translation of base pairs with respect to the helical axis was similar for major and minor C-Hg^{II}-T-containing duplexes. The minor duplex species exhibited a slightly larger x-displacement (translation of base pairs towards the grooves) for residues flanking the C-Hg^{II}-T base pairs and an increased y-displacement (translation of base pairs perpendicular to the grooves) for the C-Hg^{II}-T base pair as compared to the major duplex (Figure 5.20a). The (*C4-NH*)C-Hg^{II}-T(*N3*) connectivity of the minor species induced a perturbation of the local dimer step shift Dx parameter and a more A-form like slide Dy at the C-Hg^{II}-T base pair site (Figure 5.20b).

B- to A-transformations have been suggested to provide a mechanism for smooth bending of duplex DNA and thereby alter the accessibility of the minor groove for protein interactions.[62] Protein binding can induce kinking or smooth bending of duplex DNA and the propensity to deformation has been suggested to be a critical component for the specificity of DNA recognition by proteins. C-Hg^{II}-T-containing duplex DNA with minor metal-nucleobase connectivity exhibited a slightly curved helical structure with an axial bend of 2 ° in the center of the duplex (Figures 5.20c and 5.21). The same type of deformation was also observed in the curvature analysis of the duplexes, which compares the curvature to the nucleosome structure of DNA (PDB ID 1KX5[75]) (Figure 5.20c).[62,76] Remarkably, the central three base pairs of the minor duplex exhibits the same curvature as DNA on nucleosomes.

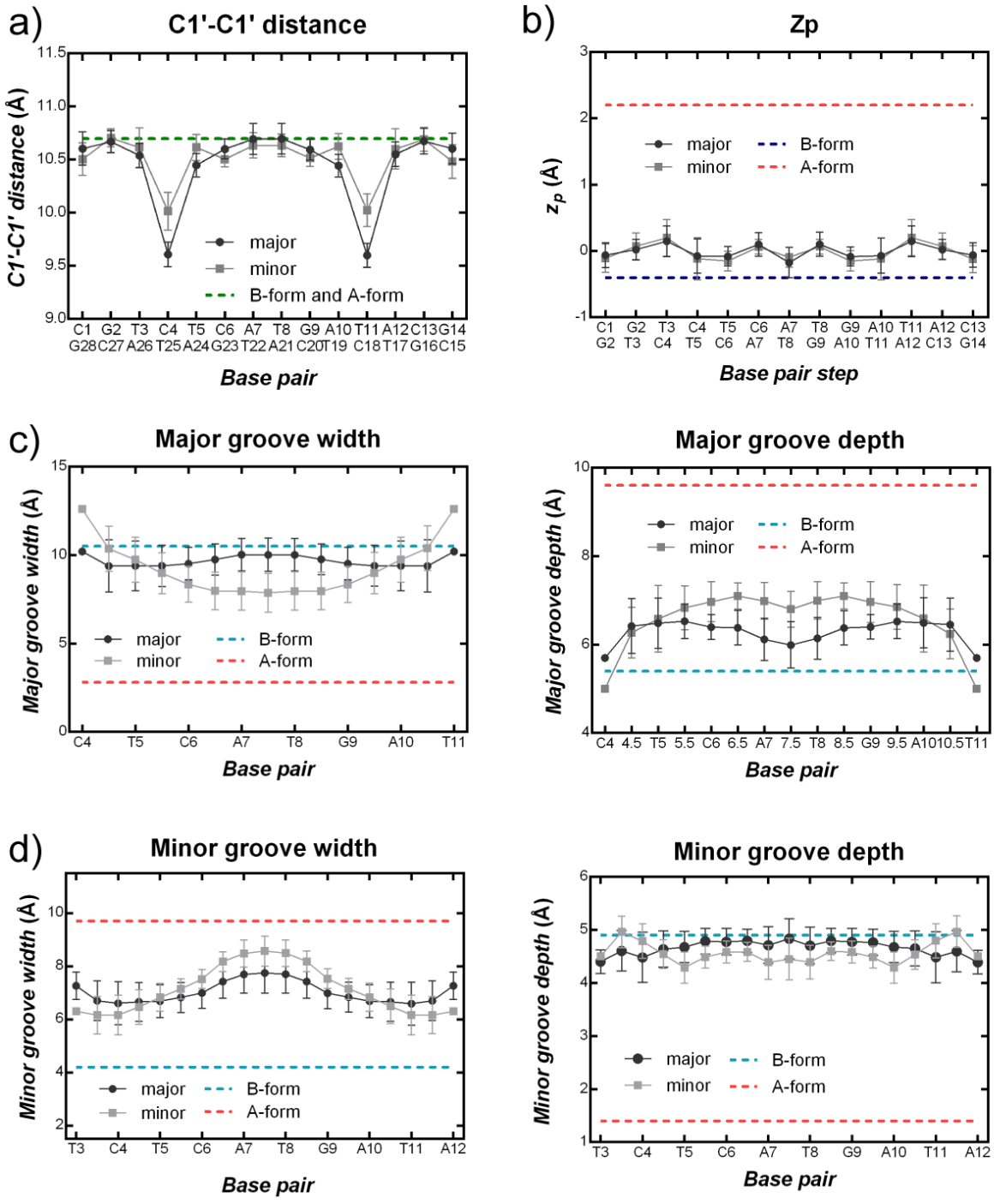

Figure 5.17. a) C1'- C1' distances in each base pair. b) Displacement of phosphate group from the middle of a base pair step (Zp). c) Major groove dimensions. d) Minor groove dimensions. C1'- C1' distance and phosphate displacement were calculated using 3DNA (a-b)[69,70] and standard A- and B- form values were taken from (ref 77) and (ref 62), respectively. Major- and minor groove dimensions were calculated with Curves+ (c-d)[65] and reference A-form and B-form values were taken from (ref 65) which analyzed crystal structures of A-DNA (PDB ID 1d13[78]) and B-DNA (PDB ID 1bna[79]) dodecamers. Reported values are mean and standard deviation of the 20 lowest energy conformations of major and minor duplex species.

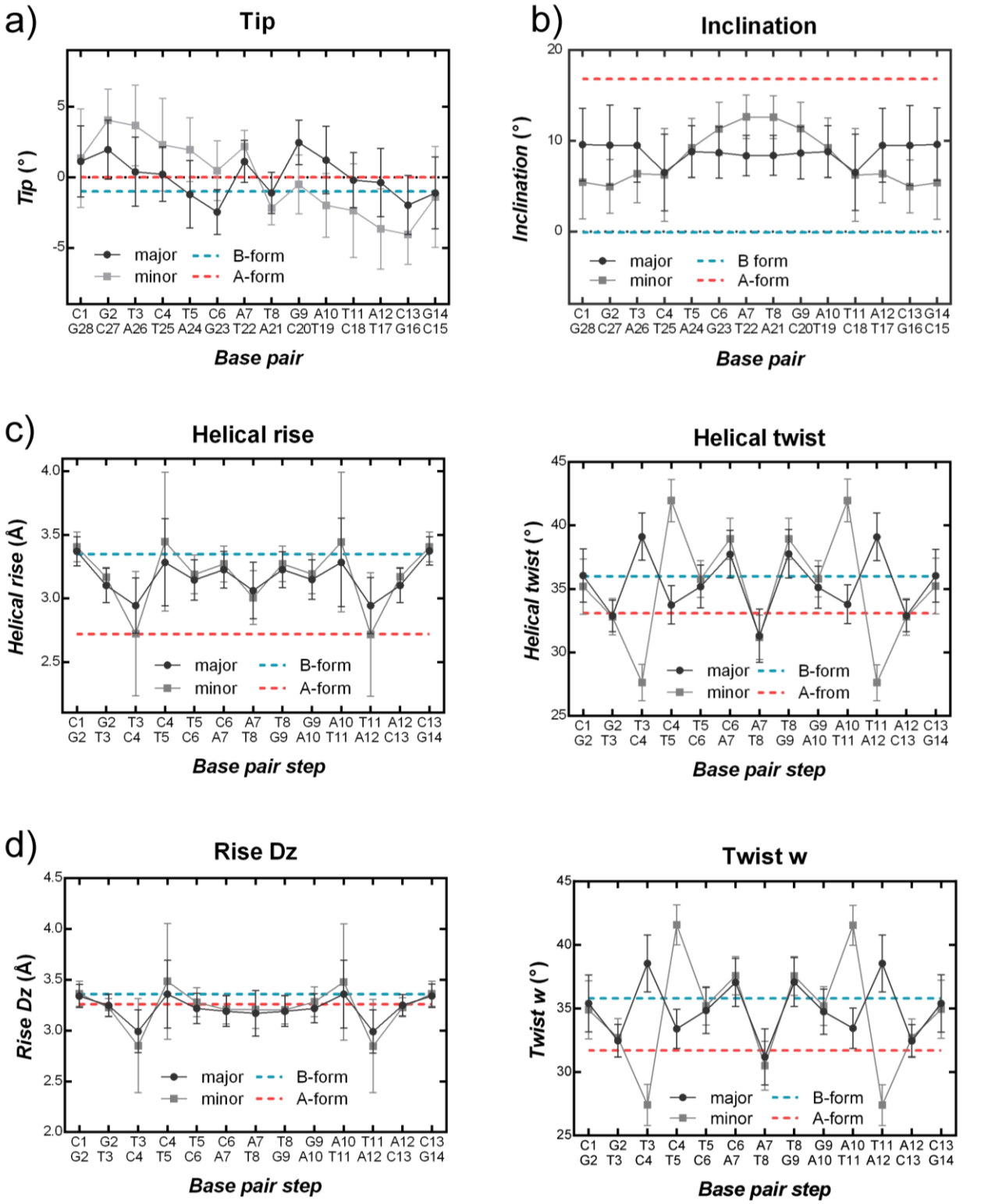

Figure 5.18. Base pair-axis parameters a) tip (rotation around the long axis of the base pair) and b) inclination of base pairs with respect to the helical axis (rotation around the short axis of the base pair). c) Helical rise (right) and helical twist angle (left). d) Rise (Dz, right) and twist angle (w, left) between base pair steps. All parameters were analyzed using Curves+[65] and represent mean and standard deviation of the 20 lowest energy conformations of major and minor duplex species. Reference A-form and B-form values were taken from (ref 65) which analyzed crystal structures of A-DNA (PDB ID 1d13[78]) and B-DNA (PDB ID 1bna[79]) dodecamers.

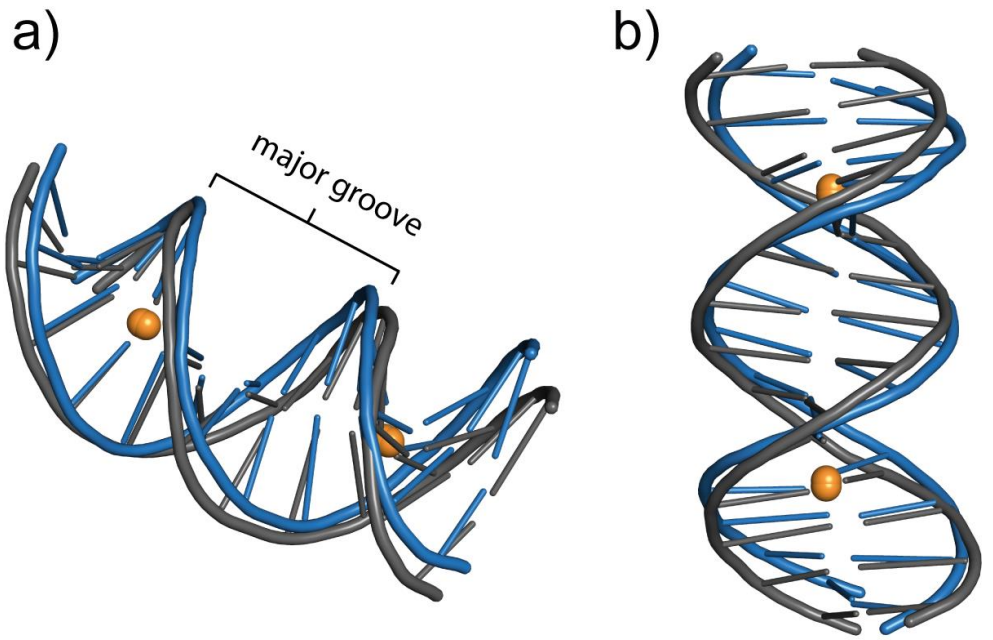

Figure 5.19. Overlay of major duplex species (grey) minor duplex species (blue). a) Side-view of the major groove. b) Side-view of overlay showing the increased inclination of the base pairs in the center of the minor duplex species (blue). Duplexes were aligned to the Hg^{II} ions (gold) and were visualized using PyMOL.[66]

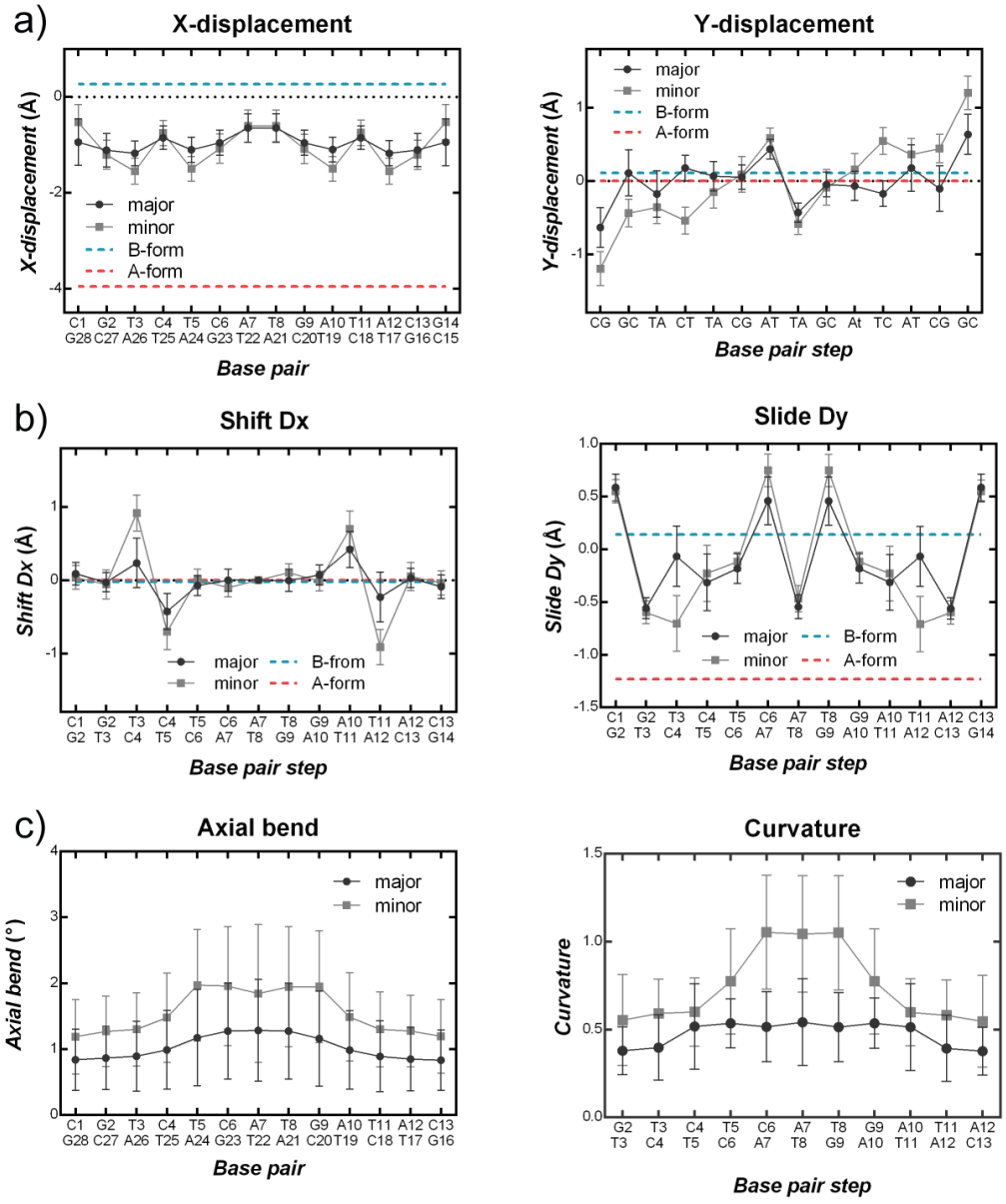

Figure 5.20. a) Translation of base pairs towards grooves (x-displacement, right) and perpendicular to the grooves (y-displacement, left). Local dimer step parameter shift (Dx, right) and slide (Dy, right) describing relative positioning of successive base pairs with respect to the x- and y-axis of the relative base pair reference frame. c) axial bend and curvature analysis of major and minor duplexes. Curvature is a dimensionless quantity normalizing the curvature to DNA on the nucleosome (curvature ~ 1).[76] All parameters were analyzed using Curves+[65] and represent mean and standard deviation of the 20 lowest energy conformations of major and minor duplex species. Reference A-form and B-form values were taken from (ref 65) which analyzed crystal structures of A-DNA (PDB ID 1d13[78]) and B-DNA (PDB ID 1bna[79]) dodecamers.

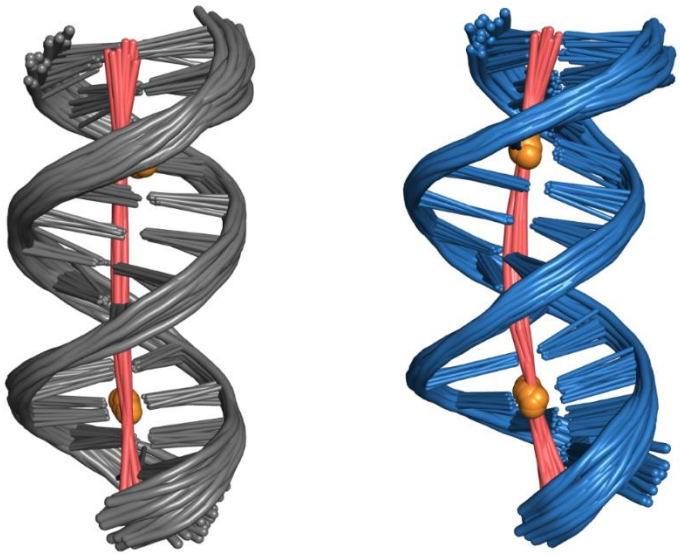

Figure 5.21. 20 lowest energy conformations of major-(grey) and minor (blue) duplex structures with inserted helical axis reference (pink) that highlights the axial bending induced by (*C4-NH*)C-Hg^{II}-T(*N3*) connectivity in the minor duplex species. The helical axis was calculated using Curves+.[65] 20 duplex conformations were aligned to the representative model containing zero outliers in the geometric quality criteria (major: model 1, minor: model 6) and visualized using PyMOL.[66]

To analyze the backbone conformations of the major-and minor duplexes we determined torsion- and pseudorotation angles and sugar pucker of the models using Curves+.[65] (Figure 5.22, Figure A26 – A27, Appendix, Table 5.3) Both duplexes exhibited similar glycosidic angles χ (-132 – -105°) which are intermediate between standard A- and B-form (A-form: -154°; B-form: -98°) (Figure A27, Appendix).[80] The largest deviations occurred at the C-Hg^{II}-T sites and T8 located in the center of the helix (-130 to -118 °), resulting in more A-form like glycosidic angles (-154 °) (Figure A27, Appendix).[80] The pseudorotation angle values (P-values = 83° – 159°), which combines the five endocyclic torsion angles, are intermediate between standard A- and B-form duplexes (Figure 5.22).[80] Interestingly, the sugar pucker amplitudes for both duplexes (mean ~27 °) were much lower than both B- and A-form amplitudes (50 ° and 41°, respectively) (Figure 5.22).[65] Flattened rings with amplitudes ranging from 20° to 30 ° can make domains of pseudorotation more accessible, thereby facilitating distortions from common C2' and C3' sugar pucker conformations of canonical B- and A-form duplexes.[81] Inspection of the 20 lowest energy models for each structure revealed a high frequency (65 – 100%) of an unusual, O4'-endo sugar pucker for residues directly coordinated to the metal ion (Table 5.3). Direct support for this was observed in the ^{3}J H1',H2' coupling constant for the Hg^{II}-coordinated cytosine residue (C4, ^{3}J H1',H2' = 6.5 Hz, Table 5.2) in the major structure that was inconsistent with both *C2*'-endo ($^{3}J_{H1'-H2'}$ = 9.5 Hz)[68] and C3'-endo (^{3}J H1',H2' = 1.5 Hz)[68] sugar conformations. Similar results were obtained for the T11 residue in the minor structure (Figure 5.16). Unfortunately, the ^{3}J H1',H2' coupling for the cytosine residue of the minor species could not be experimentally determined nor estimated from the shape of the cross peak due to overlapping signals. From a plot of ^{3}J H1',H2' as

a function of pseudorotation phase angle (P),[82] a P-value of 85° and 202° was determined for the Hg^{II}-coordinated cytosine residue of the major duplex species, which corresponded to the range of P values expected for an O4′-endo sugar pucker.[82,83] Using the *Karplus* equation[84] a torsion bond-angle of $\Phi_{1'2'}$ = 140° was calculated from the experimentally determined ^{3}J H1',H2' coupling constants, which is in excellent agreement with torsion angles observed in the solution structure models ($\Phi_{1'2'}$ = 131 °) (Figure 5.22c).[82,84] Residues flanking the metallo base pair and in the center of the duplex also exhibited a high frequency of O4'-endo and C1'-exo sugar conformations and the remaining residues adopted mostly C2'-endo sugar conformations in the models (Table 5.3). A single C3'-endo sugar puckers was observed in one of the 20 models of the major duplex. Otherwise no C3'-endo sugar puckers were observed (Table 5.3). O4'-endo and C1'-exo conformations have been previously reported to occur in mixed A/B-form conformations and in RNA/DNA hybrid structures.[85–90] Local O4'-endo sugar pucker conformations in RNA/DNA hybrids have been suggested to play a role in variable cleavage patterns by RNase H in Okazaki fragments.[86–88]

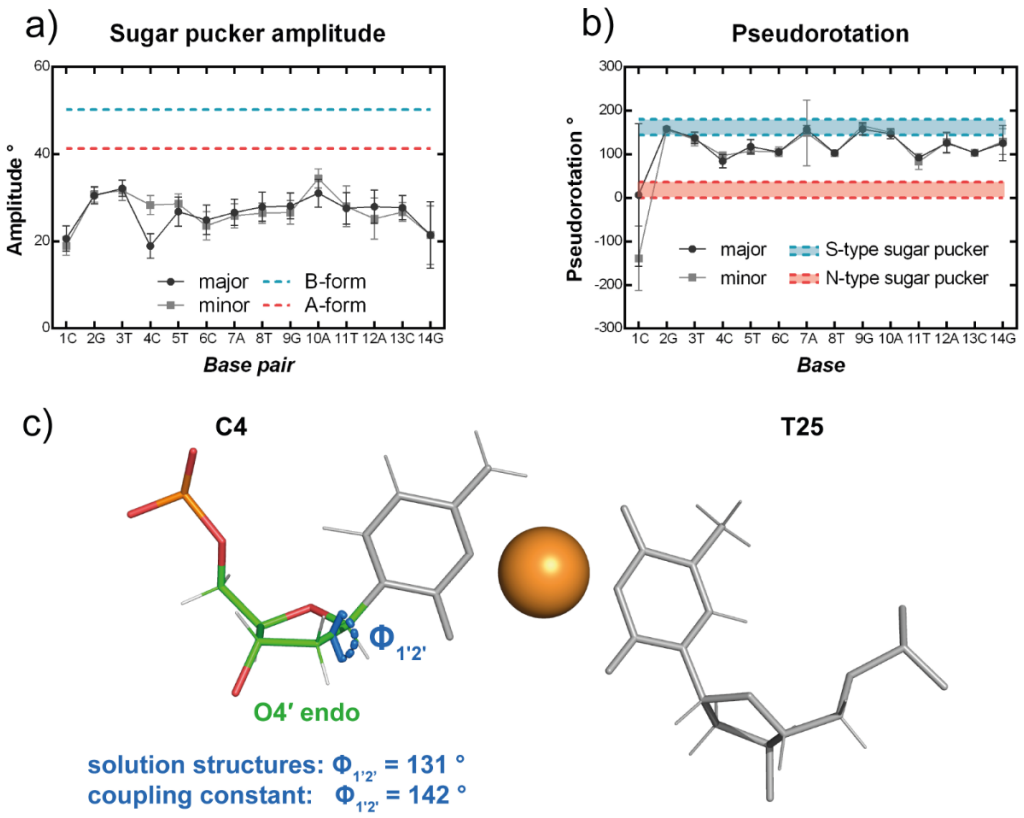

Figure 5.22. a) Sugar pucker amplitude and b) pseudorotation phase angle (P). Parameters were analyzed using Curves+[65] and represent mean and standard deviation of the 20 lowest energy conformations of major and minor duplex species. Reference A-form and B-form values for pseudorotation phase angle were taken from (ref 91) and for pucker amplitude from (ref 65) which analyzed crystal structures of A-DNA (PDB ID 1d13[78]) and B-DNA (PDB ID 1bna[79]) dodecamers. c) O4'-endo sugar pucker at the Hg^{II}-bound C4 residue of the major duplex species. The torsion angle ($\Phi_{1'2'}$ = 131 ° ± 5 °) determined from solution structures was in excellent agreement with the torsion angle calculated from the experimentally determined coupling constant ($\Phi_{1'2'}$ = 142 °) according to the *Karplus* relationship.[82,84] $\Phi_{1'2'}$ determined from the solution structures represents the mean value and standard deviation of the 20 lowest energy conformations. Figure was generated with PyMol.[66]

Table 5.3. Frequency of C2'-Endo, O4'-Endo, and C1'-Exo Sugar Pucker Conformation.[a]

Residue	C2'-endo (%)		O4'-endo (%)		C1'-exo (%)	
	major	minor	major	minor	major	minor
C1	50	5	0	0	0	0
G2	100	100	0	0	0	0
T3	50	35	0	0	50	65
C4	0	0	65	100	10	0
T5	10	0	40	55	50	45
C6	0	0	75	80	25	20
A7	95	95	0	0	5	0
T8	0	0	100	90	0	10
G9	95	100	5	0	0	0
A10	75	90	5	0	20	10
T11	0	0	100	65	0	5
A12	25	45	15	30	55	25
C13	0	0	70	100	30	0
G14	45	40	35	35	10	25

[a] % represent percentage of sugar pucker in the 20 lowest energy major and minor duplex species. Sugar pucker conformations were determined using Curves+.[65] A single C3'-endo sugar pucker was observed in one of the 20 models of the major duplex. Otherwise no C3'-endo sugar puckers were observed.

An overlay of the major and minor duplex structures illustrates that the (*C4-NH*)C-Hg^{II}-(*N3*)T connectivity of the minor duplex displaces the Hg^{II} ions, cytosine and thymidine residues towards the major groove, thereby making the Hg^{II} ions more accessible to bulk solvent (Figure 5.23). Calculations of the solvent exposed surface area (SASA) of the nucleobases and Hg^{II} ion of C-Hg^{II}-T demonstrated that C-Hg^{II}-T base pairs in the minor duplex exhibited a 20 % increase in solvent exposed surface area (SASA = 202 Å) as compared to the major duplex (SASA = 161 Å). The more solvent-exposed coordination site of Hg^{II} could explain the 10-fold increase in association and dissociation kinetics that have been reported for C-Hg^{II}-T versus T-Hg^{II}-T base pairs.[51,92] The total solvent exposed surface area (SASA) for all the nucleobases was similar for both duplexes (SASA = 1207 Å (major) and 1243 Å(minor)) and a smaller increase (12 %) in SASA was calculated for C-Hg^{II}-T base pairs together with the flanking residues, demonstrating that increase in solvent accessibility of the nucleobase residues in the minor duplex species was a local effect specific for the metallo base pair.

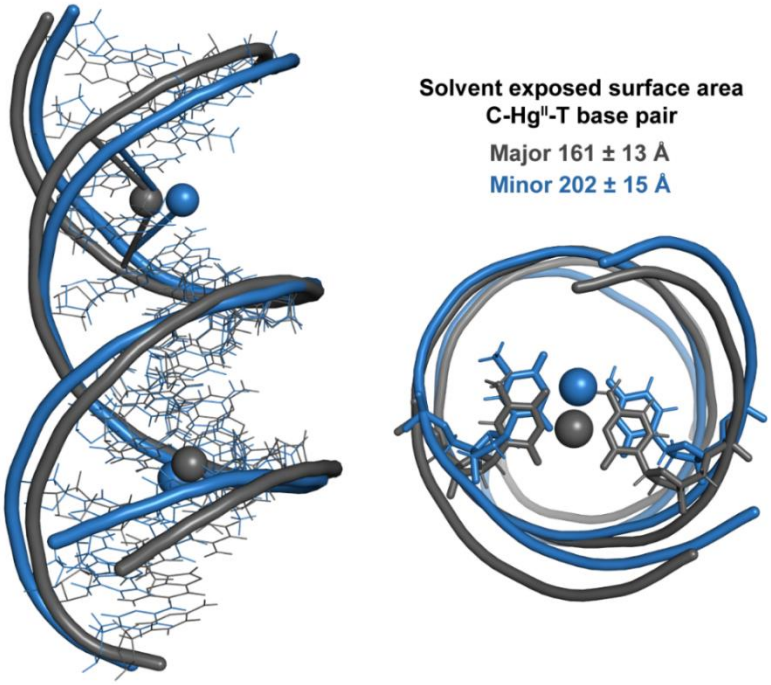

Figure 5.23. Side view (left) and top view (right) of overlay of major (grey) and minor (blue) duplex species (only one C-Hg^{II}-T base pair shown). The (*C4-NH*)C-Hg^{II}-(*N3*)T connectivity of the minor duplex displaces the Hg^{II} ion towards the major groove making it more accessible to bulk solvent (ΔSASA = 41 Å). The duplexes were aligned in the center of the helix (A7, T8, A21, T22). Solvent exposed area was calculated and figures were generated with PyMOL.[66]

5.5 Dynamics of Major – Minor Duplex Interconversion

To investigate dynamic changes in local metal ion coordination, we measured z-z exchange [^{15}N,^{1}H]-HSQC spectra with a delay before reverse INEPT. With increasing delay time (t_m), new exchange signals appeared, demonstrating that major- and minor states interconvert and that their equilibration is slow on the chemical shift NMR time scale used here (600 – 700 MHz, Figure 5.24 and 5.25). To determine rate constants of interconversion, the decreases of cross peaks and increases of exchange cross peaks were monitored as a function of delay time (t_d) at 25°C. Global fitting of integrated peak volumes versus exchange delay times using eqs 19-22[93] (Chapter 6, Experimental Procedures) furnished the rate constants (k_1 and k_{-1}) of structural interconversion, under the assumption that all proton- and nitrogen atoms have the same relaxation rate (R_1) and that the *NH* proton is converted equally to both NH_2 protons during the exchange (Figure 5.26).[93] Interconversion of major- and minor structures exhibited rate constants of $k_1 = 3.5\ s^{-1}$ and $k_{-1} = 7.7\ s^{-1}$ for the forward and reverse reactions, repectively. The Hg^{II} ions are likely to stay associated during these conformational changes, as these values are ~10^3-fold faster than the dissociation rate constants ($k_{off} \approx 10^{-3}\ s^{-1}$) of Hg^{II} from C-Hg^{II}-T base pairs in duplex DNA (Table 4.2, Chapter 4).[51]

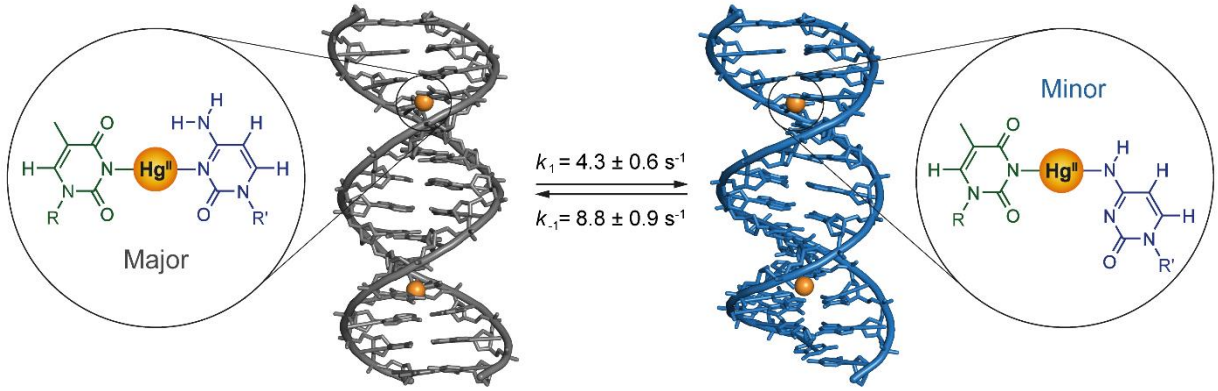

Figure 5.24. Schematic representation of structural interconversion.

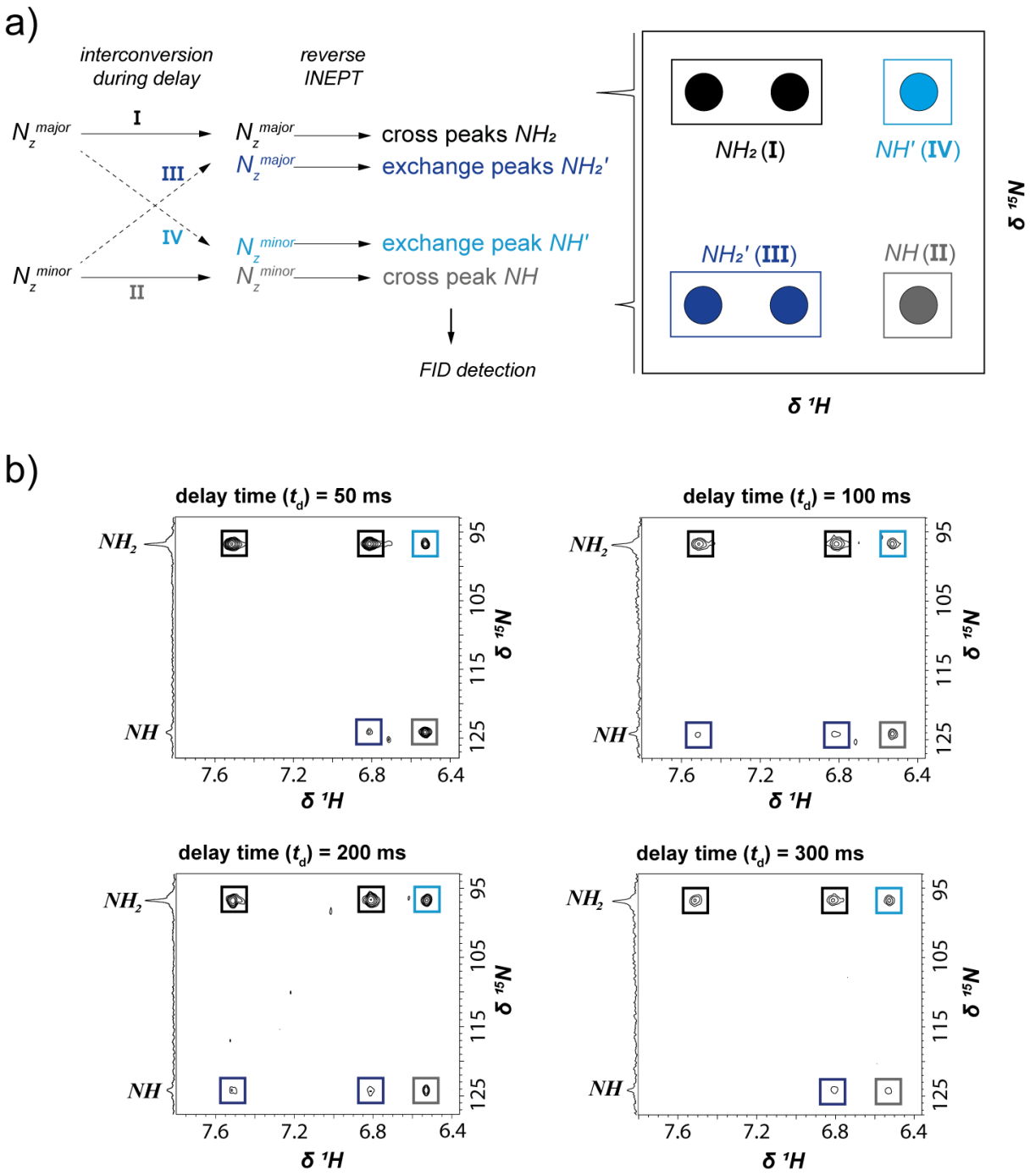

Figure 5.25. a) Schematic description of a z-z exchange [^{15}N,^{1}H]-HSQC experiment with a delay introduced before the reverse INEPT showing all possible ^{15}N z-z exchange during delay (I-IV), followed by INEPT transfer. Exchange I and II give cross peaks *NH₂* (black) and *NH* (grey), corresponding to those of [^{15}N,^{1}H]-HSQC experiments without delay (right). Interconversion of major- and minor structures during the delay results in exchange III and IV to give exchange cross peaks *NH₂'* (dark blue) and *NH'* (light blue). b) Interconversion of major and minor structures according to exchange cross peaks in z-z exchange [^{15}N,^{1}H]-HSQC spectra with various delay times before reverse INEPT at 25 °C. The DNA sample contained 0.5 mM duplex DNA and 1.5 mM of $Hg(ClO_4)_2$ in aqueous buffer (200 mM $NaClO_4$, 50 mM cacodylic acid in H_2O / D_2O (9:1) at pH = 7.8).

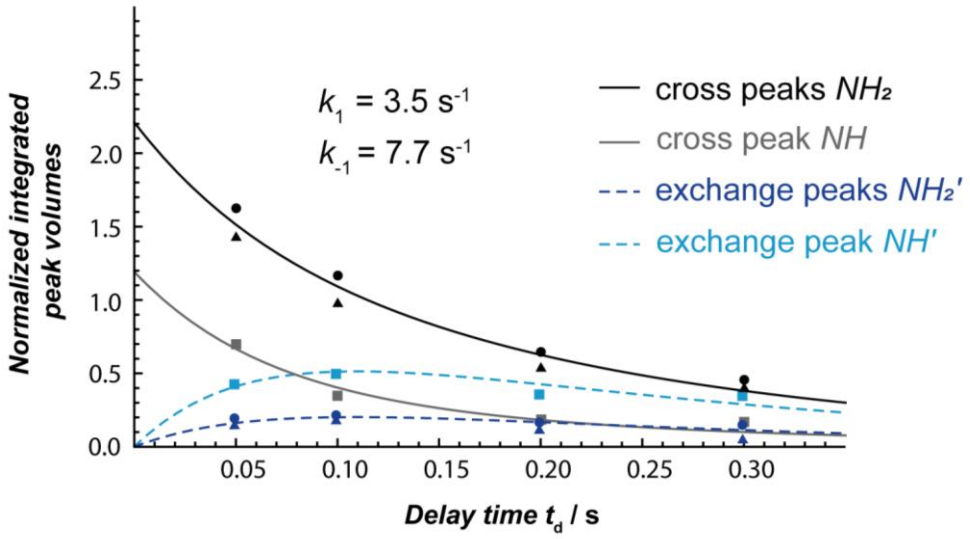

Figure 5.26. Rate constants of interconversion determined by fit of change in signal intensity of cross peaks and exchange peaks as a function of exchange delay time (t_d) (eq 19-22, Chapter 6, Experimental Procedures). For definition of signals and colors see Figure 5.25. For equations and their derivation see Chapter 6, Experimental Procedures. Both NH_2 protons were used for decreases of cross peaks NH_2 and increases of exchange peaks NH_2' (circles and triangels). A global fit was used, where the rate constants k_1, and k_{-1} were constrained to be equal for all four curves, under the assumption that all proton- and nitrogen atoms have the same relaxation rate (R_1) and that the *NH* proton is converted equally to both NH_2 protons during the exchange.

Multiple pieces of evidence suggested that the global interconversion of major and minor duplex structures was directly coupled to changes in metal-nucleobase connectivity. There are two types of metal coordination, yet only two types of helixes are observed. There is no evidence for a helix with a "mixed" metal coordination connectivity. Further evidence is found in the ROESY spectrum (Figure 5.28). Single exchange signals were observed for the Hg^{II}-bound nucleosides as well as for sugar- and aromatic proton signals of various residues throughout the duplex (Figure 5.27 and 5.28). Exchange signals can be distinguished from ROE cross peaks by the phase. ROE cross peaks are opposite in phase to the diagonal and exchange signals in phase to the diagonal (Figure 5.28). The same exchange signals were also found in the [^{1}H,^{1}H]-TOCSY spectrum in the H1'/H5 region (~ 5.0 – 6.2 ppm, Figure 5.29). Within that region, no protons belong to the same spin system. Therefore, the observed cross peaks occur by exchange and not by coupling through bonds within a spin system (Figure 5.29). Further, exchange-mediated cross peaks were observed in the aromatic → H2'/H2" region of the [^{1}H,^{1}H]-NOESY spectrum (Figure 5.27 and Figure 5.30). Together, this suggested that the two metal binding sites are directly coupled via the global conformational change.

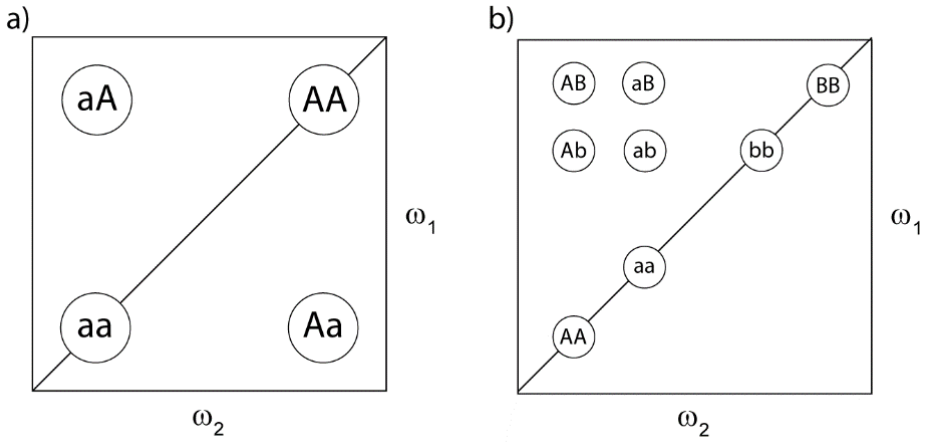

Figure 5.27. Definition of a) diagonal peaks ('AA' and 'aa') undergoing conformational interconversion to give exchange cross peaks ('aA' and 'Aa') and b) 'AB' and 'ab' NOE cross peaks undergoing conformational interconversion to give exchange-mediated NOE cross peaks 'Ab' and aB'.[94] Figures adapted from (ref 94).[94]

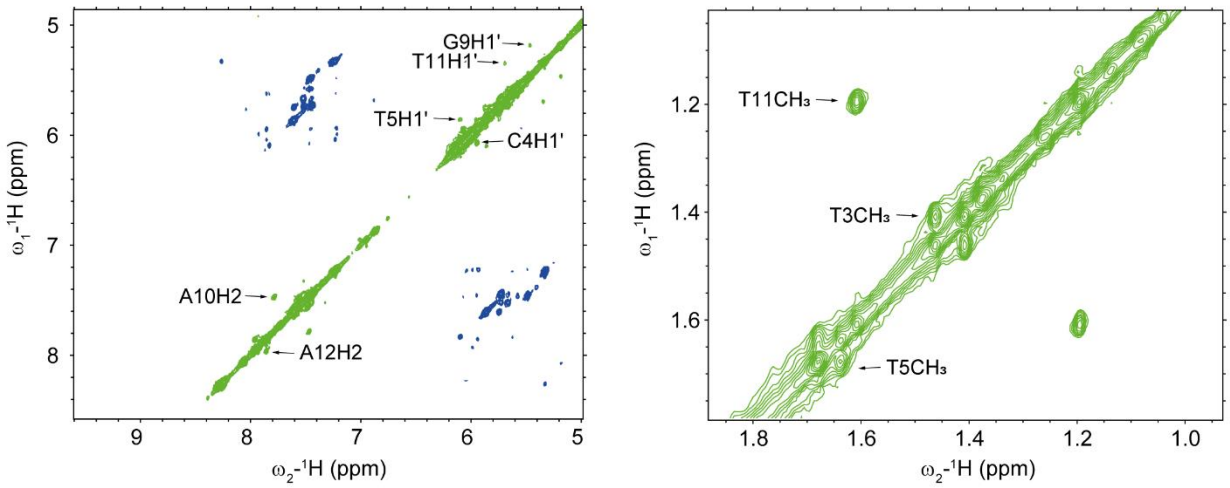

Figure 5.28. Sections of the ROESY spectrum of ODN[1] "C-Hg^{II}-T". Exchange signals can be distinguished from ROE cross peaks by the phase. ROE cross peaks are opposite in phase to the diagonal and exchange signals in phase to the diagonal. The DNA sample contained 0.4 mM duplex DNA and 1.2 mM Hg^{II} in aqueous solution of $NaClO_4$ (50 mM, D_2O, pD = 7.75) and was measured at 25 °C.

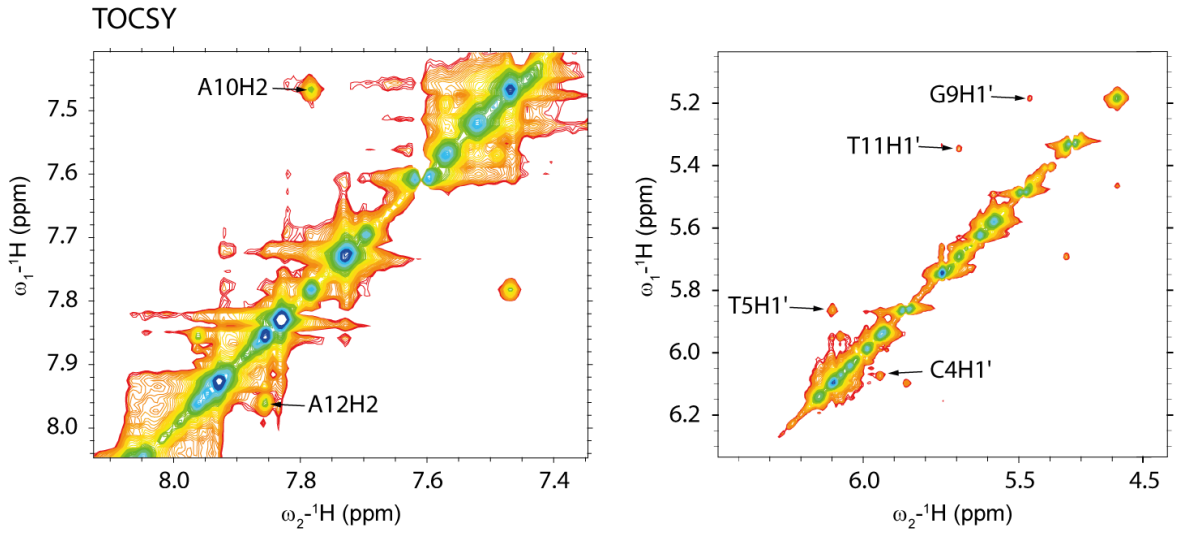

Figure 5.29. Exchange cross peaks in [^{1}H,^{1}H]-TOCSY spectrum. The DNA sample contained 0.4 mM duplex DNA and 1.2 mM Hg^{II} in aqueous solution of $NaClO_4$ (50 mM, D_2O, pD = 7.75) and was measured at 25 °C.

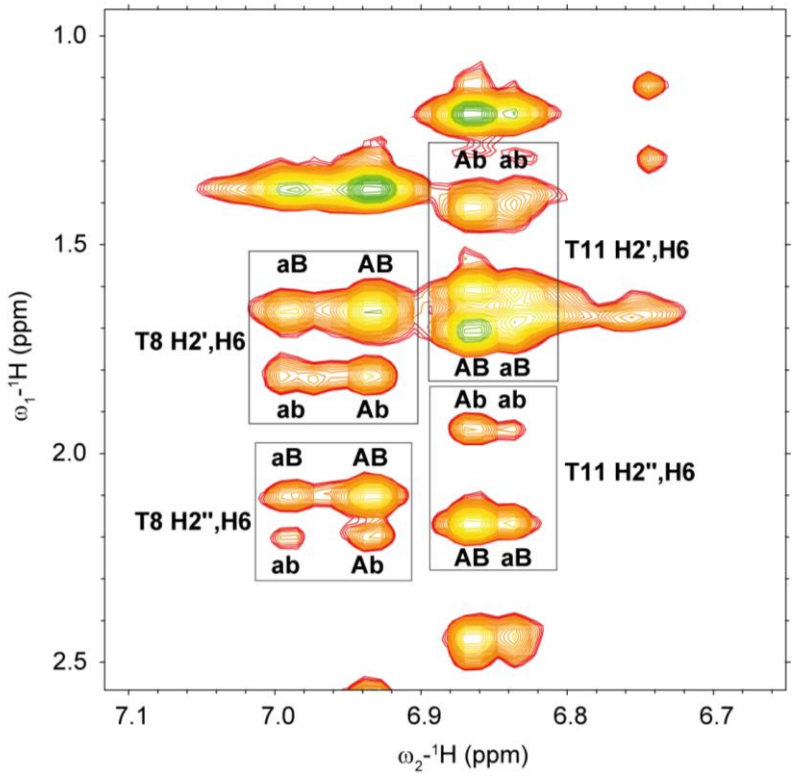

Figure 5.30. Exchange-mediated NOE cross peaks in the aromatic → H2'/H2'' region of the [^{1}H,^{1}H]-NOESY spectrum. 'AB' and 'ab' are defined as NOE cross peaks of major and minor, respectively, and 'Ab' and 'aB' exchange-mediated NOE cross peaks (Figure 5.27). The DNA sample contained 1 mM duplex DNA and 3 mM of ^{199}Hg-enriched $Hg(ClO_4)_2$ in aqueous buffer (200 mM $NaClO_4$, 50 mM cacodylic acid in H_2O / D_2O (9:1) at pH = 7.8) and was measured at 25 °C.

To determine rate constants of global interconversion of the duplexes, we measured [^{1}H,^{1}H]-NOESY spectra with various mixing times (t_m) at 25 °C (Fiugre 5.31). Selected exchange cross peaks ('Aa' and 'aA', Figure 5.31a-b, Figure A28, Appendix) and exchange-mediated NOE cross peaks ('Ab' and 'aB', Figure 5.31c, Figure A29, Appendix) were integrated, normalized to signal intensity at mixing time = 200 ms, and plotted as a function of mixing time (t_m) (Table 5.4, Figure 5.32-5.35). For definition of labels see Figure 5.27. Two NOE signals were also included to the analysis as controls (Figure 5.33). At longer mixing times, a decrease in signal intensity was observed due to auto relaxation (R_1).

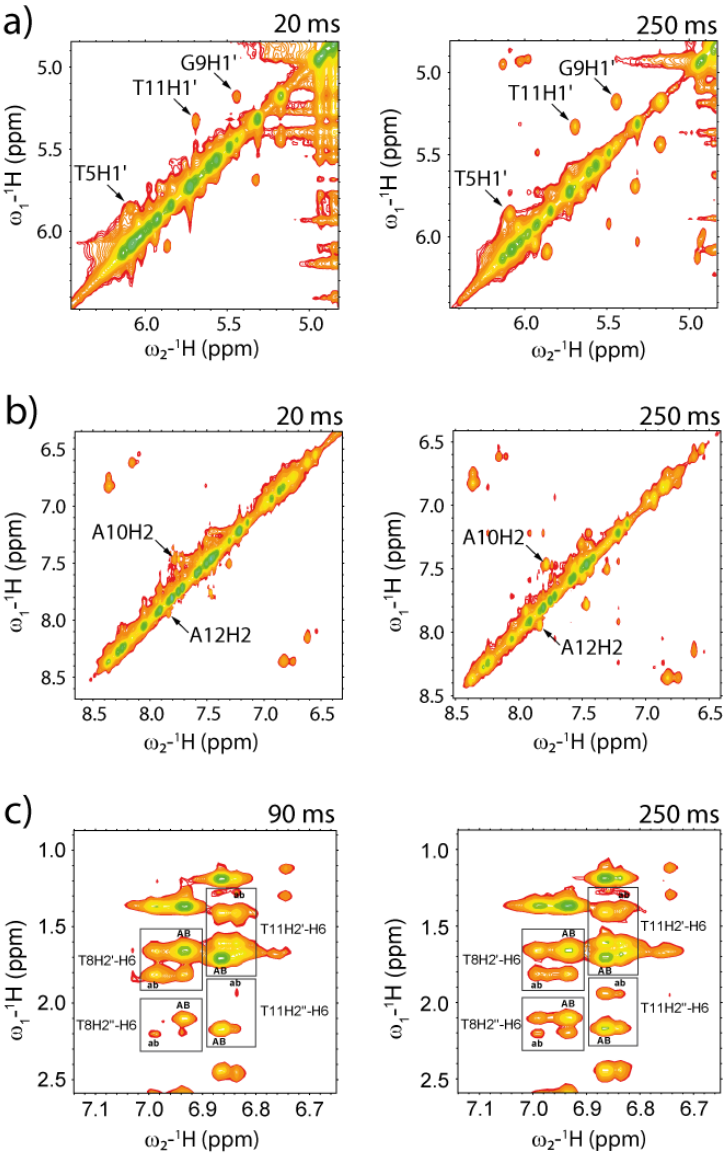

Figure 5.31. [^{1}H,^{1}H]-NOESY spectra with selected mixing times. Additional mixing times are shown in Figure A28-A29, Appendix. Changes of exchange cross peak intensities with increasing mixing time for a) H1' protons and b) H2 protons. c) Section of the aromatic → H2'/H2'' region of the[^{1}H,^{1}H]-NOESY spectra showing changes of exchange-mediated NOE cross peak intensities with increasing mixing time. The DNA sample contained 1 mM duplex DNA and 3 mM of ^{199}Hg-enriched $Hg(ClO_4)_2$ in aqueous buffer (200 mM $NaClO_4$, 50 mM cacodylic acid in H_2O / D_2O (9:1) at pH = 7.8) and was measured at 25 °C.

The area of integration of diagonal peaks ('AA' and 'aa') and exchange cross peaks ('Aa' and 'aA') (for definition of labels see Figure 5.27) were determined at various mixing times (t_m) and plotted as a function of mixing time (t_m) (Figure 5.32). Under the assumption that auto relaxation $R_{1,A} = R_{1,a}$ and cross relaxation $\sigma = 0$, change in area of integration of exchange cross peaks as a function of mixing time (t_m) can be fit with eq 1 to determine sum of rate constants $k_1 + k_{-1}$ (Figure 5.32, Table 5.4).[94,95]

$$\text{exchange cross peak 'Aa' } (t_m) = \text{ exchange cross peak 'aA' } (t_m)$$
$$= \frac{k_1 k_{-1}}{(k_1+k_{-1})^2}\, e^{-R_1 t_m}\left(1 - e^{-(k_1+k_{-1})t_m}\right) \quad (1)$$

For signals where the resolution of the diagonal peak was sufficient for integration, eq 1 can be normalized to the intensity of diagonal peaks by 'Aa' (t_m) / ('Aa' (t_m) + 'aa' (t_m)) and 'aA' (t_m) / ('aA' (t_m) + 'AA' (t_m)) to give the simplified eqs 2 and 3, from which the rate constants k_1 and k_{-1} can be determined (Figure 5.34, Table 5.4, for definition of labels see Figure 5.27).[94,95]

$$\text{normalized exchange cross peak } \frac{\text{'Aa'}(t_m)}{\text{'Aa'}(t_m)+\text{'aa'}(t_m)} = \frac{k_{-1}}{k_1+k_{-1}}\left(1 - e^{-(k_1+k_{-1})t_m}\right) \quad (2)$$

$$\text{normalized exchange cross peak } \frac{\text{'aA'}(t_m)}{\text{'aA'}(t_m)+\text{'AA'}(t_m)} = \frac{k_1}{k_1+k_{-1}}\left(1 - e^{-(k_1+k_{-1})t_m}\right) \quad (3)$$

The area of integration of NOE cross peaks ('AB' and 'ab') and exchange-mediated NOE cross peaks ('Ab' and 'aB') (for definition of labels see Figure 5.27) were determined at various mixing times (t_m). Normalized changes in area of integration of exchange-mediated cross peaks were plotted as a function of mixing time (t_m) (Figure 5.35). By dividing exchange-mediated cross peaks 'Ab' and 'aB' by the sum with its corresponding NOE cross peaks gives eq 4 and eq 5, from which the rate constants k_1 and k_{-1} can be determined (Figure 5.35, Table 5.4, under the assumption that auto relaxation $R_{1,A} = R_{1,a}$).[94,95] For derivation of equations see Chapter 6, Experimental Procedures and ref 93 – 95.

$$\text{normalized exchange} - \text{mediated NOE cross peak} \frac{\text{'aB'}(t_m)}{\text{'AB'}(t_m)+\text{'aB'}(t_m)} = \frac{k_1 - k_1\, e^{-t_m(k_1+k_{-1})}}{k_1+k_{-1}} \quad (4)$$

$$\text{normalized exchange} - \text{mediated NOE cross peak} \frac{\text{'Ab'}(t_m)}{\text{'Ab'}(t_m)+\text{'ab'}(t_m)} = \frac{k_{-1} - k_{-1}\, e^{-(k_1+k_{-1})t_m}}{k_1+k_{-1}} \quad (5)$$

with t_m = mixing time, R_1 = autorelaxation rate and k_1 and k_{-1} = rate constants of interconversion. For definition of labels 'AB', 'ab', 'Ab', and 'aB' see Figure 5.27.

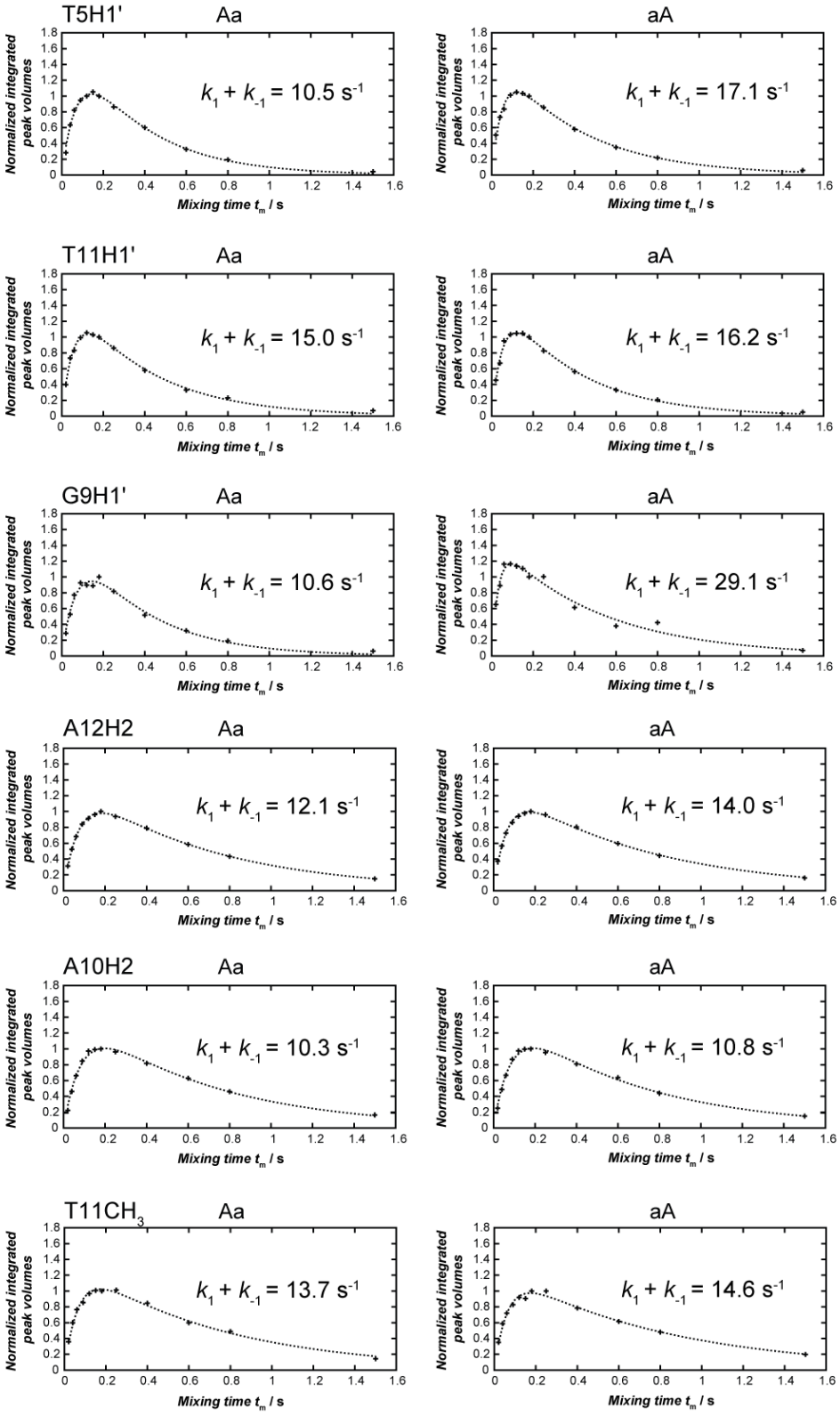

Figure 5.32. Sum of interconversion rate constants (k_1+k_{-1}) determined by fit (eq 1) of changes in cross peak intensities vs mixing time (t_m). The DNA sample contained 1 mM duplex DNA and 3 mM of ^{199}Hg-enriched $Hg(ClO_4)_2$ in aqueous buffer (200 mM $NaClO_4$, 50 mM cacodylic acid in H_2O / D_2O (9:1) at pH = 7.8) and was measured at 25 °C.

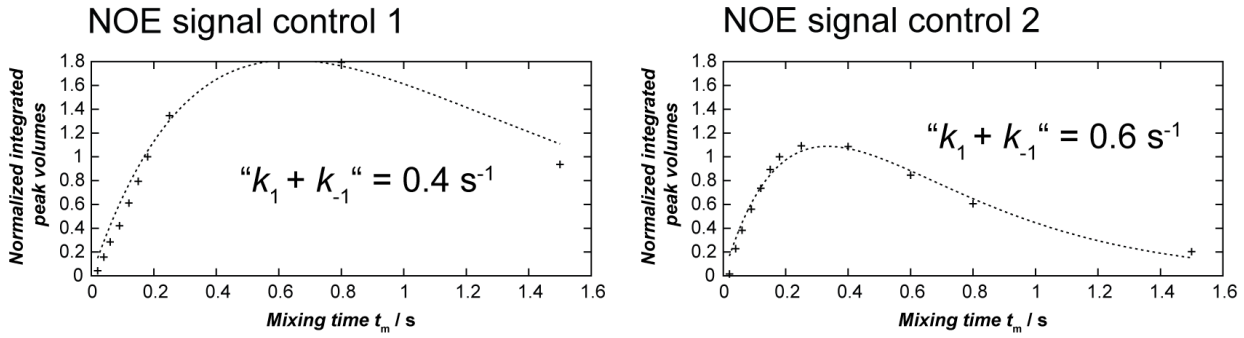

Figure 5.33. NOE signals A7H3'-H1' processed equivalent to exchange signals as control. Both examples showed large deviations from the values obtained for exchange cross peaks. The DNA sample contained 1 mM duplex DNA and 3 mM of ^{199}Hg-enriched $Hg(ClO_4)_2$ in aqueous buffer (200 mM $NaClO_4$, 50 mM cacodylic acid in H_2O / D_2O (9:1) at pH = 7.8) and was measured at 25 °C.

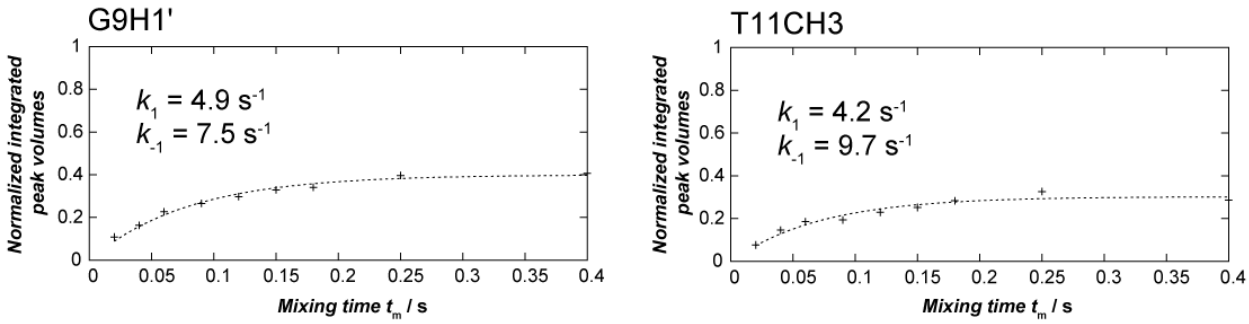

Figure 5.34. Cross peak intensities normalized to the intensities of diagonal peaks where aA (t_m) / (AA (t_m) + aA (t_m)) is plotted as a function of mixing time (t_m). Rate constants of interconversion were determined by fit with eq 2. The DNA sample contained 1 mM duplex DNA and 3 mM of ^{199}Hg-enriched $Hg(ClO_4)_2$ in aqueous buffer (200 mM $NaClO_4$, 50 mM cacodylic acid in H_2O / D_2O (9:1) at pH = 7.8) and was measured at 25 °C.

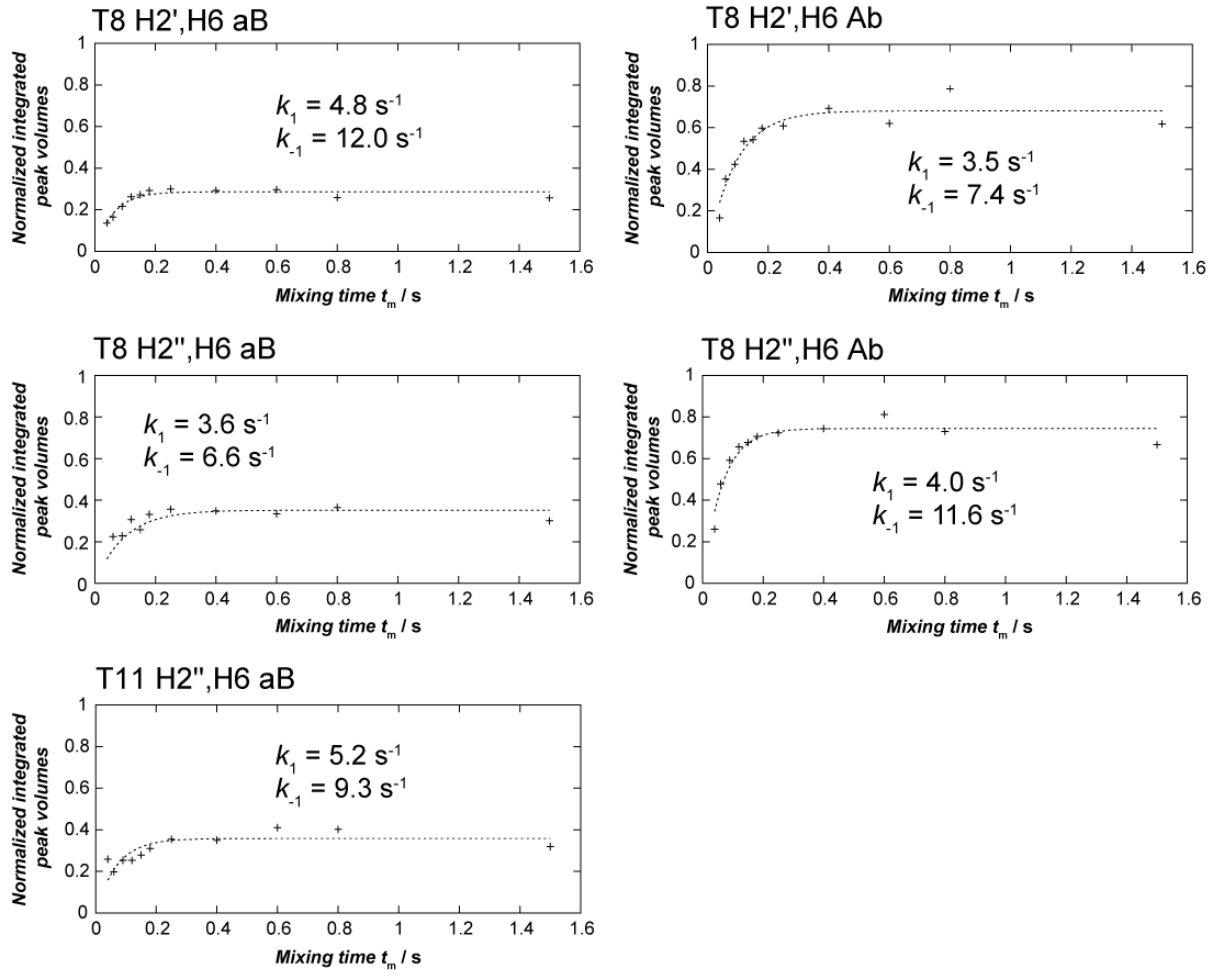

Figure 5.35. Normalized areas of integration of exchange-mediated NOE cross peaks plotted as a function of mixing time (t_m). Rate constants of interconversion were determined by fit with eq 4 ('aB') or eq 5 ('Ab'). The DNA sample contained 1 mM duplex DNA and 3 mM of ^{199}Hg-enriched $Hg(ClO_4)_2$ in aqueous buffer (200 mM $NaClO_4$, 50 mM cacodylic acid in H_2O / D_2O (9:1) at pH = 7.8) and was measured at 25 °C.

Table 5.4. Rate Constants of Duplex Interconversion[a]

	$k_1 + k_{-1}$ (s^{-1})	k_1 (s^{-1})	k_{-1} (s^{-1})
[^{15}N,^{1}H]-HSQC exchange peaks	11.2	3.5	7.7
exchange cross peaks			
T5H1'	10.5	n.d.	n.d.
T11H1'	15.0	n.d.	n.d.
G9H1'	10.6	4.9	7.5
A12H2	12.1	n.d.	n.d.
A10H2	10.3	n.d.	n.d.
T11CH3	13.7	4.2	9.7
mean ± standard deviation	12.0 ± 1.8	4.6 ± 0.4	8.6 ± 1.1
exchange-mediated NOE cross peaks			
T8H2',H6	n.d.	4.2	9.7
T8H2'',H6	n.d.	3.8	9.1
T11H2'',H6	n.d.	5.2	9.3
mean ± standard deviation	n. d.	4.4 ± 0.6	9.4 ± 0.2

[a] Sums of rate constants (k_1+k_{-1}) were determined by fitting exchange cross peak vs mixing time (t_m) with eq 1. Rate constants k_1 and k_{-1} were determined from normalized areas of integration of exchange cross peak vs mixing time (t_m) by fitting with eq 2, or from plot of changes of normalized areas of integration of exchange-mediated NOE cross peaks vs mixing time (t_m) by fit with eq 4 or 5. Values for T8H2',H6 and T8H2'',H6 were calculated as the mean of both exchange mediated NOE cross peaks. The DNA sample contained 1 mM duplex DNA and 3 mM of ^{199}Hg-enriched $Hg(ClO_4)_2$ in aqueous buffer (200 mM $NaClO_4$, 50 mM cacodylic acid in H_2O / D_2O (9:1) at pH = 7.8) and was measured at 25 °C. For residue number assignments see Figure 5.12a. For spectra see Figure 5.31 and Figures A28-A29, Appendix. For fits see Figures 5.32-35, and for fitting equations see Materials and Methods and ref 93 – 95.

The sum of rate constants $k_1 + k_{-1}$ determined by exchange cross peaks (10.5 – 15.0 s^{-1}) and rate constants k_1 (3.8 – 5.2 s^{-1}) and k_{-1} (7.5 – 9.7 s^{-1}) determined from exchange cross peaks and exchange-mediated cross peaks were in excellent agreement with rate constants of interconversion of local metal ion coordination (k_1 = 3.5 s^{-1}, k_{-1} = 7.7 s^{-1}) (Figure 5.26, Table 5.4) Furthermore, the ~2:1 ratio of rate constants (k_1 / k_{-1}) agree well with the ~3:1 equilibrium abundance of the two species. Together, these results demonstrate that dynamic changes in local metal ion coordination are directly coupled to the global interconversion of the two duplex structures. The rates of their exchange (k_1 = 4.3 ± 0.6 s^{-1}, k_{-1} = 8.8 ± 0.9 s^{-1}) are on the same time scale as many biological and material processes and can therefore serve as a low-energy barrier switch between two functional states of a duplex.

5.6 Discussion and Conclusions

"All natural" metal-mediated base pairs are potentially important in both biological and materials sciences.[31,32,41–43,96,33–40] A detailed understanding of their structures and dynamics are essential for gauging their potential applications in devices as well as their ability to interfere with biological processes.[26–28,92] We recently reported that Hg^{II} binds to C-T mismatches with similar thermodynamic stabilities as the well-known T-Hg^{II}-T base pair.[51] It was unclear, however, what type of metal coordination was exhibited by duplex DNA containing C-Hg^{II}-T base pairs. The 10-fold faster on- and off-rates of Hg^{II} to C-T compared to T-T and the less favorable entropy changes of C-Hg^{II}-T versus T-Hg^{II}-T formation suggested that C-Hg^{II}-T and T-Hg^{II}-T base pairs exhibit different coordination modes.[51] Intrigued by these observations, we investigated the binding of Hg^{II} to duplex DNA containing C-T mismatches using ^{15}N-labeled oligonucleotides and NMR spectroscopy.

^{15}N NMR spectroscopy and ^{15}N-^{199}Hg coupling revealed that Hg^{II} coordinates via two distinct binding modes to C-T mismatches to give a major species containing (*N3*)C-Hg^{II}-(*N3*)T coordination sites and a minor species with (*C4-NH*)C-Hg^{II}-(*N3*)T base pairs in a ratio of ~75% and ~25%, respectively. NMR experiments revealed two well-resolved duplexes and both duplex species exhibited characteristics of "mixed" A/B-form duplex DNA. The major species, containing two identical (*N3*)C-Hg^{II}-(*N3*)T coordination sites, exhibited a more B-form-like structure. Some notable differences in helix and base pair parameters were observed for the minor species containing two (*C4-NH*)C-Hg^{II}-(*N3*)T base pairs. The combination of deeper and narrower major groove, increased minor groove width, inclination of base pairs at the center of the helix, and higher slide of the C-Hg^{II}-T base pair to the major groove results in a more A-form like structure. Comparison of the major and minor duplex species revealed that the (*C4-NH*)C-Hg^{II}-(*N3*)T connectivity induced a displacement of the C-Hg^{II}-T base pair towards the major groove, thereby exposing the Hg^{II} ion to bulk solvent (~20 % increase in solvent exposed area). This offers an explanation for the 10-fold increase in association and dissociation observed for C-Hg^{II}-T formation compared to T-Hg^{II}-T formation.

Local structural polymorphisms of duplex DNA can provide unique recognition sites for protein binding. Larger deviations of regular B-form duplex DNA were observed for the minor structure containing (*C4-NH*)C-Hg^{II}-(*N3*)T base pairs. The minor duplex exhibited a pronounced unwinding at the C-Hg^{II}-T base pair site (28 °) and a higher twist to the neighboring step (42°) (mean helical twist B-form ~ 36 °, A-form ~ 33 °). Twist polymorphisms have been suggested to occur in regulatory regions of the genome.[64] Formation of the minor duplex species could therefore potentially influence protein binding or provide a distinct target site for small molecules to bind. An unusual O4'-endo sugar pucker was observed at the C-Hg^{II}-T site at the cytosine residue for the major duplex and at

the thymidine residue for the minor duplex. Local O4'-endo sugar pucker conformations and single sugar switches have been reported to occur in "mixed" A/B-form conformations of duplex DNA and in RNA/DNA hybrid sequences of retroviral polypurine tracts. This local sugar pucker polymorphism has been suggested to play a role in regulating RNase H activity by influencing binding of reverse transcriptase to the sugar-phosphate-backbone.[71,86–88] Formation of C-Hg^{II}-T base pairs in duplex DNA could thereby potentially alter DNA-protein binding interactions. Remarkably, major- and minor duplex species were in dynamic equilibrium. Dynamic changes in local metal ion coordination were directly coupled to the global interconversion of the two duplexes. The rates of their exchange (k_1 = 4.3 ± 0.6 s^{-1}, k_{-1} = 8.8 ± 0.9 s^{-1}) were on the same time scale as many biochemical and materials processes and can therefore serve as a low-energy barrier switch between two functional states of a duplex.

References

[1] R. E. Franklin, R. G. Gosling, *Nature,* 1953, *171*, 740–741.

[2] M. H. F. Wilkings, *Nature,* 1953, *171*, 738–740.

[3] R. E. Franklin, R. G. Gosling, *Acta Crystallogr.* 1953, *6*, 673–677.

[4] F. Dimaio, X. Yu, E. Rensen, M. Krupovic, D. Prangishvili, E. H. Egelman, *Science,* 2015, *348*, 914–917.

[5] M. Kulkarni, A. Mukherjee, *J. Chem. Phys.* 2013, *139*, 155102.

[6] E. E. Minyat, V. I. Ivanov, A. M. K. N, L. E. Minchenkova, A. K. Schyolkina, *J. Mol. Biol.* 1978, *128*, 397–409.

[7] M. Hou, S. Lin, J. P. Yuann, W. Lin, A. H. Wang, L. Kan, *Nucleic Acids Res.* 2001, *29*, 5121–5128.

[8] L. Van Dam, N. Korolev, L. Nordenskiöld, *Nucleic Acids Res.* 2002, *30*, 419–428.

[9] M. Gasior-Glogowska, K. Malek, G. Zajac, M. Baranska, *Analyst* 2016, *141*, 291–296.

[10] O. Vrana, V. Masek, V. Drazan, V. Brabec, *J. Struct. Biol.* 2007, *159*, 1–8.

[11] R. C. Todd, S. J. Lippard, *J. Inorg. Biochem.* 2010, *104*, 902–908.

[12] S. Park, S. J. Lippard, *Biochemistry* 2011, *50*, 2567–2574.

[13] A. H.-J. Wang, G. J. Quigley, F. J. Kolpak, J. L. Crawford, J. H. Jacques Boom, G. van der Marel, A. Rich, *Nature,* 1979, *282*, 680–686.

[14] P. Barraud, F. H.-T. Allain, *Curr. Top. Microbiol. Immunol.* 2012, *353*, 35–60.

[15] B. Basham, B. F. Eichman, P. S. Ho, in *Oxford Handb. Nucleic Acid Struct.* (Ed.: S. Neidle), Oxford University Press, 1999, pp. 199–252.

[16] S. Adam, P. Bourtayre, J. Liquier, E. Taillandier, *Nucleic Acids Res.* 1986, *14*, 3501–3513.

[17] B. Lippert, *Coord. Chem. Rev.* 2000, *200–202*, 487–516.

[18] B. Lippert, P. J. S. Miguel, *Acc. Chem. Res.* 2016, *49*, 1537–1545.

[19] G. H. Clever, C. Kaul, T. Carell, *Angew. Chemie - Int. Ed.* 2007, *46*, 6226–6236.

[20] Y. Takezawa, M. Shionoya, *Acc. Chem. Res.* 2012, *45*, 2066–2076.

[21] P. Scharf, J. Müller, *Chempluschem* 2013, *78*, 20–34.

[22] Y. Tanaka, J. Kondo, V. Sychrovský, J. Šebera, T. Dairaku, H. Saneyoshi, H. Urata, H. Torigoe, A. Ono, *Chem. Commun.* 2015, *51*, 17434–17360.

[23] Y. Takezawa, J. Müller, M. Shionoya, *Chem. Lett.* 2017, *46*, 622–633.

[24] B. Jash, J. Müller, *Chem. Eur. J.* 2017, *23*, 17166–17178.

[25] A. Ono, H. Torigoe, Y. Tanaka, I. Okamoto, *Chem. Soc. Rev.* 2011, *40*, 5855–5866.

[26] H. Urata, E. Yamaguchi, T. Funai, Y. Matsumura, S.-I. Wada, *Angew. Chem. Int. Ed. Engl.* 2010, *49*, 6516–6519.

[27] T. Funai, Y. Miyazaki, M. Aotani, E. Yamaguchi, O. Nakagawa, S.-I. Wada, H. Torigoe, A. Ono, H. Urata, *Angew. Chemie - Int. Ed.* 2012, *51*, 6464–6466.

[28] T. Funai, J. Nakamura, Y. Miyazaki, R. Kiriu, O. Nakagawa, A. Ono, H. Urata, *Angew. Chemie Int. Ed.* 2014, 6624–6627.

[29] O. P. Schmidt, G. Mata, N. W. Luedtke, *J. Am. Chem. Soc.* 2016, *1383*, 14733–14739.

[30] C. W. Liu, Y. W. Lin, C. C. Huang, H. T. Chang, *Biosens. Bioelectron.* 2009, *24*, 2541–2546.

[31] I. Kang, Y. Wang, C. Reagan, Y. Fu, M. X. Wang, L.-Q. Gu, *Sci. Rep.* 2013, *3*, 2381.

[32] S. J. Xiao, P. P. Hu, G. F. Xiao, W. Yi, Y. Liu, C. Z. Huang, *J. Phys. Chem. B* 2012, *116*, 9565–9569.

[33] J. Liu, Y. Lu, *Angew. Chemie - Int. Ed.* 2007, *46*, 7587–7590.

[34] K. S. Park, C. Jung, H. G. Park, *Angew. Chemie - Int. Ed.* 2010, *49*, 9757–9760.

[35] K. S. Park, C. Y. Lee, H. G. Park, *Chem. Commun.*

2016, *52*, 4868–4871.

[36] J. M. Thomas, H. Z. Yu, D. Sen, *J. Am. Chem. Soc.* 2012, *134*, 13738–13748.

[37] G. Mor-piperberg, R. Tel-vered, J. Elbaz, I. Willner, *J. Am. Chem. Soc.* 2010, *132*, 6878–6879.

[38] Z. G. Wang, J. Elbaz, I. Willner, *Nano Lett.* 2011, *11*, 304–309.

[39] S. Bi, B. Ji, Z. Zhang, J.-J. Zhu, *Chem. Sci.* 2013, *4*, 1858–1863.

[40] X. Guo, F. Seela, *Chem. Eur. J.* 2017, *23*, 11776–11779.

[41] S. Wen, T. Zeng, L. Liu, K. Zhao, Y. Zhao, X. Liu, H. Wu, *J. Am. Chem. Soc.* 2011, *133*, 18312–18317.

[42] Y. Wang, B. Ritzo, L. Gu, *RSC Adv.* 2015, *5*, 2655–2658.

[43] T. Hong, Y. Yuan, T. Wang, J. Ma, Q. Yao, X. Hua, Y. Xia, X. Zhou, *Chem. Sci.* 2017, *8*, 200–205.

[44] S. Katz, *Nature,* 1962, *68*, 569.

[45] S. Katz, *J. Am. Chem. Soc.* 1952, *74*, 2238–2245.

[46] T. Yamane, N. Davidson, *J. Am. Chem. Soc.* 1961, *83*, 2599–2607.

[47] Y. Tanaka, S. Oda, H. Yamaguchi, Y. Kondo, C. Kojima, A. Ono, *J. Am. Chem. Soc.* 2007, *129*, 244–245.

[48] T. Dairaku, K. Furuita, H. Sato, J. Šebera, K. Nakashima, J. Kondo, D. Yamanaka, Y. Kondo, I. Okamoto, A. Ono, et al., *Chem. Eur. J.* 2016, *6*, 13028–13031.

[49] H. Yamaguchi, Y. Sebera, J. Kondo, S. Oda, T. Komuro, T. Kawamura, T. Dairaku, Y. Kondo, I. Okamoto, A. Ono, et al., *Nucleic Acids Res.* 2014, *42*, 4094–4099.

[50] J. Kondo, T. Yamada, C. Hirose, I. Okamoto, Y. Tanaka, A. Ono, *Angew. Chem. Int. Ed. Engl.* 2014, *53*, 2385–2388.

[51] O. P. Schmidt, A. S. Benz, G. Mata, N. W. Luedtke, *Nucleic Acids Res.*, 2018, 46, 6470–6479.

[52] H. Torigoe, A. Ono, T. Kozasa, *Chem. Eur. J.* 2010, *16*, 13218–13225.

[53] H. Liu, C. Cai, P. Haruehanroengra, Q. Yao, Y. Chen, C. Yang, Q. Luo, B. Wu, J. Li, J. Ma, et al., *Nucleic Acids Res.* 2017, *45*, 2910–2918.

[54] Y. Miyake, H. Togashi, M. Tashiro, H. Yamaguchi, S. Oda, M. Kudo, Y. Tanaka, Y. Kondo, R. Sawa, T. Fujimoto, et al., *J. Am. Chem. Soc.* 2006, *128*, 2172–2173.

[55] H. T. Allawi, J. Santalucia, *Nucleic Acids Res.* 1998, *26*, 2694–2701.

[56] S. R. Bhaumik, K. V. R. Chary, G. Govil, K. Liu, H. T. Miles, *Biopolymers* 1997, *41*, 773–784.

[57] Y. Tanaka, A. Ono, *Dalton Trans.* 2008, 4965–74.

[58] S. Johannsen, N. Megger, D. Bo, R. K. O. Sigel, J. Müller, *Nat. Chem.* 2010, *2*, 229–234.

[59] T. Dairaku, K. Furuita, H. Sato, J. Šebera, D. Yamanaka, H. Otaki, S. Kikkawa, Y. Kondo, R. Katahira, F. Matthias Bickelhaupt, et al., *Chem. Commun. (Camb)*. 2015, *51*, 8488–91.

[60] R. S. Reid, B. Podzbyi, *J. Inorg. Chem* 1988, *195*, 183–195.

[61] L. Jen-jacobson, *Biopolymers* 1997, *44*, 153–180.

[62] X. Lu, Z. Shakked, W. K. Olson, *J. Mol. Biol* 2000, *300*, 819–840.

[63] A. G. Tsai, A. E. Engelhart, M. M. Hatmal, S. I. Houston, N. V Hud, I. S. Haworth, M. R. Lieber, *J. Biol. Chem.* 2009, *284*, 7157–7164.

[64] P. D. Dans, I. Faustino, F. Battistini, K. Zakrzewska, R. Lavery, M. Orozco, *Nucleic Acids Res.* 2014, *42*, 11304–11320.

[65] R. Lavery, M. Moakher, J. H. Maddocks, D. Petkeviciute, K. Zakrzewska, *Nucleic Acids Res.* 2009, *37*, 5917–5929.

[66] The PyMOL Molecular Graphics System, Version 2.0.7, Schrödinger, LLC., n.d.

[67] G. Varani, F. Aboul-ela, F. H. Allain, *Prog. Nucl. Magn. Reson. Spectrscopy* 1996, *29*, 51–127.

[68] H. Widmer, K. Wuthrich, *J. Magn. Reson.* 1987, *74*, 316–336.

[69] X.-J. Lu, W. K. Olson, *Nucleic Acids Res.* 2003, *31*, 5108–5121.

[70] X.-J. Lu, W. K. Olson, *Nat. Protoc.* 2008, *3*, 1213–1227.

[71] M. L. Kopka, L. Lavelle, G. W. Han, H. Ng, R. E. Dickerson, *J. Mol. Biol.* 2003, *334*, 653–665.

[72] M. Kulkarni, A. Mukherjee, *Prog. Biophys. Mol. Biol.* 2017, *128*, 63–73.

[73] R. Chandrasekaran, M. WAng, R.-G. He, L. C. Puijaner, M. A. Byler, R. P. Millane, S. Arnott, *J. Biomol. Struct. Dyn.* 1996, *13*, 1015–1027.

[74] R. Chandrasekaran, M. Wang, R.-G. He, L. C. Puijaner, M. A. Byler, R. P. Millane, S. Arnott, *J. Biomol. Struct. Dyn.* 1989, *6*, 1189–1203.

[75] C. A. Davey, D. F. Sargent, K. Luger, A. W. Maeder, T. J. Richmond, *J. Mol. Biol.* 2002, *319*, 1097–1113.

[76] M. Pasi, K. Zakrzewska, J. H. Maddocks, R. Lavery, L. I. Cnrs, I. De Biologie, *Nucleic Acids Res.* 2017, *45*, 4269–4277.

[77] W. K. Olson, M. Bansal, S. K. Burley, R. E. Dickerson, M. Gerstein, S. C. Harvey, U. Heinemann, X. Lu, S. Neidle, Z. Shakked, et al., *J. Mol. Biol.* 2001, *313*, 229–237.

[78] C. A. Frederick, G. J. Quigley, M.-K. Teng, M. Coll, G. A. van der Marel, J. H. van Boom, A. Rich, A. H.-J. Wang, *Eur. J. Biochem.* 1989, *181*, 295–307.

[79] H. R. Drew, R. M. Wing, T. Takano, C. Broka, S. Tanaka, K. Itakura, R. E. Dickerson, *Proc. Natl. Acad. Sci.* 1981, *78*, 2179–2183.

[80] G. C. K. Roberts, *NMR of Macromolecules*, Oxford University Press, New York, 1995.

[81] E. Westhoft, M. Sundaralingam, *J. Am. Chem. Soc.* 1983, *105*, 970–976.

[82] R. V Hosur, M. Ravikumar, K. V. R. Chary, A. Sheth, G. Govil, T. Zu-kun, H. T. Miles, *FEBS Lett.* 1986, *205*, 71–76.

[83] C. Altona, M. Sundaralingam, *J. Am. Chem. Soc.* 1972, *38*, 8205–8212.

[84] D. B. Davies, *Prog. Nucl. Magn. Reson. Spectrscopy* 1978, *12*, 135–225.

[85] D. Svozil, J. Kalina, M. Omelka, B. Schneider, *Nucleic Acids Res.* 2008, *36*, 3690–3706.

[86] O. Y. Fedoroff, M. Salazar, B. R. Reid, B. Departments, V. Uni, *Biochemistry* 1996, *35*, 11070–11080.

[87] T. Szyperski, M. Götte, M. Billeter, E. Perola, H. Heumann, K. Wüthrich, *J. Biomol. NMR* 1999, *13*, 343–355.

[88] O. Y. Fedoroff, M. Salazar, B. R. Reid, *J. Mol. Biol.* 1993, *233*, 509–523.

[89] J. I. Gyi, A. N. Lane, G. L. Conn, T. Brown, *Biochemistry* 1998, *37*, 73–80.

[90] X. Gaio, P. W. Jeffs, *J. Biomol. NMR* 1994, *4*, 367–384.

[91] G. C. K. Roberts, *NMR of Macromolecules*, Oxford University Press, New York, New York, 1993.

[92] O. P. Schmidt, G. Mata, N. W. Luedtke, *J. Am. Chem. Soc.* 2016, *138*, 14733–14739.

[93] N. A. Farrow, O. Zhang, J. D. Forman-Kay, L. E. Kay, *J. Biomol. NMR* 1994, *4*, 727–734.

[94] B. Choe, G. W. Cook, N. R. Krishna, *J. Magn. Reson.* 1991, *94*, 387–393.

[95] J. Jeener, B. H. Meier, P. Bachmann, R. R. Ernst, *J. Chem. Phys.* 1979, *71*, 4546–4553.

[96] Y.-W. Lin, H.-T. Ho, C. C. Huang, H.-T. Chang, *Nucleic Acids Res.* 2008, *36*, e123.

Chapter 6

Experimental Procedures

6.1 Oligonucleotides

6.1.1. DNA Synthesis and Purification

Unmodified oligonucleotides were purchased from *Sigma-Aldrich* as HPLC-purified products. ^{15}N-labeled phosphoramidites were purchased from *Cambridge Isotope Laboratories, Inc.*. ^{DMA}T[1a]- and ^{DMA}C[1b]-phosphoramidites were synthesized as previously reported. DNA oligonucleotides (21-mers) containing a single ^{DMA}T and ^{DMA}C at a variable position "X" were synthesized using standard phosphoramidite chemistry with trityl-off procedure. Self-complementary (14-mer) sequences containing a single ^{15}N-labeled thymidine and ^{15}N-labeled cytosine were synthesized using standard phosphoramidite chemistry with trityl-on procedure. DNA synthesis was performed on a 1 µmol scale using the DNA synthesizer *BioAutomation Mermade 4*, using standard synthesis conditions and reagents, except that 5% dichloroacetic acid instead of 3% trichloroacetic acid was used. To avoid ^{DMA}C deamination,[1b] automated DNA synthesis was performed under "ultramild" conditions for ^{DMA}C-containing sequences.[2] Three coupling reactions with prolonged coupling times (260 – 400 s) were performed for site-specific introduction of the modified nucleosides into oligonucleotides. Unmodified phosphoramidites were prepared as 0.1 M solutions in dry acetonitrile. ^{DMA}T-, ^{DMA}C-, ^{15}N-labeled cytosine, and ^{15}N-labeled thymidine phosphoramidites were dissolved in dry acetonitrile typically at a concentration of ~0.02 M. The synthesis of oligonucleotides was monitored using DMT deprotection. Upon completion of the sequences, the ^{DMA}T-containing oligonucleotides and ^{15}N-labeled oligonucleotides were cleaved from the solid support and deprotected by treatment with 1.2 mL of 33% aqueous ammonium hydroxide at 55 °C for 12 hours in a 1.5 mL screw-top cap tube. ^{DMA}C-containing oligonucleotides were deprotected and cleaved from the resin using K_2CO_3 in MeOH at r.t. for 5.5 h, followed by neutralization with aqueous 2 M tetraethylammonium acetate solution or with equimolar glacial acetic acid. ^{DMA}T-, and ^{DMA}C-containing oligonucleotide solutions were lyophilized to dryness and purified by HPLC column chromatography using a semi-prep C-18 reverse-phase column (YMCbasic B-22-10P 150 x 10 mm) using a *Varian*

Pro Star HPLC system. The gradient conditions were typically 5% to 10% acetonitrile over 50 minutes at 3 mL/min in 0.1 M triethylammonium acetate (TEAA, pH 7.0). Peaks were collected, lyophilized to dryness and HPLC-analyzed with an analytical column (XBridge Phenyl 3.5 μm 150 x 4.16 mm). The products were analyzed by MALDI or HR-ESI. ^{15}N-labeled oligonucleotides were purified using Glen-Pak DNA purification cartridges according to their procedure. Purified oligonucleotides were analyzed with MALDI-MS spectroscopy using THAP as matrix in a reflector-ion mode on *Bruker Ultraflextreme MALDI* mass spectrometer. The corresponding unlabeled oligonucleotide was measured in parallel. ^{15}N-labeled oligonucleotide showed a mass elevation of 5 dalton compared to the unlabeled oligonucleotide (Figure 6.1).

6.1.2. DNA Quantification and Folding

Oligonucleotide stock solutions were prepared in deionized water and their concentrations determined by absorbance at 260 nm using a molar extinction coefficient (ε_{260}) calculated using a nearest-neighbour model.[3,4] The extinction coefficients of ^{DMA}T- and ^{DMA}C-containing oligonucleotides were calculated using the base composition method by multiplying the sum of the coefficients of the individual nucleosides by a factor of 0.9 to account for base stacking interactions.[5] For calculated extinction coefficients see Tables 6.2 – 6.7. Double stranded oligonucleotides were prepared from equal amounts of complementary oligonucleotides in the indicated aqueous buffer by heating to 95 °C for 5 min, followed by slow cooling to room temperature over 4 h. For self-complementary sequences, oligonucleotides were diluted in the indicated buffer and annealed as described above.

Table 6.1. Calculated and Measured High Resolution HR-ESI MS for the ^{DMA}T-Containing DNA (X = ^{DMA}T). Monoisotopic Masses Obtained for the 10 Times Negatively Charged DNAs. MS Values Are Reported in *m*/*z*.

Name	Sequence	Molecular Formula	Calculated 10x charged *m*/*z*	Measured 10x charged *m*/*z*
X2	CXC TAA CCC TAA CCC TAA CCC	$C_{204}H_{252}N_{72}O_{122}P_{20}$	628.10535	628.10560
X13	CCC TAA CCC TAA XCC TAA CCC	$C_{204}H_{252}N_{72}O_{122}P_{20}$	628.10535	628.10894
X14	CCC TAA CCC TAA CXC TAA CCC	$C_{204}H_{252}N_{72}O_{122}P_{20}$	628.10535	628.10680
X15	CCC TAA CCC TAA CCX TAA CCC	$C_{204}H_{252}N_{72}O_{122}P_{20}$	628.10535	628.10842

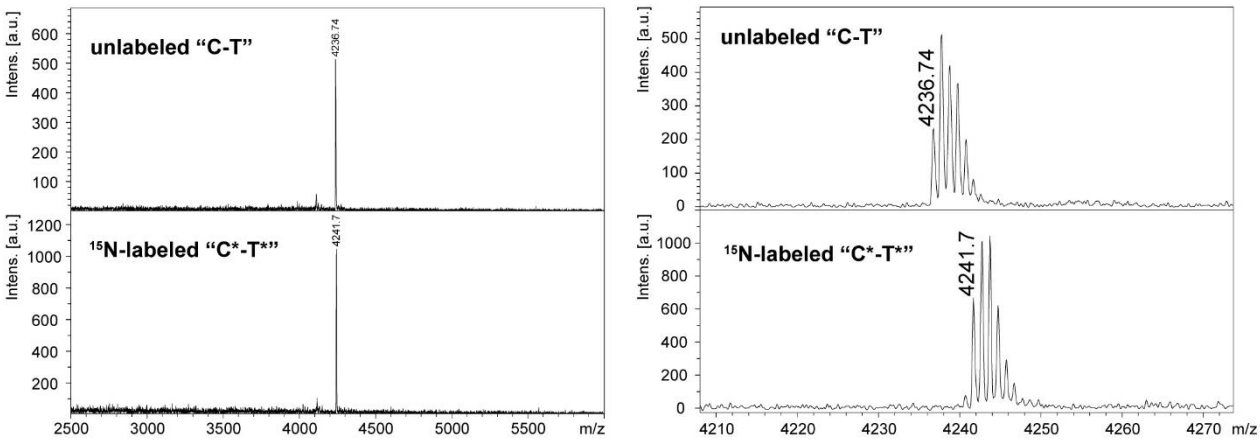

Figure 6.1. MALDI-MS analysis of unlabeled "C-T" and ^{15}N-labeled ODN1* "C*-T*" (left). ^{15}N-labeled ODN1* "C*-T*" showing a mass elevation of 5 dalton (right).

6.1.3. DNA Sequences

6.1.3.1. DNA Sequences Used in Chapter 2

Table 6.2. Names and Sequences of Duplex Oligonucleotides Used for Melting Temperatures (T_m), Photophysical Properties, Metal Ion Screening, and Stoichiometry of Hg^{II} Binding. (Y = ^{DMA}T, T, C, or A)

name		duplex sequence	ε_{260}
X2		5′-C**Y**C TAA CCC TAA CCC TAA CCC-3′	
	X2 T-A	5′-C**Y**C TAA CCC TAA CCC TAA CCC-3	186800 $M^{-1}cm^{-1}$
		3′-G**A**G ATT GGG ATT GGG ATT GGG-5′	218100 $M^{-1}cm^{-1}$
	X2 T-T	5′-C**Y**C TAA CCC TAA CCC TAA CCC-3	186800 $M^{-1}cm^{-1}$
		3′-G**T**G ATT GGG ATT GGG ATT GGG-5′	213600 $M^{-1}cm^{-1}$
	X2 C-A	5′-C**Y**C TAA CCC TAA CCC TAA CCC-3	185900 $M^{-1}cm^{-1}$
		3′-G**A**G ATT GGG ATT GGG ATT GGG-5′	218100 $M^{-1}cm^{-1}$
	X2 C-T	5′-C**Y**C TAA CCC TAA CCC TAA CCC-3	185900 $M^{-1}cm^{-1}$
		3′-G**T**G ATT GGG ATT GGG ATT GGG-5′	213600 $M^{-1}cm^{-1}$
	X2 A-A	5′-C**Y**C TAA CCC TAA CCC TAA CCC-3	191100 $M^{-1}cm^{-1}$
		3′-G**A**G ATT GGG ATT GGG ATT GGG-5′	218100 $M^{-1}cm^{-1}$
	X2 ^{DMA}T-A	5′-C**Y**C TAA CCC TAA CCC TAA CCC-3	193410 $M^{-1}cm^{-1}$
		3′-G**A**G ATT GGG ATT GGG ATT GGG-5′	218100 $M^{-1}cm^{-1}$
	X2 ^{DMA}T-T	5′-C**Y**C TAA CCC TAA CCC TAA CCC-3	193410 $M^{-1}cm^{-1}$
		3′-G**T**G ATT GGG ATT GGG ATT GGG-5′	213600 $M^{-1}cm^{-1}$
X13		5′-CCC TAA CCC TAA **Y**CC TAA CCC-3′	
	X13 T-A	5′-CCC TAA CCC TAA **Y**CC TAA CCC-3′	187800 $M^{-1}cm^{-1}$
		3′-GGG ATT GGG ATT **A**GG ATT GGG-5′	217500 $M^{-1}cm^{-1}$
	X13 T-T	5′-CCC TAA CCC TAA **Y**CC TAA CCC-3′	187800 $M^{-1}cm^{-1}$
		3′-GGG ATT GGG ATT **T**GG ATT GGG-5′	213000 $M^{-1}cm^{-1}$
	X13 C-A	5′-CCC TAA CCC TAA **Y**CC TAA CCC-3′	185900 $M^{-1}cm^{-1}$
		3′-GGG ATT GGG ATT **A**GG ATT GGG-5′	217500 $M^{-1}cm^{-1}$
	X13 C-T	5′-CCC TAA CCC TAA **Y**CC TAA CCC-3′	185900 $M^{-1}cm^{-1}$
		3′-GGG ATT GGG ATT **T**GG ATT GGG-5′	213000 $M^{-1}cm^{-1}$
	X13 A-A	5′-CCC TAA CCC TAA **Y**CC TAA CCC-3′	190700 $M^{-1}cm^{-1}$
		3′-GGG ATT GGG ATT **A**GG ATT GGG-5′	217500 $M^{-1}cm^{-1}$
	X13 ^{DMA}T-A	5′-CCC TAA CCC TAA **Y**CC TAA CCC-3′	193410 $M^{-1}cm^{-1}$
		3′-GGG ATT GGG ATT **A**GG ATT GGG-5′	217500 $M^{-1}cm^{-1}$
	X13 ^{DMA}T-T	5′-CCC TAA CCC TAA **Y**CC TAA CCC-3′	193410 $M^{-1}cm^{-1}$
		3′-GGG ATT GGG ATT **T**GG ATT GGG-5′	213000 $M^{-1}cm^{-1}$
	X13 ^{DMA}T-C	5′-CCC TAA CCC TAA **Y**CC TAA CCC-3′	193410 $M^{-1}cm^{-1}$
		3′-GGG ATT GGG ATT **C**GG ATT GGG-5′	210300 $M^{-1}cm^{-1}$
	X13 ^{DMA}T-G	5′-CCC TAA CCC TAA **Y**CC TAA CCC-3′	193410 $M^{-1}cm^{-1}$
		3′-GGG ATT GGG ATT **G**GG ATT GGG-5′	215000 $M^{-1}cm^{-1}$

Table 6.2 continued

X14		5′-CCC TAA CCC TAA C**Y**C TAA CCC-3′	
	X14 T-A	5′-CCC TAA CCC TAA C**Y**C TAA CCC-3′	186800 $M^{-1}cm^{-1}$
		3′-GGG ATT GGG ATT G**A**G ATT GGG-5′	218100 $M^{-1}cm^{-1}$
	X14 T-T	5′-CCC TAA CCC TAA C**Y**C TAA CCC-3′	186800 $M^{-1}cm^{-1}$
		3′-GGG ATT GGG ATT G**T**G ATT GGG-5′	213600 $M^{-1}cm^{-1}$
	X14 C-A	5′-CCC TAA CCC TAA C**Y**C TAA CCC-3′	185900 $M^{-1}cm^{-1}$
		3′-GGG ATT GGG ATT G**A**G ATT GGG-5′	218100 $M^{-1}cm^{-1}$
	X14 C-T	5′-CCC TAA CCC TAA C**Y**C TAA CCC-3′	185900 $M^{-1}cm^{-1}$
		3′-GGG ATT GGG ATT G**T**G ATT GGG-5′	213600 $M^{-1}cm^{-1}$
	X14 A-A	5′-CCC TAA CCC TAA C**Y**C TAA CCC-3′	191100 $M^{-1}cm^{-1}$
		3′-GGG ATT GGG ATT G**A**G ATT GGG-5′	218100 $M^{-1}cm^{-1}$
	X14 ^{DMA}T-A	5′-CCC TAA CCC TAA C**Y**C TAA CCC-3′	193410 $M^{-1}cm^{-1}$
		3′-GGG ATT GGG ATT G**A**G ATT GGG-5′	218100 $M^{-1}cm^{-1}$
	X14 ^{DMA}T-T	5′-CCC TAA CCC TAA C**Y**C TAA CCC-3′	193410 $M^{-1}cm^{-1}$
		3′-GGG ATT GGG ATT G**T**G ATT GGG-5′	213600 $M^{-1}cm^{-1}$
X15		5′-CCC TAA CCC TAA CC**Y** TAA CCC-3′	
	X15 T-A	5′-CCC TAA CCC TAA CC**Y** TAA CCC-3′	186800 $M^{-1}cm^{-1}$
		3′-GGG ATT GGG ATT GG**A** ATT GGG-5′	216900 $M^{-1}cm^{-1}$
	X15 T-T	5′-CCC TAA CCC TAA CC**Y** TAA CCC-3′	186800 $M^{-1}cm^{-1}$
		3′-GGG ATT GGG ATT GG**T** ATT GGG-5′	213000 $M^{-1}cm^{-1}$
	X15 C-A	5′-CCC TAA CCC TAA CC**Y** TAA CCC-3′	185900 $M^{-1}cm^{-1}$
		3′-GGG ATT GGG ATT GG**A** ATT GGG-5′	216900 $M^{-1}cm^{-1}$
	X15 C-T	5′-CCC TAA CCC TAA CC**Y** TAA CCC-3′	185900 $M^{-1}cm^{-1}$
		3′-GGG ATT GGG ATT GG**T** ATT GGG-5′	213000 $M^{-1}cm^{-1}$
	X15 A-A	5′-CCC TAA CCC TAA CC**Y** TAA CCC-3′	192100 $M^{-1}cm^{-1}$
		3′-GGG ATT GGG ATT GG**A** ATT GGG-5′	216900 $M^{-1}cm^{-1}$
	X15 ^{DMA}T-A	5′-CCC TAA CCC TAA CC**Y** TAA CCC-3′	193410 $M^{-1}cm^{-1}$
		3′-GGG ATT GGG ATT GG**A** ATT GGG-5′	216900 $M^{-1}cm^{-1}$
	X15 ^{DMA}T-T	5′-CCC TAA CCC TAA CC**Y** TAA CCC-3′	193410 $M^{-1}cm^{-1}$
		3′-GGG ATT GGG ATT GG**T** ATT GGG-5′	213000 $M^{-1}cm^{-1}$
	X15 ^{DMA}T-C	5′-CCC TAA CCC TAA CC**Y** TAA CCC-3′	193410 $M^{-1}cm^{-1}$
		3′-GGG ATT GGG ATT GG**C** ATT GGG-5′	211700 $M^{-1}cm^{-1}$
	X15 ^{DMA}T-G	5′-CCC TAA CCC TAA CC**Y** TAA CCC-3′	193410 $M^{-1}cm^{-1}$
		3′-GGG ATT GGG ATT GG**G** ATT GGG-5′	215000 $M^{-1}cm^{-1}$

6.1.3.2. DNA Sequences Used in Chapter 3

Table 6.3. Names and Sequences of Duplex Oligonucleotides Used for K_d, k_{on} and k_{off} Experiments (Y = ^{DMA}T or T).

name	duplex sequence	ε_{260}
X13	5′-CCC TAA CCC TAA **Y**CC TAA CCC-3′	
X13 T-T	5′-CCC TAA CCC TAA **Y**CC TAA CCC-3′	187800 $M^{-1}cm^{-1}$
	3′-GGG ATT GGG ATT **T**GG ATT GGG-5′	213000 $M^{-1}cm^{-1}$
X13 ^{DMA}T-A	5′-CCC TAA CCC TAA **Y**CC TAA CCC-3′	193410 $M^{-1}cm^{-1}$
	3′-GGG ATT GGG ATT **A**GG ATT GGG-5′	217500 $M^{-1}cm^{-1}$
X13 ^{DMA}T-T	5′-CCC TAA CCC TAA **Y**CC TAA CCC-3′	193410 $M^{-1}cm^{-1}$
	3′-GGG ATT GGG ATT **T**GG ATT GGG-5′	213000 $M^{-1}cm^{-1}$
X13 ^{DMA}T-A, X16 T-T	5′-CCC TAA CCC TAA **Y**CC TAA CCC-3′	193410 $M^{-1}cm^{-1}$
	3′-GGG ATT GGG ATT **A**GG **T**TT GGG-5′	211600 $M^{-1}cm^{-1}$
X14	5′-CCC TAA CCC TAA C**Y**C TAA CCC-3′	
X14 ^{DMA}T-A, X16 T-T	5′-CCC TAA CCC TAA C**Y**C TAA CCC-3′	193410 $M^{-1}cm^{-1}$
	3′-GGG ATT GGG ATT G**A**G **T**TT GGG-5′	212200 $M^{-1}cm^{-1}$
X15	5′-CCC TAA CCC TAA CC**Y** TAA CCC-3′	
X15 T-T	5′-CCC TAA CCC TAA CC**Y** TAA CCC-3′	193410 $M^{-1}cm^{-1}$
	3′-GGG ATT GGG ATT GG**T** ATT GGG-5′	213000 $M^{-1}cm^{-1}$
X15 T-A, X16 T-T	5′-CCC TAA CCC TAA CC**Y** TAA CCC-3′	193410 $M^{-1}cm^{-1}$
	3′-GGG ATT GGG ATT GG**A** **T**TT GGG-5′	213000 $M^{-1}cm^{-1}$
X15 ^{DMA}T-A	5′-CCC TAA CCC TAA CC**Y** TAA CCC-3′	193410 $M^{-1}cm^{-1}$
	3′-GGG ATT GGG ATT GG**A** ATT GGG-5′	216900 $M^{-1}cm^{-1}$
X15 ^{DMA}T-T	5′-CCC TAA CCC TAA CC**Y** TAA CCC-3′	193410 $M^{-1}cm^{-1}$
	3′-GGG ATT GGG ATT GG**T** ATT GGG-5′	213000 $M^{-1}cm^{-1}$
X15 ^{DMA}T-A, X16 T-T	5′-CCC TAA CCC TAA CC**Y** TAA CCC-3′	193410 $M^{-1}cm^{-1}$
	3′-GGG ATT GGG ATT GG**A** **T**TT GGG-5′	213000 $M^{-1}cm^{-1}$

Table 6.4. Names and Sequences of Duplex Oligonucleotides Used for Strand-Displacement Reactions. (Y = ^{DMA}T)

name	duplex sequence with TH = 2	invading strand I
X13	5′-CCC TAA CCC TAA **Y**CC TAA CCC-3′	
X13 ^{DMA}T-A	3′-GGG ATT GGG ATT **A**GG ATT GGG **AG**-5′	5′-CCC TAA CCC TAA **T**CC TAA CCC **TC**-3′
X13 ^{DMA}T-T	3′-GGG ATT GGG ATT **T**GG ATT GGG **AG**-5′	5′-CCC TAA CCC TAA **A**CC TAA CCC **TC**-3′
X13 ^{DMA}T-A, X10 T-T	3′-GGG ATT GGG **T**TT **A**GG ATT GGG **AG**-5′	5′-CCC TAA CCC **A**AA **T**CC TAA CCC **TC**-3′
X13 ^{DMA}T-A, X16 T-T	3′-GGG ATT GGG ATT **A**GG **T**TT GGG **AG**-5′	5′-CCC TAA CCC TAA **T**CC **A**AA CCC **TC**-3′
X14	5′-CCC TAA CCC TAA C**Y**C TAA CCC-3′	
X14 ^{DMA}T-A	3′-GGG ATT GGG ATT G**A**G ATT GGG **AG**-5′	5′-CCC TAA CCC TAA C**T**C TAA CCC **TC**-3′
X14 ^{DMA}T-T	3′-GGG ATT GGG ATT G**T**G ATT GGG **AG**-5′	5′-CCC TAA CCC TAA C**A**C TAA CCC **TC**-3′
X14 ^{DMA}T-A, X10 T-T	3′-GGG ATT GGG **T**TT G**A**G ATT GGG **AG**-5′	5′-CCC TAA CCC **A**AA C**T**C TAA CCC **TC**-3′

6.1.3.3. DNA Sequences Used in Chapter 4

Table 6.5. Names and Sequences of Duplex Oligonucleotides Used for Metal Screening Experiments and K_d, k_{on} and k_{off} Experiments for C-Hg^{II}-T base pairs (where Y = ^{DMA}T or ^{DMA}C).

name		duplex sequence	ε_{260}
X13		5'-CCC TAA CCC TAA **Y**CC TAA CCC-3'	
ODN[1]	X13 ^{DMA}T-T	5'-CCC TAA CCC TAA **Y**CC TAA CCC-3'	193410 $M^{-1}cm^{-1}$
		3'-GGG ATT GGG ATT **T**GG ATT GGG-5'	213000 $M^{-1}cm^{-1}$
ODN[2]	X13 ^{DMA}T-C	5'-CCC TAA CCC TAA **Y**CC TAA CCC-3'	193410 $M^{-1}cm^{-1}$
		3'-GGG ATT GGG ATT **C**GG ATT GGG-5'	210300 $M^{-1}cm^{-1}$
ODN[3]	X13 ^{DMA}T-G	5'-CCC TAA CCC TAA **Y**CC TAA CCC-3'	193410 $M^{-1}cm^{-1}$
		3'-GGG ATT GGG ATT **G**GG ATT GGG-5'	215000 $M^{-1}cm^{-1}$
ODN[4]	X13 ^{DMA}T-A	5'-CCC TAA CCC TAA **Y**CC TAA CCC-3'	193410 $M^{-1}cm^{-1}$
		3'-GGG ATT GGG ATT **A**GG ATT GGG-5'	217500 $M^{-1}cm^{-1}$
X14		5'-CCC TAA CCC TAA C**Y**C TAA CCC-3'	
ODN[5]	X14 ^{DMA}T-C	5'-CCC TAA CCC TAA C**Y**C TAA CCC-3'	193410 $M^{-1}cm^{-1}$
		3'-GGG ATT GGG ATT G**C**G ATT GGG-5'	211500 $M^{-1}cm^{-1}$
ODN[6]	X14 ^{DMA}C-T	5'-CCC TAA CCC TAA C**Y**C TAA CCC-3'	195210 $M^{-1}cm^{-1}$
		3'-GGG ATT GGG ATT G**T**G ATT GGG-5'	213600 $M^{-1}cm^{-1}$
X15		5'-CCC TAA CCC TAA CC**Y** TAA CCC-3'	
ODN[7]	X15 ^{DMA}T-T	5'-CCC TAA CCC TAA CC**Y** TAA CCC-3'	193410 $M^{-1}cm^{-1}$
		3'-GGG ATT GGG ATT GG**T** ATT GGG-5'	213000 $M^{-1}cm^{-1}$
ODN[8]	X15 ^{DMA}T-C	5'-CCC TAA CCC TAA CC**Y** TAA CCC-3'	193410 $M^{-1}cm^{-1}$
		3'-GGG ATT GGG ATT GG**C** ATT GGG-5'	211700 $M^{-1}cm^{-1}$
ODN[9]	X15 ^{DMA}T-G	5'-CCC TAA CCC TAA CC**Y** TAA CCC-3'	193410 $M^{-1}cm^{-1}$
		3'-GGG ATT GGG ATT GG**G** ATT GGG-5'	215000 $M^{-1}cm^{-1}$
ODN[10]	X15 ^{DMA}T-A	5'-CCC TAA CCC TAA CC**Y** TAA CCC-3'	193410 $M^{-1}cm^{-1}$
		3'-GGG ATT GGG ATT GG**A** ATT GGG-5'	216900 $M^{-1}cm^{-1}$
ODN[11]	X15 ^{DMA}C-T	5'-CCC TAA CCC TAA CC**Y** TAA CCC-3'	195210 $M^{-1}cm^{-1}$
		3'-GGG ATT GGG ATT GG**T** ATT GGG-5'	213000 $M^{-1}cm^{-1}$
ODN[12]	X15 ^{DMA}C-G	5'-CCC TAA CCC TAA CC**Y** TAA CCC-3'	195210 $M^{-1}cm^{-1}$
		3'-GGG ATT GGG ATT GG**G** ATT GGG-5'	215000 $M^{-1}cm^{-1}$
ODN[13]	X15 ^{DMA}C-G, X14 C-T	5'-CCC TAA CCC TAA C**C**Y TAA CCC-3'	195210 $M^{-1}cm^{-1}$
		3'-GGG ATT GGG ATT G**T**G ATT GGG-5'	213600 $M^{-1}cm^{-1}$
Scavenger DNA			
ODN[14]		5'-CCC TAA **C**GT GCG CAC **T**TT AGG G-3'	202400 $M^{-1}cm^{-1}$
		3'-GGG ATT **T**CA CGC GTG **C**AA TCC C-5'	

Table 6.6. Names and Sequences of Duplex Oligonucleotides Used for T_m measurements and NMR-spectroscopy.

name		duplex sequence	ε_{260}
ODN[15]	"C-T"	5'-CG T**C**T CAT GA**T** ACG-3'	133000 $M^{-1}cm^{-1}$
		3'-GC A**T**A GTA CT**C** TGC-5'	
ODN[16]	"T-T"	5'-CG T**T**T CAT GA**T** ACG-3'	133900 $M^{-1}cm^{-1}$
		3'-GC A**T**A GTA CT**T** TGC-5'	
ODN[17]	"G-T"	5'-CG T**G**T CAT GA**T** ACG-3'	136500 $M^{-1}cm^{-1}$
		3'-GC A**T**A GTA CT**G** TGC-5'	
ODN[18]	"A-T"	5'-CG T**A**T CAT GA**T** ACG-3'	139800 $M^{-1}cm^{-1}$
		3'-GC A**T**A GTA CT**A** TGC-5'	
ODN[19]	"X13 T-T"	5'-CCC TAA CCC TAA **T**CC TAA CCC-3'	187800 $M^{-1}cm^{-1}$
		3'-GGG ATT GGG ATT **T**GG ATT GGG-5'	213000 $M^{-1}cm^{-1}$
ODN[20]	"X13 C-T"	5'-CCC TAA CCC TAA **C**CC TAA CCC-3'	185900 $M^{-1}cm^{-1}$
		3'-GGG ATT GGG ATT **T**GG ATT GGG-5'	213000 $M^{-1}cm^{-1}$
ODN[21]	"X14 T-T"	5'-CCC TAA CCC TAA C**T**C TAA CCC-3'	186800 $M^{-1}cm^{-1}$
		3'-GGG ATT GGG ATT G**T**G ATT GGG-5'	213600 $M^{-1}cm^{-1}$
ODN[22]	"X14 C-T"	5'-CCC TAA CCC TAA C**C**C TAA CCC-3'	185900 $M^{-1}cm^{-1}$
		3'-GGG ATT GGG ATT G**T**G ATT GGG-5'	213600 $M^{-1}cm^{-1}$
ODN[23]	"X15 T-T"	5'-CCC TAA CCC TAA CC**T** TAA CCC-3'	186800 $M^{-1}cm^{-1}$
		3'-GGG ATT GGG ATT GG**T** ATT GGG-5'	213000 $M^{-1}cm^{-1}$
ODN[24]	"X15 C-T"	5'-CCC TAA CCC TAA CC**C** TAA CCC-3'	185900 $M^{-1}cm^{-1}$
		3'-GGG ATT GGG ATT GG**T** ATT GGG-5'	213000 $M^{-1}cm^{-1}$

6.1.3.4. DNA Sequences Used in Chapter 5

Table 6.7. Names and Sequences of Duplex Oligonucleotides Used for T_m Measurements and NMR-spectroscopy. (C* = ^{15}N-labeled C, T* = ^{15}N-labeled T).

name		duplex sequence	ε_{260}
ODN[1]	"C-T"	5'-CG TCT CAT GAT ACG-3' 3'-GC ATA GTA CTC TGC-5'	133000 $M^{-1}cm^{-1}$
ODN[1]*	"C*-T*"	5'-CG TC*T CAT GAT* ACG-3' 3'-GC AT*A GTA CTC* TGC-5'	133000 $M^{-1}cm^{-1}$
ODN[2]	"T-T"	5'-CG TTT CAT GAT ACG-3' 3'-GC ATA GTA CTT TGC-5'	133900 $M^{-1}cm^{-1}$
ODN[3]	"G-T"	5'-CG TGT CAT GAT ACG-3' 3'-GC ATA GTA CTG TGC-5'	136500 $M^{-1}cm^{-1}$
ODN[4]	"A-T"	5'-CG TAT CAT GAT ACG-3' 3'-GC ATA GTA CTA TGC-5'	139800 $M^{-1}cm^{-1}$

6.2 Thermodynamic Measurements

Equilibrium dissociation constants (K_d) were measured in three independent trials using a Horiba FluoroLog spectrofluorophotometer equipped with a speed stirrer and a temperature controller. Pre-folded duplex DNA (4 μM) in aqueous buffer (200 mM Na_2HPO_4, 100 mM citric acid, 100 mM $NaNO_3$ (pH = 7.35)), or alternatively, 10 mM sodium cacodylate-cacodylic acid, 100 mM $Na(ClO_4)_2$ (pH = 6.8) was diluted to 25 nM in a 1.5 mL cuvette. Aliquots of $Hg(ClO_4)_2$ were added while stirring at 4 °C or 25°C and the fluorescent intensity was measured after 1 h incubation.

Binding of Hg^{II} to a T-T mismatch can be modeled by eq 1, where ^{DMA}T-T represents the duplex DNA containing a ^{DMA}T-T mismatch and ^{DMA}T-Hg^{II}-T represents the duplex DNA containing a ^{DMA}T-Hg^{II}-T base pair.

$$\mathbf{^{DMA}T}\text{-T} + Hg^{II} \underset{K_d}{\overset{K_a}{\rightleftarrows}} \mathbf{^{DMA}T}\text{-}Hg^{II}\text{-T} \quad (1)$$

The dissociation constant (K_d) can be expressed by (eq 2)

$$K_d = \frac{[\mathbf{^{DMA}T}\text{–T}][Hg^{II}]}{[\mathbf{^{DMA}T}\text{-}Hg^{II}\text{-T}]} \quad (2)$$

At the half-maximal effective concentration (EC_{50}) K_d is equal to eq 3

$$K_d = [Hg^{II}]_0 - \frac{[\mathbf{^{DMA}T}\text{-T}]_0}{2} \quad (3)$$

Decrease in DNA fluorescence (f) upon Hg^{II} binding is plotted against increasing Hg^{II} concentration ($[Hg^{II}]$) and fit to a monoexponential equation (eq 4) to obtain the EC_{50} from which the dissociation constant (K_d) was calculated (eq 3). Alternatively, if decrease in DNA fluorescence (f) exhibits a biphasic quenching, the data is fit to a biphasic curve (eq 5), where Fr_1 and Fr_2 is the fractional contribution.

$$f = e^{-C[Hg^{II}]_0} \quad (4)$$

$$f = Fr_1 e^{-C_1[Hg^{II}]_0} + Fr_2 e^{-C_2[Hg^{II}]_0} \quad (5)$$

6.3 Kinetic Measurements (k_{on} and k_{off})

6.3.1. Rate Constants of Association (k_{on})

Association rate constants (k_{on}) were measured in three independent trials using a Horiba FluoroLog spectrofluorophotometer equipped with a speed stirrer and a temperature controller. Pre-folded duplex DNA (4 μM) in aqueous buffer (200 mM Na_2HPO_4, 100 mM citric acid and 100 mM $NaNO_3$) was diluted to a final concentration of 0.1 μM in a 1.5 ml cuvette. $Hg(ClO_4)_2$ (2, 4, and 6 equiv.) was added under stirring and the fluorescent intensity was measured as a function of time (λ_{ex} = 370 nm, λ_{em} = 500 nm (^{DMA}T) or λ_{em} = 510 nm (^{DMA}C)) at 25°C.

Binding of Hg^{II} can be modeled as a bimolecular reaction (eq 6) where ^{DMA}T-T represents the duplex DNA containing a ^{DMA}T-T mismatch and ^{DMA}T-Hg^{II}-T represents the duplex DNA containing the ^{DMA}T-Hg^{II}-T base pair.

$$\mathbf{^{DMA}T}\text{-T} + Hg^{II} \underset{k_{off}}{\overset{k_{on}}{\rightleftarrows}} \mathbf{^{DMA}T}\text{-}Hg^{II}\text{-T} \quad (6)$$

Given the fact that Hg^{II} is used in excess of the DNA, and that the observed dissociation of Hg^{II} from ^{DMA}T-Hg^{II}-T is much slower than the binding of Hg^{II} to the ^{DMA}T-T mismatch, the back-reaction k_{off} is neglected. The association reaction can thereby be approximated as a function of time (t) (eq 7).

$$\frac{1}{[Hg^{II}]_0 - [\mathbf{^{DMA}T}\text{-T}]_0} \ln\left(\frac{[\mathbf{^{DMA}T}\text{-T}]_0[Hg^{II}]}{[Hg^{II}]_0[\mathbf{^{DMA}T}\text{-T}]}\right) = k_{on}t \quad (7)$$

The time dependent binding can be approximated by (eq 8).

$$\frac{[\mathbf{^{DMA}T}\text{-T}]_t}{[\mathbf{^{DMA}T}\text{-T}]_0} = e^{-k_{on}[Hg^{II}]_0 t} \quad (8)$$

The decrease of the fluorescence (f) upon binding of Hg^{II} to the ^{DMA}T-T mismatch is plotted against time (t) and can be fit to the monoexponential equation (eq 9) to obtain a rate of association (r) in s^{-1}, where $r = k_{on}[Hg^{II}]_0$. Rates (r) are plotted against concentrations of Hg^{II} and the slope of the linear regression provides the association rate constant (k_{on}) in $M^{-1}s^{-1}$.

$$f = e^{-k_{on}[Hg^{II}]_0 t} \quad (9)$$

6.3.2. Rate Constants of Dissociation (k_{off})

Dissociation rate constant (k_{off}) measurements were measured in three independent trials using a 1.5 ml cuvette as for k_{on} measurements above or using a Molecular Devices Spectra spectrofluorophotometer with a temperature controller in 384-wellplates. Pre-folded duplex DNA (prepared at 4 μM or 8 μM) in aqueous buffer (200 mM Na_2HPO_4, 100 mM citric acid and 100 mM $NaNO_3$, pH = 7.35) was incubated with 2 equiv. of $Hg(ClO_4)_2$ for 3 h at rt. Then, 50 equiv. of "scavenger" DNA (Tables 6.3 and 6.5) or of an unlabeled duplex DNA of the same sequence containing a T-T mismatch was added as a passive Hg^{II} scavenger and the mixture was rapidly mixed. Samples measured in 384-well plates were overlaid with paraffin oil. The increase of fluorescent intensity was measured as a function of time (λ_{ex} = 370 nm, λ_{em} = 500 nm (^{DMA}T) or λ_{em} = 510 nm (^{DMA}C)) at 25°C. Similar results were obtained when using a scavenger duplex DNA having the same or a different sequence, suggesting the absence of any strand-displacement activity during the k_{off} measurements. The observed dissociation rates were independent of the fluorescent DNA concentrations in this range.

Hg^{II} dissociation from ^{DMA}T-Hg^{II}-T can be modeled by eq 10, where ^{DMA}T-Hg^{II}-T represents the duplex DNA containing the ^{DMA}T-Hg^{II}-T base pair and ^{DMA}T-T represents the duplex DNA containing a ^{DMA}T-T mismatch. Because of the large excess of unmodified DNA containing a T-T mismatch, the back-reaction can be neglected.

$$\mathbf{^{DMA}T}\text{-}Hg^{II}\text{-}T \xrightarrow{k_{off}} \mathbf{^{DMA}T}\text{-}T + Hg^{II} \quad (10)$$

The dissociation of Hg^{II} can be expressed as a function of time where the increase in DNA fluorescence (f) is plotted against time (t) and fit to a monoexponential equation (eq 11).

$$f = \frac{[\mathbf{^{DMA}T}\text{-}Hg^{II}\text{-}T]_t}{[\mathbf{^{DMA}T}\text{-}Hg^{II}\text{-}T]_0} = e^{-k_{off}t} \quad (11)$$

At the half-life ($t_{1/2}$) of the reaction k_{off} is equal to eq 12.

$$k_{off} = \frac{\ln(2)}{t_{1/2}} \quad (12)$$

6.4 Strand-Displacement Measurements

Strand-displacement reactions were carried out in three independent trials as previously described.[6] To pre-folded ^{DMA}T-modified duplexes DNA (4 μM) containing a 5'-overhang, an excess of invading strand was added (Table 6.4). The reaction was rapidly mixed, overlayed with paraffin oil, and changes in fluorescent intensity were measured as a function of time (λ_{ex} = 370 nm, λ_{em} = 500 nm) at 25 °C.

The strand-displacement reaction can be modeled as a bimolecular reaction (eq 13). ^{DMA}T-A represents the initial duplex, I represents the invading strand, A-I the newly formed duplex DNA, and ^{DMA}T the displaced single strand.

$$\mathbf{^{DMA}T\text{-}A} + \mathbf{I} \underset{k_{-1}}{\overset{k}{\rightleftarrows}} \mathbf{A\text{-}I} + \mathbf{^{DMA}T} \qquad (13)$$

The back-reaction (k_{-1}) was neglected due to the higher kinetic and thermodynamic stability of I-A as compared to ^{DMA}T-A. In addition, the concentration of the invading strand I ($[I]_0$ = 16 μM to 40 μM) is much higher than the initial duplex ^{DMA}T-A ($[^{DMA}T\text{-}A]_0$ = 4 μM). The change in fluorescence intensity can therefore be plotted against time and fitted by the monoexponential eq 14 to obtain a rate (r) in s^{-1}, where $r = k[I]_0$.

$$f = \frac{[\mathbf{^{DMA}T}]_t}{[\mathbf{^{DMA}T}]_0} = e^{-k[I]_0 t} \qquad (14)$$

By plotting the rates (r) against the concentration of invading strand I, the rate constant k ($M^{-1}s^{-1}$) can be determined as the slope of the linear fit.

6.5 Primer Extension Reactions

dNTP's were purchased as 100 mM solutions from *New England BioLabs Inc.* Klenow Fragment (3' → 5' *exo*-) and DNA Pol I (*E. coli*) were purchased from *New England BioLabs Inc.* Prior to use, the buffers were exchanged by ultrafiltration at 12500 x g utilizing an Amicon Ultra-0.5 centrifugal filter. The buffer solution containing Klenow Fragment (*exo*-) was exchanged with 25 mM Tris-HCl, 1 mM 3,3',3"-phosphanetriyltris (benzenesulfonic acid) trisodium salt (TPPTS), 0.1 mM EDTA and 50 % glycerol at pH = 7.40. The buffer solution containing DNA Pol I (*E. coli*) was exchanged with 25 mM Tris-HCl, 0.11 mM TPPTS, 11 μM EDTA and 50 % glycerol at pH = 7.40.

Template strands were annealed with complementary sequences and a 5' FAM-labeled primer at 10 μM each. After heating and slow cooling to rt, $Hg(ClO_4)_2$ was added (0 – 200 equiv.) and incubated for 3 h at rt. The mixture was diluted to a final concentration of 100 nM. dNTP's were then added and the reaction was started by the addition of DNA polymerase. The total reaction volume was 70 μl, and the final concentrations of each component was 100 nM template strand, 100 nM primer, 100 nM complementary strand, 2 μM dNTPs, and 50 nM Klenow Fragment (*exo*-) or 0.05 nM DNA Pol I (*E. coli*). The reaction mixture was incubated at 25 °C or 37 °C, for Klenow Fragment and DNA Pol I, respectively. Final buffer conditions were 50 mM NaCl, 10 mM $MgCl_2$ and 10 mM Tris-HCl, 8 μM TPPTS (pH = 7.90). Aliquots of each reaction (10 μl) were removed at the given time point and quenched by the addition of loading solution (10 μl, 8 M urea, 30 mM EDTA, 50 % sucrose) and heating at 90 °C for 10 min. The reaction mixtures were then placed on ice and a DTT solution (1 μl, 100 mM) was added to bind Hg^{II} thereby preventing aggregation of the DNA.[7] The reactions components were separated by gel electrophoresis on a 13 % polyacrylamide gel (1 x TBE) under denaturing conditions (8 M urea). Gels were scanned on *Typhoon FLA 9500* (λ_{ex} = 473 nm, λ_{em} = 520 nm) and analyzed using *ImageQuantTL*.

6.6 Metal Ion Screening by Fluorescence

Pre-folded duplex "X14" (8 μM) in aqueous buffer (200 mM of Na_2HPO_4, 100 mM of citric acid and 100 mM $NaNO_3$ (pH = 7.35)) was mixed 1:1 (v:v) with solutions of metal ions in the same buffer to a final concentration of 4 μM DNA and 8 μM of $Hg(ClO_4)_2$, $AgNO_3$, $CdCl_2$, $MgCl_2$, $FeCl_2$, $NiCl_2$, $Pd(NO_3)_2$, $ZnCl_2$, or $CaCl_2$ and incubated at rt for 3 h prior to each measurement. Fluorescence spectra were recorded at 25 °C using a *Molecular Devices Spectra spectrofluorophotometer* with a temperature controller in 96- or 384-well plates.

6.7 Thermal Melting Analyses (T_m)

Melting temperatures (T_m) of self-complementary sequences were determined from the changes in absorbance at 260 nm as a function of temperature in a 1 mm path length thermo-controlled, strain-free quartz cuvette on a *JASCO J-715* spectrometer equipped with a temperature control system. Solutions of pre-folded duplex DNA in aqueous buffer (200 mM $NaClO_4$, 50 mM cacodylic acid at pH = 7.0) were equilibrated at 4 °C for 20 min and slowly ramped to 90 °C with 0.5 °C steps at a rate of 25 °C / h. Where indicated, DNA samples were incubated with 2.0 equiv (relative to mismatch) of $Hg(ClO_4)_2$ or $AgNO_3$ for 3 h prior to analysis. T_m values were calculated as the first derivatives of both the heating and cooling curves measured in triplicate and averaged. Little or no hysteresis ($\leq$ 1.0 ^oC) was observed between each heating and cooling cycle. Melting temperatures (T_m) of 21-mer duplexes X13, X14, and X15 were determined from changes in the molar ellipticity at 262 nm as a function of temperature in a 1 mm path length thermo-controlled, strain-free quartz cuvette on a *JASCO J-715* spectrometer. A 5 μM solution of pre-folded duplex DNA in aqueous buffer (200 mM of Na_2HPO_4, 100 mM of citric acid and 100 mM $NaNO_3$ (pH = 7.35)) was equilibrated for 15 minutes at 5 °C and slowly ramped to 95 °C at a rate of 10 °C/h. T_m values were determined by plotting the molar ellipticity versus temperature using a dose-response non-linear regression curve and were calculated from the averaged values of heating and cooling curves. Where indicated, duplex DNA was annealed in the presence of 1.0 equiv of $Hg(ClO_4)_2$. The reproducibility of the measurement was within 0.3 °C.

6.8 Circular Dichroism (CD) Spectroscopy

Circular dichroism spectra of pre-annealed duplex DNA were measured at 4 °C or 25 °C using a 2 nm band width with 0.1 nm steps at a scanning rate of 20 nm / min in a 1 mm path length thermo-controlled strain-free quartz cuvette on a *JASCO J-715* spectrometer. Self-complementary duplex DNA (10 μM) was prepared by diluting the self-complementary sequences into aqueous buffer (200 mM $NaClO_4$, 50 mM cacodylic acid at pH = 7.0), heating to 95 °C for 5 min, and slowly cooling to room temperature over 4 h. The final pH was then adjusted to 7.8 by adding a solution of NaOH. Duplex DNAs analyzed in the presence of Hg^{II} were incubated with $Hg(ClO_4)_2$ for 3 h prior to use. 21-mer duplexes X13, X14, and X15 (5 μM) were annealed in the presence or absence of 1.0 equiv of $Hg(ClO_4)_2$ in aqueous buffer (200 mM of Na_2HPO_4, 100 mM of citric acid and 100 mM $NaNO_3$ (pH = 7.35)). CD spectra were recorded as described above, except that a scanning rate of 50 nm / min was used.

6.9 NMR Studies

6.9.1. Sample Preparation

Duplex DNA (0.5 mM or 1.0 mM) was prepared by dissolving 1.0 mM or 2.0 mM of the self-complementary sequence in aqueous buffer (200 mM $NaClO_4$, 50 mM cacodylic acid in H_2O / D_2O (9:1) at pH = 7.0), heating to 95 °C for 5 min, and slowly cooling to room temperature over 4 h. For Hg^{II} titration experiments, aliquots of $Hg(ClO_4)_2$ were added, and NMR spectra were recorded after incubating each sample for 15 min at r.t. followed by 15 min at 4 °C. ^{15}N-labeled duplex DNA (0.5 mM or 1.0 mM) was prepared by dissolving 1.0 mM or 2.0 mM of the self-complementary sequence in an aqueous buffer (200 mM $NaClO_4$, 50 mM cacodylic acid in H_2O / D_2O (9:1) at pH = 7.0) and annealed as described above. The pH was adjusted to approximately pH = 7.8 by addition of an aqueous solution of NaOH. For solution structure determination, oligonucleotides were desalted, and duplex DNA (0.4 mM) was prepared by dissolving 0.8 mM of the self-complementary sequence in an aqueous solution of $NaClO_4$ (50 mM, 90:10 H_2O/D_2O) and the pH was adjusted to 7.75 by addition of an aqueous solution of NaOH. The samples were annealed as described above and if necessary the pH was readjusted to pH = 7.75. Samples measured in D_2O were prepared in an aqueous solution of $NaClO_4$ (50 mM) and the pH was adjusted to 7.75 by addition of an aqueous solution of NaOH and annealed as described above. The sample was lyophilized, dissolved in 99.9% D_2O and the pD was adjusted to 7.35 by addition of a solution of NaOD in 99.9 % D_2O. DNA sample used for structure determination measurements was treated with Chelex-100 (BIO-RAD) for 10 min after addition of Hg^{II} (1.5 equiv with respect to mismatch) to remove unspecific Hg^{II} coordination.[8] Samples measured at 4 °C were equilibrated at 4 °C for 15 min prior to measuring.

6.9.2. NMR Spectra Measurements

^1H NMR spectra were recorded on a Bruker Avance II 500 MHz spectrometer equipped with a TXI *z*-axis gradient probe head using excitation sculpting for water suppression. Proton chemical shifts were referenced to the water line at 4.70 ppm at the given temperature. The spectra were processed with a line broadening factor of 10 Hz. [^1H,^1H]-NOESY spectra for unlabeled oligonucleotides in 200 mM $NaClO_4$, 50 mM cacodylic acid in H_2O / D_2O (9:1) at pH = 7.0 and for ^{15}N-labeled oligonucleotides (200 mM $NaClO_4$, 50 mM cacodylic acid in H_2O / D_2O (9:1) at pH = 7.8) were recorded on a Bruker Avance 600 MHz spectrometer equipped with a TCI *z*-axis gradient CryoProbe at 4 °C with mixing times 100 ms and 120 ms, respectively. Proton chemical shifts were referenced to the water line at 4.70 ppm at the given temperature. 1D ^{15}N NMR spectra were recorded on a Bruker Avance II 500 MHz spectrometer equipped with a BBO *z*-axis gradient CryoProbe at 4 °C or 25 °C using either inverse gated or no

proton decoupling. An inter-scan delay of 1 s was used with a nominal 30° pulse for excitation and the pulse sequence employed a gradient spin echo of 2.5 ms duration prior to acquisition in order to get rid of the strong background signal. The total experiment time was typically on the order of 72 h. ^{15}N chemical shifts were indirectly referenced against $^{1}\mathrm{H}$ using $\Xi = 0.101329118$.[10] The spectra were processed with a line-broadening factor of 10 Hz. ^{1}J [^{15}N,^{1}H]-HSQC spectra were recorded on a Bruker Avance II 500 MHz spectrometer equipped with a BBO *z*-axis gradient CryoProbe at 4 °C. Proton chemical shifts were referenced to the water line at 4.70 ppm at 4 °C and ^{15}N chemical shifts were indirectly referenced against $^{1}\mathrm{H}$ using $\Xi = 0.101329118$.[10] The INEPT time in the ^{1}J [^{15}N,^{1}H]-HSQC's was set to select for a 90 Hz coupling. z-z exchange ^{1}J [^{15}N,^{1}H]-HSQC spectra containing a delay time before reverse INEPT were recorded on a Bruker Avance 600 MHz spectrometer equipped with TCI *z*-axis gradient CryoProbe at 25° C. Long-range [^{15}N,^{1}H]-HSQC spectra were recorded on a Bruker Avance 600 MHz spectrometer equipped with TCI *z*-axis gradient CryoProbe at 4 °C or on a Bruker Avance 700 MHz spectrometer equipped with TXI *z*-axis gradient CryoProbe at 25 °C. The INEPT time was set to select for a 20 Hz coupling. In order to enhance sensitivity, band-selective long-range [^{15}N,^{1}H]-HSQCs were measured in some instances in which the 180° ^{15}N pulses in both INEPT blocks were replaced by band-selective pulses with a minimal excitation to the ^{15}N nuclei of the NH_2 and NH resonances. The INEPT time was set to 25 Hz coupling. Water flip-back pulses together with the WATERGATE method were used for water suppression. For solution structure determination non-exchangeable resonances were assigned from [^{1}H,^{1}H]-NOESY spectra (4 °C and 25 °C and mixing times of 60 ms and 250 ms), [^{1}H,^{1}H]-total correlation spectra (TOCSY) (4 °C, 50 ms mixing time), and [^{1}H,^{1}H]-correlation spectra (COSY) in D_2O and were recorded either on a Bruker Avance 600 MHz spectrometer equipped with a TCI *z*-axis gradient CryoProbe or on a Bruker Avance 700 MHz spectrometer equipped with TXI *z*-axis gradient CryoProbe. Exchangeable protons were assigned from [^{1}H,^{1}H]-NOESY spectra (4 °C, 150 ms mixing time) recorded on a Bruker Avance 600 MHz spectrometer equipped with a TCI *z*-axis gradient CryoProbe in H_2O/D_2O (90:10). ^{31}P spectra were recorded on a Bruker Avance II 500 MHz spectrometer equipped with a BBO *z*-axis gradient CryoProbe at 25 °C. [^{1}H,^{1}H]-Exclusive correlation spectra (E.COSY)[9] were recorded on a Bruker Avance 600 MHz spectrometer equipped with a TCI *z*-axis gradient CryoProbe.

6.9.3. HR-MS of $Hg(ClO_4)_2$

Ethylenediamine tetraacetic acid disodium salt (Na_2EDTA) (60 μM) was added to ODN1* "C*-T*" (4 μM) containing 12 μM ^{199}Hg-enriched $Hg(ClO_4)_2$. After incubating for 20 min, high-resolution electrospray mass spectra (HR-ESI-MS) of the Hg^{II}-$EDTA^{2-}$ complex were recorded on a *Bruker maXis QTOF-MS*. As control experiments the HR-ESI-MS of natural abundance $Hg(ClO_4)_2$ and ^{199}Hg-enriched $Hg(ClO_4)_2$ without DNA were recorded after incubation with Na_2EDTA. Samples were measured via continuous flow injection with a flow rate of 3 μl/min. The mass spectrometer was calibrated between *m/z* 118 and 2721 using an Agilent ESI-L low concentration tuning mix solution at a resolution of 20'000 and a mass accuracy below 2 ppm.

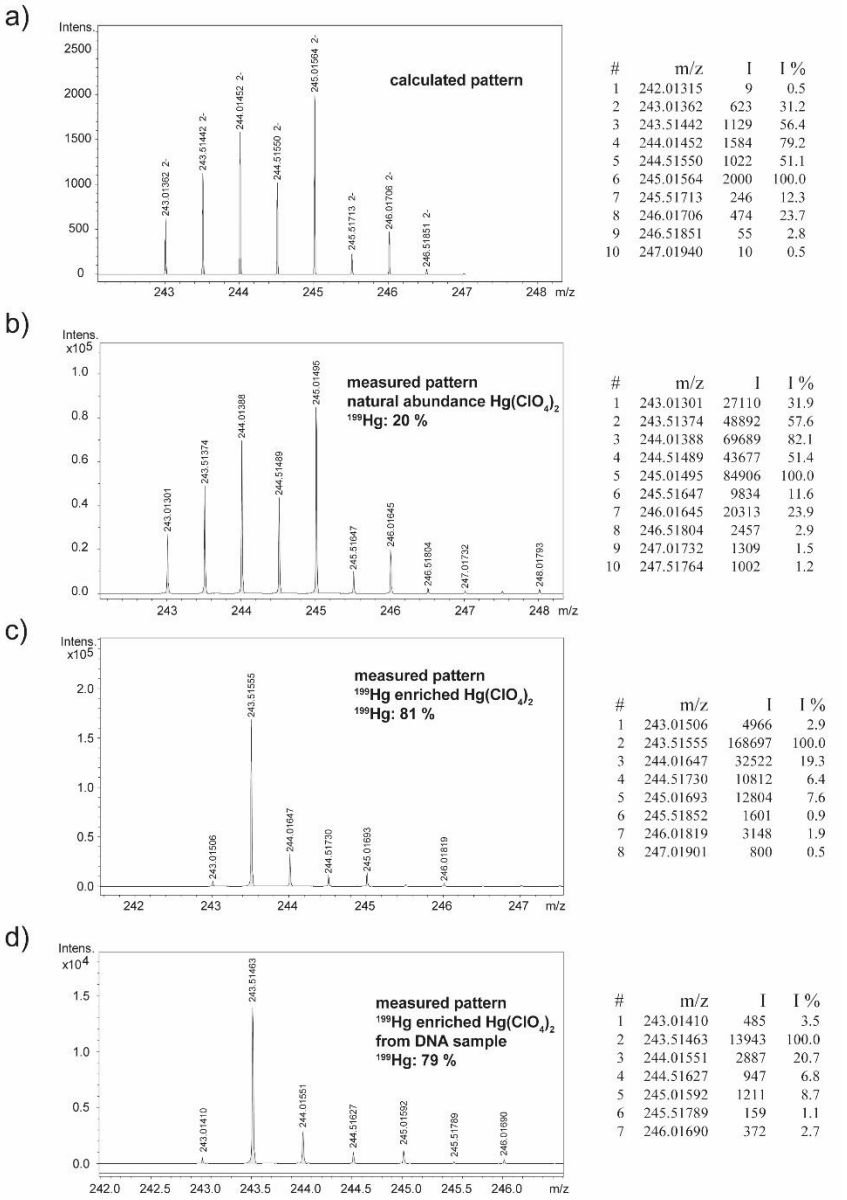

#	m/z	I	I %
1	242.01315	9	0.5
2	243.01362	623	31.2
3	243.51442	1129	56.4
4	244.01452	1584	79.2
5	244.51550	1022	51.1
6	245.01564	2000	100.0
7	245.51713	246	12.3
8	246.01706	474	23.7
9	246.51851	55	2.8
10	247.01940	10	0.5

#	m/z	I	I %
1	243.01301	27110	31.9
2	243.51374	48892	57.6
3	244.01388	69689	82.1
4	244.51489	43677	51.4
5	245.01495	84906	100.0
6	245.51647	9834	11.6
7	246.01645	20313	23.9
8	246.51804	2457	2.9
9	247.01732	1309	1.5
10	247.51764	1002	1.2

#	m/z	I	I %
1	243.01506	4966	2.9
2	243.51555	168697	100.0
3	244.01647	32522	19.3
4	244.51730	10812	6.4
5	245.01693	12804	7.6
6	245.51852	1601	0.9
7	246.01819	3148	1.9
8	247.01901	800	0.5

#	m/z	I	I %
1	243.01410	485	3.5
2	243.51463	13943	100.0
3	244.01551	2887	20.7
4	244.51627	947	6.8
5	245.01592	1211	8.7
6	245.51789	159	1.1
7	246.01690	372	2.7

Figure 6.2. HR-ESI-MS analysis of Hg^{II}-$EDTA^{2-}$ complex. a) Calculated isotopic pattern of Hg^{II}-$EDTA^{2-}$. b) Measured isotopic pattern of natural abundance Hg^{II}-$EDTA^{2-}$. c) Measured isotopic pattern of ^{199}Hg-enriched Hg^{II}-$EDTA^{2-}$. d) Measured isotopic pattern of ^{199}Hg-enriched Hg^{II}-$EDTA^{2-}$ from ODN1* **"C*-Hg^{II}-T*"** duplex DNA.

6.9.4. Structure Calculations

The integrated peak volumes from the [^{1}H,^{1}H]-NOESY spectrum measured at 25 °C with a mixing time of 250 ms were calibrated to distances using CALIBA macro in DYANA.[11] The NOE signals were grouped into four categories: (i) strong (1.8 – 3.0 Å), (ii) medium (1.8 – 4.5 Å), (iii) weak (3.0 – 6.0 Å), and very weak (4.0 – 7.0 Å).

Structure calculations were performed with XPLOR-NIH 2.46 using standard implemented force field parameters.[12] For C-Hg^{II}-T base pair residues no backbone dihedral angle-, backbone torsion angle-, or sugar pucker restraints were applied. For the other residues the following angle restraints were used: Based on ^{31}P NMR, α and ζ backbone dihedral angles were restrained to α = -70 ° ± 20 ° and ζ = -85 ° ± 20 °,[13] respectively, to exclude trans-conformation (Figure 5.15, Chapter 5).[14] Based on H1',H2', H1',H2'', H1',H3' cross peaks in [^{1}H,^{1}H]-NOESY spectra and cross peaks in [^{1}H,^{1}H]-COSY and [^{1}H,^{1}H]-TOCSY spectra, the torsion angles ß (180 ° ± 20 °)[13], γ (60 ° ± 20 °)[15], δ (140 ° ± 25 °)[15], and ε (-170 ° ± 20 °)[16] were set to B-form values. Glycosidic angles χ were restrained to -120 ± 20 Å (*anti*-conformation).[13] Planarity and H-bond distance restraints were used for all residues, except for C-Hg^{II}-T base pair residues. Hg^{II} ions were included as a 2+ positive charge. For C-Hg^{II}-T base pairs in the major duplex species, the following contraints were included based on crystal structures of similar base pairs: (i) distance *N3*(C)–*N3*(T) = 4.1 ± 0.3 Å;[17] (ii) bondlength *N3*(C)–Hg^{II} = 2.04 Å, bondlength *N3*(T)–Hg^{II} = 2.04 Å;[17] (iii) angle *N3*(T)–Hg^{II}–*N3*(C) = 180 °,[18] angle thymidine *C2*/*C4*–*N3*–Hg^{II} = 117 °,[19] angle cytosine *C2*–*N3*–Hg^{II} = 113.4 °,[20] angle cytosine *C4*–*N3*–Hg^{II} = 126.1 °.[20] For C-Hg^{II}-T base pairs in the minor duplex species, the following contraints were included based on a crystal structure of a C-Hg^{II}-T-containing duplex DNA:[21] (i) distance *N4*(C)- *N3*(T) = 4.3 ± 0.3 Å; (ii) bondlength *N4*(C)-Hg^{II} = 2.13 Å, bondlength *N3*(T)-Hg^{II} = 2.13 Å; (iii) angle *N3*(T)–Hg^{II}–*N4*(C) = 180 °, angle thymidine *C2*/*C4*–*N3*–Hg^{II} = 116 °, angle cytosine *C4*–*N4*–Hg^{II} = 118 °, angle *H*–*N4*–Hg^{II} = 120 °. H3', H4', H5', and H5'' sugar protons were only assigned for the major duplex species. For the minor duplex, same NOE-coupling patterns and NOE-cross peak intensities for the above mentioned sugar proton resonances were taken as for the major species for the structure calculation. Given the experimental C_2 symmetry observed in all NMR spectra, a non-crystallographic symmetry term was introduced for the calculations.

Starting from a strand generated based on the sequence of nucleoside residues, 2000 structures were calculated based on NOE-, dihedral-, planarity-, and H-bond distance restraints using simulated annealing. The 20 lowest energy structures were selected and used for further refinement using additional RAMA and ORIE database terms. 200 refined structures were calculated and the 20 lowest energy structures were visualized and analyzed. The representative model (major: model 1, minor: model 6) were chosen based on fewest outliers in the geometric quality criteria (standard geometry (bond lengths, bond angles, chirality, and planarity), and too-close contacts

between non-bonded atoms with unfavorable steric overlap of van der Waals shells. Root mean square deviation (r.m.s.d.) were calculated using MOLMOL[22] and duplexes were visualized using PyMOL.[23] Base-pair parameters were determined using Curves+[24] or 3DNA[25]. Structure coordinates and NMR chemical shift assignments are deposited in the Protein Data Bank as 6FY6 (major species) and 6FY7 (minor species).

6.9.5. Rate Constants of Major-Minor Duplex Interconversion

6.9.5.1. Dynamic Changes in Local Metal Ion Coordination

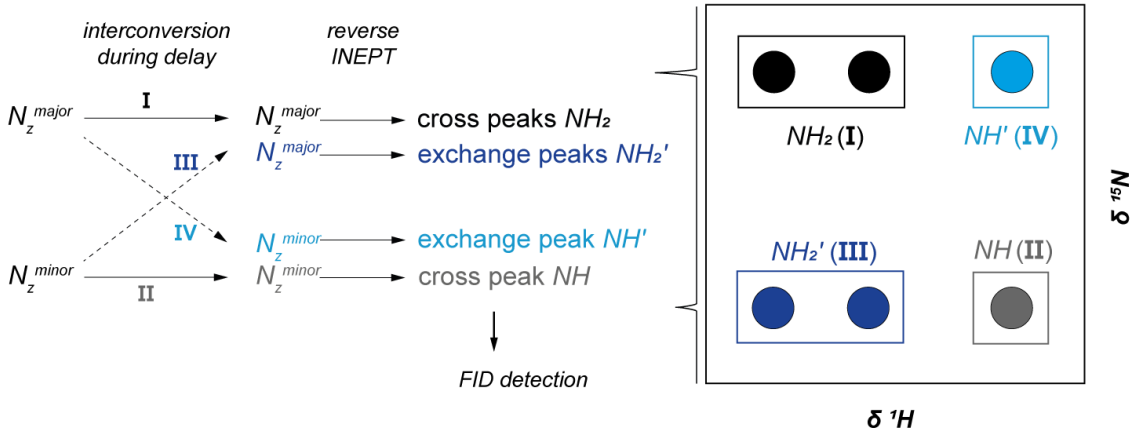

Figure 6.3. Schematic description of a [^{15}N,^{1}H]-HSQC experiment with a delay introduced before the reverse INEPT showing all possible ^{15}N z-z magnetization transfers (I-IV) (left). Exchange I and II give cross peaks NH_2 (black) and NH (grey) (right), corresponding to those of [^{15}N,^{1}H]-HSQC experiments without delay (right). Interconversion of major- and minor structures during the delay results in exchange III and IV to give exchange cross peaks NH_2' (dark blue) and NH' (light blue).

To investigate dynamic changes in local metal ion coordination, we measured z-z exchange [^{15}N,^{1}H]-HSQC with a delay before reverse INEPT. To determine rate constants of interconversion, the decreases of cross peaks and increases of exchange cross peaks were monitored as a function of delay time (t_d) at 25°C (Figure 5.25, Chapter 5). The area of integration of cross peaks (NH_2 and NH) and exchange peaks (NH_2' and NH') were taken, normalized to one of the NH_2^{major} signals (6.81/96.71 ppm) from z-z exchange [^{15}N,^{1}H]-HSQC spectrum with a delay time (t_d) = 100 ms, and plotted as a function of delay time (t_d). The rate constants of interconversion were determined by global fitting of normalized integrated peak volumes versus delay times (t_d) using eqs 19-22,[26] respectively, under the assumption that all proton- and nitrogen atoms have the same relaxation rate (R_1) and that the NH proton is converted equally to both NH_2 protons during the exchange.[26] A global fit was used, where R_1, k_1, and k_{-1} was constrained to be equal for all four curves.

The decay of NH_2 ^1J ^1H,^{15}N crosspeak can be expressed as

$$\frac{d(NH_2)}{d(t_d)} = -NH_2(t_d)(k_1 + R_1) + k_{-1}NH'(t_d) \quad (15)$$

The decay of NH ^1J ^1H,^{15}N crosspeak can be expressed as

$$\frac{d(NH)}{d(t_d)} = -NH(t_d)(k_{-1} + R_1) + k_1NH_2'(t_d) \quad (16)$$

The build-up of NH' ^1J ^1H,^{15}N crosspeak can be expressed as

$$\frac{d(NH')}{d(t_d)} = -NH'(t_d)(k_{-1} + R_1) + k_1NH_2(t_d) \quad (17)$$

The build-up of NH_2' ^1J ^1H,^{15}N crosspeaks can be expressed as

$$\frac{d(NH_2')}{d(t_d)} = -NH_2'(t_d)(k_1 + R_1) + k_{-1}NH(t_d) \quad (18)$$

with t_d = delay time, R_1 = autorelaxation rate and k_1 and k_{-1} = rate constants of interconversion.

Integration of eq 15 – 18 gives eq 19 – 22, respectively.

$$NH_2(t_d) = \frac{a_0 c\, e^{-R_1 t_d}(k_{-1} + k_1 e^{t_d(-k_1-k_{-1})})}{k_1+k_{-1}} \quad (19)$$

$$NH(t_d) = \frac{q c_0 e^{-R_1 t_d}(k_1 + k_{-1} e^{t_d(-k_1-k_{-1})})}{k_1+k_{-1}} \quad (20)$$

$$NH'(t_d) = -\frac{q a_0 e^{-R_1 t_d} k_1(-1 + e^{t_d(-k_1-k_{-1})})}{k_1+k_{-1}} \quad (21)$$

$$NH_2'(t_d) = -\frac{c c_0 k_{-1} e^{-R_1 t_d}(-1 + e^{t_d(-k_1-k_{-1})})}{k_1+k_{-1}} \quad (22)$$

with t_d = delay time, R_1 = autorelaxation rate, k_1 and k_{-1} = rate constants of interconversion and a_0 , c, c_0, and q = constants.

6.9.5.2. Rate Constants of Global Helix Interconversion

To determine rate constants of global interconversion of the duplexes, we measured [^{1}H,^{1}H]-NOESY spectra with various mixing times (t_m) at 25 °C (Figures A28 and A29, Appendix). Selected exchange cross peaks ('Aa' and 'aA', Figure 6.4a, Figure A28, Appendix) and exchange-mediated NOE cross peaks ('Ab' and 'aB', Figure 6.4b, Figure A29, Appendix) were integrated, normalized to signal intensity at mixing time = 200 ms, and plotted as a function of mixing time (t_m) (Figures 5.32 – 5.35, Chapter 5). Two NOE signals were also included to the analysis as controls (Figure 5.33, Chapter 5). At longer mixing times, a decrease in signal intensity was observed due to auto relaxation (R_1).

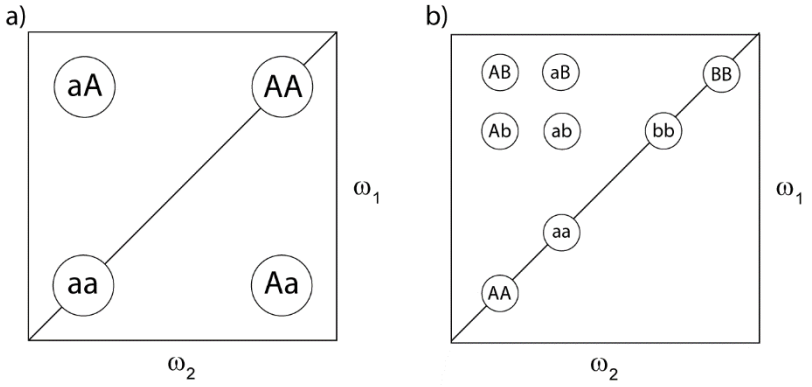

Figure 6.4. Definition of a) diagonal peaks ('AA' and 'aa') undergoing conformational interconversion to give exchange cross peaks ('aA' and 'Aa') and b) 'AB' and 'ab' NOE cross peaks undergoing conformational interconversion to give exchange-mediated NOE cross peaks 'Ab' and aB'. Figure adapted from ref 27.

Under the assumption that auto relaxation $R_{1,A} = R_{1,a}$ and cross relaxation $\sigma = 0$, change in area of integration of diagonal peaks ('AA' and 'aa') and exchange cross peaks ('Aa' and 'aA') and can be expressed by eq 23 – 25, respectively.[27,28] Fit with eq 25 of change in area of integration of exchange cross peaks as a function of mixing time (t_m) furnishes the sum of rate constants $k_1 + k_{-1}$ (Figure 5.32, Table 5.4, Chapter 5).

$$\text{diagonal peak 'AA' } (t_m) = \frac{k_{-1}}{(k_1+k_{-1})^2}\, e^{-R_1 t_m}(k_{-1} + k_1 e^{-(k_1+k_{-1})t_m}) \quad (23)$$

$$\text{diagonal peak 'aa' } (t_m) = \frac{k_1}{(k_1+k_{-1})^2}\, e^{-R_1 t_m}(k_1 + k_{-1} e^{-(k_1+k_{-1})t_m}) \quad (24)$$

$$\text{exchange cross peak 'Aa' } (t_m) = \text{ exchange cross peak 'aA' } (t_m)$$

$$= \frac{k_1 k_{-1}}{(k_1+k_{-1})^2}\, e^{-R_1 t_m}(1 - e^{-(k_1+k_{-1})t_m}) \quad (25)$$

For signals where the resolution of the diagonal peak was sufficient for integration eq 25 can be normalized to the intensity of diagonal peak by 'Aa' (t_m) / ('Aa' (t_m) + 'aa' (t_m)) and 'aA' (t_m) / ('aA' (t_m) + 'AA' (t_m)) to give the simplified eqs 26 and 27, respectively, from which the rate constants k_1 and k_{-1} can be determined (Figure 5.34, Chapter 5).[27,28]

$$\text{normalized exchange cross peak } \frac{\text{'Aa'}(t_m)}{\text{'Aa'}(t_m)+\text{'aa'}(t_m)} = \frac{k_{-1}}{k_1+k_{-1}}\left(1-e^{-(k_1+k_{-1})t_m}\right) \quad (26)$$

$$\text{normalized exchange cross peak } \frac{\text{'aA'}(t_m)}{\text{'aA'}(t_m)+\text{'AA'}(t_m)} = \frac{k_1}{k_1+k_{-1}}\left(1-e^{-(k_1+k_{-1})t_m}\right) \quad (27)$$

The area of integration of NOE cross peaks ('AB' and 'ab') and exchange-mediated NOE cross peaks ('Ab' and 'aB') (for definition of labels see Figure 6.4b, SI) were determined at various mixing times (t_m) (Figures A29, Appendix). Under the assumption that auto relaxation $R_{1,A} = R_{1,a}$, change in area of integration of NOE cross peaks as a function of mixing time (t_m) can be expressed by eqs 28 and 29.[27,28] Change in area of integration of exchange-mediated cross peaks as a function of mixing time (t_m) can be expressed by eq 30.[27,28]

$$\text{NOE cross peak 'AB' } (t_m) = \frac{k_{-1}e^{-t_m(k_1+k_{-1}+R_1+\sigma)}\,(-1+e^{2\sigma t_m})\,(k_1+k_{-1}e^{t_m(k_1+k_{-1})})}{2(k_1+k_{-1})^2} \quad (28)$$

$$\text{NOE cross peak 'ab' } (t_m) = \frac{k_1e^{-t_m(k_1+k_{-1}+R_1+\sigma)}\,(-1+e^{2\sigma t_m})\,(k_{-1}+k_1e^{t_m(k_1+k_{-1})})}{2(k_1+k_{-1})^2} \quad (29)$$

$$\text{exchange}-\text{mediated cross peak 'Ab' } (t_m) = \text{ exchange}-\text{mediated cross peak 'aB' } (t_m)$$

$$= \frac{k_1k_{-1}e^{-t_m(k_1+k_{-1}+R_1+\sigma)}\,(-1+e^{2\sigma t_m})\,(-1+e^{t_m(k_1+k_{-1})})}{2(k_1+k_{-1})^2} \quad (30)$$

By dividing exchange-mediated cross peaks 'Ab' and 'aB' over the sum with its corresponding NOE cross peak gives the simplified equations eqs 31 and 32, respectively, from which the rate constants k_1 and k_{-1} can be determined (Figure 5.35, Table 5.4, Chapter 5).[27,28]

$$\text{normalized exchange}-\text{mediated NOE cross peak}\frac{\text{'aB'}(t_m)}{\text{'AB'}(t_m)+\text{'aB'}(t_m)} = \frac{k_1-k_1\,e^{-t_m(k_1+k_{-1})}}{k_1+k_{-1}} \quad (31)$$

$$\text{normalized exchange} - \text{mediated NOE cross peak} \frac{\text{'Ab'}(t_m)}{\text{'Ab'}(t_m)+\text{'ab'}(t_m)} = \frac{k_{-1}-k_{-1}\, e^{-(k_1+k_{-1})t_m}}{k_1+k_{-1}} \quad (32)$$

with t_m = mixing time, R_1 = autorelaxation rate and k_1 and k_{-1} = rate constants of interconversion. For definition of labels 'AB', 'ab', 'Ab', and 'aB' see Figure 6.4.

REFERENCES

1. a) Mata, G; Schmidt, O. P.; Luedtke, N. W. *Chem. Commun.,* 2016, *52,* 4718; b) Mata, G.; Luedtke, N. W.; A fluorescent probe for proton-coupled folding reveals slow exchange of i-motif and duplex DNA, *J. Am. Chem. Soc.,* 2015, *137*, 699-707.
2. Schulhof,J.C.; Molko,D.; Teoule,R.; The final deprotection step in oligonucleotide synthesis is reduced to a mild and rapid ammonia treatment by using labile base-protecting groups. *Nucleic Acids Res.,* 1987, *15*, 397-416.
3. Cantor,C.R.; Warshaw,M.M.; Shapiro,H.; Oligonucleotide interactions. III. Circular dichroism studies of the conformation of deoxyoligonucleotides. *Biopolymers*, 1970*, 9*, 1059-1077.
4. Borer,P.N.; Optical properties of nucleic acids, absorption and circular dichroism spectra, in *Handbook of Biochemistry and Molecular Biology*: *Nucleic Acids*, Vol. 1, 3rd Ed., Fasman,G.D. (Ed.), CRC Press, Cleveland, Ohio, 1975, 589-595.
5. Brown,T.; Brown,D.J.S.; Modern machine-aided methods of oligodeoxyribonucleotide synthesis, In *Oligonucleotides and Analogues. A practical approach* (F.Eckstein, ed.), 1991, Oxford: IRL Press, p. 1-24.
6. a) Yurke, B.; Turberfield, A. J.; Mills, A. P.; Simmel, F. C.; Neumann, J. L. A DNA-fuelled molecular machine made of DNA, *Nature,* 2000, *406*, 605; b) Turberfield, A. J.; Mitchell, J. C.; Yurke, B.; Mills, A. P.; Blakey, M. I.; Simmel, F. C. DNA fuel for free-running nanomchines, *Phys. Rev. Lett.* 2003, *90*, 118102; c) Zhang, D. Y.; Winfree, E. *J. Am. Chem. Soc.* Control of DNA strand displacement kinetics using toehold exchange, 2009, *131*, 17303; d) Zhang, D. Y.; Seelig, G.; Dynamic DNA nanotechnology using strand-displacement reactions, *Nat. Chem.* 2011, *3*, 103; e) Genot, A. J.; Zhang, D. Y.; Bath, J.; Turberfield, A. J., Remote toehold: a mechanism for flexible control of DNA hybridization kinetics, *J. Am. Chem. Soc.* 2011, *133*, 2177; f) Tang, W.; Wang, H.; Wang, D.; Zhao, Y.; Li, N.; Liu, F., DNA tetraplexes-based toehold activation for controllable DNA strand displacement reactions, *J. Am. Chem. Soc.* 2013, *135*, 13628.
7. Urata, H.; Yamaguchi, E.; Funai, T.; Matsumura, Y.; Wada, S.-I., Incorporation of thymine nucleotides by DNA polymerases through T-Hg^{II}-T base pairing, *Angew. Chem. Int. Ed.* 2010, *49*, 6516.
8. Schmidt, O. P.; Mata, G.; Luedtke, N. W., Fluorescent base analogue reveals T-Hg^{II}-T base pairs have high kinetic stabilities that perturbs DNA metabolism, 2016, *138*, 14733.
9. Bax, A.; Lerner, L., Measurement of ^{1}H-^{1}H coupling constants in DNA fragments by 2D NMR, 1988, *79*, 429.
10. D. S. Wishart, C. G. Bigam, J. Yao, F. Abildgaard, H. J. Dyson, E. Oldfield, J. L. Markley, B. D. Sykes, ^{1}H, ^{13}C, ^{15}N chemical shift referencing in biomolecular NMR, *J. Biomol. NMR*, 1995, *6*, 135-140.
11. Güntert, P.; Mumenthaler, C.; Wüthrich K., Torsion angle dynamics for NMR structure calculation with the new program DYANA , *J. Mol. Biol.* 1997, *273*, 283.
12. a) Schwieters, C. D.; Kuszewski, J. J.; Tjandra, N.; Clore, G. M., The Xplor-NIH NMR molecular structure determination, *J. Magn. Reson*., 2003, *160*, 65-73; b) Schwieters, C. D.; Kuszewski, J. J.; Clore, G. M., Using Xplor-NIH for NMR molecular structure determination, *Progr. NMR Spectroscopy*, 2006, *48*, 47-62.

13. Tjandra, N.; Tate, S.-I.; Ono, A.; Kainosho, M.; Bax, A., The NMR structure of a DNA dodecamer in an aqueous dilute liquid crystalline phase, *J. Am. Chem. Soc.* 2000, *122*, 6190.
14. Varani, G.; Aboul-ela, F.; Allain, F. H.-T.; NMR investigation of RNA structure. *Prog. Nucl. Magn. Reson. Spectrosc.* 1996, *29*, 51.
15. Schneider, B.; Neidle, S.; Berman, H. M., Conformations of the sugar-phosphate backbone in helical DNA crystal structures, *Biopolymers*, 1997, *42*, 113.
16. Sklenar, V.; Bax, A., Measurement of ^{1}H-^{31}P NMR coupling constants in double-stranded DNA fragments, *J. Am. Chem. Soc*, 1987, *109*, 7525.
17. Kondo, J.; Yamada, T.; Hirose, C.; Okamoto, I.; Tanaka, Y.; Ono. A., Crystal structure of metallo DNA duplex containing consecutive Watson-Crick-like T-Hg(II)-T base pairs, *Angew. Chem. Int. Ed.* 2014, *53*, 2385.
18. Yamaguchi, H.; Šebera, J.; Kondo, J.; Oda, S.; Komuro, T.; Kawamura, T.; Dairaku, T.; Kondo, Y.; Okamoto, I.; Ono, A.; Burda, J. V.; Kojima, C.; Sychrovský, V.; Tanaka, Y., The structure of metallo-DNA with consecutive thymine-Hg^{II}-thymine base pairs explains positive entropy for the metallo base pair formation, *Nucleic Acids Res.*, 2014, *42*, 4094.
19. Kosturko, L. D.; Folzer, C.; Stewart, R. F., Crystal and molecular structure of a 2:1 complex of a 1-methylthymine-mercury(II), *Biochemistry*, 1974, *13*, 3949.
20. Menzer, S.; Sabar, M.; Lippert, B., Silver(I)-modified base pairs involving complementary (G, C) [guanine, cytosine] and noncomplementary (A, C) [adenine, cytosine] nucleobases. On the possible structural role of aqua ligands in metal-modified nucleobase pairs, *J. Am. Chem. Soc.*, 1992, *114*, 4644.
21. Liu, H.; Cai, C.; Haruehanroengra, P.; Yao, Q.; Chen, Y.; Yang, C.; Luo, Q.; Wu, B.; Li, J.; Ma, J.; Sheng, J.; Gan, J., Flexibility and stabilization of Hg^{II}-mediated C:T and T:T base pairs in DNA duplex, *Nucleic Acids Res.*, 2017, *45*, 2910-2918.
22. Koradi, R.; Billeter, M.; Wüthrich, K., MOLMOL: A program for display and analysis of macromolecular structures, *J. Mol. Graphics*, 1996, *14*, 51.
23. The PyMOL Molecular Graphics System, Version 2.0.7, Schrödinger, LLC.
24. Lavery, R.; Moakher, M.; Maddocks, J. H.; Petkeviciute, D.; Zakrzewska, K., Conformational analysis of nucleic acids revisited: Curves+, *Nucleic Acids Res.*, 2009, *37*, 5917.
25. a) Lu, X.-J.; Olson, W. K., 3DNA: a software package for the analysis, rebuilding and visualization of three-dimensional nucleic acid structures, *Nucleic Acids Res.* 2003, 31, 5108; b) Lu, X.-J.; Olson, W. K., 3DNA: a versatile, integrated software system for the anaylsis, rebuilding and visualization of three-dimensional nucleic-acid structures, *Nat. Protoc. 2008,* 3, 1213.
26. Farrow, N. A.; Zhang, O.; Forman-Kay, J. D.; Kay, L. E., A heteronuclear correlation experiment for simultaneous determination of 15N longitudinal decay and chemical exchange rates of systems in slow equilibrium, *J. Biomol. NMR,* 1994, *4*, 727–734.
27. Choe, B.; Cook, G. W.; Rama Krischna, N., Effect of slow conformational exchange on 2D NOESY spectra, *J. Magn. Reson.* 1991, *94*, 387-393.
28. Jeener, J.; Meier, B. H.; Bachmann, P.; Ernst, R. R., Investigation of exchange processes by two-dimensional NMR spectroscopy, *J. Chem. Phys.,* 1979, *71*, 4546–4553.

APPENDIXES

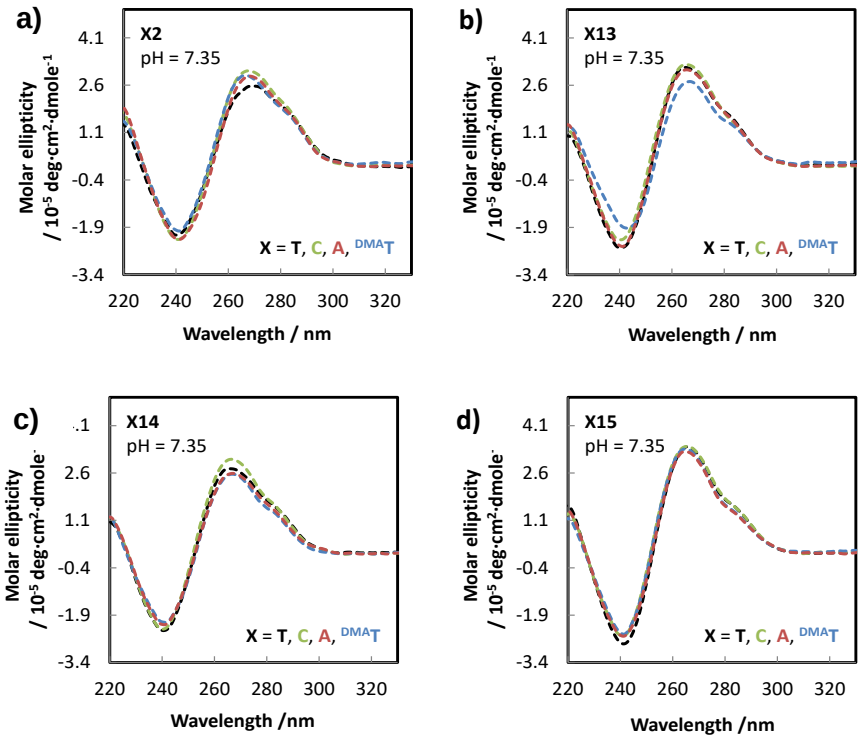

Figure A1. CD spectra of duplexes at 25 °C for: (A) X2, (B) X13, (C) X14 and (D) X15 with X = T, C, A and ^{DMA}T at pH = 7. All samples contained 5 µM of DNA in phosphate citric acid buffer (200 mM of Na_2HPO_4, 100 mM of citric acid and 100 mM NaCl).

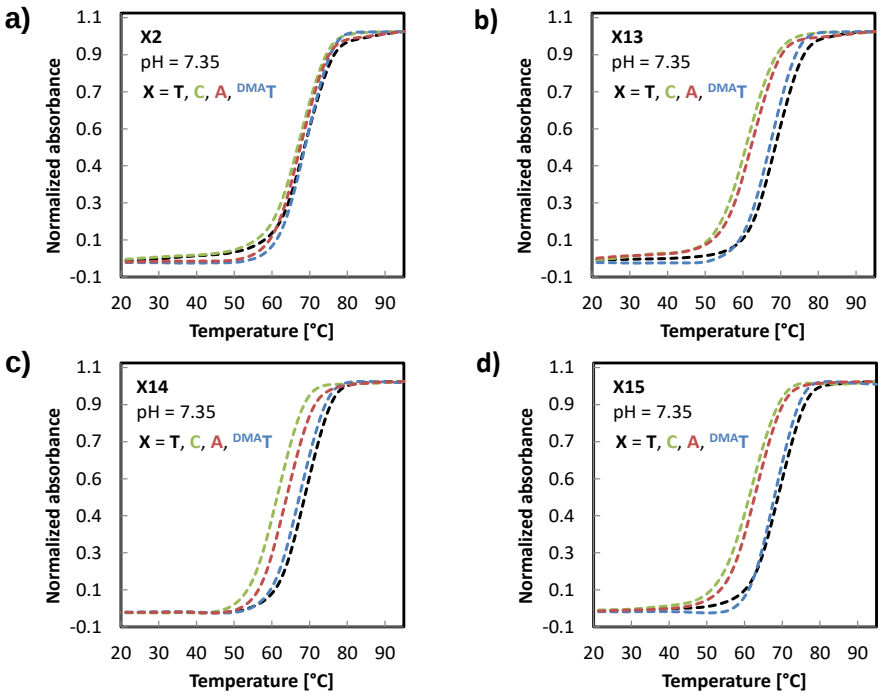

Figure A2. Thermal denaturation spectra of duplexes: (A) X2, (B) X13, (C) X14 and (D) X15 with X = T, C, A and ^{DMA}T at pH = 7.35. All samples contained 5 µM of DNA in phosphate citric acid buffer (200 mM of Na_2HPO_4, 100 mM of citric acid and 100 mM NaCl).

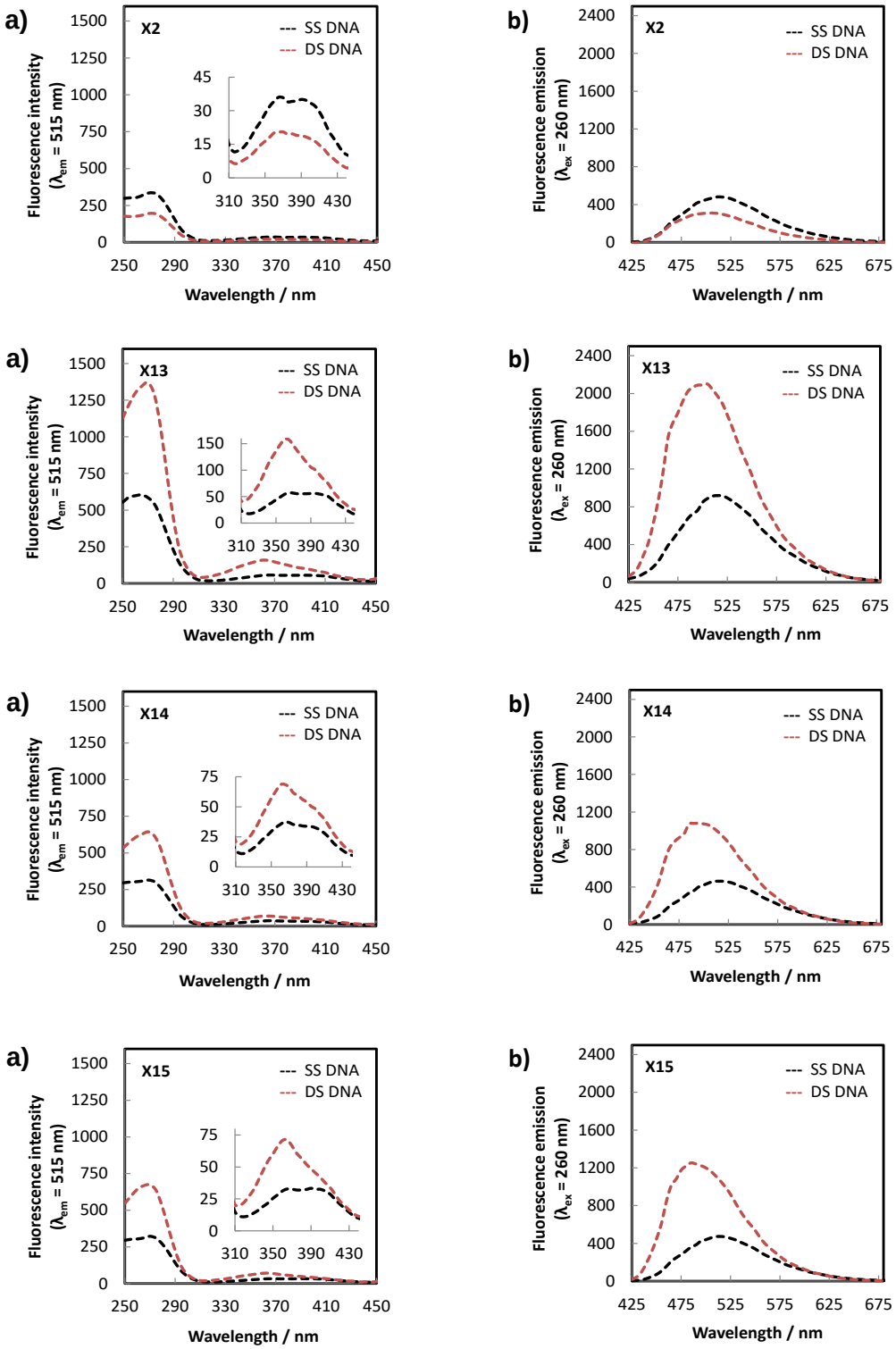

Figure A3. a) Excitation (λ_{em} = 515 nm) and b) emission spectra (λ_{ex} = 260 nm) of X2, X13, X14 and X15 prepared as unstructured, "SS" DNA (black) and double-stranded, "DS" DNA (red) with (X = ^{DMA}T). All samples contained 4 µM of DNA in phosphate citric acid buffer (20 mM of Na_2HPO_4, 10 mM of citric acid and 10 mM NaCl at pH = 7.35).

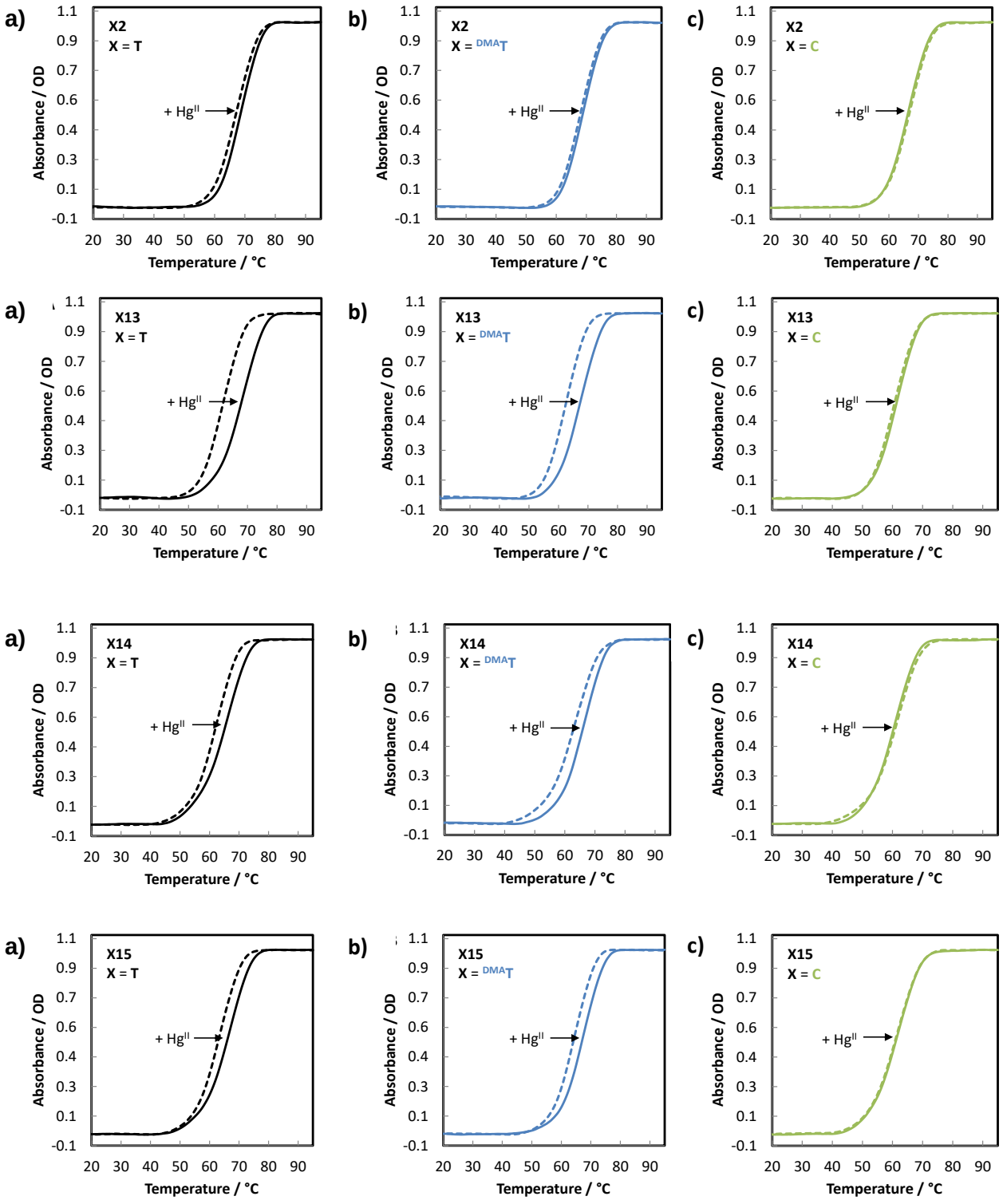

Figure A4. a) Thermal denaturation curves of duplex DNA containing X2, X13, X14 or X15 with X = (A) T, b) ^{DMA}T and c) C in the absence (---) and in the presence (—) of $Hg(ClO_4)_2$ (1.0 equiv.). The complementary strand a "T" mismatched opposite to the "X" base. All samples contained 5 µM of DNA in phosphate citric acid buffer (200 mM of Na_2HPO_4, 100 mM of citric acid and 100 mM $NaNO_3$) at pH = 7.35.

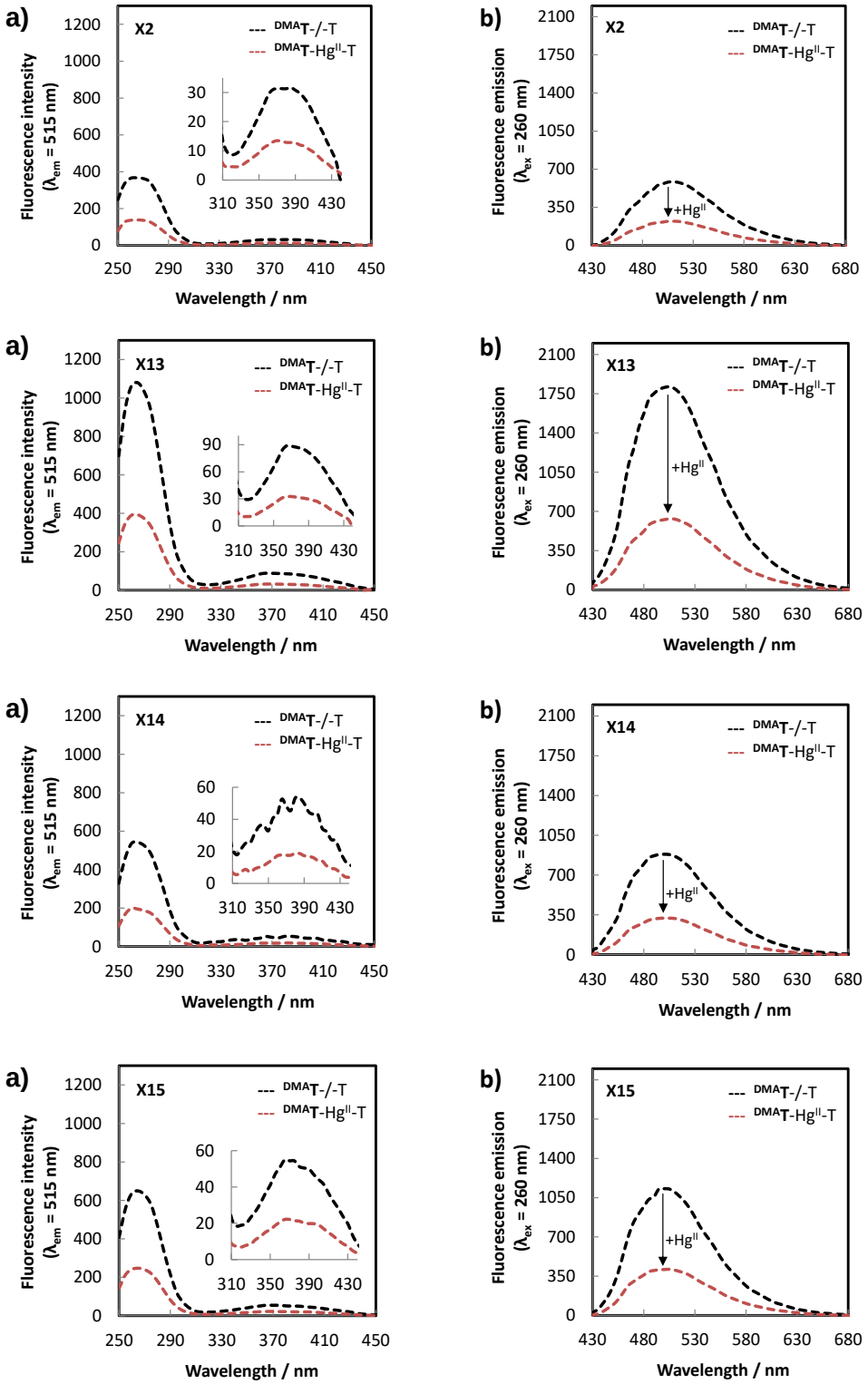

Figure A5. a) Excitation (λ_{em} = 515 nm) and b) fluorescence spectra (λ_{ex} = 260 nm) of X2, X13, X14 and X15 as double-stranded DNA with a T-/-T mismatch (black) and a T-Hg^{II}-T match (red) with (X = ^{DMA}T). All samples contained 4 µM of DNA in phosphate citric acid buffer (200 mM of Na_2HPO_4, 100 mM of citric acid and 100 mM $NaNO_3$) at pH = 7.35 with or without 1.0 eq. of Hg^{II}. The complementary strand contained a T mismatched opposite to the ^{DMA}T base.

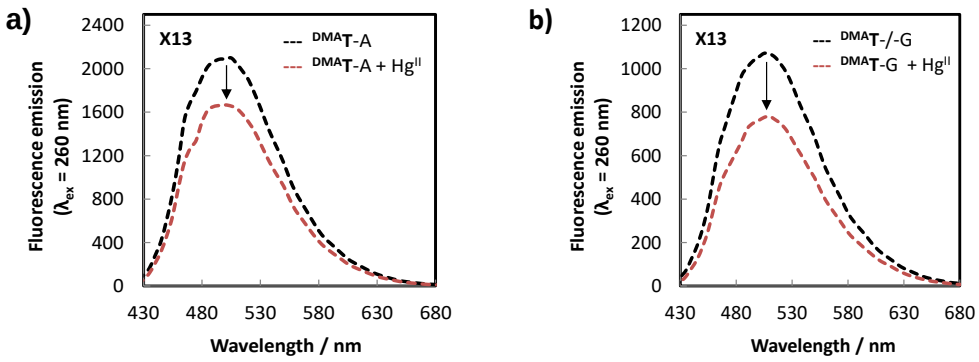

Figure A6. Fluorescence spectra (λ_{ex} = 260 nm) of X13 as double-stranded DNA containing (A) a ^{DMA}T-A base pair (black) and (B) a ^{DMA}T-G mismatched pair (black) in the presence of Hg^{II} ions (red) with (X = ^{DMA}T). All samples contain 4 μM of DNA in phosphate citric acid buffer (200 mM of Na_2HPO_4, 100 mM of citric acid and 100 mM $NaNO_3$) at pH = 7.35 with or without 1.0 eq. of Hg^{II}.

Table A1. Photophysical data of ^{DMA}T in duplex DNA.[a]

Base Pairing	Sequence	λ_{abs}[a]	λ_{em}[b]	r[c]	φ[d]	$\Delta\varphi$[e]
^{DMA}T-T	X2	375	510	0.10	0.04	-
	X13	365	505	0.09	0.13	-
	X14	385	501	0.13	0.07	-
	X15	365	500	0.12	0.08	-
^{DMA}T-Hg^{II}-T	X2	360	512	0.10	0.01	-69%
	X13	360	507	0.09	0.05	-63%
	X14	360	504	0.15	0.03	-61%
	X15	360	505	0.11	0.03	-66%

[a] λ_{abs} are reported at the most red-shifted absorbance maxima in nm, [b] λ_{em} in nm, [c] Fluorescence anisotropy (r) were calculated at pH = 7.35 (λ_{ex} = 375 nm. λ_{em} = 500 nm). [d] ^{DMA}T (φ = 0.03 at pH = 7.35 with λ_{ex} = 370 nm) was used as the fluorescent standard for calculating the relative quantum yields (φ) of ^{DMA}T in DNA. [e] Relative deviation of fluorescence quantum yield of ^{DMA}T–T mismatched duplex upon addition of Hg^{II} ions. ^{DMA}T–Hg^{II}–T base pairs were generated by the addition of 1.0 equiv. of $Hg(ClO_4)_2$ followed by heating to 90 °C for 5 min and cooled to room temperature overnight before reading. Reproducibility is within ± 30% of each reported φ value.

Table A2. Photophysical properties of ^{DMA}T-A- and ^{DMA}T-G-containing sequences in absence and presence of Hg^{II}.[a]

Base Pairing	Sequence	λ_{abs}[a]	λ_{em}[b]	r[c]	φ[d]	$\Delta\varphi$[e]
^{DMA}T-A	X13	355	504	0.09	0.20	-
	X15	355	486	0.15	0.11	-
^{DMA}T-G	X13	365	508	0.10	0.09	-
	X15	370	505	0.12	0.06	-
^{DMA}T-A + Hg^{II}	X13	365	505	0.10	0.17	ca. -13%
	X15	370	490	0.14	0.09	ca. -18%
^{DMA}T-G + Hg^{II}	X13	365	510	0.11	0.07	ca. -23%
	X15	370	505	0.13	0.06	ca. -12%

[a] λ_{abs} are reported at the most red-shifted absorbance maxima in nm, [b] λ_{em} in nm, [c] Fluorescence anisotropy (r) were calculated at pH = 7.35 (λ_{ex} = 375 nm. λ_{em} = 500 nm). [d] ^{DMA}T (φ = 0.03 at pH = 7.35 with λ_{ex} = 370 nm) was used as the fluorescent standard for calculating the relative quantum yields (φ) of ^{DMA}T in DNA. [e] Relative deviation of fluorescence quantum yield of ^{DMA}T–T mismatched duplex upon addition of 1.0 eq. of Hg^{II} ions. ^{DMA}T–Hg^{II}–T base pairs were generated by the addition of 1.0 equiv. of $Hg(ClO_4)_2$ followed by heating to 90 °C for 5 min and cooled to room temperature overnight before reading. Reproducibility is within ± 30% of each reported φ value.

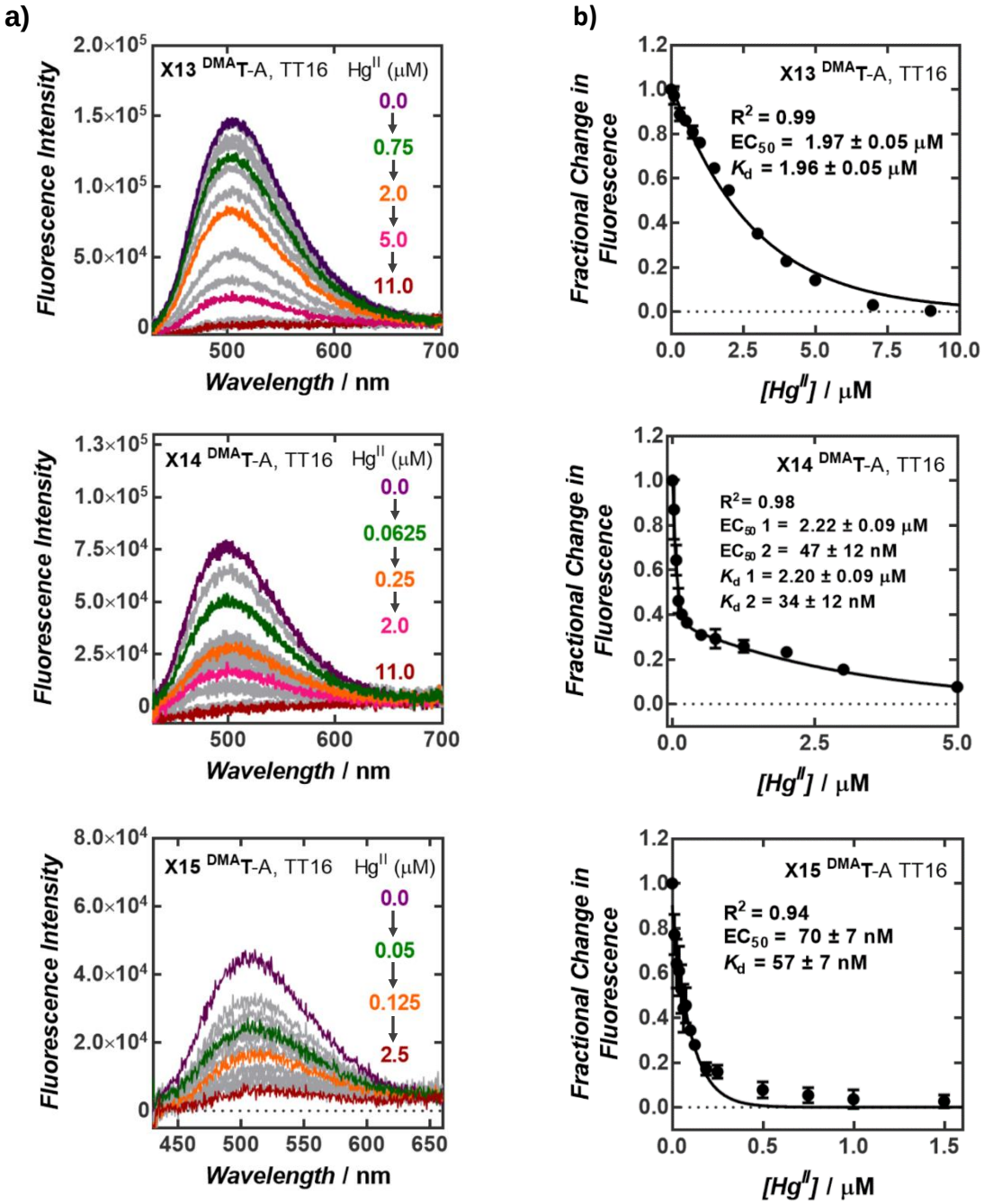

Figure A7. Fluorescence quenching of duplex DNA X13 ^{DMA}T-A, TT16 (top), X14 ^{DMA}T-A, TT16 (middle), and X15 ^{DMA}T-A, TT16 (bottom) upon addition of Hg^{II} in metal-coordinating buffer. a) Fluorescence spectra (λ_{ex} = 370 nm) of ^{DMA}T-containing duplex DNA in the absence (purple) and in the presence of variable concentrations of Hg^{II}. b) Plot of fluorescence intensity (λ_{em} = 500 nm) versus concentration of Hg^{II}. X13 ^{DMA}T-A, TT16 (top) and X15 ^{DMA}T-A, TT16 (bottom) were fit to a monoexponential curve (eq 4, Chapter 6) and X14 ^{DMA}T-A, TT16 (middle) was fit to a biphasic curve (eq 5, Chapter 6). All samples contained 25 nM DNA in aqueous buffer (200 mM Na_2HPO_4, 100 mM citric acid and 100 mM $NaNO_3$) at pH = 7.35 and were incubated with $Hg(ClO_4)_2$ at 25 °C for 1 h prior to reading.

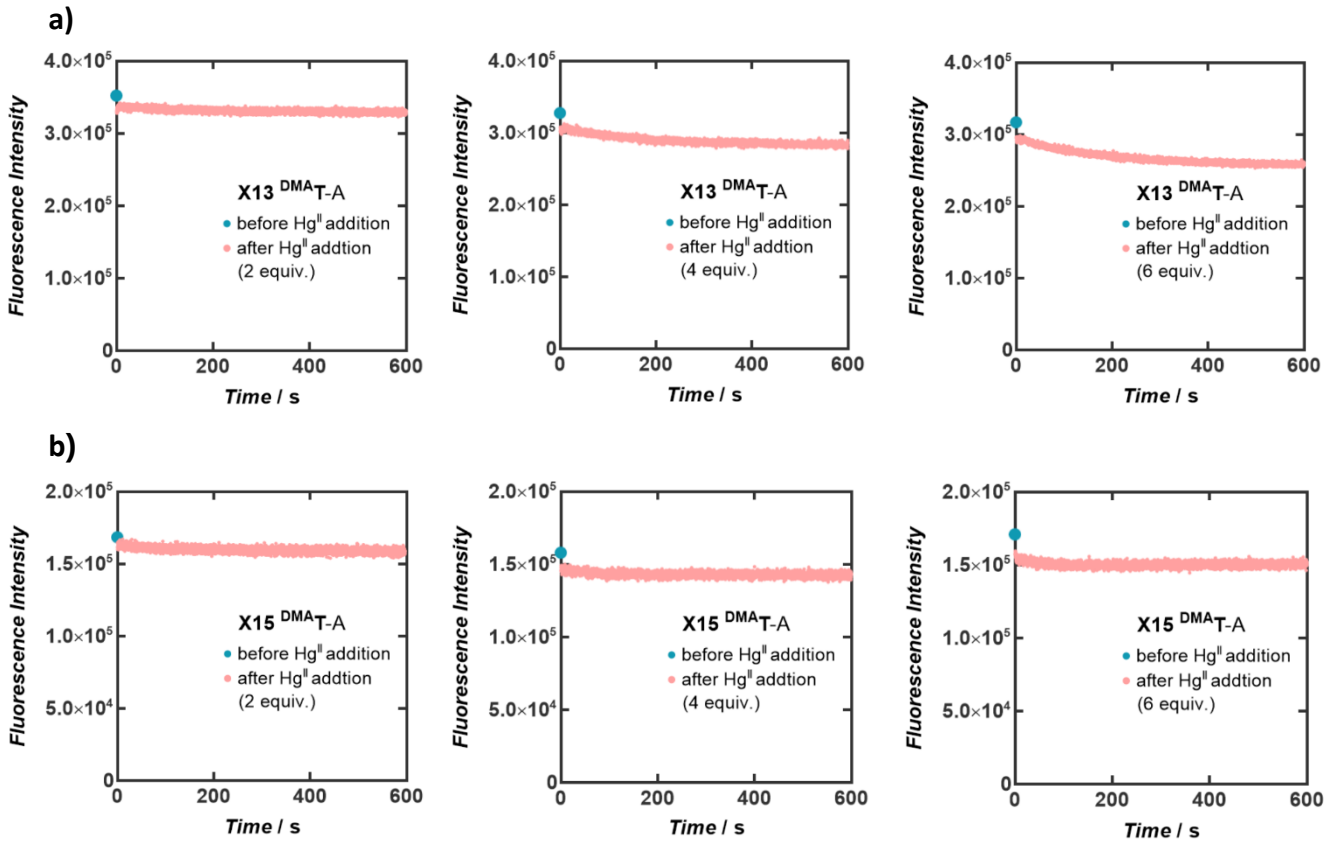

Figure A8. Nonspecific binding of Hg^{II} (2, 4, and 6 equiv) to a) X13 ^{DMA}T-A and b) X15 ^{DMA}T-A. Samples were excited at 370 nm and fluorescence was monitored at 500 nm. All samples contained 0.1 μM DNA in aqueous buffer (200 mM Na_2HPO_4, 100 mM citric acid and 100 mM $NaNO_3$) at pH = 7.35.

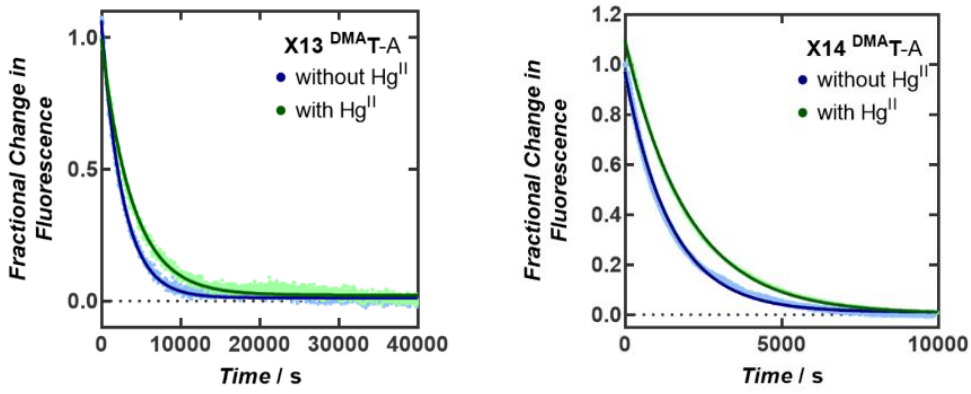

Figure A9. Strand displacement of X13 ^{DMA}T-A with and without Hg^{II} (left) and X14 ^{DMA}T-A with and without Hg^{II} (right).

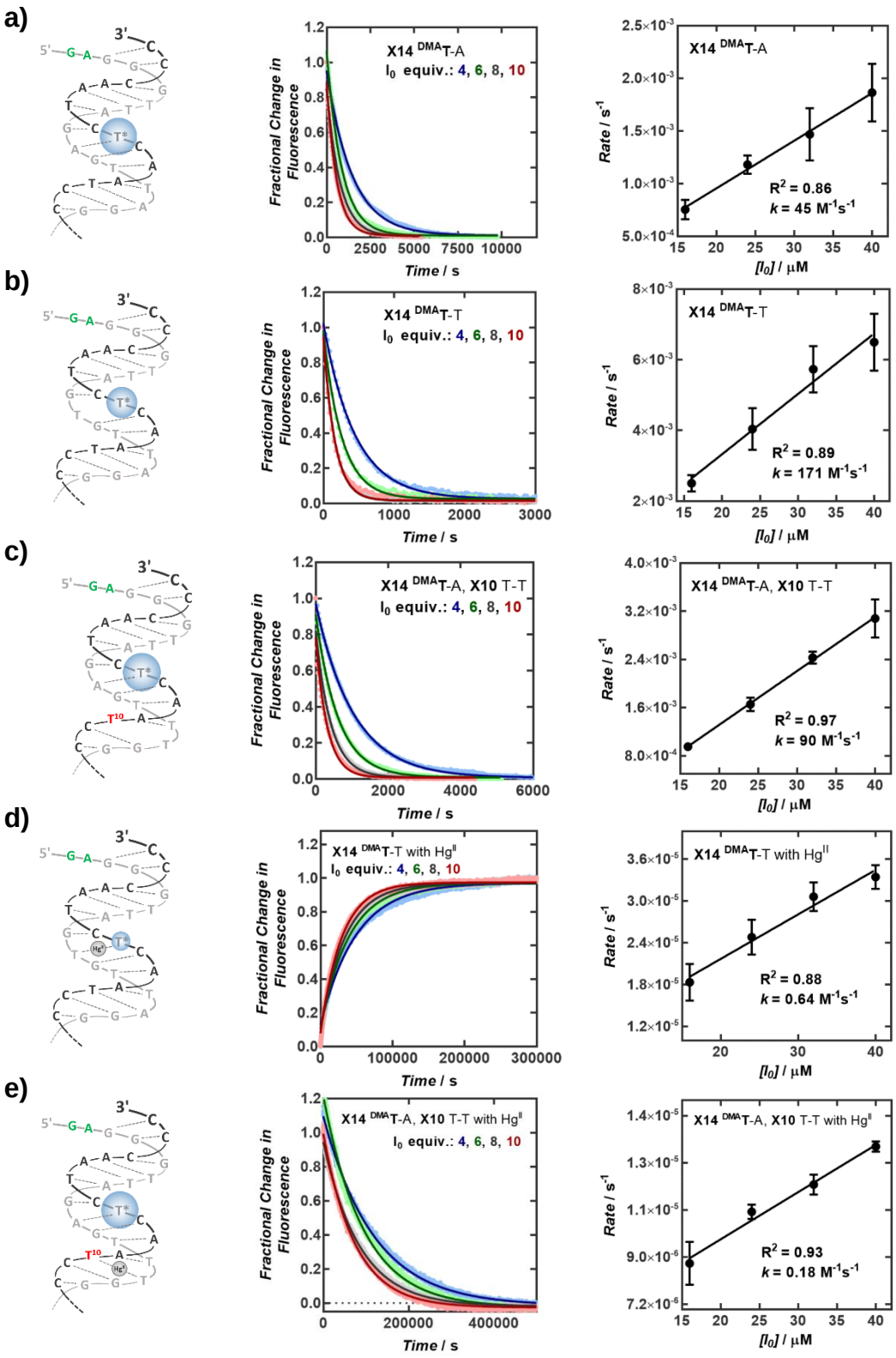

Figure A10. Duplex DNA structures (T* = ^{DMA}T) and rates of strand displacement versus invading strand (I_0) concentration for X14 containing a) ^{DMA}T-A base pair, b) ^{DMA}T-T mismatch, c) ^{DMA}T-A base pair and a T-T mismatch in position 10, d) ^{DMA}T-Hg^{II}-T base pair, e) ^{DMA}T-A base pair and a T-Hg^{II}-T base pair in position 10.

ODN1 with Klenow Fragment (*exo*-)

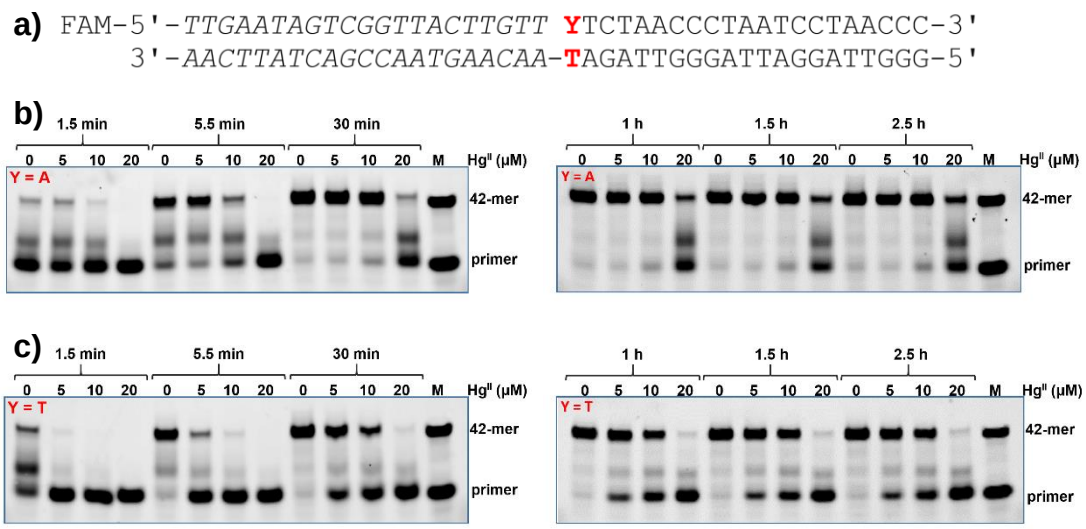

Figure A11. Gel analysis of ODN1 with Klenow Fragment (*exo*-). a) Sequence of ODN1 duplex DNA. b) DNA containing only *Watson-Crick* base pairs at various time points and Hg^{II} concentrations. c) DNA containing a T-T mismatch at the nick site at various time points and Hg^{II} concentrations. "M" = marker for primer and full-length sequence.

ODN1 with *E. coli* DNA Pol I (*exo*+)

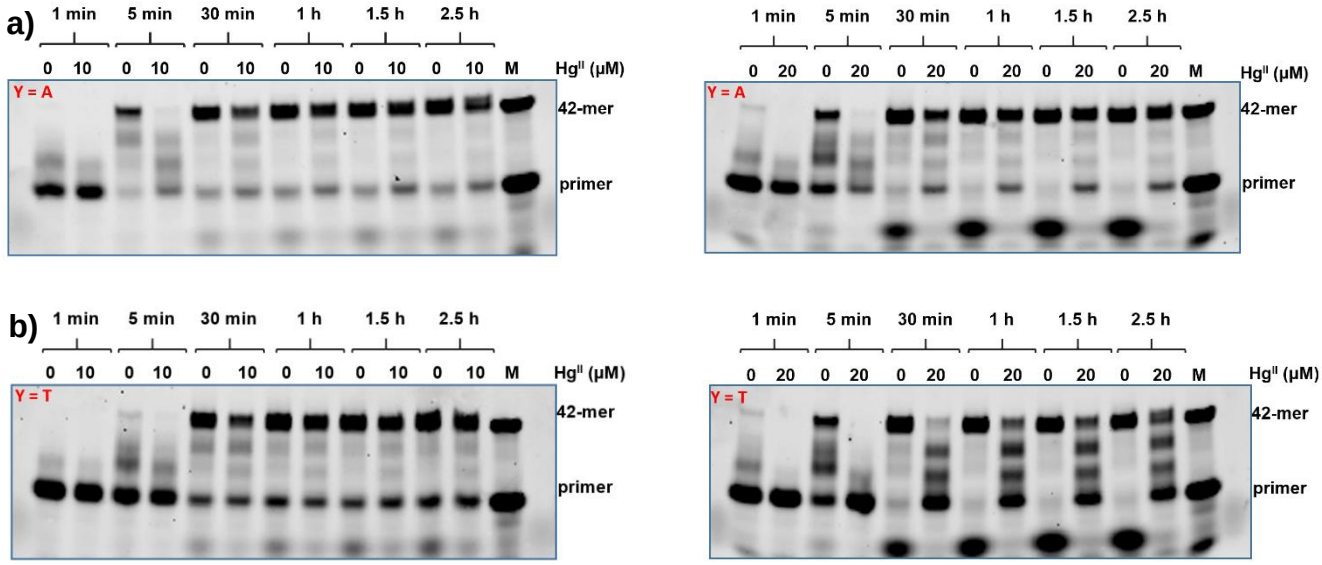

Figure A12. Gel analysis of ODN1 with DNA Pol I (*E. coli*). a) DNA containing only *Watson-Crick* base pairs at various time points and Hg^{II} concentrations. b) DNA containing a T-T mismatch at the nick site at various time points and Hg^{II} concentrations. "M" = marker for primer and full-length sequence.

ODN2 with Klenow Fragment (*exo*-)

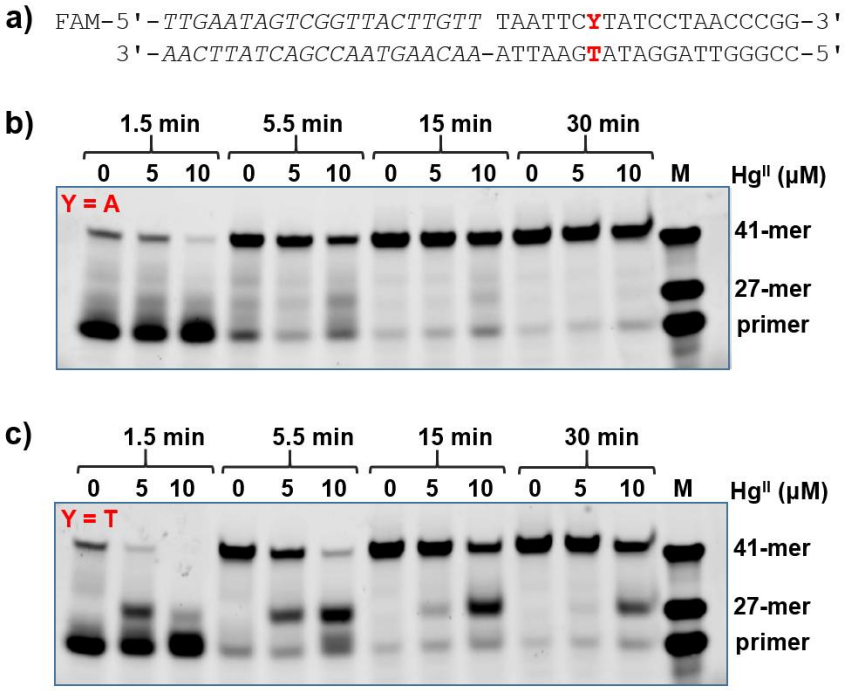

Figure A13. Gel analysis of ODN2 with Klenow Fragment (*exo*-). a) Sequence of ODN2 duplex DNA. b) DNA containing only *Watson-Crick* base pairs at various time points and Hg^{II} concentrations. c) DNA containing a T-T mismatch at various time points and Hg^{II} concentrations. "M" = marker for primer, stalled strand, and full-length sequence.

ODN2 with *E. coli* DNA Pol I (*exo*+)

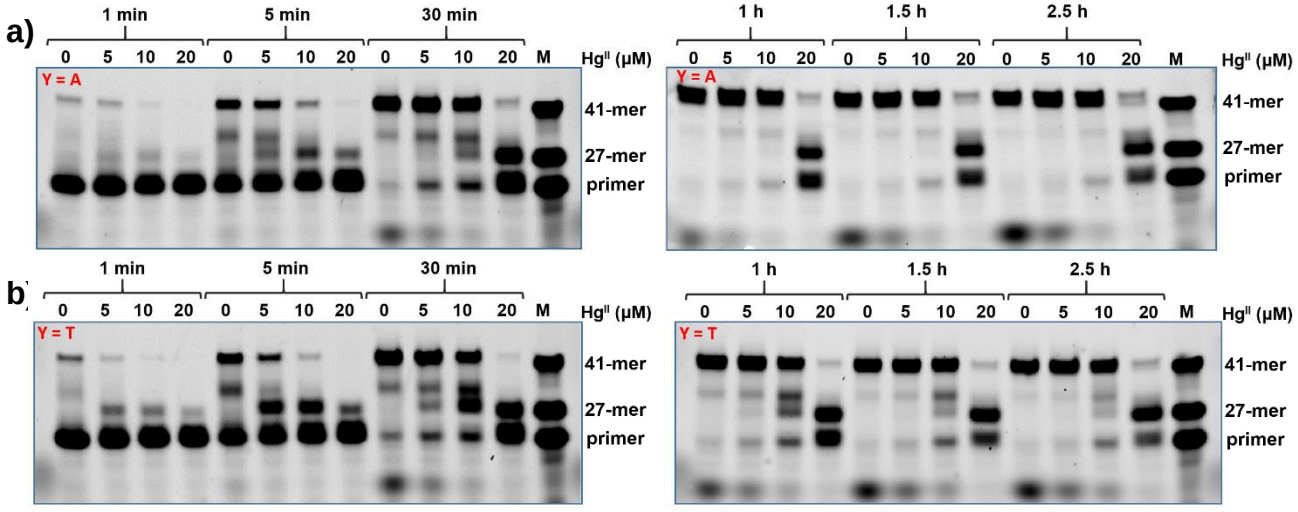

Figure A14. Gel analysis of ODN2 with DNA Pol I (*E. coli*). a) DNA containing only *Watson-Crick* base pairs at various time points and Hg^{II} concentrations. b) DNA containing a T-T mismatch at various time points and Hg^{II} concentrations. "M" = marker for primer, stalled-strand and full-length sequence.

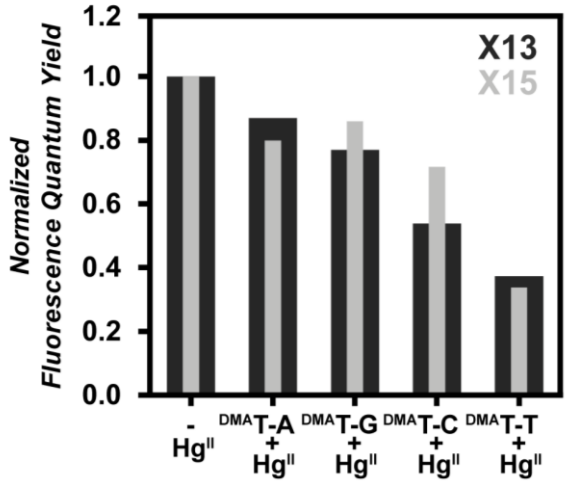

Figure A15. Normalized fluorescence quantum yields of duplexes X13 (black bars) or X15 (grey bars) containing ^{DMA}T opposite to an A, G, C, or T base upon addition of 1.0 equiv of Hg^{II} (1). All samples contained 4 μM of DNA in aqueous buffer (200 mM of Na_2HPO_4, 100 mM of citric acid and 100 mM $NaNO_3$ (pH = 7.35)) and were incubated with Hg^{II} for 3 h prior to measuring. For duplex sequences see Table 6.5.

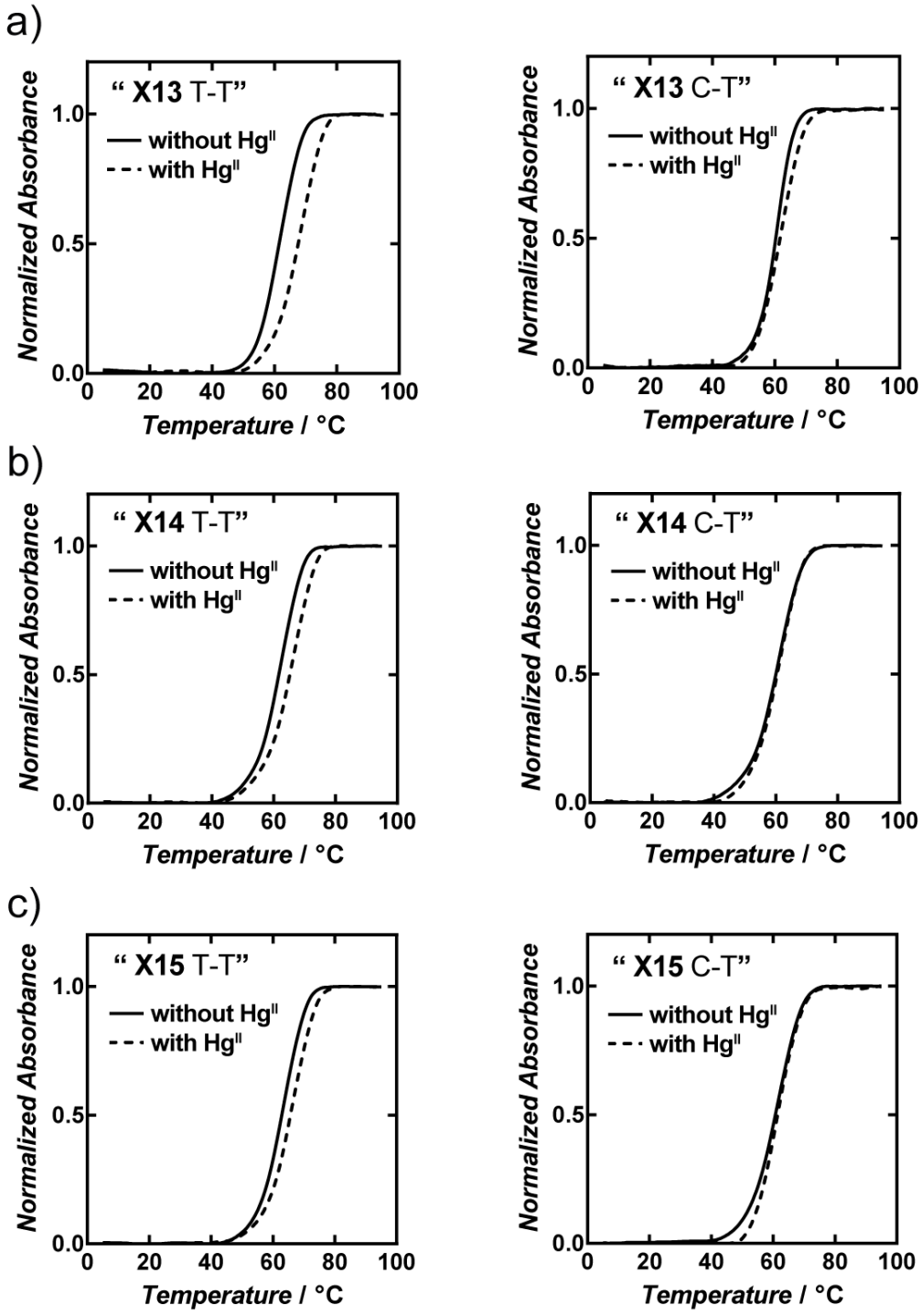

Figure A16. Thermal denaturation curves for a) "X13 T-T" (left), "X13 C-T" (right), b) "X14 T-T" (left), "X14 C-T" (right), and c) "X15 T-T" (left), "X15 C-T" (right) in the presence and absence of 1.0 equiv of Hg^{II}. Samples contained 5 μM of DNA in aqueous buffer (200 mM Na_2HPO_4, 100 mM citric acid and 100 mM $NaNO_3$) at pH = 7.35.

Table A3. Melting Temperatures (T_m) of "X13", "X14", and "X15" in Presence and Absence (+/- ΔT_m) of Hg^{II} with X = T or C[a]

Mismatch	T-T		C-T	
Sequence	-	+ Hg^{II}	-	+ Hg^{II}
"X13"	61.5	67.5 (+6.0)	60.4	61.1 (+0.7)
"X14"	61.5	65.1 (+3.6)	60.4	60.3 (-0.1)
"X15"	62.8	65.7 (+2.9)	60.6	60.9 (+0.3)

[a] The complementary strand contained a T opposite X. Samples contained 5 μM of DNA in aqueous buffer (200 mM Na_2HPO_4, 100 mM citric acid and 100 mM $NaNO_3$) at pH = 7.35.

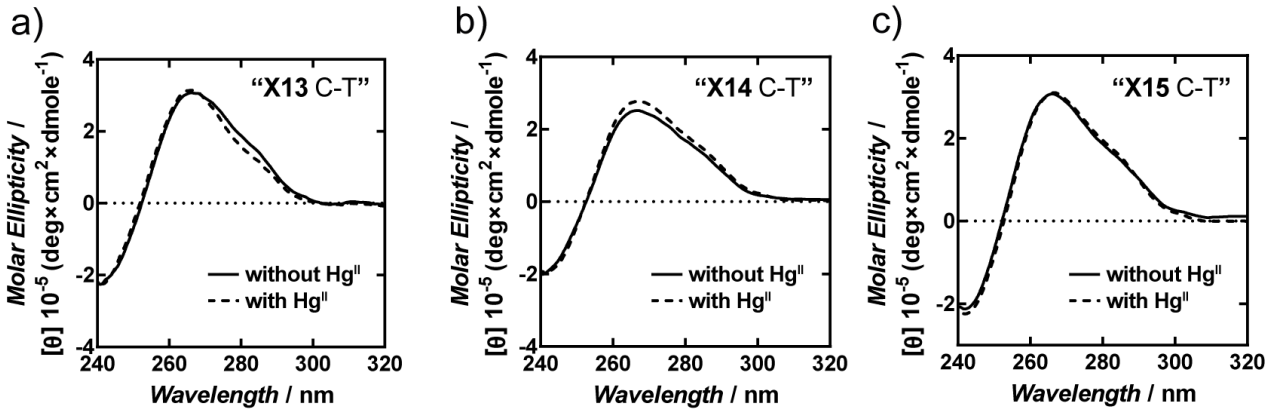

Figure A17. CD spectra of a) "X13 C-T", b) "X14 C-T", and c) "X15 C-T" in the presence and absence of 1.0 equiv of Hg^{II}. Samples contained 5 μM of DNA in aqueous buffer (200 mM Na_2HPO_4, 100 mM citric acid and 100 mM $NaNO_3$) at pH = 7.35.

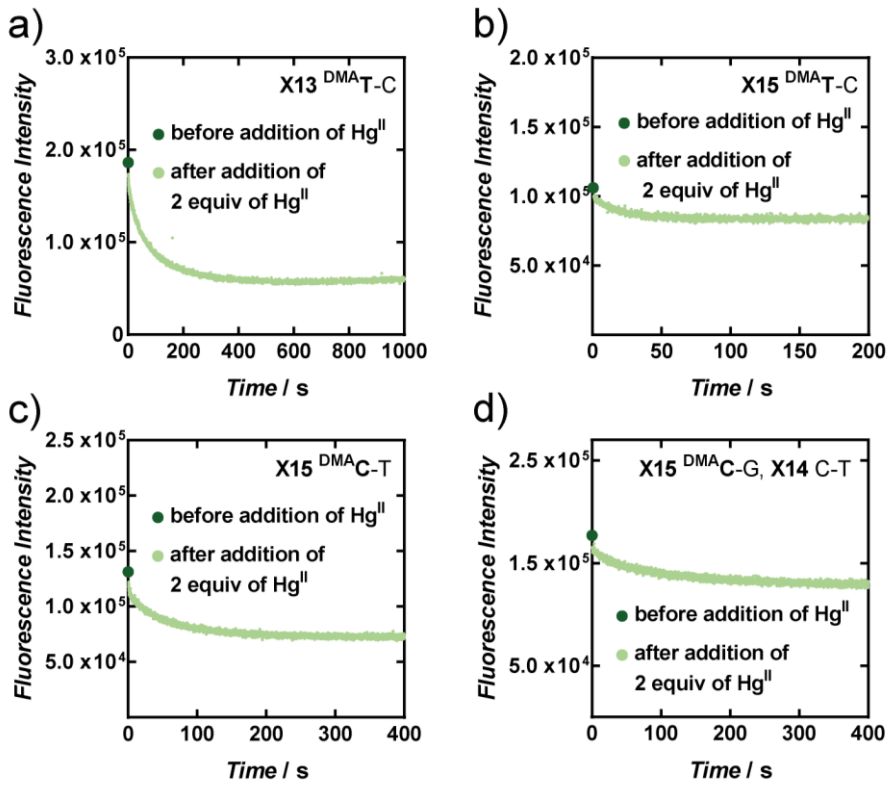

Figure A18. Addition of Hg^{II} (2.0 equiv) to a) X13 ^{DMA}T-C, b) X15 ^{DMA}T-C, c) X15 ^{DMA}C-T, and d) X15 ^{DMA}C-G, X14 C-T. Samples were excited at 370 nm and fluorescence was monitored at 500 nm (^{DMA}T) or 510 nm (^{DMA}C).. All samples contained 0.1 μM DNA in aqueous buffer (200 mM Na_2HPO_4, 100 mM citric acid and 100 mM $NaNO_3$) at pH = 7.35.

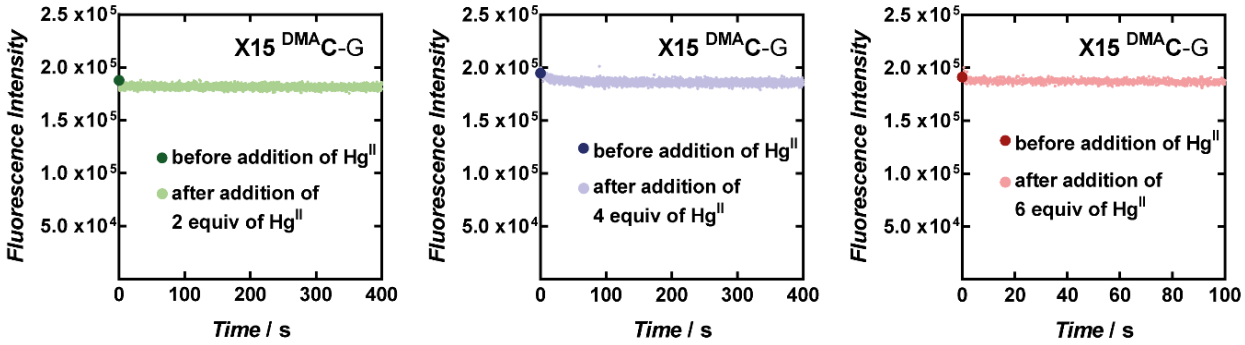

Figure A19. Nonspecific binding of 2, 4, and 6 equiv of Hg^{II} to X15 ^{DMA}C-G. Samples were excited at 370 nm and fluorescence was monitored at 510 nm. All samples contained 0.1 μM DNA in aqueous buffer (200 mM Na_2HPO_4, 100 mM citric acid and 100 mM $NaNO_3$) at pH = 7.35.

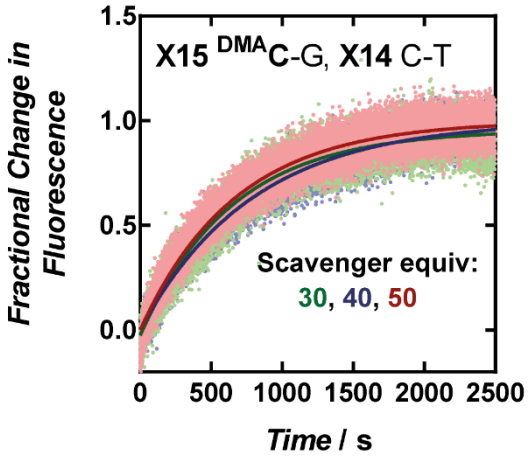

Figure A20. Dissociation of Hg^{II} from X15 ^{DMA}C-G, X14 C-Hg^{II}-T upon addition 30, 40, and 50 equiv of unlabeled, C-T-containing 'scavenger' duplex DNA. C-Hg^{II}-T base pairs were formed by pre-incubation of the DNA with 2.0 equiv of $Hg(ClO_4)_2$ for 3 h. Samples contained 0.1 μM duplex DNA in aqueous buffer (200 mM Na_2HPO_4, 100 mM citric acid and 100 mM $NaNO_3$) at pH = 7.35. DNA was incubated with $Hg(ClO_4)_2$ for 3 h prior to addition of scavenger DNA.

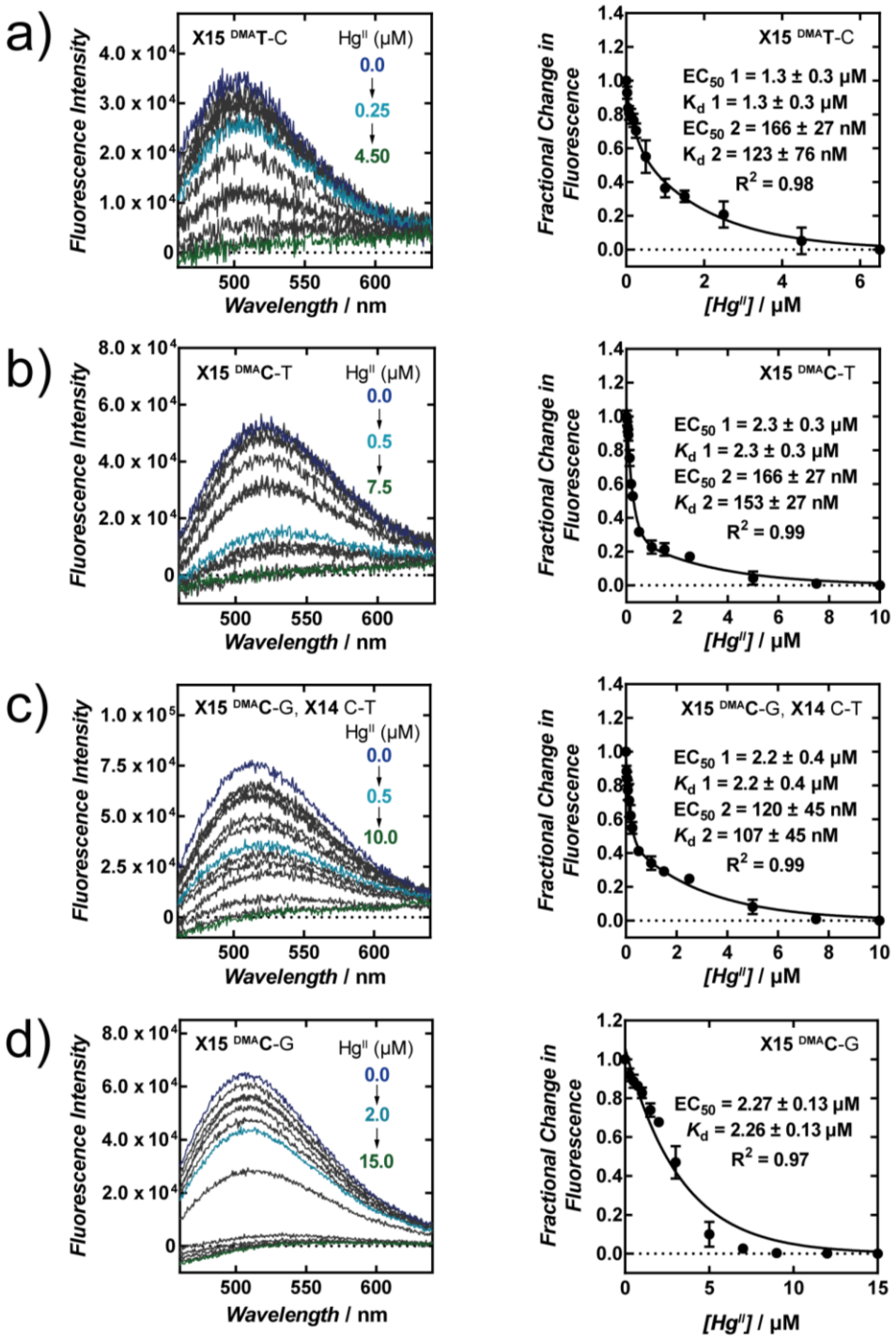

Figure A21. Fluorescence quenching of a) "X15 ^{DMA}T-C", b) "X15 ^{DMA}C-T", c) "X15 ^{DMA}C-G, X14 C-T", and d) "X15 ^{DMA}C-G" upon addition of Hg^{II}. Fluorescence spectra (λ_{ex} = 370 nm) of ^{DMA}T-, and ^{DMA}C-containing sequences in the absence (dark blue) and in the presence of variable concentrations of Hg^{II} (left). Plot of fluorescence intensity (λ_{em} = 500 nm (^{DMA}T) or 510 nm (^{DMA}C). versus concentration of Hg^{II} (right). "X15 ^{DMA}C-G" (d) was fit to a monoexponential curve (eq 4, Chapter 6). "X15 ^{DMA}T-C" (a), "X15 ^{DMA}C-T" (b) and "X15 ^{DMA}C-G, X14 C-T" (c) exhibited pronounced bi-phasic quenching and were fit to a bi-phasic curve (eq 5, Chapter 6). All samples contained 25 nM duplex DNA in aqueous buffer (200 mM of Na_2HPO_4, 100 mM of citric acid and 100 mM $NaNO_3$ (pH = 7.35)) and were incubated with $Hg(ClO_4)_2$ at 25 °C for 1 h prior to measuring.

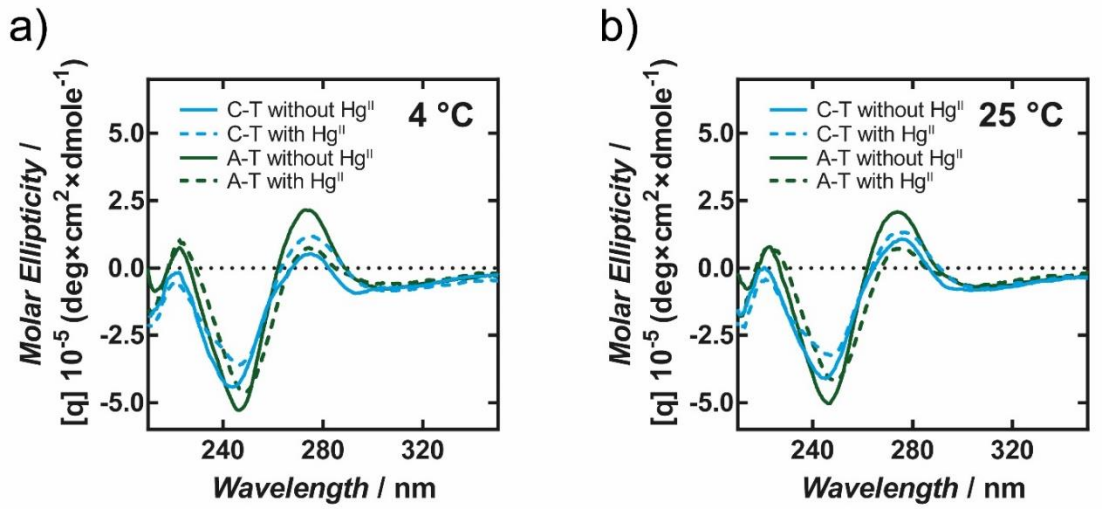

Figure A22. CD spectra for "C-T" (blue) and "T-A" (green) in the presence and absence of 2.0 equiv of Hg^{II} at a) 4°C and b) 25 °C. DNA samples contained 10 μM of pre-folded duplex DNA in aqueous buffer (200 mM $NaClO_4$, 50 mM cacodylic acid at pH = 7.8).

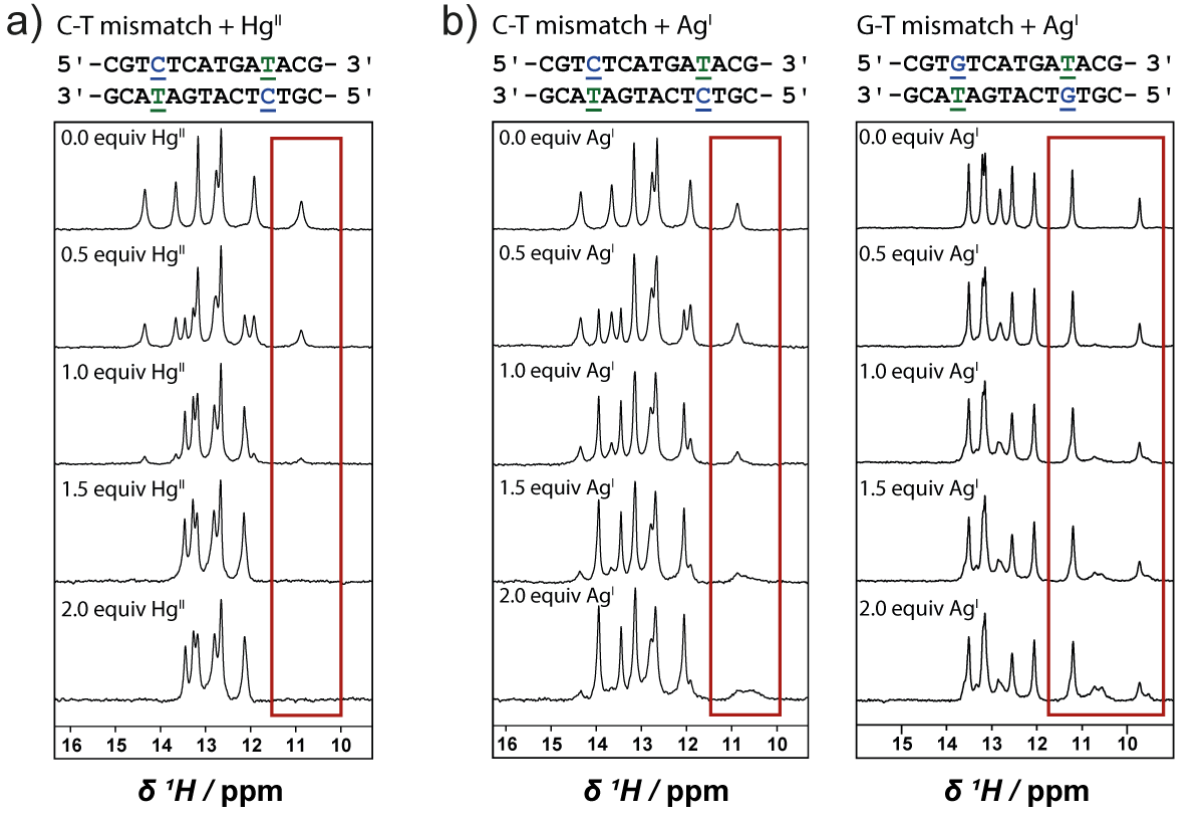

Figure A23. a) Change of imino-region of "C-T" upon addition of various equiv of Hg^{II}. b) Change of imino-region of "**C-T**" and "**G-T**" upon addition various equiv of Ag^{I}. DNA samples contained 0.1 mM duplex DNA in aqueous buffer (200 mM $NaClO_4$, 50 mM cacodylic acid in H_2O / D_2O (9:1) at pH = 7.0). All spectra were recorded at 4 °C.

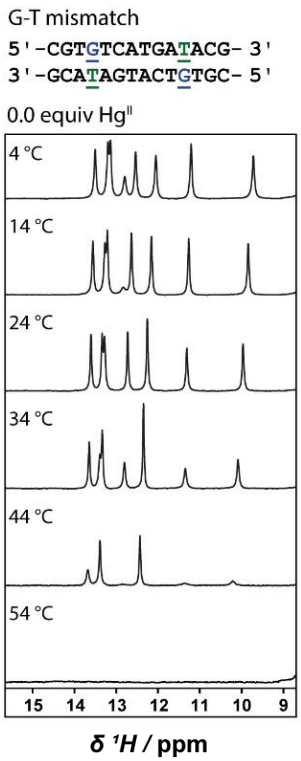

Figure A24. Melting temperature (T_m) of a) "**C-T**" in the presence (left) and absence (right) of Hg^{II} and b) "**G-T**" according to changes in the imino region of ^{1}H NMR spectra. All DNA samples contained 0.5 mM duplex DNA in aqueous buffer (200 mM $NaClO_4$, 50 mM cacodylic acid in H_2O / D_2O (9:1) at pH = 7.0).

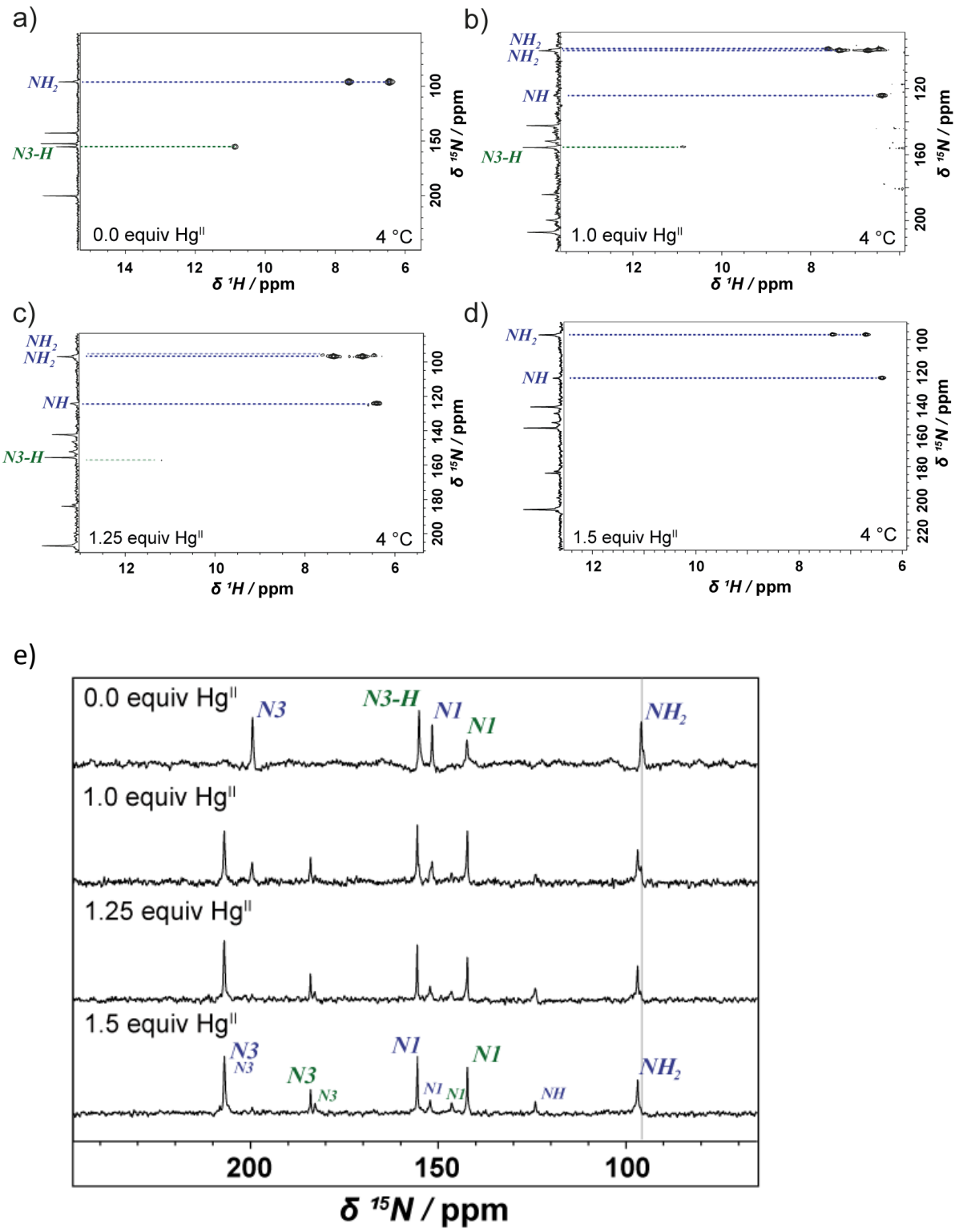

Figure A25. Formation of C-Hg^{II}-T base pairs upon addition of various equiv of Hg^{II} according to changes in [^{15}N,^{1}H]-HSQC spectra (a)-d)) and ^{15}N-spectra (e). 1.5 equiv of Hg^{II} were needed to saturate C-T mismatch containing duplex DNA and induce complete disappearance of ^{15}N signals of unbound duplex. DNA samples contained 0.5 mM duplex DNA in aqueous buffer (200 mM $NaClO_4$, 50 mM cacodylic acid in H_2O / D_2O (9:1) at pH = 7.0). Equiv of Hg^{II} given relative to mismatch. Spectra were recorded at 4 °C.

Table A4. Imino-Proton Chemical Shift Values (ppm) of ODN[1]* **"C*-T*" With and Without** Hg^{II} at 4 °C[a]

Imino-proton signal	ppm in the absence of Hg^{II}	ppm in the presence of Hg^{II}
G28	12.75	12.79 (+0.04)
G2	12.64	12.65 (+0.01)
T3	13.64	13.45 (-0.19)
T25	10.86 (*d*, ^{1}J $^{1}H,^{15}N$ = 88 Hz)	-
T5	14.33	13.26 (-1.07)
G23	11.91	12.13 (+0.22)
T22	13.15	13.17 (+0.02)

[a] Values in brackets represent chemical shift changes upon addition of Hg^{II}. The DNA sample contained 0.5 mM duplex DNA in aqueous buffer (200 mM $NaClO_4$, 50 mM cacodylic acid in H_2O / D_2O (9:1) at pH = 7.8) in the absence and the presence of 1.5 mM of $Hg(ClO_4)_2$ (1.5 equiv relative to mismatch).

Table A5. ^{15}N-Chemical Shift Values (ppm) of ODN[1]* **"C*-T*" With and Without** Hg^{II} at 25 °C.[a]

^{15}N- signal	ppm in the absence of Hg^{II}	ppm in the presence of Hg^{II}
N1 (T)	142.6	$N1^{major}$: 142.7 (+0.1) $N1^{minor}$: 146.4 (+3.8)
N3 (T)	155.2	$N3^{major}$: 184.3 (+29.1) $N3^{minor}$: 183.1 (+27.9)
N1 (C)	152.3	$N1^{major}$: 155.7 (+3.4) $N1^{minor}$: 152.5 (+0.2)
N3 (C)	200.0	$N3^{major}$: 207.2 (+7.2) $N3^{minor}$: 207.2 (+7.2)
NH_2 (C)	95.9	$C4\text{-}NH_2^{major}$: 96.7 (+0.8) $C4\text{-}NH^{minor}$: 124.1 (+28.2)

[a] Values in brackets represent chemical shift changes upon addition of Hg^{II}. The DNA sample contained 1 mM duplex DNA and 3 mM of $Hg(ClO_4)_2$ in aqueous buffer (200 mM $NaClO_4$, 50 mM cacodylic acid in H_2O / D_2O (9:1) at pH = 7.8).

Table A6. ^{15}N-Chemical Shift Values (ppm) of ODN^{1*} **"C*-T*" With and Without Hg^{II}** at 4 °C.[a]

^{15}N- signal	ppm in the absence of Hg^{II}	ppm in the presence of Hg^{II}	^{1}J ^{15}N,^{199}Hg
N1 (T)	142.3	*N1*^{major}: 142.2 (-0.1)	-
		N1^{minor}: 146.4 (+4.1)	-
N3 (T)	155.1	*N3*^{major}: 184.0 (+28.9)	1095 Hz
		N3^{minor}: 182.8 (+27.7)	*n. d.*
N1 (C)	151.6	*N1*^{major}: 155.5 (+3.9)	-
		N1^{minor}: 152.1 (+0.5)	-
N3 (C)	199.4	*N3*^{major}: 206.9 (+7.5)	114 Hz
		N3^{minor}: 206.9 (+7.5)	-
NH$_2$ (C)	95.9	*NH$_2$*^{major}: 96.9 (+1)	-
		NH^{minor}: 124.2 (+28.3)	1063 Hz

[a] Values in brackets represent chemical shift changes upon addition of Hg^{II}. The DNA sample contained 1 mM duplex DNA and 3 mM of $Hg(ClO_4)_2$ in aqueous buffer (200 mM $NaClO_4$, 50 mM cacodylic acid in H_2O / D_2O (9:1) at pH = 7.8).

Chemical Shift List Major Duplex

1DCH1'	strand A	5.816 ± 0.001
1DCH2'	strand A	2.064 ± 0.001
1DCH2"	strand A	2.473 ± 0.001
1DCH3'	strand A	4.723 ± 0.002
1DCH4'	strand A	4.096 ± 0.001
1DCH5	strand A	5.935 ± 0.001
1DCH5'	strand A	3.747 ± 0.001
1DCH6	strand A	7.679 ± 0.001
1DCH41	strand A	7.118 ± 0.003
1DCH42	strand A	8.156 ± 0.003
2DGH1'	strand A	6.059 ± 0.002
2DGH2'	strand A	2.704 ± 0.002
2DGH2"	strand A	2.841 ± 0.002
2DGH3'	strand A	4.994 ± 0.001
2DGH4'	strand A	4.399 ± 0.001
2DGH5'	strand A	4.052 ± 0.002
2DGH5"	strand A	4.132 ± 0.001
2DGH8	strand A	8.000 ± 0.001
2DGH1	strand A	12.946 ± 0.003
3DTH71	strand A	1.477 ± 0.002
3DTH1'	strand A	6.006 ± 0.002
3DTH2'	strand A	2.230 ± 0.002
3DTH2"	strand A	2.519 ± 0.002
3DTH3'	strand A	4.874 ± 0.001
3DTH4'	strand A	4.261 ± 0.002
3DTH5'	strand A	4.405 ± 0.001
3DTH6	strand A	7.292 ± 0.001
3DTH3	strand A	13.748 ± 0.003
4DCH1'	strand A	6.016 ± 0.001
4DCH2'	strand A	1.833 ± 0.002
4DCH2"	strand A	2.425 ± 0.002
4DCH3'	strand A	4.700 ± 0.002
4DCH4'	strand A	4.139 ± 0.002
4DCH5	strand A	5.555 ± 0.001
4DCH5'	strand A	4.333 ± 0.001
4DCH5"	strand A	4.241 ± 0.002
4DCH6	strand A	7.525 ± 0.001
4DCH41	strand A	6.999 ± 0.002
4DCH42	strand A	7.659 ± 0.003
5DTH71	strand A	1.749 ± 0.001
5DTH1'	strand A	6.170 ± 0.002
5DTH2'	strand A	2.499 ± 0.003
5DTH2"	strand A	2.574 ± 0.003
5DTH3'	strand A	4.945 ± 0.002
5DTH4'	strand A	4.339 ± 0.001
5DTH5'	strand A	4.117 ± 0.003
5DTH5"	strand A	4.069 ± 0.002
5DTH6	strand A	7.591 ± 0.002
5DTH3	strand A	13.472 ± 0.003
6DCH1'	strand A	5.648 ± 0.002
6DCH2'	strand A	2.033 ± 0.001
6DCH2"	strand A	2.405 ± 0.001
6DCH3'	strand A	4.878 ± 0.001
6DCH4'	strand A	4.151 ± 0.001
6DCH5	strand A	5.799 ± 0.002
6DCH6	strand A	7.511 ± 0.002
6DCH41	strand A	8.462 ± 0.002
6DCH42	strand A	7.020 ± 0.003

7DAH1'	strand A	6.213 ± 0.001	10DAH1'	strand A	6.145 ± 0.002
7DAH2	strand A	7.641 ± 0.002	10DAH2	strand A	7.538 ± 0.001
7DAH2'	strand A	2.711 ± 0.003	10DAH2'	strand A	2.527 ± 0.002
7DAH2''	strand A	2.908 ± 0.002	10DAH2''	strand A	2.784 ± 0.003
7DAH3'	strand A	5.024 ± 0.001	10DAH3'	strand A	4.920 ± 0.002
7DAH4'	strand A	4.419 ± 0.002	10DAH4'	strand A	4.424 ± 0.002
7DAH5'	strand A	4.156 ± 0.003	10DAH5'	strand A	4.258 ± 0.002
7DAH5''	strand A	4.078 ± 0.002	10DAH5''	strand A	4.177 ± 0.003
7DAH8	strand A	8.362 ± 0.001	10DAH8	strand A	8.141 ± 0.002
7DAH61	strand A	7.802 ± 0.003	10DAH61	strand A	7.749 ± 0.003
7DAH62	strand A	6.442 ± 0.002	10DAH62	strand A	6.379 ± 0.003
8DTH71	strand A	1.446 ± 0.002	11DTH71	strand A	1.267 ± 0.001
8DTH1'	strand A	5.652 ± 0.001	11DTH1'	strand A	5.763 ± 0.001
8DTH2'	strand A	1.747 ± 0.001	11DTH2'	strand A	1.800 ± 0.001
8DTH2''	strand A	2.189 ± 0.003	11DTH2''	strand A	2.241 ± 0.002
8DTH3'	strand A	4.815 ± 0.002	11DTH3'	strand A	4.820 ± 0.002
8DTH4'	strand A	4.057 ± 0.001	11DTH4'	strand A	4.107 ± 0.002
8DTH5'	strand A	4.246 ± 0.002	11DTH5'	strand A	4.184 ± 0.002
8DTH5''	strand A	4.107 ± 0.001	11DTH5''	strand A	4.023 ± 0.002
8DTH6	strand A	7.018 ± 0.002	11DTH6	strand A	6.951 ± 0.002
8DTH3	strand A	13.572 ± 0.002	12DAH1'	strand A	6.114 ± 0.002
9DGH1'	strand A	5.255 ± 0.001	12DAH2	strand A	7.926 ± 0.002
9DGH2'	strand A	2.577 ± 0.001	12DAH2'	strand A	2.744 ± 0.001
9DGH2''	strand A	2.574 ± 0.002	12DAH2''	strand A	2.775 ± 0.003
9DGH3'	strand A	4.930 ± 0.001	12DAH3'	strand A	5.019 ± 0.002
9DGH4'	strand A	4.259 ± 0.002	12DAH4'	strand A	4.416 ± 0.002
9DGH5'	strand A	4.058 ± 0.002	12DAH5'	strand A	4.113 ± 0.003
9DGH5''	strand A	4.006 ± 0.002	12DAH5''	strand A	4.022 ± 0.002
9DGH8	strand A	7.800 ± 0.002	12DAH8	strand A	8.333 ± 0.002
9DGH1	strand A	12.439 ± 0.003	12DAH61	strand A	7.616 ± 0.003

12DAH62	strand A	7.008 ± 0.002	16DGH1'	strand B	6.059 ± 0.002
13DCH1'	strand A	5.693 ± 0.002	16DGH2'	strand B	2.704 ± 0.002
13DCH2'	strand A	1.882 ± 0.001	16DGH2''	strand B	2.841 ± 0.002
13DCH2''	strand A	2.310 ± 0.001	16DGH3'	strand B	4.994 ± 0.001
13DCH3'	strand A	4.769 ± 0.003	16DGH4'	strand B	4.399 ± 0.001
13DCH4'	strand A	4.157 ± 0.001	16DGH5'	strand B	4.052 ± 0.002
13DCH5	strand A	5.401 ± 0.001	16DGH5''	strand B	4.132 ± 0.001
13DCH5'	strand A	4.244 ± 0.002	16DGH8	strand B	8.000 ± 0.001
13DCH5''	strand A	4.078 ± 0.003	16DGH1	strand B	12.946 ± 0.003
13DCH6	strand A	7.307 ± 0.001	17DTH71	strand B	1.477 ± 0.002
13DCH41	strand A	8.258 ± 0.003	17DTH1'	strand B	6.006 ± 0.002
13DCH42	strand A	6.815 ± 0.003	17DTH2'	strand B	2.230 ± 0.002
14DGH1'	strand A	6.164 ± 0.001	17DTH2''	strand B	2.519 ± 0.002
14DGH2'	strand A	2.594 ± 0.002	17DTH3'	strand B	4.874 ± 0.001
14DGH2''	strand A	2.375 ± 0.003	17DTH4'	strand B	4.261 ± 0.002
14DGH3'	strand A	4.664 ± 0.001	17DTH5'	strand B	4.405 ± 0.001
14DGH4'	strand A	4.178 ± 0.001	17DTH6	strand B	7.292 ± 0.001
14DGH5'	strand A	4.078 ± 0.002	17DTH3	strand B	13.748 ± 0.003
14DGH8	strand A	7.902 ± 0.001	18DCH1'	strand B	6.016 ± 0.001
14DGH1	strand A	13.119 ± 0.001	18DCH2'	strand B	1.833 ± 0.002
15DCH1'	strand B	5.816 ± 0.001	18DCH2''	strand B	2.425 ± 0.002
15DCH2'	strand B	2.064 ± 0.001	18DCH3'	strand B	4.700 ± 0.002
15DCH2''	strand B	2.473 ± 0.001	18DCH4'	strand B	4.139 ± 0.002
15DCH3'	strand B	4.723 ± 0.002	18DCH5	strand B	5.555 ± 0.001
15DCH4'	strand B	4.096 ± 0.001	18DCH5'	strand B	4.333 ± 0.001
15DCH5	strand B	5.935 ± 0.001	18DCH5''	strand B	4.241 ± 0.002
15DCH5'	strand B	3.747 ± 0.001	18DCH6	strand B	7.525 ± 0.001
15DCH6	strand B	7.679 ± 0.001	18DCH41	strand B	6.999 ± 0.002
15DCH41	strand B	7.118 ± 0.003	18DCH42	strand B	7.659 ± 0.003
15DCH42	strand B	8.156 ± 0.003	19DTH71	strand B	1.749 ± 0.001

19DTH1'	strand B	6.170 ± 0.002	22DTH1'	strand B	5.652 ± 0.001
19DTH2'	strand B	2.499 ± 0.003	22DTH2'	strand B	1.747 ± 0.001
19DTH2''	strand B	2.574 ± 0.003	22DTH2''	strand B	2.189 ± 0.003
19DTH3'	strand B	4.945 ± 0.002	22DTH3'	strand B	4.815 ± 0.002
19DTH4'	strand B	4.339 ± 0.001	22DTH4'	strand B	4.057 ± 0.001
19DTH5'	strand B	4.117 ± 0.003	22DTH5'	strand B	4.246 ± 0.002
19DTH5''	strand B	4.069 ± 0.002	22DTH5''	strand B	4.107 ± 0.001
19DTH6	strand B	7.591 ± 0.002	22DTH6	strand B	7.018 ± 0.002
19DTH3	strand B	13.472 ± 0.003	22DTH3	strand B	13.572 ± 0.002
20DCH1'	strand B	5.648 ± 0.002	23DGH1'	strand B	5.255 ± 0.001
20DCH2'	strand B	2.033 ± 0.001	23DGH2'	strand B	2.577 ± 0.001
20DCH2''	strand B	2.405 ± 0.001	23DGH2''	strand B	2.574 ± 0.002
20DCH3'	strand B	4.878 ± 0.001	23DGH3'	strand B	4.930 ± 0.001
20DCH4'	strand B	4.151 ± 0.001	23DGH4'	strand B	4.259 ± 0.002
20DCH5	strand B	5.799 ± 0.002	23DGH5'	strand B	4.058 ± 0.002
20DCH6	strand B	7.511 ± 0.002	23DGH5''	strand B	4.006 ± 0.002
20DCH41	strand B	8.462 ± 0.002	23DGH8	strand B	7.800 ± 0.002
20DCH42	strand B	7.020 ± 0.003	23DGH1	strand B	12.439 ± 0.003
21DAH1'	strand B	6.213 ± 0.001	24DAH1'	strand B	6.145 ± 0.002
21DAH2	strand B	7.641 ± 0.002	24DAH2	strand B	7.538 ± 0.001
21DAH2'	strand B	2.711 ± 0.003	24DAH2'	strand B	2.527 ± 0.002
21DAH2''	strand B	2.908 ± 0.002	24DAH2''	strand B	2.784 ± 0.003
21DAH3'	strand B	5.024 ± 0.001	24DAH3'	strand B	4.920 ± 0.002
21DAH4'	strand B	4.419 ± 0.002	24DAH4'	strand B	4.424 ± 0.002
21DAH5'	strand B	4.156 ± 0.003	24DAH5'	strand B	4.258 ± 0.002
21DAH5''	strand B	4.078 ± 0.002	24DAH5''	strand B	4.177 ± 0.003
21DAH8	strand B	8.362 ± 0.001	24DAH8	strand B	8.141 ± 0.002
21DAH61	strand B	7.802 ± 0.003	24DAH61	strand B	7.749 ± 0.003
21DAH62	strand B	6.442 ± 0.002	24DAH62	strand B	6.379 ± 0.003
22DTH71	strand B	1.446 ± 0.002	25DTH71	strand B	1.267 ± 0.001

25DTH1'	strand B	5.763 ± 0.001
25DTH2'	strand B	1.800 ± 0.001
25DTH2''	strand B	2.241 ± 0.002
25DTH3'	strand B	4.820 ± 0.002
25DTH4'	strand B	4.107 ± 0.002
25DTH5'	strand B	4.184 ± 0.002
25DTH5''	strand B	4.023 ± 0.002
25DTH6	strand B	6.951 ± 0.002
26DAH1'	strand B	6.114 ± 0.002
26DAH2	strand B	7.926 ± 0.002
26DAH2'	strand B	2.744 ± 0.001
26DAH2''	strand B	2.775 ± 0.003
26DAH3'	strand B	5.019 ± 0.002
26DAH4'	strand B	4.416 ± 0.002
26DAH5'	strand B	4.113 ± 0.003
26DAH5''	strand B	4.022 ± 0.002
26DAH8	strand B	8.333 ± 0.002
26DAH61	strand B	7.616 ± 0.003
26DAH62	strand B	7.008 ± 0.002
27DCH1'	strand B	5.693 ± 0.002
27DCH2'	strand B	1.882 ± 0.001
27DCH2''	strand B	2.310 ± 0.001
27DCH3'	strand B	4.769 ± 0.003
27DCH4'	strand B	4.157 ± 0.001
27DCH5	strand B	5.401 ± 0.001
27DCH5'	strand B	4.244 ± 0.002
27DCH5''	strand B	4.078 ± 0.003
27DCH6	strand B	7.307 ± 0.001
27DCH41	strand B	8.258 ± 0.003
27DCH42	strand B	6.815 ± 0.003
28DGH1'	strand B	6.164 ± 0.001
28DGH2'	strand B	2.594 ± 0.002
28DGH2''	strand B	2.375 ± 0.003
28DGH3'	strand B	4.664 ± 0.001
28DGH4'	strand B	4.178 ± 0.001
28DGH5'	strand B	4.078 ± 0.002
28DGH8	strand B	7.902 ± 0.001
28DGH1	strand B	13.119 ± 0.001

Chemical Shift List Minor Duplex

1 DC H1'	strand A	5.814 ± 0.002
1 DC H2'	strand A	2.053 ± 0.002
1 DC H2''	strand A	2.462 ± 0.001
1 DC H5	strand A	5.933 ± 0.001
1 DC H6	strand A	7.678 ± 0.002
2 DG H1'	strand A	6.094 ± 0.002
2 DG H2'	strand A	2.718 ± 0.002
2 DG H2''	strand A	2.873 ± 0.001
2 DG H8	strand A	8.017 ± 0.002
3 DT H71	strand A	1.533 ± 0.002
3 DT H1'	strand A	5.997 ± 0.003
3 DT H2'	strand A	2.179 ± 0.002
3 DT H2''	strand A	2.554 ± 0.003
3 DT H6	strand A	7.302 ± 0.002
4 DC H1'	strand A	6.147 ± 0.003
4 DC H2'	strand A	2.145 ± 0.003
4 DC H2''	strand A	2.610 ± 0.002
4 DC H5	strand A	5.554 ± 0.001
4 DC H6	strand A	7.530 ± 0.002
5 DT H71	strand A	1.709 ± 0.002
5 DT H1'	strand A	5.930 ± 0.002
5 DT H2'	strand A	2.125 ± 0.002
5 DT H2''	strand A	2.473 ± 0.002
5 DT H6	strand A	7.395 ± 0.001
6 DC H1'	strand A	5.647 ± 0.002
6 DC H2'	strand A	2.160 ± 0.001
6 DC H2''	strand A	2.468 ± 0.001
6 DC H5	strand A	5.731 ± 0.001
6 DC H6	strand A	7.592 ± 0.001
7 DA H1'	strand A	6.214 ± 0.002
7 DA H2	strand A	7.557 ± 0.000
7 DA H2'	strand A	2.676 ± 0.003
7 DA H2''	strand A	2.911 ± 0.002
7 DA H8	strand A	8.329 ± 0.002
8 DT H71	strand A	1.442 ± 0.002
8 DT H1'	strand A	5.623 ± 0.002
8 DT H2'	strand A	1.913 ± 0.001
8 DT H2''	strand A	2.303 ± 0.003
8 DT H6	strand A	7.079 ± 0.003
9 DG H1'	strand A	5.534 ± 0.002
9 DG H2'	strand A	2.593 ± 0.003
9 DG H2''	strand A	2.704 ± 0.002
9 DG H8	strand A	7.798 ± 0.001
10 DA H1'	strand A	6.156 ± 0.001
10 DA H2	strand A	7.853 ± 0.001
10 DA H2'	strand A	2.557 ± 0.003
10 DA H2''	strand A	2.822 ± 0.002
10 DA H8	strand A	8.122 ± 0.003
11 DT H71	strand A	1.678 ± 0.003
11 DT H1'	strand A	5.417 ± 0.001
11 DT H2'	strand A	1.489 ± 0.001
11 DT H2''	strand A	2.032 ± 0.002
11 DT H6	strand A	6.926 ± 0.003
12 DA H1'	strand A	6.118 ± 0.002
12 DA H2	strand A	8.031 ± 0.001
12 DA H2'	strand A	2.741 ± 0.002
12 DA H2''	strand A	2.780 ± 0.002
12 DA H8	strand A	8.308 ± 0.003
13 DC H1'	strand A	5.693 ± 0.003

13 DC H2'	strand A	1.885 ± 0.003	19 DT H2''	strand B	2.473 ± 0.002
13 DC H2''	strand A	2.308 ± 0.001	19 DT H6	strand B	7.395 ± 0.001
13 DC H5	strand A	5.400 ± 0.002	20 DC H1'	strand B	5.647 ± 0.002
13 DC H6	strand A	7.328 ± 0.002	20 DC H2'	strand B	2.160 ± 0.001
14 DG H1'	strand A	6.167 ± 0.002	20 DC H2''	strand B	2.468 ± 0.001
14 DG H2'	strand A	2.607 ± 0.001	20 DC H5	strand B	5.731 ± 0.001
14 DG H2''	strand A	2.374 ± 0.001	20 DC H6	strand B	7.592 ± 0.001
14 DG H8	strand A	7.901 ± 0.001	21 DA H1'	strand B	6.214 ± 0.002
15 DC H1'	strand B	5.814 ± 0.002	21 DA H2	strand B	7.557 ± 0.000
15 DC H2'	strand B	2.053 ± 0.002	21 DA H2'	strand B	2.676 ± 0.003
15 DC H2''	strand B	2.462 ± 0.001	21 DA H2''	strand B	2.911 ± 0.002
15 DC H5	strand B	5.933 ± 0.001	21 DA H8	strand B	8.329 ± 0.002
15 DC H6	strand B	7.678 ± 0.002	22 DT H71	strand B	1.442 ± 0.002
16 DG H1'	strand B	6.094 ± 0.002	22 DT H1'	strand B	5.623 ± 0.002
16 DG H2'	strand B	2.718 ± 0.002	22 DT H2'	strand B	1.913 ± 0.001
16 DG H2''	strand B	2.873 ± 0.001	22 DT H2''	strand B	2.303 ± 0.003
16 DG H8	strand B	8.017 ± 0.002	22 DT H6	strand B	7.079 ± 0.003
17 DT H71	strand B	1.533 ± 0.002	23 DG H1'	strand B	5.534 ± 0.002
17 DT H1'	strand B	5.997 ± 0.003	23 DG H2'	strand B	2.593 ± 0.003
17 DT H2'	strand B	2.179 ± 0.002	23 DG H2''	strand B	2.704 ± 0.002
17 DT H2''	strand B	2.554 ± 0.003	23 DG H8	strand B	7.798 ± 0.001
17 DT H6	strand B	7.302 ± 0.002	24 DA H1'	strand B	6.156 ± 0.001
18 DC H1'	strand B	6.147 ± 0.003	24 DA H2	strand B	7.853 ± 0.001
18 DC H2'	strand B	2.145 ± 0.003	24 DA H2'	strand B	2.557 ± 0.003
18 DC H2''	strand B	2.610 ± 0.002	24 DA H2''	strand B	2.822 ± 0.002
18 DC H5	strand B	5.554 ± 0.001	24 DA H8	strand B	8.122 ± 0.003
18 DC H6	strand B	7.530 ± 0.002	25 DT H71	strand B	1.678 ± 0.003
19 DT H71	strand B	1.709 ± 0.002	25 DT H1'	strand B	5.417 ± 0.001
19 DT H1'	strand B	5.930 ± 0.002	25 DT H2'	strand B	1.489 ± 0.001
19 DT H2'	strand B	2.125 ± 0.002	25 DT H2''	strand B	2.032 ± 0.002

25 DT H6	strand B	6.926 ± 0.003
26 DA H1'	strand B	6.118 ± 0.002
26 DA H2	strand B	8.031 ± 0.001
26 DA H2'	strand B	2.741 ± 0.002
26 DA H2"	strand B	2.780 ± 0.002
26 DA H8	strand B	8.308 ± 0.003
27 DC H1'	strand B	5.693 ± 0.003
27 DC H2'	strand B	1.885 ± 0.003
27 DC H2"	strand B	2.308 ± 0.001
27 DC H5	strand B	5.400 ± 0.002
27 DC H6	strand B	7.328 ± 0.002
28 DG H1'	strand B	6.167 ± 0.002
28 DG H2'	strand B	2.607 ± 0.001
28 DG H2"	strand B	2.374 ± 0.001
28 DG H8	strand B	7.901 ± 0.001

Structure Calculation and Constraints

Table A7. NMR restraints and statistics for major and minor duplex structures[a]

	Major duplex	Minor duplex
NOE-derived distance restraints[b]	646	640
C-Hg^{II}-T base pair	158	148
Intra-nucleotide	266	264
Inter-nucleotide (*i-j* = 1)	306	302
Long-range (*i-j* = ≥ 2)	74	74
Repulsive	0	0
NOE restraints per residue	23.07	22.86
NOE violation > 0.2 Å	0	0
Dihedral restraints[b,c]	168	168
Dihedral violations > 5.0 °	0	0
Hydrogen-bond restraints[b,c]	62	62
Planarity[c]	24	24
r.m.s.d (for all heavy atoms to the best structure, Å)		
Overall	1.21 ± 0.42 Å	1.09 ± 0.35 Å
Helix	1.35 ± 0.45 Å	1.20 ± 0.35 Å
C-Hg^{II}-T base pairs	0.76 ± 0.28 Å	0.75 ± 0.29 Å

[a] All statistic values are given for the 20 lowest energy structures from 200 calculated structures. [b]Experimentally derived contraints. [c]Introduced contraints.

MAJOR DUPLEX

NOE constraints

{C1}

```
assign (residue 1 and name H1')   (residue 1 and name H5)   6.00 2.00 1.00
assign (residue 1 and name H1')   (residue 1 and name H6)   3.80 2.00 0.70
assign (residue 1 and name H1')   (residue 2 and name H1')   6.00 2.00 1.00
assign (residue 1 and name H1')   (residue 2 and name H3')   6.00 2.00 1.00
assign (residue 1 and name H1')   (residue 2 and name H4')   5.00 2.00 1.00
assign (residue 1 and name H1')   (residue 2 and name H5')   3.80 2.00 0.70
assign (residue 1 and name H1')   (residue 2 and name H8)   3.80 2.00 0.70
assign (residue 1 and name H2')   (residue 1 and name H6)   2.50 0.70 0.50
assign (residue 1 and name H2')   (residue 2 and name H8)   3.80 2.00 0.70
assign (residue 1 and name H2'')  (residue 1 and name H6)   3.80 2.00 0.70
assign (residue 1 and name H2'')  (residue 2 and name H8)   2.50 0.70 0.50
assign (residue 1 and name H3')   (residue 1 and name H6)   3.80 2.00 0.70
```

```
assign (residue 1 and name H4')    (residue 1 and name H6)     5.00 2.00 1.00
assign (residue 1 and name H4')    (residue 2 and name H8)     6.00 2.00 1.00
assign (residue 1 and name H5)     (residue 1 and name H5')    6.00 2.00 1.00
assign (residue 1 and name H5)     (residue 2 and name H8)     6.00 2.00 1.00
assign (residue 1 and name H5')    (residue 1 and name H6)     3.80 2.00 0.70
assign (residue 1 and name H6)     (residue 2 and name H8)     5.00 2.00 1.00
assign (residue 1 and name H41)    (residue 2 and name H1)     5.00 2.00 1.00
assign (residue 1 and name H41)    (residue 27 and name H41)   3.80 2.00 0.70
assign (residue 1 and name H41)    (residue 28 and name H1)    3.80 2.00 0.70
assign (residue 1 and name H42)    (residue 2 and name H1)     6.00 2.00 1.00
assign (residue 1 and name H42)    (residue 28 and name H1)    5.00 2.00 1.00
assign (residue 1 and name H5)     (residue 28 and name H1)    6.00 2.00 1.00

{G2}
assign (residue 2 and name H1')    (residue 2 and name H8)     3.80 2.00 0.70
assign (residue 2 and name H1')    (residue 3 and name H51)    3.80 2.00 0.70
assign (residue 2 and name H1')    (residue 3 and name H6)     3.80 2.00 0.70
assign (residue 2 and name H2')    (residue 2 and name H8)     2.50 0.70 0.50
assign (residue 2 and name H2')    (residue 3 and name H51)    3.80 2.00 0.70
assign (residue 2 and name H2')    (residue 3 and name H6)     3.80 2.00 0.70
assign (residue 2 and name H2'')   (residue 2 and name H8)     3.80 2.00 0.70
assign (residue 2 and name H2'')   (residue 3 and name H51)    3.80 2.00 0.70
assign (residue 2 and name H2'')   (residue 3 and name H6)     3.80 2.00 0.70
assign (residue 2 and name H3')    (residue 2 and name H8)     5.00 2.00 1.00
assign (residue 2 and name H3')    (residue 3 and name H51)    5.00 2.00 1.00
assign (residue 2 and name H3')    (residue 3 and name H6)     6.00 2.00 1.00
assign (residue 2 and name H4')    (residue 2 and name H8)     5.00 2.00 1.00
assign (residue 2 and name H4')    (residue 3 and name H51)    6.00 2.00 1.00
assign (residue 2 and name H5')    (residue 2 and name H8)     3.80 2.00 0.70
assign (residue 2 and name H5'')   (residue 2 and name H8)     5.00 2.00 1.00
assign (residue 2 and name H8)     (residue 3 and name H51)    3.80 2.00 0.70
assign (residue 2 and name H8)     (residue 3 and name H6)     5.00 2.00 1.00
assign (residue 2 and name H1)     (residue 3 and name H3)     3.80 2.00 0.70
assign (residue 2 and name H1)     (residue 28 and name H1)    3.80 2.00 0.70

{T3}
assign (residue 3 and name H51)    (residue 3 and name H1')    6.00 2.00 1.00
assign (residue 3 and name H51)    (residue 3 and name H2')    5.00 2.00 1.00
assign (residue 3 and name H51)    (residue 3 and name H2'')   6.00 2.00 1.00
assign (residue 3 and name H51)    (residue 3 and name H3')    6.00 2.00 1.00
assign (residue 3 and name H51)    (residue 3 and name H4')    6.00 2.00 1.00
assign (residue 3 and name H51)    (residue 3 and name H5')    6.00 2.00 1.00
assign (residue 3 and name H51)    (residue 4 and name H5)     5.00 2.00 1.00
assign (residue 3 and name H51)    (residue 4 and name H6)     6.00 2.00 1.00
assign (residue 3 and name H1')    (residue 3 and name H6)     3.80 2.00 0.70
assign (residue 3 and name H1')    (residue 4 and name H5)     3.80 2.00 0.70
assign (residue 3 and name H1')    (residue 4 and name H6)     3.80 2.00 0.70
assign (residue 3 and name H1')    (residue 26 and name H2)    5.00 2.00 1.00
assign (residue 3 and name H2')    (residue 2 and name H1')    5.00 2.00 1.00
assign (residue 3 and name H2')    (residue 3 and name H6)     2.50 0.70 0.50
assign (residue 3 and name H2')    (residue 4 and name H5)     3.80 2.00 0.70
assign (residue 3 and name H2')    (residue 4 and name H6)     3.80 2.00 0.70
```

assign (residue 3 and name H2'') (residue 3 and name H6) 3.80 2.00 0.70
assign (residue 3 and name H2'') (residue 4 and name H5) 3.80 2.00 0.70
assign (residue 3 and name H2'') (residue 4 and name H6) 3.80 2.00 0.70
assign (residue 3 and name H3') (residue 3 and name H6) 3.80 2.00 0.70
assign (residue 3 and name H4') (residue 3 and name H6) 5.00 2.00 1.00
assign (residue 3 and name H4') (residue 4 and name H6) 6.00 2.00 1.00
assign (residue 3 and name H5') (residue 3 and name H6) 5.00 2.00 1.00
assign (residue 3 and name H6) (residue 4 and name H5) 3.80 2.00 0.70
assign (residue 3 and name H6) (residue 4 and name H6) 5.00 2.00 1.00
assign (residue 3 and name H1') (residue 2 and name H1) 6.00 2.00 1.00
assign (residue 3 and name H5'') (residue 3 and name H6) 5.00 2.00 1.00

{C4}
assign (residue 4 and name H1') (residue 4 and name H5) 6.00 2.00 1.00
assign (residue 4 and name H1') (residue 4 and name H6) 3.80 2.00 0.70
assign (residue 4 and name H1') (residue 5 and name H51) 5.00 2.00 1.00
assign (residue 4 and name H1') (residue 5 and name H6) 3.80 2.00 0.70
assign (residue 4 and name H1') (residue 5 and name H3') 6.00 2.00 1.00
assign (residue 4 and name H2') (residue 4 and name H5) 5.00 2.00 1.00
assign (residue 4 and name H2') (residue 4 and name H6) 2.50 0.70 0.50
assign (residue 4 and name H2') (residue 5 and name H51) 3.80 2.00 0.70
assign (residue 4 and name H2') (residue 5 and name H6) 3.80 2.00 0.70
assign (residue 4 and name H2'') (residue 4 and name H5) 6.00 2.00 1.00
assign (residue 4 and name H2'') (residue 4 and name H6) 3.80 2.00 0.70
assign (residue 4 and name H2'') (residue 5 and name H51) 3.80 2.00 0.70
assign (residue 4 and name H2'') (residue 5 and name H6) 3.80 2.00 0.70
assign (residue 4 and name H4') (residue 4 and name H5) 6.00 2.00 1.00
assign (residue 4 and name H4') (residue 4 and name H6) 5.00 2.00 1.00
assign (residue 4 and name H4') (residue 5 and name H6) 6.00 2.00 1.00
assign (residue 4 and name H5) (residue 3 and name H3') 6.00 2.00 1.00
assign (residue 4 and name H5) (residue 5 and name H51) 5.00 2.00 1.00
assign (residue 4 and name H5'') (residue 4 and name H6) 5.00 2.00 1.00
assign (residue 4 and name H6) (residue 4 and name H3') 3.80 2.00 0.70
assign (residue 4 and name H6) (residue 5 and name H51) 3.80 2.00 0.70
assign (residue 4 and name H6) (residue 3 and name H4') 6.00 2.00 1.00
assign (residue 4 and name H6) (residue 5 and name H6) 6.00 2.00 1.00
assign (residue 4 and name H1') (residue 3 and name H3) 6.00 2.00 1.00
assign (residue 4 and name H3') (residue 5 and name H6) 3.80 2.00 0.70
assign (residue 4 and name H41) (residue 3 and name H3) 3.80 2.00 0.70
assign (residue 4 and name H41) (residue 26 and name H2) 6.00 2.00 1.00
assign (residue 4 and name H42) (residue 3 and name H3) 5.00 2.00 1.00
assign (residue 4 and name H5) (residue 3 and name H3) 6.00 2.00 1.00
assign (residue 4 and name H5) (residue 5 and name H6) 6.00 2.00 1.00

{T5}
assign (residue 5 and name H51) (residue 5 and name H1') 6.00 2.00 1.00
assign (residue 5 and name H51) (residue 5 and name H2') 3.80 2.00 0.70
assign (residue 5 and name H51) (residue 5 and name H2'') 6.00 2.00 1.00
assign (residue 5 and name H51) (residue 5 and name H3') 6.00 2.00 1.00
assign (residue 5 and name H51) (residue 5 and name H4') 6.00 2.00 1.00
assign (residue 5 and name H51) (residue 5 and name H5') 6.00 2.00 1.00
assign (residue 5 and name H51) (residue 5 and name H5'') 6.00 2.00 1.00

```
assign (residue 5 and name H1')      (residue 5 and name H6)     3.80 2.00 0.70
assign (residue 5 and name H1')      (residue 6 and name H5)     5.00 2.00 1.00
assign (residue 5 and name H1')      (residue 6 and name H6)     3.80 2.00 0.70
assign (residue 5 and name H2')      (residue 5 and name H6)     2.50 0.70 0.50
assign (residue 5 and name H2')      (residue 6 and name H6)     3.80 2.00 0.70
assign (residue 5 and name H2'')     (residue 5 and name H6)     3.80 2.00 0.70
assign (residue 5 and name H2'')     (residue 6 and name H6)     3.80 2.00 0.70
assign (residue 5 and name H3')      (residue 5 and name H6)     3.80 2.00 0.70
assign (residue 5 and name H3')      (residue 6 and name H6)     6.00 2.00 1.00
assign (residue 5 and name H4')      (residue 5 and name H6)     5.00 2.00 1.00
assign (residue 5 and name H5')      (residue 5 and name H6)     3.80 2.00 0.70
assign (residue 5 and name H5'')     (residue 5 and name H6)     5.00 2.00 1.00
assign (residue 5 and name H6)       (residue 6 and name H5)     3.80 2.00 0.70
assign (residue 5 and name H6)       (residue 6 and name H6)     6.00 2.00 1.00
assign (residue 5 and name H3)       (residue 23 and name H1)    3.80 2.00 0.70

{C6}
assign (residue 6 and name H1')      (residue 6 and name H5)     6.00 2.00 1.00
assign (residue 6 and name H1')      (residue 6 and name H6)     3.80 2.00 0.70
assign (residue 6 and name H1')      (residue 7 and name H3')    6.00 2.00 1.00
assign (residue 6 and name H1')      (residue 7 and name H8)     3.80 2.00 0.70
assign (residue 6 and name H2')      (residue 5 and name H1')    6.00 2.00 1.00
assign (residue 6 and name H2')      (residue 6 and name H6)     2.50 0.70 0.50
assign (residue 6 and name H2')      (residue 7 and name H8)     3.80 2.00 0.70
assign (residue 6 and name H2'')     (residue 6 and name H6)     3.80 2.00 0.70
assign (residue 6 and name H2'')     (residue 7 and name H8)     3.80 2.00 0.70
assign (residue 6 and name H3')      (residue 6 and name H6)     3.80 2.00 0.70
assign (residue 6 and name H3')      (residue 7 and name H8)     5.00 2.00 1.00
assign (residue 6 and name H4')      (residue 6 and name H6)     5.00 2.00 1.00
assign (residue 6 and name H5)       (residue 5 and name H3')    6.00 2.00 1.00
assign (residue 6 and name H5)       (residue 6 and name H3')    6.00 2.00 1.00
assign (residue 6 and name H5)       (residue 7 and name H8)     6.00 2.00 1.00
assign (residue 6 and name H6)       (residue 7 and name H8)     6.00 2.00 1.00
assign (residue 6 and name H1')      (residue 5 and name H3)     6.00 2.00 1.00
assign (residue 6 and name H1')      (residue 23 and name H1)    6.00 2.00 1.00
assign (residue 6 and name H42)      (residue 22 and name H3)    6.00 2.00 1.00
assign (residue 6 and name H42)      (residue 23 and name H1)    3.80 2.00 0.70
assign (residue 6 and name H41)      (residue 5 and name H3)     3.80 2.00 0.70
assign (residue 6 and name H41)      (residue 22 and name H3)    5.00 2.00 1.00
assign (residue 6 and name H41)      (residue 23 and name H1)    2.50 0.70 0.50
assign (residue 6 and name H5)       (residue 23 and name H1)    6.00 2.00 1.00
assign (residue 6 and name H6)       (residue 23 and name H1)    6.00 2.00 1.00

{A7}
assign (residue 7 and name H1')      (residue 7 and name H2)     5.00 2.00 1.00
assign (residue 7 and name H1')      (residue 7 and name H8)     3.80 2.00 0.70
assign (residue 7 and name H1')      (residue 8 and name H51)    5.00 2.00 1.00
assign (residue 7 and name H1')      (residue 8 and name H1')    6.00 2.00 1.00
assign (residue 7 and name H1')      (residue 8 and name H6)     3.80 2.00 0.70
assign (residue 7 and name H2)       (residue 8 and name H6)     6.00 2.00 1.00
assign (residue 7 and name H2')      (residue 6 and name H1')    6.00 2.00 1.00
assign (residue 7 and name H2')      (residue 7 and name H8)     2.50 0.70 0.50
```

```
assign (residue 7 and name H2')      (residue 8 and name H51)   3.80 2.00 0.70
assign (residue 7 and name H2')      (residue 8 and name H6)    3.80 2.00 0.70
assign (residue 7 and name H2'')     (residue 6 and name H1')   6.00 2.00 1.00
assign (residue 7 and name H2'')     (residue 7 and name H8)    3.80 2.00 0.70
assign (residue 7 and name H2'')     (residue 8 and name H51)   3.80 2.00 0.70
assign (residue 7 and name H2'')     (residue 8 and name H6)    3.80 2.00 0.70
assign (residue 7 and name H3')      (residue 7 and name H8)    5.00 2.00 1.00
assign (residue 7 and name H3')      (residue 8 and name H6)    6.00 2.00 1.00
assign (residue 7 and name H4')      (residue 6 and name H1')   5.00 2.00 1.00
assign (residue 7 and name H4')      (residue 7 and name H8)    6.00 2.00 1.00
assign (residue 7 and name H5')      (residue 7 and name H8)    5.00 2.00 1.00
assign (residue 7 and name H5'')     (residue 7 and name H8)    5.00 2.00 1.00
assign (residue 7 and name H8)       (residue 8 and name H51)   5.00 2.00 1.00
assign (residue 7 and name H8)       (residue 8 and name H6)    6.00 2.00 1.00
assign (residue 7 and name H2)       (residue 22 and name H3)   2.50 0.70 0.50
assign (residue 7 and name H2)       (residue 23 and name H1)   5.00 2.00 1.00
assign (residue 7 and name H61)      (residue 22 and name H3)   2.50 0.70 0.50
assign (residue 7 and name H61)      (residue 23 and name H1)   5.00 2.00 1.00
assign (residue 7 and name H62)      (residue 22 and name H3)   3.80 2.00 0.70
assign (residue 7 and name H62)      (residue 23 and name H1)   5.00 2.00 1.00

{T8}
assign (residue 8 and name H51)      (residue 7 and name H3')   5.00 2.00 1.00
assign (residue 8 and name H51)      (residue 8 and name H1')   6.00 2.00 1.00
assign (residue 8 and name H51)      (residue 8 and name H2')   5.00 2.00 1.00
assign (residue 8 and name H51)      (residue 8 and name H2'')  6.00 2.00 1.00
assign (residue 8 and name H51)      (residue 8 and name H5')   6.00 2.00 1.00
assign (residue 8 and name H51)      (residue 8 and name H5'')  6.00 2.00 1.00
assign (residue 8 and name H51)      (residue 9 and name H8)    6.00 2.00 1.00
assign (residue 8 and name H1')      (residue 7 and name H2)    5.00 2.00 1.00
assign (residue 8 and name H1')      (residue 8 and name H6)    3.80 2.00 0.70
assign (residue 8 and name H1')      (residue 9 and name H3')   6.00 2.00 1.00
assign (residue 8 and name H1')      (residue 9 and name H8)    3.80 2.00 0.70
assign (residue 8 and name H2')      (residue 8 and name H6)    2.50 0.70 0.50
assign (residue 8 and name H2')      (residue 9 and name H8)    3.80 2.00 0.70
assign (residue 8 and name H2'')     (residue 8 and name H6)    3.80 2.00 0.70
assign (residue 8 and name H2'')     (residue 9 and name H8)    3.80 2.00 0.70
assign (residue 8 and name H4')      (residue 8 and name H6)    5.00 2.00 1.00
assign (residue 8 and name H5')      (residue 7 and name H1')   3.80 2.00 0.70
assign (residue 8 and name H5'')     (residue 7 and name H1')   5.00 2.00 1.00
assign (residue 8 and name H6)       (residue 8 and name H5')   5.00 2.00 1.00
assign (residue 8 and name H6)       (residue 8 and name H5'')  6.00 2.00 1.00
assign (residue 8 and name H6)       (residue 9 and name H8)    5.00 2.00 1.00
assign (residue 8 and name H1')      (residue 8 and name H3)    5.00 2.00 1.00
assign (residue 8 and name H3)       (residue 9 and name H1)    5.00 2.00 1.00

{G9}
assign (residue 9 and name H1')      (residue 9 and name H8)    3.80 2.00 0.70
assign (residue 9 and name H1')      (residue 10 and name H4')  5.00 2.00 1.00
assign (residue 9 and name H1')      (residue 10 and name H5')  3.80 2.00 0.70
assign (residue 9 and name H1')      (residue 10 and name H5'') 5.00 2.00 1.00
assign (residue 9 and name H1')      (residue 10 and name H8)   3.80 2.00 0.70
```

```
assign (residue 9 and name H2')      (residue 9 and name H8)     2.50 0.70 0.50
assign (residue 9 and name H2')      (residue 10 and name H8)   3.80 2.00 0.70
assign (residue 9 and name H2'')     (residue 9 and name H8)    3.80 2.00 0.70
assign (residue 9 and name H2'')     (residue 10 and name H8)   3.80 2.00 0.70
assign (residue 9 and name H3')      (residue 9 and name H8)    5.00 2.00 1.00
assign (residue 9 and name H4')      (residue 9 and name H8)    6.00 2.00 1.00
assign (residue 9 and name H5')      (residue 9 and name H8)    3.80 2.00 0.70
assign (residue 9 and name H5'')     (residue 9 and name H8)    5.00 2.00 1.00
assign (residue 9 and name H8)       (residue 10 and name H8)   5.00 2.00 1.00
assign (residue 9 and name H1')      (residue 9 and name H1)    6.00 2.00 1.00

{A10}
assign (residue 10 and name H1')     (residue 9 and name H1')   6.00 2.00 1.00
assign (residue 10 and name H1')     (residue 10 and name H2)   5.00 2.00 1.00
assign (residue 10 and name H1')     (residue 10 and name H8)   3.80 2.00 0.70
assign (residue 10 and name H1')     (residue 11 and name H51)  5.00 2.00 1.00
assign (residue 10 and name H1')     (residue 11 and name H6)   3.80 2.00 0.70
assign (residue 10 and name H2)      (residue 11 and name H6)   6.00 2.00 1.00
assign (residue 10 and name H2')     (residue 10 and name H8)   2.50 0.70 0.50
assign (residue 10 and name H2')     (residue 11 and name H51)  3.80 2.00 0.70
assign (residue 10 and name H2')     (residue 11 and name H6)   3.80 2.00 0.70
assign (residue 10 and name H2'')    (residue 10 and name H8)   3.80 2.00 0.70
assign (residue 10 and name H2'')    (residue 11 and name H51)  3.80 2.00 0.70
assign (residue 10 and name H2'')    (residue 11 and name H6)   3.80 2.00 0.70
assign (residue 10 and name H3')     (residue 10 and name H8)   5.00 2.00 1.00
assign (residue 10 and name H3')     (residue 11 and name H51)  5.00 2.00 1.00
assign (residue 10 and name H3')     (residue 11 and name H6)   6.00 2.00 1.00
assign (residue 10 and name H4')     (residue 11 and name H51)  6.00 2.00 1.00
assign (residue 10 and name H5')     (residue 10 and name H8)   5.00 2.00 1.00
assign (residue 10 and name H8)      (residue 10 and name H4')  5.00 2.00 1.00
assign (residue 10 and name H8)      (residue 10 and name H5'')  5.00 2.00 1.00
assign (residue 10 and name H8)      (residue 11 and name H51)  3.80 2.00 0.70
assign (residue 10 and name H8)      (residue 11 and name H6)   6.00 2.00 1.00
assign (residue 10 and name H2)      (residue 19 and name H3)   2.50 0.70 0.50
assign (residue 10 and name H61)     (residue 19 and name H3)   2.50 0.70 0.50
assign (residue 10 and name H62)     (residue 19 and name H3)   3.80 2.00 0.70

{T11}
assign (residue 11 and name H51)     (residue 11 and name H1')  6.00 2.00 1.00
assign (residue 11 and name H51)     (residue 11 and name H2')  5.00 2.00 1.00
assign (residue 11 and name H51)     (residue 11 and name H2'')  6.00 2.00 1.00
assign (residue 11 and name H51)     (residue 11 and name H3')  6.00 2.00 1.00
assign (residue 11 and name H51)     (residue 11 and name H4')  6.00 2.00 1.00
assign (residue 11 and name H51)     (residue 11 and name H5')  6.00 2.00 1.00
assign (residue 11 and name H51)     (residue 12 and name H8)   6.00 2.00 1.00
assign (residue 11 and name H1')     (residue 10 and name H2)   5.00 2.00 1.00
assign (residue 11 and name H1')     (residue 11 and name H6)   3.80 2.00 0.70
assign (residue 11 and name H1')     (residue 12 and name H3')  6.00 2.00 1.00
assign (residue 11 and name H1')     (residue 12 and name H4')  5.00 2.00 1.00
assign (residue 11 and name H1')     (residue 12 and name H8)   3.80 2.00 0.70
assign (residue 11 and name H2')     (residue 11 and name H6)   2.50 0.70 0.50
assign (residue 11 and name H2')     (residue 12 and name H8)   3.80 2.00 0.70
```

```
assign (residue 11 and name H2")      (residue 11 and name H6)   3.80 2.00 0.70
assign (residue 11 and name H2")      (residue 12 and name H8)   2.50 0.70 0.50
assign (residue 11 and name H4')      (residue 11 and name H6)   5.00 2.00 1.00
assign (residue 11 and name H5')      (residue 11 and name H6)   5.00 2.00 1.00
assign (residue 11 and name H5")      (residue 11 and name H6)   5.00 2.00 1.00
assign (residue 11 and name H6)       (residue 10 and name H4')  6.00 2.00 1.00
assign (residue 11 and name H6)       (residue 11 and name H3')  3.80 2.00 0.70
assign (residue 11 and name H6)       (residue 12 and name H8)   5.00 2.00 1.00
assign (residue 11 and name H1')      (residue 10 and name H2)   5.00 2.00 1.00

{A12}
assign (residue 12 and name H1')      (residue 11 and name H1')  6.00 2.00 1.00
assign (residue 12 and name H1')      (residue 12 and name H2)   5.00 2.00 1.00
assign (residue 12 and name H1')      (residue 12 and name H8)   3.80 2.00 0.70
assign (residue 12 and name H1')      (residue 13 and name H1')  5.00 2.00 1.00
assign (residue 12 and name H1')      (residue 13 and name H5)   5.00 2.00 1.00
assign (residue 12 and name H1')      (residue 13 and name H6)   3.80 2.00 0.70
assign (residue 12 and name H2)       (residue 13 and name H5)   6.00 2.00 1.00
assign (residue 12 and name H2)       (residue 13 and name H6)   6.00 2.00 1.00
assign (residue 12 and name H2)       (residue 18 and name H5)   6.00 2.00 1.00
assign (residue 12 and name H2)       (residue 18 and name H6)   6.00 2.00 1.00
assign (residue 12 and name H2')      (residue 12 and name H8)   2.50 0.70 0.50
assign (residue 12 and name H2')      (residue 13 and name H5)   3.80 2.00 0.70
assign (residue 12 and name H2')      (residue 13 and name H6)   3.80 2.00 0.70
assign (residue 12 and name H2")      (residue 12 and name H8)   3.80 2.00 0.70
assign (residue 12 and name H2")      (residue 13 and name H5)   3.80 2.00 0.70
assign (residue 12 and name H2")      (residue 13 and name H6)   3.80 2.00 0.70
assign (residue 12 and name H3')      (residue 12 and name H8)   3.80 2.00 0.70
assign (residue 12 and name H3')      (residue 13 and name H5)   6.00 2.00 1.00
assign (residue 12 and name H3')      (residue 13 and name H6)   6.00 2.00 1.00
assign (residue 12 and name H4')      (residue 12 and name H8)   6.00 2.00 1.00
assign (residue 12 and name H5')      (residue 12 and name H8)   3.80 2.00 0.70
assign (residue 12 and name H5")      (residue 12 and name H8)   5.00 2.00 1.00
assign (residue 12 and name H8)       (residue 13 and name H5)   3.80 2.00 0.70
assign (residue 12 and name H8)       (residue 13 and name H6)   5.00 2.00 1.00
assign (residue 12 and name H2)       (residue 16 and name H1)   3.80 2.00 0.70
assign (residue 12 and name H2)       (residue 17 and name H3)   2.50 0.70 0.50
assign (residue 12 and name H61)      (residue 17 and name H3)   3.80 2.00 0.70
assign (residue 12 and name H62)      (residue 17 and name H3)   5.00 2.00 1.00

{C13}
assign (residue 13 and name H1')      (residue 12 and name H2)   5.00 2.00 1.00
assign (residue 13 and name H1')      (residue 13 and name H5)   6.00 2.00 1.00
assign (residue 13 and name H1')      (residue 13 and name H6)   3.80 2.00 0.70
assign (residue 13 and name H1')      (residue 14 and name H8)   3.80 2.00 0.70
assign (residue 13 and name H2')      (residue 13 and name H5)   5.00 2.00 1.00
assign (residue 13 and name H2')      (residue 13 and name H6)   2.50 0.70 0.50
assign (residue 13 and name H2')      (residue 14 and name H8)   3.80 2.00 0.70
assign (residue 13 and name H2")      (residue 13 and name H5)   6.00 2.00 1.00
assign (residue 13 and name H2")      (residue 13 and name H6)   3.80 2.00 0.70
assign (residue 13 and name H2")      (residue 14 and name H8)   2.50 0.70 0.50
assign (residue 13 and name H4')      (residue 13 and name H5)   6.00 2.00 1.00
```

```
assign (residue 13 and name H4')      (residue 13 and name H6)    5.00 2.00 1.00
assign (residue 13 and name H5)       (residue 12 and name H4')   6.00 2.00 1.00
assign (residue 13 and name H5)       (residue 14 and name H8)    6.00 2.00 1.00
assign (residue 13 and name H5')      (residue 13 and name H6)    5.00 2.00 1.00
assign (residue 13 and name H5")      (residue 13 and name H6)    5.00 2.00 1.00
assign (residue 13 and name H6)       (residue 14 and name H8)    5.00 2.00 1.00
assign (residue 13 and name H1')      (residue 16 and name H1)    6.00 2.00 1.00
assign (residue 13 and name H3')      (residue 13 and name H6)    3.80 2.00 0.70
assign (residue 13 and name H3')      (residue 14 and name H8)    5.00 2.00 1.00
assign (residue 13 and name H41)      (residue 16 and name H1)    2.50 0.70 0.50
assign (residue 13 and name H41)      (residue 17 and name H3)    5.00 2.00 1.00
assign (residue 13 and name H42)      (residue 16 and name H1)    3.80 2.00 0.70
assign (residue 13 and name H42)      (residue 17 and name H3)    5.00 2.00 1.00
assign (residue 13 and name H42)      (residue 14 and name H1)    6.00 2.00 1.00
assign (residue 13 and name H5)       (residue 16 and name H1)    6.00 2.00 1.00
assign (residue 13 and name H6)       (residue 16 and name H1)    6.00 2.00 1.00

{G14}
assign (residue 14 and name H1')      (residue 14 and name H8)    3.80 2.00 0.70
assign (residue 14 and name H2')      (residue 14 and name H8)    2.50 0.70 0.50
assign (residue 14 and name H2")      (residue 14 and name H8)    3.80 2.00 0.70
assign (residue 14 and name H3')      (residue 14 and name H8)    5.00 2.00 1.00
assign (residue 14 and name H4')      (residue 14 and name H8)    5.00 2.00 1.00
assign (residue 14 and name H5')      (residue 14 and name H8)    3.80 2.00 0.70

{T22}
assign (residue 22 and name H1')      (residue 21 and name H2)    5.00 2.00 1.00

{C15}
assign (residue 15 and name H1')      (residue 15 and name H5)    6.00 2.00 1.00
assign (residue 15 and name H1')      (residue 15 and name H6)    3.80 2.00 0.70
assign (residue 15 and name H1')      (residue 16 and name H1')   6.00 2.00 1.00
assign (residue 15 and name H1')      (residue 16 and name H3')   6.00 2.00 1.00
assign (residue 15 and name H1')      (residue 16 and name H4')   5.00 2.00 1.00
assign (residue 15 and name H1')      (residue 16 and name H5')   3.80 2.00 0.70
assign (residue 15 and name H1')      (residue 16 and name H8)    3.80 2.00 0.70
assign (residue 15 and name H2')      (residue 15 and name H6)    2.50 0.70 0.50
assign (residue 15 and name H2')      (residue 16 and name H8)    3.80 2.00 0.70
assign (residue 15 and name H2")      (residue 15 and name H6)    3.80 2.00 0.70
assign (residue 15 and name H2")      (residue 16 and name H8)    2.50 0.70 0.50
assign (residue 15 and name H3')      (residue 15 and name H6)    3.80 2.00 0.70
assign (residue 15 and name H4')      (residue 15 and name H6)    5.00 2.00 1.00
assign (residue 15 and name H4')      (residue 16 and name H8)    6.00 2.00 1.00
assign (residue 15 and name H5)       (residue 15 and name H5')   6.00 2.00 1.00
assign (residue 15 and name H5)       (residue 16 and name H8)    6.00 2.00 1.00
assign (residue 15 and name H5')      (residue 15 and name H6)    3.80 2.00 0.70
assign (residue 15 and name H6)       (residue 16 and name H8)    5.00 2.00 1.00
assign (residue 15 and name H41)      (residue 16 and name H1)    5.00 2.00 1.00
assign (residue 15 and name H41)      (residue 13 and name H41)   3.80 2.00 0.70
assign (residue 15 and name H41)      (residue 14 and name H1)    3.80 2.00 0.70
assign (residue 15 and name H42)      (residue 16 and name H1)    6.00 2.00 1.00
assign (residue 15 and name H42)      (residue 14 and name H1)    5.00 2.00 1.00
```

```
assign (residue 15 and name H5)      (residue 14 and name H1)   6.00 2.00 1.00

{G16}
assign (residue 16 and name H1')     (residue 16 and name H8)   3.80 2.00 0.70
assign (residue 16 and name H1')     (residue 17 and name H51)  3.80 2.00 0.70
assign (residue 16 and name H1')     (residue 17 and name H6)   3.80 2.00 0.70
assign (residue 16 and name H2')     (residue 16 and name H8)   2.50 0.70 0.50
assign (residue 16 and name H2')     (residue 17 and name H51)  3.80 2.00 0.70
assign (residue 16 and name H2')     (residue 17 and name H6)   3.80 2.00 0.70
assign (residue 16 and name H2")     (residue 16 and name H8)   3.80 2.00 0.70
assign (residue 16 and name H2")     (residue 17 and name H51)  3.80 2.00 0.70
assign (residue 16 and name H2")     (residue 17 and name H6)   3.80 2.00 0.70
assign (residue 16 and name H3')     (residue 16 and name H8)   5.00 2.00 1.00
assign (residue 16 and name H3')     (residue 17 and name H51)  5.00 2.00 1.00
assign (residue 16 and name H3')     (residue 17 and name H6)   6.00 2.00 1.00
assign (residue 16 and name H4')     (residue 16 and name H8)   5.00 2.00 1.00
assign (residue 16 and name H4')     (residue 17 and name H51)  6.00 2.00 1.00
assign (residue 16 and name H5')     (residue 16 and name H8)   3.80 2.00 0.70
assign (residue 16 and name H5")     (residue 16 and name H8)   5.00 2.00 1.00
assign (residue 16 and name H8)      (residue 17 and name H51)  3.80 2.00 0.70
assign (residue 16 and name H8)      (residue 17 and name H6)   5.00 2.00 1.00
assign (residue 16 and name H1)      (residue 17 and name H3)   3.80 2.00 0.70
assign (residue 16 and name H1)      (residue 14 and name H1)   3.80 2.00 0.70

{T17}
assign (residue 17 and name H51)     (residue 17 and name H1')   6.00 2.00 1.00
assign (residue 17 and name H51)     (residue 17 and name H2')   5.00 2.00 1.00
assign (residue 17 and name H51)     (residue 17 and name H2")  6.00 2.00 1.00
assign (residue 17 and name H51)     (residue 17 and name H3')   6.00 2.00 1.00
assign (residue 17 and name H51)     (residue 17 and name H4')   6.00 2.00 1.00
assign (residue 17 and name H51)     (residue 17 and name H5')   6.00 2.00 1.00
assign (residue 17 and name H51)     (residue 18 and name H5)   5.00 2.00 1.00
assign (residue 17 and name H51)     (residue 18 and name H6)   6.00 2.00 1.00
assign (residue 17 and name H1')     (residue 17 and name H6)   3.80 2.00 0.70
assign (residue 17 and name H1')     (residue 18 and name H5)   3.80 2.00 0.70
assign (residue 17 and name H1')     (residue 18 and name H6)   3.80 2.00 0.70
assign (residue 17 and name H1')     (residue 12 and name H2)   5.00 2.00 1.00
assign (residue 17 and name H2')     (residue 16 and name H1')  5.00 2.00 1.00
assign (residue 17 and name H2')     (residue 17 and name H6)   2.50 0.70 0.50
assign (residue 17 and name H2')     (residue 18 and name H5)   3.80 2.00 0.70
assign (residue 17 and name H2')     (residue 18 and name H6)   3.80 2.00 0.70
assign (residue 17 and name H2")     (residue 17 and name H6)   3.80 2.00 0.70
assign (residue 17 and name H2")     (residue 18 and name H5)   3.80 2.00 0.70
assign (residue 17 and name H2")     (residue 18 and name H6)   3.80 2.00 0.70
assign (residue 17 and name H3')     (residue 17 and name H6)   3.80 2.00 0.70
assign (residue 17 and name H4')     (residue 17 and name H6)   5.00 2.00 1.00
assign (residue 17 and name H4')     (residue 18 and name H6)   6.00 2.00 1.00
assign (residue 17 and name H5')     (residue 17 and name H6)   5.00 2.00 1.00
assign (residue 17 and name H6)      (residue 18 and name H5)   3.80 2.00 0.70
assign (residue 17 and name H6)      (residue 18 and name H6)   5.00 2.00 1.00
assign (residue 17 and name H1')     (residue 16 and name H1)    6.00 2.00 1.0
assign (residue 17 and name H5")     (residue 17 and name H6)   5.00 2.00 1.00
```

{C18}
assign (residue 18 and name H1') (residue 18 and name H5) 6.00 2.00 1.00
assign (residue 18 and name H1') (residue 18 and name H6) 3.80 2.00 0.70
assign (residue 18 and name H1') (residue 19 and name H51) 5.00 2.00 1.00
assign (residue 18 and name H1') (residue 19 and name H6) 3.80 2.00 0.70
assign (residue 18 and name H1') (residue 19 and name H3') 6.00 2.00 1.00
assign (residue 18 and name H2') (residue 18 and name H5) 5.00 2.00 1.00
assign (residue 18 and name H2') (residue 18 and name H6) 2.50 0.70 0.50
assign (residue 18 and name H2') (residue 19 and name H51) 3.80 2.00 0.70
assign (residue 18 and name H2') (residue 19 and name H6) 3.80 2.00 0.70
assign (residue 18 and name H2") (residue 18 and name H5) 6.00 2.00 1.00
assign (residue 18 and name H2") (residue 18 and name H6) 3.80 2.00 0.70
assign (residue 18 and name H2") (residue 19 and name H51) 3.80 2.00 0.70
assign (residue 18 and name H2") (residue 19 and name H6) 3.80 2.00 0.70
assign (residue 18 and name H4') (residue 18 and name H5) 6.00 2.00 1.00
assign (residue 18 and name H4') (residue 18 and name H6) 5.00 2.00 1.00
assign (residue 18 and name H4') (residue 19 and name H6) 6.00 2.00 1.00
assign (residue 18 and name H5) (residue 17 and name H3') 6.00 2.00 1.00
assign (residue 18 and name H5) (residue 19 and name H51) 5.00 2.00 1.00
assign (residue 18 and name H5") (residue 18 and name H6) 5.00 2.00 1.00
assign (residue 18 and name H6) (residue 18 and name H3') 3.80 2.00 0.70
assign (residue 18 and name H6) (residue 19 and name H51) 3.80 2.00 0.70
assign (residue 18 and name H6) (residue 17 and name H4') 6.00 2.00 1.00
assign (residue 18 and name H6) (residue 19 and name H6) 6.00 2.00 1.00
assign (residue 18 and name H1') (residue 17 and name H3) 6.00 2.00 1.00
assign (residue 18 and name H3') (residue 19 and name H6) 3.80 2.00 0.70
assign (residue 18 and name H41) (residue 17 and name H3) 3.80 2.00 0.70
assign (residue 18 and name H41) (residue 12 and name H2) 6.00 2.00 1.00
assign (residue 18 and name H42) (residue 17 and name H3) 5.00 2.00 1.00
assign (residue 18 and name H5) (residue 17 and name H3) 6.00 2.00 1.00
assign (residue 18 and name H5) (residue 19 and name H6) 6.00 2.00 1.00

{T19}
assign (residue 19 and name H51) (residue 19 and name H1') 6.00 2.00 1.00
assign (residue 19 and name H51) (residue 19 and name H2') 3.80 2.00 0.70
assign (residue 19 and name H51) (residue 19 and name H2") 6.00 2.00 1.00
assign (residue 19 and name H51) (residue 19 and name H3') 6.00 2.00 1.00
assign (residue 19 and name H51) (residue 19 and name H4') 6.00 2.00 1.00
assign (residue 19 and name H51) (residue 19 and name H5') 6.00 2.00 1.00
assign (residue 19 and name H51) (residue 19 and name H5") 6.00 2.00 1.00
assign (residue 19 and name H1') (residue 19 and name H6) 3.80 2.00 0.70
assign (residue 19 and name H1') (residue 20 and name H5) 5.00 2.00 1.00
assign (residue 19 and name H1') (residue 20 and name H6) 3.80 2.00 0.70
assign (residue 19 and name H2') (residue 19 and name H6) 2.50 0.70 0.50
assign (residue 19 and name H2') (residue 20 and name H6) 3.80 2.00 0.70
assign (residue 19 and name H2") (residue 19 and name H6) 3.80 2.00 0.70
assign (residue 19 and name H2") (residue 20 and name H6) 3.80 2.00 0.70
assign (residue 19 and name H3') (residue 19 and name H6) 3.80 2.00 0.70
assign (residue 19 and name H3') (residue 20 and name H6) 6.00 2.00 1.00
assign (residue 19 and name H4') (residue 19 and name H6) 5.00 2.00 1.00
assign (residue 19 and name H5') (residue 19 and name H6) 3.80 2.00 0.70

```
assign (residue 19 and name H5")      (residue 19 and name H6)    5.00  2.00  1.00
assign (residue 19 and name H6)       (residue 20 and name H5)    3.80  2.00  0.70
assign (residue 19 and name H6)       (residue 20 and name H6)    6.00  2.00  1.00
assign (residue 19 and name H3)       (residue 9 and name H1)     3.80  2.00  0.70

{C20}
assign (residue 20 and name H1')      (residue 20 and name H5)    6.00  2.00  1.00
assign (residue 20 and name H1')      (residue 20 and name H6)    3.80  2.00  0.70
assign (residue 20 and name H1')      (residue 21 and name H3')   6.00  2.00  1.00
assign (residue 20 and name H1')      (residue 21 and name H8)    3.80  2.00  0.70
assign (residue 20 and name H2')      (residue 19 and name H1')   6.00  2.00  1.00
assign (residue 20 and name H2')      (residue 20 and name H6)    2.50  0.70  0.50
assign (residue 20 and name H2')      (residue 21 and name H8)    3.80  2.00  0.70
assign (residue 20 and name H2")      (residue 20 and name H6)    3.80  2.00  0.70
assign (residue 20 and name H2")      (residue 21 and name H8)    3.80  2.00  0.70
assign (residue 20 and name H3')      (residue 20 and name H6)    3.80  2.00  0.70
assign (residue 20 and name H3')      (residue 21 and name H8)    5.00  2.00  1.00
assign (residue 20 and name H4')      (residue 20 and name H6)    5.00  2.00  1.00
assign (residue 20 and name H5)       (residue 19 and name H3')   6.00  2.00  1.00
assign (residue 20 and name H5)       (residue 20 and name H3')   6.00  2.00  1.00
assign (residue 20 and name H5)       (residue 21 and name H8)    6.00  2.00  1.00
assign (residue 20 and name H6)       (residue 21 and name H8)    6.00  2.00  1.00
assign (residue 20 and name H1')      (residue 19 and name H3)    6.00  2.00  1.00
assign (residue 20 and name H1')      (residue 9 and name H1)     6.00  2.00  1.00
assign (residue 20 and name H42)      (residue 8 and name H3)     6.00  2.00  1.00
assign (residue 20 and name H42)      (residue 9 and name H1)     3.80  2.00  0.70
assign (residue 20 and name H41)      (residue 19 and name H3)    3.80  2.00  0.70
assign (residue 20 and name H41)      (residue 8 and name H3)     5.00  2.00  1.00
assign (residue 20 and name H41)      (residue 9 and name H1)     2.50  0.70  0.50
assign (residue 20 and name H5)       (residue 9 and name H1)     6.00  2.00  1.00
assign (residue 20 and name H6)       (residue 9 and name H1)     6.00  2.00  1.00


{A21}
assign (residue 21 and name H1')      (residue 21 and name H2)    5.00  2.00  1.00
assign (residue 21 and name H1')      (residue 21 and name H8)    3.80  2.00  0.70
assign (residue 21 and name H1')      (residue 22 and name H51)   5.00  2.00  1.00
assign (residue 21 and name H1')      (residue 22 and name H1')   6.00  2.00  1.00
assign (residue 21 and name H1')      (residue 22 and name H6)    3.80  2.00  0.70
assign (residue 21 and name H2)       (residue 22 and name H6)    6.00  2.00  1.00
assign (residue 21 and name H2')      (residue 20 and name H1')   6.00  2.00  1.00
assign (residue 21 and name H2')      (residue 21 and name H8)    2.50  0.70  0.50
assign (residue 21 and name H2')      (residue 22 and name H51)   3.80  2.00  0.70
assign (residue 21 and name H2')      (residue 22 and name H6)    3.80  2.00  0.70
assign (residue 21 and name H2")      (residue 20 and name H1')   6.00  2.00  1.00
assign (residue 21 and name H2")      (residue 21 and name H8)    3.80  2.00  0.70
assign (residue 21 and name H2")      (residue 22 and name H51)   3.80  2.00  0.70
assign (residue 21 and name H2")      (residue 22 and name H6)    3.80  2.00  0.70
assign (residue 21 and name H3')      (residue 21 and name H8)    5.00  2.00  1.00
assign (residue 21 and name H3')      (residue 22 and name H6)    6.00  2.00  1.00
assign (residue 21 and name H4')      (residue 20 and name H1')   5.00  2.00  1.00
assign (residue 21 and name H4')      (residue 21 and name H8)    6.00  2.00  1.00
```

assign (residue 21 and name H5') (residue 21 and name H8) 5.00 2.00 1.00
assign (residue 21 and name H5'') (residue 21 and name H8) 5.00 2.00 1.00
assign (residue 21 and name H8) (residue 22 and name H51) 5.00 2.00 1.00
assign (residue 21 and name H8) (residue 22 and name H6) 6.00 2.00 1.00
assign (residue 21 and name H2) (residue 8 and name H3) 2.50 0.70 0.50
assign (residue 21 and name H2) (residue 9 and name H1) 5.00 2.00 1.00
assign (residue 21 and name H61) (residue 8 and name H3) 2.50 0.70 0.50
assign (residue 21 and name H61) (residue 9 and name H1) 5.00 2.00 1.00
assign (residue 21 and name H62) (residue 8 and name H3) 3.80 2.00 0.70
assign (residue 21 and name H62) (residue 9 and name H1) 5.00 2.00 1.00

{T22}
assign (residue 22 and name H51) (residue 21 and name H3') 5.00 2.00 1.00
assign (residue 22 and name H51) (residue 22 and name H1') 6.00 2.00 1.00
assign (residue 22 and name H51) (residue 22 and name H2') 5.00 2.00 1.00
assign (residue 22 and name H51) (residue 22 and name H2'') 6.00 2.00 1.00
assign (residue 22 and name H51) (residue 22 and name H5') 6.00 2.00 1.00
assign (residue 22 and name H51) (residue 22 and name H5'') 6.00 2.00 1.00
assign (residue 22 and name H51) (residue 23 and name H8) 6.00 2.00 1.00
assign (residue 22 and name H1') (residue 21 and name H2) 5.00 2.00 1.00
assign (residue 22 and name H1') (residue 22 and name H6) 3.80 2.00 0.70
assign (residue 22 and name H1') (residue 23 and name H3') 6.00 2.00 1.00
assign (residue 22 and name H1') (residue 23 and name H8) 3.80 2.00 0.70
assign (residue 22 and name H2') (residue 22 and name H6) 2.50 0.70 0.50
assign (residue 22 and name H2') (residue 23 and name H8) 3.80 2.00 0.70
assign (residue 22 and name H2'') (residue 22 and name H6) 3.80 2.00 0.70
assign (residue 22 and name H2'') (residue 23 and name H8) 3.80 2.00 0.70
assign (residue 22 and name H4') (residue 22 and name H6) 5.00 2.00 1.00
assign (residue 22 and name H5') (residue 21 and name H1') 3.80 2.00 0.70
assign (residue 22 and name H5'') (residue 21 and name H1') 5.00 2.00 1.00
assign (residue 22 and name H6) (residue 22 and name H5') 5.00 2.00 1.00
assign (residue 22 and name H6) (residue 22 and name H5'') 6.00 2.00 1.00
assign (residue 22 and name H6) (residue 23 and name H8) 5.00 2.00 1.00
assign (residue 22 and name H1') (residue 22 and name H3) 5.00 2.00 1.00
assign (residue 22 and name H3) (residue 23 and name H1) 5.00 2.00 1.00

{G23}
assign (residue 23 and name H1') (residue 23 and name H8) 3.80 2.00 0.70
assign (residue 23 and name H1') (residue 24 and name H4') 5.00 2.00 1.00
assign (residue 23 and name H1') (residue 24 and name H5') 3.80 2.00 0.70
assign (residue 23 and name H1') (residue 24 and name H5'') 5.00 2.00 1.00
assign (residue 23 and name H1') (residue 24 and name H8) 3.80 2.00 0.70
assign (residue 23 and name H2') (residue 23 and name H8) 2.50 0.70 0.50
assign (residue 23 and name H2') (residue 24 and name H8) 3.80 2.00 0.70
assign (residue 23 and name H2'') (residue 23 and name H8) 3.80 2.00 0.70
assign (residue 23 and name H2'') (residue 24 and name H8) 3.80 2.00 0.70
assign (residue 23 and name H3') (residue 23 and name H8) 5.00 2.00 1.00
assign (residue 23 and name H4') (residue 23 and name H8) 6.00 2.00 1.00
assign (residue 23 and name H5') (residue 23 and name H8) 3.80 2.00 0.70
assign (residue 23 and name H5'') (residue 23 and name H8) 5.00 2.00 1.00
assign (residue 23 and name H8) (residue 24 and name H8) 5.00 2.00 1.00
assign (residue 23 and name H1') (residue 23 and name H1) 6.00 2.00 1.00

{A24}
assign (residue 24 and name H1') (residue 23 and name H1') 6.00 2.00 1.00
assign (residue 24 and name H1') (residue 24 and name H2) 5.00 2.00 1.00
assign (residue 24 and name H1') (residue 24 and name H8) 3.80 2.00 0.70
assign (residue 24 and name H1') (residue 25 and name H51) 5.00 2.00 1.00
assign (residue 24 and name H1') (residue 25 and name H6) 3.80 2.00 0.70
assign (residue 24 and name H2) (residue 25 and name H6) 6.00 2.00 1.00
assign (residue 24 and name H2') (residue 24 and name H8) 2.50 0.70 0.50
assign (residue 24 and name H2') (residue 25 and name H51) 3.80 2.00 0.70
assign (residue 24 and name H2') (residue 25 and name H6) 3.80 2.00 0.70
assign (residue 24 and name H2") (residue 24 and name H8) 3.80 2.00 0.70
assign (residue 24 and name H2") (residue 25 and name H51) 3.80 2.00 0.70
assign (residue 24 and name H2") (residue 25 and name H6) 3.80 2.00 0.70
assign (residue 24 and name H3') (residue 24 and name H8) 5.00 2.00 1.00
assign (residue 24 and name H3') (residue 25 and name H51) 5.00 2.00 1.00
assign (residue 24 and name H3') (residue 25 and name H6) 6.00 2.00 1.00
assign (residue 24 and name H4') (residue 25 and name H51) 6.00 2.00 1.00
assign (residue 24 and name H5') (residue 24 and name H8) 5.00 2.00 1.00
assign (residue 24 and name H8) (residue 24 and name H4') 5.00 2.00 1.00
assign (residue 24 and name H8) (residue 24 and name H5") 5.00 2.00 1.00
assign (residue 24 and name H8) (residue 25 and name H51) 3.80 2.00 0.70
assign (residue 24 and name H8) (residue 25 and name H6) 6.00 2.00 1.00
assign (residue 24 and name H2) (residue 5 and name H3) 2.50 0.70 0.50
assign (residue 24 and name H61) (residue 5 and name H3) 2.50 0.70 0.50
assign (residue 24 and name H62) (residue 5 and name H3) 3.80 2.00 0.70

{T25}
assign (residue 25 and name H51) (residue 25 and name H1') 6.00 2.00 1.00
assign (residue 25 and name H51) (residue 25 and name H2') 5.00 2.00 1.00
assign (residue 25 and name H51) (residue 25 and name H2") 6.00 2.00 1.00
assign (residue 25 and name H51) (residue 25 and name H3') 6.00 2.00 1.00
assign (residue 25 and name H51) (residue 25 and name H4') 6.00 2.00 1.00
assign (residue 25 and name H51) (residue 25 and name H5') 6.00 2.00 1.00
assign (residue 25 and name H51) (residue 26 and name H8) 6.00 2.00 1.00
assign (residue 25 and name H1') (residue 24 and name H2) 5.00 2.00 1.00
assign (residue 25 and name H1') (residue 25 and name H6) 3.80 2.00 0.70
assign (residue 25 and name H1') (residue 26 and name H3') 6.00 2.00 1.00
assign (residue 25 and name H1') (residue 26 and name H4') 5.00 2.00 1.00
assign (residue 25 and name H1') (residue 26 and name H8) 3.80 2.00 0.70
assign (residue 25 and name H2') (residue 25 and name H6) 2.50 0.70 0.50
assign (residue 25 and name H2') (residue 26 and name H8) 3.80 2.00 0.70
assign (residue 25 and name H2") (residue 25 and name H6) 3.80 2.00 0.70
assign (residue 25 and name H2") (residue 26 and name H8) 2.50 0.70 0.50
assign (residue 25 and name H4') (residue 25 and name H6) 5.00 2.00 1.00
assign (residue 25 and name H5') (residue 25 and name H6) 5.00 2.00 1.00
assign (residue 25 and name H5") (residue 25 and name H6) 5.00 2.00 1.00
assign (residue 25 and name H6) (residue 24 and name H4') 6.00 2.00 1.00
assign (residue 25 and name H6) (residue 25 and name H3') 3.80 2.00 0.70
assign (residue 25 and name H6) (residue 26 and name H8) 5.00 2.00 1.00
assign (residue 25 and name H1') (residue 24 and name H2) 5.00 2.00 1.00

{A26}

assign (residue 26 and name H1') (residue 25 and name H1') 6.00 2.00 1.00
assign (residue 26 and name H1') (residue 26 and name H2) 5.00 2.00 1.00
assign (residue 26 and name H1') (residue 26 and name H8) 3.80 2.00 0.70
assign (residue 26 and name H1') (residue 27 and name H1') 5.00 2.00 1.00
assign (residue 26 and name H1') (residue 27 and name H5) 5.00 2.00 1.00
assign (residue 26 and name H1') (residue 27 and name H6) 3.80 2.00 0.70
assign (residue 26 and name H2) (residue 27 and name H5) 6.00 2.00 1.00
assign (residue 26 and name H2) (residue 27 and name H6) 6.00 2.00 1.00
assign (residue 26 and name H2) (residue 4 and name H5) 6.00 2.00 1.00
assign (residue 26 and name H2) (residue 4 and name H6) 6.00 2.00 1.00
assign (residue 26 and name H2') (residue 26 and name H8) 2.50 0.70 0.50
assign (residue 26 and name H2') (residue 27 and name H5) 3.80 2.00 0.70
assign (residue 26 and name H2') (residue 27 and name H6) 3.80 2.00 0.70
assign (residue 26 and name H2") (residue 26 and name H8) 3.80 2.00 0.70
assign (residue 26 and name H2") (residue 27 and name H5) 3.80 2.00 0.70
assign (residue 26 and name H2") (residue 27 and name H6) 3.80 2.00 0.70
assign (residue 26 and name H3') (residue 26 and name H8) 3.80 2.00 0.70
assign (residue 26 and name H3') (residue 27 and name H5) 6.00 2.00 1.00
assign (residue 26 and name H3') (residue 27 and name H6) 6.00 2.00 1.00
assign (residue 26 and name H4') (residue 26 and name H8) 6.00 2.00 1.00
assign (residue 26 and name H5') (residue 26 and name H8) 3.80 2.00 0.70
assign (residue 26 and name H5") (residue 26 and name H8) 5.00 2.00 1.00
assign (residue 26 and name H8) (residue 27 and name H5) 3.80 2.00 0.70
assign (residue 26 and name H8) (residue 27 and name H6) 5.00 2.00 1.00
assign (residue 26 and name H2) (residue 2 and name H1) 3.80 2.00 0.70
assign (residue 26 and name H2) (residue 3 and name H3) 2.50 0.70 0.50
assign (residue 26 and name H61) (residue 3 and name H3) 3.80 2.00 0.70
assign (residue 26 and name H62) (residue 3 and name H3) 5.00 2.00 1.00

{C27}

assign (residue 27 and name H1') (residue 26 and name H2) 5.00 2.00 1.00
assign (residue 27 and name H1') (residue 27 and name H5) 6.00 2.00 1.00
assign (residue 27 and name H1') (residue 27 and name H6) 3.80 2.00 0.70
assign (residue 27 and name H1') (residue 28 and name H8) 3.80 2.00 0.70
assign (residue 27 and name H2') (residue 27 and name H5) 5.00 2.00 1.00
assign (residue 27 and name H2') (residue 27 and name H6) 2.50 0.70 0.50
assign (residue 27 and name H2') (residue 28 and name H8) 3.80 2.00 0.70
assign (residue 27 and name H2") (residue 27 and name H5) 6.00 2.00 1.00
assign (residue 27 and name H2") (residue 27 and name H6) 3.80 2.00 0.70
assign (residue 27 and name H2") (residue 28 and name H8) 2.50 0.70 0.50
assign (residue 27 and name H4') (residue 27 and name H5) 6.00 2.00 1.00
assign (residue 27 and name H4') (residue 27 and name H6) 5.00 2.00 1.00
assign (residue 27 and name H5) (residue 26 and name H4') 6.00 2.00 1.00
assign (residue 27 and name H5) (residue 28 and name H8) 6.00 2.00 1.00
assign (residue 27 and name H5') (residue 27 and name H6) 5.00 2.00 1.00
assign (residue 27 and name H5") (residue 27 and name H6) 5.00 2.00 1.00
assign (residue 27 and name H6) (residue 28 and name H8) 5.00 2.00 1.00
assign (residue 27 and name H1') (residue 2 and name H1) 6.00 2.00 1.00
assign (residue 27 and name H3') (residue 27 and name H6) 3.80 2.00 0.70
assign (residue 27 and name H3') (residue 28 and name H8) 5.00 2.00 1.00
assign (residue 27 and name H41) (residue 2 and name H1) 2.50 0.70 0.50

```
assign (residue 27 and name H41)     (residue 3 and name H3)     5.00  2.00  1.00
assign (residue 27 and name H42)     (residue 2 and name H1)     3.80  2.00  0.70
assign (residue 27 and name H42)     (residue 3 and name H3)     5.00  2.00  1.00
assign (residue 27 and name H42)     (residue 28 and name H1)    6.00  2.00  1.00
assign (residue 27 and name H5)      (residue 2 and name H1)     6.00  2.00  1.00
assign (residue 27 and name H6)      (residue 2 and name H1)     6.00  2.00  1.00

{G28}
assign (residue 28 and name H1')     (residue 28 and name H8)    3.80  2.00  0.70
assign (residue 28 and name H2')     (residue 28 and name H8)    2.50  0.70  0.50
assign (residue 28 and name H2'')    (residue 28 and name H8)    3.80  2.00  0.70
assign (residue 28 and name H3')     (residue 28 and name H8)    5.00  2.00  1.00
assign (residue 28 and name H4')     (residue 28 and name H8)    5.00  2.00  1.00
assign (residue 28 and name H5')     (residue 28 and name H8)    3.80  2.00  0.70

{T8}
assign (residue 8 and name H1')      (residue 7 and name H2)     5.00  2.00  1.00


!-------------------------------------------------------------------------------
```

H-bond for base pair fix

```
{C1-G28}
{GUA28}                {CYT1}
assign (resid 28 and name H1)        (resid 1 and name N3)      1.90 0.20 0.20
assign (resid 28 and name N1)        (resid 1 and name N3)      2.90 0.30 0.30
assign (resid 28 and name O6)        (resid 1 and name H41)     2.00 0.20 0.20
assign (resid 28 and name O6)        (resid 1 and name N4)      2.90 0.30 0.30
assign (resid 28 and name H21)       (resid 1 and name O2)      2.00 0.20 0.20
assign (resid 28 and name N2)        (resid 1 and name O2)      2.90 0.30 0.30

{G2-C27}
{GUA2}                 {CYT27}
assign (resid 2 and name H1)         (resid 27 and name N3)     1.90 0.20 0.20
assign (resid 2 and name N1)         (resid 27 and name N3)     2.90 0.30 0.30
assign (resid 2 and name O6)         (resid 27 and name H41)    2.00 0.20 0.20
assign (resid 2 and name O6)         (resid 27 and name N4)     2.90 0.30 0.30
assign (resid 2 and name H21)        (resid 27 and name O2)     2.00 0.20 0.20
assign (resid 2 and name N2)         (resid 27 and name O2)     2.90 0.30 0.30


{T3-A26}
{THY3}                 {ADE26}
assi (resi 3 and name  H3)           (resi 26  and name  N1)    1.90 0.10 0.10
assi (resi 3 and name  N3)           (resi 26  and name  N1)    2.90 0.10 0.10
assi (resi 3 and name  O4)           (resi 26  and name  H61    1.90 0.10 0.10
assi (resi 3 and name  O4)           (resi 26  and name  N6)    2.90 0.10 0.10

{C+4-T+25}
{THY+25}               {CYT+4}
```

```
assi (resi 25 and name  N3)          (resi 4  and name  N3)      4.10 0.30 0.30

{T5-A24}
{THY5}              {ADE24}
assi (resi 5 and name  H3)           (resi 24  and name  N1)     1.90 0.10 0.10
assi (resi 5 and name  N3)           (resi 24  and name  N1)     2.90 0.10 0.10
assi (resi 5 and name  O4)           (resi 24  and name  H61)    1.90 0.10 0.10
assi (resi 5 and name  O4)           (resi 24  and name  N6)     2.90 0.10 0.10

{C6-G23}
{GUA23}               {CYT6}
assign (resid 23 and name H1)        (resid 6 and name N3)       1.90 0.20 0.20
assign (resid 23 and name N1)        (resid 6 and name N3)       2.90 0.30 0.30
assign (resid 23 and name O6)        (resid 6 and name H41)      2.00 0.20 0.20
assign (resid 23 and name O6)        (resid 6 and name N4)       2.90 0.30 0.30
assign (resid 23 and name H21)       (resid 6 and name O2)       2.00 0.20 0.20
assign (resid 23 and name N2)        (resid 6 and name O2)       2.90 0.30 0.30

{A7-T22}
{THY22}             {ADE7}
assi (resi 22 and name  H3)          (resi 7  and name  N1)      1.90 0.10 0.10
assi (resi 22 and name  N3)          (resi 7  and name  N1)      2.90 0.10 0.10
assi (resi 22 and name  O4)          (resi 7  and name  H61)     1.90 0.10 0.10
assi (resi 22 and name  O4)          (resi 7  and name  N6)      2.90 0.10 0.10

{T8-A21}
{THY8}              {ADE21}
assi (resi 8 and name  H3)           (resi 21  and name  N1)     1.90 0.10 0.10
assi (resi 8 and name  N3)           (resi 21  and name  N1)     2.90 0.10 0.10
assi (resi 8 and name  O4)           (resi 21  and name  H61)    1.90 0.10 0.10
assi (resi 8 and name  O4)           (resi 21  and name  N6)     2.90 0.10 0.10

{G9-C20}
{GUA9}               {CYT20}
assign (resid 9 and name H1)         (resid 20 and name N3)      1.90 0.20 0.20
assign (resid 9 and name N1)         (resid 20 and name N3)      2.90 0.30 0.30
assign (resid 9 and name O6)         (resid 20 and name H41)     2.00 0.20 0.20
assign (resid 9 and name O6)         (resid 20 and name N4)      2.90 0.30 0.30
assign (resid 9 and name H21)        (resid 20 and name O2)      2.00 0.20 0.20
assign (resid 9 and name N2)         (resid 20 and name O2)      2.90 0.30 0.30

{A10-T19}
{THY19}             {ADE10}
assi (resi 19 and name  H3)          (resi 10  and name  N1)     1.90 0.10 0.10
assi (resi 19 and name  N3)          (resi 10  and name  N1)     2.90 0.10 0.10
assi (resi 19 and name  O4)          (resi 10  and name  H61)    1.90 0.10 0.10
assi (resi 19 and name  O4)          (resi 10  and name  N6)     2.90 0.10 0.10

{T+11-C+18}
{THY+11}            {CYT+18}
assi (resi 11 and name  N3)          (resi 18  and name  N3)     4.10 0.30 0.30
```

{A12-T17}
{THY17} {ADE12}
assi (resi 17 and name H3) (resi 12 and name N1) 1.90 0.10 0.10
assi (resi 17 and name N3) (resi 12 and name N1) 2.90 0.10 0.10
assi (resi 17 and name O4) (resi 12 and name H61) 1.90 0.10 0.10
assi (resi 17 and name O4) (resi 12 and name N6) 2.90 0.10 0.10

{C13-G16}
{GUA16} {CYT13}
assign (resid 16 and name H1) (resid 13 and name N3) 1.90 0.20 0.20
assign (resid 16 and name N1) (resid 13 and name N3) 2.90 0.30 0.30
assign (resid 16 and name O6) (resid 13 and name H41) 2.00 0.20 0.20
assign (resid 16 and name O6) (resid 13 and name N4) 2.90 0.30 0.30
assign (resid 16 and name H21) (resid 13 and name O2) 2.00 0.20 0.20
assign (resid 16 and name N2) (resid 13 and name O2) 2.90 0.30 0.30

{G14-C15}
{GUA14} {CYT15}
assign (resid 14 and name H1) (resid 15 and name N3) 1.90 0.20 0.20
assign (resid 14 and name N1) (resid 15 and name N3) 2.90 0.30 0.30
assign (resid 14 and name O6) (resid 15 and name H41) 2.00 0.20 0.20
assign (resid 14 and name O6) (resid 15 and name N4) 2.90 0.30 0.30
assign (resid 14 and name H21) (resid 15 and name O2) 2.00 0.20 0.20
assign (resid 14 and name N2) (resid 15 and name O2) 2.90 0.30 0.30

!---

Angles for sugar puckering

```
restraints dihedral
        nassign=1000

 for $1 in (

{====>}   {* Select nucleotides to be restrained. *}

 1 2 3 5 6 7 8 9 10 12 13 14 15 16 17 19 20 21 22 23 24 26
27 28
        ) loop dihe

  evaluate($a=$1+1)
  evaluate($b=$1-1)

  assign  ( resid $b and name O3' )
            ( resid $1 and name P )
            ( resid $1 and name O5' )
    ( resid $1 and name C5' ) 50.0  -70.0 20.0 2 {* alpha *}

  assign  ( resid $1 and name P )
            ( resid $1 and name O5' )
            ( resid $1 and name C5' )
    ( resid $1 and name C4' ) 50.0  180.0 20.0 2 {* beta *}

  assign  ( resid $1 and name O5' )
            ( resid $1 and name C5' )
            ( resid $1 and name C4' )
  ( resid $1 and name C3' ) 50.0   60.0 20.0 2 {* gamma *}

  assign  ( resid $1 and name c5' )
            ( resid $1 and name c4' )
            ( resid $1 and name c3' )
    ( resid $1 and name o3' ) 50.0  140.0 25.0 2 {* delta *}

  assign  ( resid $1 and name c4' )
            ( resid $1 and name c3' )
            ( resid $1 and name o3' )
  ( resid $a and name P )   50.0 -170.0 20.0 2 {* epsilon *}

  assign  ( resid $1 and name C3' )
            ( resid $1 and name O3' )
            ( resid $a and name P )
      ( resid $a and name O5' ) 50.0  -85.0 20.0 2 {* zeta *}


 end loop dihe

 for $1 in (

{====>}                  {* Select purines to be restrained.
*}

 2 7 9 10 12 14 16 21 23 24 26 28
        ) loop dihe

   assign  ( resid $1 and name O4' )
             ( resid $1 and name C1' )
             ( resid $1 and name N9 )
         ( resid $1 and name C4 ) 50.0 -120.0 20.0 2 {* chi *}

end loop dihe


 for $1 in (

{====>}                  {* Select pyrimidines to be
restrained. *}

 1 3 5 6 8 13 15 17 19 20 22 27
        ) loop dihe

 assign  ( resid $1 and name O4' )
           ( resid $1 and name C1' )
           ( resid $1 and name N1 )
     ( resid $1 and name C2 ) 50.0 -120.00 20.0 2 {* chi *}

end loop dihe


!---------------------------------------------------------------------
```

Restraints plane

```
group
select= ((resid 28 and (name n1 or name c6 or name c2))
or
        (resid 1 and (name n3)))
 weight=20.0
 end

group
select= ((resid 2 and (name n1 or name c6 or name c2))
or
        (resid 27 and (name n3)))
 weight=20.0
 end

group
select= ((resid 26 and (name n1 or name c6 or name c2))
or
        (resid 3 and (name n3)))
 weight=50.0
 end

group
select= ((resid 24 and (name n1 or name c6 or name c2))
or
        (resid 5 and (name n3)))
 weight=30.0
 end

group
select= ((resid 23 and (name n1 or name c6 or name c2))
or
        (resid 6 and (name n3)))
 weight=50.0
 end

group
select= ((resid 7 and (name n1 or name c6 or name c2))
or
        (resid 22 and (name n3)))
 weight=50.0
 end

group
select= ((resid 21 and (name n1 or name c6 or name c2))
or
        (resid 8 and (name n3)))
 weight=50.0
 end

group
select= ((resid 9 and (name n1 or name c6 or name c2))
or
        (resid 20 and (name n3)))
 weight=50.0
 end

group
select= ((resid 10 and (name n1 or name c6 or name c2))
or
        (resid 19 and (name n3)))
 weight=30.0
 end

group
select= ((resid 12 and (name n1 or name c6 or name c2))
or
        (resid 17 and (name n3)))
 weight=50.0
 end

group
select= ((resid 16 and (name n1 or name c6 or name c2))
or
        (resid 13 and (name n3)))
 weight=20.0
 end

group
select= ((resid 14 and (name n1 or name c6 or name c2))
or
        (resid 15 and (name n3)))
 weight=20.0
 end

group
select= ((resid 28 and (name n1)) or
        (resid 1 and (name n3 or name c2 or name c4)))
 weight=20.0
 end

group
select= ((resid 2 and (name n1)) or
        (resid 27 and (name n3 or name c2 or name c4)))
 weight=20.0
 end

group
select= ((resid 26 and (name n1)) or
        (resid 3 and (name n3 or name c2 or name c4)))
 weight=50.0
 end
```

```
group
select= ((resid 24 and (name n1)) or
         (resid 5 and (name n3 or name c2 or name c4)))
 weight=30.0
 end

group
select= ((resid 23 and (name n1)) or
         (resid 6 and (name n3 or name c2 or name c4)))
 weight=50.0
 end

group
select= ((resid 7 and (name n1)) or
         (resid 22 and (name n3 or name c2 or name c4)))
 weight=50.0
 end

group
select= ((resid 21 and (name n1)) or
         (resid 8 and (name n3 or name c2 or name c4)))
 weight=50.0
 end

group
select= ((resid 9 and (name n1)) or
         (resid 20 and (name n3 or name c2 or name c4)))
 weight=50.0
 end

group
select= ((resid 10 and (name n1)) or
         (resid 19 and (name n3 or name c2 or name c4)))
 weight=30.0
 end

group
select= ((resid 12 and (name n1)) or
         (resid 17 and (name n3 or name c2 or name c4)))
 weight=50.0
 end

group
select= ((resid 16 and (name n1)) or
         (resid 13 and (name n3 or name c2 or name c4)))
 weight=20.0
 end

group
select= ((resid 14 and (name n1)) or
         (resid 15 and (name n3 or name c2 or name c4)))
 weight=20.0
 end

end
!------------------------------------------------------------------------------
```

MINOR DUPLEX

NOE constraints

{C1}

```
assign (residue 1 and name H1')      (residue 1 and name H5)      6.00 2.00 1.00
assign (residue 1 and name H1')      (residue 1 and name H6)      3.80 2.00 0.70
assign (residue 1 and name H1')      (residue 2 and name H1')     6.00 2.00 1.00
assign (residue 1 and name H1')      (residue 2 and name H3')     6.00 2.00 1.00
assign (residue 1 and name H1')      (residue 2 and name H4')     5.00 2.00 1.00
assign (residue 1 and name H1')      (residue 2 and name H5')     3.80 2.00 0.70
assign (residue 1 and name H1')      (residue 2 and name H8)      3.80 2.00 0.70
assign (residue 1 and name H2')      (residue 1 and name H6)      2.50 0.70 0.50
assign (residue 1 and name H2')      (residue 2 and name H8)      3.80 2.00 0.70
assign (residue 1 and name H2'')     (residue 1 and name H6)      3.80 2.00 0.70
assign (residue 1 and name H2'')     (residue 2 and name H8)      2.50 0.70 0.50
assign (residue 1 and name H3')      (residue 1 and name H6)      3.80 2.00 0.70
assign (residue 1 and name H4')      (residue 1 and name H6)      5.00 2.00 1.00
assign (residue 1 and name H4')      (residue 2 and name H8)      6.00 2.00 1.00
assign (residue 1 and name H5)       (residue 1 and name H5')     6.00 2.00 1.00
assign (residue 1 and name H5)       (residue 2 and name H8)      6.00 2.00 1.00
assign (residue 1 and name H5')      (residue 1 and name H6)      3.80 2.00 0.70
assign (residue 1 and name H6)       (residue 2 and name H8)      5.00 2.00 1.00
assign (residue 1 and name H41)      (residue 2 and name H1)      5.00 2.00 1.00
assign (residue 1 and name H41)      (residue 27 and name H41)    3.80 2.00 0.70
assign (residue 1 and name H41)      (residue 28 and name H1)     3.80 2.00 0.70
assign (residue 1 and name H42)      (residue 2 and name H1)      6.00 2.00 1.00
assign (residue 1 and name H42)      (residue 28 and name H1)     5.00 2.00 1.00
assign (residue 1 and name H5)       (residue 28 and name H1)     6.00 2.00 1.00
```

{G2}

```
assign (residue 2 and name H1')      (residue 2 and name H8)      3.80 2.00 0.70
assign (residue 2 and name H1')      (residue 3 and name H51)     3.80 2.00 0.70
assign (residue 2 and name H1')      (residue 3 and name H6)      3.80 2.00 0.70
assign (residue 2 and name H2')      (residue 2 and name H8)      2.50 0.70 0.50
assign (residue 2 and name H2')      (residue 3 and name H51)     3.80 2.00 0.70
assign (residue 2 and name H2')      (residue 3 and name H6)      3.80 2.00 0.70
assign (residue 2 and name H2'')     (residue 2 and name H8)      3.80 2.00 0.70
assign (residue 2 and name H2'')     (residue 3 and name H51)     3.80 2.00 0.70
assign (residue 2 and name H2'')     (residue 3 and name H6)      3.80 2.00 0.70
assign (residue 2 and name H3')      (residue 2 and name H8)      5.00 2.00 1.00
assign (residue 2 and name H3')      (residue 3 and name H51)     5.00 2.00 1.00
assign (residue 2 and name H3')      (residue 3 and name H6)      6.00 2.00 1.00
assign (residue 2 and name H4')      (residue 2 and name H8)      5.00 2.00 1.00
assign (residue 2 and name H4')      (residue 3 and name H51)     6.00 2.00 1.00
assign (residue 2 and name H5')      (residue 2 and name H8)      3.80 2.00 0.70
assign (residue 2 and name H5'')     (residue 2 and name H8)      5.00 2.00 1.00
assign (residue 2 and name H8)       (residue 3 and name H51)     3.80 2.00 0.70
assign (residue 2 and name H8)       (residue 3 and name H6)      5.00 2.00 1.00
assign (residue 2 and name H1)       (residue 3 and name H3)      3.80 2.00 0.70
```

```
assign (residue 2 and name H1)      (residue 28 and name H1)    3.80 2.00 0.70

{T3}
assign (residue 3 and name H51)     (residue 3 and name H1')    6.00 2.00 1.00
assign (residue 3 and name H51)     (residue 3 and name H2')    5.00 2.00 1.00
assign (residue 3 and name H51)     (residue 3 and name H2'')   6.00 2.00 1.00
assign (residue 3 and name H51)     (residue 3 and name H3')    6.00 2.00 1.00
assign (residue 3 and name H51)     (residue 3 and name H4')    6.00 2.00 1.00
assign (residue 3 and name H51)     (residue 3 and name H5')    6.00 2.00 1.00
assign (residue 3 and name H51)     (residue 4 and name H5)     5.00 2.00 1.00
assign (residue 3 and name H51)     (residue 4 and name H6)     6.00 2.00 1.00
assign (residue 3 and name H1')     (residue 3 and name H6)     3.80 2.00 0.70
assign (residue 3 and name H1')     (residue 4 and name H5)     3.80 2.00 0.70
assign (residue 3 and name H1')     (residue 4 and name H6)     3.80 2.00 0.70
assign (residue 3 and name H1')     (residue 26 and name H2)    5.00 2.00 1.00
assign (residue 3 and name H2')     (residue 2 and name H1')    5.00 2.00 1.00
assign (residue 3 and name H2')     (residue 3 and name H6)     2.50 0.70 0.50
assign (residue 3 and name H2')     (residue 4 and name H5)     3.80 2.00 0.70
assign (residue 3 and name H2')     (residue 4 and name H6)     3.80 2.00 0.70
assign (residue 3 and name H2'')    (residue 3 and name H6)     3.80 2.00 0.70
assign (residue 3 and name H2'')    (residue 4 and name H5)     3.80 2.00 0.70
assign (residue 3 and name H2'')    (residue 4 and name H6)     3.80 2.00 0.70
assign (residue 3 and name H3')     (residue 3 and name H6)     3.80 2.00 0.70
assign (residue 3 and name H4')     (residue 3 and name H6)     5.00 2.00 1.00
assign (residue 3 and name H4')     (residue 4 and name H6)     6.00 2.00 1.00
assign (residue 3 and name H5')     (residue 3 and name H6)     5.00 2.00 1.00
assign (residue 3 and name H6)      (residue 4 and name H5)     3.80 2.00 0.70
assign (residue 3 and name H6)      (residue 4 and name H6)     5.00 2.00 1.00
assign (residue 3 and name H1')     (residue 2 and name H1)     6.00 2.00 1.00
assign (residue 3 and name H5'')    (residue 3 and name H6)     5.00 2.00 1.00

{C4}
assign (residue 4 and name H1')     (residue 4 and name H5)     6.00 2.00 1.00
assign (residue 4 and name H1')     (residue 4 and name H6)     3.80 2.00 0.70
assign (residue 4 and name H1')     (residue 5 and name H51)    5.00 2.00 1.00
assign (residue 4 and name H1')     (residue 5 and name H6)     3.80 2.00 0.70
assign (residue 4 and name H1')     (residue 5 and name H3')    6.00 2.00 1.00
assign (residue 4 and name H2')     (residue 4 and name H5)     5.00 2.00 1.00
assign (residue 4 and name H2')     (residue 4 and name H6)     2.50 0.70 0.50
assign (residue 4 and name H2')     (residue 5 and name H51)    3.80 2.00 0.70
assign (residue 4 and name H2')     (residue 5 and name H6)     3.80 2.00 0.70
assign (residue 4 and name H2'')    (residue 4 and name H5)     6.00 2.00 1.00
assign (residue 4 and name H2'')    (residue 4 and name H6)     3.80 2.00 0.70
assign (residue 4 and name H2'')    (residue 5 and name H51)    3.80 2.00 0.70
assign (residue 4 and name H2'')    (residue 5 and name H6)     3.80 2.00 0.70
assign (residue 4 and name H4')     (residue 4 and name H5)     6.00 2.00 1.00
assign (residue 4 and name H4')     (residue 4 and name H6)     5.00 2.00 1.00
assign (residue 4 and name H4')     (residue 5 and name H6)     6.00 2.00 1.00
assign (residue 4 and name H5)      (residue 3 and name H3')    6.00 2.00 1.00
assign (residue 4 and name H5)      (residue 5 and name H51)    3.80 2.00 0.70
assign (residue 4 and name H5)      (residue 5 and name H6)     5.00 2.00 1.00
assign (residue 4 and name H5'')    (residue 4 and name H6)     5.00 2.00 1.00
```

assign (residue 4 and name H6) (residue 4 and name H3') 3.80 2.00 0.70
assign (residue 4 and name H6) (residue 5 and name H51) 3.80 2.00 0.70
assign (residue 4 and name H6) (residue 3 and name H4') 6.00 2.00 1.00
assign (residue 4 and name H6) (residue 5 and name H6) 6.00 2.00 1.00
assign (residue 4 and name H1') (residue 3 and name H3) 6.00 2.00 1.00
assign (residue 4 and name H3') (residue 5 and name H6) 3.80 2.00 0.70
assign (residue 4 and name H5) (residue 3 and name H3) 6.00 2.00 1.00
assign (residue 4 and name H5) (residue 5 and name H6) 6.00 2.00 1.00

{T5}
assign (residue 5 and name H51) (residue 5 and name H1') 6.00 2.00 1.00
assign (residue 5 and name H51) (residue 5 and name H2') 3.80 2.00 0.70
assign (residue 5 and name H51) (residue 5 and name H2") 6.00 2.00 1.00
assign (residue 5 and name H51) (residue 5 and name H3') 6.00 2.00 1.00
assign (residue 5 and name H51) (residue 5 and name H4') 6.00 2.00 1.00
assign (residue 5 and name H51) (residue 5 and name H5') 6.00 2.00 1.00
assign (residue 5 and name H51) (residue 5 and name H5") 6.00 2.00 1.00
assign (residue 5 and name H51) (residue 6 and name H5) 3.80 2.00 0.70
assign (residue 5 and name H1') (residue 5 and name H6) 3.80 2.00 0.70
assign (residue 5 and name H1') (residue 6 and name H5) 5.00 2.00 1.00
assign (residue 5 and name H1') (residue 6 and name H6) 3.80 2.00 0.70
assign (residue 5 and name H2') (residue 5 and name H6) 2.50 0.70 0.50
assign (residue 5 and name H2') (residue 6 and name H6) 3.80 2.00 0.70
assign (residue 5 and name H2") (residue 5 and name H6) 3.80 2.00 0.70
assign (residue 5 and name H2") (residue 6 and name H6) 3.80 2.00 0.70
assign (residue 5 and name H3') (residue 5 and name H6) 3.80 2.00 0.70
assign (residue 5 and name H3') (residue 6 and name H6) 6.00 2.00 1.00
assign (residue 5 and name H4') (residue 5 and name H6) 5.00 2.00 1.00
assign (residue 5 and name H5') (residue 5 and name H6) 3.80 2.00 0.70
assign (residue 5 and name H5") (residue 5 and name H6) 5.00 2.00 1.00
assign (residue 5 and name H6) (residue 6 and name H5) 3.80 2.00 0.70
assign (residue 5 and name H6) (residue 6 and name H6) 6.00 2.00 1.00
assign (residue 5 and name H3) (residue 23 and name H1) 3.80 2.00 0.70

{C6}
assign (residue 6 and name H1') (residue 6 and name H5) 6.00 2.00 1.00
assign (residue 6 and name H1') (residue 6 and name H6) 3.80 2.00 0.70
assign (residue 6 and name H1') (residue 7 and name H3') 6.00 2.00 1.00
assign (residue 6 and name H1') (residue 7 and name H8) 3.80 2.00 0.70
assign (residue 6 and name H1') (residue 24 and name H2) 5.00 2.00 1.00
assign (residue 6 and name H2') (residue 5 and name H1') 6.00 2.00 1.00
assign (residue 6 and name H2') (residue 6 and name H6) 2.50 0.70 0.50
assign (residue 6 and name H2') (residue 7 and name H8) 3.80 2.00 0.70
assign (residue 6 and name H2") (residue 6 and name H6) 3.80 2.00 0.70
assign (residue 6 and name H2") (residue 7 and name H8) 3.80 2.00 0.70
assign (residue 6 and name H3') (residue 6 and name H6) 3.80 2.00 0.70
assign (residue 6 and name H3') (residue 7 and name H8) 5.00 2.00 1.00
assign (residue 6 and name H4') (residue 6 and name H6) 5.00 2.00 1.00
assign (residue 6 and name H5) (residue 5 and name H3') 6.00 2.00 1.00
assign (residue 6 and name H5) (residue 6 and name H3') 6.00 2.00 1.00
assign (residue 6 and name H5) (residue 7 and name H8) 6.00 2.00 1.00
assign (residue 6 and name H6) (residue 7 and name H8) 5.00 2.00 1.00

assign (residue 6 and name H1') (residue 5 and name H3) 6.00 2.00 1.00
assign (residue 6 and name H1') (residue 23 and name H1) 6.00 2.00 1.00
assign (residue 6 and name H42) (residue 22 and name H3) 6.00 2.00 1.00
assign (residue 6 and name H42) (residue 23 and name H1) 3.80 2.00 0.70
assign (residue 6 and name H41) (residue 5 and name H3) 3.80 2.00 0.70
assign (residue 6 and name H41) (residue 22 and name H3) 5.00 2.00 1.00
assign (residue 6 and name H41) (residue 23 and name H1) 2.50 0.70 0.50
assign (residue 6 and name H5) (residue 23 and name H1) 6.00 2.00 1.00
assign (residue 6 and name H6) (residue 23 and name H1) 6.00 2.00 1.00

{A7}
assign (residue 7 and name H1') (residue 7 and name H2) 5.00 2.00 1.00
assign (residue 7 and name H1') (residue 7 and name H8) 3.80 2.00 0.70
assign (residue 7 and name H1') (residue 8 and name H51) 5.00 2.00 1.00
assign (residue 7 and name H1') (residue 8 and name H1') 6.00 2.00 1.00
assign (residue 7 and name H1') (residue 8 and name H6) 3.80 2.00 0.70
assign (residue 7 and name H2) (residue 8 and name H6) 6.00 2.00 1.00
assign (residue 7 and name H2') (residue 6 and name H1') 6.00 2.00 1.00
assign (residue 7 and name H2') (residue 7 and name H8) 2.50 0.70 0.50
assign (residue 7 and name H2') (residue 8 and name H51) 3.80 2.00 0.70
assign (residue 7 and name H2') (residue 8 and name H6) 3.80 2.00 0.70
assign (residue 7 and name H2'') (residue 6 and name H1') 6.00 2.00 1.00
assign (residue 7 and name H2'') (residue 7 and name H8) 3.80 2.00 0.70
assign (residue 7 and name H2'') (residue 8 and name H51) 3.80 2.00 0.70
assign (residue 7 and name H2'') (residue 8 and name H6) 3.80 2.00 0.70
assign (residue 7 and name H3') (residue 7 and name H8) 5.00 2.00 1.00
assign (residue 7 and name H3') (residue 8 and name H6) 6.00 2.00 1.00
assign (residue 7 and name H4') (residue 6 and name H1') 5.00 2.00 1.00
assign (residue 7 and name H4') (residue 7 and name H8) 6.00 2.00 1.00
assign (residue 7 and name H5') (residue 7 and name H8) 5.00 2.00 1.00
assign (residue 7 and name H5'') (residue 7 and name H8) 5.00 2.00 1.00
assign (residue 7 and name H8) (residue 8 and name H51) 5.00 2.00 1.00
assign (residue 7 and name H8) (residue 8 and name H6) 6.00 2.00 1.00
assign (residue 7 and name H2) (residue 22 and name H3) 2.50 0.70 0.50
assign (residue 7 and name H2) (residue 23 and name H1) 5.00 2.00 1.00
assign (residue 7 and name H61) (residue 22 and name H3) 2.50 0.70 0.50
assign (residue 7 and name H61) (residue 23 and name H1) 5.00 2.00 1.00
assign (residue 7 and name H62) (residue 22 and name H3) 3.80 2.00 0.70
assign (residue 7 and name H62) (residue 23 and name H1) 5.00 2.00 1.00

{T8}
assign (residue 8 and name H51) (residue 7 and name H3') 5.00 2.00 1.00
assign (residue 8 and name H51) (residue 8 and name H1') 6.00 2.00 1.00
assign (residue 8 and name H51) (residue 8 and name H2') 5.00 2.00 1.00
assign (residue 8 and name H51) (residue 8 and name H2'') 6.00 2.00 1.00
assign (residue 8 and name H51) (residue 8 and name H5') 6.00 2.00 1.00
assign (residue 8 and name H51) (residue 8 and name H5'') 6.00 2.00 1.00
assign (residue 8 and name H51) (residue 9 and name H8) 6.00 2.00 1.00
assign (residue 8 and name H1') (residue 7 and name H2) 5.00 2.00 1.00
assign (residue 8 and name H1') (residue 8 and name H6) 3.80 2.00 0.70
assign (residue 8 and name H1') (residue 9 and name H3') 6.00 2.00 1.00
assign (residue 8 and name H1') (residue 9 and name H8) 3.80 2.00 0.70

```
assign (residue 8 and name H1')      (residue 7 and name H2)      5.00 2.00 1.00
assign (residue 8 and name H2')      (residue 8 and name H6)      2.50 0.70 0.50
assign (residue 8 and name H2')      (residue 9 and name H8)      3.80 2.00 0.70
assign (residue 8 and name H2'')     (residue 8 and name H6)      3.80 2.00 0.70
assign (residue 8 and name H2'')     (residue 9 and name H8)      3.80 2.00 0.70
assign (residue 8 and name H4')      (residue 8 and name H6)      5.00 2.00 1.00
assign (residue 8 and name H5')      (residue 7 and name H1')     3.80 2.00 0.70
assign (residue 8 and name H5'')     (residue 7 and name H1')     5.00 2.00 1.00
assign (residue 8 and name H6)       (residue 8 and name H5')     5.00 2.00 1.00
assign (residue 8 and name H6)       (residue 8 and name H5'')    6.00 2.00 1.00
assign (residue 8 and name H6)       (residue 9 and name H8)      5.00 2.00 1.00
assign (residue 8 and name H1')      (residue 8 and name H3)      5.00 2.00 1.00
assign (residue 8 and name H3)       (residue 9 and name H1)      5.00 2.00 1.00

{G9}
assign (residue 9 and name H1')      (residue 9 and name H8)      3.80 2.00 0.70
assign (residue 9 and name H1')      (residue 10 and name H4')    5.00 2.00 1.00
assign (residue 9 and name H1')      (residue 10 and name H5')    3.80 2.00 0.70
assign (residue 9 and name H1')      (residue 10 and name H5'')   5.00 2.00 1.00
assign (residue 9 and name H1')      (residue 10 and name H8)     3.80 2.00 0.70
assign (residue 9 and name H2')      (residue 9 and name H8)      2.50 0.70 0.50
assign (residue 9 and name H2')      (residue 10 and name H8)     3.80 2.00 0.70
assign (residue 9 and name H2'')     (residue 9 and name H8)      3.80 2.00 0.70
assign (residue 9 and name H2'')     (residue 10 and name H8)     3.80 2.00 0.70
assign (residue 9 and name H3')      (residue 9 and name H8)      5.00 2.00 1.00
assign (residue 9 and name H4')      (residue 9 and name H8)      6.00 2.00 1.00
assign (residue 9 and name H5')      (residue 9 and name H8)      3.80 2.00 0.70
assign (residue 9 and name H5'')     (residue 9 and name H8)      5.00 2.00 1.00
assign (residue 9 and name H8)       (residue 10 and name H8)     5.00 2.00 1.00
assign (residue 9 and name H1')      (residue 9 and name H1)      6.00 2.00 1.00

{A10}
assign (residue 10 and name H1')     (residue 9 and name H1')     6.00 2.00 1.00
assign (residue 10 and name H1')     (residue 10 and name H2)     5.00 2.00 1.00
assign (residue 10 and name H1')     (residue 10 and name H8)     3.80 2.00 0.70
assign (residue 10 and name H1')     (residue 11 and name H51)    3.80 2.00 0.70
assign (residue 10 and name H1')     (residue 11 and name H6)     3.80 2.00 0.70
assign (residue 10 and name H2')     (residue 10 and name H8)     2.50 0.70 0.50
assign (residue 10 and name H2')     (residue 11 and name H51)    3.80 2.00 0.70
assign (residue 10 and name H2')     (residue 11 and name H6)     3.80 2.00 0.70
assign (residue 10 and name H2'')    (residue 10 and name H8)     3.80 2.00 0.70
assign (residue 10 and name H2'')    (residue 11 and name H51)    3.80 2.00 0.70
assign (residue 10 and name H2'')    (residue 11 and name H6)     3.80 2.00 0.70
assign (residue 10 and name H3')     (residue 10 and name H8)     5.00 2.00 1.00
assign (residue 10 and name H3')     (residue 11 and name H51)    5.00 2.00 1.00
assign (residue 10 and name H3')     (residue 11 and name H6)     6.00 2.00 1.00
assign (residue 10 and name H4')     (residue 11 and name H51)    6.00 2.00 1.00
assign (residue 10 and name H5')     (residue 10 and name H8)     5.00 2.00 1.00
assign (residue 10 and name H8)      (residue 10 and name H4')    5.00 2.00 1.00
assign (residue 10 and name H8)      (residue 10 and name H5'')   5.00 2.00 1.00
assign (residue 10 and name H8)      (residue 11 and name H51)    3.80 2.00 0.70
assign (residue 10 and name H8)      (residue 11 and name H6)     5.00 2.00 1.00
```

assign (residue 10 and name H2) (residue 19 and name H3) 2.50 0.70 0.50
assign (residue 10 and name H61) (residue 19 and name H3) 2.50 0.70 0.50
assign (residue 10 and name H62) (residue 19 and name H3) 3.80 2.00 0.70

{T11}
assign (residue 11 and name H51) (residue 11 and name H1') 6.00 2.00 1.00
assign (residue 11 and name H51) (residue 11 and name H2') 5.00 2.00 1.00
assign (residue 11 and name H51) (residue 11 and name H3') 6.00 2.00 1.00
assign (residue 11 and name H51) (residue 11 and name H4') 6.00 2.00 1.00
assign (residue 11 and name H51) (residue 11 and name H5') 6.00 2.00 1.00
assign (residue 11 and name H1') (residue 10 and name H2) 5.00 2.00 1.00
assign (residue 11 and name H1') (residue 11 and name H6) 3.80 2.00 0.70
assign (residue 11 and name H1') (residue 12 and name H3') 6.00 2.00 1.00
assign (residue 11 and name H1') (residue 12 and name H4') 5.00 2.00 1.00
assign (residue 11 and name H1') (residue 12 and name H8) 3.80 2.00 0.70
assign (residue 11 and name H2') (residue 11 and name H6) 2.50 0.70 0.50
assign (residue 11 and name H2') (residue 12 and name H8) 3.80 2.00 0.70
assign (residue 11 and name H2") (residue 11 and name H6) 3.80 2.00 0.70
assign (residue 11 and name H2") (residue 12 and name H8) 2.50 0.70 0.50
assign (residue 11 and name H4') (residue 11 and name H6) 5.00 2.00 1.00
assign (residue 11 and name H5') (residue 11 and name H6) 5.00 2.00 1.00
assign (residue 11 and name H5") (residue 11 and name H6) 5.00 2.00 1.00
assign (residue 11 and name H6) (residue 10 and name H4') 6.00 2.00 1.00
assign (residue 11 and name H6) (residue 11 and name H3') 3.80 2.00 0.70
assign (residue 11 and name H6) (residue 12 and name H8) 5.00 2.00 1.00
assign (residue 11 and name H1') (residue 10 and name H2) 5.00 2.00 1.00

{A12}
assign (residue 12 and name H1') (residue 11 and name H1') 6.00 2.00 1.00
assign (residue 12 and name H1') (residue 12 and name H2) 5.00 2.00 1.00
assign (residue 12 and name H1') (residue 12 and name H8) 3.80 2.00 0.70
assign (residue 12 and name H1') (residue 13 and name H1') 5.00 2.00 1.00
assign (residue 12 and name H1') (residue 13 and name H5) 5.00 2.00 1.00
assign (residue 12 and name H1') (residue 13 and name H6) 3.80 2.00 0.70
assign (residue 12 and name H2) (residue 13 and name H5) 6.00 2.00 1.00
assign (residue 12 and name H2) (residue 13 and name H6) 6.00 2.00 1.00
assign (residue 12 and name H2) (residue 18 and name H5) 6.00 2.00 1.00
assign (residue 12 and name H2) (residue 18 and name H6) 6.00 2.00 1.00
assign (residue 12 and name H2') (residue 12 and name H8) 2.50 0.70 0.50
assign (residue 12 and name H2') (residue 13 and name H5) 3.80 2.00 0.70
assign (residue 12 and name H2') (residue 13 and name H6) 3.80 2.00 0.70
assign (residue 12 and name H2") (residue 12 and name H8) 3.80 2.00 0.70
assign (residue 12 and name H2") (residue 13 and name H5) 3.80 2.00 0.70
assign (residue 12 and name H2") (residue 13 and name H6) 3.80 2.00 0.70
assign (residue 12 and name H3') (residue 12 and name H8) 3.80 2.00 0.70
assign (residue 12 and name H3') (residue 13 and name H5) 6.00 2.00 1.00
assign (residue 12 and name H3') (residue 13 and name H6) 6.00 2.00 1.00
assign (residue 12 and name H4') (residue 12 and name H8) 6.00 2.00 1.00
assign (residue 12 and name H5') (residue 12 and name H8) 3.80 2.00 0.70
assign (residue 12 and name H5") (residue 12 and name H8) 5.00 2.00 1.00
assign (residue 12 and name H8) (residue 13 and name H5) 3.80 2.00 0.70

assign (residue 12 and name H8) (residue 13 and name H6) 5.00 2.00 1.00
assign (residue 12 and name H2) (residue 16 and name H1) 3.80 2.00 0.70
assign (residue 12 and name H2) (residue 17 and name H3) 2.50 0.70 0.50
assign (residue 12 and name H61) (residue 17 and name H3) 3.80 2.00 0.70
assign (residue 12 and name H62) (residue 17 and name H3) 5.00 2.00 1.00

{C13}
assign (residue 13 and name H1') (residue 12 and name H2) 5.00 2.00 1.00
assign (residue 13 and name H1') (residue 13 and name H5) 6.00 2.00 1.00
assign (residue 13 and name H1') (residue 13 and name H6) 3.80 2.00 0.70
assign (residue 13 and name H1') (residue 14 and name H8) 3.80 2.00 0.70
assign (residue 13 and name H2') (residue 13 and name H5) 5.00 2.00 1.00
assign (residue 13 and name H2') (residue 13 and name H6) 2.50 0.70 0.50
assign (residue 13 and name H2') (residue 14 and name H8) 3.80 2.00 0.70
assign (residue 13 and name H2") (residue 13 and name H5) 6.00 2.00 1.00
assign (residue 13 and name H2") (residue 13 and name H6) 3.80 2.00 0.70
assign (residue 13 and name H2") (residue 14 and name H8) 2.50 0.70 0.50
assign (residue 13 and name H4') (residue 13 and name H5) 6.00 2.00 1.00
assign (residue 13 and name H4') (residue 13 and name H6) 5.00 2.00 1.00
assign (residue 13 and name H5) (residue 12 and name H4') 6.00 2.00 1.00
assign (residue 13 and name H5) (residue 14 and name H8) 6.00 2.00 1.00
assign (residue 13 and name H5') (residue 13 and name H6) 5.00 2.00 1.00
assign (residue 13 and name H5") (residue 13 and name H6) 5.00 2.00 1.00
assign (residue 13 and name H6) (residue 14 and name H8) 5.00 2.00 1.00
assign (residue 13 and name H1') (residue 16 and name H1) 6.00 2.00 1.00
assign (residue 13 and name H3') (residue 13 and name H6) 3.80 2.00 0.70
assign (residue 13 and name H3') (residue 14 and name H8) 5.00 2.00 1.00
assign (residue 13 and name H41) (residue 16 and name H1) 2.50 0.70 0.50
assign (residue 13 and name H41) (residue 17 and name H3) 5.00 2.00 1.00
assign (residue 13 and name H42) (residue 16 and name H1) 3.80 2.00 0.70
assign (residue 13 and name H42) (residue 17 and name H3) 5.00 2.00 1.00
assign (residue 13 and name H42) (residue 14 and name H1) 6.00 2.00 1.00
assign (residue 13 and name H5) (residue 16 and name H1) 6.00 2.00 1.00
assign (residue 13 and name H6) (residue 16 and name H1) 6.00 2.00 1.00

{G14}
assign (residue 14 and name H1') (residue 14 and name H8) 3.80 2.00 0.70
assign (residue 14 and name H2') (residue 14 and name H8) 2.50 0.70 0.50
assign (residue 14 and name H2") (residue 14 and name H8) 3.80 2.00 0.70
assign (residue 14 and name H3') (residue 14 and name H8) 5.00 2.00 1.00
assign (residue 14 and name H4') (residue 14 and name H8) 5.00 2.00 1.00
assign (residue 14 and name H5') (residue 14 and name H8) 3.80 2.00 0.70

{C15}
assign (residue 15 and name H1') (residue 15 and name H5) 6.00 2.00 1.00
assign (residue 15 and name H1') (residue 15 and name H6) 3.80 2.00 0.70
assign (residue 15 and name H1') (residue 16 and name H1') 6.00 2.00 1.00
assign (residue 15 and name H1') (residue 16 and name H3') 6.00 2.00 1.00
assign (residue 15 and name H1') (residue 16 and name H4') 5.00 2.00 1.00
assign (residue 15 and name H1') (residue 16 and name H5') 3.80 2.00 0.70
assign (residue 15 and name H1') (residue 16 and name H8) 3.80 2.00 0.70
assign (residue 15 and name H2') (residue 15 and name H6) 2.50 0.70 0.50

```
assign (residue 15 and name H2')     (residue 16 and name H8)     3.80 2.00 0.70
assign (residue 15 and name H2'')    (residue 15 and name H6)     3.80 2.00 0.70
assign (residue 15 and name H2'')    (residue 16 and name H8)     2.50 0.70 0.50
assign (residue 15 and name H3')     (residue 15 and name H6)     3.80 2.00 0.70
assign (residue 15 and name H4')     (residue 15 and name H6)     5.00 2.00 1.00
assign (residue 15 and name H4')     (residue 16 and name H8)     6.00 2.00 1.00
assign (residue 15 and name H5)      (residue 15 and name H5')    6.00 2.00 1.00
assign (residue 15 and name H5)      (residue 16 and name H8)     6.00 2.00 1.00
assign (residue 15 and name H5')     (residue 15 and name H6)     3.80 2.00 0.70
assign (residue 15 and name H6)      (residue 16 and name H8)     5.00 2.00 1.00
assign (residue 15 and name H41)     (residue 16 and name H1)     5.00 2.00 1.00
assign (residue 15 and name H41)     (residue 13 and name H41)    3.80 2.00 0.70
assign (residue 15 and name H41)     (residue 14 and name H1)     3.80 2.00 0.70
assign (residue 15 and name H42)     (residue 16 and name H1)     6.00 2.00 1.00
assign (residue 15 and name H42)     (residue 14 and name H1)     5.00 2.00 1.00
assign (residue 15 and name H5)      (residue 14 and name H1)     6.00 2.00 1.00

{G16}
assign (residue 16 and name H1')     (residue 16 and name H8)      3.80 2.00 0.70
assign (residue 16 and name H1')     (residue 17 and name H51)    3.80 2.00 0.70
assign (residue 16 and name H1')     (residue 17 and name H6)     3.80 2.00 0.70
assign (residue 16 and name H2')     (residue 16 and name H8)     2.50 0.70 0.50
assign (residue 16 and name H2')     (residue 17 and name H51)    3.80 2.00 0.70
assign (residue 16 and name H2')     (residue 17 and name H6)     3.80 2.00 0.70
assign (residue 16 and name H2'')    (residue 16 and name H8)     3.80 2.00 0.70
assign (residue 16 and name H2'')    (residue 17 and name H51)    3.80 2.00 0.70
assign (residue 16 and name H2'')    (residue 17 and name H6)     3.80 2.00 0.70
assign (residue 16 and name H3')     (residue 16 and name H8)     5.00 2.00 1.00
assign (residue 16 and name H3')     (residue 17 and name H51)    5.00 2.00 1.00
assign (residue 16 and name H3')     (residue 17 and name H6)     6.00 2.00 1.00
assign (residue 16 and name H4')     (residue 16 and name H8)     5.00 2.00 1.00
assign (residue 16 and name H4')     (residue 17 and name H51)    6.00 2.00 1.00
assign (residue 16 and name H5')     (residue 16 and name H8)     3.80 2.00 0.70
assign (residue 16 and name H5'')    (residue 16 and name H8)     5.00 2.00 1.00
assign (residue 16 and name H8)      (residue 17 and name H51)    3.80 2.00 0.70
assign (residue 16 and name H8)      (residue 17 and name H6)     5.00 2.00 1.00
assign (residue 16 and name H1)      (residue 17 and name H3)     3.80 2.00 0.70
assign (residue 16 and name H1)      (residue 14 and name H1)     3.80 2.00 0.70

{T17}
assign (residue 17 and name H51)     (residue 17 and name H1')    6.00 2.00 1.00
assign (residue 17 and name H51)     (residue 17 and name H2')    5.00 2.00 1.00
assign (residue 17 and name H51)     (residue 17 and name H2'')   6.00 2.00 1.00
assign (residue 17 and name H51)     (residue 17 and name H3')    6.00 2.00 1.00
assign (residue 17 and name H51)     (residue 17 and name H4')    6.00 2.00 1.00
assign (residue 17 and name H51)     (residue 17 and name H5')    6.00 2.00 1.00
assign (residue 17 and name H51)     (residue 18 and name H5)     5.00 2.00 1.00
assign (residue 17 and name H51)     (residue 18 and name H6)     6.00 2.00 1.00
assign (residue 17 and name H1')     (residue 17 and name H6)     3.80 2.00 0.70
assign (residue 17 and name H1')     (residue 18 and name H5)     3.80 2.00 0.70
assign (residue 17 and name H1')     (residue 18 and name H6)     3.80 2.00 0.70
assign (residue 17 and name H1')     (residue 12 and name H2)     5.00 2.00 1.00
```

assign (residue 17 and name H2') (residue 16 and name H1') 5.00 2.00 1.00
assign (residue 17 and name H2') (residue 17 and name H6) 2.50 0.70 0.50
assign (residue 17 and name H2') (residue 18 and name H5) 3.80 2.00 0.70
assign (residue 17 and name H2') (residue 18 and name H6) 3.80 2.00 0.70
assign (residue 17 and name H2'') (residue 17 and name H6) 3.80 2.00 0.70
assign (residue 17 and name H2'') (residue 18 and name H5) 3.80 2.00 0.70
assign (residue 17 and name H2'') (residue 18 and name H6) 3.80 2.00 0.70
assign (residue 17 and name H3') (residue 17 and name H6) 3.80 2.00 0.70
assign (residue 17 and name H4') (residue 17 and name H6) 5.00 2.00 1.00
assign (residue 17 and name H4') (residue 18 and name H6) 6.00 2.00 1.00
assign (residue 17 and name H5') (residue 17 and name H6) 5.00 2.00 1.00
assign (residue 17 and name H6) (residue 18 and name H5) 3.80 2.00 0.70
assign (residue 17 and name H6) (residue 18 and name H6) 5.00 2.00 1.00
assign (residue 17 and name H1') (residue 16 and name H1) 6.00 2.00 1.0
assign (residue 17 and name H5'') (residue 17 and name H6) 5.00 2.00 1.00

{C18}
assign (residue 18 and name H1') (residue 18 and name H5) 6.00 2.00 1.00
assign (residue 18 and name H1') (residue 18 and name H6) 3.80 2.00 0.70
assign (residue 18 and name H1') (residue 19 and name H51) 5.00 2.00 1.00
assign (residue 18 and name H1') (residue 19 and name H6) 3.80 2.00 0.70
assign (residue 18 and name H1') (residue 19 and name H3') 6.00 2.00 1.00
assign (residue 18 and name H2') (residue 18 and name H5) 5.00 2.00 1.00
assign (residue 18 and name H2') (residue 18 and name H6) 2.50 0.70 0.50
assign (residue 18 and name H2') (residue 19 and name H51) 3.80 2.00 0.70
assign (residue 18 and name H2') (residue 19 and name H6) 3.80 2.00 0.70
assign (residue 18 and name H2'') (residue 18 and name H5) 6.00 2.00 1.00
assign (residue 18 and name H2'') (residue 18 and name H6) 3.80 2.00 0.70
assign (residue 18 and name H2'') (residue 19 and name H51) 3.80 2.00 0.70
assign (residue 18 and name H2'') (residue 19 and name H6) 3.80 2.00 0.70
assign (residue 18 and name H4') (residue 18 and name H5) 6.00 2.00 1.00
assign (residue 18 and name H4') (residue 18 and name H6) 5.00 2.00 1.00
assign (residue 18 and name H4') (residue 19 and name H6) 6.00 2.00 1.00
assign (residue 18 and name H5) (residue 17 and name H3') 6.00 2.00 1.00
assign (residue 18 and name H5) (residue 19 and name H51) 3.80 2.00 0.70
assign (residue 18 and name H5) (residue 19 and name H6) 5.00 2.00 1.00
assign (residue 18 and name H5'') (residue 18 and name H6) 5.00 2.00 1.00
assign (residue 18 and name H6) (residue 18 and name H3') 3.80 2.00 0.70
assign (residue 18 and name H6) (residue 19 and name H51) 3.80 2.00 0.70
assign (residue 18 and name H6) (residue 17 and name H4') 6.00 2.00 1.00
assign (residue 18 and name H6) (residue 19 and name H6) 6.00 2.00 1.00
assign (residue 18 and name H1') (residue 17 and name H3) 6.00 2.00 1.00
assign (residue 18 and name H3') (residue 19 and name H6) 3.80 2.00 0.70
assign (residue 18 and name H5) (residue 17 and name H3) 6.00 2.00 1.00
assign (residue 18 and name H5) (residue 19 and name H6) 6.00 2.00 1.00

{T19}
assign (residue 19 and name H51) (residue 19 and name H1') 6.00 2.00 1.00
assign (residue 19 and name H51) (residue 19 and name H2') 3.80 2.00 0.70
assign (residue 19 and name H51) (residue 19 and name H2'') 6.00 2.00 1.00
assign (residue 19 and name H51) (residue 19 and name H3') 6.00 2.00 1.00
assign (residue 19 and name H51) (residue 19 and name H4') 6.00 2.00 1.00

```
assign (residue 19 and name H51)    (residue 19 and name H5')   6.00 2.00 1.00
assign (residue 19 and name H51)    (residue 19 and name H5'')  6.00 2.00 1.00
assign (residue 19 and name H51)    (residue 20 and name H5)    3.80 2.00 0.70
assign (residue 19 and name H1')    (residue 19 and name H6)    3.80 2.00 0.70
assign (residue 19 and name H1')    (residue 20 and name H5)    5.00 2.00 1.00
assign (residue 19 and name H1')    (residue 20 and name H6)    3.80 2.00 0.70
assign (residue 19 and name H2')    (residue 19 and name H6)    2.50 0.70 0.50
assign (residue 19 and name H2')    (residue 20 and name H6)    3.80 2.00 0.70
assign (residue 19 and name H2'')   (residue 19 and name H6)    3.80 2.00 0.70
assign (residue 19 and name H2'')   (residue 20 and name H6)    3.80 2.00 0.70
assign (residue 19 and name H3')    (residue 19 and name H6)    3.80 2.00 0.70
assign (residue 19 and name H3')    (residue 20 and name H6)    6.00 2.00 1.00
assign (residue 19 and name H4')    (residue 19 and name H6)    5.00 2.00 1.00
assign (residue 19 and name H5')    (residue 19 and name H6)    3.80 2.00 0.70
assign (residue 19 and name H5'')   (residue 19 and name H6)    5.00 2.00 1.00
assign (residue 19 and name H6)     (residue 20 and name H5)    3.80 2.00 0.70
assign (residue 19 and name H6)     (residue 20 and name H6)    6.00 2.00 1.00
assign (residue 19 and name H3)     (residue 9 and name H1)     3.80 2.00 0.70

{C20}
assign (residue 20 and name H1')    (residue 20 and name H5)    6.00 2.00 1.00
assign (residue 20 and name H1')    (residue 20 and name H6)    3.80 2.00 0.70
assign (residue 20 and name H1')    (residue 21 and name H3')   6.00 2.00 1.00
assign (residue 20 and name H1')    (residue 21 and name H8)    3.80 2.00 0.70
assign (residue 20 and name H1')    (residue 10 and name H2)    5.00 2.00 1.00
assign (residue 20 and name H2')    (residue 19 and name H1')   6.00 2.00 1.00
assign (residue 20 and name H2')    (residue 20 and name H6)    2.50 0.70 0.50
assign (residue 20 and name H2')    (residue 21 and name H8)    3.80 2.00 0.70
assign (residue 20 and name H2'')   (residue 20 and name H6)    3.80 2.00 0.70
assign (residue 20 and name H2'')   (residue 21 and name H8)    3.80 2.00 0.70
assign (residue 20 and name H3')    (residue 20 and name H6)    3.80 2.00 0.70
assign (residue 20 and name H3')    (residue 21 and name H8)    5.00 2.00 1.00
assign (residue 20 and name H4')    (residue 20 and name H6)    5.00 2.00 1.00
assign (residue 20 and name H5)     (residue 19 and name H3')   6.00 2.00 1.00
assign (residue 20 and name H5)     (residue 20 and name H3')   6.00 2.00 1.00
assign (residue 20 and name H5)     (residue 21 and name H8)    6.00 2.00 1.00
assign (residue 20 and name H6)     (residue 21 and name H8)    5.00 2.00 1.00
assign (residue 20 and name H1')    (residue 19 and name H3)    6.00 2.00 1.00
assign (residue 20 and name H1')    (residue 9 and name H1)     6.00 2.00 1.00
assign (residue 20 and name H42)    (residue 8 and name H3)     6.00 2.00 1.00
assign (residue 20 and name H42)    (residue 9 and name H1)     3.80 2.00 0.70
assign (residue 20 and name H41)    (residue 19 and name H3)    3.80 2.00 0.70
assign (residue 20 and name H41)    (residue 8 and name H3)     5.00 2.00 1.00
assign (residue 20 and name H41)    (residue 9 and name H1)     2.50 0.70 0.50
assign (residue 20 and name H5)     (residue 9 and name H1)     6.00 2.00 1.00
assign (residue 20 and name H6)     (residue 9 and name H1)     6.00 2.00 1.00

{A21}
assign (residue 21 and name H1')    (residue 21 and name H2)    5.00 2.00 1.00
assign (residue 21 and name H1')    (residue 21 and name H8)    3.80 2.00 0.70
assign (residue 21 and name H1')    (residue 22 and name H51)   5.00 2.00 1.00
assign (residue 21 and name H1')    (residue 22 and name H1')   6.00 2.00 1.00
```

assign (residue 21 and name H1') (residue 22 and name H6) 3.80 2.00 0.70
assign (residue 21 and name H2) (residue 22 and name H6) 6.00 2.00 1.00
assign (residue 21 and name H2') (residue 20 and name H1') 6.00 2.00 1.00
assign (residue 21 and name H2') (residue 21 and name H8) 2.50 0.70 0.50
assign (residue 21 and name H2') (residue 22 and name H51) 3.80 2.00 0.70
assign (residue 21 and name H2') (residue 22 and name H6) 3.80 2.00 0.70
assign (residue 21 and name H2") (residue 20 and name H1') 6.00 2.00 1.00
assign (residue 21 and name H2") (residue 21 and name H8) 3.80 2.00 0.70
assign (residue 21 and name H2") (residue 22 and name H51) 3.80 2.00 0.70
assign (residue 21 and name H2") (residue 22 and name H6) 3.80 2.00 0.70
assign (residue 21 and name H3') (residue 21 and name H8) 5.00 2.00 1.00
assign (residue 21 and name H3') (residue 22 and name H6) 6.00 2.00 1.00
assign (residue 21 and name H4') (residue 20 and name H1') 5.00 2.00 1.00
assign (residue 21 and name H4') (residue 21 and name H8) 6.00 2.00 1.00
assign (residue 21 and name H5') (residue 21 and name H8) 5.00 2.00 1.00
assign (residue 21 and name H5") (residue 21 and name H8) 5.00 2.00 1.00
assign (residue 21 and name H8) (residue 22 and name H51) 5.00 2.00 1.00
assign (residue 21 and name H8) (residue 22 and name H6) 6.00 2.00 1.00
assign (residue 21 and name H2) (residue 8 and name H3) 2.50 0.70 0.50
assign (residue 21 and name H2) (residue 9 and name H1) 5.00 2.00 1.00
assign (residue 21 and name H61) (residue 8 and name H3) 2.50 0.70 0.50
assign (residue 21 and name H61) (residue 9 and name H1) 5.00 2.00 1.00
assign (residue 21 and name H62) (residue 8 and name H3) 3.80 2.00 0.70
assign (residue 21 and name H62) (residue 9 and name H1) 5.00 2.00 1.00

{T22}
assign (residue 22 and name H51) (residue 21 and name H3') 5.00 2.00 1.00
assign (residue 22 and name H51) (residue 22 and name H1') 6.00 2.00 1.00
assign (residue 22 and name H51) (residue 22 and name H2') 5.00 2.00 1.00
assign (residue 22 and name H51) (residue 22 and name H2") 6.00 2.00 1.00
assign (residue 22 and name H51) (residue 22 and name H5') 6.00 2.00 1.00
assign (residue 22 and name H51) (residue 22 and name H5") 6.00 2.00 1.00
assign (residue 22 and name H51) (residue 23 and name H8) 6.00 2.00 1.00
assign (residue 22 and name H1') (residue 21 and name H2) 5.00 2.00 1.00
assign (residue 22 and name H1') (residue 22 and name H6) 3.80 2.00 0.70
assign (residue 22 and name H1') (residue 23 and name H3') 6.00 2.00 1.00
assign (residue 22 and name H1') (residue 23 and name H8) 3.80 2.00 0.70
assign (residue 22 and name H1') (residue 21 and name H2) 5.00 2.00 1.00
assign (residue 22 and name H2') (residue 22 and name H6) 2.50 0.70 0.50
assign (residue 22 and name H2') (residue 23 and name H8) 3.80 2.00 0.70
assign (residue 22 and name H2") (residue 22 and name H6) 3.80 2.00 0.70
assign (residue 22 and name H2") (residue 23 and name H8) 3.80 2.00 0.70
assign (residue 22 and name H4') (residue 22 and name H6) 5.00 2.00 1.00
assign (residue 22 and name H5') (residue 21 and name H1') 3.80 2.00 0.70
assign (residue 22 and name H5") (residue 21 and name H1') 5.00 2.00 1.00
assign (residue 22 and name H6) (residue 22 and name H5') 5.00 2.00 1.00
assign (residue 22 and name H6) (residue 22 and name H5") 6.00 2.00 1.00
assign (residue 22 and name H6) (residue 23 and name H8) 5.00 2.00 1.00
assign (residue 22 and name H1') (residue 22 and name H3) 5.00 2.00 1.00
assign (residue 22 and name H3) (residue 23 and name H1) 5.00 2.00 1.00

{G23}

```
assign (residue 23 and name H1')      (residue 23 and name H8)     3.80 2.00 0.70
assign (residue 23 and name H1')      (residue 24 and name H4')    5.00 2.00 1.00
assign (residue 23 and name H1')      (residue 24 and name H5')    3.80 2.00 0.70
assign (residue 23 and name H1')      (residue 24 and name H5'')   5.00 2.00 1.00
assign (residue 23 and name H1')      (residue 24 and name H8)     3.80 2.00 0.70
assign (residue 23 and name H2')      (residue 23 and name H8)     2.50 0.70 0.50
assign (residue 23 and name H2')      (residue 24 and name H8)     3.80 2.00 0.70
assign (residue 23 and name H2'')     (residue 23 and name H8)     3.80 2.00 0.70
assign (residue 23 and name H2'')     (residue 24 and name H8)     3.80 2.00 0.70
assign (residue 23 and name H3')      (residue 23 and name H8)     5.00 2.00 1.00
assign (residue 23 and name H4')      (residue 23 and name H8)     6.00 2.00 1.00
assign (residue 23 and name H5')      (residue 23 and name H8)     3.80 2.00 0.70
assign (residue 23 and name H5'')     (residue 23 and name H8)     5.00 2.00 1.00
assign (residue 23 and name H8)       (residue 24 and name H8)     5.00 2.00 1.00
assign (residue 23 and name H1')      (residue 23 and name H1)     6.00 2.00 1.00

{A24}
assign (residue 24 and name H1')      (residue 23 and name H1')    6.00 2.00 1.00
assign (residue 24 and name H1')      (residue 24 and name H2)     5.00 2.00 1.00
assign (residue 24 and name H1')      (residue 24 and name H8)     3.80 2.00 0.70
assign (residue 24 and name H1')      (residue 25 and name H51)    3.80 2.00 0.70
assign (residue 24 and name H1')      (residue 25 and name H6)     3.80 2.00 0.70
assign (residue 24 and name H2')      (residue 24 and name H8)     2.50 0.70 0.50
assign (residue 24 and name H2')      (residue 25 and name H51)    3.80 2.00 0.70
assign (residue 24 and name H2')      (residue 25 and name H6)     3.80 2.00 0.70
assign (residue 24 and name H2'')     (residue 24 and name H8)     3.80 2.00 0.70
assign (residue 24 and name H2'')     (residue 25 and name H51)    3.80 2.00 0.70
assign (residue 24 and name H2'')     (residue 25 and name H6)     3.80 2.00 0.70
assign (residue 24 and name H3')      (residue 24 and name H8)     5.00 2.00 1.00
assign (residue 24 and name H3')      (residue 25 and name H51)    5.00 2.00 1.00
assign (residue 24 and name H3')      (residue 25 and name H6)     6.00 2.00 1.00
assign (residue 24 and name H4')      (residue 25 and name H51)    6.00 2.00 1.00
assign (residue 24 and name H5')      (residue 24 and name H8)     5.00 2.00 1.00
assign (residue 24 and name H8)       (residue 24 and name H4')    5.00 2.00 1.00
assign (residue 24 and name H8)       (residue 24 and name H5'')   5.00 2.00 1.00
assign (residue 24 and name H8)       (residue 25 and name H51)    3.80 2.00 0.70
assign (residue 24 and name H8)       (residue 25 and name H6)     5.00 2.00 1.00
assign (residue 24 and name H2)       (residue 5 and name H3)      2.50 0.70 0.50
assign (residue 24 and name H61)      (residue 5 and name H3)      2.50 0.70 0.50
assign (residue 24 and name H62)      (residue 5 and name H3)      3.80 2.00 0.70

{T25}
assign (residue 25 and name H51)      (residue 25 and name H1')     6.00 2.00 1.00
assign (residue 25 and name H51)      (residue 25 and name H2')    5.00 2.00 1.00
assign (residue 25 and name H51)      (residue 25 and name H3')    6.00 2.00 1.00
assign (residue 25 and name H51)      (residue 25 and name H4')    6.00 2.00 1.00
assign (residue 25 and name H51)      (residue 25 and name H5')    6.00 2.00 1.00
assign (residue 25 and name H1')      (residue 24 and name H2)     5.00 2.00 1.00
assign (residue 25 and name H1')      (residue 25 and name H6)     3.80 2.00 0.70
assign (residue 25 and name H1')      (residue 26 and name H3')    6.00 2.00 1.00
assign (residue 25 and name H1')      (residue 26 and name H4')    5.00 2.00 1.00
assign (residue 25 and name H1')      (residue 26 and name H8)     3.80 2.00 0.70
```

assign (residue 25 and name H2') (residue 25 and name H6) 2.50 0.70 0.50
assign (residue 25 and name H2') (residue 26 and name H8) 3.80 2.00 0.70
assign (residue 25 and name H2") (residue 25 and name H6) 3.80 2.00 0.70
assign (residue 25 and name H2") (residue 26 and name H8) 2.50 0.70 0.50
assign (residue 25 and name H4') (residue 25 and name H6) 5.00 2.00 1.00
assign (residue 25 and name H5') (residue 25 and name H6) 5.00 2.00 1.00
assign (residue 25 and name H5") (residue 25 and name H6) 5.00 2.00 1.00
assign (residue 25 and name H6) (residue 24 and name H4') 6.00 2.00 1.00
assign (residue 25 and name H6) (residue 25 and name H3') 3.80 2.00 0.70
assign (residue 25 and name H6) (residue 26 and name H8) 5.00 2.00 1.00
assign (residue 25 and name H1') (residue 24 and name H2) 5.00 2.00 1.00

{A26}
assign (residue 26 and name H1') (residue 25 and name H1') 6.00 2.00 1.00
assign (residue 26 and name H1') (residue 26 and name H2) 5.00 2.00 1.00
assign (residue 26 and name H1') (residue 26 and name H8) 3.80 2.00 0.70
assign (residue 26 and name H1') (residue 27 and name H1') 5.00 2.00 1.00
assign (residue 26 and name H1') (residue 27 and name H5) 5.00 2.00 1.00
assign (residue 26 and name H1') (residue 27 and name H6) 3.80 2.00 0.70
assign (residue 26 and name H2) (residue 27 and name H5) 6.00 2.00 1.00
assign (residue 26 and name H2) (residue 27 and name H6) 6.00 2.00 1.00
assign (residue 26 and name H2) (residue 4 and name H5) 6.00 2.00 1.00
assign (residue 26 and name H2) (residue 4 and name H6) 6.00 2.00 1.00
assign (residue 26 and name H2') (residue 26 and name H8) 2.50 0.70 0.50
assign (residue 26 and name H2') (residue 27 and name H5) 3.80 2.00 0.70
assign (residue 26 and name H2') (residue 27 and name H6) 3.80 2.00 0.70
assign (residue 26 and name H2") (residue 26 and name H8) 3.80 2.00 0.70
assign (residue 26 and name H2") (residue 27 and name H5) 3.80 2.00 0.70
assign (residue 26 and name H2") (residue 27 and name H6) 3.80 2.00 0.70
assign (residue 26 and name H3') (residue 26 and name H8) 3.80 2.00 0.70
assign (residue 26 and name H3') (residue 27 and name H5) 6.00 2.00 1.00
assign (residue 26 and name H3') (residue 27 and name H6) 6.00 2.00 1.00
assign (residue 26 and name H4') (residue 26 and name H8) 6.00 2.00 1.00
assign (residue 26 and name H5') (residue 26 and name H8) 3.80 2.00 0.70
assign (residue 26 and name H5") (residue 26 and name H8) 5.00 2.00 1.00
assign (residue 26 and name H8) (residue 27 and name H5) 3.80 2.00 0.70
assign (residue 26 and name H8) (residue 27 and name H6) 5.00 2.00 1.00
assign (residue 26 and name H2) (residue 2 and name H1) 3.80 2.00 0.70
assign (residue 26 and name H2) (residue 3 and name H3) 2.50 0.70 0.50
assign (residue 26 and name H61) (residue 3 and name H3) 3.80 2.00 0.70
assign (residue 26 and name H62) (residue 3 and name H3) 5.00 2.00 1.00

{C27}
assign (residue 27 and name H1') (residue 26 and name H2) 5.00 2.00 1.00
assign (residue 27 and name H1') (residue 27 and name H5) 6.00 2.00 1.00
assign (residue 27 and name H1') (residue 27 and name H6) 3.80 2.00 0.70
assign (residue 27 and name H1') (residue 28 and name H8) 3.80 2.00 0.70
assign (residue 27 and name H2') (residue 27 and name H5) 5.00 2.00 1.00
assign (residue 27 and name H2') (residue 27 and name H6) 2.50 0.70 0.50
assign (residue 27 and name H2') (residue 28 and name H8) 3.80 2.00 0.70
assign (residue 27 and name H2") (residue 27 and name H5) 6.00 2.00 1.00
assign (residue 27 and name H2") (residue 27 and name H6) 3.80 2.00 0.70

```
assign (residue 27 and name H2'')    (residue 28 and name H8)    2.50  0.70  0.50
assign (residue 27 and name H4')     (residue 27 and name H5)    6.00  2.00  1.00
assign (residue 27 and name H4')     (residue 27 and name H6)    5.00  2.00  1.00
assign (residue 27 and name H5)      (residue 26 and name H4')   6.00  2.00  1.00
assign (residue 27 and name H5)      (residue 28 and name H8)    6.00  2.00  1.00
assign (residue 27 and name H5')     (residue 27 and name H6)    5.00  2.00  1.00
assign (residue 27 and name H5'')    (residue 27 and name H6)    5.00  2.00  1.00
assign (residue 27 and name H6)      (residue 28 and name H8)    5.00  2.00  1.00
assign (residue 27 and name H1')     (residue 2 and name H1)     6.00  2.00  1.00
assign (residue 27 and name H3')     (residue 27 and name H6)    3.80  2.00  0.70
assign (residue 27 and name H3')     (residue 28 and name H8)    5.00  2.00  1.00
assign (residue 27 and name H41)     (residue 2 and name H1)     2.50  0.70  0.50
assign (residue 27 and name H41)     (residue 3 and name H3)     5.00  2.00  1.00
assign (residue 27 and name H42)     (residue 2 and name H1)     3.80  2.00  0.70
assign (residue 27 and name H42)     (residue 3 and name H3)     5.00  2.00  1.00
assign (residue 27 and name H42)     (residue 28 and name H1)    6.00  2.00  1.00
assign (residue 27 and name H5)      (residue 2 and name H1)     6.00  2.00  1.00
assign (residue 27 and name H6)      (residue 2 and name H1)     6.00  2.00  1.00

{G28}
assign (residue 28 and name H1')     (residue 28 and name H8)    3.80  2.00  0.70
assign (residue 28 and name H2')     (residue 28 and name H8)    2.50  0.70  0.50
assign (residue 28 and name H2'')    (residue 28 and name H8)    3.80  2.00  0.70
assign (residue 28 and name H3')     (residue 28 and name H8)    5.00  2.00  1.00
assign (residue 28 and name H4')     (residue 28 and name H8)    5.00  2.00  1.00
assign (residue 28 and name H5')     (residue 28 and name H8)    3.80  2.00  0.70

!-------------------------------------------------------------------------------
```

H-bond_for base pair fix

```
{C1-G28}
{GUA28}                {CYT1}
assign (resid 28 and name H1)        (resid 1 and name N3)     1.90 0.20 0.20
assign (resid 28 and name N1)        (resid 1 and name N3)     2.90 0.30 0.30
assign (resid 28 and name O6)        (resid 1 and name H41)    2.00 0.20 0.20
assign (resid 28 and name O6)        (resid 1 and name N4)     2.90 0.30 0.30
assign (resid 28 and name H21)       (resid 1 and name O2)     2.00 0.20 0.20
assign (resid 28 and name N2)        (resid 1 and name O2)     2.90 0.30 0.30

{G2-C27}
{GUA2}                 {CYT27}
assign (resid 2 and name H1)         (resid 27 and name N3)    1.90 0.20 0.20
assign (resid 2 and name N1)         (resid 27 and name N3)    2.90 0.30 0.30
assign (resid 2 and name O6)         (resid 27 and name H41)   2.00 0.20 0.20
assign (resid 2 and name O6)         (resid 27 and name N4)    2.90 0.30 0.30
assign (resid 2 and name H21)        (resid 27 and name O2)    2.00 0.20 0.20
assign (resid 2 and name N2)         (resid 27 and name O2)    2.90 0.30 0.30

{T3-A26}
{THY3}                 {ADE26}
```

```
assi (resi 3 and name  H3)          (resi 26  and name  N1)   1.90 0.10 0.10
assi (resi 3 and name  N3)          (resi 26  and name  N1)   2.90 0.10 0.10
assi (resi 3 and name  O4)          (resi 26  and name  H61)  1.90 0.10 0.10
assi (resi 3 and name  O4)          (resi 26  and name  N6)   2.90 0.10 0.10

{C+4-T+25}
{THY+25}            {CYT+4}
assi (resi 25 and name  N3)         (resi 4  and name  N4)    4.3 0.30 0.30

{T5-A24}
{THY5}              {ADE24}
assi (resi 5 and name  H3)          (resi 24  and name  N1)   1.90 0.10 0.10
assi (resi 5 and name  N3)          (resi 24  and name  N1)   2.90 0.10 0.10
assi (resi 5 and name  O4)          (resi 24  and name  H61)  1.90 0.10 0.10
assi (resi 5 and name  O4)          (resi 24  and name  N6)   2.90 0.10 0.10

{C6-G23}
{GUA23}             {CYT6}
assign (resid 23 and name H1)       (resid 6 and name N3)     1.90 0.20 0.20
assign (resid 23 and name N1)       (resid 6 and name N3)     2.90 0.30 0.30
assign (resid 23 and name O6)       (resid 6 and name H41)    2.00 0.20 0.20
assign (resid 23 and name O6)       (resid 6 and name N4)     2.90 0.30 0.30
assign (resid 23 and name H21)      (resid 6 and name O2)     2.00 0.20 0.20
assign (resid 23 and name N2)       (resid 6 and name O2)     2.90 0.30 0.30

{A7-T22}
{THY22}             {ADE7}
assi (resi 22 and name  H3)         (resi 7  and name  N1)    1.90 0.10 0.10
assi (resi 22 and name  N3)         (resi 7  and name  N1)    2.90 0.10 0.10
assi (resi 22 and name  O4)         (resi 7  and name  H61)   1.90 0.10 0.10
assi (resi 22 and name  O4)         (resi 7  and name  N6)    2.90 0.10 0.10

{T8-A21}
{THY8}              {ADE21}
assi (resi 8 and name  H3)          (resi 21  and name  N1)   1.90 0.10 0.10
assi (resi 8 and name  N3)          (resi 21  and name  N1)   2.90 0.10 0.10
assi (resi 8 and name  O4)          (resi 21  and name  H61)  1.90 0.10 0.10
assi (resi 8 and name  O4)          (resi 21  and name  N6)   2.90 0.10 0.10

{G9-C20}
{GUA9}              {CYT20}
assign (resid 9 and name H1)        (resid 20 and name N3)    1.90 0.20 0.20
assign (resid 9 and name N1)        (resid 20 and name N3)    2.90 0.30 0.30
assign (resid 9 and name O6)        (resid 20 and name H41)   2.00 0.20 0.20
assign (resid 9 and name O6)        (resid 20 and name N4)    2.90 0.30 0.30
assign (resid 9 and name H21)       (resid 20 and name O2)    2.00 0.20 0.20
assign (resid 9 and name N2)        (resid 20 and name O2)    2.90 0.30 0.30

{A10-T19}
{THY19}             {ADE10}
assi (resi 19 and name  H3)         (resi 10  and name  N1)   1.90 0.10 0.10
assi (resi 19 and name  N3)         (resi 10  and name  N1)   2.90 0.10 0.10
```

```
assi (resi 19 and name  O4)          (resi 10  and name  H61)  1.90 0.10 0.10
assi (resi 19 and name  O4)          (resi 10  and name  N6)   2.90 0.10 0.10

{T+11-C+18}
{THY+11}             {CYT+18}
assi (resi 11 and name  N3)          (resi 18  and name  N4)   4.30 0.30 0.30

{A12-T17}
{THY17}              {ADE12}
assi (resi 17 and name  H3)          (resi 12  and name  N1)   1.90 0.10 0.10
assi (resi 17 and name  N3)          (resi 12  and name  N1)   2.90 0.10 0.10
assi (resi 17 and name  O4)          (resi 12  and name  H61)  1.90 0.10 0.10
assi (resi 17 and name  O4)          (resi 12  and name  N6)   2.90 0.10 0.10

{C13-G16}
{GUA16}              {CYT13}
assign (resid 16 and name H1)        (resid 13 and name N3)   1.90 0.20 0.20
assign (resid 16 and name N1)        (resid 13 and name N3)   2.90 0.30 0.30
assign (resid 16 and name O6)        (resid 13 and name H41)  2.00 0.20 0.20
assign (resid 16 and name O6)        (resid 13 and name N4)   2.90 0.30 0.30
assign (resid 16 and name H21)       (resid 13 and name O2)   2.00 0.20 0.20
assign (resid 16 and name N2)        (resid 13 and name O2)   2.90 0.30 0.30

{G14-C15}
{GUA14}              {CYT15}
assign (resid 14 and name H1)        (resid 15 and name N3)   1.90 0.20 0.20
assign (resid 14 and name N1)        (resid 15 and name N3)   2.90 0.30 0.30
assign (resid 14 and name O6)        (resid 15 and name H41)  2.00 0.20 0.20
assign (resid 14 and name O6)        (resid 15 and name N4)   2.90 0.30 0.30
assign (resid 14 and name H21)       (resid 15 and name O2)   2.00 0.20 0.20
assign (resid 14 and name N2)        (resid 15 and name O2)   2.90 0.30 0.30

!---------------------------------------------------------------------------
```

Angles for sugar puckering

```
restraints dihedral
        nassign=1000

 for $1 in (

{====>}            {* Select nucleotides to be restrained. *}

 1 2 3 5 6 7 8 9 10 12 13 14 15 16 17 19 20 21 22 23 24 26
27 28
        ) loop dihe


evaluate($a=$1+1)
                                          evaluate($b=$1-1)


assign  ( resid $b and name O3' )
          ( resid $1 and name P )
          ( resid $1 and name O5' )
     ( resid $1 and name C5' ) 50.0  -70.0 20.0 2 {* alpha *}

assign  ( resid $1 and name P )
          ( resid $1 and name O5' )
          ( resid $1 and name C5' )
      ( resid $1 and name C4' ) 50.0  180.0 20.0 2 {* beta *}

 assign  ( resid $1 and name O5' )
          ( resid $1 and name C5' )
          ( resid $1 and name C4' )
   ( resid $1 and name C3' ) 50.0   60.0 20.0 2 {* gamma *}

assign  ( resid $1 and name c5' )
          ( resid $1 and name c4' )
          ( resid $1 and name c3' )
     ( resid $1 and name o3' ) 50.0  140.0 25.0 2 {* delta *}

 assign  ( resid $1 and name c4' )
          ( resid $1 and name c3' )
           ( resid $1 and name o3' )
  ( resid $a and name P )   50.0 -170.0 20.0 2 {* epsilon *}

assign  ( resid $1 and name C3' )
          ( resid $1 and name O3' )
          ( resid $a and name P )
       ( resid $a and name O5' ) 50.0  -85.0 20.0 2 {* zeta *}


 end loop dihe
```

```
 for $1 in (

{====>}                {* Select purines to be restrained. *}

 2 7 9 10 12 14 16 21 23 24 26 28
        ) loop dihe

assign  ( resid $1 and name O4' )
          ( resid $1 and name C1' )
          ( resid $1 and name N9 )
      ( resid $1 and name C4 ) 50.0 -120.0 20.0 2 {* chi *}

end loop dihe


 for $1 in (

{====>}            {* Select pyrimidines to be restrained. *}

 1 3 5 6 8 13 15 17 19 20 22 27
        ) loop dihe

assign  ( resid $1 and name O4' )
          ( resid $1 and name C1' )
          ( resid $1 and name N1 )
    ( resid $1 and name C2 ) 50.0 -120.00 20.0 2 {* chi *}

end loop dihe

!---------------------------------------------------------------------------
```

```
restraints plane

group
select= ((resid 28 and (name n1 or name c6 or name c2))
or
        (resid 1 and (name n3)))
 weight=20.0
 end

group
select= ((resid 2 and (name n1 or name c6 or name c2))
or
        (resid 27 and (name n3)))
 weight=20.0
 end

group
select= ((resid 26 and (name n1 or name c6 or name c2))
or
        (resid 3 and (name n3)))
 weight=50.0
 end

group
select= ((resid 24 and (name n1 or name c6 or name c2))
or
        (resid 5 and (name n3)))
 weight=30.0
 end

group
select= ((resid 23 and (name n1 or name c6 or name c2))
or
        (resid 6 and (name n3)))
 weight=50.0
 end

group
select= ((resid 7 and (name n1 or name c6 or name c2))
or
        (resid 22 and (name n3)))
 weight=50.0
 end

group
select= ((resid 21 and (name n1 or name c6 or name c2))
or
        (resid 8 and (name n3)))
 weight=50.0
 end

group
select= ((resid 9 and (name n1 or name c6 or name c2))
or
        (resid 20 and (name n3)))
 weight=50.0
 end

group
select= ((resid 10 and (name n1 or name c6 or name c2))
or
        (resid 19 and (name n3)))
 weight=30.0
 end

group
select= ((resid 12 and (name n1 or name c6 or name c2))
or
        (resid 17 and (name n3)))
 weight=50.0
 end

group
select= ((resid 16 and (name n1 or name c6 or name c2))
or
        (resid 13 and (name n3)))
 weight=20.0
 end

group
select= ((resid 14 and (name n1 or name c6 or name c2))
or
        (resid 15 and (name n3)))
 weight=20.0
 end

group
select= ((resid 28 and (name n1)) or
        (resid 1 and (name n3 or name c2 or name c4)))
 weight=20.0
 end

group
select= ((resid 2 and (name n1)) or
        (resid 27 and (name n3 or name c2 or name c4)))
 weight=20.0
 end

group
select= ((resid 26 and (name n1)) or
        (resid 3 and (name n3 or name c2 or name c4)))
 weight=50.0
 end
```

```
group
select= ((resid 24 and (name n1)) or
         (resid 5 and (name n3 or name c2 or name c4)))
 weight=30.0
 end

group
select= ((resid 23 and (name n1)) or
         (resid 6 and (name n3 or name c2 or name c4)))
 weight=50.0
 end

group
select= ((resid 7 and (name n1)) or
         (resid 22 and (name n3 or name c2 or name c4)))
 weight=50.0
 end

group
select= ((resid 21 and (name n1)) or
         (resid 8 and (name n3 or name c2 or name c4)))
 weight=50.0
 end

group
select= ((resid 9 and (name n1)) or
         (resid 20 and (name n3 or name c2 or name c4)))
 weight=50.0
 end

group
select= ((resid 10 and (name n1)) or
         (resid 19 and (name n3 or name c2 or name c4)))
 weight=30.0
 end

group
select= ((resid 12 and (name n1)) or
         (resid 17 and (name n3 or name c2 or name c4)))
 weight=50.0
 end

group
select= ((resid 16 and (name n1)) or
         (resid 13 and (name n3 or name c2 or name c4)))
 weight=20.0
 end

group
select= ((resid 14 and (name n1)) or
         (resid 15 and (name n3 or name c2 or name c4)))
 weight=20.0
 end

end
!--------------------------------------------------------------------
```

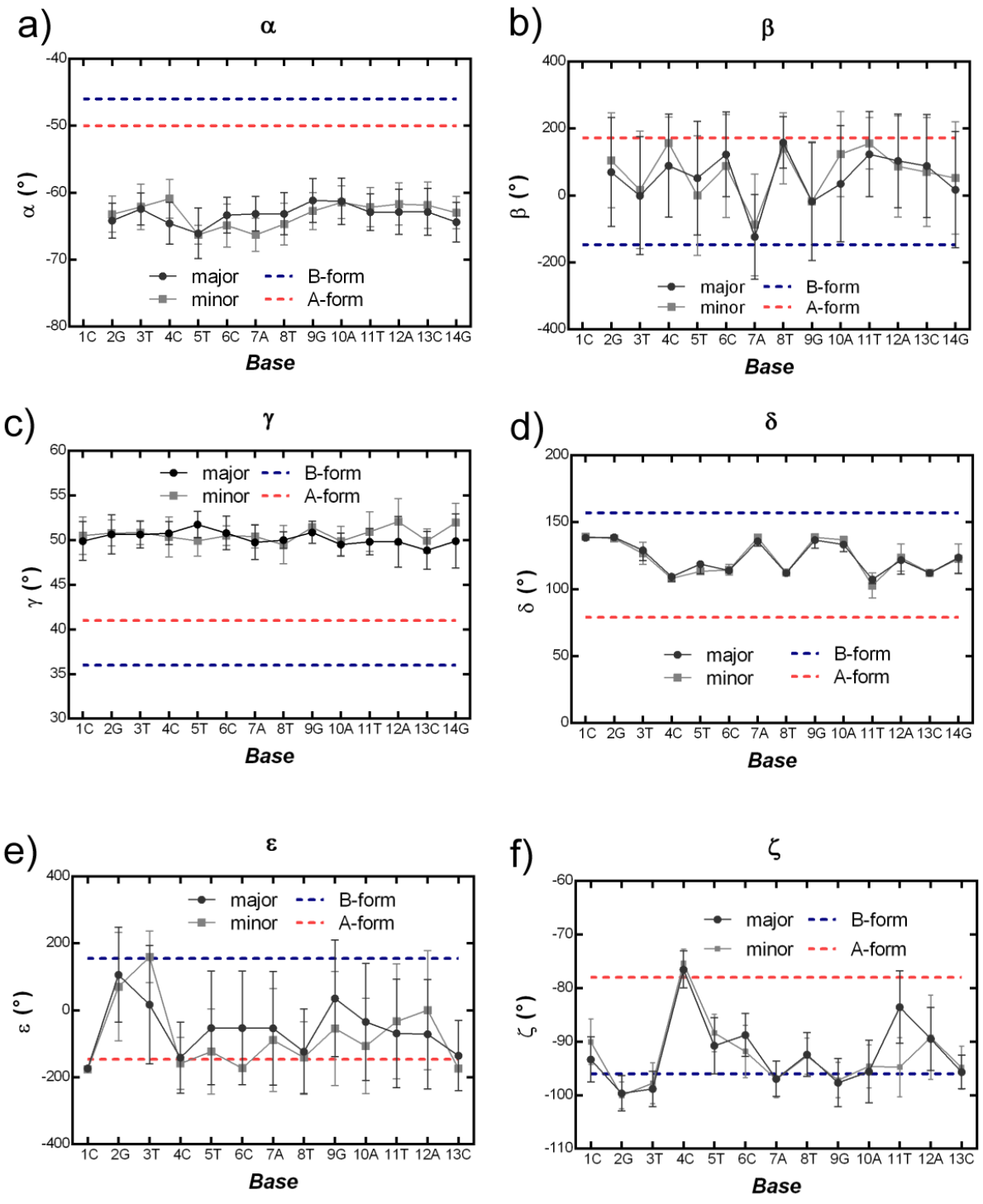

Figure A26. Backbone conformational parameters: a) α-torsion angle (O3'-P-O5'-C5'), b) ß-torsion angle (P-O5'-C5'-C4'), c) γ-torsion angle (O5'-C5'- C4'- C3'), d) δ-torsion angle (C5'- C4'- C3'- O3'), e) ε-torsion angle (C4'- C3'- O3'-P) f) ζ-torsion angle (C3'-O3'-P-O5'). Reference A-form and B-form values were taken from (G. C. K. Roberts, *NMR of Macromolecules*, Oxford University Press, New York, 1993).

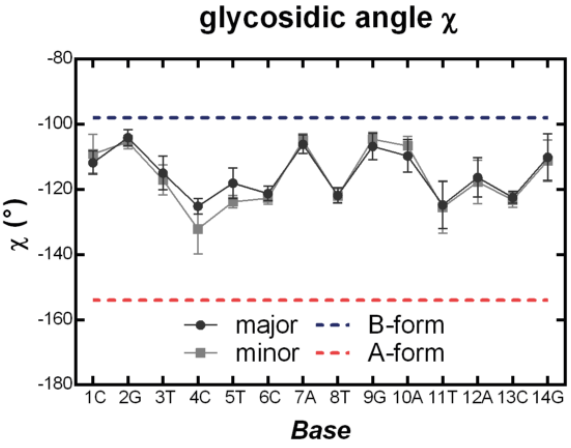

Figure A27. Glycosidic angle χ. Parameters were analyzed using Curves+ and represent mean and standard deviation of the 20 lowest energy conformations of major and minor duplex species. Reference A-form and B-form values were taken from (G. C. K. Roberts, *NMR of Macromolecules*, Oxford University Press, New York, 1993)

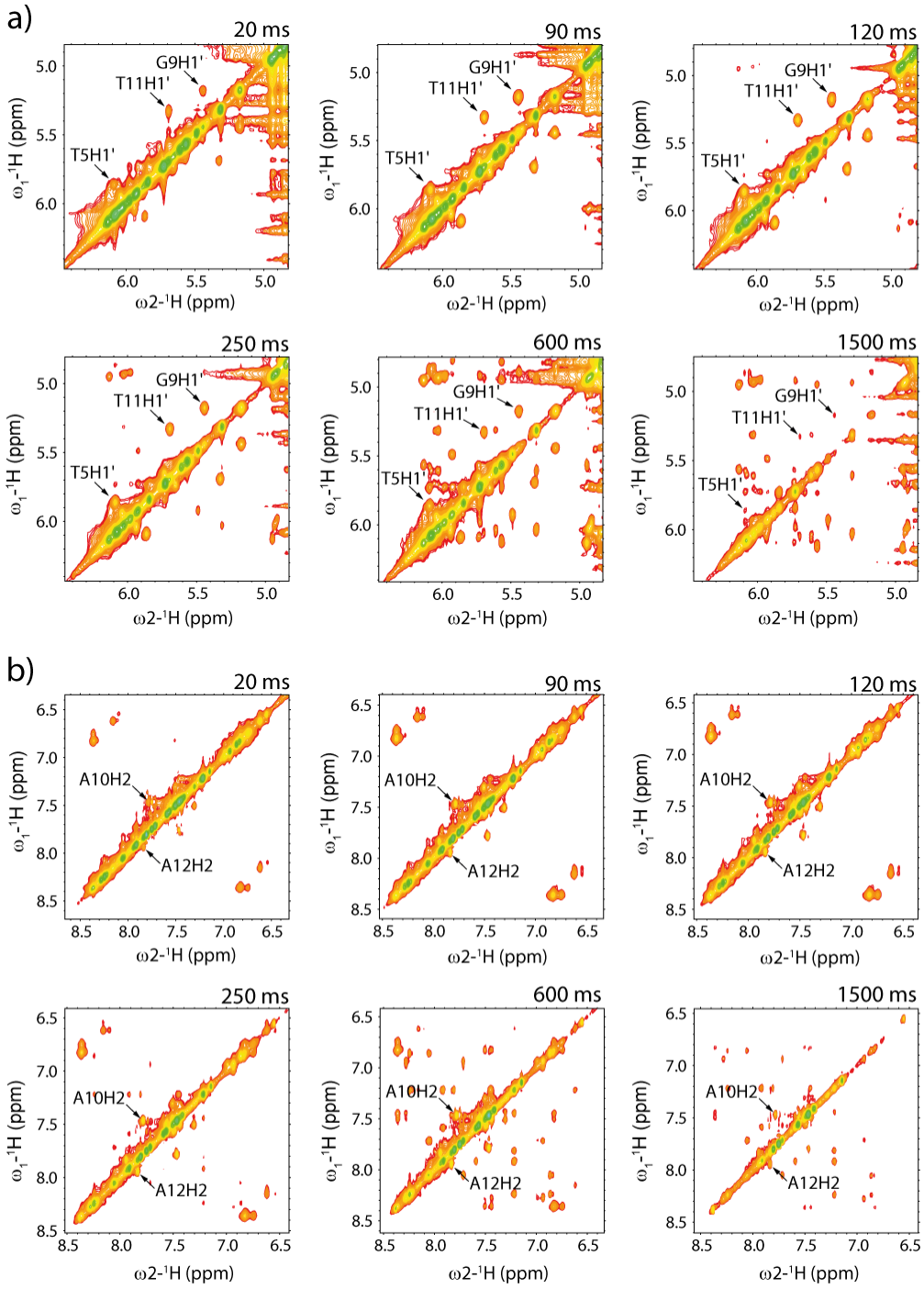

Figure A28. [^{1}H,^{1}H]-NOESY spectra with selected mixing times ranging 20 ms to 1.5 s. Change of exchange cross peak intensity as a function of mixing time for a) H1' protons and b) H2 protons. The DNA sample contained 1 mM duplex DNA and 3 mM of ^{199}Hg-enriched $Hg(ClO_4)_2$ in aqueous buffer (200 mM $NaClO_4$, 50 mM cacodylic acid in H_2O / D_2O (9:1) at pH = 7.8).

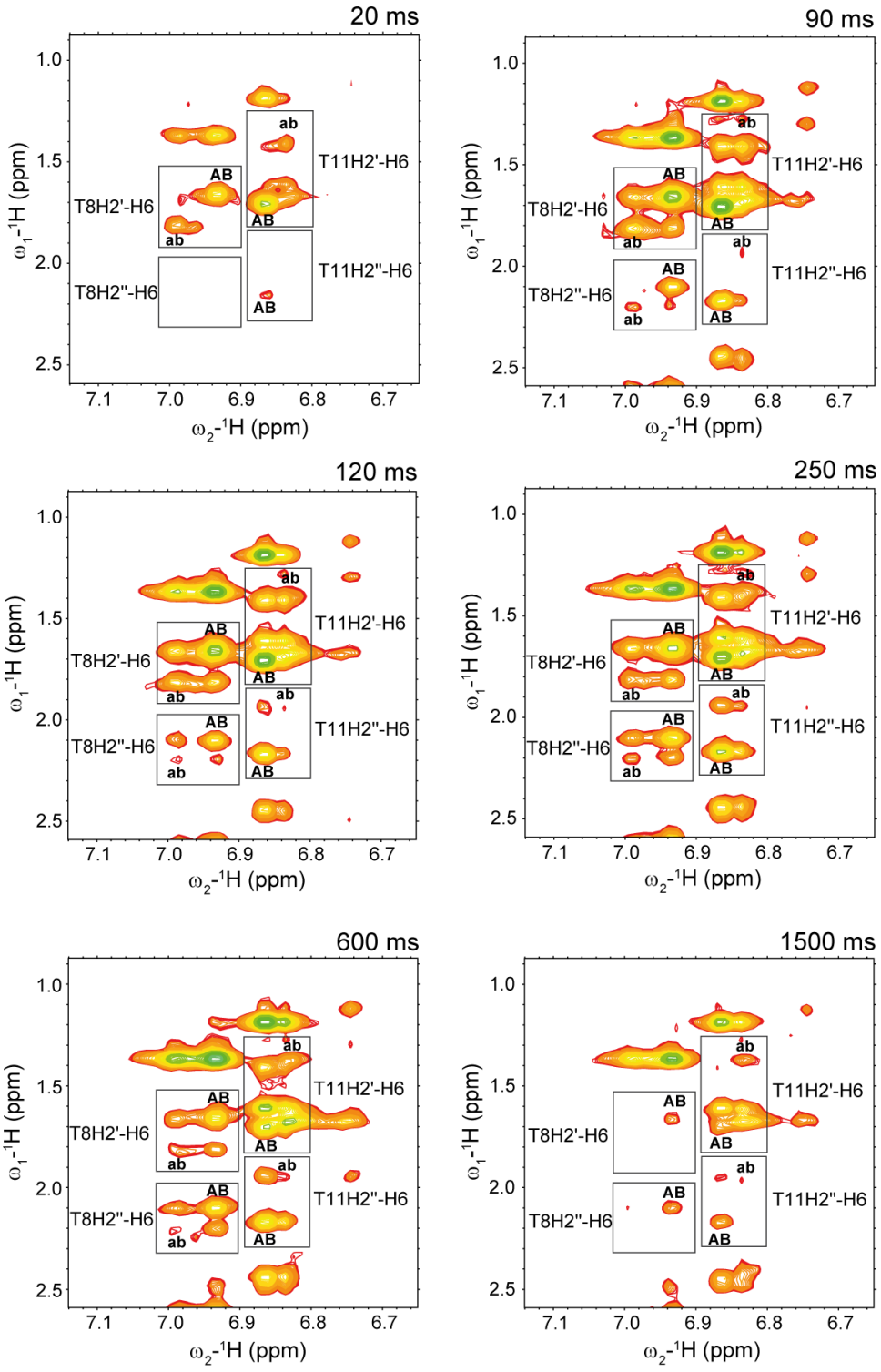

Figure A29. [^{1}H,^{1}H]-NOESY spectra with selected mixing times ranging 20 ms to 1.5 s. Change of exchange-mediated NOE cross peak intensity as a function of mixing time for. The DNA sample contained 1 mM duplex DNA and 3 mM of ^{199}Hg-enriched $Hg(ClO_4)_2$ in aqueous buffer (200 mM $NaClO_4$, 50 mM cacodylic acid in H_2O / D_2O (9:1) at pH = 7.8).

Abbreviations and Symbols

A	Adenine
C	Cytosine
CD	Circular dichroism
COSY	Correlation spectroscopy
DFT	Density functional theory
DMA	Dimethylaniline
DMT	Dimethoxytrityl
DNA	2'-Deoxyribonucleic acid
EC_{50}	Half maximal effective concentration
EDTA	Ethylenediaminetetraacetic acid
ESI	Electrospray ionization
EC_{50}	Half maximal effective concentration
FAM	Fluorescein amidite
FRET	Förster resonance energy transfer
G	Guanine
HPLC	High performance liquid chromatography
HOMO	Highest occupied molecular orbital
HSQC	Heteronuclear signle quantum coherence spectroscopy
LUMO	Lowest unoccupied molecular orbital
MS	Mass spectrometry
NMR	Nuclear magnetic resonance
NOE	Nuclear Overhauser effect
NTP	Nucleoside triphosphate
PDB	Protein data bank
Pol	Polymerase
ppm	Parts per million
r.m.s.d.	Root meen square deviation
RNA	Ribonucleic acid
ROESY	Rotating-frame nuclear Overhauser effect correlation spectroscopy
RT	Room temperature
T	Thymidine
TBE	Tris-borate-EDTA buffer
TOCSY	Total correlation spectroscopy
TPPTS	Phosphanetriyltris(benzenesulfonic acid) trisodium salt
UV	Ultraviolet

r	Fluorescence anisotropy
ϕ	Quantum yield
n	Refractive index
ηt	Energy transfer
λ_{ex}	Excitation wavelength
λ_{em}	Emission wavelength
λ_{abs}	Absorbance wavelength
E_{T30}	Solvent polarity parameter
k	Rate constant
$t_{½}$	Half-life
ε	Molar extinction coefficient
δ	Chemical shift
J	Coupling constant
T_m	Thermal melting temperature

Chapter 7

Conclusions and Summary

7.1 Summary

Characterization of Metal-Mediated Base Pairs in Duplex DNA Using Fluorescent Nucleoside Analogs and NMR Spectroscopy

All biological information essential for life is stored and encoded in nucleic acids. Duplex DNA is a highly dynamic molecule and can fold into a variety of single-stranded and double helical structures. Non-duplex DNA structures and local polymorphisms have been suggested to play regulatory roles in gene expression and other cellular processes by providing unique recognition sites for proteins and small molecules. Given the polyanionic nature of nucleic acids, DNA molecules are accompanied by metal ions. In addition to stabilizing secondary DNA structures, metal ions can induce conformational changes, mediate protein-DNA binding interactions, and act as catalytic co-factors for ribozyme catalysis. Transition metal ions exhibit a wide variety of binding sites on nucleic acids and in some cases, can dramatically stabilize pairing interactions of "all natural" nucleosides by the formation of metal-mediated base pairs. T-Hg^{II}-T base pairs provided the first examples of "all natural" metal-mediated base pairs composed of nucleobase mismatches coordinated to a transition metal ion. Structurally analogous C-Ag^{I}-C have also been reported, and in both cases, little or no impact on the global structure of the B-form duplex was observed. The formation and properties of "all natural" metallo base pairs have broad implications in material and biological sciences. Previous studies have demonstrated that T-Hg^{II}-T can serve as a functional mimic of T-A base pairs by stabilizing T-T during DNA primer extension, and by causing enzymatic misincorporation of dTTP across from thymidine in vitro and possibly in vivo.

The kinetic and thermodynamic parameters of local, site-specific metal-mediated base pair formation in duplex DNA are important for understanding their potential biological and material properties, however, there are no previous studies that report these values. Fluorescent nucleobase analogs (FBAs) can facilitate highly sensitive biophysical measurements with single-base resolution, however, there are no previous examples of native, site-specific metal-nucleobase binding interactions being directly reported by an FBA. This would provide a powerful tool for determining the kinetic and thermodynamic parameters of local metal binding reactions. Our goal was to develop a fluorescence based assay to detect and characterize metallo base pair formation and investigate their potential impact on dynamic processes involving DNA. We envisioned the use of oligonucleotides containing fluorescent thymidine and cytosine analogs to determine kinetic and thermodynamic parameters of Hg^{II}-mediated base pairs and thereby shed light on potential mechanisms for the cytotoxic and mutagenic activities associated with Hg^{II} exposure. With this goal, we recently synthesized a new fluorescent thymidine mimic "^{DMA}T" that exhibits same base pairing preferences and same pK_a as native thymine residues. Duplexes containing ^{DMA}T-A base pairs exhibited the same global structures and thermal stabilities as wild-type duplexes containing T-A base pairs. The quantum yield of ^{DMA}T (ϕ = 0.03 in water) increased upon its incorporation into duplex DNA (ϕ = 0.11 – 0.20) where its fluorescent properties were highly sensitive to nucleobase hydration, ionization, and base pairing. Thermal melting temperature analysis of ^{DMA}T-T- and T-T-mismatch containing oligonucleotides in the presence and absence of 1.0 equiv of Hg^{II} demonstrated the excellent mimicry of ^{DMA}T for thymidine residues in the demanding context of T-Hg^{II}-T base pair. Addition of Hg^{II} to ^{DMA}T-T-mismatch containing oligonucleotides induced bi-phasic fluorescence quenching. Steep slopes were observed between 0.0 and 1.0 equiv of added Hg^{II} as a result of ^{DMA}T-T specific binding, and shallow slopes between 2.0 and 3.0 equiv, due to non-specific interactions. These results demonstrated that the fluorescent properties of ^{DMA}T can be utilized to monitor site-specific binding of Hg^{II} ions to ^{DMA}T-T sites and provided the first example of using fluorescent nucleobase analogs to monitor a specific binding reaction between DNA and Hg^{II} ions.

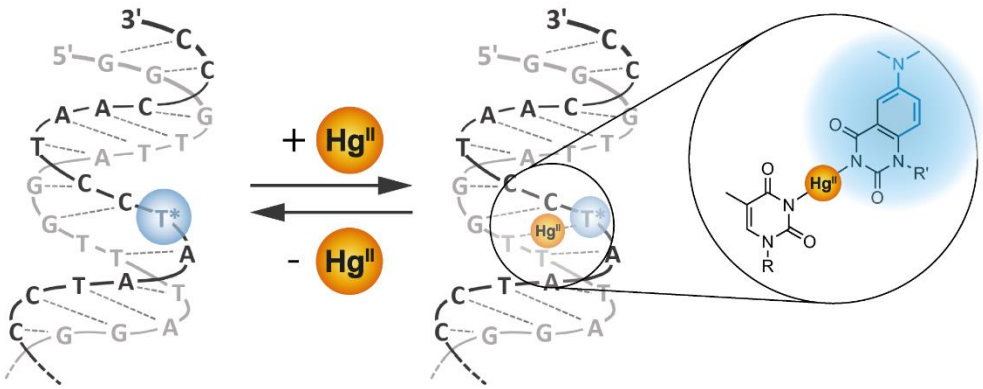

The fluorescent properties of ^{DMA}T-A base pairs were highly sensitive to mercury binding reactions at T-T mismatches located at an adjacent site or one base pair away. This allowed the use of ^{DMA}T-containing oligonucleotides for the first fluorescence-based study of direct, site-specific metal binding reactions involving unmodified nucleobases in duplex DNA. Given the exceptionally high sensitivity of fluorescent measurements, we were able to directly assess the local kinetic and thermodynamic parameters of T-Hg^{II}-T base pairs by monitoring changes in ^{DMA}T-fluorescence of ^{DMA}T-T- and ^{DMA}T-A-containing duplex DNA. Hg^{II} exhibited high affinity binding interactions to duplexes containing ^{DMA}T-T and T-T mismatches, with equilibrium dissociation constants of K_d = 34–77 nM. Duplex DNA containing ^{DMA}T-A and no T-T mismatch, in contrast, showed local, nonspecific Hg^{II} binding affinities of $K_d \approx 2.0\ \mu M$. Tracking time-dependent changes in fluorescence intensity of ^{DMA}T-containing duplexes revealed that T-Hg^{II}-T binding interactions were characterized by surprisingly slow association and dissociation rate constants ($k_{on} \approx 10^4$–$10^5\ M^{-1}s^{-1}$, $k_{off} \approx 10^{-4}$–$10^{-3}\ s^{-1}$) with half-lives ($t_{1/2}$) in the range of 0.3–1.3 h, demonstrating the exceptionally high kinetic stabilities of T-Hg^{II}-T base pairs. Most biochemical processes take place on the time scale of microseconds to seconds. To evaluated whether the exceptionally high kinetic stabilities of T-Hg^{II}-T base pairs could pose significant barriers to dynamic processes involving DNA, we investigated the kinetics of strand-displacement reactions and primer extension by DNA polymerase. Our results demonstrated that T-Hg^{II}-T base pairs pose a significant barrier towards DNA-DNA strand-displacement reactions and inhibit enzymatic DNA synthesis by inducing a pronounced stalling of the DNA polymerase and termination of DNA synthesis at the site of the T-Hg^{II}-T base pair. These results revealed that T-Hg^{II}-T base pairs have a high potential to disrupt DNA metabolism *in vivo* and offer a potential mechanism for the cytotoxic activities that are associated with Hg^{II} exposure.

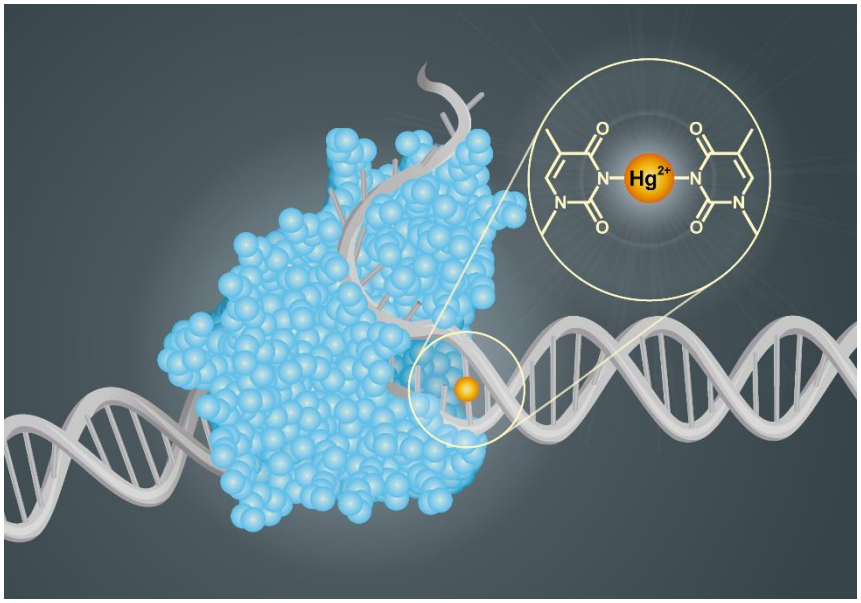

Metal-mediated base pairs expand the repertoire of helical structures and dynamics available to duplex nucleic acids, thereby tuning their biological and materials properties. In recent years, a wide variety of other metallated base pairs have been observed in crystals of non-B-form nucleic acids. Among those, a C-Hg^{II}-T base pair was found in short, A-form duplex DNA where the metal ion was unexpectedly bound to the exocyclic amine (*N4*) of a deprotonated cytosine residue and to the *N3* of a deprotonated thymidine. In contrast to T-Hg^{II}-T and C-Ag^{I}-C, however, little or no change was observed in the thermal melting temperatures of duplexes containing C-T mismatches upon addition of Hg^{II}. This result could be interpreted as the absence of a strong binding interaction, but this is not the case.

We characterized binding reactions of Hg^{II} and Ag^{I} to C-T mismatches in duplex DNA using fluorescent nucleobase analogs ^{DMA}T and ^{DMA}C, thermal denaturation and ^{1}H NMR. Our results demonstrated that Hg^{II}, but not Ag^{I}, exhibits high-affinity, stoichiometric binding of C-T mismatches in duplex DNA. C-Hg^{II}-T base pairs exhibited thermodynamic stabilities (K_d = 10 – 153 nM) that were very similar to those of widely-studied T-Hg^{II}-T base pairs. Both association and dissociation kinetics were approximately 10-fold faster to C-T ($k_{on} \approx 10^5$ $M^{-1}s^{-1}$, $k_{off} \approx 10^{-3}s^{-1}$) as compared to T-T mismatches ($k_{on} \approx 10^4$ $M^{-1}s^{-1}$, $k_{off} = 10^{-4}s^{-1}$). In addition to revealing the high thermodynamic and kinetic stabilities of C-Hg^{II}-T base pairs, our results demonstrated that fluorescent nucleobase analogs enable highly sensitive detection and characterization of metal-mediated base pairs – even in situations where metal binding has little or no impact on the thermal stability of the duplex. Temperature-dependent K_d measurements suggested that less favorable entropy changes of C-Hg^{II}-T versus T-Hg^{II}-T formation are responsible for the negligible impact that Hg^{II} had on the thermal stabilities of DNA duplexes containing C-T mismatches (ΔT_m = 1 – 4 °C) as compared to T-T mismatches (ΔT_m = 6 – 19 °C). Together with the results of the kinetic analysis, these results suggest that C-Hg^{II}-T and T-Hg^{II}-T base pairs exhibit different metal binding modes.

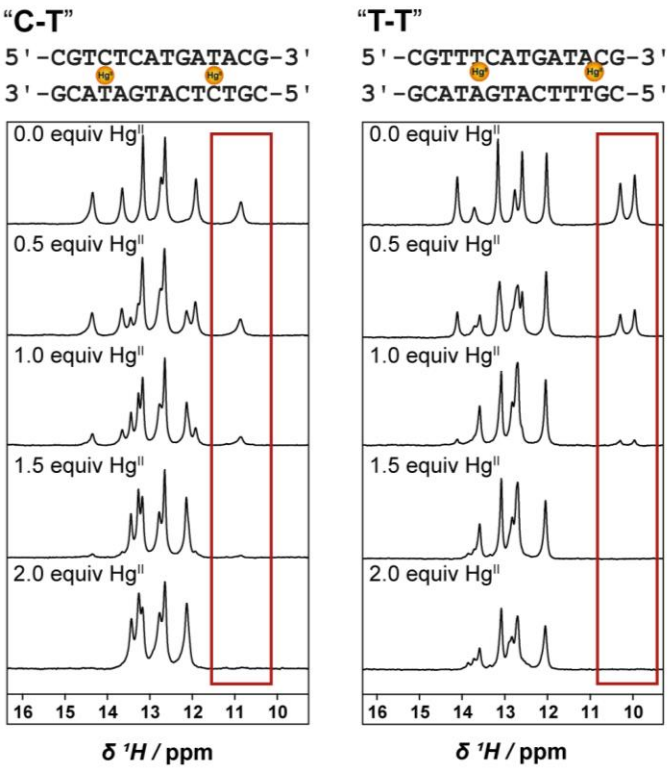

With the goal to investigate the exact metal coordination site of Hg^{II} to C-T-mismatch containing duplex DNA, we synthesized site-specific ^{15}N-labeled oligonucleotides. ^{15}N NMR spectroscopy and ^{15}N-^{199}Hg coupling revealed that Hg^{II} coordinates via two binding sites to C-T mismatches to give a major species containing (*N3*)C-Hg^{II}-(*N3*)T coordination sites and a minor species with (*C4-NH*)C-Hg^{II}-(*N3*)T base pairs in a ratio of ~75% and ~25%, respectively. To investigate the effect of C-Hg^{II}-T formation on the global helical structure of duplex DNA, we solved the solution structures of C-Hg^{II}-T-containing oligonucleotides. NMR experiments revealed two well-resolved duplexes and both structures exhibited characteristics of "mixed" A/B-form duplex DNA. The major species, containing two identical (*N3*)C-Hg^{II}-(*N3*)T coordination sites, adopted a more B-form duplex DNA structure and the minor species, containing two (*C4-NH*)C-Hg^{II}-(*N3*)T base pairs, exhibited more A-form like character. Remarkably, the major- and minor duplex species were in dynamic equilibrium. Dynamic changes in local metal ion coordination were directly coupled to the global interconversion of the two duplexes. The rates of their exchange (k_1 = 4.3 ± 0.6 s^{-1}, k_{-1} = 8.8 ± 0.9 s^{-1}) were on the same time scale as many biochemical and materials processes and can therefore serve as a low-energy barrier switch between two functional states of a duplex.

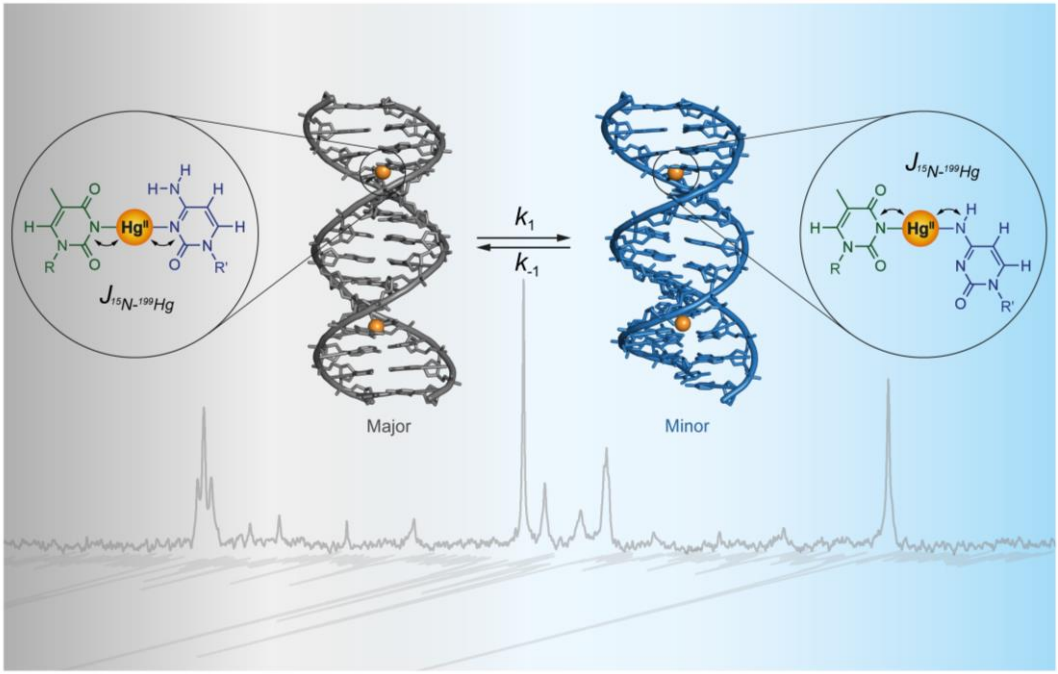

By incorporating fluorescent thymidine and cytosine analogs into oligonucleotides we developed a novel fluorescence based assay to detect and characterize metallo base pair formation. The exceptionally high sensitivity of the fluorescent nucleobase analogs provided a powerful tool to study kinetic and thermodynamic parameters of site-specific metal binding reactions and revealed their effects on dynamic processes involving DNA. In addition to offering a potential mechanism for the cytotoxic effects associated with Hg^{II} exposure, NMR experiments provided the first example of a reversible, metal-coupled switch of alternative helical structures of DNA in dynamic equilibrium.

7.2 Zusammenfassung

Charakterisierung von Metallvermittelten Basenpaaren in Duplex-DNA unter Verwendung von fluoreszierenden Nukleosidanaloga und NMR-Spektroskopie

Alle für das Leben essentiellen biologischen Informationen werden in Nukleinsäuren kodiert und gespeichert. Duplex-DNA ist ein hochdynamisches Molekül und kann sich zu einer Vielzahl von einzelsträngigen und doppelsträngigen Strukturen falten. Einzelsträngige DNA Strukturen und lokale Polymorphismen können regulatorische Rollen bei der Genexpression und anderen zellulären Prozessen übernehmen, indem sie einzigartige Erkennungsstellen für Proteine und kleine Moleküle darstellen. Angesichts der polyanionischen Natur von Nukleinsäuren binden sie sich an Metallionen. Zusätzlich zur Stabilisierung sekundärer DNA-Strukturen können Metallionen Konformationsänderungen induzieren, Protein-DNA Bindungen vermitteln und als katalytische Kofaktoren für die Ribozymkatalyse wirken. Übergangsmetallionen koordinieren an verschiedene Bindungsstellen von Nukleinsäuren und können in einigen Fällen Paarungswechselwirkungen von natürlichen Nukleosiden durch die Bildung metallvermittelter Basenpaaren dramatisch stabilisieren. T-Hg^{II}-T-Basenpaare lieferten die ersten Beispiele für „ganz natürliche“ Metall-vermittelten Basenpaare. Ein metallvermitteltes Basenpaar kann durch die koordination von Übergangsmetallen an Nukleobasen-Fehlpaarungen gebildet werden. Strukturell analoge C-Ag^{I}-C wurden ebenfalls beschrieben, und in beiden Fällen wurde nur ein geringer oder gar kein Einfluss auf die globale Struktur des B-Form-Duplex beobachtet. Die Bildung und Eigenschaften von "ganz natürlichen" Metall-Basenpaaren haben weitreichende Auswirkungen auf die Materialwissenschaften und die Biologie. Frühere Studien haben gezeigt, dass T-Hg^{II}-T als funktionelle Nachahmung von T-A-Basenpaaren dienen können, indem T-T während der DNA-Primerextension stabilisiert wird und in vitro, und möglicherweise auch in vivo, eine enzymatische Fehlinkorporation von dTTP durch Thymin verursacht wird.

Die kinetischen und thermodynamischen Parameter der lokalen, ortsspezifischen Metall-vermittelten Basenpaarbildung in Duplex-DNA sind wichtig für das Verständnis ihrer potenziellen biologischen und Materialeigenschaften. Es gibt jedoch noch keine Studien, die diese Werte untersucht haben. Fluoreszierende Nukleobasenanaloga können hochempfindliche biophysikalische Messungen mit Einzelbasenauflösung ermöglichen, es gibt jedoch noch keine Beispiele für native, ortsspezifische Bindungswechselwirkungen von Metallnukleobasen, die direkt von einem fluoreszierenden Nukleobasenanaloga berichtet werden. Dies würde ein

leistungsfähiges Werkzeug zur Bestimmung der kinetischen und thermodynamischen Parameter lokaler Metallbindungsreaktionen liefern. Unser Ziel war es, einen fluoreszenz-basierten Assay zu entwickeln, um die Bildung von Metallo-Basenpaaren zu detektieren, zu charakterisieren und deren mögliche Auswirkungen auf dynamische Prozesse der DNA zu untersuchen. Wir haben uns vorgestellt, Oligonukleotide mit fluoreszierenden Thymidin und Cytosin analoga zur Bestimmung der kinetischen und thermodynamischen Parameter von Hg^{II}-vermittelten Basenpaaren zu verwenden und damit mögliche Mechanismen für die zytotoxischen und mutagenen Aktivitäten von Hg^{II} aufzudecken. Mit diesem Ziel haben wir kürzlich ein neues fluoreszierendes Thymidin-Mimetikum "^{DMA}T" synthetisiert, das die gleichen Basenpaarungspräferenzen und denselben pKs wie natives Thymin aufweist. Doppelsträngige DNA, die ^{DMA}T-A-Basenpaare enthielten, zeigten die gleichen globalen Strukturen und thermischen Stabilitäten wie doppelsträngige DNA, die T-A-Basenpaare enthielten. Die Quantenausbeute von ^{DMA}T ($\varphi = 0.03$ in Wasser) war kleiner als nach dem Einbau in Duplex-DNA ($\varphi = 0.11$ - 0.20), wo seine fluoreszierenden Eigenschaften sehr empfindlich gegenüber Nucleobasenhydratation, Ionisierung und Basenpaarung waren. Die Thermische Schmelztemperaturanalyse von ^{DMA}T-T- und T-T-Fehlpaarungen, die Oligonucleotide in Gegenwart und Abwesenheit von 1.0 Äquivalent Hg^{II} enthielten, beschrieben die ausgezeichnete Nachahmung von ^{DMA}T für natürliches Thymidin im anspruchsvollen Kontext des T-Hg^{II}-T-Basenpaars. Zugabe von Hg^{II} zu Oligonukleotiden, die eine ^{DMA}T-T-Fehlpaarung enthielten, induzierte eine bi-phasische Fluoreszenzlöschung. Eine steile Steigung wurde beobachtet zwischen 0.0 und 1.0 Äquivalent von hinzugefügtem Hg^{II} als Ergebnis von spezifischer Bindung zu ^{DMA}T-T und eine flache Steigung zwischen 2.0 und 3.0 Äquivalenten aufgrund von nicht-spezifischen Bindungen. Diese Ergebnisse zeigten auf, dass die fluoreszierenden Eigenschaften von ^{DMA}T genutzt werden können, um die ortsspezifische Bindung von Hg^{II}-Ionen an ^{DMA}T-T zu verfolgen, und lieferten das erste Beispiel für die Verwendung fluoreszierender Nukleobasenanaloge um spezifische Bindungsreaktion zwischen DNA und Hg^{II}-Ionen aufzuzeigen.

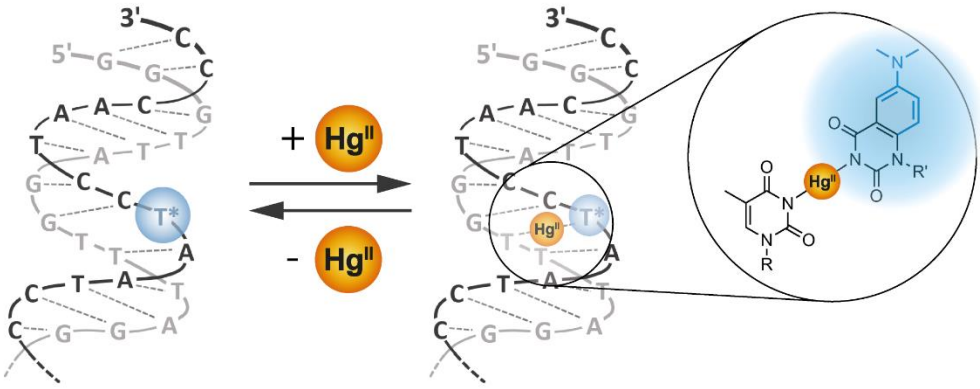

Die Fluoreszenzeigenschaften von ^{DMA}T-A-Basenpaaren waren sehr empfindlich gegenüber Quecksilberbindungsreaktionen an T-T-Fehlpaarungen, die an einer benachbarten Stelle oder ein Basenpaar entfernt waren. Dies ermöglichte die Verwendung von ^{DMA}T-haltigen Oligonukleotiden für die erste fluoreszenzbasierte Untersuchung von direkten, ortsspezifischen Metallbindungsreaktionen unter Beteiligung nicht-modifizierter Nukleobasen in Duplex-DNA. Aufgrund der außergewöhnlich hohen Sensitivität von Fluoreszenzmessungen, konnten wir die lokalen kinetischen und thermodynamischen Parameter von T-Hg^{II}-T-Basenpaaren direkt verfolgen, indem wir Veränderungen der ^{DMA}T-Fluoreszenz von ^{DMA}T-T- und ^{DMA}T-A-haltiger Duplex-DNA beobachteten. Hg^{II} zeigte hochaffine Bindungswechselwirkungen gegenüber doppelsträngiger DNA, die ^{DMA}T-T- und T-T-Fehlpaarungen enthielten, mit Gleichgewichtsdissoziationskonstanten von K_d = 34–77 nM. Duplex-DNA, die ^{DMA}T-A und keine T-T-Fehlpaarung enthielt, zeigte dagegen lokale, unspezifische Hg^{II}-Bindungsaffinitäten von Kd ≥ 2.0 μM. Das Verfolgung von zeitabhängigen Änderungen der Fluoreszenzintensität von ^{DMA}T-haltigen Duplexen zeigte, dass T-Hg^{II}-T-Bindungen durch überraschend langsame Assoziations- und Dissoziationsgeschwindigkeitskonstanten ($k_{on} \approx 10^4$–10^5 M^{-1} s^{-1}, $k_{off} \approx 10^{-4}$–10^{-3} s^{-1}) beschrieben werden. Dies, zusammen mit Halbwertszeiten ($t_{1/2}$) im Bereich von 0.3–1.3 h, zeigten die außergewöhnlich hohen kinetischen Stabilitäten von T-Hg^{II}-T-Basenpaaren auf. Die meisten biochemischen Prozesse finden auf der Zeitskala von Mikrosekunden bis Sekunden statt. Um herauszufinden, ob die außergewöhnlich hohen kinetischen Stabilitäten von T-Hg^{II}-T-Basenpaaren signifikante Barrieren für dynamische Prozesse mit DNA darstellen könnten, untersuchten wir die Kinetik von Strangverdrängungsreaktionen und die Primerverlängerung durch DNA-Polymerase. Unsere Ergebnisse zeigten, dass T-Hg^{II}-T-Basenpaare eine signifikante Barriere gegen DNA-DNA-Strangverdrängungsreaktionen darstellen und die enzymatische DNA-Synthese hemmen, indem sie einen ausgeprägten Stillstand der DNA-Polymerase und die Beendigung der DNA-Synthese an der Stelle des T-Hg^{II}-T-Basenpaars induzierten. Diese Ergebnisse zeigten, dass T-Hg^{II}-T-Basenpaare ein hohes Potenzial haben, den DNA-Metabolismus in vivo zu stören. Dies könnte einen potenziellen Mechanismus für die zytotoxische Aktivität von Hg^{II} darstellen.

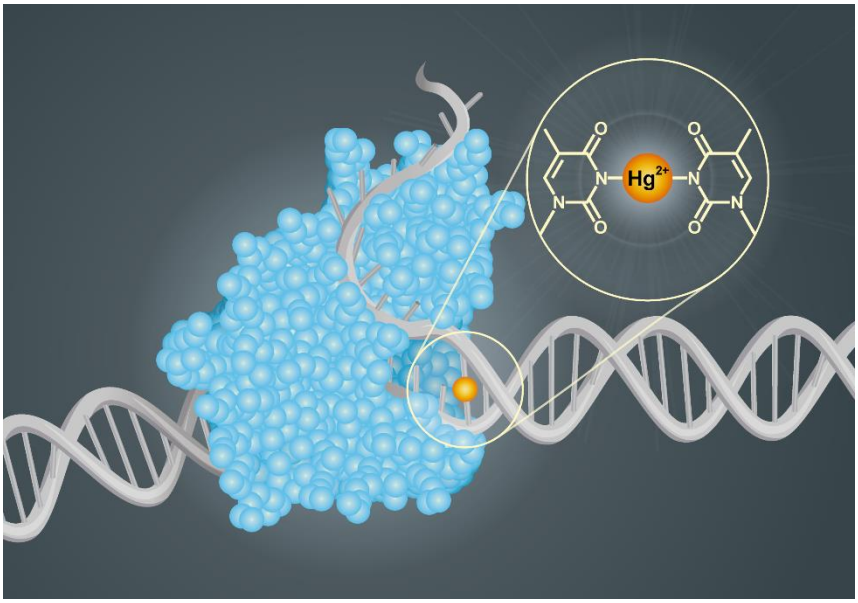

Metallvermittelte Basenpaare erweitern das Repertoire an helikalen Strukturen und Dynamiken, die Duplex-Nukleinsäuren zur Verfügung stehen, und können dadurch gebraucht werden um die biologischen und materiellen Eigenschaften zu verändern. In den letzten Jahren wurde eine große Vielzahl anderer metallvermittelten Basenpaare in Kristallen von Nukleinsäuren gefunden, die nicht eine B-Helix aufweisten. Unter diesen war ein C-Hg^{II}-T-Basenpaar in einer kurzen A-Form-Duplex-DNA, wobei das Metallion unerwartet an das exocyclische Amin (*N4*) eines deprotonierten Cytosinrests und an das *N3* eines deprotonierten Thymidins gebunden war. Im Gegensatz zu T-Hg^{II}-T und C-Ag^{I}-C wurde jedoch durch Zugabe von Hg^{II} wenig oder keine Änderung der thermischen Schmelztemperaturen von den Duplexen beobachtet, die C-T-Fehlpaarung enthielten. Dieses Ergebnis könnte als das Fehlen einer starken Bindungswechselwirkung interpretiert werden, dies ist jedoch nicht der Fall.

Wir charakterisierten Bindungsreaktionen von Hg^{II} und Ag^{I} mit Duplex-DNA, die C-T-Fehlpaarungen enthielten, durch fluoreszierende Nucleobasenanaloga ^{DMA}T und ^{DMA}C, thermischer Denaturierung und ^{1}H-NMR. Unsere Ergebnisse zeigten, dass Hg^{II}, aber nicht Ag^{I}, eine stöchiometrische Bindung von C-T-Fehlpaarungen mit hoher Affinität in Duplex-DNA eingeht. C-Hg^{II}-T-Basenpaare zeigten thermodynamische Stabilitäten (Kd = 10–153 nM), die denen der gut untersuchten T-Hg^{II}-T-Basenpaare sehr ähnlich waren. Sowohl die Assoziations- als auch die Dissoziationskinetik waren im Vergleich zu T-T-Fehlpaarungen ($k_{on} \approx 10^4$ $M^{-1}s^{-1}$, $k_{off} \approx 10^{-4}$ s^{-1}) ca. 10-mal schneller gegenüber C-T-Fehlpaarungen ($k_{on} \approx 10^5$ $M^{-1}s^{-1}$, $k_{off} \approx 10^{-3}$ s^{-1}). Zusätzlich zu den hohen thermodynamischen und kinetischen Stabilitäten von C-Hg^{II}-T-Basenpaaren zeigten unsere Ergebnisse, dass fluoreszierende Nucleobasenanaloga eine hochsensitive Detektion und Charakterisierung metallvermittelter Basenpaare ermöglichen – selbst in Situationen, in denen die Metallbindung wenig oder keine Auswirkungen auf

die thermische Stabilität des Duplexes hat. Temperaturabhängige K_d-Messungen legen nahe, dass weniger günstige Entropieänderungen der C-Hg^{II}-T- im Vergleich zu T-Hg^{II}-T-Bildung für den vernachlässigbaren Einfluss von Hg^{II} auf die thermischen Stabilitäten von DNA-Doppelsträngen mit C-T-Fehlpaarungen verantwortlich sind (ΔT_m = 1–4 °C) im Vergleich zu T-T-Fehlpaarungen (ΔT_m = 6–19 °C). Zusammen mit den Ergebnissen der kinetischen Analyse legen diese Ergebnisse nahe, dass C-Hg^{II}-T- und T-Hg^{II}-T-Basenpaare unterschiedliche Metallbindungsmoden aufweisen.

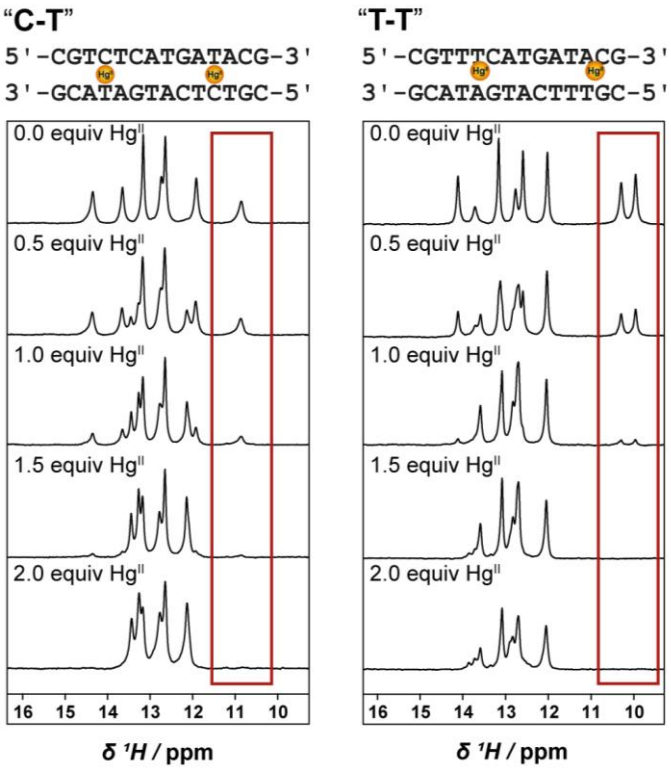

Mit dem Ziel, die genaue Metallkoordinationsstelle von Hg^{II} zu Duplex-DNA, die C-T-Fehlpaarungen enthalten, zu untersuchen, synthetisierten wir ortsspezifische ^{15}N-markierte Oligonukleotide. ^{15}N-NMR-Spektroskopie und ^{15}N-^{199}Hg-Kopplungen zeigten, dass Hg^{II} über zwei Bindungsarten an C-T-Fehlpaarungen koordiniert. Die Hauptspezies (~ 75%) weist (*N3*)C-Hg^{II}-(*N3*)T-Koordinationsstellen auf und die Nebenspezies (~ 25%) (*C4-NH*)C-Hg^{II}-(N3)T-Basenpaare. Um den Effekt der C-Hg^{II}-T-Bildung auf die globale helikale Struktur von Duplex-DNA zu untersuchen, haben wir die dreidimensionale Struktur von C-Hg^{II}-T-haltigen Oligonukleotiden gelöst. NMR-Experimente lieferten zwei gut aufgelöste Duplex Strukturen und beide zeigten Eigenschaften von "gemischter" A/B-Form-Duplex-DNA auf. Die Hauptspezies, die zwei identische (*N3*)C-Hg^{II}-

(*N3*)T-Koordinationsstellen enthielt, nahm eine doppelsträngige B-Form Duplex-DNA-Struktur an, und die Nebenspezies, die zwei (*C4-NH*)C-Hg^{II}-(*N3*)T Basenpaare enthielt, nahmen mehr A-Form Charakter an. Bemerkenswerterweise befanden sich die Haupt- und Neben-Duplex-Spezies in einem dynamischen Gleichgewicht. Dynamische Änderungen in der lokalen Metallionenkoordination waren direkt an die globale Interkonversion der beiden Duplex Strukturen gekoppelt. Die Geschwindigkeitsraten ihrer Interkonversion (k_1 = 4.3 ± 0.6 s^{-1}, k_{-1} = 8.8 ± 0.9 s^{-1}) waren im gleichen Zeitmaßstab wie viele biochemische und materielle Prozesse und können daher als niederenergetischer Barrierenschalter zwischen zwei funktionellen Duplex-DNA Zuständen dienen.

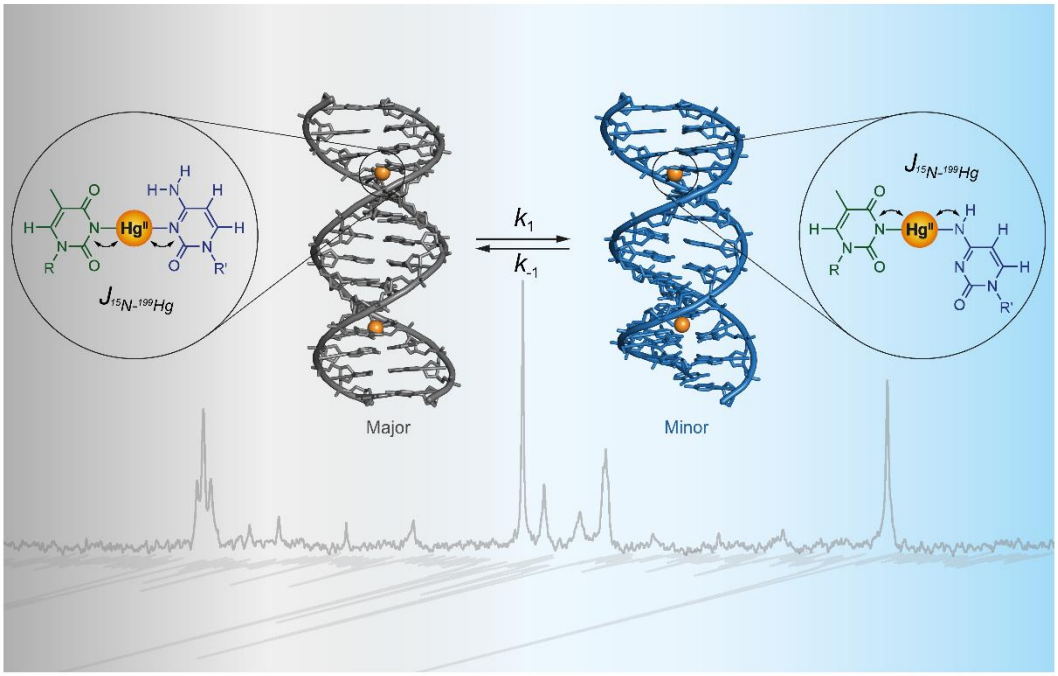

Durch den Einbau fluoreszierender Thymidine und Cytosinanaloga in Oligonukleotide wurde ein neuartiger fluoreszenzbasierter Assay zur Detektion und Charakterisierung der Bildung von Metallobasenpaaren entwickelt. Die außergewöhnlich hohe Empfindlichkeit der fluoreszierenden Nucleobasenanaloga lieferte ein leistungsfähiges Werkzeug, um kinetische und thermodynamische Parameter ortsspezifischer Metallbindungsreaktionen zu untersuchen und ihre Auswirkungen auf dynamische Prozesse mit DNA zu zeigen. Zusätzlich zu einem möglichen Mechanismus für den zytotoxischen Effekte von Hg^{II}, lieferten NMR-Experimente das erste Beispiel für einen reversiblen, metallgekoppelten Wechsel alternativer helikaler DNA-Strukturen im dynamischen Gleichgewicht.

Olivia Schmidt

CURRICULUM VITAE

Department of Chemistry, University of Zurich, Winterthurerstrasse 190, CH-8057 Zurich

Email: olivia.schmidt@chem.uzh.ch; Mobile phone number: +41 77 418 46 61

Education

PhD student, Chemistry, University of Zurich, Department of Chemistry, Zurich, Switzerland **12/2013 – present**

Mentor: Prof. Dr. Nathan W. Luedtke

"Characterization of Metal-Mediated Base Pairs in DNA Utilizing Fluorescent Nucleoside Analogs"

MSc, Chemistry, University of Zurich, Institute of Organic Chemistry, Zurich, Switzerland **09/2011 – 11/2013**

(completed with 5.6 / 6)

Mentor: Prof. Dr. Nathan W. Luedtke

"Metal Binding and Catalysis by Pyridine-Modified DNA"

BSc, Chemistry, University of Zurich, Institute of Organic Chemistry, Zurich, Switzerland **09/2008 – 06/2011**

(completed with 5.1 / 6)

Minor in Biochemistry (completed with 5.4 / 6)

Zurich University of the Arts, Department of Music, Zurich, Switzerland **08/2007 – 09/2008**

Foundation course on the drum set in jazz music

Swiss Confederate Maturity, Kantonsschule Hohe Promenade, Zurich Switzerland **08/2000 – 09/2006**

Research Experience

Synthesis

Synthetic Organic Chemistry, Planning and executing multistep synthesis involving air- and water-sensitive reactions.

DNA synthesis, Oligonucleotide synthesis on solid support and incorporation of non-natural nucleobases into oligonucleotides.

Techniques

NMR Spectroscopy, Characterization and structure determination of small molecules using 1D- and 2D-experiments; investigation of Hg^{II} binding to duplex DNA using ^{1}H-,^{15}N-, ^{199}Hg-, and 2D experiments.

UV/Vis/Fluorescence Spectroscopy, Thermodynamic and kinetic analyses of metal binding to modified oligonucleotides; kinetic analyses of DNA-DNA strand displacement; quantum yield calculations; analyses of electrostatic potential of duplex DNA.

CD Spectroscopy, Secondary structure determination of oligonucleotides and melting temperature calculations; investigation of porphyrin binding to duplex DNA.

HPLC, Purification of oligonucleotides by reverse phase HPLC; catalysis, evaluating the diastereo- and enantioselectivity of Cu^{II} catalyzed *Diels Alder* reactions.

ESI/MS, Characterization of small molecules and oligonucleotides.

Enzymatic DNA Synthesis, Primer extension assays by DNA polymerases.

Polyacrylamide Gel Electrophoresis, Secondary structure determination of oligonucleotides; kinetic analyses of enzymatic DNA synthesis.

Personal Skills

Language skills, German (mother tongue); English (fluent spoken, excellent written skills); French (school knowledge).

Digital competences, MS-Office, ChemOffice, Origin, Prism, Topspin, Scifinder, Adobe Illustrator.

Awards

Best Poster Presentation, XVIIth Symposium on Chemistry of Nucleic Acid Components **06/2017**

Český Krumlov, Czech Republic

Best Oral Presentation, SCS Fall meeting 2016. Meeting of the Swiss Chemical Society **09/2016**

Zurich, Switzerland, **2016**

Alfred Werner Fund, Scholarship awarded for BSc degree **11/2012**

Teaching Experience

Teaching and Supervision

Practical Organic Chemistry, Laboratory course for 2nd year chemistry students (3 semesters; 380 h)

Organic Chemistry Lectures, Preparing and giving exercises to 2nd year chemistry students (3 semesters, 180 h)

Practical General Chemistry, Laboratory course for 1st year medicine students (2 semesters, 300 hours)

Research Project Supervision, Research internship (Alexander Walter); Master thesis (Andrea Benz)

Contributions to Conferences

Poster

Gordon Research Conference on Nucleosides, Nucleotides and Oligonucleotides **06/2017**

Newport, United States

17SCNAC XVIIth Symposium on Chemistry of Nucleic Acid Components **06/2017**

Český Krumlov, Czech Republic

Beilstein Organic Chemistry Symposium on Nucleic Acid Chemistry **10/2016**

Prien am Chiemsee, Germany

Graduate School of Chemical and Molecular Sciences Zurich Retreat **01/2015**

Zuoz, Switzerland

Oral

SCS Fall Meeting of the Swiss Chemical Society, Zurich, Switzerland **09/2016**

Doktorandentag, Au, Switzerland **06/2016**

Publications

6. Olivia P. Schmidt, Simon Jurt, Silke Johannsen, Roland K. O. Sigel, Nathan W. Luedtke, Dynamic structural polymorphism of a metallo DNA double helix, Manuscript in preparation for submission to *Nature Chemistry*.

5. Olivia P. Schmidt, Andrea S. Benz, Guillaume Mata, Nathan W. Luedtke, Hg^{II} binds to C-T mismatches with high affinity, *Nucleic Acids Res.* **2018**, *46*, 6470.

4. Olivia P. Schmidt, DNA polymerase inhibition by high kinetic stability of T-Hg^{II}-T base pairs, *Chimia*, **2017**, *71*, 181.

3. Theodor Marsoner, Olivia P. Schmidt, Therese Triemer, Nathan W. Luedtke, DNA-targeted inhibition of MGMT, *ChemBioChem*, **2017**, *18*, 894.

2. Olivia P. Schmidt, Guillaume Mata, Nathan W. Luedtke, Fluorescent base analogue reveals T-Hg^{II}-T base pairs have high kinetic stabilities that perturb DNA metabolism, *J. Am. Chem. Soc.* **2016**, *138*, 14733. [Highlighted by *Chimia*].

1. Guillaume Mata, Olivia P. Schmidt, Nathan W. Luedtke, A fluorescent surrogate of thymidine in duplex DNA, *Chem. Commun.* **2016**, *52*, 4718.